Technological Interventions for Value Addition of Polyherbal Spent Materials from Ayurvedic Industries

by

Billu Abraham

AcSIR Registration No. 10CC19A39002
RMIT University Registration No. S3989165

A thesis submitted under
AcSIR-RMIT Joint (Cotutelle) Ph.D Program
for the award of the degree of

DOCTOR OF PHILOSOPHY
in
SCIENCE

Under the supervision of

Dr. P. Nisha (Supervisor)
Dr. Anjineyulu Kothakota (Co-Supervisor)

CSIR-National Institute for Interdisciplinary Science and Technology
Thiruvananthapuram, Kerala -695019

Academy of Scientific and Innovative Research
AcSIR Headquarters, CSIR-HRDC campus
Sector 19, Kamla Nehru Nagar,
Ghaziabad, U.P. – 201 002, India

Prof. Benu Adhikari (Senior Supervisor)
Prof. Nitin Mantri (Associate Supervisor)
Prof. Charles Brennan (Associate Supervisor)

School of Science,
Bundoora Campus

Royal Melbourne Institute of Technology (RMIT) University,
Plenty Road, Bundoora, Victoria -3083,
Australia

January 2025

राष्ट्रीय अंतर्विषयी विज्ञान तथा प्रौद्योगिकी संस्थान
वैज्ञानिक तथा औद्योगिक अनुसंधान परिषद् | विज्ञान तथा प्रौद्योगिकी मंत्रालय, भारत सरकार
इंडस्ट्रियल इस्टेट पी.ओ., पाप्पनंकोड, तिरुवनंतपुरम, भारत-695 019

CSIR-NATIONAL INSTITUTE FOR INTERDISCIPLINARY SCIENCE AND TECHNOLOGY (CSIR-NIIST)
Council of Scientific & Industrial Research | Ministry of Science and Technology, Govt. of India
Industrial Estate P.O., Pappanamcode, Thiruvananthapuram, India-695 019

CERTIFICATE

This is to certify that the work incorporated in this Ph.D. thesis entitled, "**Technological Interventions for Value Addition of Polyherbal Spent Materials from Ayurvedic Industries**" submitted by Billu Abraham to the Academy of Scientific and Innovative Research (AcSIR) in fulfillment of the requirements for the award of the Degree of Doctor of Philosophy in Science, embodies original research work carried out by the student.

We, further certify that this work has not been submitted to any other University or Institution in part or full for the award of any degree or diploma. Research materials obtained from other sources and used in this research work have been duly acknowledged in the thesis. Images, illustrations, figures, tables, etc., used in the thesis from other sources, have also been duly cited and acknowledged.

Billu 30/01/2025	K. Anj 30.01.25	30/01/25
Billu Abraham	**Dr.Anjineyulu Kothakota**	**Dr. P. Nisha**
	Co-Supervisor	**Supervisor**

30-01-2025
Thiruvananthapuram

STATEMENTS OF ACADEMIC INTEGRITY

I Billu Abraham, a Ph.D. student of the Academy of Scientific and Innovative Research (AcSIR) with Registration No.10CC19A39002 hereby undertake that, the thesis entitled **"Technological Interventions for Value Addition of Polyherbal Spent Materials from Ayurvedic Industries"** has been prepared by me and that the document reports original work carried out by me and is free of any plagiarism in compliance with the UGC Regulations on *"Promotion of Academic Integrity and Prevention of Plagiarism in Higher Educational Institutions (2018)"* and the CSIR Guidelines for *"Ethics in Research and in Governance(2020)".*

Billu Abraham
Date: 30-01-2025
Place: Thiruvananthapuram

---

lt is hereby certified that the work done by the student, under my supervision, is plagiarism-free in accordance with the UGC Regulations on *"Promotion of Academic Integrity and Prevention of Plagiarism in Higher Educational Institutions {2018)"* and the CSlR Guidelines for *"Ethics in Research and in Governance (2020)".*

K. Anji 30/01/25

सी एस आई आर CSIR भारत का नवाचार इंजन The Innovation Engine of India
niist
डॉ. अन्जिनेयुलु कोत्ताकोटा
Dr. ANJINEYULU KOTHAKOTA
वरिष्ठ वैज्ञानिक/ Senior Scientist
कृषि संसाधन एवं पौद्योगिकी प्रभाग
Agro Processing and Technology Division
सी एस आई आर-राष्ट्रीय अंतर्विषयी विज्ञान तथा प्रौद्योगिकी संस्थान
CSIR-National Institute for Interdisciplinary Science and Technology (NIIST), Govt. of India
तिरुवनन्तपुरम/ Thiruvananthapuram-695 019.

30/01/25

Dr. P. Nisha.
Date: 30-01-2025
Place: Thiruvananthapuram

Acknowledgment

Firstly, I am deeply grateful to Almighty God for granting me the strength, resilience, and clarity needed to see this work through. I extend my sincere thanks to the Council of Scientific and Industrial Research (CSIR) for providing the CSIR-SRF direct fellowship, and to AcSIR and RMIT University, Melbourne, for facilitating my joint PhD program.

I am particularly indebted to my supervisor, Dr. P. Nisha, Senior Principal Scientist, for her invaluable guidance, expertise, and relentless support throughout my research journey. Her mentorship has been transformative, and I feel privileged to have had the opportunity to work under her guidance. I also express my gratitude to my co-supervisor, Dr. Anjineyulu Kothakota, Senior Scientist, for his constant encouragement and insightful contributions.

My deepest appreciation extends to my senior supervisor, Prof. Benu Adhikari at RMIT University, for his expertise, support, and feedback, which enriched my research immensely. I am equally grateful to my associate supervisors, Prof. Nitin Mantri and Prof. Charles Brennan, for their constructive insights and guidance, which greatly enhanced the quality of my work.

I extend my deep gratitude to Dr. A. Ajayaghosh and Dr. C. Anandharamakrishnan (former and present Directors) for providing the necessary facilities for this research. Special thanks to former AcSIR coordinators, Dr. C.H. Suresh and Dr. Karunakaran Venugopal, as well as the current coordinator, Dr. P. Jayamurthy, for their support in academic matters.

I am honored to extend special thanks to Distinguished Prof. Suresh Bhargava, the mastermind behind the AcSIR-RMIT program, for his vision and leadership. I am also grateful to Mr. Tae Kim for facilitating smooth transitions with his insightful emails and discussions, and to Prof. Samantha Richardson and Prof. Jayani Chandrapala, who guided me through the completion of RMIT milestones and coursework.

I emphatically thank the members of my doctoral advisory committee, Dr. K. G. Raghu, Dr. Sashidhar B.S, and Dr. Jayamoorthy P., for their esteemed guidance, professional expertise, and timely cooperation during the course of my research. I am also deeply grateful to Er. M.M. Sreekumar, Dr. Dileep Kumar, Dr. K. G. Raghu (former heads), and Er. Venugopalan V.V., Head of the Department, Agro Processing and Technology Division, CSIR-NIIST, Trivandrum, for their support and encouragement.

I am especially thankful to Mr. Pratheesh, whom I regard as a brother, for his unwavering support and constant assistance whenever needed, as well as the kindness and encouragement of his parents. My gratitude also extends to Mr. Peer Mohamed for rheology and thermal analysis, Soumini for NMR, Viji for MALDI, Hareesh for SEM analysis, Amal for FTIR, Kiran Mohan for TEM, and Sreejith, Jerin, Merin, and Aswathi for their academic support.

It has been a privilege to work in NIIST, where I had the pleasure of collaborating with many outstanding colleagues. I extend my gratitude to my senior and junior colleagues, including Dr. Arun, Liza, Shini, Dr. Resmitha, Dr. Nayana, Dr. Sithara, Dr. Sannya, Dr. Padma, Dr. Navami, Dr. Kavya, Nidhina, Sudhina, Dr. Chinthu, Abhijit, Reshma, Archana, Nisha, Sandhya, Hari, Noor,

Titto, Ramees, Treeza, Dr. Cally Makebe, Anupama Tuluwani, Evan, Abin, Nishana, Shaheena, Parvathi, Aiswarya, Meghana, Dr. Prabha, Dr. Eveline, Dr. Sruthi, Dr. Anagha, Anusha, Dr. Poornima, Ashin, Dr. Taniya, Dr. Raveena, Dr. Roopasree, Dr. Lakshmi, Dr. Juby,

Dr. Jesmina, Gopika, Shenjo, Theertha, Dr. Drishya, Dr. Soumya, Dr. Salin, Dr. Genu, Dr. Sree Lakshmi, Dr. Swapna, Dr. Anupama, Dr. Preetha, Dr. Shyni, Dr. Kavitha, Surjith, Silpa, Anoop, Nandhu, Kiran, Thaejus, Krishna priya, Rahul, Sanooj, Arun, Anju, Gayatri, Arun, Midhun, Merin, Sooraj, Arun, Nandhu, Aswin, Jijo, Sreenandhu, Jasim, Jibin, Fahad, Deepak, Adarsh, Rajeev, Camphel and Vishnu.

I sincerely thank Heba, my junior group member, for her constant support and encouragement throughout the final stages of my research. I extend my heartfelt gratitude to Dr. Bineesh, my supervisor Dr. Nisha's husband, for his constant motivation and invaluable suggestions, which have contributed significantly to my journey. I also thank their daughters, Aintzza and Avishka, for their kindness and support. I am deeply grateful to my childhood friend Tobin, now an optometrist in Australia, and his wife Shiljha, for their unwavering encouragement and daily calls, which have been a great source of strength. My sincere thanks also go to my dear friend Athira A.S. (Athi) for her steadfast support and companionship through every high and low. I am equally thankful to Shyamaettan and Krishnakumar for their limitless support and always being available to clarify my doubts and assist with anything I needed.

Sreepuram House, where I stayed during my time at NIIST, holds a special place in my heart as a home filled with cherished memories. I also extend my gratitude to my M.Sc. friend Rothish, who has been by my side, providing invaluable encouragement and insights throughout this journey.

I wish to thank the staff of the Microscopy and Microanalysis Facility (RMMF), Micro Nano Research Facility (MNRF), and the Analytical Chemistry and Food Science and Innovation Centre at RMIT for their technical support. A special thanks goes to my friends and colleagues at RMIT- Dr. Zijiya, Dr. Mehran Ghasemlou, Kanjana Singh, Yogesh, Dr. Kingshuk, Nazila, Linh, Zahra, Jayani, Yuxin, Nethra, Sanka, Billy, Harshveer, Sooraj, Dr. Joe, Dr. Zimar, Emmanuavel, Dr. Prashant, Dr. Prem, Dileep, Jeet, Anooj, Aditya, Avinash, Sunil, Prajakta, Dr. Chaitali Dekiwadia, Dr. Lillian, Andre, Spiros, Yan, Mina, and Maryam—for their helpful advice and camaraderie.

I express my deepest appreciation to my family. My parents, the late Mr. Babu Abraham and Mrs. Sally Abraham, have been my pillars of strength, and their unwavering support and love have been a constant source of inspiration. I am also grateful to my brother Bino and his wife Susan for their understanding and encouragement throughout this journey. To all those whose names may not appear individually here but who have supported me in countless ways, I extend my heartfelt thanks. Lastly, and most importantly, I thank Almighty God for His grace and blessings, which have guided me through this academic milestone in my life.

Once I thank you to all
Billu Abraham

DEDICATED TO MY DEAR

APPA AND AMMA

Table of Contents

Thesis title page		
Certificate		i
Statement of integrity		ii
Acknowledgment		iii
Table of contents		vi
List of abbreviations		xv
List of units and symbols		xix
List of figures		xxi
List of graphical abstract		xxiv
List of tables		xxv
Summary		1
Chapter 1	**Introduction**	4
1.1	**Introduction**	5
1.2	**Importance of the thesis work**	7
1.3	**Research questions**	9
1.4	**Objectives**	9
1.5	**Expected outcomes**	10
1.6	**Outline of thesis**	10
	References	13
Chapter 2A	**Literature Review**	17
	Status and prospects of valorisation of Ayurvedic spent materials	
	Abstract	18
2A.1	**Introduction**	19
2A.2	**Ayurvedic formulations and Dashamoola**	22
2A.2.1	Dashamoola: Composition, therapeutic applications	22
2A.2.2	Dashamoolarishta: A key Dashamoola product	24
2A.3	**Spent materials generation in the Ayurvedic industry**	26
2A.3.1	Types of spent material generated	26
2A.3.2	Occurrence of Dashamoola spent material (DSM)	28
2A.3.3	Current disposal practices and associated challenges	29
2A.4	**Prospects and benefits of valorisation**	31
2A.4.1	Potential for creating value-added products	31
2A.4.1.1	Applications of residual bioactive compounds	32

2A.4.1.2	Utilisation of lignocellulosic biomass	32
2A.4.1.3	Nanotechnology innovations	34
2A.4.1.4	Biopolymer advancements in Pickering emulsions	34
2A.4.2	Benefits of valorisation	36
2A.5	Challenges, gaps in knowledge, and research directions	38
2A.5.1	Key challenges	38
2A.5.2	Gaps in knowledge	38
2A.5.3	Future prospects	39
2A.6	**Conclusion**	40
	References	40
Chapter 2B	**Literature Review**	51
	Lignin-based nanomaterials for food and pharmaceutical applications: recent trends and future outlook	
	Abstract	52
2B.1	**Introduction**	53
2B.2	**Sources of lignin**	55
2B.3	**Applications of lignin**	60
2B.3.1	Food industry applications	61
2B.3.1.1	Emulsion	66
2B.3.1.2	Packaging	67
2B.3.1.3	Nutrient delivery	68
2B.3.2	Pharmaceutical applications	69
2B.3.2.1	Hydrogels for drug delivery	69
2B.3.2.1.a	Cross-linking method	69
2B.3.2.1.b	ATRP and RAFT methods	70
2B.3.2.1.c	Copolymerization method	70
2B.3.2.1.d	Ultrasonication method	70
2B.3.2.1.e	Wet spinning method	71
2B.3.3	Tissue engineering applications	73
2B.3.4	Lignin composites with biological activity	75
2B.3.4.1	Antioxidant activity	75
2B.3.4.2	Antimicrobial properties	77
2B.3.4.3	Lignin composites for drug delivery systems	78
2B.3.4.4	Lignin composites for wound healing	79
2B.3.4.5	Lignin for disease prevention	80
2B.4	**Recent trends in lignin research: nanolignin**	96
2B.4.1	The rationale for nanolignin preparation	96
2B.4.1.1	Nanolignin from mechanical processes	98

2B.4.1.2	Nanolignin from solvent shifting method	99
2B.4.1.3	Nanolignin from pH shifting technique	99
2B.4.1.4	Nanolignin from template-based synthesis technique	99
2B.4.1.5	Nanolignin from ice-segregation-induced self-assembly method	100
2B.4.1.6	Nanolignin from aerosol process	100
2B.4.1.7	Nanolignin from electrospinning method	100
2B.4.1.8	Nanolignin from supercritical fluid processes	101
2B.4.1.9	Nanolignin from solvent antisolvent precipitation	101
2B.4.1.10	Nanolignin from acoustic cavitation assisted nanoparticles preparation	102
2B.4.1.11	Nanolignin from SERSL	102
2B.4.1.12	Nanolignin from green synthesis process	102
2B.4.1.13	Nanolignin from hydroxymethylation	102
2B.4.1.14	Nanolignin from wheat pulping black liquor	103
2B.4.1.15	Nanolignin from supercritical antisolvent technology	103
2B.4.1.16	Nanolignin from chemomechanical methods	103
2B.4.1.17	Nanolignin from self-assembly	104
2B.4.2	Applications of nanolignin	104
2B.4.2.1	Food packaging	105
2B.4.2.2	Nanolignin as a radical scavenger/antioxidant	106
2B.4.2.3	Nanolignin as a carrier	106
2B.4.2.4	Solid and porous particles/structures	108
2B.4.2.5	Nanolignin for oral disease and tissue regeneration	109
2B.4.2.6	Nanolignin as a UV blocker	109
2B.4.2.7	Nanolignin as adsorbent	110
2B.4.2.8	Nanolignin as supercapacitor	110
2B.4.2.9	Nanolignin as surfactant	111
2B.4.3	United nations sustainable development goal (UNSDG) achieved with the development of nanolignins	111
2B.5	**Future perspectives**	112
2B.6	**Conclusion**	113
	References	113
Chapter 3	**Phytochemical rich extract from the spent material generated from industrial Dashamoola preparation (a medicinal Ayurvedic decoction)**	135

	with antioxidant, antidiabetic and anti-inflammatory potential	
	Abstract	136
3.1	**Introduction**	138
3.2	**Materials and methods**	139
3.2.1	Chemicals and plant material	139
3.2.2	Proximate composition and mineral analysis	140
3.2.3	Preparation of the extracts	140
3.2.4	High-performance thin layer chromatography (HPTLC)	141
3.2.5	Fourier transform infrared spectrum (FTIR)	141
3.2.6	Phytochemical analysis of spent Dashamoola	142
3.2.6.1	Determination of total phenolic content (TPC)	142
3.2.6.2	Determination of total flavonoid content (TFC)	142
3.2.7	Chemical profiling and quantification using LCMS/MS	142
3.2.8	Antioxidant analysis of Dashamoola spent material	145
3.2.8.1	DPPH Radical scavenging activity	145
3.2.8.2	ABTS Assay	145
3.2.8.3	Nitric oxide radical scavenging assay	145
3.2.9	Antidiabetic assay of Dashamoola spent material	146
3.2.9.1	α -amylase inhibition assay	146
3.2.9.2	α - glucosidase inhibition assay	147
3.2.9.3	Glucose uptake assay	147
3.2.10	Anti-inflammatory activity of spent Dashamoola	148
3.2.10.1	Inhibition of albumin denaturation	148
3.2.10.2	Inhibition of antiproteinase action	148
3.2.10.3	Nitric oxide inhibition assay	149
3.3	**Results and discussion**	150
3.3.1	Proximate analysis of DSM	150
3.3.2	Comparative evaluation of phytochemicals by HPTLC	150
3.3.3	Fourier transform infrared spectroscopy (FTIR)	152
3.3.4	Total phenolic content (TPC) and flavonoid content (TFC)	153
3.3.5	Profiling and quantification using LC-MS/MS	154
3.3.6	Evaluation of antioxidant efficiency	157
3.3.7	In vitro antidiabetic assay	158
3.3.8	Glucose uptake assay	159
3.3.9	In vitro anti-inflammatory assay	161

3.4	**Conclusion**	164
	References	165
Chapter 4	**Lignin nanoparticles from Ayurvedic industry spent materials: Applications in Pickering emulsions for curcumin and vitamin D_3 encapsulation**	175
	Abstract	176
4.1	**Introduction**	178
4.2	**Material and methods**	180
4.2.1	Material and chemicals	180
4.2.2	Isolation of lignin from DSM	180
4.2.3	Preparation of nano lignin	180
4.2.4	Zeta potential and particle size	181
4.2.5	Characterization of LNP	181
4.2.5.1	Purity of extracted lignin	181
4.2.5.2	Functional group analysis of LNP using FTIR	181
4.2.5.3	Determining the molecular weight of LNP	181
4.2.5.4	NMR characterization of LNP	182
4.2.5.5	Analysis of phenolic content	182
4.2.5.6	Surface composition of LNP	182
4.2.5.7	Thermal degradation of LNP	182
4.2.5.8	Thermal characteristics of LNP	183
4.2.5.9	Crystalline and amorphous content of LNP	183
4.2.5.10	Contact angle	183
4.2.5.11	Microscopic surface morphology	184
4.2.5.12	Internal structure of LNP	184
4.2.6	Preparation of O/W Pickering emulsions	184
4.2.6.1	Rheological properties	184
4.2.6.2	Microstructure of emulsions	185
4.2.6.3	Creaming index	185
4.2.6.4	Encapsulation efficiency	186
4.2.6.5	Cell viability assay	186
4.2.6.7	Storage stability	187
4.2.7	Statistical analysis	187
4.3	**Results and discussion**	188
4.3.1	Characterization of extracted lignin	188
4.3.1.1	Chemical composition	188
4.3.1.2	Bonding and elemental composition	191
4.3.1.3	Thermal behaviour	192
4.3.1.4	Surface morphology and microstructure	194

4.3.2	Characteristics of Pickering emulsion	194
4.3.2.1	Particle size and zeta potential	197
4.3.2.2	Colour analysis of emulsions	198
4.3.2.3	Viscometrical and rheological behaviour	199
4.3.2.4	Molecular level interactions in emulsions	201
4.3.3	Toxicity	202
4.3.4	Storage stability of Pickering emulsion	203
4.4	**Conclusion**	206
	References	207
Chapter 5	**Nutrient-rich puffed snacks developed using blended flours and lignin Pickering emulsions containing curcumin and vitamin D_3**	218
	Abstract	219
5.1	**Introduction**	221
5.2	**Materials and methods**	223
5.2.1	Materials	223
5.2.2	Preparation of O/W Pickering emulsions	224
5.2.3	Preparation of extruded snacks	224
5.2.4	Extrusion process	224
5.2.5	Analysis of the physical and functional attributes of extrudates	226
5.2.5.1	Proximate composition of flours and extrudates	226
5.2.5.2	Estimation of dietary fiber	227
5.2.5.3	Expansion ratio	227
5.2.5.4	Bulk density	228
5.2.5.5	Colour analysis	228
5.2.5.6	Texture analysis	228
5.2.5.7	Sensory analysis	229
5.2.5.8	Cross-sectional microscopic images	229
5.2.5.9	Observing microscopic morphology	229
5.2.5.10	Stability of curcumin and vitamin D_3	230
5.2.6	Statistical analysis	230
5.3	**Results and discussion**	230
5.3.1	Nutritional profile of extruded snacks	230
5.3.2	Bulk density and expansion ratio	233
5.3.3	Texture profile analysis	235
5.3.4	Colour analysis	237
5.3.5	Sensory profile of snacks	239
5.3.6	Microstructural analysis	241

5.3.7	Stability of bioactives in lignin-encapsulated extrudates	242
5.4	**Conclusion**	245
	References	245
Chapter 6	**Cellulose and lignin nanoparticles from an Ayurvedic waste stream for essential oil-based active packaging to extend shelf life of perishable fruit**	255
	Abstract	256
6.1	**Introduction**	258
6.2	**Materials and methods**	260
6.2.1	Raw material selection and source	260
6.2.2	Chemicals and reagents	260
6.2.3	Fruit selection	261
6.2.4	Nano-cellulose (NCP) and nano lignin (LNP) extraction from DSM	261
6.2.5	Characterization of NCP	262
6.2.5.1	Particle size and zeta potential of NCP	263
6.2.5.2	Observation of microstructure	263
6.2.5.3	Functional group analysis of NCP using FTIR	263
6.2.5.4	Thermal degradation of NCP	263
6.2.5.5	Surface composition of NCP	263
6.2.5.6	Crystalline and amorphous content of NCP	264
6.2.6	Preparation and characterization of emulsions	264
6.2.6.1	Particle size and zeta potential	264
6.2.7	Film casting preparation	265
6.2.8	Characterization of films	266
6.2.8.1	Thickness of films	266
6.2.8.2	Water contact angle analysis	266
6.2.8.3	Water vapor transmission rate (WVTR)	266
6.2.8.4	Measurement of colour parameters	266
6.2.8.5	Microstructure analysis	267
6.2.8.6	Measurement of mechanical properties	267
6.2.8.7	Thermal degradation of films	267
6.2.8.8	Thermal characteristics of films	267
6.2.8.9	Crystalline and amorphous content of films	268
6.2.8.10	Film transparency	268
6.2.8.11	Antioxidant properties of films	268
6.2.8.12	Antibacterial assays of films	268
6.2.9	Assessment of preservation effect on strawberry	269

6.2.9.1	Colour analysis of strawberry	269
6.2.9.2	Hardness of strawberry	269
6.2.9.3	pH of strawberry	270
6.2.10	Statistical analysis	270
6.3	**Results and discussion**	270
6.3.1	Characterization of extracted lignin and cellulose from DSM	270
6.3.2	Compositional analysis of NCP	273
6.3.3	Emulsion preparation and characterization	275
6.3.4	Essential oil-infused bioactive PVOH film and its characterization	276
6.3.4.1	Physical properties of films	277
6.3.5	Surface morphology of films	279
6.3.6	Mechanical properties of films	281
6.3.7	FTIR, thermal properties, and UV transmittance of films	283
6.3.8	Antioxidant and antimicrobial activity of films	286
6.3.9	Application of films to extend the shelf life of strawberries	288
6.3.9.1	Storage studies of strawberry	289
6.4	**Conclusion**	291
	References	292
Chapter 7	**General discussion, conclusion and recommendation**	305
7.1	**Overview of research work**	306
7.2	**Key findings, general discussion, and conclusion**	308
7.2.1	Extraction and bioactive potential of phenolic compounds from DSM	308
7.2.2	Development and application of lignin nanoparticles	309
7.2.3	Fortification of extruded snacks using nanolignin from DSM	309
7.2.4	Creating active packaging films using NCP and LNP from DSM	310
7.3	**Contribution made by the thesis to the body of knowledge**	310
7.4	**Recommendations for future work**	313
	References	314
	AcSIR course work	316
	Abstract	317

Details of publications emanating from the thesis work 318
List of publications not related to thesis 318
List of posters and orals presented 321
Contributions to Academic Conferences 322
SCI Publications 325

List of abbreviations

ABTS	2,2'-azino-bis(3-ethylbenzothiazoline-6-sulphonic acid)
ACL-THF	Acetylated Lignin-Tetrahydrofuran
Ag-NPs	Silver Nanoparticles
AL	Alkali Lignin
ALNP	Alkali Lignin Nanoparticles
ANOVA	Analysis of Variance
AOAC	Association of Official Analytical Chemists
C_TTO	Nano Cellulose Powder with Tea Tree Oil
CE	Collision Energy
CG	Corn Grits
CH	Chitosan
CH_3COOH	Glacial Acetic Acid
CL_TTO	Cellulose-Lignin with Tea Tree Oil
CN	Chitin Nanofibrils
CTAB	Cetyltrimethylammonium Bromide
Cu	Curcumin
DA	Dashamoola Arishta
DDS	Drug Delivery Systems
DE	Dashamoola Extract
DHP	Dehydrogenative Polymerization
DL	Detection Limit
DLNP	Dioxane Lignin Nanoparticles
DLS	Dynamic Light Scattering
DMEM	Dulbecco's Modified Eagle's Medium
DPPH	2,2-Diphenyl-1-picrylhydrazyl
DSC	Differential Scanning Calorimetry
DSME	Dashamoola Spent Material Extract
DTG	Derivative Thermogravimetric
E.E	Encapsulation Efficiency
ECM	Extracellular Matrix
EPS	Extruded Puffed Snacks
ESH	Epichlorohydrin
FBS	Fetal Bovine Serum
Fe-LNP	Iron-Lignin Nanoparticles
FTIR	Fourier Transform Infrared Spectroscopy
GAE	Gallic Acid Equivalent
GLUT4	Glucose Transporter Type 4
GMA	Glycidyl Methacrylate
HCl	Hydrochloric Acid

HPLC	High-Performance Liquid Chromatography
HPLC-DAD	High-Performance Liquid Chromatography with Diode-Array Detector
HPTLC	High-Performance Thin Layer Chromatography
HRP	Horseradish Peroxidase
HSQC	Heteronuclear Single-Quantum Coherence
HSV	Herpes Simplex Virus
HTST	High-Temperature Short-Time
IC_{50}	Half-maximal Inhibitory Concentration
L_TTO	Lignin Nanoparticles with Tea Tree Oil
LB	Luria-Bertani (Broth)
LC-MS/MS	Liquid Chromatography-Mass Spectrometry
LMNP	Lignin-Melanin Core-Shell Nanoparticles
LMWL	Low Molecular Weight Lignin
Ln	Lignin Solutions
LnE+Cu+vD_3	Lignin Emulsion Loaded with Curcumin and Vitamin D_3
LNP	Lignin Nanoparticles
LPC	Lignin-Poly(diallyl dimethylammonium chloride) Complexes
LPE	Lignin Pickering Emulsion
LPS	Lipopolysaccharides
LVE	Linear Viscoelastic Region
MIC	Minimum Inhibitory Concentration
MNP	Melanin Core-Shell Nanoparticles
MTT	3-(4,5-dimethylthiazol-2-yl)-2,5-diphenyltetrazolium bromide
NCP	Nano Cellulose Powder
NR	Natural Rubber
NREL	National Renewable Energy Laboratory
O/W	Oil in Water
PAHs	Polycyclic Aromatic Hydrocarbons
PBAT	Poly(butylene adipate-co-terephthalate)
PBS	Phosphate-Buffered Saline
PCL	Polycaprolactone
PDI	Polydispersity Index
PEG	Polyethylene Glycol
PGLNs	Polymer-Grafted Lignin Nanoparticles
PLA	Polylactic Acid
PMF	Pearl Millet Flour
PMMA	Polymethyl Methacrylate
PNP	Patented and Proprietary Products
PVA	Polyvinyl Alcohol

PVOH	Polyvinyl Alcohol
QE	Quercetin Equivalent
QL	Quantitation Limit
RAFT	Reversible Addition-Fragmentation Chain Transfer
RH	Relative Humidity
ROS	Reactive Oxygen Species
RSV	Resveratrol
RTE	Ready-To-Eat
SCF	Spent Coconut Flour
SCP	Standard Cellulose Powder
SD	Standard Deviation
SDGs	Sustainable Development Goals
SDS	Sodium Dodecyl Sulfate
SEM	Scanning Electron Microscopy
SERSL	Steam Exploded Rice Straw Lignin
SLP	Standard Lignin Powder
SLRM	Self-Assembled Lignin Micelles
SPF	Sun Protection Factor
SPSS	Statistical Package for the Social Sciences
T_0	Onset Temperature
TC	Conclusion Temperature
TEAC	Trolox Equivalent Antioxidant Capacity
TEM	Transmission Electron Microscopy
TG	Thermal Gravimetric
TGA	Thermogravimetric Analysis
TO	Onset Temperature
TP	Peak Temperature
T_p	Peak Temperature
TPA	Texture Profile Analysis
TTO	Tea Tree Oil
T_x	Conclusion Temperature
UNSDG	United Nations Sustainable Development Goal
UV-Vis	Ultraviolet-Visible Spectroscopy
UW	Unwrapped
vD_3	Vitamin D_3
VOCs	Volatile Organic Compounds
WAXD	Wide-Angle X-ray Diffraction
WCA	Water Contact Angle
WHO	World Health Organization
WVTR	Water Vapour Transmission Rate

XPS	X-ray Photoelectron Spectroscopy
XRD	X-ray Diffraction
YI	Yellowness Index
ΔE	Total Colour Change

List of units and symbols

g/cm^3	Grams per cubic centimeter
ppm	Parts per million
N	Newton
°C	Degrees Celsius
mm	Millimeters
%	Percentage
% w/v	Weight/volume percentage
mg GAE/g	Milligrams gallic acid equivalent per gram
mg QE/g	Milligrams quercetin equivalent per gram
µg/mL	Micrograms per milliliter
µg/g	Micrograms per gram
µg/L	Micrograms per liter
mM	Millimolar
nm	Nanometers
cm^{-1}	Wavenumber
minutes	Time in minutes
cm	Centimeters
hours	Time in hours
°C	Temperature
%	Percentage
mL	Milliliters
nm	Nanometers
mV	Millivolts
g	Grams
KDa	Kilodaltons
m/s^2	Gravitational acceleration
rpm	Revolutions per minute
rad/s	Radians per second
Pa·s	Pascal-second
mg	Milligrams
mg/mL	Milligrams per milliliter
kV	Kilovolts
mW/cm^2	Milliwatts per square centimeter
µg/g	Micrograms per gram
g/cm^3	Grams per cubic centimeter
ppm	Parts per million
N	Newton
°C	Degrees Celsius
mm	Millimeters
%	Percentage

Wb %	Wet basis percentage
rpm	Revolutions per minute
µm	Micrometer
nm	Nanometers
mV	Millivolts
µm	Micrometers
g/m²·day	Grams per square meter per day
°	Degrees
cm^{-1}	Wavenumbers
°C	Degrees Celsius
%	Percentage
MPa	Megapascals
N	Newtons
AU	Absorbance Units
µL	Microliters
g	Grams
kV	Kilovolts
eV	Electron volts
°2θ	Degrees two-theta

List of Figures		Page
Chapter 1	**Introduction**	
Fig. 1.1	Overview of the four experimental chapters of the thesis, outlining the experimental work conducted.	13
Chapter 2A	**Literature Review** **Status and prospects of valorisation of Ayurvedic spent materials**	
Fig. 2A.1	Classification of valiyapanchamoola (larger plants) and laghupanchamoola (smaller plants) with corresponding species used in Ayurvedic formulations.	24
Fig. 2A.2	Commercial Dashmoolarishta products from various brands.	25
Fig. 2A.3	Dashamoola spent material (DSM) - a byproduct generated from the production of Dashamoolarishta.	28
Fig. 2A.4	Schematic of lignocellulosic biomass components derived from plant sources.	33
Fig. 2A.5	Schematic representation of Pickering emulsion	35
Chapter 2B	**Literature Review** **Lignin-based nanomaterials for food and pharmaceutical applications: recent trends and future outlook**	
Fig. 2B.1	Lignin extraction method using alkali.	57
Fig. 2B.2	Applications of lignin.	61
Fig. 2B.3	Nanolignin preparation method.	96
Fig. 2B.4	Applications of nanolignin.	105
Chapter 3	**Phytochemical rich extract from the spent material generated from industrial Dashamoola preparation (a medicinal Ayurvedic decoction) with antioxidant, antidiabetic and anti-inflammatory potential**	
Fig. 3.1	TLC Plate views (I and II) and corresponding HPTLC chromatograms (III and IV) of DE and DSME at 254 and 366 nm.	151
Fig. 3.2	FTIR spectra of Dashamoola raw extract (DE) & Dashamoola spent material extract (DSME).	153
Fig. 3.3	LC-MS/MS analysis of compounds in DE & DSME.	156
Fig. 3.4	LC-MS/MS chromatograms showing (a) standard polyphenols (150 ppb mix), (b) DE, and (c) DSME.	157
Fig. 3.5	The effect of DSME extract on L6 myoblast and RAW 264.7 cell viability by MTT assay.	160

Fig. 3.6	Glucose uptake (2-NBDG) in L6 myoblast cells observed under confocal microscopy (BD Falcon).	161
Fig. 3.7	NO production inhibition assay by griess reagent.	164
Chapter 4	**Lignin nanoparticles from Ayurvedic industry spent materials: applications in Pickering emulsions for curcumin and vitamin D_3 encapsulation**	
Fig. 4.1	Images of lignin solution at different pH levels (4-10), and lignin solution size & zeta potential data	188
Fig. 4.2	2D-NMR spectroscopy, FTIR spectroscopy comparison of SLP and LNP	189
Fig. 4.3	XPS analysis: Survey spectrum and curve fitting for carbon and oxygen in SLP and LNP	192
Fig. 4.4	Thermal and structural analyses: TGA, DSC, and XRD for SLP and LNP	193
Fig. 4.5	Microscopic characterization of LNP (SEM, TEM), and contact angle measurement	195
Fig. 4.6	Formation of lignin emulsion, LNP concentration effects, and fluorescence microscopy of emulsions	196
Fig. 4.7	Viscosity curves, amplitude sweep, frequency sweep, FTIR analysis, and toxicity of lignin emulsions	200
Fig. 4.8	HPLC chromatograph: Encapsulation efficiency for curcumin and vitamin D_3 in emulsions	202
Fig. 4.9	Visual stability images of emulsions (LnE+Cu+vD_3) under room and refrigeration temperatures	203
Fig. 4.10	Particle size, zeta potential, and colour value changes in emulsions during 90-day storage	205
Chapter 5	**Nutrient-rich puffed snacks developed using blended flours and lignin Pickering emulsions containing curcumin and vitamin D_3**	
Fig. 5.1	Flowchart of extrusion process to produce EPS: C1 - Control, S1 – EPS with blended flour, S2 – EPS with LPE.	226
Fig. 5.2a	Bulk density content in the extrudates.	235
Fig. 5.2b	Expansion ratio of extruded puffed snacks (EPS).	235
Fig. 5.3	Texture profile of extruded puffed snacks. All parameters expressed in Newton (N). Significant differences marked.	237
Fig. 5.4	Sensory profiles of extruded puffed snacks: corn grit (C1), blended flour (S1), and S2 with LPE.	240

Fig. 5.5a-c	Microscopic images of extruded puffed snacks (optical microscopy).	242
Fig. 5.5d-f	Microscopic images of extruded puffed snacks (SEM).	242
Fig. 5.6	HPLC chromatograms of extruded snacks showing bioactive stability.	244
Chapter 6	**Cellulose and lignin nanoparticles from an Ayurvedic waste stream for essential oil-based active packaging to extend shelf life of perishable fruit**	
Fig. 6.1	Characteristics of nanocellulose powder (NCP) obtained from Dashamoola spent material (DSM).	273
Fig. 6.2	XPS analysis of NCP obtained from Dashamoola spent material (DSM).	274
Fig. 6.3	Visual images of tea tree oil emulsions with cellulose (C_TTO), lignin (L_TTO), and their combination (CL_TTO).	276
Fig. 6.4	Analysis of polyvinyl alcohol (PVOH) treatments showing photographic appearance and mechanical flexibility.	281
Fig. 6.5	Mechanical profiles of PVOH composites.	283
Fig. 6.6	Polyvinyl alcohol (PVOH)-based films with lignin, cellulose, and tea tree oil additives.	286
Fig. 6.7	Antioxidant (DPPH scavenging) and antimicrobial (E. coli inhibition) activities of pure PVOH films.	288
Fig. 6.8	Strawberry preservation studies under room temperature and refrigeration conditions.	289
Fig. 6.9	Storage performance of strawberries wrapped in different films over 14 days.	291

Graphical abstracts		Page
Fig. 1	Graphical abstract showing the extraction, chemical profiling, and bioactivity evaluation of Dashamoola Spent Material (DSM).	137
Fig. 2	Graphical abstract showing lignin extraction, nanoparticle formation, and emulsion preparation with curcumin and vitamin D_3.	177
Fig. 3	Graphical abstract showing extruded snacks from blended flours and lignin Pickering emulsions with curcumin and vitamin D_3	220
Fig. 4	Graphical abstract showing the process of obtaining cellulose and lignin from DSM and their application in making active packaging films.	257

List of Tables **Page**

Chapter 2A	**Status and Prospects of Valorisation of Ayurvedic Spent Materials**	
Table 2A.1	Medicinal importance of plants used to formulate Dashamoola	23
Table 2A.2	Value-added products and applications of ayurvedic materials	27
Chapter 2B	**Lignin-based nanomaterials for food and pharmaceutical applications: recent trends and future outlook**	
Table 2B.1	Major sources and classifications of lignin.	57
Table 2B.2	Extraction techniques, advantages, disadvantages, and applications of lignin-sourced raw materials.	62
Table 2B.3	Summary of the studies on the food applications of lignin.	81
Table 2B.4	Summary of the studies on the pharmaceutical applications of lignin.	84
Table 2B.5	Comparison of typical lignin and nanolignin.	97
Chapter 3	**Phytochemical rich extract from the spent material generated from industrial Dashamoola preparation (a medicinal Ayurvedic decoction) with antioxidant, antidiabetic and anti-inflammatory potential**	
Table 3.1	The analytical performance of the LC–MS/MS method of 28 compounds.	144
Table 3.2	HPTLC data of DE and DSME at 254 nm.	152
Table 3.3	Antioxidant, anti-diabetic, and anti-inflammation activity of DE and DSME.	158
Chapter 4	**Lignin nanoparticles from Ayurvedic industry spent materials: applications in Pickering emulsions for curcumin and vitamin D_3 encapsulation**	
Table 4.1	Lignin characterized by GPC, IR, UV	190
Table 4.2	Lignin emulsions of size, zeta, and colour values	198
Chapter 5	**Nutrient-rich puffed snacks developed using blended flours and lignin Pickering emulsions containing curcumin and vitamin D_3**	
Table 5.1	Nutritional profile of EPS from corn grit (C1), blended flour (S1), and blended flour infused with curcumin and D_3 (S2).	232
Table 5.2	Colour analysis of EPS at different combinations of blended flour.	239

Chapter 6	**Cellulose and lignin nanoparticles from an Ayurvedic waste stream for essential oil-based active packaging to extend shelf life of perishable fruit**	
Table 6.1	Preparation ratio PVOH, PVOH-C_TTO, PVOH-L_TTO, and PVOH-CL_TTO.	265
Table 6.2	Particle size, PDI and zeta of emulsion tea tree oil with cellulose (C_TTO), lignin (L_TTO), and their combination (CL_TTO).	276
Table 6.3	Properties of PVOH-based films with tea tree oil, cellulose, and lignin.	279

Summary

This thesis investigates the valorisation of Dashamoola spent material (DSM), a significant waste stream in the Ayurvedic industry. DSM is produced in substantial quantities as a by-product of manufacturing Dashamoola concoction, a traditional mixture derived from ten medicinal plants. Building on the premise that DSM contains valuable lignocellulosic biomass (e.g. cellulose and lignin) and health-promoting phenolic compounds, this research explores their extraction, modification, and application in value-added products. Currently discarded as waste, DSM is proposed as a promising source of phenolic compounds, cellulose, and lignin, which could be modified, characterised, and utilised in emulsions, nutrient-rich food formulations, and active packaging.

The introduction chapter establishes the context by highlighting the growing manufacture of Ayurvedic formulations, driven by increasing demand, which has led to a concurrent rise in associated waste streams, including DSM. The lack of effective valorisation of these waste streams is exacerbating environmental challenges and resulting in the underutilisation of a valuable resource. Despite their potential, the Ayurvedic industry has yet to systematically valorise its waste streams to address this issue. This chapter underscores the significance of valorising Ayurvedic waste streams, using DSM as an example to extract, modify, and apply phenolic compounds, cellulose, and lignin as valuable ingredients. This approach aligns with circular economy principles and provides a pathway to address the sustainability concerns of the Ayurvedic industry.

The first experimental chapter focuses on the extraction of phenolic compounds from DSM through an optimised pathway, followed by the identification and characterisation of key compounds. The analyses identified several valuable phenolic compounds in Dashamoola spent material extracts (DSME), including shikimic acid (83.2 mg/g), gallic acid (51.2 mg/g), epicatechin (26.3 mg/g), naringenin (25.0 mg/g), and vanillic acid (14.1 mg/g). The results demonstrated that the DSME possessed significant antioxidant, antidiabetic, and anti-

inflammatory properties, as evidenced by DPPH data. DSME also showed showed significant anti-inflammatory capability closely matching with that of aspirin. DSME did not show adverse health effects as cell tolerability was up to 500 μg/mL in L6 myoblast and RAW 264.7 cells. These findings highlight DSME's potential as a promising candidate for incorporation into health-promoting foods and nutraceuticals. These results establish DSM as a valuable source of high-value phenolic compounds.

The second experimental chapter focuses on the extraction and characterisation of lignin from DSM and its conversion into lignin nanoparticles (LNPs). The LNPs were effective, as natural stabilisers, to stabilise Pickering emulsions for 90 days. These emulsions were able to load 87.9% curcumin and 72.6% of Vitamin D_3. Cell line studies confirmed the non-toxic nature of the emulsions, with LnE+Cu+vD_3 causing only 29.3% and 34.9% cell death in L6 and RAW 264.7 cells, respectively, at the highest concentration (50 μg/mL). These findings establish that lignin nanoparticles derived from DSM can serve as effective Pickering emulsifiers and encapsulating materials for high-value unstable compounds.

The third experimental chapter explores the application of LNP-stabilised Pickering emulsions in creating nutrient-fortified extruded snacks. LNP-stabilised emulsions containing curcumin and vitamin D_3 were incorporated into the blended flour feed and then extruded. The resulting fortified snacks retained curcumin and vitamin D_3 bioavailability and improved their thermal stability by 69.0% and 65.7%, respectively. Thse findings highlight the potential of LNP-stabilised emulsions to protect functional compounds and create nutrient-rich snack foods, helping to address micronutrient deficiencies while contributing to the valorisation of Ayurvedic spent materials.

The fourth experimental chapter focuses on the development of active and biodegradable packaging films using lignin and cellulose nanoparticles (LNPs and NCPs) derived from DSM. The films were produced using polyvinyl alcohol (PVOH) as the matrix, incorporating NCPs and LNPs and tea tree oil (TTO, 16% w/v) as functional additives. The resulting films exhibited

antimicrobial, antioxidant (85% DPPH scavenging), and UV-blocking (95% transmittance reduction) properties without compromising mechanical strength. Nanocellulose provided structure-reinforcing properties, LNPs contributed antioxidant activity and UV-blocking, and tea tree oil exhibited strong antimicrobial efficacy against E. coli. These films extended the shelf life of strawberries by 14 days under chilling conditions. These findings highlight the potential of LNPs and nanocellulose, derived from DSM, in creating sustainable active packaging solutions, extending the shelf life of perishable foods while valorising Ayurvedic waste streams.

As summarised above, DSM is a valuable source of phenolic compounds, cellulose, and lignin, which can be extracted, transformed, and applied in food and other industries. This thesis demonstrates the feasibility and importance of valorising DSM and similar Ayurvedic spent materials by using these components to produce emulsions, encapsulate unstable nutrients, develop nutritionally enriched snacks, and create active, biodegradable packaging. These findings have important implications for valorising waste in the Ayurvedic industry, promoting sustainability and waste reduction. This thesis makes a significant contribution to knowledge by advancing the extraction, transformation, and application of phenolic compounds, cellulose, and lignin from DSM. It also establishes a foundation for exploring the sustainable use of other waste streams of the Ayurvedic sector. The contribution of this work is reflected in four papers (three in Q1 journals) and one manuscript currently under review, underscoring its value to the field.

Chapter-1
Introduction

1.1. Introduction

Ayurveda, one of the oldest systems of medicine in the world, originated in India over 5,000 years ago. It emphasizes a holistic approach to health, integrating natural therapies, dietary practices, and lifestyle modifications to promote physical, mental, and spiritual well-being. A cornerstone of Ayurveda is its reliance on natural ingredients such as herbs, minerals, and oils, which are processed into a wide range of therapeutic formulations (Chimankar et al., 2020). However, these processes often generate significant waste streams, raising concerns about the environmental impact and resource efficiency of Ayurvedic manufacturing practices. Addressing these challenges through the sustainable management and value addition of such by-products is not only an environmental imperative but also aligns with Ayurveda's foundational principles of harmony with nature (Swathi & Sundaravadivelu, 2023). Furthermore, Ayurveda's practices emphasize a deeper understanding of the interconnectedness between the natural ingredients used in formulations and the environment, making the valorisation of its waste streams both relevant and necessary in contemporary research.

In recent decades, Ayurveda has gained global recognition for its effectiveness in addressing chronic illnesses and lifestyle-related disorders. The growing prevalence of these conditions has attracted renewed interest in natural and sustainable healthcare solutions. Ayurvedic formulations, rooted in the polyherbal principle of combining multiple plant-based ingredients, are commonly acknowledged for their holistic therapeutic efficacy. Among these, Dashamoola stands out as a traditional remedy of significant importance (Nagarkar, 2016). Comprising the roots of ten medicinal plants, Dashamoola has been a cornerstone of Ayurvedic treatment for centuries, known for its anti-inflammatory, antipyretic, and respiratory benefits. It is particularly effective in managing complex health conditions such as arthritis, fever, and bronchial disorders (Taru et al., 2022). The rising demand for Dashamoola and similar

Ayurvedic formulations has greatly increased their production volumes, which has concurrently led to the generation of larger waste streams.

The manufacturing of Ayurvedic formulations generates substantial quantities of waste material, commonly referred to as Ayurvedic spent materials, including Dashamoola spent material (DSM). These waste streams pose significant environmental and economic challenges. The DSM is primarily composed of lignocellulosic biomass, including cellulose, lignin, and various bioactive compounds such as polyphenols. These compounds are known for their antioxidant, anti-inflammatory, and antimicrobial properties, making DSM a valuable resource with untapped potential. The lack of effective utilization strategies, however, results in DSM being treated as waste. This not only represents a missed opportunity to harness its latent value but also contributes to environmental degradation through improper disposal methods (Abraham et al., 2023).

The disposal of DSM and other Ayurvedic spent materials often involves traditional methods such as open dumping, burning, or discarding into water bodies, resulting in significant environmental damage. Open dumping contaminates soil and groundwater through toxic leachate, while burning releases greenhouse gases and particulate matter, contributing to air pollution. Discarding waste into water bodies disrupts aquatic ecosystems, causing oxygen depletion and eutrophication. These practices pose risks to ecosystems and human health, underscoring the urgent need for innovative and sustainable waste management solutions in the Ayurvedic industry.

Given the environmental challenges posed by traditional waste disposal methods, the valorisation of Ayurvedic spent materials, including DSM, is of vital importance for resource utilization and the mitigation of environmental impacts. By transforming low-value waste streams into valuable ingredients, valorisation contributes to the circular economy. This approach also enhances the economic sustainability of the Ayurvedic industry. DSM, with its

rich composition of bioactive compounds and structural biopolymers (e.g., cellulose and lignin), is particularly well-suited for valorisation (Abraham et al., 2024). For instance, polyphenols extracted from DSM can be used in nutraceuticals and functional foods (Abraham et al., 2020). Similarly, lignin and cellulose can be processed into and included as functional materials in sustainable packaging, drug delivery, and cosmetics.

Lignin nanoparticles (LNPs) are among the most promising materials in the valorisation of DSM. As natural stabilizers, LNPs play a crucial role in the development of Pickering emulsions-emulsions stabilized by solid particles instead of conventional emulsifiers (Abraham et al., 2023). These emulsions offer enhanced stability and can be utilized for encapsulating bioactive compounds like curcumin and vitamin D_3. The encapsulation process not only improves the stability and bioavailability of these compounds but also broadens their applicability across multiple industries, including pharmaceuticals, functional foods, and cosmetics (Lizundia et al., 2021).

Nanocellulose, another potential valorized product of DSM, is a versatile material with applications across various fields. With exceptional mechanical properties, high surface area, and biodegradability, nanocellulose is an ideal candidate for partially substituting or fully replacing conventional plastics in some packaging applications (Kirtania et al., 2024). Its incorporation into biodegradable films enhances strength and barrier properties, making them suitable for preserving perishable goods and reducing plastic waste.

1.2. Importance of the thesis work

The importance of valorizing DSM extends beyond industrial benefits; it contributes to advancing sustainability within the Ayurvedic industry. By providing pathways for transforming the underutilized waste streams of traditional industries into functional materials, this work exemplifies how modern technologies can be harnessed to address the challenges they face. Recent innovations in nanotechnology and green extraction methods enable the

efficient recovery of valuable compounds from DSM. Environmentally friendly processes, such as solvent-free extraction and supercritical fluid extraction, implemented in this work, minimize waste generation while enhancing the recovery of bioactive compounds (Abraham et al., 2020; Abraham et al., 2023). In essence, this research underscores the pivotal role of technological innovation in driving sustainability across traditional industries.

This research explores the potential of valorized extracts of DSM in various applications, including nutraceuticals, emulsifiers, and components of sustainable packaging. It aims to establish a comprehensive framework for effectively utilizing Ayurvedic spent materials to address the environmental and industrial challenges faced by the industry. By providing pathways for extracting, modifying, and applying the bioactive (e.g., phenolic compound-rich extracts) and structural components (e.g., cellulose and lignin) of DSM, this work contributes to the integration of circular economy principles into the Ayurvedic sector (Abraham et al., 2024). The findings are expected to inspire further research and innovation in this important traditional industry.

The valorisation of DSM is an important step toward ensuring the sustainability of the Ayurvedic industry. The outcomes presented in this thesis not only address the environmental challenges posed by Ayurvedic waste streams but also demonstrate how these underutilized byproducts can be transformed into valuable ingredients and products. Ultimately, the study highlights how the implementation of cutting-edge technologies, such as nanotechnology and green extraction, can drive progress in Ayurvedic and similar traditional industries toward a more sustainable and resource-efficient future.

1.3. Research questions

This thesis addressed the following questions:

1. Does Dashamoola spent material (DSM) contain biologically active phytochemicals with antioxidant, antidiabetic, and anti-inflammatory potential?
2. What are the physicochemical properties of lignin nanoparticles extracted from DSM, and can they stabilize Pickering emulsions for encapsulating unstable compounds (e.g., curcumin and vitamin D_3)?
3. Can the above-mentioned lignin-based Pickering emulsions be utilized to fortify extruded snacks and improve their nutritional value?
4. Can nanocellulose and nano-lignin extracted from DSM, combined with tea tree oil, be used to produce active packaging films that extend the shelf life of fruits?

1.4. Objectives

The aim of this thesis was to explore the valorisation of Dashamoola spent material (DSM) by extracting and characterizing its bioactive compounds and structural polymers (cellulose and lignin) and applying them in innovative products, such as Pickering emulsions, extruded snacks, and active packaging.

The specific objectives of this research were to:

1. Develop an optimal process for extracting and recovering bioactive phytochemicals from DSM and characterize their antioxidant, antidiabetic, and anti-inflammatory properties.
2. Investigate the application of lignin nanoparticles in Pickering emulsions for encapsulating curcumin and vitamin D_3 as model health-promoting compounds.
3. Formulate nutrient-fortified model extruded snacks by incorporating lignin-stabilized Pickering emulsions into coconut spent flour and millet.

4. Evaluate the efficacy of PVOH films infused with nanocellulose, nano-lignin, and tea tree oil emulsions in extending the shelf life of strawberries as a model fruit.

1.5. Expected outcomes

1. Optimized method for extracting and characterizing bioactive phytochemicals from DSM.
2. Development of stable and effective Pickering emulsions using lignin nanoparticles.
3. Nutritional and sensorially improved extruded snacks fortified with DSM-derived materials.
4. Creation of active packaging films containing nanocellulose and nanolignin from DSM with enhanced UV-blocking and antimicrobial properties with ability to extend the shelf life of representative fruits.

1.6. Outline of thesis

This thesis is structured into seven chapters, each addressing a specific aspect of the valorisation of Ayurvedic spent materials (Fig. 1.1). Dashamoola spent material (DSM) was used as the representative spent material of Ayurvedic waste stream. The chapters are outlined as follows:

Chapter 1: Introduction

The first chapter provides the foundational background and rationale for this research. It highlights the environmental and economic challenges posed by the waste generated during the production of Ayurvedic formulations. The chapter underscores the importance of valorizing Ayurvedic spent materials, particularly DSM, as a pathway toward sustainability. The research questions, objectives, and expected outcomes are presented, setting the stage for the subsequent chapters.

Chapter 2: Literature review

This chapter reviews existing literature on the valorisation of Ayurvedic spent materials, with a focus on the extraction of bioactive compounds and the development of lignin- and cellulose-

based nanomaterials. It outlines the current state of research on DSM, identifies knowledge gaps, and highlights opportunities for innovation in waste valorisation. Additionally, it reviews the extraction, characterization, and potential applications of lignin and cellulose as valorized materials relevant to Ayurvedic spent materials, including DSM. Notably, the lignin and cellulose section of this chapter has been published as a review paper in *Science of the Total Environment* (Abraham et al., 2023).

Chapter 3: Extraction of bioactive phytochemicals from DSM

This chapter presents the findings of research conducted to optimize methods for extracting bioactive compounds from DSM. The antioxidant, antidiabetic, and anti-inflammatory properties of the extracted phytochemicals are presented and discussed, highlighting the therapeutic potential of DSM-derived compounds. The phytochemical-rich extract obtained from the DSM decoction showed its potential for applications in health-promoting food formulations. The content of this chapter has been published in *Industrial Crops and Products* (Abraham et al., 2020).

Chapter 4: Development of lignin nanoparticles and Pickering emulsions

This chapter explores the preparation and characterization of lignin nanoparticles (LNPs) derived from DSM. It focuses on the application of LNPs in stabilizing Pickering emulsions for the encapsulation of bioactive compounds, using curcumin and vitamin D_3 as models. The chapter highlights the physicochemical properties and advantages of LNP-stabilized emulsions, emphasizing their role in improving the stability and bioavailability of encapsulated compounds. The content of this chapter has been published in *Food Chemistry* (Abraham et al., 2024).

Chapter 5: Nutritional fortification of extruded snacks

This chapter investigates the application of lignin-stabilized Pickering emulsions in the formulation of nutrient-fortified extruded snacks. The formulation includes blended flours and Pickering emulsions containing curcumin and vitamin D_3, resulting in snacks with significantly

improved nutritional and sensory attributes. It presents data and explanations on the proximate composition, sensory evaluation, and bioactive retention in the fortified snacks. This research underscores the potential of lignin nanoparticles as delivery vehicles for unstable yet valuable compounds in the creation of healthy snack foods. The content of this chapter has been published in RSC *Sustainable Food Technology* (Abraham et al., 2025).

Chapter 6: Development of active packaging films

This chapter focuses on the development of active and biodegradable packaging films using nanocellulose and lignin nanoparticles derived from DSM. The films are evaluated for their mechanical properties, antimicrobial activity, UV-blocking properties, and efficacy in extending the shelf life of perishable fruits, with strawberries used as the model. The incorporation of essential oils enhances the active properties of the films. The content of this chapter has been published in *International Journal of Biological Macromolecules* (Abraham et al., 2025).

Chapter 7: Conclusions and future directions

This final chapter synthesizes the key findings documented in the experimental chapters (Chapters 3 to 6), draws overall conclusions, and discusses their implications for the valorisation of waste streams in the Ayurvedic industry. It articulates the contributions made by the findings presented in this thesis to the body of knowledge on waste valorisation and the application of valorized materials. Recommendations are also made for future research to advance knowledge and explore innovative opportunities for further valorisation of Ayurvedic spent materials. The thesis concludes by envisioning the continuous application of interdisciplinary science to achieve higher levels of valorisation and contribution to the circular economy within the Ayurvedic sector.

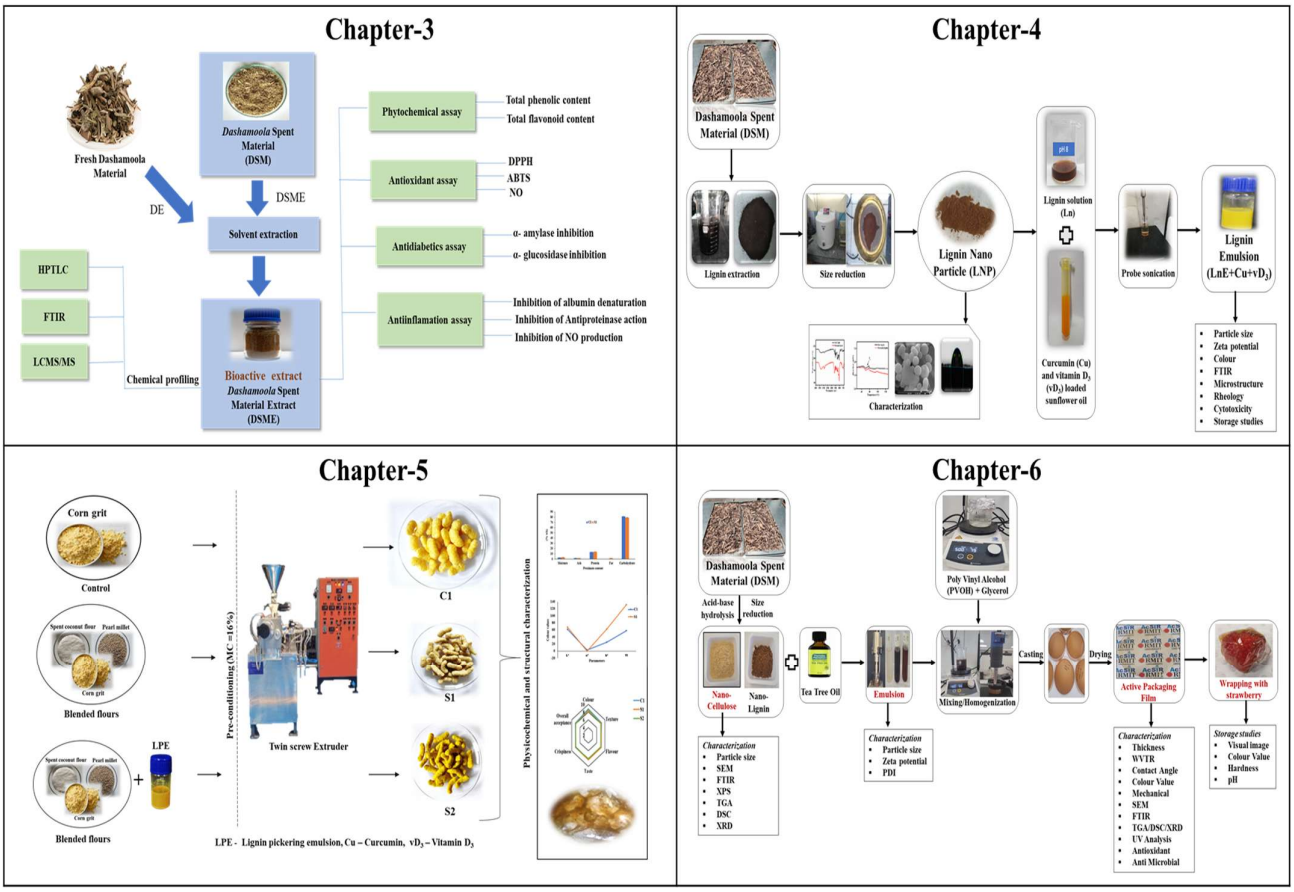

Fig. 1.1. Overview of the four experimental chapters of the thesis, outlining the experimental work conducted.

References

Abraham, B., Reshmitha, T. R., Navami, M. M., George, L., Venugopalan, V. V., & Nisha, P. (2020). Phytochemical rich extract from the spent material generated from Industrial Dashamoola preparation (a medicinal Ayurvedic decoction) with antioxidant, antidiabetic and anti-inflammatory potential. *Industrial crops and products*, 151, 112451. https://doi.org/10.1016/j.indcrop.2020.112451.

Abraham, B., Shakeela, H., Devendra, LP, Arun, KB, Ragavan, KV, Brennan, C., & Nisha, P. (2024). Lignin nanoparticles from Ayurvedic industry spent materials: Applications in Pickering emulsions for curcumin and vitamin D_3 encapsulation. *Food Chemistry*, 458, 140284. https://doi.org/10.1016/j.foodchem.2024.140284

Abraham, B., Syamnath, V. L., Arun, K. B., Zahra, P. F., Anjusha, P., Kothakotta, A., & Nisha, P. (2023). Lignin-based nanomaterials for food and pharmaceutical applications: Recent trends and future outlook. *Science of The Total Environment*, 881, 163316. https://doi.org/10.1016/j.scitotenv.2023.163316.

Chimankar, R.P., Tawalare, K.A., & Mishra, S.A. (2020). Prevention of lifestyle disorders with basic principles of Ayurveda. International Ayurvedic Medical Journal, (Online), 4487-4492. https://doi.org/10.46607/iamj3008092020

Debnath, P. K., Banerjee, S., Debnath, P., Mitra, A., & Mukherjee, P. K. (2015). Ayurveda–opportunities for developing safe and effective treatment choices for the future. In Evidence-based validation of herbal medicine (pp. 427-454). Elsevier. https://doi.org/10.1016/B978-0-12-800874-4.00020-9

Dhadse, S., Alam, S. N., & Rao, M. M. (2021). Development of nutrient rich biofertilizer by co-vermistabilization of aquatic weeds using herbal pharmaceutical wastewater along with sediment of lake. Bioresource Technology Reports, 13, 100633. https://doi.org/10.1016/j.biteb.2021.100633

Gopinath, N. (2020). Industrial Manufacture of Traditional Ayurvedic Medicines. In Ayurveda in The New Millennium (pp. 41-70). CRC Press.

Gupta, P. K., Raghunath, S. S., Prasanna, D. V., Venkat, P., Shree, V., Chithananthan, C., & Geetha, K. (2019). An update on overview of cellulose, its structure and applications. Cellulose, 201(9), 84727.

Inglis, K. (2012). Ayurveda: Asian Secrets of Wellness, Beauty and Balance. Tuttle Publishing.

Jairu, D., & Acharya, S. K. (2019). Herbal the harvest: The business profitability and ecological sustenance in India. Call for Editorial Board Members, 5(1), 47. DOI: http://dx.doi.org/10.21088/ijab.2454.7964.5119.7

Kirtania, M.D., Chakraborty, S., Barik, A., & Dey, S. (2024). Sources and Applications of Nano Cellulose Tailored Materials. In Nanocellulose-Sources, Preparations, and Applications. IntechOpen. DOI: 10.5772/intechopen.113935

Kizhakkeveettil, A., Parla, J., Patwardhan, K., Sharma, A., & Sharma, S. (2024). History, Present and Prospects of Ayurveda. In History, Present and Prospect of World Traditional Medicine (pp. 1-72). https://doi.org/10.1142/9789811282171_0001

Nagarkar, B. E (2016). Studies on anti inflammatory potential of dashamoola formulations and its dosage forms and# 8195. http://hdl.handle.net/10603/148786

Rajan, R., Robin, D. T., & Vandanarani, M. (2019). Biomedical waste management in Ayurveda hospitals–current practices and future prospectives. *Journal of Ayurveda and integrative medicine*, 10(3), 214-221. https://doi.org/10.1016/j.jaim.2017.07.011

Swathi, K., & Sundaravadivelu, S. (2023). Ayurveda and Transdisciplinary Approaches: A Way Forward towards Personalized and Preventive Medicine. *Indian Journal of Pharmaceutical Sciences*, *85* (6), 1574-1585.

Taru, P., Syed, S., Kute, P., Shikalgar, M., Kad, D., & Gadakh, A. (2022). Dashamoola: A systematic overview. GIS-Zeitschrift fü Geoinformatik, 9, 1334-1345.

Yance, D. R. (2013). Adaptogens in medical herbalism: elite herbs and natural compounds for mastering stress, aging, and chronic disease. Simon and Schuster.

Yarin, T., Dutta, B., Murmu, D. K., Medda, P., & Das, S. (2022). Valorisation of medicinal and aromatic plant waste. *J Pharm Innov*, 11 (1), 532-537.

Zhao, Q., Fan, L., Li, J., & Zhong, S. (2024). Pickering emulsions stabilized by biopolymer-based nanoparticles or hybrid particles for the development of food packaging films: A review. *Food Hydrocolloids*, 146, 109185. https://doi.org/10.1016/j.foodhyd.2023.109185

Chapter 2A

Literature Review

Status and Prospects of Valorisation of Ayurvedic Spent Materials

Abstract:

Ayurveda, an ancient Indian medical system, emphasises natural remedies for holistically maintaining health. The growing global demand for Ayurvedic products has resulted in significant waste generation, including spent plant residues, liquid effluents, and packaging waste, posing environmental challenges. Current waste disposal practices, such as open dumping and burning, are exacerbating environmental degradation, highlighting the need for innovative strategies. This section of the literature review explores the valorisation of Ayurvedic spent materials as a sustainable approach to waste management, with a focus on creating value-added products such as nutraceuticals and biopolymers. Particular emphasis is placed on the composition and therapeutic applications of Dashamoola, a polyherbal formulation, and the valorisation potential of Dashamoola Spent Material (DSM), a by-product of its processing in Ayurvedic formulations. The application of advances in nanotechnology and biopolymer science enables the transformation of lignocellulosic biomass into high-performance materials, biodegradable packaging, and nutrient delivery systems. This review highlights the environmental, economic, and societal benefits of valorisation, including reduced pollution, new revenue streams, and healthy products. It also addresses challenges such as variability in raw materials, high technological costs, and regulatory limitations, while identifying knowledge gaps in the characterisation of waste streams and the scalability of recovery technologies. By examining the intersection of traditional Ayurvedic practices and modern sustainability goals, this review provides a framework for advancing waste management practices, fostering environmental conservation, and supporting the circular economy.

Keywords: Ayurvedic waste valorisation, Dashamoola, nanotechnology, lignocellulosic biomass, sustainable practices

2A.1. Introduction

Ayurveda is one of the oldest medical systems in the world and originated in India over 5,000 years ago. The term 'Ayurveda' is derived from the Sanskrit words 'Ayur' (life) and 'Veda' (knowledge) and translates as the 'science of life' (Chimankar et al., 2020). Ayurveda adopts a holistic approach, emphasising the balance of the three doshas (mind-body energies): Vata (air and space), Pitta (fire and water), and Kapha (earth and water), which are believed to govern physiological and psychological functions (Kizhakkeveettil et al., 2024; Swathi & Sundaravadivelu, 2023; Shah, 2019).Unlike Western medicine that focuses predominantly on curing diseases, Ayurveda integrates preventive and curative measures, including natural therapies, dietary interventions, yoga, meditation, and purification practices such as Panchakarma (five actions) (Chauhan et al., 2023; Debnath et al., 2015). This comprehensive approach considers physical, mental, and spiritual well-being as interconnected and equally important for maintaining health (Luhaste, 2023).

In recent decades, Ayurveda has gained global recognition as an alternative medicine system. Its eco-friendly and sustainable principles resonate with the rising global demand for natural health practices (Bhattacharya, 2024). The global Ayurveda market size was estimated at USD 14.4 billion in 2023 and is projected to grow at a Compound Annual Growth Rate (CAGR) of 27.2% from 2024 to 2030 due to growing consumer awareness of Ayurvedic benefits (Grand View Research, 2024). Ayurvedic formulations such as Chyawanprash (a rejuvenating herbal jam), Ashwagandha (Indian ginseng, renowned for its stress-relieving and energy-boosting properties), and Triphala (a traditional blend of three fruits used for digestion and detoxification) have become household names for their health and therapeutic benefits (Thakur et al., 2012; Sarkar et al., 2023; Agarwal et al., 2018). Exports of Ayurvedic and herbal products from India increased from USD 479.6 million (3,967.4 crores INR) in FY21 to USD 606.2 million (5,014.3 crores INR) in FY23, reflecting a significant rise in global demand (Grand

View Research, 2024). The endorsement of Ayurveda by the World Health Organisation (WHO) as a form of traditional medicine has further legitimised its role in addressing chronic and lifestyle-related diseases (Anand et al., 2022; Maier, 2021). Additionally, the rising demand for organic and natural personal care products infused with Ayurvedic ingredients like neem, turmeric, and sandalwood has fueled industry growth, solidifying Ayurveda's position in the wellness sector (Grand View Research, 2024). The widespread adaptation of Ayurveda in wellness centres, spas, and integrative health programmes has established it as a key player in the global wellness industry. (Mukerji & Prasher, 2016).

Despite its popularity, the rapid expansion of Ayurvedic industries has resulted in significant environmental challenges. These industries generate a diverse range of waste materials, including spent plant residues, liquid effluents, and packaging waste. Improper disposal of these materials is causing adverse environmental impacts such as soil degradation, water pollution, and air quality issues (Rajan et al., 2019). Plant residues, often rich in lignocellulosic biomass, are discarded or incinerated, contributing to greenhouse gas emissions. Liquid effluents containing high concentrations of organic matter and bioactive compounds are frequently released without treatment into water bodies, causing eutrophication and endangering aquatic ecosystems (Mukerji & Prasher, 2016). Non-biodegradable packaging waste used in the Ayurvedic Industry adds to the environmental burden, further highlighting the need for sustainable waste management practices.

The challenges associated with Ayurvedic waste management are exacerbated by factors such as variability in raw materials, lack of standardised protocols, and high costs of waste treatment technologies. Limited awareness among producers and inadequate policy frameworks further hinder sustainable practices in this sector (Swathi & Sundaravadivelu, 2023). These challenges

underscore the need for innovative approaches to manage Ayurvedic waste effectively and sustainably.

Valorisation of Ayurvedic spent materials offers a transformative solution. By converting waste into value-added products, industries can significantly reduce their environmental footprint while creating economic opportunities. Residual bioactive compounds in spent plant materials can be extracted and utilised in the development of nutraceuticals, pharmaceuticals, and functional foods (Espro et al., 2021). Lignocellulosic biomass, a major component of Ayurvedic waste, can be converted into biopolymers, bioethanol, and bioplastics, contributing to the circular economy (Debnath et al., 2015). Valorisation also supports resource conservation, reduces pollution, and creates green jobs, aligning with global sustainability goals (Bhattacharya, 2024).

This part of the Literature review chapter aims to explore the current status and future prospects of valorising Ayurvedic spent materials, focusing on their composition, challenges, and applications. By highlighting innovative waste management practices and technologies, it seeks to promote sustainability within the Ayurvedic industry. The review provides a comprehensive understanding of key aspects related to Ayurvedic formulations and their sustainable practices. It begins with an overview of Ayurvedic formulations, focusing on Dashamoola – a polyherbal Ayurvedic formulation- and its therapeutic applications. The discussion then transitions to the generation of Ayurvedic spent materials, specifically Dashamoola Spent Material (DSM), highlighting its characteristics, environmental impacts, and current disposal practices. Next, the review explores technological advancements in the valorisation of Ayurvedic waste, emphasising nanotechnology and biopolymers. Finally, it summarises the benefits of waste valorisation while addressing challenges and future directions for integrating sustainability practices into Ayurvedic practices.

2A.2. Ayurvedic formulations and Dashamoola

Ayurvedic preparations are based on either single herbs (e.g., *Curcuma longa* (turmeric) and *Azadirachta indica* (neem) or polyherbal formulations (e.g., Dashamoola – roots of 10 medicinal plants and herbs, Triphala – a combination of three fruits: *Emblica officinalis* (amla), *Terminalia bellirica* (bibhitaki), and *Terminalia chebula* (haritaki). Polyherbal formulations are integral to Ayurvedic medicine, emphasizing the synergistic effects of multiple herbs to enhance therapeutic efficacy (Rajini et al., 2023; Agarwal et al., 2018). Unlike single-herb remedies, which primarily target specific dosha imbalances, polyherbal treatments address a broader spectrum of health concerns. These formulations are designed to balance Vata, Pitta, and Kapha doshas simultaneously, enabling a holistic approach to health management (Kotmire et al., 2024). Polyherbal formulations also allow Ayurvedic practitioners to tailor treatments to individual *prakriti* (body constitution), ensuring personalized care. This adaptability not only enhances efficacy but also minimizes potential side effects, as the combined effects of the herbs work in harmony to mitigate adverse reactions (Mahale, 2023). Polyherbal formulations like Dashamoola exemplify this principle, providing comprehensive solutions for a range of health conditions.

2A.2.1. Dashamoola: composition, therapeutic applications, and significance

Dashamoola, translating to "ten roots," is a classical Ayurvedic formulation comprising the roots of ten medicinal plants (Table 2A.1). These roots are divided into two categories (Nagarkar, 2016; Swathi et al., 2023) (Fig. 2A.1):

Table 2A.1. Medicinal importance of plants used to formulate Dashamoola

Category	Plant Name (Scientific Name)	Medicinal Importance
Valiyapanchamoola (Larger Plants)	Bilwa (*Aegle marmelos*)	Known for its digestive and anti-inflammatory properties.
	Agnimantha (*Clerodendrum phlomidis*)	Promotes vitality and supports respiratory health.
	Shyonaka (*Oroxylum indicum*)	Effective in managing joint pain and inflammation.
	Patala (*Stereospermum suaveolens*)	Supports immunity and respiratory function.
	Gambhari (*Gmelina arborea*)	Enhances strength and addresses skin and digestive disorders.
Laghupanchamoola (Smaller Plants)	Brihati (*Solanum indicum*)	Treats asthma and other respiratory ailments.
	Kantakari (*Solanum xanthocarpum*)	Relieves bronchitis and acts as an expectorant.
	Shalaparni (*Desmodium gangeticum*)	Known for its pain-relieving and adaptogenic properties.
	Prishniparni (*Uraria picta*)	Supports fever management and general immunity.
	Gokshura (*Tribulus terrestris*)	Improves urinary health and vitality.

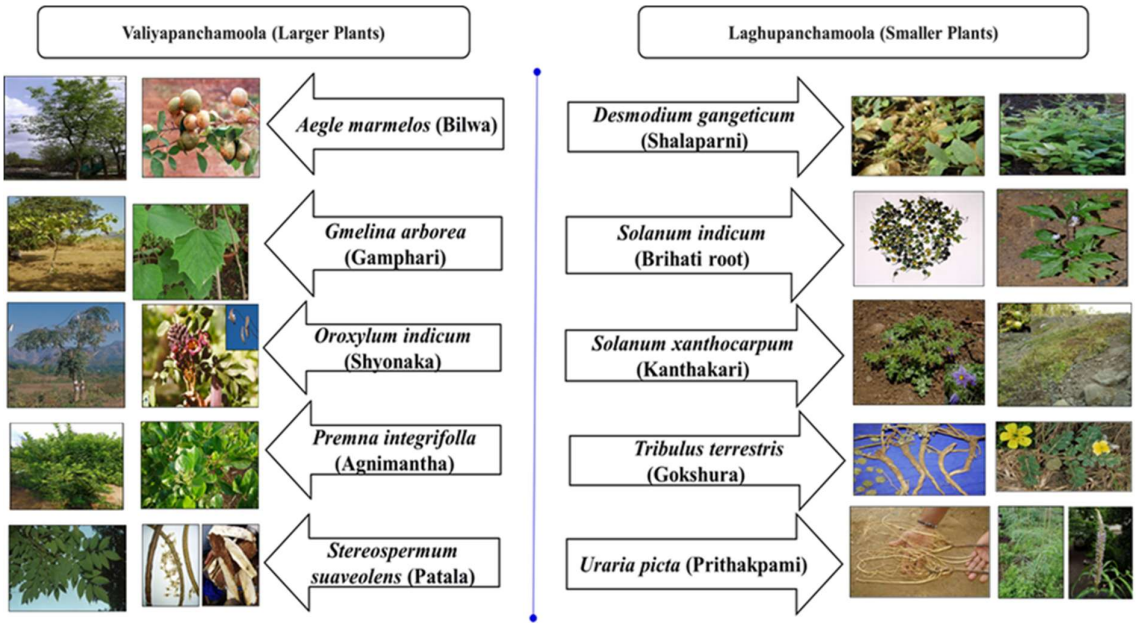

Fig. 2A.1. Classification of Valiyapanchamoola (larger plants) and Laghupanchamoola (smaller plants) with corresponding species used in Ayurvedic formulations.

Each root contributes distinct therapeutic properties, including anti-inflammatory, analgesic, expectorant, and adaptogenic effects. Together, they create a balanced formulation that addresses multiple health concerns. For instance, Valiyapanchamoola primarily targets Vata imbalances, while Laghupanchamoola focuses on Kapha-related disorders (Nagarkar, 2016).

Therapeutically, Dashamoola is known for its ability to reduce inflammation, enhance respiratory health, and support metabolic functions (Parekar et al., 2015; Swathi et al., 2023). It is commonly used to manage arthritis, asthma, and digestive disorders. The formulation's comprehensive action makes it a cornerstone of Ayurvedic medicine, reflecting its emphasis on harmony and balance (Kumar et al., 2017; Taru et al., 2022).

2A.2.2. Dashamoolarishta: A key Dashamoola product and its applications

Dashamoolarishta is a fermented herbal decoction derived from Dashamoola, recognised in Ayurveda as a *rasayana* (rejuvenative) for its adaptogenic and restorative properties (Fig.

2A.2). The fermentation process enhances the bioavailability of its active compounds, such as tannins, flavonoids, and alkaloids, contributing to its therapeutic efficacy (Athira et al., 2022). With its systemic action, Dashamoolarishta addresses dosha imbalances, making it a versatile formulation in Ayurvedic practice (Prabhune et al., 2019). In India, annual production of Dashamoolarishta is approximately 15 lakh litres, reflecting its high demand in the Ayurvedic industry (Shetty et al., 2017; Sebastiani et al., 2022). However, this growing demand has led to concerns about the availability of raw materials, particularly the roots required for Dashamoola, which are often subject to seasonal and geographic limitations. This scarcity poses challenges to sustainable production and highlights the need for resource management strategies in the Ayurvedic sector.

Fig. 2A.2. Commercial Dashmoolarishta products from various brands.

Therapeutically, Dashamoolarishta is used for postnatal care by restoring strength and vitality after childbirth, while its adaptogenic properties aid in emotional stability and recovery. It supports respiratory health by managing asthma, bronchitis, and airway inflammation, and enhances digestive functions, alleviating issues like indigestion and bloating. Additionally, its anti-inflammatory properties help treat arthritis and gout, while its antioxidant-rich components combat fatigue and improve immunity (Mohite et al., 2014). Through these multifaceted benefits, Dashamoolarishta remains a cornerstone in Ayurvedic therapy, addressing a wide range of health conditions holistically (Pawar et al., 2013).

2A.3. Spent materials generation in the Ayurvedic industry

The Ayurvedic industry, rooted in traditional practices and reliant on natural raw materials, faces increasing challenges due to the rising global demand for its products. This growing demand has led to substantial waste generation, including plant residues, liquid effluents, and packaging waste, which pose significant environmental and logistical challenges (Raju et al., 2024). Ayurvedic formulations such as decoctions, oils, and powders depend heavily on plant-based resources, and their processing leaves behind various types of spent materials (Table 2A.2). Proper management of these wastes is essential to ensure environmental sustainability and uphold the Ayurvedic principle of balance and harmony (Abdulhameed et al., 2020; Kularatne, 2024; Yadevendra et al., 2019).

2A.3.1. Types of spent material generated in Ayurvedic formulations production

Ayurvedic formulations are created through processes such as collection, drying, grinding, extraction, and formulation, which generate several types of waste (Kularatne, 2024; Abdulhameed et al., 2020).

Plant residues: Ayurvedic production involves various plant parts such as roots, stems, bark, leaves, flowers, and seeds. After the active compounds, including alkaloids, flavonoids, and tannins, are extracted, a significant amount of fibrous residue remains. These residues, referred to as "spent materials," form the bulk of Ayurvedic waste. For example, the preparation of Dashamoolarishta leaves behind large quantities of root material after fermentation and extraction, often discarded as waste despite its potential for secondary applications (Abdulhameed et al., 2020).

Spent extraction solids: The extraction of active principles using mediums like water, alcohol, or oils generates solid waste composed of fibrous plant material and inert remnants. While these solids retain traces of bioactive compounds, improper disposal can negatively impact the environment, contributing to waste accumulation and pollution (Gopinath, 2020).

Liquid waste: Liquid effluents are produced during processes such as decoction preparation and fermentation. These wastes often contain plant extracts, solvent residues, and by-products of fermentation. If untreated, they pose a significant risk of water pollution by contaminating nearby water bodies and disrupting aquatic ecosystems (Kularatne, 2024; Abdulhameed et al., 2020).

Packaging waste: Ayurvedic products are typically packaged in materials like plastic, glass, or cardboard. The increased production and popularity of Ayurvedic products have resulted in a growing volume of discarded packaging materials, which contribute to environmental pollution, particularly when disposed of carelessly (Kularatne, 2024; Gopinath, 2020).

Table 2A.2. Value-added products and applications of ayurvedic materials

Spent Material	Value-Added Product/Process	Application	Reference
Dashamoola spent material	Extraction of bioactive compounds (polyphenols, flavonoids)	Antioxidant, anti-inflammatory, antidiabetic properties	Abraham et al., 2023
Ashwagandha spent roots	Bioactive-rich extract for nutraceutical formulations	Adaptogenic and stress-relief supplements	Sarkar et al., 2023
Neem spent leaves	Neem oil extraction and biopesticide formulation	Agricultural pest control, medicinal uses	Ojo et al., 2024
Turmeric spent residue	Curcumin recovery and nano-encapsulation	Enhanced bioavailability in food & pharma	Mahjoubin et al., 2020
Triphala spent material	Polyphenol recovery for functional beverages	Antioxidant and gut health benefits	Agarwal et al., 2018
Brahmi spent biomass	Extracts for cognitive health supplements	Memory enhancement and neuroprotection	Preethy et al., 2018
Spent black pepper	Piperine extraction and microencapsulation	Bioavailability enhancement in nutraceuticals	Prabhu et al., 2015
Spent cumin	Essential oil recovery and antioxidant-rich extracts	Flavoring agent, antimicrobial applications	Arun et al., 2018

2A.3.2. Occurrence of Dashamoola spent material (DSM)

Dashamoola Spent Material (DSM) is a by-product generated during the preparation of Ayurvedic formulations such as Dashamoolarishta (Fig. 2A.3). The process involves the extraction and fermentation of the roots of ten medicinal plants that make up Dashamoola. After the active compounds are extracted for formulations, significant quantities of fibrous residues remain, referred to as DSM. It primarily consists of lignocellulosic biomass and trace amounts of bioactive compounds such as tannins and flavonoids (Abraham et al., 2020). The Ayurvedic industry generates approximately 1,000 tons of DSM annually, making it a valuable waste stream for potential utilisation.

Fig. 2A.3. Dashamoola spent material (DSM) — a byproduct generated from the production of Dashamoolarishta.

Despite its promising composition, DSM is often considered waste and discarded without exploring its potential applications. This material is typically left to accumulate at production sites, incinerated, or disposed of in landfills, contributing to environmental concerns. However, its fibrous nature and residual bioactive content suggest its suitability for secondary uses, including the development of biofertilisers, compost, or even bioenergy applications. Understanding the occurrence and characteristics of DSM is critical for transitioning the Ayurvedic industry towards more sustainable waste management practices (Abraham et al., 2020).

2A.3.3. Current disposal practices and associated challenges

The Ayurvedic industry, despite its reliance on natural materials, faces significant challenges in waste disposal. Traditional waste management methods, such as open dumping, burning, and disposal into water bodies or agricultural fields, are still prevalent in India and other regions where Ayurveda is practised. These unsustainable practices fail to mitigate the environmental burden of Ayurvedic waste and contribute to soil degradation, water pollution, and air quality issues (Rajan et al., 2019; Posada, 2017; Resmi et al., 2022).

- **Open dumping and landfill**

One of the common methods of disposing of Ayurvedic spent materials is open dumping or landfill disposal. While these methods may seem convenient, they result in significant environmental harm (Rajan et al., 2019; Patel et al., 2024):

Soil degradation: Open dumping and landfill disposal disrupt the natural soil ecosystem. Decomposing organic matter alters soil pH and releases excess nutrients, which can lead to reduced fertility and loss of native vegetation (Kularatne, 2024).

Methane emissions: Organic waste in landfills decomposes to produce methane, a greenhouse gas 25 times more potent than carbon dioxide, significantly contributing to climate change (Patel et al., 2024).

Leachate formation: Waste in landfills generates leachate, a toxic liquid that seeps into the soil and contaminates groundwater. This leachate contains organic materials and plant by-products harmful to both soil fertility and human health when it reaches water sources (Kularatne, 2024).

- **Burning of herbal waste**

In rural areas, where proper waste management systems are lacking, burning herbal waste remains a common practice. While seemingly a quick solution, this method creates several environmental challenges (Xin et al., 2019; Maj et al., 2019):

Air pollution: Burning releases airborne pollutants, including carbon dioxide, carbon monoxide, particulate matter, volatile organic compounds (VOCs), and polycyclic aromatic hydrocarbons (PAHs). These pollutants pose serious risks to human health, such as respiratory and cardiovascular issues (Marcelino et al., 2023).

Greenhouse gas emissions: Combustion generates carbon dioxide and other gases, worsening global warming and ozone depletion. Despite these impacts, burning remains a widely practised method of waste disposal (Maj et al., 2019; Meng et al., 2017).

- **Discarding into water bodies**

Some Ayurvedic processing units discharge spent plant materials and liquid waste into nearby rivers, lakes, or streams, assuming this will dilute the pollution. However, such practices result in severe ecological consequences (Puri et al., 2021; Rajan et al., 2019; WHO, 2003):

Water pollution: Biodegradation of waste in water bodies depletes oxygen levels, harming aquatic organisms and disrupting ecosystems (WHO, 2003; Puri et al., 2021).

Eutrophication: Excess nutrients, particularly nitrogen and phosphorus, promote algal blooms, a process known as eutrophication. This depletes oxygen in water, degrading quality and threatening aquatic life (Dhadse et al., 2021).

- **Use in agricultural fields**

Some Ayurvedic companies claim that herbal waste can act as natural manure and often dump spent materials onto agricultural lands. While organic matter can improve soil quality, this practice is not without risks (Tao et al., 2021; Lubbe & Verpoorte, 2011):

Soil contamination: Bioactive compounds in Ayurvedic waste can disrupt soil microorganisms and alter pH levels, negatively impacting crop yields and nutrient cycles (Rajan et al., 2019).

Water runoff: During rainfall, surface runoff carries nutrients and bioactive agents into nearby water bodies, exacerbating water pollution and eutrophication (Srivastava et al., 2010).

Accumulation at production sites: Inadequate waste treatment often leads to waste accumulation at processing sites. Decomposing waste generates odours, attracts insects, and produces leachate, which seeps into the soil and contaminates groundwater (Abdulhameed et al., 2020).

The environmental impacts of these practices underscore the urgent need for modern, sustainable waste management solutions within the Ayurvedic industry. Addressing soil degradation, water pollution, and air quality issues will not only mitigate ecological harm but also align the industry's operations with global sustainability goals.

2A.4. Prospects and benefits of valorisation of Ayurvedic spent materials

The valorisation of Ayurvedic spent materials offers promising prospects for creating sustainable, high-value products that align with global environmental and economic goals. By leveraging residual bioactive compounds and lignocellulosic biomass, industries can not only reduce waste but also develop innovative solutions across various sectors such as pharmaceuticals, nutraceuticals, and packaging. The following sections outline specific opportunities and applications.

2A.4.1. Potential for creating value-added products

The Ayurvedic industry generates significant quantities of waste materials, including plant residues and liquid effluents, that hold immense potential for transformation into value-added products. Most of the Ayurvedic preparations are based on aqueous decoctions and oil extracts and therefore there is substantial retention of the bioactive phytochmeicals in the residue. By extracting valuable components such as bioactive compounds and lignocellulosic biomass, these waste materials can be repurposed into a range of innovative applications across pharmaceuticals, nutraceuticals, sustainable materials, and bioenergy. This approach not only mitigates environmental challenges but also contributes to the principles of sustainability and the circular economy (Yarin et al., 2022; Abraham et al., 2020).

The valorisation of these by-products involves advanced technologies, including the extraction of residual bioactives and the conversion of lignocellulosic materials into high-value products. With increasing global demand for natural, eco-friendly solutions, the Ayurvedic industry is uniquely positioned to lead in the development of sustainable alternatives while reducing its ecological footprint by further valourization of its by-products (Kularatne, 2024).

2A.4.1.1. Applications of residual bioactive compounds

Residual bioactive compounds in Ayurvedic spent materials, such as tannins, flavonoids, alkaloids, and polyphenols, exhibit diverse therapeutic and functional properties. These compounds can be extracted and utilised in various industries:

Pharmaceuticals and nutraceuticals: Tannins and flavonoids are valuable as natural antioxidants, anti-inflammatory agents, and antimicrobial agents. Their integration into supplements and medications offers solutions for chronic diseases and immunity enhancement (Abraham et al., 2020).

Food and beverage industry: Residual bioactives can act as natural preservatives or functional ingredients, replacing synthetic additives. Flavonoids, for instance, are being explored for their potential to enhance the shelf life and nutritional value of products (Espro et al., 2021).

Cosmetics: Polyphenols and alkaloids are increasingly used in skincare formulations for their rejuvenating and anti-ageing effects, providing eco-friendly alternatives to synthetic chemicals. The recovery and commercialisation of these compounds provide an opportunity for waste reduction while creating products with high market demand, thereby aligning with sustainable business practices (Kularatne, 2024).

2A.4.1.2. Utilisation of lignocellulosic biomass

Lignocellulosic biomass, a major component of Ayurvedic spent materials, comprises lignin, cellulose, and hemicellulose (Fig. 2A.4). These components can be repurposed into materials and energy solutions, offering significant industrial and environmental benefits:

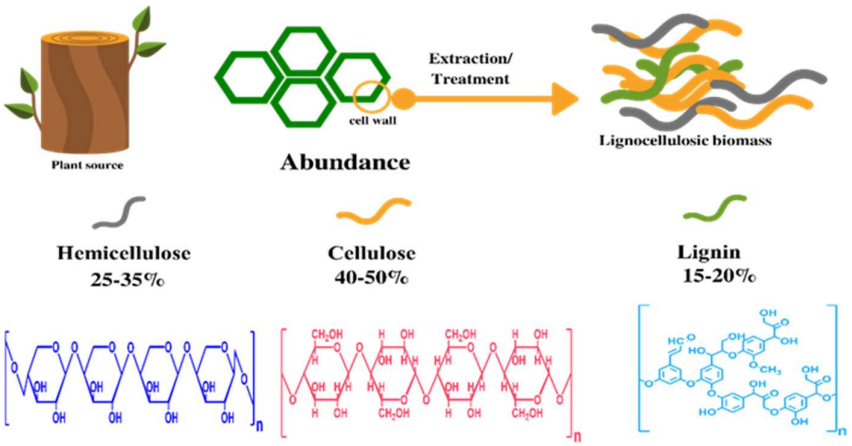

Fig. 2A.4. Schematic of lignocellulosic biomass components derived from plant sources.

Bioenergy and biofuels: Cellulose and hemicellulose can be converted into bioethanol, providing a renewable alternative to fossil fuels. This application contributes to the global shift towards cleaner energy sources (Gupta et al., 2019; Liu et al., 2019; Abraham et al., 2023).

Sustainable packaging: Cellulose-based films and composites are being developed as biodegradable packaging materials, addressing the environmental challenges posed by plastic waste.

High-performance materials: Lignin can be transformed into advanced products such as carbon fibres, adhesives, and biopolymers. Nano-lignin, for example, is gaining popularity for its use in drug delivery systems, antioxidant formulations, and lightweight composites in automotive and aerospace industries (Abraham et al., 2023).

By effectively utilising lignocellulosic biomass, the Ayurvedic industry can reduce waste, conserve resources, and contribute to sustainable development. This valorisation aligns with both environmental goals and economic opportunities, positioning the industry as a leader in innovative waste management strategies (Kularatne, 2024).

2A.4.1.3. Nanotechnology innovations: development and applications of nano lignin and nano cellulose

Nanotechnology offers transformative potential for the valorisation of Ayurvedic spent materials, particularly in the development of nano lignin and nano cellulose. These nanoscale materials, derived from lignocellulosic biomass, possess unique structural and functional properties that make them highly desirable for various industrial and biomedical applications (Vickram et al., 2023).

Nano-lignin: Nano-lignin is increasingly gaining attention for its antioxidant, antimicrobial, and UV-blocking properties. It is being developed for use in drug delivery systems, where its ability to encapsulate and protect bioactive compounds can enhance the efficacy and stability of medications. Additionally, nano-lignin is employed in high-performance coatings, adhesives, and antioxidant formulations for food and cosmetic industries (Abraham et al., 2024).

Nano cellulose: Nano cellulose, derived from cellulose fibres, exhibits remarkable mechanical strength, high surface area, and biocompatibility. Its applications include the development of biodegradable composites, flexible electronics, and water purification membranes. In food and pharmaceutical sectors, nano-cellulose is used as a stabiliser in emulsions, a carrier for active ingredients, and a matrix for controlled drug release (Kularatne, 2024).

By integrating nanotechnology into the utilisation of Ayurvedic spent materials in recovery of lignocellulosic mass and converting to nanomaterials, the industry can produce sustainable, high-value products that address the growing demand for eco-friendly and functional materials.

2A.4.1.4. Biopolymer advancements in Pickering emulsions, active packaging, and nutrient delivery

Pickering emulsions, emulsions stabilised by solid particles, are gaining attention in various applications in food, pharmaceuticals and cosmetics. The lignin and cellulose from Ayurvedic

spent materials offers innovative solutions for applications such as Pickering emulsions, active packaging, and nutrient delivery systems (Pandita et al., 2024). These biopolymer-based advancements contribute to reducing reliance on synthetic materials while addressing the demand for sustainability.

Pickering emulsions: Biopolymers, such as nano-lignin and nano-cellulose, serve as stabilisers in Pickering emulsions, which are emulsions stabilised by solid particles instead of surfactants. These emulsions are gaining popularity in food and pharmaceutical applications due to their enhanced stability and reduced use of synthetic additives (Fig. 2A.5). For instance, nano-lignin-based emulsions can encapsulate sensitive bioactives like curcumin and vitamins, ensuring better protection and controlled release (Abraham et al., 2024).

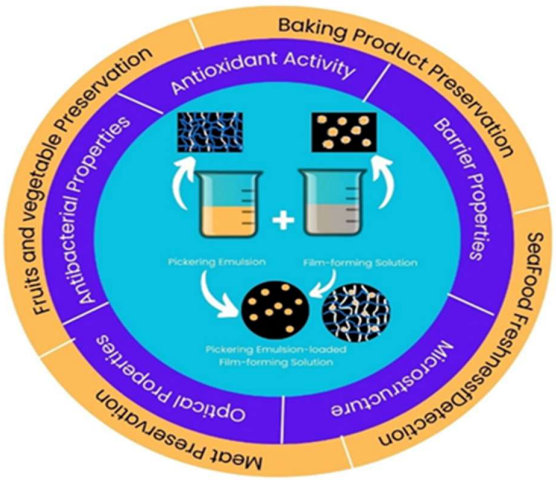

Fig. 2A.5. Schematic representation of Pickering emulsion-loaded film-forming solutions and their applications in food preservation (Zhao et al., 2024).

Active packaging: Biopolymers derived from Ayurvedic spent materials, particularly lignin and cellulose, are used in developing active packaging solutions and biodegradable packaging materials (Zhao et al., 2024). These materials provide antioxidant and antimicrobial functionalities, extending the shelf life of perishable goods. For example, cellulose-based films

infused with nano-lignin can inhibit microbial growth and protect against oxidation, reducing food waste and promoting sustainability (Kularatne, 2024).

Nutrient delivery systems: Biopolymers play a crucial role in creating nutrient delivery systems by acting as carriers for vitamins, minerals, and other bioactive compounds. Nano-cellulose, with its high surface area and biocompatibility, is particularly effective in encapsulating and delivering nutrients in a controlled manner. These systems find applications in functional foods, dietary supplements, and targeted drug delivery, offering improved efficacy and consumer benefits (Rayees et al., 2024).

By advancing biopolymer applications in these areas, the Ayurvedic industry can create sustainable, innovative products that meet consumer needs while minimising environmental impact.

2A.4.2. Benefits of valorisation

The valorisation of Ayurvedic spent materials offers a holistic range of benefits, addressing environmental, economic, and societal challenges while aligning with global sustainability goals. By converting waste into value-added products, the Ayurvedic industry can reduce its environmental impact, foster economic growth, and contribute to societal well-being (Kumar et al., 2024).

Environmental benefits: Valorisation significantly reduces the environmental burden caused by Ayurvedic waste disposal. By utilising plant residues and lignocellulosic biomass to create phytochemicals, bioplastics, and other high-value products, the industry can mitigates pollution and promotes resource conservation. For instance, reusing lignin and cellulose from spent materials prevents methane emissions from landfills and reduces water pollution caused by untreated effluents. Moreover, replacing synthetic materials with biodegradable alternatives reduces dependency on fossil fuels and minimises the accumulation of plastic waste, contributing to a circular economy (Maity, 2023; Abraham et al., 2024; Kularatne, 2024). The

phytochemicals could be converted to nutraceuticals or patented and proprietary products (PNP products).

Economic benefits: The valorisation of spent materials creates new revenue streams for the Ayurvedic industry by converting waste into marketable products such as nutraceuticals, pharmaceuticals, and eco-friendly packaging. These high-value products tap into growing consumer demand for sustainable and health-promoting solutions. Additionally, the development and adoption of advanced valorisation technologies generate green jobs, fostering local and regional economic growth. By aligning with global trends in sustainability, the Ayurvedic industry can enhance its competitiveness while reducing production costs through efficient resource use (Rayees et al., 2024).

Societal benefits: Valorisation contributes to the development of sustainable health and wellness products, offering natural alternatives to synthetic chemicals. Bioactive compounds recovered from Ayurvedic spent materials can be incorporated into functional foods, dietary supplements, and personal care products, addressing the increasing demand for eco-friendly and health-conscious products. Furthermore, reducing environmental pollution through waste valorisation improves public health outcomes, while the development of sustainable practices strengthens the social responsibility of the Ayurvedic industry. These advancements ensure long-term societal benefits by promoting healthier lifestyles and preserving environmental integrity (Abraham et al., 2024).

By integrating these environmental, economic, and societal benefits, the valorisation of Ayurvedic spent materials emerges as a transformative strategy for sustainable development. It not only addresses pressing global challenges but also positions the Ayurvedic industry as a leader in eco-innovation and sustainability.

2A.5. Challenges, gaps in knowledge, and research directions

The valorisation of Ayurvedic spent materials offers immense potential for sustainability and innovation. However, its implementation faces several challenges and knowledge gaps that require targeted research and strategic interventions to unlock its full potential.

2A.5.1. Key challenges

One of the primary challenges in the valorisation of Ayurvedic spent materials is the variability in raw materials. Ayurvedic formulations utilise a wide range of plant species, each with distinct properties and compositions. This inconsistency complicates the standardisation of valorisation processes and affects the reproducibility of high-value products. Another significant hurdle is the high technological costs associated with advanced techniques such as extraction and purification of biopolymer extraction and application of nanotechnology. These technologies often require substantial investment, making them inaccessible to small and medium-sized enterprises in the Ayurvedic sector. Regulatory limitations further compound these issues, as the lack of clear policies and certification standards impedes the adoption of sustainable practices and restricts the market potential of valorised products (Abraham et al., 2024; Rayees et al., 2024).

2A.5.2. Gaps in knowledge

Despite progress in research, critical gaps in knowledge hinder the optimisation of Ayurvedic waste valorisation. One major gap is the lack of systematic studies focusing on the unique characteristics of different waste streams, such as plant residues, liquid effluents, and packaging waste. Each stream requires tailored approaches for efficient management, but comprehensive data on their composition and properties is limited. Additionally, fundamental information about the chemical and physical characteristics of Ayurvedic spent materials under varying processing conditions is still missing, which restricts the development of efficient recovery technologies. Furthermore, many of the applied or proposed technologies, such as

nano-lignin and nano-cellulose production, have not been rigorously evaluated for their efficiency, scalability, or environmental impact. This lack of evaluation leaves their industrial potential underexplored and limits their adoption in large-scale applications (Wang et al., 2023; Beladjine et al., 2023).

2A.5.3. Future prospects

Addressing these challenges and gaps requires strategic research directions and policy support. Enhanced methods for bioactive recovery can significantly increase the profitability and sustainability of valorisation processes. Developing cost-effective technologies to extract valuable compounds such as tannins, flavonoids, and alkaloids will expand the commercial potential of Ayurvedic spent materials. Progress in the utilisation of lignocellulosic biomass, particularly for creating biodegradable materials, biofuels, and nanomaterials, is vital for broadening the scope of waste valorisation. Scaling up the production of nano-lignin and nano-cellulose, as well as exploring their applications in industries such as food, pharmaceuticals, and packaging, could drive innovation and sustainability (Bangar et al., 2021; Rayees et al., 2024). Moreover, the establishment of robust policy frameworks is crucial to supporting waste management practices in the Ayurvedic industry. This includes incentivising sustainable practices, providing certifications for value-added products, and creating infrastructure to facilitate waste processing. Strengthened collaboration between researchers, policymakers, and industry stakeholders will ensure the integration of traditional Ayurvedic practices with modern sustainability goals, paving the way for transformative advancements in waste management and valorisation (Sinha et al., 2025; Verma et al., 2024; Kularatne, 2024).

2A.6. Conclusion

This section of review of Ayurvedic spent materials highlights the significant potential of utilising polyphenol-rich extracts, nanocellulose, and lignin for sustainable and innovative applications. Current research emphasises the therapeutic and functional benefits of bioactive compounds, such as antioxidants and anti-inflammatory agents, derived from Ayurvedic waste streams. Likewise, lignin and nanocellulose have shown considerable promise as key components in the development of biodegradable materials, advanced delivery systems, and eco-friendly packaging. Nonetheless, notable gaps remain in the systematic study of the unique characteristics of different Ayurvedic waste streams, as well as in the assessment of the efficiency and scalability of proposed technologies.

This review forms the basis for addressing these gaps through the valorisation of Ayurvedic spent materials, serving as a rationale for the subsequent experimental chapters. It provides a framework for investigating bioactive recovery methods, developing lignin nanoparticles for stabilising emulsions, incorporating these systems into nutrient-fortified products, and designing active packaging materials. Integrating modern technological advances into traditional Ayurvedic practices will address gaps in the utilisation and valorisation of Ayurvedic spent materials, drive product innovation, and promote environmental sustainability.

References

Abdulhameed, S., Surendran O, N., & Haridas, M. (2020). Recycling and Reuse of Ayurvedic Pharma Industry Wastes. Valorisation of Agro-industrial Residues–Volume I: Biological Approaches, 203-217. https://doi.org/10.1007/978-3-030-39137-9_10

Abraham, B., Reshmitha, T. R., Navami, M. M., George, L., Venugopalan, V. V., & Nisha, P. (2020). Phytochemical rich extract from the spent material generated from Industrial Dashamoola preparation (a medicinal Ayurvedic decoction) with antioxidant, antidiabetic and

anti-inflammatory potential. Industrial crops and products, 151, 112451. https://doi.org/10.1016/j.indcrop.2020.112451.

Abraham, B., Shakeela, H., Devendra, LP, Arun, KB, Ragavan, KV, Brennan, C., & Nisha, P. (2024). Lignin nanoparticles from Ayurvedic industry spent materials: Applications in Pickering emulsions for curcumin and vitamin D_3 encapsulation. *Food Chemistry*, *458*, 140284. https://doi.org/10.1016/j.foodchem.2024.140284

Abraham, B., Syamnath, V. L., Arun, K. B., Zahra, P. F., Anjusha, P., Kothakotta, A., & Nisha, P. (2023). Lignin-based nanomaterials for food and pharmaceutical applications: Recent trends and future outlook. *Science of The Total Environment*, 881, 163316. https://doi.org/10.1016/j.scitotenv.2023.163316.

Agarwal, P., Goyal, A., & Vaishnav, R. (2018). Comparative quality assessment of three different marketed brands of Indian polyherbal formulation-triphala churna. *Biomedical Journal*, 2(9). doi: 10.26717/BJSTR.2018.05.001237

Anand, U., Tudu, C.K., Nandy, S., Sunita, K., Tripathi, V., Loake, G.J., & Proćków, J. (2022). Ethnodermatological use of medicinal plants in India: From ayurvedic formulations to clinical perspectives–A review. *Journal of ethnopharmacology,* 284, 114744. https://doi.org/10.1016/j.jep.2021.114744

Arun, K. B., Chandran, J., Venugopal, V. V., Madhavankutty, T. S., & Nisha, P. (2018). Spent cumin seeds generated from ayurvedic industry as a source of bioactive compounds for nutraceutical/functional food applications. *Journal of Food Processing and Preservation*, *42*(1), e13392.

Athira, N., Awasthi, V., Thamara, K., & Kumar, S. (2022). Pharmacological potential of polyherbal ayurvedic formulations–a review. *Asian J Pharm Clin Res*, *15*(11), 14-20. http://dx.doi.org/10.22159/ajpcr.2022v15i11.45703

Bangar, S. P., & Whiteside, W. S. (2021). Nano-cellulose reinforced starch bio composite films-A review on green composites. *International journal of biological macromolecules,* 185, 849-860. https://doi.org/10.1016/j.ijbiomac.2021.07.017

Beladjine, M., Albert, C., Sintès, M., Mekhloufi, G., Gueutin, C., Nicolas, V., & Huang, N. (2023). Pickering emulsions stabilized with biodegradable nanoparticles for the co-encapsulation of two active pharmaceutical ingredients. *International Journal of Pharmaceutics,* 637, 122870. https://doi.org/10.1016/j.ijpharm.2023.122870

Bhattacharya, S. (2024). Application of a Novel Nanotherapeutic Strategy in Ayurvedic Treatment. In Emerging Applications of Novel Nanoparticles (pp. 199-228). Cham: Springer Nature Switzerland. https://doi.org/10.1007/978-3-031-57843-4_8

Chauhan, A., Semwal, D. K., & Joshi, S. K. (2023). An Overview of Biotechnological Applications in Ayurveda: Amalgamation of Modern Techniques and Science. *Current Traditional Medicine*, 9(1), 23-32. https://doi.org/10.2174/2215083808666220211161918

Chimankar, R.P., Tawalare, K.A., & Mishra, S.A. (2020). Prevention of lifestyle disorders with basic principles of Ayurveda. *International Ayurvedic Medical Journal*, (Online), 4487-4492. https://doi.org/10.46607/iamj3008092020

Debnath, P. K., Banerjee, S., Mitra, A., & Mukherjee, P. K. (2015). Ayurveda–opportunities for developing safe and effective treatment choices for the future. In Evidence-based validation of herbal medicine (pp. 427-454). Elsevier. https://doi.org/10.1016/B978-0-12-800874-4.00020-9

Dhadse, S., Alam, S. N., & Rao, M. M. (2021). Development of nutrient rich biofertilizer by co-vermistabilization of aquatic weeds using herbal pharmaceutical wastewater along with sediment of lake. *Bioresource Technology Reports,* 13, 100633. https://doi.org/10.1016/j.biteb.2021.100633

Espro, C., Paone, E., Mauriello, F., Gotti, R., Uliassi, E., Bolognesi, M. L., & Luque, R. (2021). Sustainable production of pharmaceutical, nutraceutical and bioactive compounds from biomass and waste. *Chemical Society Reviews*, *50*(20), 11191-11207. doi: 10.1039/D1CS00524C

Gopinath, N. (2020). Industrial Manufacture of Traditional Ayurvedic Medicines. In Ayurveda in The New Millennium (pp. 41-70). CRC Press.

Grand View Research. (2024). *Ayurveda market size, share & trends analysis report: Segment forecasts, 2024-2030*. Grand View Research. https://www.grandviewresearch.com

Gupta, P. K., Raghunath, S. S., Prasanna, D. V., Venkat, P., Shree, V., Chithananthan, C., & Geetha, K. (2019). An update on overview of cellulose, its structure and applications. *Cellulose*, 201(9), 84727.

Kizhakkeveettil, A., Parla, J., Patwardhan, K., Sharma, A., & Sharma, S. (2024). History, Present and Prospects of Ayurveda. In History, Present and Prospect of World Traditional Medicine (pp. 1-72). https://doi.org/10.1142/9789811282171_0001

Kotmire, S., Desai, A., & Chougule, N. (2024). The advances in polyherbal formulation. *Journal of Pharmacognosy and Phytochemistry*, *13*(1), 210-221. doi: 10.22271/phyto.2024.v13.i1c.14828

Kularatne, R. K. A. (2024). Biomedical waste generation at Ayurveda hospitals in South Asia: A mini review of the composition, quantities and characteristics. *Waste Management & Research*, 42(2), 95-110. https://doi.org/10.1177/0734242X231178225

Kumar, I., Kumar, U., Singh, P.K., Singh, R.P., Madheshiya, P., & Kharwar, S. (2024). Utilizing Residual Biomass from Medicinal and Aromatic Plants: Scope for Value Enhancement. In Medicinal and Aromatic Plants: Current Research Status, Value-Addition to

Their Waste, and Agro-Industrial Potential (Vol II) (pp. 185-202). Cham: Springer Nature Switzerland. https://doi.org/10.1007/978-3-031-64601-0_13

Kumar, S., Dobos, G. J., & Rampp, T. (2017). The significance of ayurvedic medicinal plants. *Journal of evidence-based complementary & alternative medicine,* 22(3), 494-501. https://doi.org/10.1177/21565872166713

Liu, X., Lin, Q., Yan, Y., Peng, F., Sun, R., & Ren, J. (2019). Hemicellulose from plant biomass in medical and pharmaceutical application: A critical review. *Current medicinal chemistry*, 26(14), 2430-2455. https://doi.org/10.2174/0929867324666170705113657

Lubbe, A., & Verpoorte, R. (2011). Cultivation of medicinal and aromatic plants for specialty industrial materials. *Industrial crops and products*, 34(1), 785-801. https://doi.org/10.1016/j.indcrop.2011.01.019

Luhaste, V. (2023). Maharishi Ayurveda Integrated Approach to Mental Health: The Effect of Maharishi Ayurveda Treatments for Anxiety and Depression Symptoms. A Mixed Methods Study Within a Whole Systems Research Project (WSR). Maharishi University of Management.

Mahale, P. (2023). Determinants of Customers' Trust in Ayurvedic Products–A Review. International Journal of Case Studies in Business, IT and Education (IJCSBE), 7(4), 429-458. https://doi.org/10.47992/IJCSBE.2581.6942.0330

Mahjoubin, M., Rezaei, S., Kesharwani, P., & Sahebkar, A. (2024). Nanospheres for curcumin delivery as a precision nanomedicine in cancer therapy. *Journal of Biomaterials Science, Polymer Edition*, *35*(14), 2250-2274.

Maier, K. (2021). Energetic Herbalism: A Guide to Sacred Plant Traditions Integrating Elements of Vitalism, Ayurveda, and Chinese Medicine. Chelsea Green Publishing.

Maity, S. (2023). Sustainable Healthcare: Medicinal Plants and Environmental Balance in Ayurveda. A Basic Overview of Environment and Sustainable Development [Volume: 2], 166. https://doi.org/10.52756/boesd.2023.e02.011

Maj, G., Najda, A., Klimek, K., & Balant, S. (2019). Estimation of energy and emissions properties of waste from various species of mint in the herbal products industry. *Energies*, 13(1), 55. https://doi.org/10.3390/en13010055

Marcelino, S., Gaspar, P. D., & Paço, A. (2023). Sustainable waste management in the production of medicinal and aromatic plants—A systematic review. *Sustainability*, 15(18), 13333. https://doi.org/10.3390/su151813333

Meng, X., Wen, Z., Qian, Y., & Yu, H. (2017). Evaluation of cleaner production technology integration for the Chinese herbal medicine industry using carbon flow analysis. *Journal of Cleaner Production*, 163, 49-57. https://doi.org/10.1016/j.jclepro.2015.10.067

Mohite, S., Kapoor, E., Nagarkar, B., & Mohite, S. S. (2014). Evaluation of efficacy of dashmoolarishta in cervicitis: a proof-of-concept study. *World J Pharm Sci*, 3(6), 1526-1532.

Nagarkar, B. E (2016). Studies on anti inflammatory potential of dashamoola formulations and its dosage forms and# 8195. http://hdl.handle.net/10603/148786

Ojo, S. K. S., Ojo, A. M., Ayo, I. O., Oluwole, B. R., & Otugboyega, J. O. (2024). Nanobioinsecticides Derived from Neem-Based Preparations. *Handbook of Agricultural Biotechnology*, *4*, 27-68.

Pandita, G., de Souza, C.K., Gonçalves, M.J., Jasińska, J.M., Jamróz, E., & Roy, S. (2024). Recent progress on Pickering emulsion stabilized essential oil added biopolymer-based film for food packaging applications: A review. *International Journal of Biological Macromolecules*, 132067. https://doi.org/10.1016/j.ijbiomac.2024.132067

Parekar, R. R., Bolegave, S. S., Marathe, P. A., & Rege, N. N. (2015). Experimental evaluation of analgesic, anti-inflammatory and anti-platelet potential of Dashamoola. *Journal of Ayurveda and integrative medicine,* 6(1), 11. doi: 10.4103/0975-9476.146565

Patel, S., Das, P., Priyadarshi, M., Babbar, M., Hussain, A., & Bharat, T. V. (2024). Anaerobic digestion of herbal waste: a waste to energy option. *Environmental Monitoring and Assessment,* 196(7), 600. https://doi.org/10.1007/s10661-024-12769-x

Pawar, N., Kogje, A., Bhondave, P., Nagarkar, Kulkarni, R., Harsulkar, Y., & Jagtap, H. (2013). Comparative free radical scavenging and anti-inflammatory potential of branded market samples of an Ayurvedic formulation: Dashamoolarishta. *Int J Pharma Bio Sci*, 4, 789-799.

Posada, E. (2017). The Ayurveda natural medicine system and its environmental implications. *Environ Sci Ind J*, 13(4), 144.

Prabhu, G. R. D., Kiran, C. R., Sundaresan, A., Mony, R. S., & Venugopalan, V. V. (2015). Process development studies for recovery of bio active isolates from spent black pepper generated from ayurvedic industry. *Industrial Crops and Products*, *66*, 144-149.

Prabhune, A., & Mohite, S. (2019). Clinical Efficacy of Modified Dashmoolarishta in Cervicitis. *International Journal of Innovative Knowledge Concepts*, 7, 4.

Preethy H, A., Venkatakrishnan, Y. B., Ramakrishnan, V., & Krishnan, U. M. (2024). A network pharmacological approach for the identification of potential therapeutic targets of Brahmi Nei–a complex traditional Siddha formulation. *Journal of Biomolecular Structure and Dynamics*, 1-24.

Puri, I., & Pargotra, P. P. (2021). Biomedical waste & its disposal in Ayurvedic Hospitals: Awareness and practices. *Journal of Ayurveda and Integrated Medical Sciences*, 6(3), 164-169.

Rajan, R., Robin, D. T., & Vandanarani, M. (2019). Biomedical waste management in Ayurveda hospitals–current practices and future prospectives. Journal of Ayurveda and integrative medicine, 10(3), 214-221. https://doi.org/10.1016/j.jaim.2017.07.011

Rajini, P. S., & Muralidhara, M. (2023). Therapeutic efficacy of ayurvedic polyherbal formulations (PHF): Interactive mechanisms and broad-spectrum activities against neurological disorders. In Ayurvedic Herbal Preparations in Neurological Disorders (pp. 89-111). Academic Press. https://doi.org/10.1016/B978-0-443-19084-1.00024-7

Raju, S., & Das, M. (2024). Medicinal plants industry in India: Challenges, opportunities and sustainability. doi : 10.5958/0975-6892.2024.00001.7

Rayees, R., Gani, A., Noor, N., Ayoub, A., & Ashraf, Z. U. (2024). General approaches to biopolymer-based Pickering emulsions. *International Journal of Biological Macromolecules*, 131430. https://doi.org/10.1016/j.ijbiomac.2024.131430

Resmi, B. G., Yadav, C. R., & Abhilash, M. (2022). Impact of environmental toxicity on health in ayurvedic parlance. *Int J Community Med Public Health*, 9, 3326-34. https://dx.doi.org/10.18203/2394-6040.ijcmph20222043

Sarkar, R., Basak, BB, & Das, M. (2023). Bioprospection of above ground biomass from ashwagandha plant: A waste valorisation approach. Indian Horticulture , 68 (5), 49-52.

Sebastiani, G., Navarro-Tapia, E., Almeida-Toledano, L., Serra-Delgado, M., Paltrinieri, A. L., García-Algar, Ó., & Andreu-Fernández, V. (2022). Effects of antioxidant intake on fetal

development and maternal/neonatal health during pregnancy. *Antioxidants*, 11(4), 648. https://doi.org/10.3390/antiox11040648

Shah, S. (2019). Ayurveda: The conventional Indian medicine system and its global practice. *Himalayan Journal of Health Sciences*, 13-33. https://doi.org/10.22270/ijist.v4i1.36

Shetty, Y. C., Godbharle, S., Brahma, S., Salgaonkar, S., & Rege, N. N. (2017). Evaluation of oral multi-herbal preparation of Dashmoolarishta on mice model of osteoarthritis. *Journal of Basic and Clinical Physiology and Pharmacology*, 28(6), 583-591. https://doi.org/10.1515/jbcpp-2016-0141

Sinha, A., Sidana, S., Rao, G. M., Rathore, N., Raj, S., Jha, A., & Kumar, V. (2025). Application of Artificial Intelligence in Ayurvedic Science Healthcare Practices: A Detailed Survey. *Ethical Dimensions of AI Development*, 437-466.

Srivastava, N. K., Ram, L. C., & Masto, R. E. (2010). Role of selected riparian herbs in reducing soil erosion and nutrient loss under simulated rainfall. *Environmental Earth Sciences*, 61(2), 405-417. https://doi.org/10.1007/s12665-009-0353-5

Swathi, K., & Sundaravadivelu, S. (2023). Ayurveda and Transdisciplinary Approaches: A Way Forward towards Personalized and Preventive Medicine. *Indian Journal of Pharmaceutical Sciences*, 85(6), 1574-1585.

Tao, W., Jin, J., Zheng, Y., & Li, S. (2021). Current advances of resource utilization of herbal extraction residues in China. *Waste and biomass valorization*, 1-16. https://doi.org/10.1007/s12649-021-01428-8

Taru, P., Syed, S., Kute, P., Shikalgar, M., Kad, D., & Gadakh, A. (2022). Dashamoola: A systematic overview. GIS-Zeitschrift fü Geoinformatik, 9, 1334-1345.

Thakur, M., Weng, A., Fuchs, H., Sharma, V., Bhargava, C. S., Chauhan, N. S., & Bhargava, S. (2012). Rasayana properties of Ayurvedic herbs: Are polysaccharides a major contributor. *Carbohydrate polymers*, 87(1), 3-15. https://doi.org/10.1016/j.carbpol.2011.08.035

Verma, S. K., Pandey, M., Sharma, A., & Singh, D. (2024). Exploring Ayurveda: principles and their application in modern medicine. *Bulletin of the National Research Center*, 48 (1), 77. https://doi.org/10.1186/s42269-024-01231-0

Vickram, A. S., Kumar, G., Dey, N., Karunakaran, R., Anbarasu, K., Patel, A. K., & Ponnusamy, V. K. (2023). Valorisation of nano-based lignocellulosic derivatives to procure commercially significant value-added products for biomedical applications. *Environmental Research*, 216, 114400. https://doi.org/10.1016/j.envres.2022.114400

Wang, K., Zhu, M., Yang, Z., Bai, L., Huan, S., & Wang, C. (2023). Sustainable production of stable lignin nanoparticle-stabilized Pickering emulsions via Cellulose Nanofibril-Induced Depletion Effect. *ACS Sustainable Chemistry & Engineering*, 11(24), 9132-9142. https://doi.org/10.1021/acssuschemeng.3c01972

World Health Organization. (2003). WHO guidelines on good agricultural and collection practices [GACP] for medicinal plants. World Health Organization.

Xin, S., Huang, F., Liu, X., Mi, T., & Xu, Q. (2019). Torrefaction of herbal medicine wastes: Characterization of the physicochemical properties and combustion behaviors. *Bioresource technology*, 287, 121408. https://doi.org/10.1016/j.biortech.2019.121408

Yadevendra, Y., Sani, S., Sharma, K.C., Hema, P., & Rajesh, A.K. (2019). A novel ayurvedic techniques approach for value addition of waste materials.

Yarin, T., Dutta, B., Murmu, D. K., Medda, P., & Das, S. (2022). Valorisation of medicinal and aromatic plant waste. *J Pharm Innov*, 11 (1), 532-537.

Zhao, Q., Fan, L., Li, J., & Zhong, S. (2024). Pickering emulsions stabilized by biopolymer-based nanoparticles or hybrid particles for the development of food packaging films: A review. *Food Hydrocolloids*, 146, 109185. https://doi.org/10.1016/j.foodhyd.2023.109185

Chapter-2B

Lignin-based nanomaterials for food and pharmaceutical applications: Recent trends and future outlook

Abstract

Small particles of size range from 1 to 100 nm are referred to as nanoparticles. Nanoparticles have tremendous applications in various sectors including the areas of food and pharmaceutics. They are being prepared from various natural sources widely. Lignin is one such sources that deserves a special mention due to its ecological compatibility, accessibility, abundance, and low cost. This amorphous heterogeneous phenolic polymer is the second most abundant molecule in nature after cellulose. Apart from being used as a biofuel source, lignin is less explored for its potential at nano level. In plants, lignin exhibits cross linking structures with cellulose and hemicellulose. To benefit from the untapped potential of lignin in high-value-added applications, numerous advancements have taken place in synthesizing nanolignins for manufacturing lignin-based materials. Lignin and lignin-based nanoparticles have numerous applications, but in this review, we are particularly focusing on the applications at food and pharmaceutical sectors. The exercise we undertake has great relevance as it helps scientists and industries gain valuable insights into lignin's capabilities and exploit its physical and chemical properties to facilitate the development of future lignin-based materials. We have summarized the available lignin resources and its potential in food and pharmaceutical industries at various levels. This review attempts to understand various methods adopted for the preparation of nanolignin. Furthermore, the unique properties of nano-lignin-based materials and their applications in fields including packaging industry, emulsions, nutrient delivery, drug delivery hydrogels, tissue engineering, and biomedical applications were well-discussed.

Keywords: Lignin, nanolignin, antioxidant activity, nutrient delivery, drug delivery

2B.1. Introduction

The principal components of plant biomass created by plants consist of cellulose, hemicellulose, and lignin. Lignin is the most widely distributed aromatic polymer, and it participates with cellulose and hemicellulose to shape and toughen plant cell walls. According to recent reports, the paper industry produces nearly 50 million tons of biomass by-products annually worldwide. Unfortunately, 98%of this organic chunk is either burned for generating energy or disposed of directly into sewage systems, leading to serious environmental consequences. That leaves 2% of the biomass material for industrial use, especially for creating valuable lignin-based products (Pham et al., 2023). Lignin also accounts for one-fifth of the total biomass available on the planet (Pham et al., 2023, Bajwa et al., 2019). Together, they form a reinforced structure resembling a supra-molecular scaffold capable of providing physical and chemical durability to the cell when encountering infections and enzymatic, and chemical destruction (Xie et al., 2018). Mostly lignin (up to 35%) gets stored in the middle lamella of plants like jute, cotton, industrial hemp, and wood pulp. Lignin types viz lignosulfonates (88%), kraft lignin (9%), and the emerging sulfur-free organosolv accounting for 2% represent the lignin market. By 2025, lignin's valuation is expected to reach $913.1 million if current trends continue (Pham et al., 2023, Bajwa et al., 2019). Lignin has a variety of industrial applications, including sterile biomedical device modules, food packaging materials, toughened entities for tissue engineering, and deliverable drug carriers, among others. Lignin also adds value to consumer goods owing to its intrinsic UV shielding qualities, antioxidant capability, chemical stability, and physical toughness. Several publications discuss how lignin helps in value addition and shelf-life extension (Akbarian et al., 2022).

Augustin Pyramus de Candolle introduced the moniker lignum, and Peter Klason proposed a coniferyl alcohol-packed lignin skeleton to explain the chemical composition of lignin (Bajwa et al., 2019). Lignin is a polymer made up of three monolignols-*p*-hydroxyphenyl (H), guaiacyl

(G), and syringyl (S) units. Substituted phenolic groups like p-coumaryl, coniferyl, and sinapyl are spatially ordered in a lignin biomolecule, allowing for a wide range of functional entities and linkages. The interplay between H, G, and S units in lignin contributes to their heterogeneity, yielding numerous functional groups and linkages. About 50% of all linkages come from the aryl ether-O-4 linkage (Sethupathy et al., 2022).

Previously, the only way to obtain organic constituents and usable energy from lignin-loaded industrial spent materials and residues was by burning them. The H, S, and G subunits produced by the radical coupling process of phenylpropanoid units provide the structural foundation for lignin. Because of their heterogeneous character, recovering lignin in its native state for structural elucidation becomes laborious. Recent near-perfect recoveries of milled wood lignin (MWL) and cellulolytic enzyme lignin (CEL) provide a resolution to this problem to an extent (Bertella and Luterbacher, 2020). Previous lignin research focused on its role in the pulp and paper industry, as lignin was dumped as waste by the industry. Because of that, studies were limited to the structural elucidation and chemical profiling (Sharma et al., 2020).

In their natural form, lignins are polysaccharide-bound structures entangled in cellulose and hemicellulose with irregular distribution patterns (Sharma et al., 2020). Plant source, treatment criteria, extraction plan, and other factors influence the physicochemical properties of lignin. Agricultural and industrial by-products such as pulp and paper (Tortora et al., 2014), bagasse (Bertolo et al., 2019), herbal and agro-waste materials (Abraham et al., 2020), wood, and other organic wastes have copious amounts of lignin. In contrast, individual plant parts, grass, and other organic wastes yield significantly low levels of lignin (Sethupathy et al., 2022).

Recently, lignin-derived composites have drawn the attention of researchers and industrialists since their nanoforms improved durability and added multitudinous value to products such as rubber, textiles, and other materials. Compared to nano-sized lignins, native lignin fails to deliver the expected interaction and performance-boosting capabilities when treated as a single

entity (Parvathy et al., 2020). When impregnated with gluten-containing nanostructures, nanolignins exhibited improved thermal, mechanical, UV-shielding, and water-sensing capacity. Nanolignins combined with chitosan have shown up to 83% methyl orange scavenging capabilities in contaminated water systems. A study found that the morphology of lignin nanoparticles provides better dispersibility and stability for up to two months. They produced uniformly dispersed nanolignins using acoustic irradiation sans chemical intervention (Gilca et al., 2015). Encapsulating cationic polyelectrolyte layers onto nanolignins loaded with silver ions can form biodegradable and eco-friendly fill-in for silver nanoparticles. The polyelectrolyte surface facilitates contact with the bacterial cell membrane, kills a wide range of bacteria, particularly quaternary-amine-resistant *Ralstonia* sp., *Pseudomonas aeruginosa*, and *E. coli*, when combined with silver ions (Richter et al., 2015).

Many applications involving lignin are in the pipeline, and the need for superior materials to improve performances and evade life threats is rising. That is why we think it is high time to shed light on these overlooked abundant, ecofriendly, and biocompatible components.

2B.2. Sources of lignin

The major sources of lignin include plants, agro-processing residues and in India from ayurvedic industries as spent materials. The different sources of lignin are summarized in Table 2B.1.

Lignin in the plant cell walls perform various physiological functions. Pine variety called Brazilwood, bamboo species such as *Bambusa vulgaris* and *Chusquea oxylepis*, *Festuca arundinacea* belonging to grass species, elephant grass (*Pennisetum purpureum*), Zea mays, red clover, bagasse (*Saccharum hibridas*) from sugar cane, and lucerne (*Medicago sativa*) are all good sources of lignin.

Using agricultural by-products for lignin synthesis has several advantages on the techno-economic-environmental front due to the accessibility to various eco-friendly methods. The agro processing residual biomass generates economically viable homogeneous nanoscale

coatings and sterile biopolymeric materials for food packaging. Sugar cane, rice, wheat, and maize are the four crops that contribute the most lignocellulosic biomass to the global agro-industry, with the remainder of the crops contributing only marginally. Bioethanol synthesis from lignin-rich agricultural by-products using environmentally friendly technology involving enzymes and engineered yeasts has the potential to contribute to energy security (Haldar et al., 2022).

The Ayurveda drug industry uses over a thousand plants and plant parts to manufacture drugs. Dumping these inorganic wastes exacerbates the accumulation of a large volume of industrial biomass in landfills (Vinardell et al., 2017). Several studies point to the judicious use of plant-based spent materials containing lignin portions. Our team has already revealed the potential of water-miscible bioactive trapped inside massive chunks of lignocellulose spent material abandoned by the Ayurveda medicine industry (Abraham et al., 2020). Due to incomplete extraction with popular solvents mentioned in Ayurvedic texts (water, milk, ghee, oil, etc.), herbal leftovers remained a reservoir of phytochemicals till further extraction. Vinardell et al. investigated the biological significance of lignin fractions generated from the babul tree (*Acacia nilotica*), a medicinal herb used in ayurvedic decoctions. Extraction methods of lignin from spent materials showing in Fig. 2B.1. Study by Vinardell et al. support the use of bio-transformed lignin from medicinal plants in the food, pharmaceutical, and cosmetic industries (Vinardell et al., 2017).

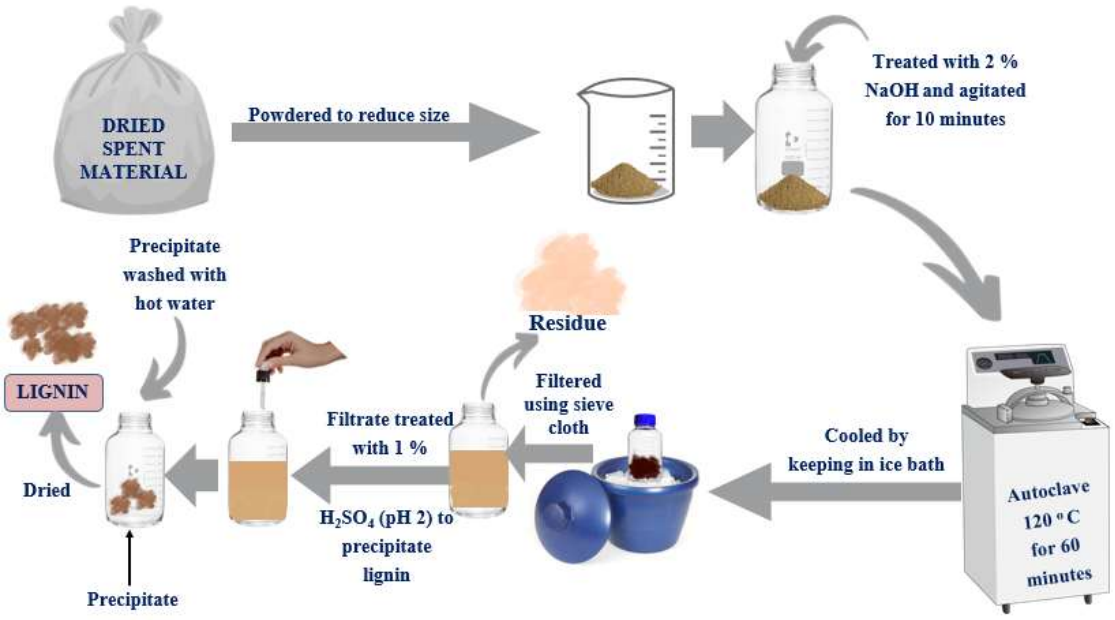

Fig. 2B.1. Lignin extraction method using Alkali.

Table 2B.1: Major sources and classifications of lignin

Source	Image	Classification	References
Wood		Sulfite lignin (Lignosulfonates)	Lora, 2008
Wood (Black liquors)		Kraft lignin	Ekeberg et al., 2006
Non-wood fibers, annual plants		Soda lignin (Alkali lignin)	Gosselink et al., 2004

Annual plants		Aquasolv lignin	Zhuang et al., 2016
Methanol extracts of fresh birch (*Betula pendula*) xylem		Brauns' lignins	Hiltunen et al., 2006
Middle lamella of the plant cell walls	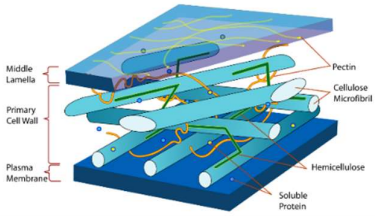	Milled wood lignin (Björkman's lignin)	Claudia et al., 2011
Residue left after polysaccharides hydrolysis of the carbohydrates in finely milled wood	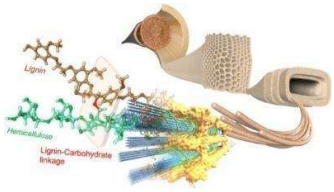	Milled wood enzyme lignin (MWEL)	Agrawal et al., 2014
Solvent-soluble fraction of MWEL		Cellulase enzyme lignin	Agrawal et al., 2014
Hardwood and wheat straw		Organosolv lignin	Prakash et al., 2015

Insoluble residue portion after removing the ash by concentrated acid hydrolysis of the plant tissues	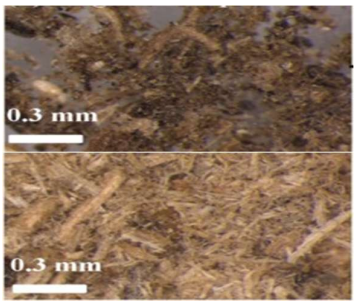	Klason lignin	Chen, 2015
Hardwood species such as aspen		Steam explosion lignin	Gellerstedt and Henriksson, 2008
Corn stalk		Organosolv ethanol lignin (OEL)	Wang et al., 2019
Bamboo		Lignin–carbohydrate complexes	Huang et al., 2018

Artocarpus heterophyllus		Bio composite lignin–chitosan	Jaganathan et al., 2018
Birch wood		Poly (lactic acid)–lignin biocomposites	Spiridon et al., 2018
Oil palm empty fruit bunches		Lignocellulosic	Medina et al., 2016
Avermectin encapsulated with acetylated lignin and benzoylated lignin		Pulp-making black liquor	Zhou et al., 2019

2B.3. Applications of lignin

Lignin has a wide range of applications in various industrial sectors, such as the food and pharmaceutical industries (Fig. 2B.2).

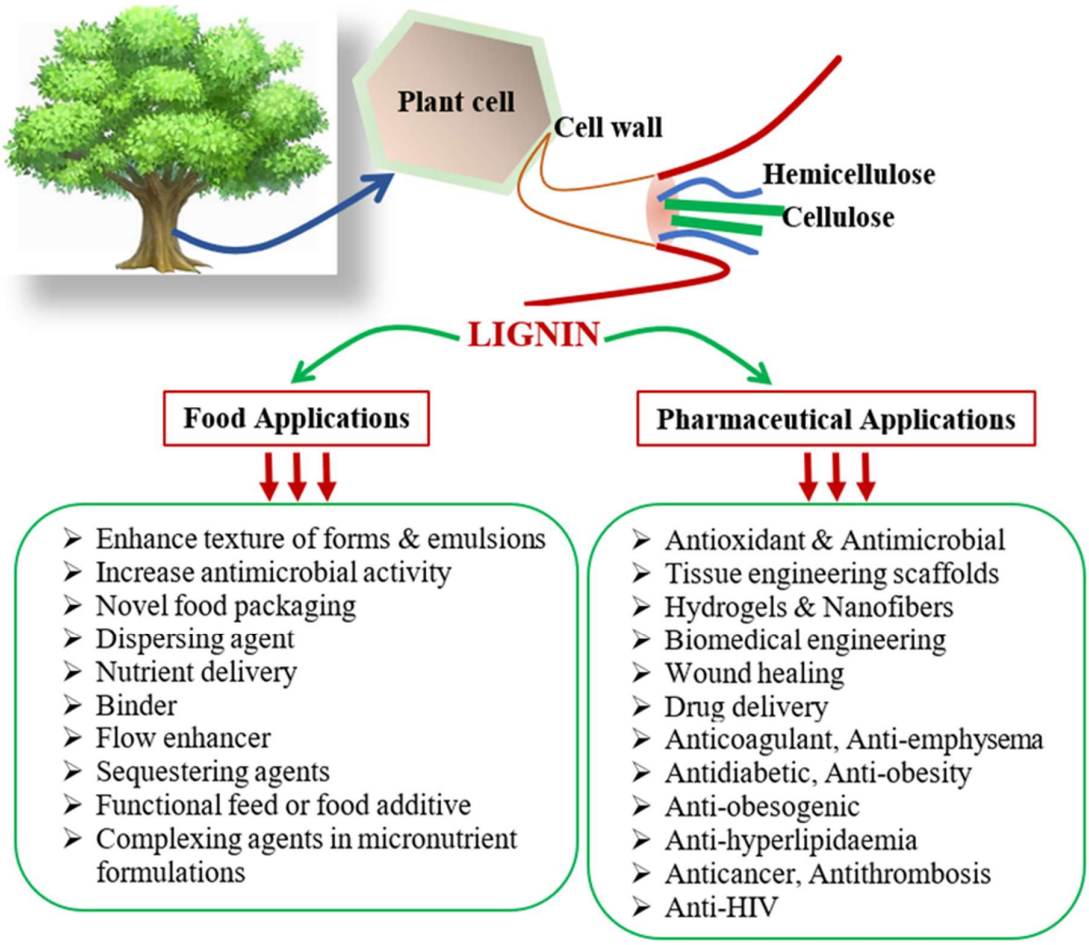

Fig. 2B.2. Applications of lignin

2.B.3.1. Food industry applications

The food industry constantly strives to find new functional entities to improve the quality of food that leaves factories. Such functional foods will contain health-promoting components that can improve nutrient absorption by filtering out undesirable chemicals in the gastrointestinal tract (Gil-Chávez et al., 2019).

The zero-waste concept is a widely held concept that dictates the maximum utilization of plant-derived raw materials. Several allied and non-allied sectors will benefit if the agro-food industries fixate on adopting such a policy for a low-cost alternative out of lignocellulosic biomass (Sharma et al., 2020). The applications of lignin in food industries are depicted in

Table 2B.2: Extraction techniques, advantages, disadvantages and application of lignin sourced raw materials

Raw material	Extraction method	Advantage	Disadvantage	Application	References
Wood	Aqueous dioxane extraction of milled wood	Better selectivity for the hydrolysis of lignin. This extraction process significantly increased yield and methoxyl content of the isolated lignin.	Dioxane is not recommendable from an environmental perspective as it uses toxic solvents. .	Agriculture, manufacturing, cosmetics, construction and biomedicine.	Lora et al., 2008; Chen et al., 2015
Wood (Black liquors)	Hydrophobic Interaction Chromatography (HIC) method to separate lignosulphonates and kraft lignins into seven distinctive peaks according to hydrophobicity.	Water soluble	Complexity and irregularity of the molecular structure of lignin.	As dispersion agent in concrete, in ceramics, as dispersants in textile dyeing, in pesticides, and as binders in briquetting and animal feed.	Ekeberg et al., 2006
Non-wood fibers, annual plants	Novel, sulphur chemical free-pulping process, which called the NovaFiber process	Anti-oxidant, UV stabiliser and low cost of lignin	Heterogeneity, odour and colour problems of lignin-based products.	Functional additive in commodity plastics like polyethylene and polypropylene	Gosselink et al., 2004
Annual plants	Liquid hot water pretreatment of lignocellulosic biomass.	Minimizes the formation of degradation products,	The residual lignin, structural characteristics, high solid	Production of high value-added products and biorefinery	Zhuang et al., 2016

		Reduces high water consumption and energy input	loading and end products negatively influence enzymatic hydrolysis of cellulose	of cellulosic ethanol.	
Methanol extracts of fresh birch (*Betula pendula*) xylem	Brauns lignin extracted with neutral alcoholic solvents.	Attractive light colour of the wood	Vacuum drying of sawn birch timber (dark in colour) causes discolouration.	Woodworking industry, wood panel products	Hiltunen et al., 2006
Middle lamella of the spruce (*Picea abies* and *Picea mariana*) and beech (Fagus) wood	Bjorkman method with slight modification. The biomass is saturated with toluene prior to milling (48 h) and the milled material is mixed with 1,4-dioxone/water solution and is stirred (24 h) at ambient temperature. After centrifugation, evaporate solvent from supernatants to separate milled wood lignin.	Quicker extraction method. Structural changes of lignin is relatively small during the separation process	Extraction is difficult due to the chemical bonds that exist between lignin and the carbohydrates. Lignin has a very high molecular weight and may form a three-dimensional network.	Anti-microbial and anti-HIV effects. It used as biological carriers.	Claudia et al., 2011
Finely Milled wood	Lignin isolated from Finely-milled wood, the cellulolytic enzymes are used.	Prevents scaling in hot and cooling waters and dissolves micronutrients in liquid fertilizers. Plentiful functional groups and low toxicity	Some carbohydrate cannot be removed by prolonged and repetitive enzymatic treatments or by purification methods during lignin isolation.Lower durability, poor fibre-matrix adhesion	As sequestering agents, as a dispersant in battery, as a dust suppressant, as a food additives, in cement, and in blends.	Ganasan et al., 2022; Agrawal et al., 2014
Hardwood and wheat straw	Methanol/H_2O(60/40 ,v/v); 0.1%HCl; 85°C, 4h.	The treatment of Hardwood	Extraction efficiency is very less	Antioxidant addi-	Prakash et al., 2015

		and wheat straw with aqueous organic acids is very well suitable for separation of lignins.		tive in pharmaceuticals, cosmetics and the food industries.	
Insoluble residue portion after removing the ash by concentrated acid hydrolysis of the plant tissues	Benzene and Ethanol; 72% conc. H_2SO_4 (30°C, 4 h); diluted to 3% (2 h); the insoluble substrate is weighed as lignin	Most direct and the most reliable method	Unstable physical and chemical properties	As packaging materials.	Chen, 2015
Hardwood species such as aspen	Comprehensive milling of the plant material, followed by solvent extraction with dioxane and further purification	More amount of lignin can be isolated.	Presence of minor carbohydrate impurities	Catalysts, adsorbents, ion exchangers	Gellerstedt and Henriksson, 2008
Corn stalk	Ionic liquids including [Hnmp]Cl, [Hnmp]CH_3SO_3 and [Hnmp]H_2PO_4:Acetone/water(1:1,v/v), 50~90°C, 30~180min	Ionic liquids provides a good environment for lignin extraction and enzymatic hydrolysis for corn stalk	Ionic liquids is their relatively high cost compared to conventional organic solvents	Suitable for adhesive formulation or other composite biomass applications due to better thermal stability	Wang et al., 2019
Bamboo	Formic acid/Acetic acid/water(30/50/20, %v/v), 50~107°C, 30~180min	Produces a light-coloured acetic acid bamboo lignin microsphere with excellent UV absorbance. Has a small particle size and large interval space	It shows less unsaturated structure and fewer methoxyl groups.	Addresses the staining issue and facilitates the marketing promotion of lignin sunscreens.	Zhang et al., 2019

Artocarpus heterophyllus fruit peels	Treat fruit peel powder with dil H_2SO_4 (0.2 mol/L, 180 °C, 300 W); the resultant product 0.1 g dissolved in 7 ml of H_2SO_4 and microwave irradiation, filtration; washed with DD water; dried at 100 °C.	Higher porosity of lignin encouraged the water availability into the polymeric network of biocomposites	Sulphuric acid requiring neutralization and purification.	Wound healing (skin burns).	Jaganathan et al., 2018
Birch wood	Extracted with Hydrotopic solution with the addition of formic acid and hydrogen peroxide	Use of environmentally friendly hydrotopic process to extract lignin from industrial birch wood chips	Hydrotopic solvents are not cost effective.	Biomedical applications.	Spiridon et al., 2018
Oil palm empty fruit bunches	93%(w/w) acetic acid aqueous;0.3% (w/w) HCl; 115℃, 3h.	Majority are lignocellulosic materials, consisting of an estimated cellulosic content of 30–50%, 15–35% of hemicelluloses and about 20–30% of lignin.	Lower strength, variable quality and poor moisture resistance.	Cosmetics, pharmaceutical, polymers resins and biofuels.	Medina et al., 2016
Avermectin (AVM) encapsulated with acetylated lignin (ACAL) and benzoylated lignin (BZAL)	ACAL and BZAL were obtained from the chemical modification of alkali lignin with CH_3COCl and C_7H_5ClO, respectively	Lignin used as shell material to prepare AVM-loaded nanospheres showed good controlled	Low yield of production and irreugalar morphology.	Tissue engineering or regeneration, artificial muscles, and strong underwater antifouling materials.	Zhou et al., 2019

		release and anti-photolysis properties			

2B.3.1.1. Emulsion

An emulsion is a stable concoction of liquids which are unblendable due to phase separation. The emulsification process allows unblendable liquids to stabilize and remain as a single unit. Food emulsions exhibit phase separation due to their inherent instability. The adsorptive nature of certain emulsifiers and their ability to lower the interfacial tension allows for the synthesis of finely divided emulsion. The food industry uses emulsions to make products, such as mayonnaise, salad creams, and beverages. The pharmaceutical industry uses it to make medications like ointments, and cosmetic and personal care products, including creams, lotions, sunscreens, hair sprays, and many more. A cohort from Finland demonstrated the application of wood-based lignin as a stabilizer, thickener, and texture enhancer in yogurt, baked, and meat products (Aura, 2018). As evidenced by Gil-Chávez et al., calorie-free lignin used to make fluffy muffins can be a replacement for egg components used for the baking process. In addition to being indigestible, lignin-rich foods help lower blood cholesterol and total calories (Gil-Chávez et al., 2019).

Kraft lignin modified with tannic acid have the potential to stabilize oil. Additionally, during ring-opening polymerization through re-oxidation, tannic acid yielded a form of lignin with improved carboxylate density and solubility. These types of lignin have potential application in stabilizing oil (hexadecane) in water emulsion systems (Gharehkhani et al., 2018). Lignosulfonates are part of pest and herb controlling formulations, colourants, and pigments as a stabilizer (Calvo-Flores et al., 2010). By tweaking the acidity and salinity, it is possible to enhance the stabilizing properties of amphiphilic lignin obtained from soda and kraft lignin.

The new functionalized lignins formed were due to molecular affinity between the two liquid phases (Rojas et al., 2007).

2B.3.1.2. Packaging

The food industry is looking for greener alternatives to traditional food packaging materials due to the adverse consequences of petroleum-derived materials, aluminum cans, and PFCs - perfluorinated organic compounds (Tayeb et al., 2020). Due to its crosslinking properties, lignin finds application in food-grade biofilms to have a unique spatial arrangement that aids flexibility and stability (Sharma et al., 2020). Consumer products with lignin-incorporated packaging materials containing chitosan have a longer shelf life because they are impervious to moisture and pathogenic bacteria (Yang et al., 2016). Recently, biofilms reinforced with lignin were developed from oil palm black liquor spent materials using glycerol. These films demonstrated increased plasticity, and thermal, mechanical, and water-repellent properties (Bhat et al., 2013).

Javed et al. exploited the incorporation of ammonium zirconium carbonate (AZC) cross-linker onto affixed lignin to improve the storage modulus of pure starch, thereby preventing or reducing coating dissolution of the support material (Javed et al., 2018). Tayeb et al. used a type of filtration to create ultrathin biopolymer wafer (16 g/m^2) coatings of lignin-containing cellulose nanofibrils (LCNF) and cellulose nanofibrils (CNF). Both LCNF and CNF favored physical and chemical properties such as tensile strength, water vapor permeability, moisture repellency, and oxygen transmission rate. When incubated with cooking oils, LCNF performed well as a leak-proof coating with improved mechanical qualities, giving a leak-free environment for five months. The findings show that wood-derived lignin candidates may outperform traditional fluorocarbon methods (Tayeb et al., 2020).

Cationic wood nanofiber (CWNF) biofilms derived from cationized sawdust contain lignin as a key component. The lignin component of the system improved UV and oxygen shielding

capability, and optical transparency while quelling oxygen transmission and swelling tendencies under stimulated conditions, either alone or in combination. According to the study, such eco-friendly CWNF will eventually phase out oil-featured plastics from the packaging sector one day. Their application in electronic equipment such as solar batteries is due to their excellent UV absorbing capability (Sirviö et al., 2020). When used in conjunction with a bar coater, Tamminen et al. propose esterified softwood lignin as a model packaging material capable of generating a uniform coat on paperboard. This wood-based barrier architecture utilizes tall oil fatty acid-mediated esterification and is a more environmentally friendly and long-lasting alternative to its oil-based counterparts (Tamminen et al., 2014).

2B.3.1.3. Nutrient delivery

The use of nanoparticles to distribute nutrients has emerged as a promising field in the functional food business, attracting the attention of scientists and academics alike. The sole purpose of the diet is to ensure that the nutrient content of the consumed food gets delivered to the consumer with minimal loss. Gil-Chávez et al. cite a patent filed by the Dutch company DSM that turned lignin into a makeshift transport molecule for vitamins and natural colouring components like carotenoids (Gil-Chávez et al., 2019). Another study by Dinari using the atom transfer radical polymerization (ATRP) method underpins the ability of lignin-derived nanogels as a potent delivery vehicle for curcumin (CUR). The synthesised lignin-based nanogels (lignin-g-P(NIPAM-co-DMAEMA) nanogel (LNDNG) exhibited superior curcumin loading capacity (49.69%), encapsulation efficiency (92.62%) and cumulative release amount (65.36% after 72 h), making it a promising candidate for the safe and efficient future nutrient delivery system (Dinari et al.,2021).

2B.3.2. Pharmaceutical applications

2B.3.2.1. Hydrogels for drug delivery

Hydrogel technology's applications in designing novel drug delivery systems and smart hydrogels have grown in stature, and it has never looked back. Hydrogels, as smart polymers, have been at the forefront of setting industry standards for better targeted and controlled drug administration for many years (TCDD). Smart hydrogels are non-toxic, biodegradable, and biocompatible, making them ideal for replacing conventional hydrogels.

Because of the hydrophilic nature of the biopolymer, chemical and physical variants of hydrogels can retain large amounts of water in their intrinsic 3D framework (Ahmed, 2015). The hydrophilicity of monomeric and polymeric subunits (chemically induced) is essential to forming stable biopolymers. Such biopolymers will have cross-linked fabric and a rigid covalent backbone. In contrast, physical hydrogels rely heavily on network formation mediated by weak intermolecular forces (IMF) and shape-restricting molecular entanglements (Truong et al., 2021). Hydrogels are part of regenerative medicine as a moisture-controlling ingredient in food packaging and the development of diagnostic devices (Ahmed, 2015).

Techniques used to synthesize lignin-derived hydrogels include a). cross-linking, b). atom transfer radical polymerization (ATRP) and reversible addition-fragmentation chain-transfer (RAFT), c). polymerization and copolymerization, d). ultrasonication and e). wet spinning.

2B.3.2.1. a. Cross-linking method

Crosslinking prevents hydrophilic components of hydrogel from dissolution upon coming in contact with an aqueous environment. Larrañeta et. al demonstrated a convenient method to synthesise lignin-based hydrogels for biomedical purposes from high molecular weight lignin by fusing lignin with poly(ethylene glycol) and poly(methyl vinyl ether-co-maleic acid) via esterification. The investigators managed to cross-link the numerous alcohol groups present in the selected lignin with GAN (Gantrez) as the crosslinker and used PEG molecules with

varying molecular weights to reinforce the final material. They also showed how to accelerate the solid-state synthesis using microwave (MW). Apart from GAN, other investigators, such as Sharma et al., used N, N - methylenebisacrylamide (MBAm) as a cross-linking agent, known for working effectively as a cross-linking agent and a monomer that improves efficiency, production, and swelling capacity of the resultant graft (Dacrory et al., 2018).

2B.3.2.1. b. ATRP and RAFT methods

The ATRP (atom transfer radical polymerization) method utilizes the reactivity of organic halide precursor and monomeric forms of acrylonitrile to produce lignin-based hydrogels. On the other hand, Azobisisobutyronitrile (AIBN) initiator- lignin core complex achieves polymerization through radical reaction.

RAFT and ATRP ensue by regulating radicals by reversibly converting active polymeric radicals to produce dormant polymer chains (Truong et al., 2021). Although effective at synthesizing hydrogels, both techniques own drawbacks, such as substandard influence over molecular weight and distribution. Also, it is nearly impossible to create such hydrogels with preset capabilities and a stable copolymer structure.

2B.3.2.1. c. Copolymerization method

Copolymerization of lignin-derived hydrogels from diverse monomeric species can be achieved by treating catalytic initiators, cross-linking agents, or graft copolymerization. For instance, lignosulfonate g-acrylic acid hydrogels from acrylic acid when copolymerized with lignosulfonates. Acrylamide monomer-mediated graft copolymerization is also a viable technique to synthesize lignin hydrogels. Copolymerization is advantageous because it affords stable forms of commercial-grade biopolymers with improved mechanical properties and impact strength (Nguyen et al.,2022; Wu et al., 2017).

2B.3.2.1. d. Ultrasonication method

This method exploits the rheological changes affecting reaction media when subjected to high-frequency sound waves. The sound waves cause low-pressure areas in the medium and create cavitation bubbles. By exploiting the properties of these cavitation bubbles it is possible to afford hydrogels (Sharma and Kumar, 2020). Lignosulphonate-grafted poly (acrylic acid-co-poly (vinyl pyrrolidone) were produced by subjecting the pH-dependent methodology to ultra-sonication (Wang et al., 2016). The low monomer conversion and high power requirements for ultra-sonication reduces its industrial applications.

2B.3.2.1. e. Wet spinning method

It is economical and eco-friendly to generate a sustainable bio-based material on a sub-micron scale. With the introduction of shear stress, the approach self-assembles the growing hydrogel and then reshapes it in a multi-hierarchical arrangement. A prepolymer, a coagulation solution, and a receiving pool with a collector roller are the three essential components of traditional wet spinning. Wet spinning is a helpful way of assisting tissue regeneration, cell communication, and other biomimetic structures without compromising the functionality and architecture of the anticipated biological product.

Polyethylene glycol (PEG) is a suitable candidate for the hydro gelling of working models for drug delivery purposes. Another recent innovation in hydrogel-assisted drug delivery is the reactive extrusion procedure. In response to the catalytic impact of sodium hypophosphite, lignin and related biopolymers undergo plasticization. As a result, citric acid backbones hold the network together. The formed hydrogels exhibited superior swelling properties when regulated by pH and acted as a switch to control the diffusion of liquids and particles. Furthermore, extruding hydrogels with a catalyst reduces the likelihood of degradation, making the reactive extrusion method a viable choice for systemic drug transportation (Farhat et al., 2017).

Using lignin-derived hydrogels as a sterile surface-spanning coating material for medical devices can save lives. Concerns about resistant superbugs and cross-contamination during equipment handling and drug elution led to the development of a hydrogel with antimicrobial capabilities and the ability to keep the proposed medicine inside the hydrophobic bubble for up to four days. This achievement was accomplished by esterifying lignin with PEG and poly (methyl vinyl ether-co-maleic acid), resulting in a fluid absorption capability of 500%. Larrañeta et al. found that PEG 10,000 coatings were effective against a wide range of pathogenic microorganisms, including *S. aureus* and *Proteus mirabilis* (Larrañeta et al., 2018). Recent studies established the role of sodium lignosulphonate-grafted poly (acrylic acid-co-poly (vinyl pyrrolidone) hydrogel (SLS-g-P(AA-co-PVP) as a drug delivery platform. They investigated amoxicillin uptake, transportation, and release in simulated conditions without the involvement of enzymes which helped to evade acidic conditions of the gastric milieu. The researchers evaluated the elasticity of the concerned hydrogels in intestine-like settings and discovered that pH had a significant impact on the hydrogel's releasing capabilities. Swelling ratios of hydrogels were also a factor in determining the biopolymer's ability to retain water (Wang et al., 2016).

Inert and biocompatible characteristics of cellulose allow for bypassing the immune reaction that would otherwise be impossible with lignin alone. A cost-effective cellulose-lignin pair successfully prolonged the release of bioactive chemicals like phenolics. The complex can enhance desired output in all living systems by securing bioactive lignin inside the cellulose covering. The more swelling capacity a hydrogel has, the more polyphenols it can hold, which, in turn, is determined by the amount of lignin it contains. Hydrogels of this type are a good fit for drug delivery systems. A recent study tried to achieve controlled release of metronidazole and lysozyme standards. The results from the experiment revealed that the desired effect came from the viscosity of the hydrogel (Dong et al., 2018).

2B.3.3. Tissue engineering applications

Tissue engineering is an area of research concerned with developing biocompatible alternatives for restoring, maintaining, and improving tissue integrity and performance. Scaffolding techniques, facilitated by the characteristics of both synthetic and natural polymers, are used in biological substitutes. Tissue engineering has typically used cells from the source material and factors that guide the regular functioning of tissues. To provide the appropriate extracellular environment ex vivo, several biomimetic components and structural proteins, such as elastin and collagen, are combined.

The coupling of chitin and lignin facilitates the production of nonwoven polymer composites with a natural feel and acceptability. Such biocompatible tissue scaffolds resembled an extracellular matrix (ECM). After undergoing mild electrospinning, they enhanced optimal tissue regeneration without inducing immunogenicity. Their interaction promoted wound healing, and anti-inflammatory and anti-aging effects on a nanometric level (Morganti et al., 2018).

In one of the electro-spun methods, multi-component biomaterials containing chitin, lignin, and poly(glycerol sebacate) (PGS) gained bactericidal properties against *E. coli* and *Staphylococcus aureus*. The amount of PGS in the solution contributes to the structural integrity and strength of the hybrid biopolymer, and an optimum level of 15% offers maximum mechanical strength. This lignin-based hybrid is ideal for wound dressing because its ECM mimics the microstructure of the unwoven network and has antibacterial properties (Abudula et al., 2018).

Ultrafine biopolymers are formed by ring-opening polymerization when lignin combines with polyesters (polycaprolactone, PCL, and poly (L-lactic acid), PLLA). These polymers have fibrous 3D networks that can reach nanoscale thickness. Electrospinning takes place without a solvent, and the resulting biomaterial provides optimum conditions for cell growth and

multiplication while also providing the necessary mechanical strength. Lignin must be kept between 10% and 30% to achieve these benefits (Kai et al., 2017). PCL featured lignin-based biopolymers created via the electrospinning method to yield ECM-like ultra-fine polymeric structures with 10% wt lignin. Such scaffolds have outstanding elastic characteristics, bio-eco compatibility, pore size, and void fraction at optimum levels. Moreover, optimum pore size and void fraction of the nanocomposites are prerequisites for adequate cell adhesion and development (Salami et al., 2017).

A group of researchers used a solvent-less ring-opening polymerization approach involving lignin/PCL to create an antioxidant-rich bio scaffold capable of assisting in the regeneration, growth, and translational enhancement of neurons and supporting cells, including Schwann cells at various developmental stages. Experiments with hematopoietic cells from the bone marrow also yielded similar results (Wang et al., 2018). Copolymerization occurs when lignin interacts with PCL and polymethyl methacrylate (PMMA). These non-immunogenic electro-spun nanostructures afford biomaterials with superior properties favoring proper cell proliferation and adhesion (Kai et al., 2015).

When lignin and alginate gelatinize in CO_2, aerogels with physical and rheological properties ideal for tissue engineering are formed. By limiting the solubility of the alginate component, lignin was observed to enhance the functioning of the produced aerogels by creating a niche conducive to average cell growth, differentiation, and adhesion. The inherent stability of lignin aided in slowing the biopolymer's degradation rate, which in turn boosted bone tissue regeneration (Quraishi et al., 2015).

Lignin is a biomolecule that can change the intrinsic mechanical properties of other substances, allowing them to participate in bone tissue regeneration via tissue engineering. For example, lignin derived from OPEFB's (oil palm empty fruit bunches) black lye promotes preferential cross-linking of epichlorohydrin (ESH) following acid treatment, resulting in hydrogels with

mechanical qualities required for a solid 3D network. The optimal lignin/agarose hydrogel includes 5% lignin and agarose each, with a maximum ESH content of 10 mL. (Sathawong et al., 2018). Similarly, adding 3% lignin to chitosan improves the tensile strength and stiffness of the bone tissue fabrication candidate (Wang et al., 2016). The resulting PLA/lignin mesh had enhanced tensile strength when reinforced with lignin (7-15%), which was not possible with a lower amount of lignin. The human osteosarcoma cell line did not show any form of immune response to such a composite structure (Spiridon et al., 2018). Because of their potential to solve solubility issues and unique thermal behavior, bioactive integrated metal implants produced from bio/eco-friendly scaffolds like organosolv/lignin are utilized to repair fractured bone tissue and regain functionality. When mixed with hydroxyapatite at varying concentrations, organosolv/lignin improved the bioactivity of titanium implants. By replacing titanium with silver, the produced biomaterial becomes more antibacterial, especially against *S. aureus* (Ganasan et al., 2022, Erakovic et al., 2014).

Heat treatment of wood constituents impacts the chemical makeup and the overall mechanical capabilities of polymer-ridden timber matrices. It is capable of creating implants with dimensional stability and low moisture content. To determine the lifetime of such biopolymer implants, regular histometrical and histological evaluations are necessary. During postoperative radiological follow-up in a trial with birch wood-derived bone implants for rabbit femur bone regeneration, the trabecular bone region of the affected femur supported the implant via intracondylar implantation. In addition to birch wood, other researchers used beech, juniper, and ash wood for biomaterial-assisted bone healing (Rekola et al., 2009).

2B.3.4. Lignin composites with biological activity

2B.3.4.1. Antioxidant activity

Daily, biological systems produce reactive oxygen species (ROS) such as H_2O_2, superoxide ions, NO_3^-, NaClO, and OH due to various routine metabolic activities involving oxygen. These

toxic chemical entities are a severe threat to the proper functioning of cells and tissues, increasing the risk of developing life-threatening and debilitating health problems over time. When ROS affects the stable existence of biomolecules in cells, premature aging, cancer, type 2 diabetes, and autoimmune disorders start forming (Liguori et al., 2018).

By utilizing poly (butylene succinate) via hot-melt extrusion, researchers produced lignin-based composite materials with antioxidant potential (Domínguez-Robles et al., 2019). Previous studies have reported free radicals to be inhibited by lignin-carbohydrate complexes (LCCs) derived from poplar and bamboo. By up-regulating the antioxidant activity of the concerned enzymes, these complexes successfully scavenged reactive oxygen species (ROS) in both animal models (zebrafish) and *in vitro* (RAW 264.7 cells) (Dong et al., 2019). Lignin binds to PLA and castor oil to create customizable composites that can form fibrous interlocks when 3D printed. Following extrusion at 200°C, these composites achieve exceptional antioxidant and mechanical characteristics essential for biomedical and wound healing applications. An optimal mesh can accommodate up to 3% (w/w) lignin content in its filamentous PLA structure (Domnguez-Robles et al., 2019). Lignin-based biomaterials are also employed to counteract the onset of ROS-mediated hyperglycemia. The α-amylase activity of *Acacia nilotica* lignin-rich wood produced promising in vitro free radical scavenging results (Barapatre et al., 2015). In another study involving lignin-derived metabolic intervention for curbing hyperglycemia, lignosulfonic acid (LS) was able to non-competitively inhibit the activity of the intestinal α-glucosidase enzyme and lower the absorption of 2-deoxy-glucose by glucose transporters (Hasegawa et al., 2015). Lignophenols (LPs) have been shown to play a crucial role in the chemoprotective aspect of Streptozotocin-induced diabetic nephropathy and localized oxidative stress. LPs commit to this by increasing oxygen delivery to the damaged organ and combating the mechanisms that cause glomerular fibrosis and MCR-mRNA expression (Sato et al., 2009).

2B.3.4.2. Antimicrobial properties

Sepsis is one of the most common causes of death in the world. The systemic invasion of microbes triggers it; hence, keeping medical devices, pharmaceuticals, and consumer items free of infectious agents becomes a challenging task (Greenhalgh et al., 2019). The synergistic effect of various phenolic groups and benzene moieties in lignin nanoparticles leads to bactericidal properties (Zhang et al., 2019; Reshmy et al., 2022). Acacia wood lignin, combined with poly vinyl alcohol (PVA) and AgNF (silver nanofibers), generates 3D networks that are resistant to microbial diseases. In a standard agar well diffusion test, such scaffoldings were efficient against *B. circulans* (1.3 ± 0.08 cm) and *E. coli* (1.1 ± 0.05 cm). Nanofibrous mats like these can be found in specialized applications such as membrane filters, sterile textiles, and wound-healing dressings (Aadil et al., 2018).

The chitosan/LS nanoparticles are another fascinating lignin-featured combination that works effectively against *E. coli, S. aureus*, and *B. subtilis* unfavorable effects. The lignin portion was found to decimate the bacterial presence, as demonstrated by the turbidimetric test (Kim et al., 2013). Lee et al. successfully created a system based on Lignin/PVA composite networks with near-100% antibacterial efficacy against *S. aureus* and excellent UV shielding (UPF >50). PVA nanostructures containing lignin-decorated t-MWNTs (thin multi-walled nanotubes) inhibited the growth of *S. aureus* strains by 68.7% after 18 hours compared to PVA nanofibers, according to another study by the same research group. Such thermally stable reinforced nanofibers are excellent for initiating dermal wound healing (Lee et al., 2018).

Biocompatible silver-doped lignin mats (Silver/hydroxyapatite/lignin) with superior bactericidal capability against *Pseudomonas aeruginosa, S. aureus,* and *Candida famata* provide an industrial application for the development of implants requiring immunologically inert biofilms (Jankovi'c et al., 2015). Lignin nanoparticles (LNPs) can form multifunctional ternary systems with chitosan and PVA, thereby enhancing the antimicrobial and antioxidant

potential of the resulting composite hydrogels. Both 1 and 3-weight percent LNPs incorporated hydrogels exhibited antagonistic activity towards the growth of *S. aureus* 8325-4 and *E. coli* RB, allowing for their use in the packaging industry, wound healing fabrics, and targeted drug delivery systems. Moreover, LNP hydrogels synergistically improved the overall physical stability of the entire structure, making this versatile composite association a valuable addition to the pipeline (Yang et al., 2018). In a recent contribution, biomaterial featuring lignin/chitosan against *E. coli* and *Klebsiella* yielded a zone of inhibition of ~0.9 mm and ~1.1 mm for *E. coli* and *Klebsiella*, respectively (Jaganathan et al., 2018). The way the herpes simplex virus (HSV-1) undergoes inhibition by the nonsulfated cinnamic acid-derived lignopolymer ascertains the antiviral nature of lignin. The study found the overall efficacy of carboxylated lignopolymer to be 1000 times better at restricting the cellular entry of enveloped viruses than previous anti-HIV drug candidates.

Lignosulfonic acid inhibits the replication of the R5 and X4 virus types and HSV-2 through various cellular mechanisms, including blocking the gp120 viral protein from T cell adhesion and preventing CD4+ T cell bystander activation from already infected T cells. It is worth noting that this achievement was accomplished without compromising the efficacy of popular antivirals like acyclovir, LabyA1, or PRO2000 (Gordts et al., 2015). *Pimpinella anisum* has antiviral lignin-carbohydrate-protein complexes effective against common viruses infecting humans li HCMV, HSV-1, HSV-2, and measles. Upon treating these extracts with RAW 264.7 cells, they increased cytokine levels, as demonstrated by the increased IL-1 and IL-10 (Lee et al., 2011).

2B.3.4.3. Lignin composites for drug delivery systems

A subpar maize starch biofilm may be efficiently transformed into a very stable pH-dependent (inversely proportional) drug delivery system with better thermal and mechanical properties by adding 2 wt % hazelnut-derived lignin. In a traditional in vitro release assay that lasted ten

days, such thermoplastics successfully transported and delivered the standard antibiotic ciprofloxacin, with peak release occurring within 60 minutes. Lignin-graft-PDLA (LG-g-PDLA), a superior antioxidative and anticancer filler, improves the properties of an otherwise hostile environment created by PLLA nanocomposites for light-sensitive drugs like trans-resveratrol (t-RSV). The filler efficiently shields the drug from UV radiation after it forms a stereo complex and actively participates in the prolonged release of t-RSV, which can be fine-tuned by changing the filler content. LG-g-PDLA also improved the system's overall toughness and thermal stability (Liu et al., 2018).

2B.3.4.4. Lignin composites for wound healing

Wound dressing fabric influences how the injured region initiates and promotes healing. Currently, sterile garments and fibers such as cotton wool, gauze bandages, and various cotton composites meet the requirement. An optimal dressing material allows for proper ventilation, pain relief, the absorption of serosanguinous discharge from wounds, and the prevention of sepsis. Recent advances in lignin research aim to develop user-friendly biocompatible dressing materials that keep the wound hydrated while meeting other healing requirements (Ravishankar et al., 2019).

Physical cross-links involving ionic bonds from an inherently weak chitosan-PVA composite permit 3D scaffolds of lignin-based hydrogels capable of withstanding stress levels (up to 46.87 MPa) required to evade deformation due to tensile strain. Histomorphological analysis of murine wound models suggested accelerated regeneration and increased protein adsorption capacity. Other benefits of such hydrogels include improved antibacterial and antioxidative activities and the ability to condition wound sites by regulating biological factors for appropriate healing, making them suitable for wound dressing (Zhang et al., 2019). A biocompatible hydrogel made of chitosan and alkali lignin with substantial wound regeneration potential was mentioned in a recent study. The hydrogel responded remarkably well in a scratch

assay featuring mouse fibroblast cell lines (NIH 3T3). The bio composite was able to regulate cell migration which is imperative for wound healing (Ravishankar et al., 2019).

Bacterial cellulose dehydrogenase polymer, a biofilm made from microbial cellulose and lignin, was created to improve wound healing and reduce pain while preventing infection. The large swelling capacity and bactericidal activity are helpful for therapies that require sustained drug release, such as delayed wound healing (Zmejkoski et al., 2018). The same researchers had previously created a hydrogel (DHP-Alg) compatible with human epithelial cells and had antibacterial activity against *Staphylococcus aureus*, *Pseudomonas aeruginosa*, *Salmonella Typhimurium*, and *Listeria monocytogenes* strains. When blended in 1:2 (w/v) of DHP: Alg(alginate), the participating hydrogel exhibited good MICs or minimal inhibitory concentrations (0.002-0.90 mg/mL) and MBCs (0.004-1.25 mg/mL) (Spasojević et al., 2016).

2B.3.4.5. Lignin for disease prevention

Lignin is the major component of the medication $CDSO_3$, used to treat emphysema, a lung disease marked by ruptured alveoli and shortness of breath. Here, low molecular weight lignin (LMWLs) with sulfated caffeic acid moiety ameliorated the disease condition by down-regulating neutrophil elastase (an aberrant protein marker), oxidation, and inflammation. As a result, its efficacy as a biocompatible anti-emphysema agent with triple benefits was established beyond doubt. The flow of blood through arteries is affected by high cholesterol levels. The presence of total cholesterol in the blood increases the risk of life-threatening illnesses like myocardial infarction and stroke. Lignophenols reduce cholesterol levels by regulating oleic acid-induced apo-B lipoproteins produced by HepG2 cells (Norikura et al., 2010). The research reveals that LP interventions at the transcriptional and translational levels are responsible for the desired result (Saluja et al., 2013). The pharmaceutical applications of lignin are summarized in Table 2B.3.

Table 2B.3: Summary of the studies on the food applications of lignin

Product	**Usage**	**Feedstock lignin**	**Lignin Content (wt %)**	**Reaction/Process Condition**	**References**
Wood-derived products	Texture improvers, thickening agent, emulsion, foam stabilizers, reduce oxidation in food products	Kraft lignin	Up to 80%	Evaluation of 1- and 2-naphthol, formaldehyde (chemical additives) during hydrothermal pre-treatments of pine, birch, and willow wood followed by the incorporation of the residual hydrolysis lignin in polylactic acid (PLA)-based composites.	Aura, 2018
Wood-derived products	For baking muffins, to substitute whole eggs and egg yolks	VTT tested lignin	15 or 25%	By hot pressing from four different industrial sources	Gil-Chávez et al., 2019
Water-soluble lignin with a high anionic charge density	Stabilizer for oil (hexadecane) in water (O/W) emulsions	Water-soluble lignin	20 - 32%	Initially, lignin and tannic acid underwent both oxidation and transesterification reactions. Later, re-oxidized tannic acid afforded a ring-opened product that enhanced carboxylate group content and hydrophilicity of modified lignin.	Gharehkhani et al., 2018

Vanillin	Flavoring agent in foods and beverages	Lignin sulfonates or kraft lignin	N/A	Oxidation reaction was catalyzed with recycled copper catalyst.	Calvo-Flores et al., 2010
Polymeric amphiphiles	Stabilization of emulsions	Kraft and soda lignin	4 -5%	Reaction condition involves oxidation with recycled copper catalyst. Emulsions with various oils (including crude oils) can be formulated and their properties rationalized according to lignin surface activity as a function of pH and salinity.	Rojas et al., 2007
Paper-Based Oil Barrier Packaging	Holding commercially available cooking oils without leakage for over five months and excellent resistance to grease.	Lignin-containing cellulose nanofibrils	23%	The process involves a filtration technique that mimics the addition of material at the wet end of a paper machine. Thin films (16 g/m2) from lignin-containing cellulose nanofibrils and cellulose nanofibrils form on paper substrates. Further analyses reveal the surface, barrier and mechanical attributes of the samples.	Tayeb et al., 2020
Biopolymer-based packaging substance	Filler material in biopolymer-based packaging	Lignocellulosic biomass	15% to 25%	Valorisation of agri-food-industrial by-products	Sharma et al., 2020

Novel sago starch-based food packaging films	Good thermo mechanical properties, barrier properties, and seal strength with improved water resistance.	Lignin isolated from oil palm black liquor waste.	1, 2, 3, 4 and 5% v/w.	Prepared through casting method from sago palm (*Metroxylon sagu*) starch (in the form of film matrix with 30% w/w glycerol as plasticizer) by adding lignin isolated from oil palm black liquor waste (from empty fruit bunch), as a reinforcing material (1, 2, 3, 4 and 5% v/w).	Bhat et al., 2013
Plasticized starchy films	Modifying tensile resistance	Lignosulfonates	10%	Films were prepared from wheat starch and crude commercial lignosulfonates in the presence of glycerol, either by thermal moulding or by casting.	Baumberger et al., 1997
Lignin-containing coatings	Packaging materials	Kraft lignin	19-17%	Starch solution was added to the lignin solution, stirred at 100–300 rpm, followed by the addition of glycerol and AZC solution.	Javed et al., 2018
Lignin-containing cellulose nanofibrils (LCNF)	Packaging materials	Kraft lignin	N/A	Thin films (16 g/m^2) from LCNF and CNF were formed on paper substrates through filtration technique.	Tayeb et al., 2020

Lignin-containing cationic wood nanofiber (CWNF) films	Packaging materials	Unbleached spruce sawdust	28.6 wt%	CWNF films were fabricated using the solvent-casting method: CWNF suspension was diluted, sonicated for 10 minutes, poured on a polystyrene tray and stored at 50% relative humidity (RH).	Sirviö et al., 2020
Lignin esterified with TOFA	Barrier material in fiber-based packaging material	Softwood lignin		Lignin esterified with tall oil fatty acid (TOFA) and tested as barrier material in fiber-based packaging material.	Tamminen et al., 2014

Table 2B.4: Summary of the studies on the pharmaceutical applications of lignin

Product	**Usage**	**Feedstock lignin**	**Lignin Content (wt %)**	**Reaction/Process Condition**	**References**
Drug delivery hydrogels	Drug delivery systems	Kraft lignin	Up to 80%	Used micro-extruder at 120 °C for 2 or 5 min of recirculation and 20 to 200 wt % citric acid.	Farhat et al., 2017
PEG-lignin hydrogels	Medical material coatings based on their resistance to infection and the ability to release drugs over several days.	Klason lignin and acid soluble lignin	10% (w/w)	7.5 g of Ethanol/water (70% v/v) containing 10% (w/w) of LIG, 5% (w/w) of GAN and 5% (w/w) of GLY or PEG dried for 48 h, oven-dried at 80°C for 24 h and placed in an ethanol/water (70% v/v) solution for a week.	Larrañeta et al., 2018

SLS-g-P(AA-co-PVP) hydrogels	Deliver amoxicillin drug to the intestine.	Sodium Lignosulphonate	N/A	Involves free-radical polymerization- SLS and sodium hydrate mixing, followed by the addition of acrylic acid, PVP, NMBA and APS. The whole solution was stirred for an additional 30 min and transferred to an ultrasonic reactor.	Wang et al., 2016
Cellulose–lignin hydrogels	Controlled release of polyphenols by lignin.	Steam explosion lignin from aspen wood	N/A	Cross-linking reaction between cellulose in alkaline solution, lignin and epichlorohydrin for 8 h, at 80 °C.	Ciolacu et al., 2012
Microcrystalline cellulose hydrogel	Lignin controlled release of drug metronidazole.	N/A	6.3%	Hydrolysis of bleached cellulose fibers and unbleached brown fibers. The mechanical treatment after hydrolysis enables dispersal of the cellulose into gel-like material.	Dong et al., 2018
Collagen hydrogels	Lignin controlled release rate of the cancer drug doxorubicin	Alkali lignin	N/A	Promotes the formation of layer-by-layer films using tannic acid and lignin dipped into collagen hydrogel for 30 s and then washing twice in pH-adjusted distilled water for 15 s each.	Choi et al., 2016
Pectin and lignin hydrogels	Deliver β-glucuronidase and estrogens	Wheat stems lignin and oak lignin	5%	4% citrus pectin heated to 40°C, extruded into 100 mL of a 0.34 M aqueous CaCl2 solution and mixed with 2.5% lignin.	Borisenkov et al., 2015

Scaffolds of chitin-lignin	Support cellular activity, optimize tissue regeneration without eliciting any undesirable local or systemic response	N/A	N/A	Nanoscale lignin obtained by the solution-precipitation method was allowed to complex with chitin nanofibril.	Morganti et al., 2018
Scaffolds of Chitin/lignin/poly (glycerol sebacate)	Create hybrid nonwoven scaffolds.	Bio-lignin	0.1 wt %	chitin nanofibrils (30 wt%),bio-lignin, PEO (7wt%) mixed with (deionized water(62.9 wt %) to produce the sol-gel mixture followed by the mixing of sol-gel and PGS solutions via electrospinning.	Abudula et al., 2018
Lignin-based copolymer	Tissue engineering	Alkali lignin	10–30 wt%	Alkali lignin, ε-caprolactone, L-lactide, and tin(II) 2-ethylhexanoate were mixed, stirred (130 °C,24 h, N2atm), and cooled. Added chloroform and centrifuged to obtain supernatant which was then washed with ether/ methanol mixed solvent and dried(50 °C,24 h)	Kai et al., 2017
Polymeric scaffold fibers	Enhance the biological response of the cells with the	N/A	10 wt.% Lignin	Varying ratios (100, 95:5, 90:10, and 85:15) of lignin was added to the PCL solution containing 1 ml dichloromethane. The mixture was	Salami et al., 2017

	mechanical signals			stirred for 1 h, sonicated for 20 s, and applied into a 1-ml syringe of ELS. Desired scaffolds form on aluminium foil attached to the rotating drum.	
Scaffolds of PCL/lignin nanofibers	Promote cell proliferation of both BMSCs and Schwann cells, enhance myelin basic protein expressions of Schwann cells, stimulate neurite outgrowth of DRG neurons and exhibit antioxidant properties	Alkali lignin	N/A	After reacting ε-caprolactone (6 g) with Tin(II) 2-ethyl hexanoate (0.5 wt% of monomer as the catalyst) and purging with N2 for 30 min, the mixture underwent stirring at 130°C for 24 h. The resulting mixture was dissolved in chloroform, and the unreacted lignin was centrifuged at 5000 rpm for 5 min. The precipitate (lignin-PCL) was collected and dried in a vacuum oven at 50°C for 24 h.	Wang et al., 2018
Aerogels using alginate and lignin	Scaffolds for tissue engineering	N/A	N/A	0.5 mL of DHP in DMSO was added to sodium alginate (0.2 g) in 9.5 mL of distilled water. Further addition of 0.5% (w/ v) CaCl2 yielded the gel.	Quraishi et al., 2015

Lignin/hydroxyapatite and lignin/β-tricalcium phosphate systems	Bone tissue engineering	Brazilian wood biomass lignin	20% and 40%	HA and β-TCP were obtained by wet precipitation synthesis, dried at 110 ºC for 4h and mixed with lignin. The resulting mix was transformed into disks under pressure and sintered at 900ºC/1h.	Mansur et al., 2005
Lignin-agarose hydrogel	Higher mechanical properties than pure agarose gels	Kraft black liquor	5%	Chemical cross linking of 5%lignin and 5% agarose by 10 ml of epichlorohydrin	Sathawong et al., 2018
Lignin-chitosan microfibers	Influence mechanical properties	Alkali lignin	3%	Chitosan (0.15 g) was mixed with 10 ml of 1% acetic acid solution and was then stirred at 700 rpm for 4h. Further addition of lignin accompanied by stirring at 700rpm for 24hr and subsequent wet spinning technique facilitates fabrication.	Wang et al., 2016
(PLA)-lignin composites	Reduce crystallization of poly (lactic acid)	Kraft lignin	15%	PLA and lignin was dried (48 h, 40 °C), batches melt mixed with PLA in the micro-compounding system, extrude injection moulded	Anwer et al., 2015
PLA-lignin composites	Increase the tensile strength	Organosolv lignin from birch wood and Kraft lignin from softwood	7–15%	PLA pellets (50 ºC) and lignin (80 ºC) were dried, compounding procedure at 175 ºC for 10 min, 60 rpm, compression moulding, using a Carver press.	Spiridon et al., 2018

Hydroxyapatite/lignin composite coatings	Bioactive coating for titanium implants	Organosolv lignin	0.5–10%	Electrophoretic deposition of HAP/Lig and Ag/HAP/Lig coatings on Titanium-HAP/Lig and Ag/HAP/Lig suspensions via ultrasonication lasting 30 min. Titanium plate forms the working electrode with an EPD voltage range of 50 to 100 V and deposition time ranging from 30 s to 5 min.	Erakovic et al., 2014
Heat-treated birch wood	Osteoconductivity	N/A	N/A	The wood material was heated at 140 °C and 200 °C under normal atmospheric pressure for 2h.	Rekola et al., 2009
Lignin\PBS composites	Antibacterial and antioxidant properties	kraft lignin	up to 15% w/w	Employed brabender plastograph internal mixing machine for adding lignin to PBS matrix at 150 °C, 80 rpm and 10 min. The mixture was cooled, milled using a blade mill and stored.	Domínguez-Robles et al., 2019
Lignin-carbohydrate complexes	Prevent the reduction of antioxidant enzyme activity.	LCC from bamboo and poplar	44.1%-47.8%	RAW 264.7 cells were co-incubated with ROS fluorescent probe for 30 min after adding 50 μg/mL LCCs-Bjorkman solution and 100 μmol/L of H_2O_2. Evaluation of ROS was achieved by the Flow cytometry technique.	Dong et al., 2019

3D printed meshes	Wound healing	Kraft lignin	0.5 to 3%	Vortexed PLA pellets (40 g) and castor oil (40 µL) before adding and vortexing lignin and tetracycline powder. Allows for the extrusion of filaments, discs and squares and 3D-printed using Ultimaker 3FFF system.	Domínguez-Robles et al., 2019
Alkali lignin	To act against hyperglycemia	Alkali lignin	N/A	Alkali lignin extraction and microbial biotransformation by ligninolytic fungus.	Barapatre et al., 2015
Lignosulfonic acid	Suppress the rise in blood glucose level	N/A	N/A	LS acid was added to 0.2 U/ml alpha-glucosidase in 50 mM PBS and incubated for 30 min at 25°C. Added PNP Gluc solution followed by Na_2CO_3 to terminate the reaction.	Hasegawa et al., 2015
Lignophenols	Excess oxidative stress, infiltration and activation of macrophages and glomerular expansion in STZ-induced diabetic kidneys	N/A	N/A	The LPs were mixed with a standard commercial laboratory diet and provided to diabetic rats	Sato et al., 2009
PVA/Acacia wood lignin/silver nanofibers	Act against *B. circulans* and *E. coli*	Acacia wood lignin	1 wt%	PVA and lignin were blended in a 9:1 ratio in 10 mL of methanol: water (60:40) and stirred for 2 h.	Aadil et al., 2018

				Stirred again after adding silver nanoparticles and then sonicated.	
Chitosan/lignosulfonates nanoparticles	Antagonist for *S. aureus*, *E. coli* and *B. subtilis*	Hardwood lignin	N/A	Sonochemical formation of particles by incorporation of CS and LS solutions, 30 mL and 15 mL, respectively, in the presence of 5 mL of the organic phase (vegetal oil).	Kim et al., 2013
Lignin/(PVA) nanocomposite fibers	99.9% reduction rate against *S.aureus,* excellent UV protection	Alkali lignin	50 and 85 wt%	The lignin/PVA solutions was stirred at 80^0C for 6 h and then electrospun under various spinning conditions.	Lee et al., 2019
Lignin/decorated thin multi-walled carbon nanotubes in poly(vinylalcohol) nanocomposites	68.7% bacterial growth decrease of *S. aureus*	N/A	N/A	tMWNTs were synthesized via chemical vapor deposition (CVD) method and was added to lignin solutions and subjected to sonication.	Lee et al., 2018
Silver/hydroxyapatite/lignin thin films	Act against the microbial colonization of *S. aureus, P. aeruginosa* and *C. famata*	Organosolv Lignin	1 % w/v	Ag: HA powders (10 % w/v) and Lig (1 % w/v) were dissolved in distilled water, vortexed and flash-frozen in a liquid nitrogen-cooled copper container. Later, it was mounted on a cryogenic holder, rotated at 10 rpm and irradiated with a laser beam.	Jankovi´c et al., 2015
Gelatin/lignin films	inhibitors for *B. subtilis*			H-bonding between gelatin-lignin via cholinium citrate.	Mehta et al., 2019

Polyvinyl alcohol/lignin/chitosan hydrogels	Greater than 95% cell reduction in *E. coli* and greater than 85% in *S. aureus*	Pristine lignin	1 and 3%	PVA was diluted in deionized water at 20% (wt/v) under magnetic stirring at 90 °C for 4 h. An aqueous dispersion of LNPs was added and sonicated for 5 min at 40 % amplitude. Chitosan was dissolved in water containing glacial acetic acid (1% v/v) under magnetic stirring at 40 °C for 12 h and was mixed with PVA/LNPs solution.	Yang et al., 2018
Polylactide/silver/lignin nanoparticles	100% cell reduction of *L. monocytogenes*	Organosolv lignin	40 mg	PLA (4 g) was added to the AgNPs solution and stirred continuously at 22±2 °C for 48 h. The mix was cast onto a Teflon film-coated glass plate, dried, and then conditioned in a humidity chamber.	Shankar et al., 2018
Artocarpus heterophyllus peel lignin/chitosan Biocomposites	Inhibition zone for *E. coli* and *Klebsiella*	*Artocarpus heterophyllus* peel lignin	1%,3%,5 %	Lignin was added to chitosan medium (15 mg in 10 ml of 1% acetic acid), sonicated at 100 W for 5 h and fabricated via freezing drying methods.	Jaganathan et al., 2018

Carboxylated lignin polymer	Act as an antagonist to HIV-1, dengue, Kaposi's sarcoma-associated herpes virus, and hepatitis C virus.	Caffeic acid and ferulic acid lignin	N/A	Caffeic/ferulic acid and H2O2 were added to 50 mL of 10 mg HRP in 10 mM sodium phosphate buffer at pH 8 for 5h.	Thakkar et al., 2010
Lignosulfonic acid	Anti-HIV and anti-HSV activity	N/A	2.5%	Mice exposed to HSV-2 G suspension were treated with 50 µl of 2.5% LA, 5% acyclovir, 1% tenofovir for 5 days.	Gordts et al., 2015
Lignin-Carbohydrate-Protein Complexes	Antiviral activity against herpes simplex virus type1 and type 2, human cytomegalovirus (HCMV) and measles virus	*Pimpinella anisum* lignin		HSV-2 suspension and precooled (3hr) LCC were mixed at 40C, washed with PBS wash (3 times) before diluting (10-fold PBS) the cell pellet. Finally, added vero cell monolayers (35mm dish) and performed a plaque assay.	Lee et al., 2011
Lignin– starch biodegradable films	Release of Ciprofloxacin	Alkali lignin	1.2, 1.6, 2.0 and 2.4wt%	Starch and lignin were added to 20 mL water (constant stirring at 100°C) containing 0.5 mL glycerol as a plasticizer and heated for 5min. Dried biofilms were placed in vials containing 15 mL of Ciprofloxacin (172 mg/L) for 72 h at 208°C and dried at 408°C	Çalgeris et al., 2012

Drug-loaded poly(L-lactide)/lignin stereocomplex film	Release of trans - resveratrol	Alkaline lignin	10% (w/w)	PLLA and LG-g-PDLA were dissolved in chloroform, sonicated for 5 min and trans-RSV acetone solution appended. The mixture was poured onto a smooth and framed PTFE plate and kept in a 40 °C vacuum.	Liu et al., 2018
Banana-chitosan film	Wound healing	N/A	N/A	Chitosan powder was dissolved in 2% acetic acid solution and stirred for 4 hours with 1 ml glycerol as a plasticizer. Mixed with banana peel powder, dried at 40°C for 24 h followed by another drying at 40°C for 4 h.	Rihayat et al., 2019
Lignin–chitosan–PVA composite hydrogel	Wound healing	Sulfite papermaking pulp lignin	10 wt%	Chitosan dissolved in acetic acid solution (500 rpm for 5 h), PVA dissolved into water (90 °C,6 h) and lignin dissolved into deionized water (500 rpm ,5 h). The solution was mixed (1000 rpm, 5 h) and frozen at −18 °C for 8 h.	Zhang et al., 2019
Chitosan-alkali lignin hydrogel	Wound healing	Alkali lignin	10%	Hydrogels and crosslinked films of chitosan and alkali lignin obtained by ionotropic cross-linking.	Ravishankar et al., 2019
Bacteria cellulose and lignin model polymer (BCDHP)	Wound healing		N/A	DHP synthesis by the action of CA, H2O2, and horseradish peroxidase prepared in phosphate	Zmejkoski et al., 2018

				buffer(pH 7.3). DHP was centrifuged and washed in double-distilled water. Finally, the precipitate was air-dried and dissolved in a 5% dimethyl sulfoxide (DMSO) water solution.	
DHP-alginate hydrogel	Wound healing		1% (w/v)	DHP in DMSO solution and sodium alginate solution were mixed and CaCl2 0.5% w/ v was added.	Spasojević et al., 2016
Unsulfated or sulfated low molecular weight lignins	Therapeutic use in emphysema	Caffeic acid, ferulic acid or sinapic acid	N/A	LMWLs were synthesized chemoenzymatically from three 4-hydroxycinnamic acids.	Saluja et al., 2013
Lignophenols	Regulation of apo-B secretion, decreases cellular total cholesterol	Native lignin from Japanese cedar	N/A	Phase-separation system consisting of cresol and sulfuric acid.	Norikura et al., 2010

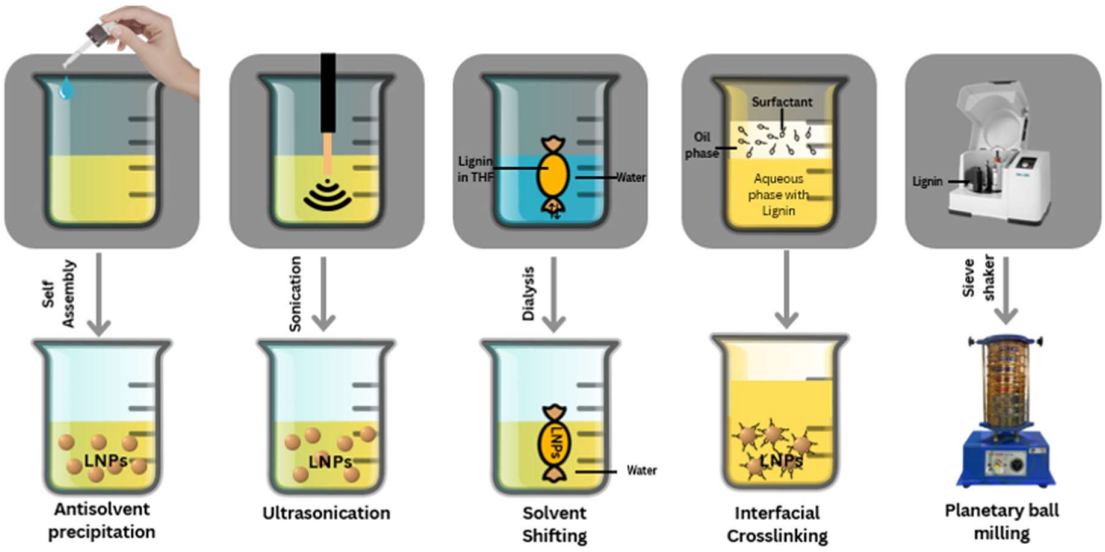

Fig. 2B.3. Nanolignin Preparations method

2B.4. Recent trends in lignin research: Nanolignin

2B.4.1. The rationale for nanolignin preparation

The most attractive features of lignocellulosic residues are their eco-friendliness, availability, and inherent bioactive characteristics. By harnessing the powers of nanotechnology, nanolignin has the potential to drive future nano-based medical interventions, diagnostics, and food sectors. Environmental and nanotechnology research is gaining traction due to the constant development of recyclable lignin-containing biomass. Several scientific improvements and patents relevant to enhanced lignin use, particularly in nano lignin-based products, have been made in the last decade (Dey et al., 2022). Nanolignin preparation methods showing in Fig. 2B.3.

A comparison of lignin and nanolignin is described in Table 2B.5. The following section discusses the available methods to synthesize nanolignin from native lignin.

Table 2B.5: Comparison of typical lignin and nanolignin

Properties	**Normal lignin**	**Nanolignin**	**Source**
Mechanical properties	Good mechanical properties	**Advantages:** Improved stiffness, strength, toughness, thermal stability and barrier properties. Performs better in comparison to traditional composites due to the higher specific surface of the nanofillers.	Cai et al., 2008
UV blocking	Better UV blocking property due to phenolic, ketone and other chromophores	**Advantages:** 30% increase in UV protective activity Exhibits a broader absorption band in the longer wavelength region and shows a shoulder towards the longer wavelength region SPF value of the sunscreens increases with decreasing size of lignin colloidal spheres.	Li et al., 2016
Antimicrobial property	Successful antimicrobial properties against various microorganisms due to the polyphenolic compounds of lignin	**Advantages:**Increased antimicrobial effect due to huge surface area, more functional and polyphenolic sidechains on their surface, and increased contact area.	Nada et al., 1989
Radical-scavenging capacity, reducing power, and superoxide radical scavenging activity.	Effective free-radical scavenger, capable of reducing oxygen radicals, retard and inhibit oxidation reactions	**Advantages:** Nanoscale polar OS lignin has improved radical-scavenging capacity, reducing power, superoxide radical scavenging activity and water solubility than non-nano scale lignin.	Dizhbite et al., 2004
Pickering emulsion	Under acidic conditions at pH 4, lignin forms particles with an average size of 182 nm. These particles form a Pickering emulsion.	**Advantages:** Nanoparticles grafted with surface-active polymer chains can decrease surface and interfacial tensions and create stable Pickering emulsions.	Wei et al., 2012

Carbonized lignin nanofibers	Produced carbon fibers from commercially available Kraft lignin.	**Advantages:** Increased tensile strength and modulus of carbon fibers were observed with decreasing fiber diameter.	Kadla et al., 2002
Adsorption capacity	Lignin-derived adsorbing materials exhibited relatively low adsorption capacity and poor affinity for specific heavy metal ions due to small surface areas (large size) and lack of functionalities. For example, 31.6 mg/g was the adsorption capacity of alkaline lignin for Cr(VI).	**Advantages:** Excellent adsorption capability toward different kinds of heavy metal ions Ex: lignin-based nano-trap (LBNT). LBNT is expected to possess reduced particle size for enhancing diffusion and contacting frequency, strong metal binding groups on the surface affordable to different kinds of heavy metal ions with excellent adsorption capability, and the surface-dispersed binding sites in control of loading heavy metal ions facilitating further multiple use.	Albadarin et al., 2011

2B.4.1.1. Nanolignin from mechanical processes

The milling process is one of the most widely used methods for synthesizing nanolignins from plant sources. It is a cost-effective technique for obtaining lignins with nanomolecular particle sizes (Sharma and Kumar, 2020). For example, homogenizing 5 g/L kraft lignin at 15 K rpm for 4 hours yields 500 nm kraft lignin-derived nanolignin. Furthermore, a sonication-based acoustic approach produces stable 10-20 nm nanolignin with a uniform dispersion of 0.7% lignin suspension derived from wheat straw and Sarkanda grass. 20 kHz sound waves and 600 W input for an hour in a homogenous stable nanodispersion of size 10-20 nm are ideal circumstances for such nanoscale formation without free radicals (Gilca et al., 2015).

2B.4.1.2. Nanolignin from solvent shifting method

Under the effect of polarity considerations of the involved lignin substrates, a strictly regulated solvent shift approach can produce mid-sized nanolignins despite their low yield. Dimethyl sulfoxide, acetone/water, tetrahydrofuran, and acetone are the chosen solvents for this procedure (Sharma and Kumar, 2020). Using tetrahydrofuran and water, the solvent-shifting approach produced small nanolignin with a particle size of 221 ± 10 nm, whereas kraft lignin created lignin nanoparticles with a 200-500 nm size (Figueiredo et al., 2017).

2B.4.1.3. Nanolignin from pH shifting technique

Stable nanostructures with densely arranged lignin moieties form by precipitating extremely porous lignin nanoparticles by shifting the pH. Such stable nanoparticles are the result of two independent stages. The first attempt features Indulin AT in ethylene glycol solution followed by adding aqueous HCl. The second method uses a mixture of lignin and aqueous sodium hydroxide, which produces the required precipitates when combined with HNO_3. The first approach yielded pH stable (1-9) biodegradable nanoparticles. The second method produced environmentally safe nanolignins that are stable below pH 5. Lignin sourced nanostructures do not affect the growth of model microorganisms such as *Chlamydomonas reinhardtii* and *Saccharomyces cerevisiae*, ensuring cell viability (Sharma and Kumar, 2020).

2B.4.1.4. Nanolignin from template-based synthesis technique

Caicedo et al. used template synthesis to create lignin-derived nanomaterials. The process is initiated by Schiff's base reaction between the aldehyde groups of thioglycolate lignin and their amino counterparts in the activated alumina membrane (APTES). Polymerization starts after adding hydroxycinnamaldehydes, hydroxycinnamates, or hydroxycinnamyl alcohols in the presence of appropriate catalysts such as HRP (horseradish peroxidase) and H_2O_2. As a result, nanotubes with 15 nm thick walls and nanowires with a 200 nm inner diameter form. These nanomaterials can also be bio-functionalized after being placed on the lignin base layer.

(Caicedo et al., 2012). Reductant-mediated template synthesis of lignin molecules affords uniformly dispersed 45-55 nm pseudo spherical silver nanoparticles with antimicrobial activity. Although template synthesis has various advantages, it is also responsible for the toxicity factor of surfactants such as SDS and CTAB. Other limiting factors that undermine the overall effectiveness of this method are issues related to purification and the removability of source materials (Sharma and Kumar, 2020).

2B.4.1.5. Nanolignin from ice-segregation-induced self-assembly method

Initially, a monomer unit-containing solution is frozen (Sharma and Kumar, 2020). As a result of this process, ice crystals form, which continue to develop and segregate the polymer phase. Under the effect of a revolving drum (300 rpm) and liquid nitrogen (77 K) as a coolant, homogenous lignin nanofiber scaffolds form with alkali lignin as the source material (Spender et al., 2012).

2B.4.1.6. Nanolignin from aerosol process

Using an atomizer, this approach creates a continuous loop of aerosol. After passing through a heating tube, the aerosol is captured by a low-pressure impactor, which collects the sorted fractions of the required nanoparticle. This highly reproducible one-step method accurately assembles dried nanoparticles based on size and shape. This approach helps produce lignin nanoparticles with particle sizes ranging from 30 to 200 nanometers (Sharma and Kumar, 2020).

2B.4.1.7. Nanolignin from electrospinning method

The electrospinning method requires a polymer solution as a starting material for nanolignin formation. The mixture can travel through a 100 m wide nozzle that acts as an electrode/auxiliary electrode system after being mixed with an appropriate solvent. For nanolignin production using the electrospinning process, the desired E-field level is 100-500 kV/m (Sharma and Kumar, 2020).

2B.4.1.8. Nanolignin from supercritical fluid processes

Nanolignin synthesis with supercritical fluids like CO_2 is beneficial since it is inexpensive, non-flammable, and non-toxic (Sharma and Kumar, 2020). CO_2 also has a favorable critical temperature and pressure of 304.3 K and 7.4 MPs, making it an ideal choice for supercritical fluid-mediated processes. Fine lignin nanoparticles of 144 nm are formed by reacting CO_2 and acetone with lignin at 30 MPs and 35 °C. The compressed CO_2 antisolvent Technique can make environmentally friendly LNPs (Myint et al., 2016). The process starts by pumping CO_2 to a cooler kept at 258.2 K and then transferring it to the precipitator, where it gets liquefied. Following the stabilization of the precipitating unit, lignin solution was added to the obtained lignin nanoparticles after weighing. The resulting mixture was subjected to sonication for half an hour at room temperature and sprayed via a nozzle dictated by flow rate presets. The particles that make it to the filter paper are collected. CO_2 immiscible compounds are not suitable for this Technique (Sharma and Kumar, 2020).

2B.4.1.9. Nanolignin from solvent antisolvent precipitation

The slow addition of a prepared lignin solution to an antisolvent such as water is used in this procedure. Polarity of antisolvent differs from that of the organic solvent used to dissolve lignin before antisolvent treatment. Water is a popular antisolvent because lignin is immiscible or sparingly soluble (Sharma and Kumar, 2020). In one work, both soft (alkali lignin) and hardwood (dioxin lignin) lignins were treated with the antisolvent precipitation approach to produce 80 to 104 nm lignin particles (ALNP and DLNP) with strong UV shielding and radical scavenging properties. For this, the contributors employed acetone and water with constant stirring (300 rpm) at 20°C (Yearla and Padmasree, 2016). The Technique's drawbacks include the colloid system's instability, the shape of the formed nanoparticles, and the solvents' irremovable nature (Sharma and Kumar, 2020).

2B.4.1.10. Nanolignin from acoustic cavitation assisted nanoparticles preparation

Gilca et al. prepared stable lignin nanoparticles from lignin (0.7%) suspension by taking advantage of this method. The aqueous solution was then subjected to acoustic treatment via an ultrasonic probe outputting a 20 KHz frequency at 600 W for an hour. The resulting uniform nanosuspension was allowed to dry under mild conditions (Gilca et al., 2015).

2B.4.1.11. Nanolignin from SERSL

Steam exploded rice straw lignin (SERSL) is an alternative source for the synthesis of LNPs. Initially, castor oil (20 wt.%) and SERSL solution mixture underwent stirring to afford a homogenous solution. By maintaining a nitrogen setting, 20 mL HCl (1 M) was introduced in drops at 50°C for 4 h. Nascent lignin nanoparticles formed were subjected to thorough washing with water and ethanol until a pH of 7 was reached (Rahman et al., 2018).

2B.4.1.12. Nanolignin from green synthesis process

The use of precursor materials (kraft lignin and organosolv) in a unique technique for manufacturing LNPs resulted in nanoparticles with diameters ranging from 45 to 250 nm. Kraft (Indulin AT) guided synthesis begins when a solution of 0.25 g kraft in 50 mL ethylene glycol is vortexed (30 min) and filtered through a 0.45 μm pore size syringe filter. Particles emerge after quickly adding 1-3 mL of 0.025 M nitric acid to 5 mL of the filtered solution in a scintillation vial with continual shaking. The acetone/organosolv stock solution (0.25 organosolv in 50 mL acetone) was subjected to the same initial vortexing and filtration stages in the second approach. Finally, supersaturated lignin was phase-separated into LNPs by adding 9.2 mL water to a 1 mL filtrate solution (Richter et al., 2016).

2B.4.1.13. Nanolignin from hydroxymethylation

Popa et al. demonstrated the role of hydroxymethylation in the synthesis of lignin nanoparticles in a study. Initially, 10 g of lignin derived from wheat straw and Sarkanda grass produced lignin suspension in water (47 mL) upon stirring continuously at room temperature for 120 min. The

resulting lignin dispersion was then treated with a 50% solution containing 1.29 g sodium hydroxide and a 25% solution containing 3.14 g ammonium hydroxide while mechanically shaken for 2 hours (for catalysis). A 37% solution containing 6.7 g formaldehyde was allowed to react for 4 hours in the next phase, kept at 85ºC. Next, a recovery stage with 1 N HCl (pH 2) yielded a precipitate, centrifuged to obtain a solid phase. The portion was washed twice with water and dried to obtain LNPs (Popa et al., 2011).

2B.4.1.14. Nanolignin from wheat pulping black liquor

This method is suitable for transforming non-uniform clusters of lignin-derived polymers into uniformly distributed spherical colloidal nanoparticles. In one such study, pulping black liquor formed the source of alkali lignin, which was then purified and acetylated. For that, acetylated lignin-tetrahydrofuran (ACL–THF) solution (1 mg/mL) was prepared by adding tetrahydrofuran to the solution followed by water. The hydrophobic nature of acetylated lignin molecules in the ACL-THF solution started to promote the formation of colloids, as evidenced by the sudden rise in the scattered light intensity of the solution. The critical water content of 44 vol % facilitated the formation of spherical colloids (Qian et al., 2014).

2B.4.1.15. Nanolignin from supercritical antisolvent technology

The supercritical antisolvent approach is a viable way to produce lignin-based nanoparticles from rugose wood elements. It comprises a combination of techniques, including precipitation, dissolution, centrifugation, and CO_2 supercritical equipment. They used carbonic acid as the antisolvent of choice in the patented technology for producing industrial-grade xylogen NPs.

2B.4.1.16. Nanolignin from chemomechanical methods

This patented chemo-mechanical process enabled the synthesis of size-controlled xylogen nanoparticles with a particle size of up to 26 nm. The procedure begins with alkali treatment of the extract, followed by grinding to a particle size of less than 0.2 mm and freeze-drying the colloid sol to obtain xylogen NPs with an average particle size of 30 nm (Zhiming et al., 2013).

2B.4.1.17. Nanolignin from self-assembly

When used as fillers in natural rubber, stable lignin nanoparticles of 100 nm made from industrial sulfate lignin accelerated vulcanization. Colloidal LPCs were mixed with a 2% poly (diallyl dimethylammonium chloride) (PDADMAC) solution in an alkaline pH to make these electrostatically assembled NR/LPCs (Natural Rubber/ Lignin-Poly (diallyl dimethylammonium chloride) (PDADMAC) complexes (LPCs) composites (pH 12). The obtained solution was coprecipitated with H_2SO_4 (pH 2), yielding a mixture. Filtering, washing, and vacuum drying at 50°C culminate in fabricating the NR/LPCs nanocomposites (Jiang et al., 2013).

2B.4.2. Applications of nanolignin

Despite lignin's universal abundance, it is seldom considered for high-end applications. Because of their particle size and surface area, biopolymers such as lignin exhibit remarkable physical and chemical properties. Large and highly complex compounds like lignin can be broken down to nanoscale levels. Nanolignin has the advantage of being mechanically and thermally stable particles with superior antioxidant, bactericidal, UV shielding, and stabilizing capabilities than native lignin molecules. By valorizing the input feedstock, nanometric lignin particles can leverage the biorefining sector (Ponnusamy et al., 2019; Akbarian et al., 2022). The following section discusses the application of nanoscale lignin in different aspects (Fig. 2B.4).

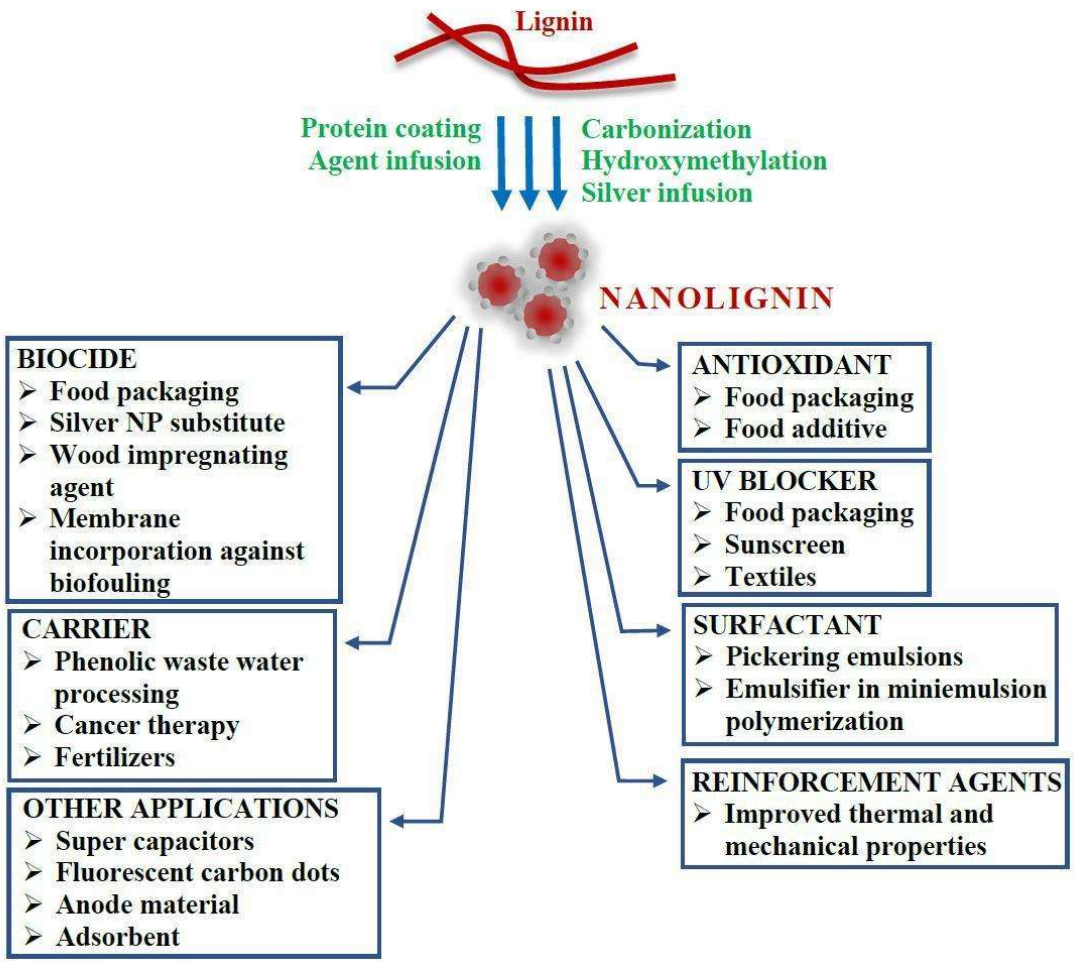

Fig. 2B.4. Applications of nanolignin

2B.4.2.1. Food packaging

The biggest challenge faced by the food packaging industry is the lack of low-cost, biodegradable packaging with antimicrobial properties. Since impending contamination hazards threaten each packaging stage, the development of nanometric kraft lignin labeled with silver NPs could be one such solution. For this, Indulin AT was precipitated by pH shifting and treated with Ag-NPs in an aqueous $AgNO_3$ solution. These silver-tagged lignin NPs were able to efficiently neutralize both gram-negative and gram-positive food-borne pathogens (Richter et al., 2015).

Yang's team contributed to the industry by developing a three-component polymeric covering that had shown significant action against *Pseudomonas syringae* pv. tomato (Pst), a plant

pathogen. LNPs and cellulose nanocrystals were deposited on PLA with and without a glycidyl methacrylate (GMA) graft using a melt extrusion method. The reinforced PLA biofilm (1 and 3 wt% of lignin) also exhibited good UV protection and nucleation. By incorporating chitosan in the skeleton, the same group executed solvent casting with binary and ternary coatings. As a result, PVA/CH/LNP nanocomposites could suppress *Erwinia carotovora* subsp. *carotovora* and *Xanthomonas arboricola pv. Pruni*. These encouraging findings highlight the efficacy and use of lignin nanoparticles as a safe and low-cost food packaging option (Yang et al., 2016).

2B.4.2.2. Nanolignin as a radical scavenger/antioxidant.

LNPs impart antioxidant functionality to systems courtesy of functional groups and inherent complexity. These factors promote hydrogen donation, an antagonist of oxidation and free radical formation (Chauhan, 2019). The antioxidant and radical scavenging potential of nanometric lignin composites are one of the most sought-after entities in the present-day food, pharma, and cosmetic industries. Lu et al. employed acetone as a solvent and supercritical CO_2 as an antisolvent. Upon estimation, the reducing power and radical scavenging potential of the nanolignins showed improvements (Lu et al., 2012).

Transparent polymeric composite structures of PLA-fused LNPs with strong antioxidant properties were recently described (Tian et al., 2017). In an investigation, dioxane lignin nanoparticles (DLNP) and alkali lignin nanoparticles (ALNP) were effective in protecting E. coli against radiation-induced death. Compared to the control, nano lignin production using an alkaline solution precipitation approach had a 3.3 times greater free radical scavenging capability. The nanolignin's bioavailability, smaller dimensions, and larger surface area are most likely to have contributed to the nanolignin's potency (Yearla and Padmasree, 2016).

2B.4.2.3. Nanolignin as a carrier

Biocompatible substrates like lignin, both at micron and sub-micron levels) with low immunogenicity are used for a targeted treatment regime. Capsular, hollow, and porous forms, and solid structures with pores, are two types of lignin nanocarriers (Akbarian et al., 2022).

A lignosulfonate capsule with hollow porous structures carrying hydrophobic bioactive molecules, such as coumarin-6, is an example of a pH-sensitive nanometric drug carrier. Embedding β-thiopropionate (acid-labile functionality) on the shell surface enables drug delivery to the target site in response to a matching pH. These acoustically synthesized capsular carriers with allyl-grafts typically have a 50-300 nm diameter range and are formed in an oil-in-water emulsion system (Chen et al., 2016). Tortora et al. explored the production of coumarin-6 microcapsular carriers generated from kraft lignin. 0.3 to 1.1 μm sized microcapsules can be produced by a high-frequency acoustic-driven synthesis of oil-laden lignin microcapsules at the water/oil portion of oil in water emulsion. Furthermore, after internalization into hamster ovary cells, this method showed low immunogenicity and toxicity (Tortora et al., 2014). The release patterns of coumarin were similar in both cases. When loaded with bioactive supplements like polyphenols and essential oils, these nanocapsules have the potential to cure skin-related ailments (Akbarian et al., 2022).

Yiamsawas et al. developed stable lignin-derived nanocapsules of 150-200 nm diameter at the water-cyclohexane interface. Reduced cross-linking agent (lignosulfonic acid), enzyme degradation, increased temperature, and inversely proportional pH levels improved the release rates of the resulting nanocarriers. The same authors also describe an effective 2-propylpyridine-loaded kraft lignin-derived nanocapsules possessing an oil phase and lignin core (Yiamsawas et al., 2017).

Cytotoxicity of carbon nanotubes to living cells restricts their application in the human body. The ability of biocompatible lignin nanotubes to transfect HeLa cells after DNA adsorption makes them an appropriate solution to this problem. In a study comparing the cytotoxicity of

both nanostructures on HeLa cells, lignin nanotubes exhibited a tolerance threshold ten times higher than carbon nanotubes. Recently, self-assembled micelles of lignin (SLRM) origin that encapsulated horseradish peroxidase (HRP) enzyme inside its hydrophilic core exhibited improved enzymatic activity upon immobilization. The SLRM core structure boosts HRP's overall activity, enabling bioremediation of phenol-contaminated wastewater at pH4 (Zhong et al., 2016). Reusable colloidal cationic lignin nanospheres enable ester synthesis by helping to attach entrapped hydrolases onto the platform (Sipponen et al., 2018). The pH of the medium impacts the stability of novel biocompatible LNPs encapsulating water-soluble Rhodamine 6G. Green synthesis of nanoparticles utilizing a hydrotropic solution includes self-assembling LNPs made of aqueous sodium p-toluene sulfonate. These nanoparticles demonstrated a long-term drug release profile while encapsulating hydrophobic molecules with 90% efficiency (Chen et al., 2018).

2B.4.2.4. Solid and porous particles/structures

The use of novel bionanomaterials and nanocarriers is important in the fight against neoplasm. Shortcomings of conventional and targeted cancer therapies lie in the mode of delivery of the proposed drug. LNPs tasked to encapsulate test compounds against cancer must preserve the target medication from premature degradation and allow for ligand-assisted tumor penetration. Modifying LNPs with targeting entities help to attain enhanced cellular interaction during the treatment. Various cell lines treated with complex spherical LNPs containing iron molecules (Fe-LNPs and Fe_3O_4-LNPs) exhibited low polydispersity, low toxicity, insignificant in vitro hemolysis, and H_2O_2 generation at a stable pH of 7.4. Also, BZL (benzazulenein) cancer cell lines' cytotoxic effect was boosted by pure lignin nanoparticles (Figueiredo et al., 2017). The use of magnetic Resveratrol (RSV)-loaded lignin nanoparticles (AL/RSV/Fe3O4 NPs) in cytological and animal experiments was a success against proliferating cancer cells. The work focused on creating green chemistry-based self-assembled AL-based unmodified lignin

nanocomposites. The magnetic drug-loaded delivery method improved long-term drug release, allowing optimal drug accumulation and tumor shrinkage (Dai et al., 2017). The overall performance of these innovative technologies makes it possible to test them in real-world circumstances.

2B.4.2.5. Nanolignin for oral disease and tissue regeneration

As a virus-inhibiting agent, solubilized nanolignin in the form of [125I]-labeled LCC (lignin carbohydrate complex) has medical potential (Sakagami et al., 2017). A recent study examined the effect of combining electropositive chitin nanofibrils (CN) with LNPs. The bactericidal and anti-inflammatory capabilities of the formed CN-LG particles (163 nm) possessed a wide range of industrial and medicinal applications, including skin-related disorders. CN-LG matrix helps tissue regeneration by establishing a barrier against microbial proliferation at the wound site, in addition to being a chemoattractant. Also, these compounds can be administered to in vitro cultures of human keratinocytes and human mesenchymal stromal cells for potential use in skin contact applications (Danti et al., 2019).

2B.4.2.6. Nanolignin as a UV blocker

Lignin is an excellent candidate for a sun blocker ingredient in some lignin-derived sunscreens since it is non-oxidizable. The addition of LNPs enhanced the native SPF value of plain creams significantly (1.03 versus 1.26-2.23 for amalgamations) (Chauhan, 2019). In another study, when exposed to 400 nm light, a transparent PLA-tagged LNP matrix containing 4 wt% LNPs offered UV protection of up to 80%. (Tian et al., 2017). Value-addition of sunscreens with photoprotective LNPs/ZnO sourced from Agave tequilana enhanced the SPF value of the sunscreen as evidenced by the extent of blocking of UV-B and UV-C rays (Hernandez et al., 2016). The poly (butylene adipate-coterephthalate) (PBAT) matrix forms biofilms with improved mechanical and thermal stability when combined with various LNP combinations of melanin core-shell nanoparticles (MNP) and lignin-melanin core-shell nanoparticles (LMNP).

Poly(butylene adipate-coterephthalate) (PBAT) matrix associates with various LNP combinations of melanin core-shell nanoparticles (MNP) and lignin−melanin core−shell nanoparticles (LMNP) to form biofilms with enhanced mechanical and thermal stability. Also, they absorbed more than 80% of incoming UV-B rays when NPs concentrations ranged between 0.5 -5.0 wt% (Xing et al., 2019). A study dedicated to investigating the effect of the development of sunscreens with lignin and lignin-based colloidal micelles of different shapes and sizes revealed that of all blend types, sunscreen with colloidal spheres exhibited the most protection owing to the presence of phenolic groups in lignin molecules.

Although UV-absorbing clothes containing LNPs are rare, they protect from damaging UV rays without impairing the fabric's basic texture. A study found that nanolignins with silicone emulsion offered the garments antibacterial and antistatic properties. Such application-level initiatives could lead to the development of fabrics that protect wearers from more challenging environmental threats like viruses and fungi in the future. The role of nanolignins as a versatile finish agent is detailed in a study that used lignin obtained from coconut fibers to treat cotton and linen textiles. Apart from being UV resistant, both fabrics showed significant action against *S. aureus* and *K. pneumonia*. The antioxidant capacity of the participating nanolignin impregnated fabrics was confirmed by their radical scavenging activity (Juikar et al., 2017).

2B.4.2.7. Nanolignin as adsorbent

Xiao's team had previously produced a functionalized metal-organic scaffold that efficiently scavenges heavy metal ions and microorganisms. Their study further bolstered its bactericidal property against *E. coli* (99.68%) and *S. aureus* (99.76%) when tagged with silver metal (Xiao et al., 2018, Liu et al., 2022).

2B.4.2.8. Nanolignin as supercapacitor

LNPs can act as excellent ultra-capacitors when conditioned with a KOH (6 M) electrolyte solution. Activation of lignin-derived microspheres and precursors (LAC-M and LAC-P)

resulted in profound capacitive (at 50 mV/s) and rate performance (at a particular current range of 0.05 - 100 A/g) features. When soda lignin from spruce wood is carbonized and activated, carbon fibers (ACFs) with submicron thickness and high porosity form. These acts can be used as ultra-capacitors with a storage capacity of 8.1 Wh/kg. A study that investigated alkaline lignin as ultra-capacitors vouched for the ability of the resulting fibrous mats to be used as an anode material in a conventional Li-ion battery. Such composites are expected to have a specific capacity of 445 mAh/g and a capacitance retention rate of about 90% after 6000 charge/discharge cycles (Yu et al., 2018).

2B.4.2.9. Nanolignin as surfactant

In the food and pharmaceutical industry, the use of submicron-level (320 nm) kraft lignin NPs as surfactants form a stable Pickering emulsion with different-sized hexadecane droplets. These lignin-derived surfactants offer a cost-effective and recyclable form of lignin NPs (182 nm) that renders pH responsiveness to styrene-in-water Pickering emulsions by generating insoluble particles at pH 4. RAFT-mediated grafting of kraft lignin particles with polyacrylamide functionality yields polymer-grafted lignin nanoparticles (PGLNs) that control aggregation strength without affecting interfacial interactions required to form Pickering emulsions. Furthermore, the emulsion's comparatively rapid creaming property did not affect Ostwald's ripening and coalescence for months (Qian et al., 2014).

2B.4.3. United Nations Sustainable Development Goal (UNSDG) achieved with the development of nanolignins

The use of nanolignins can guide the development of sustainable and environment-friendly food and pharmaceutical products, which aligns with the United Nations Sustainable Development Goal 12 (UNSDG 12) - Responsible Consumption and Production. Nanolignin-derived products can also give access to the costly healthcare system because it follows UNSDG 3, which endorses Good Health and Well-being. Additionally, food and

pharmaceutical applications containing nanolignins components can potentially create more job opportunities and hence support the UNSDG 8 - Decent Work and Economic Growth. Furthermore, lignin-based nanomaterials also contribute to UNSDG 13 - Climate Action as it addresses some environmental problems facing the food and pharmaceutical industries, such as waste and pollution.

2B.5. Future perspectives

Lignin, an undervalued natural polymer, is rapidly gaining importance, especially with the application of nano-technological innovations. Most patents involving lignin deal with the production of nanolignin, which shows the vast potential of nanolignin. Based on our current knowledge of lignin and lignin nanoparticles and considering the existing gaps in technologies adopted for nanoparticle development, we have to enlist future actions that are feasible enough to overcome the hurdles in this area. It is necessary that studies should focus on the following areas in order to meet sustainable standards and ensure their safety and effectiveness, greener processes for the synthesis of lignin and nanolignin that use more affordable, environmentally friendly, and easily recoverable solvents are essential. To accomplish lignin and nanolignin industrialization and speedy commercialization, scale-up processes may call for investments in large-scale, quick, low-cost, energy-efficient in manufacturing methods. It is essential to do a life cycle analysis of a nanolignin biorefinery. Discovering and creating new nanolignin that could substitute carbon-intensive synthetic nanoparticles and nanoparticles made from other natural sources are novel applications of nanolignin. The viability and marketing of nanolignins will be improved by this. Prior to clinical trials, the safety, interactions, and efficacy of freshly synthesized lignin and nanolignins should be assessed using in silico, in vitro, and in vivo approaches. These results are necessary to obtain regulatory agency permission and move on to the next phase of nano lignin utilization.

2B.6. Conclusion

A comparison between lignin and nano lignin shows vastly improved properties for nanolignin than non-nanolignin. This includes enhanced mechanical, UV blocking, radical-scavenging capacity, reducing power, superoxide radical scavenging activity, ability to form pickering emulsion, and adsorption capacity for nanolignin. The unique properties of lignin and nano lignin enable its application in other fields like the packaging industry, emulsions, nutrient delivery, drug delivery hydrogels, tissue engineering, and biomedical applications, which will be an excellent opening for human needs. Since these nanoscales and non-nano scale lignin has a wide range of properties, lignin applications will continue to undergo extensive research in the coming years. The findings and insights included in this review will give a different perspective on the potential applications of nanolignins in the food and pharma industries. The article also analyses the challenges and opportunities presented by useful nanolignins, which help researchers, policymakers, and industry professionals plan their nano-lignin-centred investigations with a clear mind about the possible challenges and limitations of the technology.

References

Aadil, K.R., Mussatto, S.I., Jha, H., 2018. Synthesis and characterization of silver nanoparticles loaded poly (vinyl alcohol)-lignin electrospun nanofibers and their antimicrobial activity. *Int. J. Biol. Macromol.* 120, 763–767. https://doi.org/10.1016/j.ijbiomac.2018.08.109.

Abraham, B., Reshmitha, T.R., Navami, M.M., George, L., Venugopalan, V.V., Nisha, P., 2020. Phytochemical rich extract from the spent material generated from Industrial dashamoola preparation (a medicinal ayurvedic decoction) with antioxidant, antidiabetic and anti-inflammatory potential. *Ind. Crops Prod.* 151, 112451. https://doi:10.1016/j.indcrop.2020.112451.

Abudula, T., Gzara, L., Simonetti, G., Alshahrie, A., Salah, N., Morganti, P., Chianese, A., Fallahi, A., Tamayol, A., Bencherif, S.A., Memic, A., 2018. The effect of poly (glycerol sebacate) incorporation within hybrid chitin-lignin sol–gel nanofibrous scaffolds. *Materials* 11 (3), 451. https://doi.org/10.3390/ma11030451.

Agrawal, A., Kaushik, N., Biswas, S., 2014. Derivatives & applications of lignin – An insight. *The Scitech. J.* 01 (7), 30-36.

Ahmed, E.M., 2015. Hydrogel: preparation, characterization, and applications: A review. *J. Adv. Res.* 6 (2), 105–121. https://doi.org/10.1016/j.jare.2013.07.006.

Akbarian, A., Andooz, A., Kowsari, E., Ramakrishna, S., Asgari, S., Cheshmeh, Z.A., 2022. Challenges and opportunities of lignocellulosic biomass gasification in the path of circular bioeconomy. *Bioresour. Technol,* 127774. https://doi.org/10.1016/j.biortech.2022.127774.

Albadarin, A.A.H., Al-Muhtaseb, N.A., Al-laqtah, G.M., Walker, S.J., Allen, M.N.M., Ahmad, 2011. Biosorption of toxic chromium from aqueous phase by lignin: mechanism, effect of other metal ions and salts. Chem. Eng. J. 169, 20–30. https://doi.org/10.1016/j.cej.2011.02.044.

Anwer, M.A.S., Naguib, H.E., Celzard, A., Fierro, V., 2015. Comparison of the thermal, dynamic mechanical and morphological properties of PLA-Lignin & PLA-Tannin particulate green composites. *Compos. B. Eng.* 82, 92–99. https://doi.org/10.1016/j.compositesb.2015.08.028.

Aura, A., 2018. MLM Wood components to boost the quality of food products. Wood components to boost the quality of food products [media]. Available from: http://www.vttresearch.com/media/news/wood-components-to-boostthe-quality-of-food-products.

Bajwa, D., Pourhashem, G., Ullah, A.H., Bajwa, S., 2019. A concise review of current lignin production, applications, products and their environment impact. *Ind. Crops Prod.* 139. https://doi:10.1016/j.indcrop.2019.111526.

Barapatre, A., Aadil, K.R., Tiwary, B.N., Jha, H., 2015. In vitro antioxidant and antidiabetic activities of biomodified lignin from Acacia nilotica wood. *Int. J. Biol. Macromol.* 75, 81–89. https://doi.org/10.1016/j.ijbiomac.2015.01.012.

Baumberger, S., Lapierre, C., Monties, B., Lourdin, D., Colonna, B., 1997. Preparation and properties of thermally moulded and cast lignosulfonates-starch blends. *Ind. Crops. Prod.* 6, 253–258.

Bertella, S., Luterbacher, J.S., 2020. Lignin Functionalization for the Production of Novel Materials. *Trends Chem.* 2 (5), 440–453. https://doi.org/10.1016/j.trechm.2020.03.001.

Bertolo, M.R.V., Brenelli de Paiva, L.B., Nascimento, V.M., Gandin, C.A., Neto, M.O., Driemeier, C.E., Rabelo, S.C., 2019. Lignins from sugarcane bagasse: Renewable source of nanoparticles as pickering emulsions stabilizers for bioactive compounds encapsulation. *Ind. Crops Prod.* 140, 111591. https://doi:10.1016/j.indcrop.2019.111591.

Bhat, R., Abdullah, N., Din, R.H., Tay, G.S., 2013. Producing novel sago starch-based food packaging films by incorporating lignin isolated from oil palm black liquor waste. *J. Food Eng.* 119, 707–713.

Borisenkov, M.F., Karmanov, A.P., Kocheva, L.S., Markov, P.A., Istomina, E.I., Bakutova, L.A., Popov, S.V., 2015. Adsorption of β-glucuronidase and estrogens on pectin/lignin hydrogel particles. *Int. J. Polym. Mater*. 65 (9), 433–441. https://doi.org/10.1080/00914037.2015.1129955.

Cai, X., Riedl, B., Zhang, S. Y., Wan, H., 2008. The impact of the nature of nanofillers on the performance of wood polymer nanocomposites. *Compos. Part A Appl. Sci. Manuf.* 39, 727-737. https://doi.org/10.1016/j.compositesa.2008.02.004.

Caicedo, H.K., Dempere, L.A., Vermerris, W., 2012. Template-mediated synthesis and bio-functionalization of flexible lignin-based nanotubes and nanowires. *Nanotechnology* 23, 105605–105617. https://doi.org/10.1088/0957-4484/23/10/105605.

Çalgeris, İ., Çakmakçı, E., Ogan, A., Kahraman, M.V., Kayaman-Apohan, N., 2012. Preparation and drug release properties of lignin–starch biodegradable films. *Starch-Stärke* 64 (5), 399–407. https://doi.org/10.1002/star.201100158.

Calvo-Flores, F.G., Dobado, J.A., 2010. Lignin as renewable raw material. *Chem. Sus. Chem.* 3 (11), 1227–1235.

Chauhan, P.S., 2019. Lignin nanoparticles: Eco-friendly and versatile tool for new era. *Bioresour. Technol. Rep.* 100374. https://doi:10.1016/j.biteb.2019.100374.

Chen, H., 2015. Lignocellulose biorefinery feedstock engineering. *Lignocellulose Biorefin. Eng.* 37–86.

Chen, L., Zhou, X., Shi, Y., Gao, B., Wu, J., Kirk, T.B., Xue, W., 2018. Green synthesis of lignin nanoparticle in aqueous hydrotropic solution toward broadening the window for its processing and application. *Chem. Eng. J.* 346, 217–225. https://doi:10.1016/j.cej.2018.04.020.

Chen, N., Dempere, L.A., Tong, Z., 2016. Synthesis of pH-responsive lignin-based nanocapsules for controlled release of hydrophobic molecules. *ACS Sustain. Chem. Eng.* 4 (10), 5204–5211. https://doi:10.1021/acssuschemeng.6b01209.

Choi, D., Heo, J., Park, J.H., Jo, Y., Jeong, H., Chang, M., Hong, J., 2016. Nano-film coatings onto collagen hydrogels with desired drug release. *J. Ind. Eng. Chem.* 36, 326–333. https://doi.org/10.1016/j.jiec.2016.02.023.

Ciolacu, D., Oprea, A.M., Anghel, N., Cazacu, G., Cazacu, M., 2012. New cellulose–lignin hydrogels and their application in controlled release of polyphenols. *Mater. Sci. Eng. C.* 32 (3), 452–463. https://doi.org/10.1016/j.msec.2011.11.018.

Claudia, C., Federica, M., Marco, S., 2011. Milled wood lignin: a linear oligomer. *Biomacromol.* 12, 3928–3935.

Dacrory, S., Abou-Yousef, H., Abouzeid, R. E., Kamel, S., Abdel-aziz, M. S., El-badry, M., 2018. Antimicrobial cellulosic hydrogel from olive oil industrial residue. *Int. J. Biol. Macromol.* 117, 179-188. https://doi.org/10.1016/j.ijbiomac.2018.05.179.

Dai, L., Liu, R., Hu, L.Q., Zou, Z.F., Si, C.L., 2017. Lignin nanoparticle as a novel green carrier for the efficient delivery of resveratrol. *ACS Sustain. Chem. Eng.* 5 (9), 8241–8249. https://doi:10.1021/acssuschemeng.7b01903.

Danti, S., Trombi, L., Fusco, A., Azimi, B., Lazzeri, A., Morganti, P., Donnarumma, G., 2019. Chitin nanofibrils and nanolignin as functional agents in skin regeneration. *Int. J. Mol. Sci.* 20 (11), 2669. https://doi:10.3390/ijms20112669.

Demirci, F., Yildirim, K., Kocer, H.B., 2018. Antimicrobial open-cell polyurethane foams with quaternary ammonium salts. *J. Appl. Polym. Sci.* 135 (9), 45914. https://doi.org/10.1002/app.45914.

Dey, N., Kumar, G., Vickram, A.S., Mohan, M., Singhania, R.R., Patel, A.K., Dong, C.D., Anbarasu, K., Thanigaivel, S. and Ponnusamy, V.K., 2022. Nanotechnology-assisted production of value-added biopotent energy-yielding products from lignocellulosic biomass

refinery–a review. *Bioresour. Technol.,* 344, p.126-171. https://doi.org/10.1016/j.biortech.2021.126171

Dinari, A., Abdollahi, M., Sadeghizadeh, M., 2021. Design and fabrication of dual responsive lignin-based nanogel via "grafting from" atom transfer radical polymerization for curcumin loading and release. *Scientific Reports,* 11(1), 1962. https://doi.org/10.1038/s41598-021-81393-3

Dizhbite, T., Telysheva, G., Jurkjane, V., Viesturs, U., 2004. Characterization of the radical scavenging activity of lignins - natural antioxidants. *Bioresour. Technol.* 95, 309–317. https://doi.org/10.1016/j.biortech.2004.02.024.

Domínguez-Robles, J., Larrañeta, E., Fong, M.L., Martin, N.K., Irwin, N.J., Mutjé, P., Delgado-Aguilar, M., 2019. Lignin/poly (butylene succinate) composites with antioxidant and antibacterial properties for potential biomedical applications. *Int. J. Biol. Macromol.* 145, 92–99. https://doi.org/10.1016/j.ijbiomac.2019.12.146.

Domínguez-Robles, J., Martin, N., Fong, M., Stewart, S., Irwin, N., Rial-Hermida, M., Larrañeta, E., 2019. Antioxidant PLA composites containing lignin for 3D printing applications: A potential material for healthcare applications. *Pharmaceutics* 11 (4), 165. https://doi.org/10.3390/pharmaceutics11040165.

Domínguez-Robles, J., Peresin, M.S., Tamminen, T., Rodríguez, A., Larrañeta, E., Jääskeläinen, A. S., 2018. Lignin-based hydrogels with “super-swelling” capacities for dye removal. *Int. J. Biol. Macromol.* 115, 1249–1259. https://doi.org/10.1016/j.ijbiomac.2018.04.044.

Dong, H., Zheng, Yu, P., Jiang, Q., Wu, Y., Huang, C., Yin, B., 2019. Characterization and application of lignin-carbohydrate complexes from lignocellulosic materials as antioxidant for

scavenging in vitro and in vivo reactive oxygen species. *ACS Sustain. Chem. Eng.* 8 (1), 256–266. https://doi.org/10.1021/acssuschemeng.9b05290.

Dong, Y., Paukkonen, H., Fang, W., Kontturi, E., Laaksonen, T., Laaksonen, P., 2018. Entangled and colloidally stable microcrystalline cellulose matrices in controlled drug release. *Int. J. Pharm.* 548 (1), 113–119. https://doi.org/10.1016/j.ijpharm.2018.06.022.

Ekeberg, D., Gretland, K.S., Gustafsson, J., Bråten, S.M., 2006. Characterisation of lignosulphonates and kraft lignin by hydrophobic interaction chromatography. *Analytica. Chimica. Acta.* 565(1), 121–128.

Erakovic, S., Jankovic, A., Tsui, G.C.P., Tang, C.Y., Miskovic-Stankovic, V., Stevanovic, T., 2014. Novel bioactive antimicrobial lignin containing coatings on titanium obtained by electrophoretic deposition. *Int. J. Mol. Sci.* 15, 12294–12322.

Farhat, W., Venditti, R., Mignard, N., Taha, M., Becquart, F., Ayoub, A., 2017. Polysaccharides and lignin based hydrogels with potential pharmaceutical use as a drug delivery system produced by a reactive extrusion process. *Int. J. Biol. Macromol.* 104, 564–575. https://doi.org/10.1016/j.ijbiomac.2017.06.037.

Figueiredo, P., Lintinen, K., Kiriazis, A., Hynninen, V., Liu, Z., Bauleth-Ramos, T., Rahikkala, A., Correia, A., Kohout, T., Sarmento, B., Yli-Kauhaluoma, J., Hirvonen, J., Ikkala, O., Kostiainen, M.A., Santos, H. A., 2017. In vitro evaluation of biodegradable lignin-based nanoparticles for drug delivery and enhanced antiproliferation effect in cancer cells. *Biomaterials* 121, 97–108. https://doi.org/10.1016/j.biomaterials.2016.12.034.

Ganasan, E., Mohd Yusoff, H., Azmi, A. A., Chia, P. W., Lam, S. S., Kan, S. Y., Teo, C. K., 2022. Food additives for the synthesis of metal nanoparticles: a review. *Environmental Chemistry Letters,* 1-14. https://doi.org/10.1007/s10311-022-01473-2

Gellerstedt, G., Henriksson, G., 2008. Lignins: major sources, structure and properties, in: Belgacem, M.N., Gandini, A. (Eds.), Monomers, Polymers and Composites from Renewable Resources, pp. 201–224.

Gharehkhani, S., Ghavidel, N., Fatehi, P., 2018. Kraft lignin-tannic acid as a green stabilizer for oil/water emulsion. *ACS Sustainable Chem. Eng.* 2370–2379.

Gîlca, I.A., Popa, V.I., 2013. Study on biocidal properties of some nanoparticles based on epoxy lignin. *Cellul. Chem. Technol.* 47, 3–4.

Gilca, I.A., Popa, V.I., Crestini, C., 2015. Obtaining lignin nanoparticles by sonication. *Ultrason. Sonochem.* 23, 369–375. https://doi:10.1016/j.ultsonch.2014.08.02.

Gil-Chávez, J., Gurikov, P., Hu, X., Meyer, R., Reynolds, W., Smirnova, I., 2019. Application of novel and technical lignins in food and pharmaceutical industries: structure-function relationship and current challenges. *Biomass Conv. Bioref.* https://doi:10.1007/s13399-019-00458-6.

Gordts, S.C., Férir, G., D'huys, T., Petrova, M.I., Lebeer, S., Snoeck, R., Schols, D., 2015. The low-cost compound lignosulfonic acid (LA) exhibits broad-spectrum anti-HIV and anti-HSV activity and has potential for microbicidal applications. *PLOS One* 10 (7), e0131219. https://doi.org/10.1371/journal.pone.0131219.

Gosselink, R., Snijder, M., Kranenbarg, A., Keijsers, E., de Jong, E., Stigsson, L., 2004. Characterisation and application of Nova Fiber lignin. *Ind. Crops. Prod*. 20, 191-203.

Greenhalgh, R., Dempsey-Hibbert, N.C., Whitehead, K.A., 2019. Antimicrobial strategies to reduce polymer biomaterial infections and their economic implications and considerations. *Int. Biodeter. Biodegr.* 136, 1–14. https://doi.org/10.1016/j.ibiod.2018.10.005.

Gupta, A.K., Mohanty, S., Nayak, S.K., 2015. Influence of addition of vapor grown carbon fibers on mechanical, thermal and biodegradation properties of lignin nanoparticle filled bio-poly (trimethylene terephthalate) hybrid nanocomposites. *RSC Adv.* 5 (69), 56028–56036. https://doi:10.1039/c5ra07828h.

Haghdan, S., Renneckar, S., Smith, G. D., 2016. Sources of lignin. Lignin in Polym. Compos. 1–11.

Haldar, D., Shabbirahmed, A.M., Singhania, R.R., Chen, C.W., Dong, C.D., Ponnusamy, V.K., Patel, A.K., 2022. Understanding the management of household food waste and its engineering for sustainable valorization-A state-of-the-art review. *Bioresour. Technol.* p.127390. https://doi.org/10.1016/j.biortech.2022.127390

Hasegawa, Y., Kadota, Y., Hasegawa, C., Kawaminami, S, 2015. Lignosulfonic Acid-Induced Inhibition of Intestinal Glucose Absorption. *J. Nutr. Sci. Vitaminol.* 61 (6), 449–454. https://doi.org/10.3177/jnsv.61.449.

Hernandez, G.J.M., Escalante, A., Murillo Vazquez, R.N., Delgado, E., Gonzalez, F.J., Toriz, G., 2016. Use of agave tequilana-lignin and zinc oxide nanoparticles for skin photoprotection. *J. Photochem. Photobiol.* 163, 156-161. https://doi.org/10.1016/j.jphotobiol.2016.08.027.

Hiltunen, E., Alvila, L., Pakkanen, T.T., 2006. Characterization of brauns' lignin from fresh and vacuum-dried birch (*Betula pendula*) wood. *Wood Sci. Technol.* 40, 575.

Huang, C., Tang, S., Zhang, W., Tao, Y., Lai, C., Li, X., Yong, Q., 2018. Unveiling the structural properties of lignin–carbohydrate complexes in bamboo residues and its functionality as antioxidants and immunostimulants. *ACS Sustain. Chem. Eng.* 69, 12522–12531.

Jaganathan, G., Manivannan, K., Lakshmanan, S., Sithique, M.A., 2018. Fabrication and characterization of *Artocarpus heterophyllus* waste derived lignin added chitosan

biocomposites for wound dressing application. *Sustain. Chem. Pharm.* 10, 27–32. https://doi.org/10.1016/j.scp.2018.08.002.

Jankovi´c, A., Erakovi´c, S., Ristoscu, C., 2015. Structural and biological evaluation of lignin addition to simple and silver-doped hydroxyapatite thin films synthesized by matrix-assisted pulsed laser evaporation. *J. Mater. Sci. Mater. Med.* 26 (1), 17. https://doi.org/10.1007/s10856-014-5333-y.

Javed, A., Ullsten, H., Rättö, P., Järnström, L., 2018. Lignin-containing coatings for packaging materials. Nord. Pulp. Paper Res. J. 33 (3), 548–556.

Jiang, C., He, H., Jiang, H., Ma, L., Jia, D. M., 2013. Nano-lignin filled natural rubber composites: Preparation and characterization. eXPRESS. *Polym. Lett.* 7 (5), 480–493. https://doi.org/10.3144/expresspolymlett.2013.44.

Juikar, S.J., Vigneshwaran, N., 2017. Microbial production of coconut fiber nanolignin for application onto cotton and linen fabrics to impart multifunctional properties. *Surf. Interfaces.* 9, 147–153. https://doi:10.1016/j.surfin.2017.09.006.

Kadla, J., Kubo, S., Venditti, R., Gilbert, R., Compere, A., Griffith, W., 2002. Lignin-based carbon fibers for composite fiber applications. Carbon N. Y. 40, 2913–2920. https://doi.org/10.1016/S0008-6223(02)00248-8.

Kai, D., Jiang, S., Low, Z.W., Loh, X.J., 2015. Engineering highly stretchable lignin-based electrospun nanofibers for potential biomedical applications. *J. Mater. Chem.* A. B. 3 (30), 6194–6204. https://doi.org/10.1039/c5tb00765h.

Kai, D., Zhang, K., Jiang, L., Wong, H.Z., Li, Z., Zhang, Z., Loh, X.J., 2017. Sustainable and antioxidant lignin–polyester copolymers and nanofibers for potential healthcare applications. *ACS. Sustain. Chem. Eng.* 5, 6016–6025. https://doi.org/10.1021/acssuschemeng.7b00850.

Kim, S., Fernandes, M.M., Matamá, T., Loureiro, A., Gomes, A.C., Cavaco-Paulo, A., 2013. Chitosan–lignosulfonates sono-chemically prepared nanoparticles: characterisation and potential applications. *Colloid. Surf. B.* 103, 1–8. https://doi.org/10.1016/j.colsurfb.2012.10.033.

Larrañeta, E., Imízcoz, M., Toh, J.X., Irwin, N.J., Ripolin, A., Perminova, A., Donnelly, R.F., 2018. Synthesis and characterization of lignin hydrogels for potential applications as drug eluting antimicrobial coatings for medical materials. *ACS. Sustain. Chem. Eng.* 6 (7), 9037–9046. https://doi.org/10.1021/acssuschemeng.8b01371.

Lee, E., Song, Y., Lee, S., 2019. Crosslinking of lignin/poly (vinyl alcohol) nanocomposite fiber webs and their antimicrobial and ultraviolet-protective properties. *Tex. Res. J.* 89 (1), 3–12. https://doi.org/10.1177/0040517517736468.

Lee, E.S., Kim, Y.O., Ha, Y.M., Lim, D., Hwang, J.Y., Kim, J., Park, M., Cho, J.W., Jung, Y.C., 2018. Antimicrobial properties of lignin-decorated thinmulti-walled carbon nanotubes in poly (vinyl alcohol) nanocomposites. *Europ. Polym. J.* 105, 79–84. https://doi.org/10.1016/j.eurpolymj.2018.05.014.

Lee, J.B., Yamagishi, C., Hayashi, K., Hayashi, T., 2011. Antiviral and immunostimulating effects of lignin-carbohydrate-protein complexes from *Pimpinella anisum*. *Biosci. Biotechnol. Biochem.* 75 (3), 459–465. https://doi.org/10.1271/bbb.100645.

Li, H., Deng, Y., Wu, H., Ren, Y., Qiu, X., Zheng, D., Li, C., 2016. Self-assembly of kraft lignin into nanospheres in dioxane-water mixtures. *Holzforschung* 70, 725–731. https://doi:10.1515/hf-2015-0238.

Liguori, I., Russo, G., Curcio, F., Bulli, G., Aran, L., Della-Morte, D., Gargiulo, G., Testa, G., Cacciatore, F., Bonaduce, D., Abete, P., 2018. Oxidative stress, aging, and diseases. *Clin. Interv. Aging.* 26 (13), 757-772. https://doi:10.2147/CIA.S158513.

Liu, J., Wu, J., Lu, Y., Zhang, H., Hua, Q., Bi, R., Rojas, O., Renneckar, S., Fan, S., Xiao, Z., Saddler, J., 2022. The pre-addition of “blocking” proteins decreases subsequent cellulase adsorption to lignin and enhances cellulose hydrolysis. *Bioresour. Technol.* p.128276. https://doi.org/10.1016/j.biortech.2022.128276

Liu, R., Dai, L., Zou, Z., Si, C., 2018. Drug-loaded poly (L-lactide)/lignin stereocomplex film for enhancing stability and sustained release of trans-resveratrol. *Int. J. Biol. Macromol.* 119, 1129–1136. https://doi.org/10.1016/j.ijbiomac.2018.08.040

Lora, J., 2008. Industrial commercial lignins: sources, properties and applications. In: Monomers, polymers and composites from renewable resources. Elsevier, pp. 225–241.

Ma, Z., Wang, J., Zhou, H., Zhang, Y., Yang, Y., Liu, X., Wang, S., 2018. Relationship of thermal degradation behavior and chemical structure of lignin isolated from palm kernel shell under different process severities. *Fuel Process. Technol.* 181, 142–156.

Mansur, H.S., Mansur, A.A., Bicallho, S.M., 2005. Lignin-hydroxyapatite/tricalcium phosphate biocomposites: SEM/EDX and FTIR characterization. Key. *Eng. Mater.* 284–286: 745–748. https://doi.org/10.4028/www.scientific.net/KEM.284-286.745

Medina, J.D.C., Woiciechowski, A.L., Filho, A.Z., Bissoqui, L., Noseda, M.D., Vandenberghe, L.P., de S., Zawadzki, S.F., Soccol, C.R., 2016. Biological activities and thermal behavior of lignin from oil palm empty fruit bunches as potential source of chemicals of added value. *Ind. Crops. Prod.* 94, 630–637.

Mehta, M.J., Kumar, A., 2019. Ionic liquid stabilized gelatin-lignin films: a potential UV-shielding material with excellent mechanical and antimicrobial properties. *Chem. A. Eur. J.* 25 (5), 1269–1274. https://doi.org/10.1002/chem.201803763.

Morganti, P., Danti, S., Coltelli, M.B., 2018. Chitin and lignin to produce biocompatible tissues. *Res. Clin. Dermatol.* 1, 5–11.

Myint, A. A., Lee, H. W., Seo, B., Son, W. S., Yoon, J., Yoon, T. J., Lee, Y. W, 2016. One pot synthesis of environmentally friendly lignin nanoparticles with compressed liquid carbon dioxide as an antisolvent. *Green. Chem.* 18(7), 2129–2146. https://doi.org/10.1039/c5gc02398j

Nada, A.M.A., El-Diwany, A.I., Elshafei, A.M., 1989. Infrared and antimicrobial studies on different lignins. *Acta Biotechnol.* 9, 295–298. https://doi.org/10.1002/abio.370090322

Nguyen, N. T. T., Nguyen, L. M., Nguyen, T. T. T., Liew, R. K., Nguyen, D. T. C., Van Tran, T., 2022. Recent advances on botanical biosynthesis of nanoparticles for catalytic, water treatment and agricultural applications: a review. *Science of the total environment*, 154160. https://doi.org/10.1016/j.scitotenv.2022.154160

Norikura, T., Mukai, Y., Fujita, S., Mikame, K., Funaoka, M. and Sato, S., 2010. Lignophenols Decrease Oleate-Induced Apolipoprotein-B Secretion in HepG2 Cells. *Basic Clin. Pharmacol. Toxicol.* 107(4), pp.813-817. https://doi.org/10.1111/j.1742-7843.2010.00575.x

Norikura, T., Mukai, Y., Fujita, S., Mikame, K., Funaoka, M. and Sato, S., 2010. Lignophenols Decrease Oleate-Induced Apolipoprotein-B Secretion in HepG2 Cells. *Basic Clin. Pharmacol. Toxicol.* 107(4), pp.813-817. https://doi.org/10.1111/j.1742-7843.2010.00575.x

Nypelö, T.E., Carrillo, C.A., Rojas, O.J., 2015. Lignin supracolloids synthesized from (W/O) microemulsions: Use in the interfacial stabilization of pickering systems and organic carriers for silver metal. *Soft Matter* 11, 2046–2054. https://doi.org/10.1039/c4sm02851a

Parvathy, G., Sethulekshmi, A.S., Jayan, J.S., Raman, A., Saritha, A. 2020. Lignin based nano-composites: Synthesis and applications. *Process Saf. Environ. Prot.* 145, 395-410. https://doi:10.1016/j.psep.2020.11.017

Pham, C. D., Dang, M. D., Ly, T. B., Tran, K. D., Vo, N. T., Do, N. H., Le, P. K., 2023. A review of the extraction methods and advanced applications of lignin-silica hybrids derived from natural sources. *International Journal of Biological Macromolecules,* 123175. https://doi.org/10.1016/j.ijbiomac.2023.123175

Ponnusamy, V.K., Nguyen, D.D., Dharmaraja, J., Shobana, S., Banu, J.R., Saratale, R.G., Chang, S.W. and Kumar, G., 2019. A review on lignin structure, pretreatments, fermentation reactions and biorefinery potential. *Bioresour. Technol.* 271, pp.462-472. https://doi.org/10.1016/j.biortech.2018.09.070

Popa, V.I., Capraru, A.M., Grama, S., Malutan, T., 2011. Nanoparticles based on modified lignins with biocide properties. *Cellul. Chem. Technol.* 45 (3), 221–226. https://www.researchgate.net/publication/265234734_Nanoparticles_based_on_modified_lignins_with_biocide_properties

Prakash, A., Singh, R., Balagurumurthy, B., Bhaskar, T., Arora, A.K., Puri, S.K., 2015. Thermochemical valorization of lignin, in: Pandey, A., Bhaskar, T., Sukumaran, R.K. (Eds.), Recent Advances in Thermo-Chemical Conversion of Biomass, pp. 455–478.

Qian, Y., Deng, Y., Qiu, X., Li, H., Yang, D., 2014. Formation of uniform colloidal spheres from lignin, a renewable resource recovered from pulping spent liquor. Green Chem. 16 (4), 2156. https://doi.org/10.1039/c3gc42131g.

Qian, Y., Zhang, Q., Qiu, X., Zhu, S., 2014. CO_2-responsive diethylaminoethyl-modified lignin nanoparticles and their application as surfactants for CO_2/N_2-switchable pickering emulsions. *Green Chem.* 16, 4963–4968. https://doi.org/10.1039/C4GC01242A

Quraishi, S., Martins, M., Barros, A.A., Gurikov, P., Raman, S.P., Smirnova, I., Reis, R.L., 2015. Novel non-cytotoxic alginate–lignin hybrid aerogels as scaffolds for tissue engineering. *J. Supercrit. Fluid.* 105, 1–8. https://doi.org/10.1016/j.supflu.2014.12.026

Rahman, O. ur, Shi, S., Ding, J., Wang, D., Ahmad, S., Yu, H., 2018. Lignin nanoparticles: synthesis, characterization and corrosion protection performance. *New J. Chem.* 42 (5), 3415–3425. https://doi.org/10.1039/c7nj04103a

Ravishankar, K., Venkatesan, M., Desingh, R.P., Mahalingam, A., Sadhasivam, B., Subramaniyam, R., Dhamodharan, R., 2019. Biocompatible hydrogels of chitosan-alkali lignin for potential wound healing applications. *Mater. Sci. Eng.* C. 102, 447–457. https://doi.org/10.1016/j.msec.2019.04.038

Rekola, J., Aho, A.J., Gunn, J., Matinlinna, J., Hirvonen, J., Viitaniemi, P., Vallittu, P.K., 2009. The effect of heat treatment of wood on osteoconductivity. *Acta Biomater.* 5 (5), 1596–1604. https://doi.org/10.1016/j.actbio.2009.01.018

Reshmy, R., Balakumaran, P.A., Divakar, K., Philip, E., Madhavan, A., Pugazhendhi, A., Sirohi, R., Binod, P., Awasthi, M.K. and Sindhu, R., 2022. Microbial valorization of lignin: Prospects and challenges. *Bioresour. Technol.* 344, p.126240. https://doi.org/10.1016/j.biortech.2021.126240

Richter, A.P., Bharti, B., Armstrong, H.B., Brown, J.S., Plemmons, D., Paunov, V.N., Velev, O.D., 2016. Synthesis and characterization of biodegradable lignin nanoparticles with tunable surface properties. *Langmuir* 32 (25), 6468–6477. https://doi.org/10.1021/acs.langmuir.6b01088

Richter, A.P., Brown, J.S., Bharti, B., Wang, A., Gangwal, S., Houck, K., Cohen Hubal, E.A., Paunov, V.N.,Stoyanov, S.D., Velev, O.D., 2015. An environmentally benign antimicrobial nanoparticle based on a silver-infused lignin core. *Nat. Nanotechnol.* 10, 817–823. https://doi.org/10.1038/nnano.2015.141

Rihayat, T., Suryani, Siregar, J. P., Zaimahwati, Salmyah, Helmi, Sariadi, Fitria, Satriananda, Putra, A., Fona, Z., Juanda, Raudah, Mawaddah, Nurhanifa, Riskina, S., Syahputra, W., Jaafar,

J., 2019. Wound dressing based on banana peels waste and chitosan by strengthening lignin as wound healing medicine. IOP Conference Series: *Mater. Sci. Eng.* C. 506, 012056. https://doi.org/10.1088/1757-899x/506/1/012056

Rojas, O.J., Bullon, J., Ysambertt, F., Forgiarini, A., Salager, J.L., Argyropoulos, D. 2007. Lignins as Emulsion Stabilizers. 953, 182-199. https://doi.org/10.1021/bk-2007-0954.ch012

Sakagami, H., Sheng, H., Yasui, T., Fukuchi, K., Oizumi, T., Ohno, H., Nakashima, H., 2017. Therapeutic potential of solubilized nanolignin against oral diseases, in: Andronescu, E., Grumezescu, A.M., (Eds.), Nanostructures for Oral Medicine, pp. 545–576. https://doi:10.1016/b978-0-323-47720-8.00019-5

Salami, M.A., Kaveian, F., Rafienia, M., Samandari, S.S., Khandan, A., Naeimi, M., 2017. Electrospun polycaprolactone/lignin-based nanocomposite as a novel tissue scaffold for biomedical applications. *J. Med. Signals Sens.* 7 (4), 228–238. https://doi.org/10.4103/jmss.JMSS_11_17

Saluja, B., Thakkar, J.N., Li, H., Desai, U.R., Sakagami, M., 2013. Novel low molecular weight lignins as potential anti-emphysema agents: In vitro triple inhibitory activity against elastase, oxidation and inflammation. *Pulm. Pharmacol. Ther*. 26 (2), 296–304. https://doi.org/10.1016/j.pupt.2012.12.009.

Sathawong, S., Sridach, W., Techato, K., 2018. Lignin: Isolation and preparing the lignin based hydrogel. *J. Environ. Chem. Eng*. 6 (5), 5879–5888.

Sato, S., Mukai, Y., Yamate, J., Norikura, T., Morinaga, Y., Mikame, K., Fujita, S, 2009. Lignin-derived lignophenols attenuate oxidative and inflammatory damage to the kidney in streptozotocin-induced diabetic rats. Free Radic. Res. 43 (12), 1205–1213. https://doi.org/10.3109/10715760903247264

Sethupathy, S., Morales, G.M., Gao, L., Wang, H., Yang, B., Jiang, J., Sun, J., Zhu, D., 2022. Lignin valorization: status, challenges and opportunities. *Bioresour. Technol*. pp.126696. https://doi.org/10.1016/j.biortech.2022.126696

Shankar, S., Rhim, J.W., Won, K., 2018. Preparation of poly (lactide)/lignin/silver nanoparticles composite films with UV light barrier and antibacterial properties. *Int. J. Biol. Macromol.* 107, 1724–1731. https://doi.org/10.1016/j.ijbiomac.2017.10.038.

Sharma, S., Kumar, A. (Eds.), 2020. Lignin. Springer Series on Polymer and Composite Materials. pp. 298. https://doi:10.1007/978-3-030-40663-9.

Sharma, S., Sharma, A., Mulla, S.I., Pant, D., Sharma, T., Kumar, A., 2020. Lignin as potent industrial biopolymer: An introduction. In S. Sharma & A. Kumar (Eds.), Lignin: biosynthesis and transformation for ndustrial applications, 1–15. https://doi.org/10.1007/978-3-030-40663-9_1.

Sipponen, M.H., Farooq, M., Koivisto, J., Pellis, A., Seitsonen, J., Österberg, M., 2018. Spatially confined lignin nanospheres for biocatalytic ester synthesis in aqueous media. *Nat. Commun.* 9 (1) 2300. https://doi:10.1038/s41467-018-04715-6

Sirviö, J.A., Ismail, M.Y., Zhang, K., Tejesvi, M.V., Ämmälä, A., 2020. Transparent lignin-containing wood nanofiber films with UV-blocking, oxygen barrier, and anti-microbial properties. *J. Mater. Chem. A*, 8, 7935-7946.

Spasojević, D., Zmejkoski, D., Glamočlija, J., Nikolić, M., Soković, M., Milošević, V., Radotić, K., 2016. Lignin model compound in alginate hydrogel: a strong antimicrobial agent with high potential in wound treatment. *Int. J. Antimicrob. Agents*. 48 (6), 732–735. https://doi.org/10.1016/j.ijantimicag.

Spender, J., Demers, A.L., Xie, X., Cline, A.E., Earle, M.A., Ellis, L.D., Neivandt, D.J., 2012. Method for production of polymer and carbon nanofibers from water-soluble polymers. *Nano. Lett*. 12, 3857–3860. https://doi.org/10.1021/nl301983d

Spiridon, I., 2018. Biological and pharmaceutical applications of lignin and its derivatives: a minireview. *Cellul. Chem. Technol*. 52(7–8), 543–550.

Spiridon, I., Tanase, C.E., 2018. Design, characterization and preliminary biological evaluation of new lignin-PLA biocomposites. *Int. J. Biol. Macromol.* 114, 855–863.

Sun, Y., Ma, Y., Fang, G., Ren, S., Fu, Y, 2016. Controlled pesticide release from porous composite hydrogels based on lignin and polyacrylic acid. BioResources 11 (1), 2361–2371.

Sun, Y., Yang, L., Lu, X., He, C., 2015. Biodegradable and renewable poly (lactide)–lignin composites: synthesis, interface and toughening mechanism. *J. Mater. Chem.* A 3, 3699–3709. https://doi.org/10.1039/C4TA05991C

Tamminen, T., Ropponen, T., Eva-Lena, H., Poppius-Levlin, K., 2014. Functionalized lignin and method of producing the same. United States Patent No. 2014/0243511A1. Available at: https://patentimages.storage.googleapis.com/02/05/ad/8b6bff013f0857/US20140243511A1.pdf

Tayeb, H.A., Tajvidi, M., Bousfield, D., 2020. Paper-Based Oil Barrier packaging using lignin-containing cellulose nanofibrils. *Molecules* 25 (6), 1344.

Thakkar, J.N., Tiwari, V., Desai, U.R., 2010. Nonsulfated, cinnamic acid-based lignins are potent antagonists of HSV-1 entry into cells. *Biomacromolecules* 11 (5), 1412–1416. https://doi.org/10.1021/bm100161u

Tian, D., Hu, J., Chandra, R.P., Saddler, J.N., Lu, C., 2017. Valorizing recalcitrant cellulolytic enzyme lignin via lignin nanoparticles fabrication in an integrated biorefinery. ACS *Sustain. Chem. Eng.* 5 (3), 2702–2710. https://doi.org/10.1021/acssuschemeng.6b03043

Tortora, M., Cavalieri, F., Mosesso, P., Ciaffardini, F., Melone, F., Crestini, C., 2014. Ultrasound driven assembly of lignin into microcapsules for storage and delivery of hydrophobic molecules. *Biomacromolecules* 15 (5), 1634–1643. https://doi:10.1021/bm500015j

Truong, N.P., Jones, G.R., Bradford, K.G.E., 2021. A comparison of RAFT and ATRP methods for controlled radical polymerization. *Nat. Rev. Chem.* 5, 859–869. https://doi.org/10.1038/s41570-021-00328-8.

United Nations World Tourism Organization., 2018. Tourismand the Sustainable Development Goals–Journey to2030.

Vinardell, M.P., Mitjans, M., 2017. Lignins and their derivatives with beneficial effects on human health. *Int . J. Mol. Sci.* 18 (6), 1219.

Wang, J., Tian, L., Luo, B., Ramakrishna, S., Kai, D., Loh, X.J., Mo, X., 2018. Engineering PCL/lignin nanofibers as an antioxidant scaffold for the growth of neuron and schwann cell. *Colloid Surface B.* 169, 356–365. https://doi.org/10.1016/j.colsurfb.2018.05.021 2016.08.014

Wang, K., Loo, L.S., Goh, K.L., 2016. A facile method for processing lignin reinforced chitosan biopolymer microfibres: Optimising the fibre mechanical properties through lignin type and concentration. *Mater. Res. Express*. 3, 035301.

Wang, L., Ago, M., Borghei, M., Ishaq, A., Papageorgiou, A.C., Lundahl, M., Rojas, O.J., 2019. Conductive carbon microfibers derived from wet-spzun lignin/nanocellulose hydrogels. ACS. *Sustain. Chem. Eng*. 7 (6), 6013–6022. https://doi.org/10.1021/acssuschemeng.8b06081

Wang, X., Zhou, Z., Guo, X., He, Q., Chen, H., Ge, C., 2016. Ultrasonic-assisted synthesis of sodium lignosulfonate-grafted poly (acrylic acid-co-poly (vinyl pyrrolidone) hydrogel for drug delivery. *RSC Adv.* 6(42), 35550–35558. https://doi.org/10.1039/C6RA03398A

Wei, Z., Yang, Y., Yang, R., Wang, C., 2012. Alkaline lignin extracted from furfural residues for pH-responsive Pickering emulsions and their recyclable polymerization. *Green Chem*. 14, 3230. https://doi.org/10.1039/C2GC36278C

Wu, S., Zhang, Y., Han, J., Xie, Z., Xu, J., Guo, B., 2017. Copolymerization with polyether segments improves the mechanical properties of biodegradable polyesters. *ACS Omega.* 2 (6), 2639-2648. https://doi.org/10.1021/acsomega.7b00517.

Xiao, D., Ding, W., Zhang, J., Ge, Y., Wu, Z., Li, Z., 2018. Fabrication of a versatile lignin-based nano-trap for heavy metal ion capture and bacterial inhibition. *Chem. Eng.* J. https://doi:10.1016/j.cej.2018.10.037

Xie, M., Muchero, W., Bryan, A.C., Yee, K., Guo, H.B., Zhang, J., 2018. A 5-enolpyruvylshikimate 3-phosphate synthase functions as a transcriptional repressor in populus. *Plant Cell* 30, 1645–1660. https://doi:10.1105/tpc.18.00168

Xing, Q., Buono, P., Ruch, D., Dubois, P., Wu, L., Wang, W.J., 2019. Biodegradable UV blocking films through core-shell lignin-melanin nanoparticles in poly (butylene adipate-co-terephthalate). Acs *Sustain.Chem.Eng*.7, 4147-4157. https://doi.org/10.1021/acssuschemeng.8b05755

Yang, M., Zhao, W., Singh, S., Simmons, B., Cheng, G., 2019. On the solution structure of kraft lignin in ethylene glycol and its implication for nanoparticle preparation. *Nanoscale.Adv*.1, 299-304. https://doi.org/10.1039/C8NA00042E

Yang, W., Fortunati, E., Bertoglio, F., Owczarek, J.S., Bruni, G., Kozanecki, M., Kenny, J.M., Torre, L., Visai, L., Puglia, D., 2018. Polyvinyl alcohol/chitosan hydrogels with enhanced antioxidant and antibacterial properties induced by lignin nanoparticles. *Carbohyd. Polym.* 181, 275–284. https://doi.org/10.1016/j.carbpol.2017.10.084.

Yang, W., Owczarek, J.S.S., Fortunati, E., Kozanecki, M., Mazzaglia, A., Balestra, G.M.M., Kenny, J.M.M., Torre, L., Puglia, D., 2016. Antioxidant and antibacterial lignin nanoparticles in polyvinyl alcohol/chitosan films for active packaging. *Ind. Crops Prod.* 94, 800–811. https://doi.org/10.1016/j.indcrop.2016.09.061

Yearla, S. R., Padmasree, K., 2016. Preparation and characterisation of lignin nanoparticles: evaluation of their potential as antioxidants and UV protectants. *J. Exp. Nanoscience* 11, 289–302. https://doi.org/10.1080/17458080.2015.1055842

Yiamsawas, D., Beckers, S.J., Lu, H., Landfester, K., Wurm, F.R. 2017. Morphology-controlled synthesis of lignin nanocarriers for drug delivery and carbon materials. ACS *Biomater. Sci. Eng*. 3, 2375–2383. https://doi.org/10.1021/acsbiomaterials.7b00278

Yin, H., Liu, L., Wang, X., Wang, T., Zhou, Y., Liu, B., Lü, X., 2018. A novel flocculant prepared by lignin nanoparticles-gelatin complex from switch grass for the capture of *Staphylococcus aureus* and *Escherichia coli*. Colloids Surf. A Physicochem. Eng. Asp. 545, 51–59. https://doi:10.1016/j.colsurfa.2018.02.033

Yu, B., Chang, Z., Zhang, Y., Wang, C., 2018. Preparation and formation mechanism of size-controlled lignin based microsphere by reverse phase polymerization. *Mater. Chem. Phys*. 203, 97–105. https://doi:10.1016/j.matchemphys.2017.08.039

Zhang, X., Zhou, Y., Xiong, W., Wei, W., Jiang, W., 2022. Co-production of xylose, lignin, and ethanol from eucalyptus through a choline chloride-formic acid pretreatment. *Bioresour. Technol.* 359, p.127502. https://doi.org/10.1016/j.biortech.2022.127502

Zhang, Y., Jiang, M., Zhang, Y., Cao, Q., Wang, X., Han, Y., Zhou, J., 2019. Novel lignin–chitosan–PVA composite hydrogel for wound dressing. *Mater. Sci. Eng. C*. 104, 110002. https://doi.org/10.1016/j.msec.2019.110002

Zhen, X., Li, H., Xu, Z., Wang, Q., Zhu, S., Wang, Z., Yuan, Z., 2021. Facile synthesis of lignin-based epoxy resins with excellent thermal-mechanical performance. *Int. J. Biol. Macromol.* 182, 276-285. https://doi:10.1016/J.IJBIOMAC.2021.03.203

Zhiming, L., Chao, L., Haiying, W., 2013. Preparation method of nanolignin with controllable particle size. Chinese Patent CN. 103145999A. https://patents.google.com/patent/CN103145999A/en.

Zhong, X., Qian, Y., Huang, J., Yang, D., Deng, Y., Qiu, X., 2016. Fabrication of lignosulfonate vesicular reverse micelles to immobilize horseradish peroxidase. *Ind. Eng. Chem. Res*. 55, 2731–2737. https://doi.org/10.1021/acs.iecr.5b04939

Zhou, Y., Wang, D., Yang, D., Qiu, X., Li, Y., 2019. Avermectin loaded nanosphere prepared from acylated alkali lignin showed anti-photolysis property and controlled release performance. *Ind. Crops. Prod.* 137, 453–459.

Zhuang, X., Wang, W., Yu, Q., Qi, W., Wang, Q., Tan, X., Zhou, G., Yuan, Z., 2016. Liquid hot water pretreatment of lignocellulosic biomass for bioethanol production accompanying with high valuable products. *Bioresour. Technol.* 199, 68–75.

Zmejkoski, D., Spasojević, D., Orlovska, I., Kozyrovska, N., Soković, M., Glamočlija, J., Radotić, K., 2018. Bacterial cellulose-lignin composite hydrogel as a promising agent in chronic wound healing. *Int. J. Biol. Macromol.* 118, 494–503. https://doi.org/10.1016/j.ijbiomac.2018.06.067

Chapter-3

Phytochemical rich extract from the spent material generated from Industrial Dashamoola preparation (a medicinal Ayurvedic decoction) with antioxidant, antidiabetic and anti-inflammatory potential

Abstract

Dashamoola Arishta (DA), an age-old Ayurvedic formulation, is considered as panacea for inflammation-related ailments. As water is used as the solvent in DA preprations, the active ingredients are not extracted out completely and remain in the spent material (DSM). The phytochemicals extracted from Dashamoola fresh and Dashamoola spent material using 70% (v/v) ethanol (DE & DSME respectively) were characterized using HPTLC which suggested retension of considerable amount of phytochemicals in DSME. Studies on the total phenolic and flavonoid content indicated polyphenol and/or flavonoid-rich matrix. LCMS/MS analysis of DSME confirmed the presence of polyphenols, especially shikimic acid (83.225 mg/g), gallic acid (51.261 mg/g), epicatechin (26.300 mg/g), naringenin (25.054 mg/g) and vanillic acid (14.147 mg/g). The antioxidant potential of DE and DSME evaluated in terms of DPPH (IC_{50} 98.19 & 68.17 µg/mL), ABTS (IC_{50} 44.2 & 17.8 µg/mL) and NO (IC_{50} 881 & 738 µg/mL) assays indicated better activity of DSME. DSME showed better antidiabetic potential as inferred from α-amylase and α-glucosidase inhibition assays. The anti-inflammatory capability of DSME was evaluated using protein denaturation assay which showed an IC_{50} value of 61.17 µg/mL against 95.04 & 100.12 µg/mL for DE and aspirin, resepctively. DSME (IC_{50} of 60.8 µg/mL) closely contested with aspirin (IC_{50} of 70.1 µg/mL) in the proteinase inhibition assay. RAW 264.7 cells subjected to LPS-induced NO production further strengthens the scope of preliminary antioxidant results. Safety of DSME was established by MTT assay in L6 myoblast and RAW 264.7 cells with tolerability reaching up to 500 µg/mL concentration. The present study indicates the potential of DSM for further value addition, as a source of bioactives with immense nutraceutical/therapeutic properties.

Keywords: Dashamoola spent material, phytochemical assay, antioxidant activity, antidiabetic activity, anti-inflammatory activity

Graphical abstract

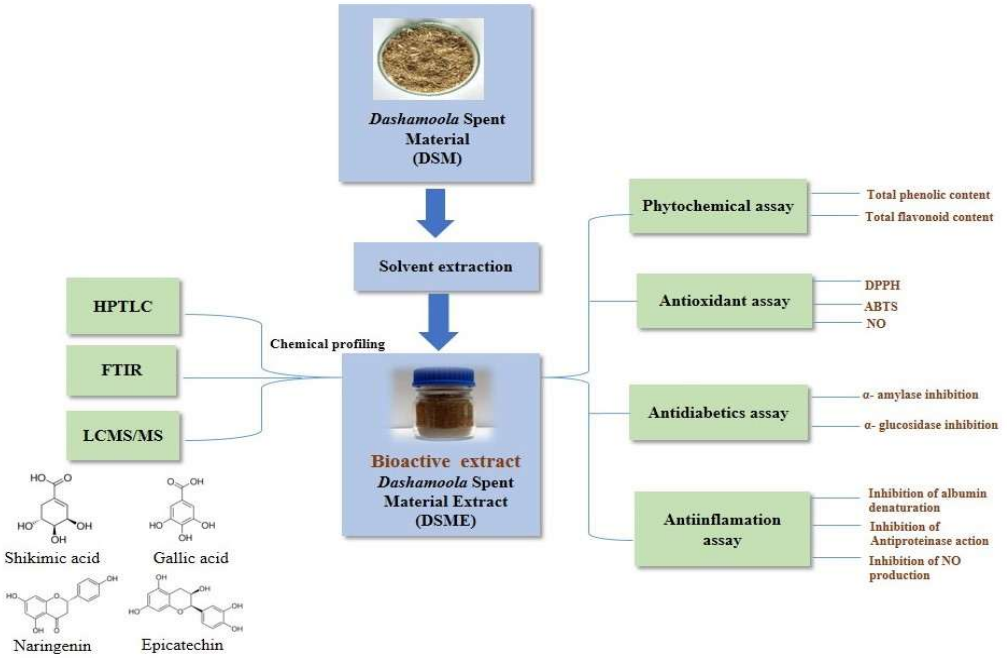

Fig. 1. Graphical abstract showing the extraction, chemical profiling, and bioactivity evaluation of Dashamoola Spent Material (DSM).

Highlights

- Dashamoola is a combination of ten herbal plant roots prescribed in Ayurveda.
- Bioactivity of Dashamoola spent material extract (DSME) was characterized by LCMS/MS.
- Shikimic acid, gallic acid, epicatechin & naringenin were the major polyphenols in DSME.
- DSME was analysed for TPC & TFC; antioxidant potential was proven by DPPH, ABTS & NO.
- Antidiabetic & anti-inflammatory activity of DSME were confirmed by various assays.

3.1. Introduction

Ayurveda, an indigenous system of traditional medicine, is being practiced for over thousands of years. It generally focuses on plant-based medicines for the management of various diseases (Randive et al., 2014). Scientific validation of the traditional medicines are being attempted to trace clues regarding contributing factors in ameliorating debilitating disease conditions (Tungcharoen et al., 2018). Dashamoola is an ayurvedic polyherbal formulation prepared from ten different plant roots, based on traditional Ayurvedic text 'Sahasrayogam'. The plants used in Dashamoola preparation are known to possess therapeutical potential against certain health ailments (Awasthi & Pandey, 2015) which include the roots of ten medicinal plans - five bigger plants called "Valiyapanchamoola" and five smaller plants called "Laghupanchamoola" as recorded in Ayurvedic texts (Vyas et al., 2011). Valiyapanchamoola is a combination of *Stereospermum suaveolens* (Patala) *Premna integrifolla* (Agnimantha), *Aeglemarmelos* (Bilwa) *Gmelinaarborea* (Gamphari) and *Oroxylum indicum* (Shyonaka). Laghupanchamoola category includes *Desmodium gangeticum* (Shalaparni), *Uraria picta* (Prithakpami), *Solanum indicum* (Brihati root), *Solanum xanthocarpum* (Kanthakari) and *Tribulus terrestris* (Gokshura) (Nagarkar et al., 2013). All the plants in Dashmoola are endowed with medicinal properties, mainly anti-inflammatory, hypoglycemic, antihypertensive, vasodilator, analgesic, anti-cholestrolemic, antirheumatic, antioxidant and anti-fever (Nanda & Tiwari, 2016). In the above context, dashamoola plays a versatile role in the biological and pharmacological aspects (Rao, M.L., & Savithramma, N., 2011). There are several products with "dashamoola" as the main ingredient as described in Ayurvedic classics (Karunagoda et al., 2010; Irshad et al., 2009). The need for dashamoola in the market is on the rise because of its utility in preparing various formulations (Nagarkar, B., & Jagtap, S., 2017; Sudhanshu et al., 2012).

In most of the Ayurvedic preparations, water is used as the solvent, and therefore, most of the time active ingredients are not extracted out completely. Therefore, there is great possibility of

retaining phytochemicals with potential biological activity in the spent material. Similar studies conducted on spent cumin (Arun et al., 2018) and black pepper (Prabhu et al., 2015) revealed the potential for value addition of Ayurvedic spent materials as a rich source of bioactives for further formulions in the form of functional foods and nutraceuticals.

Utilization of spent materials generated from Ayurveda industries have got great relevance as the availability of plant materials are getting diminished due to the high demand for the medicinal plants in various preparations and also due to the threat of extinction. The Ayurvedic industries are investigating possibilities for preserving the medicinal plants by various means. One such activity includes the utilization of spent materials for further value addition. In this context, spent materials generated from Ayurveda industries are investigated and found to possess promising biological activities (Arun et al., 2018). Some of the plants used in Dashamoola are becoming extinct, and therefore, the re-utilization of the spent materials for the ayurvedic/nutraceutical preparations, if found potential, could be of high relevance. The medicinal plants in the 'Dashamoola' are reported to possess antioxidant, anti-inflammatory and hypoglycemic action (Nanda & Tiwari, 2016). As Ayurvedic medicine preparations employ water-based decoctions of medicinal plants and other ingredients, the Dashamoola spent materials (DSM in the present study) may retain a major part of the bioactive phytochemicals. Based on this hypothesis, the objectives of the present study is to compare the phytochemical content of DSM with that of fresh dashamoola extract and to evaluate its antioxidant, antidiabetic and anti-inflammatory potential. From this study, we expect to gain valuable information about the compounds that are retained in the spent materials and their potential in encompassing inflammation and diabetes.

3.2. Materials and methods

3.2.1. Chemicals and plant material

2,2'-azino-bis(3-ethylbenzothiazoline-6-sulphonic acid) (ABTS), 2,2-diphenyl-1-picrylhydrazyl (DPPH), α-glucosidase, α-amylase, acarbose, trolox, ascorbic acid polyphenol

standards, dulbecco's modified eagle's media (DMEM), fetal bovine serum (FBS), horse serum, rosiglitazone, 4-nitrophenyl α-D-glucopyranoside, 3-(4,5-dime thylthiazol-2-yl)-2,5-diphenyl tetrazolium bromide (MTT), gallic acid, dimethyl sulfoxide (DMSO), lipopolysaccharides (LPS), dexamethasone, aspirin, trypsin, casein, perchloric acid, Griess reagent were procured from Sigma Aldrich Chemicals (St. Louis, MO, USA). Folin–Ciocalteu reagent, sodium chloride (NaCl), ethylene diamine tetraacetic acid (EDTA), sodium carbonate (Na_2CO_3), tris-HCl, potassium hydroxide (KOH) were obtained from MERK. Trypsin-EDTA, antibiotic-antimycotic were purchased from Gibco Invitrogen (Carlsbad, CA, USA). 2-NBDG (2-(N-(7-nitrobenz-2-oxa-1,3-diazol-4-yl) amino)-2-deoxyglucose) was procured from Molecular Probe (Invitrogen Life Technologies, Carlsbad, CA, USA). All the reagents used were of high-quality analytical grade.

Fresh Dashamoola raw materials in the proportion as used for the Ayurveda preparations and corresponding spent Dashamoola materials were supplied by M/s. Kottakkal Arya Vaidyasala, Kottakkal, Kerala, India (M/s. AVS Kottakkal Ltd).

3.2.2. Proximate composition and mineral analysis of Dashamoola spent materials (DSM)

Initially, moisture content (AOAC method 930.15) of the oven-dried (105°C) DSM was estimated in triplicates. For this, dried samples were allowed to cool in a desiccator before weighing. Weighed samples used for the estimation of ash content (AOAC method 923.03) were heated (550°C) in a muffle furnace with for 16 h. Micro-Kjeldahl method furnished protein content in the samples by converting resultant nitrogen to protein (multiplying by 6.25). Fat content was determined By using the soxhlet extraction method (AOAC method 920.39) and the total carbohydrate content was calculated based on the difference method.

3.2.3. Preparation of the extracts

The dried raw and spent sample powder (40-60 mesh size) were extracted with 70% ethanol by hot extraction method using soxhlet apparatus lasting 6 hours. The extracts were filtered

and then concentrated using a rotary evaporator (Heidolph, Germany). The concentrate was then lyophilized (VirTis Genesis, USA) and stored at -4°C until use the lyophilized samples were then subjected to various analysis as described below.

3.2.4. High-performance thin layer chromatography (HPTLC)

The 70 % ethanolic extract of 1 g Fresh Dashamoola (DE) and 1g spent Dashamoola (DSME) (10 mL) was dissolved in 10 mL of methanol. Pre-activated HPTLC Silica gel 60 F_{254} plates (10 × 10 cm; Merck, Darmstadt, Germany) was employed to perform chromatography. Then, the plates were submitted to densitometric scanning on a CAMAG scanner III at 490 nm. Using an automatic applicator in HPTLC (Linomat-V with N_2 flow, CAMAG Repostar 3, Switzerland), extracts were applied 8mm above one end of each plate forming 6mm wide bands. Before commencing chromatography, the plates were subjected to an activation process involving methanolic prewashing (60°C for 5 minutes). Scanning speed of 40 mm s^{-1} and slit size of 5 × 0.45 mm were ensured for the analysis that utilized a mobile phase constituting Toluene: Ethyl acetate: Formic acid: Methanol (7:5:1:0.5). Plates were developed on a twin glass chamber (10 × 10 cm) filled with the mobile phase. Plates were then air-dried, derivatized, and then heated to 105 °C for 5 min. Derivatization of chromatogram makes use of the Camag glass reagent spray (5% sulfuric acid in methanol). After 30 minutes, plates were observed using Camag UV cabinet at 254 and 366 nm (Kumar et al., 2015).

3.2.5. Fourier transform infrared spectrum (FTIR)

FTIR spectroscopy was used for characterizing the functional groups of phytochemicals present in DE and DSME. The spectra were recorded using the Bruker FT-IR (Germany) spectrometer in the wavenumber range between 4000 to 400 cm^{-1}.

3.2.6. Phytochemical analysis of spent Dashamoola

3.2.6.1. Determination of total phenolic content (TPC)

Estimation of Phenolic content in DSME was done using Folin-Ciocalteau reagent with gallic acid (1-1000 µg/mL) serving as standard (Singleton, V.L., & Rossi, J.A., 1965). Reaction mixtures containing 100-500 µL of DSME and Folin–Ciocalteu reagent (0.5 mL) mixed with 20% sodium carbonate were incubated for 90 minutes at 760 nm on a Shimadzu ultraviolet-visible 2600 (UV) spectrophotometer (Kyoto, Japan). The volume of the reaction mixtures was made up with distilled water. Gallic acid equivalent (mg/100g) of DSME was plotted and the resulting standard curve was used for the quantification of polyphenols.

3.2.6.2. Determination of total flavonoid content (TFC)

Flavonoid content in DSME was estimated by aluminum chloride method (Chang et al., 2002). Initially, varying concentrations of quercetin (20-100 µg) and DSME (100–500 µL) were prepared. To the samples, 0.3 mL of aluminium chloride (10%), sodium nitrite (5%) and 2 mL NaOH were added. The final volume (10 mL) of the reaction mixtures were attained by adding distilled water. After the reaction, absorbance of each sample was read at 510 nm using a spectrophotometer (Shimadzu ultraviolet-visible 2600 (UV) spectrophotometer (Kyoto, Japan).

3.2.7. Chemical profiling and quantification using LCMS/MS

The quantitative analysis of 28 compounds – catechol, catechin, quinine, naringenin, tocopherol, gallic acid, chlorogenic acid, epicatechin, syringic acid, vanillic acid, caffeic acid, epigallocatechin, ferulic acid, myricetin, quercetin, p-Coumaric acid, luteolin, apigenin, kaempferol, rutin, diadzein, hesperetin, shikimic acid, ellagic acid, morin, genistein, cinnamic acid, and chrysin were performed by LC-MS/MS system (Nexera with LCMS-8045, Shimadzu Corporation, Kyoto, Japan) - HPLC (Nexera LC-30AD) equipped with an autosampler (SIL-30AC), temperature-controlled column oven (CTO-20AC) and prominence diode array

detector (SPD-M20A) coupled to triple quadrupole mass spectrometer (Nexera with LCMS-8045, Shimadzu Corporation, Kyoto, Japan). Working standards were prepared by diluting the stock solution with water concentration ranging from 0.01- 1 µg/ml. The quantification of all the polyphenols was carried out on Shimadzu Shim-pack GISS C18 column (150 X 2.1 mm i.d, 1.9 µm) that used water / formic acid (100/0.1%) mobile phase for solvent A and 100 % methanol for solvent B. Polyphenols were eluted with a linear gradient system as follows: 0.5 – 1.9 min 5% of solvent B, 2.0 – 10.0 min 98% of solvent B, 10.1 – 15 min 98% of solvent B and 15.1 – 17 min 5% of solvent B, a flow rate of 0.3 mL/min, the injection volume was 10 µl and oven temperature of 40 °C. Positive and negative modes of multiple reaction-monitoring (MRM) mode were operated during LC-MS/MS with electrospray ionization (ESI). LC-MS/MS data were collected and processed by Lab Solutions software (Shimadzu, Kyoto, Japan). An interface temperature of 400°C was conditioned for ionization, desolvation line temperature of 300°C, heat block temperature of 400°C, nebulizing gas flow (nitrogen) at 3 L/min and drying gas flow (nitrogen) at 10 L/min. Each calibration solution was analyzed in triplicate, and the average value of the results was used as the representative for each point. The results obtained are represented as polyphenols in µg/g with SD (n = 3). The values are statistically significant as F>F critical one-tail. Therefore, the variances of the two populations are unequal. The analytical performance of the LC-MS/MS method is given in Table 3.1.

Table 3.1: The analytical performance of the LC–MS/MS method of 28 compounds.

Compounds	R_t (min)	Parent ion (m/z)	Molecular Ion (m/z)	Ion Mode	CE (V)	Calibration equation	r^2	Linear Range (µg/L)	DL/QL (µg/L)
1. Catechol (PA)	1.87	111.20	78.95/64.10	+ve	-9/-25	y=387.253x+7.0483e+006	0.986	5-50	0.07/0.23
2. Catechin (F)	6.75	291.20	139.10/165.05	+ve	-15/-13	y=10393.1x-16953.5	0.993	5-150	2.20/6.68
3. Quinine (A)	6.88	325.20	307.10/184.05	+ve	-24/-28	y=70839.3x+3503.38	0.996	5-150	0.27/0.81
4. Naringenin (F)	7.28	273.20	153.05/147.15	+ve	-17/-21	y=5753.24x-13117.0	0.992	5-150	0.78/2.37
5. Tocopherol (V)	12.87	429.50	163.15/205.05	+ve	-22/-23	y=12257.5x-27446.3	0.993	5-150	2.31/7.01
6. Gallic acid (PA)	1.91	169.20	125.05/81.00	-ve	17/17	y=2779.60x+1214.12	0.992	5-150	3.20/9.70
7. Chlorogenic acid (PA)	6.81	353.00	191.20/92.90	-ve	16/43	y=10282.0x+16136.9	0.997	5-150	1.27/3.85
8. Epicatechin (F)	6.77	289.00	245.20/205.20	-ve	14/16	y=2231.57x-3359.76	0.993	5-150	7.08/21.46
9. Syringic acid (PA)	7.20	197.20	182.20/123.05	-ve	14/24	y=941.096x+12146.4	0.996	5-150	10.44/31.65
10. Vanillic acid (PA)	6.79	167.20	152.10/108.10	-ve	17/19	y=8887.775x+2823.33	0.991	5-150	14.35/43.48
11. Caffeic acid (PA)	6.91	179.20	135.15/134.10	-ve	16/30	y=31106.3x-2363.27	0.995	5-150	0.49/1.49
12. Epigallocatechin (F)	2.01	456.90	169.15/125.05	-ve	17/40	y=904.191x-524.176	0.987	5-50	2.90/8.79
13. Ferulic acid (PA)	7.36	193.20	134.00/178.00	-ve	15/10	y=2014.91x+171906	0.992	5-50	4.37/13.23
14. Myricetin (F)	7.65	317.00	151.20/179.20	-ve	25/19	y=15064.0x-14109.0	0.995	5-150	0.25/0.75
15. Quercetin (F)	7.92	301.20	151.05/179.00	-ve	22/18	y=48446.6x+52582.0	0.991	5-150	0.62/1.88
16. p-Coumaric acid (PA)	7.34	163.00	119.15/93.10	-ve	15/33	y=12379.7x+41113.6	0.992	5-150	2.13/6.46
17. Luteolin (F)	7.92	285.20	151.10/175.05	-ve	25/25	y=29060.1x+177101	0.991	5-150	0.27/0.83
18. Apigenin (F)	8.18	269.20	149.05/151.00	-ve	23/25	y=26104.3x-13101.5	0.993	5-150	0.48/1.45
19. Kaempferol (F)	7.83	285.20	159.15/187.05	-ve	31/27	y=1243.29x-487.739	0.993	5-150	1.44/4.36
20. Rutin (F)	7.34	609.20	300.00/301.15	-ve	38/34	y=25186.6x+9234.48	0.995	5-150	0.08/0.23
21. Diadzein (F)	7.91	252.90	208.20/224.15	-ve	29/25	y=8324.16x-13781.5	0.981	5-150	0.71/2.16
22. Hesperetin (F)	7.86	301.20	164.10/286.05	-ve	25/18	y=17857.8x-14187.8	0.993	5-150	0.57/1.73
23. Shikimic acid (PA)	1.76	172.90	111.20	-ve	11	y=864.091x+63809.9	0.969	5-150	5.79/17.55
24. Ellagic acid (PA)	7.56	300.90	185.10/145.20	-ve	31/40	y=648.613x+9964.71	0.992	5-150	2.28/6.92
25. Morin (F)	7.74	301.20	151.00/149.15	-ve	20/25	y=49085.8x+113300	0.994	5-150	0.59/1.79
26. Genistein (F)	7.81	269.20	133.20/132.05	-ve	31/46	y=11955.6x-6477.21	0.990	5-150	0.59/1.79
27. Cinnamic acid (PA)	7.93	147.00	103.05	-ve	13	y=628.783x+1513.72	0.993	5-150	6.60/20.01
28. Chrysin (F)	8.39	252.90	62.95/143.20	-ve	32/27	y=20464.6x-17508.2	0.996	5-150	0.41/1.26

PA-Phenolic acid, A- Alkaloid, F- Flavonoid, V- Vitamin, Rt – Retention time, DL- Detection Limit, QL- Quantitation Limit

3.2.8. Antioxidant analysis of Dashamoola spent material

3.2.8.1. 2,2-diphenyl-1-picrylhydrazyl (DPPH) radical scavenging activity

DPPH scavenging activity of DSME was estimated using a 130mM DPPH solution. The reaction was allowed to take place between 2.5 mL of DPPH and 500 µL of DE / DSME (10 – 250 µg/mL) and ascorbic acid (1 – 10 µg/mL) (Brand-Williams et al., 1995). Following this, the mixture was vortexed and incubated in the dark for 90 minutes at 33°C. The absorbance of the assay mixture was read at 517 nm using UV/VIS spectrophotometer 2600 (Shimadzu, Japan) at 517nm. The following equation was used to calculate IC_{50} (µg/mL) values.

$$\%\ Inhibition = \frac{Absorbance\ of Control - Absorbanc\ \ of\ Sample}{Absorbance\ of\ Control} \times 100 \quad (1).$$

3.2.8.2. 2, 2'-azino-bis (3-ethylbenzothiazoline-6-sulphonic acid) (ABTS) assay

ABTS assay uses radical cations prepared from 2 mM (0.0548 g in 50 ml) ABTS dissolved in distilled water (Re et al., 1999). Apart from ABTS, potassium persulfate 70 mM (0.0189 g in 1mL) was also prepared. A reaction mixture containing 200 µL of potassium persulfate and 50 mL of ABTS were prepared and used post 2 hours of mixing. Solutions of DE and DSME were prepared at varying concentrations (1 – 100 µg/mL) by adding 0.3 mL of ABTS radical cation and 1.7 mL phosphate buffer (pH 7.4). Trolox (1 – 10 µg/mL) was used as positive control for the assay absorbance was read at 734 nm, with triplicate values recorded for DE, DSME and Trolox .

$$\text{Inhibition (\%)} = 100 \times (A_0 - A_1)/A_0 \quad (2).$$

Where absorbance of the control and DE/DSME /standard are A_0 and A_1, respectively. IC_{50} values were determined from the curve obtained by plotting % inhibition and concentration. The IC_{50} value is indirectly proportional to antioxidant capacity.

3.2.8.3. Nitric oxide (NO) radical scavenging assay

Nitric oxide radical scavenging assay revolves around the production of nitrite ions and the subsequent spectrophotometric measurement of the resulting chromophore at 546 nm

(Govindarajan et al., 2003). At physiological pH, nitric oxide gets released from sodium nitroprusside, which further reacts with oxygen to form nitrite ions. In the presence of nitric oxide scavengers, nitrite ion production plummets as these scavengers competitively use up the oxygen levels. Greiss reagent (1% sulphanilamide, 2% O-phosphoric acid and 0.1% of N-(1- naphthyl) ethylenediamine dihydrochloride) is used to estimate the nitrite ion concentration. Approximately 1 mL of sodium nitroprusside (5mM) was mixed with varying concentrations of DE and DSME (200-1000 µg/ml) in phosphate buffer (pH 7.4, 0.1 M), followed by incubation at 25°C for 2 h. Post incubation, 1.5 mL of Greiss reagent was added after the removal of the same volume of the reaction mixture. The resulting chromophore is formed in two steps- diazotization and coupling with Greiss reagent components. The absorbance of DE, DSME, ascorbic acid (10 – 500 µg/mL) and control tubes was measured at 546 nm after the formation of chromophores.

3.2.9. Antidiabetic assay of Dashamoola spent material

3.2.9.1. α -amylase inhibition assay

The assay method described by Xiao (Xiao et al., 2006) depends on the starch-iodine test for assessing α-amylase enzyme inhibition. The most active methanolic extract form was selected for the assay. Intitially, varying concentrations of DE and DSME (50 – 250 µg/mL) extracts were added to the mixture, followed by the addition of 0.02 M sodium phosphate buffer (pH 6.9) and 6 mM NaCl. 1 U/mL of porcine pancreatic α-amylase was added to all the mixtures which was then incubated at 50^{o} C for 30 min post addition of soluble starch (1% w/v). Finally, iodine reagent (5 mM I_2 and 5 mM KI) was added prior to stopping the reaction using 1 M HCl. Absorbance of the samples was read at 580 nm on a multiplate reader (Synergy 4 Biotek multiplate reader, USA). Wells without any extract was used as control, and a known amylase inhibitor, Acarbose (1 – 25 µg/mL), was used as the positive control. The percentage of amylase enzyme inhibition was calculated using the following equation.

$$\%\ Inhibition = \frac{Absorbance\ of Control - Absorbance\ of\ Sample}{Absorbance\ of\ Control} \times 100 \quad (3).$$

3.2.9.2. α - glucosidase inhibition assay

α-glucosidase assay followed in this study is based on the procedure of Adisakwattana (Adisakwattana et al., 2004), with slight modifications. This assay aims at estimating the IC_{50} values of samples spectrophotometrically. Initially, 200 µL of DE and DSME (50 – 250 µg/mL) were premixed with 20 µL of α -glucosidase (1.25 U/mL) and was incubated at RT for 5 min. The extracts were dissolved in 50 mM potassium phosphate buffer (pH 6.8) before premixing. To the samples, 200 µL of 50 mM phosphate-buffered 4-nitrophenyl α-D-glucopyranoside (1mM) was added to initiate the reaction and incubated the reaction mixture for 20-minutes at room temperature. The addition of 500 µL of 1M Na_2CO_3, terminates the reaction leaving a final volume of 1.5 mL in the reaction tubes. Quantity of p-nitrophenol released during the reaction was determined by reading samples at 405 nm using a microplate reader (BioTek Instruments Inc. Winooski, VT). Concentrations ranging from 10 – 100 µg/mL was used for acarbose (positive control). Glucosidase activity (IC_{50} values) of the extract was calculated based on the triplicate values obtained during spectrophotometric analysis.

$$\%\ Inhibition = \frac{Absorbance\ of Control - Absorbanc\ \ of\ Sample}{Absorbance\ of\ Control} \times 100 \quad (4).$$

3.2.9.3. Glucose uptake assay

3.2.9.3.1. Cell culture conditions

L6 myoblast was obtained from NCCS, Pune, India. L6 Myoblasts were nurtured in Dulbecco's modified eagle's medium (DMEM) containing 10% fetal bovine serum (FBS) and 1% antibiotic-antimycotic solution. A humidified ambience (37°C, 5% CO_2) was set up for the growth of the cells. The cells were seeded at a density of 1x 10^3 cells/well on 24 well-plates and 96-well black plates (BD Biosciences, Franklin Lakes, NJ, United States) for different assays.

3.2.9.3.2. Cell viability assay

The cellular toxicity of DSME on L6 cells was determined by the MTT assay (Mosmann, T., 1983). The cells were seeded and cultured in 96 well plate for 24h and then the cells were incubated with various concentrations of DSME (10 – 500 µg/mL) containing complete DMEM medium for 24 h. After incubation, 100 µL of MTT (0.5 mg/mL) was added to all wells and kept at dark for 4 h. After discarding the MTT medium, 200 µL of DMSO was added to solubilize the formed formazan by shaking. Then, the absorbance was measured at 570 nm using the microplate reader (Synergy4 Biotek multiplate reader, USA). The untreated cells were used as control.

Glucose uptake assay was done in differentiated L6 myoblast cell line as described by Chen (Chen et al., 2010) with minor modifications. Cells were seeded in 96-black well plates and allowed to differentiate into myotubes as described above. The assays were performed at 70% cell confluency, the cells were washed with phosphate-buffered saline (PBS), and treated with DSME extract at two different concentrations 50 µg/mL and 100 µg/mL in low glucose media for 24 hrs. After incubation, cells were incubated with 2-NBDG in PBS at 37 ℃ for 30 min. Cells were then incubated and subjected to washing with phosphate buffer (pH 7.4), and observed under confocal microscopy (Pathway 855, BD Bioscience, USA).

3.2.10. Anti-inflammatory activity of spent Dashamoola

3.2.10.1. Inhibition of albumin denaturation

Anti-inflammatory activity of DE and DSME extract was determined using inhibition of albumin denaturation assay with minor modification (Mizushima, Y., & Kobayashi, M., 1968 and Sakat et al., 2010). Different concentrations of DE and DSME (10 – 250 µg/mL) and 1% bovine albumin was mixed, and the pH of the mixture was adjusted using 1N HCl. The Reaction mixture was incubated for 20 min at 37 ºC, and then temperature increased to 60 ºC for 30 min. After incubation, the samples were cooled and turbidity was read at 660 nm using

a microplate reader (Synergy4 Biotek multiplate reader, USA). Reaction mixture without samples was used as control and aspirin (10 – 250 µg/mL) was used as standard. Experiments were done in triplicates. Percentage inhibition of protein denaturation was determined using the following equation:

Percentage inhibition = (Abs Control – Abs Sample) X 100/ Abs control (5).

3.2.10.2. Inhibition of antiproteinase action

The antiproteinase test was performed according to Oyedepo and Sakat with slight modification (Oyedepo, O.O., & Femurewa, A.J., 1995 and Sakat et. al., 2010). The reaction mixture with 0.06 mg trypsin, 20 mM Tris HCl buffer (pH 7.4), and different concentrations (10 – 250 µg/ml) of DE / DSME and aspirin (10 – 250 µg/mL) was incubated for 5 min at 37ºC. Then, 0.8 % (w/v) casein was added to the mixture and incubated for 20 min to arrest the reaction. After incubation, 70% perchloric acid was added to the reaction mixture. Absorbance of the supernanant from the resulting cloudy suspension was read at 210 nm using multiplate reader (Synergy4 Biotek multiplate reader, USA) against buffer as blank and samples without extract as control. The experiments were done individually in triplicates. Percentage inhibition of proteinase inhibitory activity was determined using the equation below.

Percentage inhibition = (Abs control –Abs sample) X100/ Abs control (6)

3.2.10.3. Nitric oxide inhibition assay

RAW 264.7 cells were procured from ATCC (American Type Culture Collection, Manassas, United States). The cells were maintained in the same way as described under 3.2.9.3.1. The cell viability was estimated using the MTT assay as per the protocol given under 3.2.9.3.2

NO released from immune cells was evaluated in the cultured supernatant media (Green *et al.*, 1982). After pretreatment of DSME extract for 2h, LPS (lipopolysaccharide, 5 µg/mL) was added to all the wells except that of the negative control. After 24 h incubation, all the treated cells in the culture media (100 µL) underwent treatment with 0.1 mL Griess reagent (1%

sulfanilamide, 0.1% naphthylethylene diamine in 2.5% phosphoric acid solution) at ambient temperature for 10 min. The reaction mixture in the 96 well plates were then read at 540 nm using multiplate reader (Synergy4 Biotek multiplate reader, USA). Results were then calibrated using absorbance values obtained from dexamethasone standard.

3.2.11. Statistical analysis

Experimental data provided are mean ± SD (standard deviation) derived from triplicate measurements of values recorded from respective assays. All the data were then subjected Duncan's multiple range tests which is used to assess the significance of mean differences obtained during the initial one-way analysis of variance (ANOVA) using SPSS, standard version7.5.1 (SPSS Inc., USA) and the significance was accepted at $p \leq 0.05$.

3.3. Results and discussion

3.3.1. Proximate analysis of DSM

Proximate analysis of Dashamoola Spent Material (DSM) serves as a toolkit to assess the macronutrient content in it. The proximate composition of DSM were, moisture content - 8.68 ± 0.070%; ash content 3.62 ± 0.049%; fat content 0.90 ± 0.007%; crude protein content: 3.34 ± 0.028% and carbohydrate content: 83.46 ± 0.431%. Thus carbohydrates turned out to be the major macronutrient in DSM.

3.3.2. Comparative evaluation of phytochemicals in DE and DSME by HPTLC

Preliminary evaluation of the phytochemical content of DE and DSME by HPTLC was performed to confirm the retention of bioactive compounds in the spent materials. First glimpse into the distribution pattern of bioactive compounds among DE and DSME was obtained through HPTLC. It is evident from the fluorescence behavior that DSME is enriched with phenolic compounds (Stanek, N., & Jasicka-Misiak, I., 2018). HPTLC fingerprint yielded similar banding pattern and graphs for DE and DSME (Fig. 3.1). Interestingly, highest area (AU) was recorded by DSME (89874.8). Similar R_f values in DE and DSME indicates the

presence of shared bioactive compounds in DSME which were retained even after industrial arishta preparation process (Table 3.2).

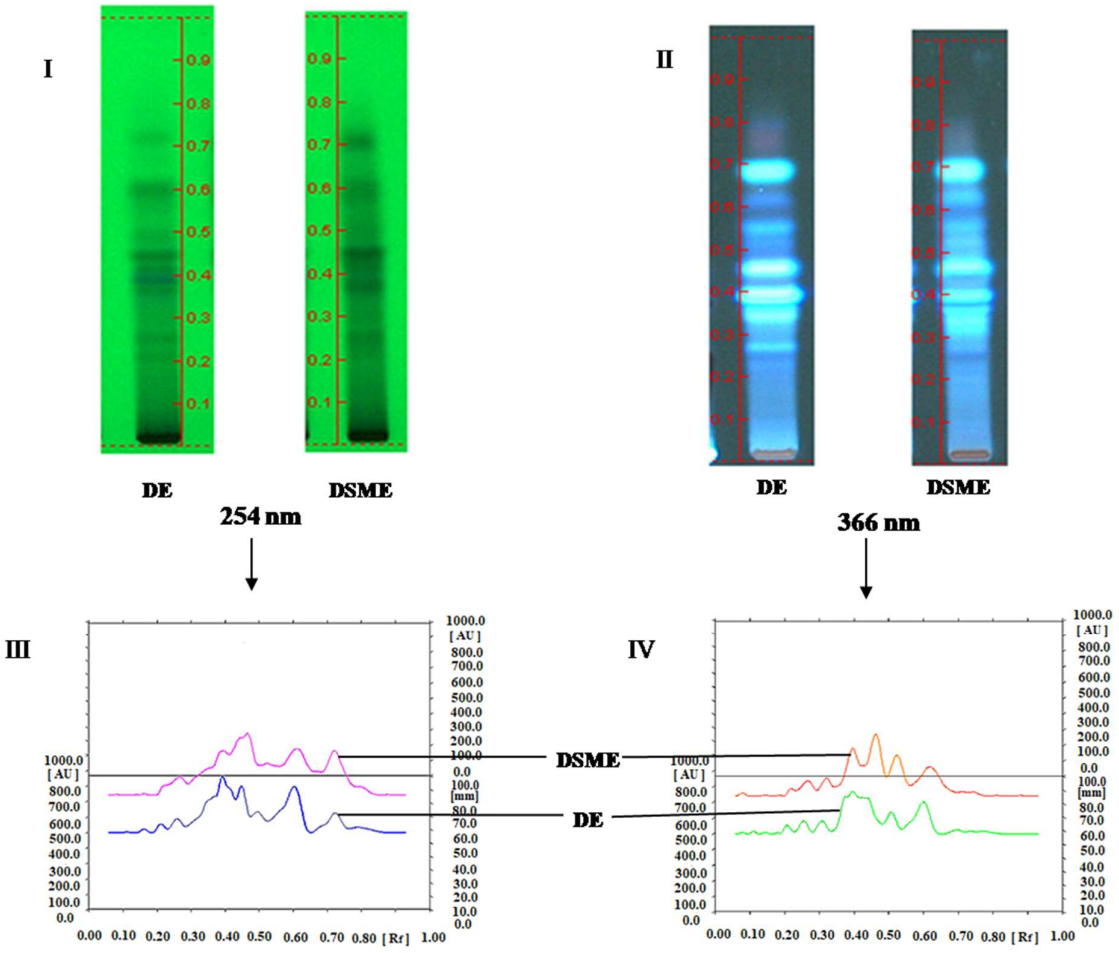

Fig. 3.1. TLC Plate views (I and II) and the corresponding HPTL chromatograms (III and IV) of DE, DSME at 254 and 366 nm.

Table 3.2: HPTLC data of DE and DSME at 254 nm.

DE				DSME			
Peak no.	R_f Value	Area (AU)	% Area	Peak no.	R_f Value	Area (AU)	% Area
1	0.16	374.2	0.61	1	-	-	-
2	0.21	1162.1	1.88	2	-	-	-
3	0.26	2532.5	4.10	3	0.27	5578.6	6.21
4	0.39	22992.6	37.26	4	0.39	17912.9	19.93
5	0.45	7651.4	12.40	5	0.46	22175.3	24.67
6	0.49	4536.5	7.36	6	0.52	9149.0	10.18
7	0.60	15380.6	24.93	7	0.61	18826.4	20.95
8	0.72	5356.3	8.68	8	0.72	14673.3	16.32
9	0.79	1717.2	2.78	9	0.79	1559.3	1.74
Total		61703.4	100%			89874.8	100%

3.3.3. Fourier transform infrared spectroscopy (FTIR)

FTIR spectra of DE and DSME are depicted in Fig. 3.2 presence of phenolic compounds and alcohols has created a broad band at 3334 cm^{-1} owing to the vibratory stretching of the −OH group. Peak formation at 1031 cm^{-1} is from the carboxylic acid carbonyl (C=O) groups contributed by the phenolics. Additionally, −CH bending vibrations (1450−1317 cm^{-1}), C−C stretching vibrations (1612 cm^{-1}) and aliphatic −CH stretching (2936 cm^{-1}) were also recorded (Karattu Veedu et al., 2019). Interestingly DSME was able to retain most of the functional groups from DE.

These striking similarities in HPTLC and FTIR analysis lead to further investigation of DSME using phytochemical assays and LC-MS/MS and other bioactive assays.

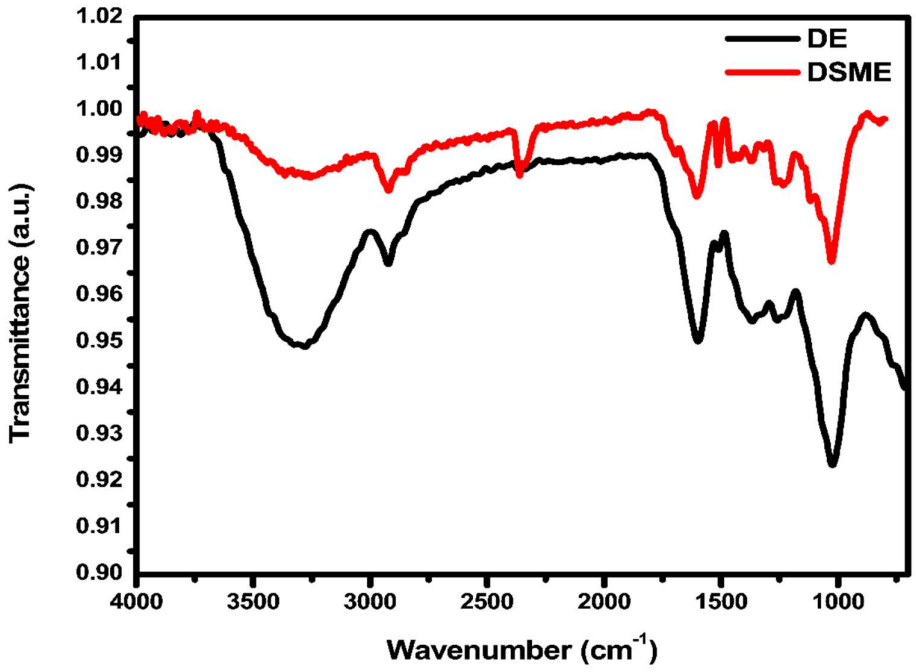

Fig. 3.2. FTIR spectra of Dashamoola raw extract (DE) & Dashamoola Spent Material Extract (DSME).

3.3.4. Determination of total phenolic content (TPC) and total flavonoid content (TFC) in DSME extract

Total phenolic content (TPC) was determined with gallic acid (1 mg/ml) as standard. A calibration curve was obtained that provided a linear equation, using which the phenolic content in DSME was calculated. Phenolic concentration in DSME (143.032 ± 5.0432 mg GAE/g dry weight) clearly suggested its potent antioxidant activity. Quercetin standard (1 mg/ml) was used to determine the total flavonoid content in DSME. The linear equation derived from the standard calibration plot was employed for the assessment of total flavonoids in the extract. Flavonoid content in the sample was estimated to be 62.92 ± 0.981 mg QE/g dry weight.

The total phenolic content of residue from bacaba fruit (Barros et al., 2017), spent coffee (Marina Ramón-Gonçalves et al., 2019), and spent cumin (Arun et al., 2018) was reported to

be 0.11 GAE/g, 15.38 GAE/g, 9–29 mg GAE/g and 1.20 mg GAE/g, respectively. The flavonoid content bacaba fruit residue was 0.086 QE/g, coffee spent 11–27 mg QE/g DW, and spent cumin 3.10 mg QE/g DW. Compare to these reports, DSME possesses much higher phytochemicals.

3.3.5. Profiling and quantification of compounds using LC-MS/MS

A comparative LCMS/MS profiling of DE and DSME clearly suggest that DSME possess more phytochmeicals (Fig. 3.3). The corresponding chromatograms of the standard compounds, DE and DSME are given in Fig. 3.4a, 3.4b and 3.4c respectively. These bioactive compounds are known for their effectiveness in curbing reactive oxidative species (ROS), diabetis, inflammation, cancer, and so on. Shikimic acid (83.225 mg/g) was found to be the most abundant one followed by gallic acid (51.261 mg/g), epicatechin (26.300 mg/g), naringenin (25.054 mg/g) and vanillic acid (14.147 mg/g) indicates the phytochemical richness of DSME in ameliorating disease conditions. Shikimic acid is the key ingredient of the oseltamivir phosphate, the drug used to treat human influenza (WHO, 1980) and also reported to possesses vital neuroprotective capability alongside a key role in preventing blood clots (Estévez et al., 2012). Anticancer, herbicidal and antimicrobial role of shikimic acid makes it the starting material for the synthesis of the drugs (Cuellar et al., 2015) which is directly isolated from the plant source (Hao et al., 2015). Gallic acid ((3,4,5-trihydroxybenzoic acid) and chlorogenic acid (5.158 mg/g) have the ability to fight viral and microbial infections (Sorrentino et al., 2018) alongside stabilizing obesity and hypertension by affecting lipid metabolism (Naveed et al., 2018). Gallic acid is a potent bile stimulator with profound antioxidant efficacy (Anand et al., 1997), anticancerous (Asci et al., 2017; Ho et al., 2010 Yoshioka et al., 2000, Nam et al., 2016; Madlener et al., 2007), hepatoprotective (Jadon et al., 2006). Antioxidant properties of gallic acid are leveraged for the natural colour enhancement of fruit-based beverages (Navruz et al., 2016; Roidoung et al., 2016) and as an oxidation

barrier in double emulsions (Silva et al., 2018). Studies based on epicatechin shed insight into improved insulin sensitivity and evading hyper and hypoglycemia in human test groups (Cremonini et al., 2019). By inhibiting NF-KB production (Fraga et al., 2011) and by exerting various protective actions on the gastrointestinal tract, epicatechin delivers direct benefit for the smooth functioning of the body (Oteiza et al., 2018). Naringenin is indeed a very interesting flavanone carrying a spectrum of biological activity ranging from anti-inflammatory, fibrosis, and even neoplasm (Du et al., 2009; Zeng et al., 2018). Even though lesser in quantity when compared to other polyphenols, ellagic acid (7.311mg/g), tocopherol (5.615mg/g), syringic acid (5.257mg/g), p-Coumaric acid (4.687mg/g), apigenin (3.752mg/g), chrysin (3.299mg/g) were also identified and quantified. The trend followed by HPTLC was also observable in LCMS/MS results as the quantity of some of the detected compounds were more pronounced in DE (Fig. 3.3). The reason for this behavior could be attributed to the fact that 70% ethanol system used for extraction was efficient in leaching out compounds of varying polarities along with physical properties of the compounds, source of the plant materials used, etc. (Chekroun-Bechlaghem et al., 2019; Dehghan et al., 2016). Scientific investigations suggest that these polyphenols possess higher antioxidant capability (Guitard et al., 2016; Kilic et al., 2014; Lesjak et al., 2018; Hodgson et al., 2004; Kyriakis et al., 2015). From the LCMS/MS data, it can be inferred that DSME houses much promising biologically active of phenolic and flavonoid compounds as compared to some of the spent materials already reported (Marina Ramón-Gonçalves et al., 2019; Arun et al., 2018). Therefore, we further explored the antioxidant activities of the extract by in vitro biochemical analysis. Therefore, we further explored the antioxidant activities of the extract by in vitro biochemical analysis.

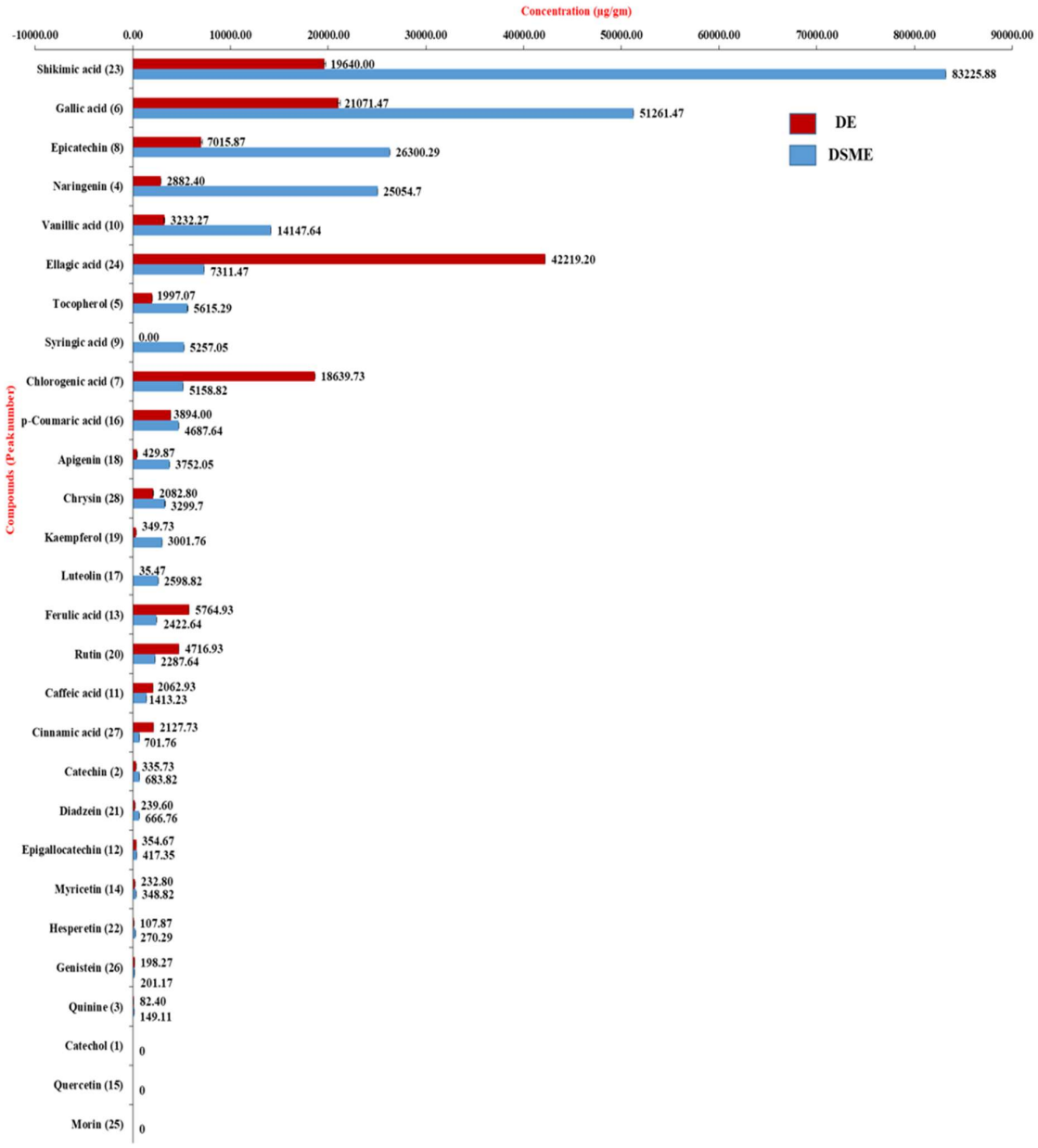

Fig. 3.3. LCMS/MS analysis of compounds in DE & DSME.

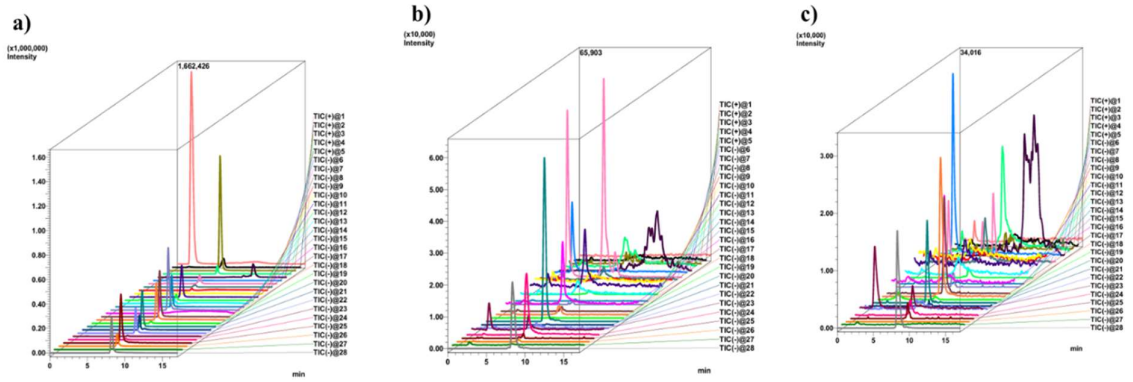

Fig. 3.4. LC-MS/MS chromatogram showing a) standard Polyphenols (150 ppb mix) b) DE c) DSME

1-Catechol, 2-Catechin, 3-Quinine, 4-Naringenin, 5-Tocopherol, 6-Gallic acid, 7-Chlorogenic acid, 8-Epicatechin, 9-Syringic acid, 10-Vanillic acid, 11-Caffeic acid, 12-Epigallocatechin, 13-Ferulic acid, 14-Myricetin, 15-Quercetin, 16-p-Coumaric acid, 17-Luteolin, 18-Apigenin, 19-Kaempferol, 20-Rutin, 21-Diadzein, 22-Hesperetin, 23-Shikimic acid, 24-Elagic acid, 25-Morin, 26-Genistein, 27-Cinnamic acid and 28-Chrysin.

3.3.6. Evaluation of antioxidant efficiency

The degree of scavenging (expressed as IC_{50} value) of free radicals formed during various antioxidant assays is employed to assess the efficiency of a sample in curbing biological oxidation stress in vitro (Frankel. E.N., & Meyer, A.S., 2000). The IC_{50} value (Table 3.3) of DE and DSME against DPPH free radical was found to be 98.19 ± 1.11, 68.17 ± 1.54 µg/mL, and that of standard gallic acid was 2.3 ± 0.09 µg/mL. ABTS assay is yet another tool that measures the extent of antioxidant capacity by trapping $ABTS^{+}$ free radicals. The results are expressed as TEAC value (Trolox equivalent antioxidant capacity) in comparison with the standard Trolox. TEAC of the sample is the concentration equivalent of extract to that of the activity shown by Trolox. TEAC values for 50% reduction in free radicals were 44.2 ± 0.98, 17.8 ± 1.03, and 2.8 ± 0.32 µg/ml for DE, DSME, and Trolox, respectively. Nitric oxide (NO) production in the body is under the strict regulatory control of various biomolecules, including hormones and cytokines. Although NO plays a vital role in maintaining cellular homeostasis,

the overproduction of NO can be deleterious to physiological stability. NO can be viewed as markers of inflammation when expressed for a long period. In addition to inflammation, NO is also seen elevated in patients suffering from cancer, Parkinson's disease (PD), arthritis, and diabetes, (Zou et al., 2002). NO scavenging activity of methanolic extract of DE and DSME was 881 ±1.67, 738 ±1.02 µg/ml, respectively. The standard Vitamin C exhibited an IC_{50} value of 238 ±1.13 µg/ml (Table 3.3).

Table 3.3: Antioxidant, anti-diabetic and anti-inflammation activity of DE and DSME.

Sample	**Anti-oxidant Assays** (IC_{50} - µg/mL)			**Anti-diabetic Assays** (IC_{50} - µg/mL)		**Anti-inflammatory Assays** (IC_{50} - µg/mL)	
	DPPH	ABTS	NO	α-amylase	α-glucosidase	Albumin denaturation	Proteinase Inhibition
Standard	Gallic acid	Trolox	Ascorbic acid	Acarbose	Acarbose	Aspirin	Aspirin
	2.3 ± 0.09	2.8 ± 0.32	238 ± 1.13	6.27 ± 0.92	54.67 ± 1.32	100.12 ± 0.06	70.1 ± 0.01
DE	98.19 ± 1.11	44.2 ± 0.98	881 ± 1.67	154.07 ± 1.57	102.91 ± 0.24	95.04 ± 0.01	78.6 ± 0.01
DSME	68.17 ± 1.54*	17.8 ± 1.03*	738 ± 1.02*	129.19 ± 0.84*	77.03 ± 0.92*	61.17 ± 0.00*	60.8 ± 0.00*

*Each value represents mean ± SD (standard deviation) from triplicate measurements. DSME significantly different from DE; (p value ≤0.05).

3.3.7. In vitro antidiabetic assay

α-amylase found in the saliva and pancreatic juice is a hydrolizing enzyme that cleaves alpha 1, 4 glucosidic bonds in starch, thereby exposing the resulting oligosaccharides for the final conversion to glucose, leading to elevated blood glucose level (Hanhineva et al., 2010). On the other hand, α-glucosidases found in the intestinal cells aid absorption by catalyzing undigested carbohydrates to monosaccharides (Kim et al., 2010). Therefore, inhibitors of α-glucosidases and α-amylase are responsible for the lowering of postprandial blood sugar levels by delaying

the availability of the respective enzymes. Hence, the antidiabetic potential of DE and DMSE was evaluated in terms of inhibition of the action of digestive enzymes. The α-amylase inhibition of DE and DSME recorded IC_{50} values of 154.07 ± 1.57 and 129.19 ± 0.84 µg/mL, respectively, whereas that of acarbose was 6.27 ± 0.92 µg/mL (Table 3.3). The IC_{50} values of DE and DSME in α -glucosidase inhibition assay were 102.91 ± 0.24 and 54.67± 1.32 µg/mL, respectively, while that of the standard (acarbose) was 77.03 ± 0.92 µg/mL (Table 3.3). It can be seen that DSME demonstrated superior activity over DE in all the test assays. This striking inhibitory potential of both the extract can be explained based on the molecular structure of the bioactive compounds present. Polyphenols and flavonoids are made of glycoside linkages, whose presence and structural variations cause enzyme inhibition (Wang et al., 2018). Plant extracts with high antioxidant potential have shown strong antidiabetic capacity during in vitro tests involving α-amylase and α-glucosidase enzymes (Sobeh et al., 2017; Sekhon-Loodu, S., & Rupasinghe, H. P., 2019). Synergistic effect of bioactive compounds presents in the samples including cholorogenic acid, caffeic acid, etc may have caused amelioration during the tests (Chiou et al., 2017; Aras et al., 2019).

3.3.8. Glucose uptake assay

The role of skeletal muscle in rendering glucose homeostasis and oxidation is well documented (Engeli et al., 2012). Increasing the uptake of glucose by skeletal muscle cells has been one of the important targets for anti-diabetes therapy (Arha, 2017). It is known that glucose uptake mediated by the upregulation and expression of GLUT4 found in adipose tissue is key to an increase in sensitivity to insulin. In the case of type 2 diabetes, the cells including skeletal muscle cells fail to uptake glucose, creating an imbalance in the glucose homeostasis that leads to the onset of hyperglycemia. As DSME exhibited significant anti-diabetic properties, as established in the preliminary screening, it prompted us to carry out further studies to assess its efficacy in inducing glucose uptake in L6 myoblast.

Cytotoxicity effect of DSME on cell growth and survival was studied using the MTT assay. L6 myoblast cell lines were able to tolerate up to 500 µg/mL DSME while maintaining desirable cell viability of above 70% (Fig. 3.5). These results indicated that DSME extract did not cause any cytotoxicity in cells in vitro. Therefore, concentrations of DSME below this level (50 µg/mL and 100 µg/mL) were selected for the cellular experiments.

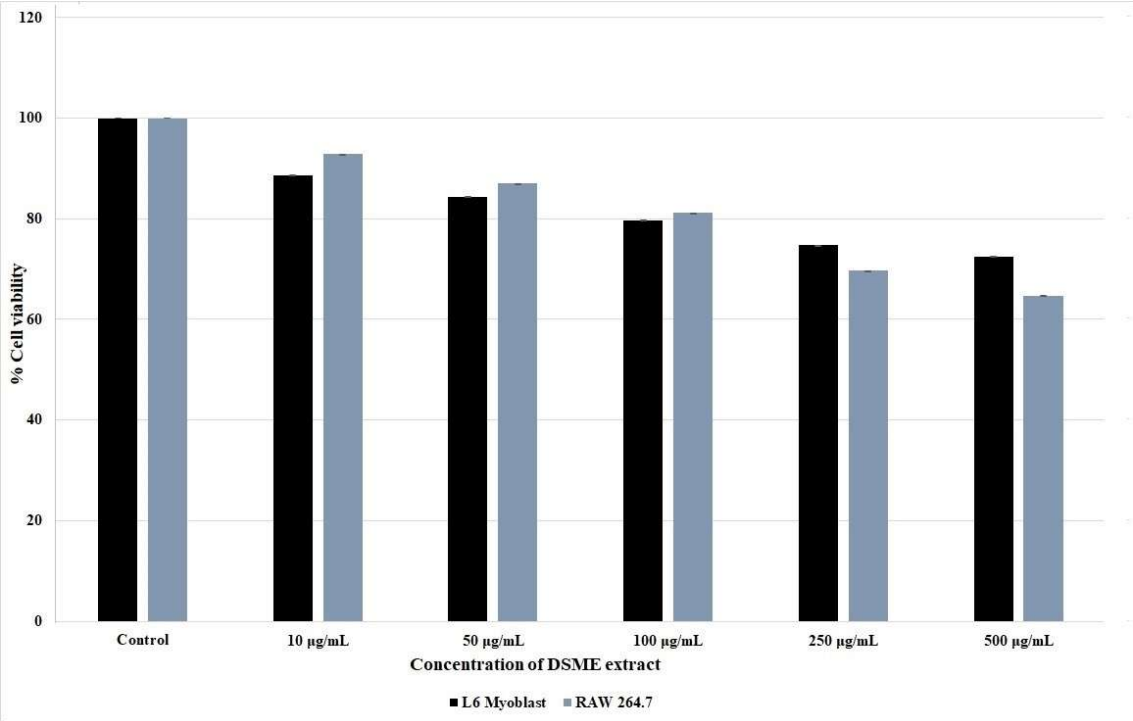

Fig. 3.5. The effect of DSME extract on L6 myoblast and RAW 264.7 cells viability by MTT assay (The data represents mean ± SD of three independent experiment).

Glucose uptake efficacy of DSME was tested in glucose fluorescent analog, 2-NBDG (10 mM) L6 myoblast aided by confocal imaging Fig. 3.6 shows increased 2-NBDG uptake as evidenced by the increased fluorescent intensity in participant cells. However, the activity was less than the metformin, a standard drug used as the positive control, as can be noted from the higher fluorescent intensity under identical experimental conditions. As can be seen, the treatment of cells with DSME induced cellular uptake of 2-NBDG, indicating its intervention in diabetes management, presumably by GLUT4 translocation process.

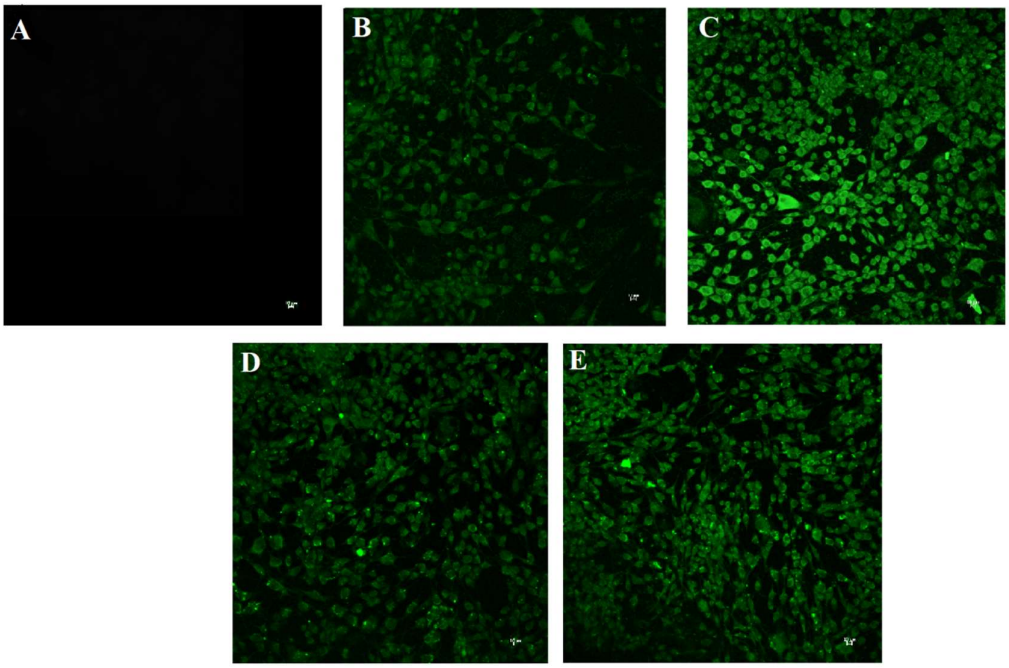

Fig. 3.6. Glucose uptake (2-NBDG) in L6 myoblast cells was observed under confocal microscopy (BD Falcon). Images A to E depicts A- Blank, B- control, C- Metformin, D- 50µg/mL DSME, E- 100µg/mL DSME.

3.3.9. In vitro anti-inflammatory assay

The anti-inflammatory activity of DSME was assessed in terms of inhibition of albumin denaturation, antiproteinase action, and NO production by RAW 264.7 cells.

3.3.9.1. Albumin denaturation inhibition by DSME extract

Protein denaturation is a process in which proteins lose their structural conformation due to external stress or any substances, such as strong base or acid or heat. When denatured, most of the biological proteins lose their biological function. Denaturation of proteins is known to be the main course of inflammation (Mizushima, Y., & Kobayashi, M., 1968 and Sakat et al., 2010). As a part of the examination of the mechanism of the anti-inflammatory activity of DE and DSME, its ability to inhibit protein denaturation was studied. The results suggest that DSME extract was effective in inhibiting heat-induced albumin denaturation. DE and DSME demonstrated IC_{50} values of 95.04 ± 0.019 and 61.17 ± 0.004 µg/mL respectively against

inhibition of protein denaturation that was much better than aspirin (100.12 ± 0.061 μg/mL), the standard anti-inflammation drug (Table 3.3). Thus, DSME resulted in higher inhibition when compared to DE and aspirin.

3.3.9.2. Proteinase inhibition by DSME extract

Proteinase enzymes (proteinases) have been associated with arthritic reactions. Neutrophils are known to be a rich source of proteinase and are confined inside cellular components like lysosomes. It was reported that the proteinase secreted by leukocytes plays an important role in the development of tissue damage during inflammatory reactions and a significant level of defense was provided by proteinase inhibitors. According to Das and Chatterjee (1995), a significant level of protection was provided by proteinase inhibitors. The IC_{50} value of DSME in anti-proteinase assay produced 60.8 ± 0.003 μg/mL inhibitory activity whereas that of aspirin was 70.1 ± 0.012 μg/mL (Table 3.3). DE on the otherhand inhibited proteinase activity (IC_{50} 78.6 ± 0.015 μg/mL) in a compatitive manner but with less effectiveness than aspirin and DSME. DSME exhibited the highest anti-proteinase activity among all the test groups. The presence of bioactives in DSME might have contributed to their anti-inflammatory activity.

The cytotoxicity of the DSME on RAW 264.7 cells indicated cell viability above 70% on treatment of the cells with DSME at a concentration up to 500 μg/mL, and therefore, concentrations of DSME below this level (50 μg/mL and 100 μg/mL) were selected for other cellular experiments. DSME was also able to establish potent anti-inflammatory activity against LPS-induced NO formation in RAW 264.7 cell line (at 10–500 μg/mL concentrations) by significantly lowering nitrite concentration in nitrite estimation assay.

3.3.9.3. Effect of DSME on NO production by RAW 264.7 cells

Estimation of inhibited NO produced by RAW 264.7 cells was carried out using Griess reagent. Cellular acquisition of anti-inflammatory capability is reflected in the lowering of NO production post antigenic challenge. Unstimulated cells were found to produce fewer NO when

compared to LPS treated (5 μg/mL) RAW 264.7 macrophage cells. Effectiveness of DSME extract (10–500 μg/mL) in neutralizing LPS-induced NO generation can be drawn from the results obtained in vitro. (Fig. 3.7). At 500 μg/mL, it can be clearly seen that DSME was able to retard NO production in a concentration-dependent manner, an activity superior to dexamethasone which served as the positive control. Evidence from this assay proves the potency of DSME in combating inflammation. There are instances in which ethanolic extract with high NO scavenging activity exhibited superior anti-inflammatory potential by impacting transcription factors leading to inhibition of cytokine production (Junior et al., 2020). Individual herbs that constitute Dashamoola were reported to have anti-inflammatory, antipyretic, analgesic properties, supported by various studies. Individual anti-inflammation contributions from *Uraria picta* root (Kale et al., 2012) and *Solanum indicum* Linn. fruits (Deb et al., 2014) have been documented in separate studies. Synergistic effects of the retained, flavonoids and phenolic acids in DSME could have attributed to the observed beneficial effects in vitro.

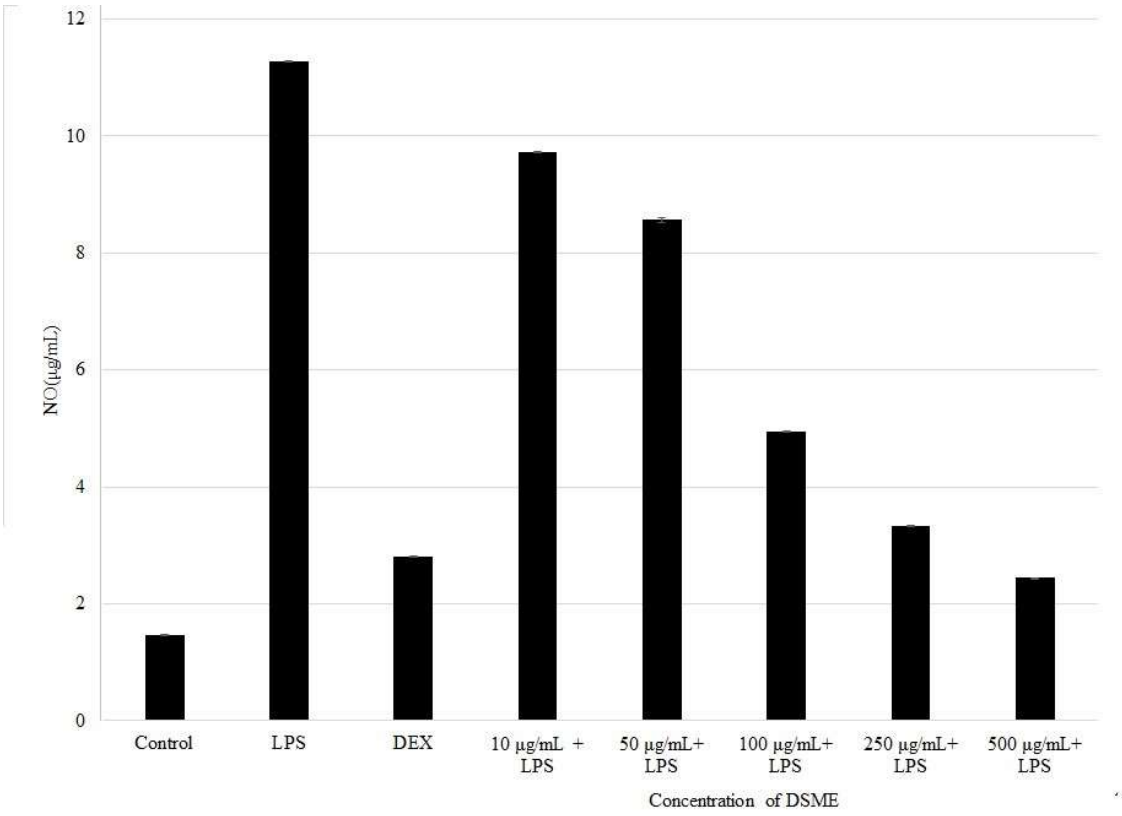

Fig. 3.7. NO Production inhibition assay by Griess reagent.

3.4. Conclusion

The study confirmed the retention of bioactive phytochmeicals in the spent dashamoola material. The HPTLC and LCMS/ms analysis of the DSME revealed the presence of phytochemicals wih immense biological potential. Further studies on the antioxidant activities suggested promising activity which was better than the fresh extract itself. DSME demonsrated potential antidiabetic and anti-inflammatory capabilities in vitro. Retention of residual phytochemical in DSME with confirmed biological activity caters to the needs of several foods, nutraceutical and pharmaceutical industries. If proven in vivo, the spent materilas from the related industries could be utilized for the further value addition e.g. development of nutraceutical products or active ingredeint isolation. Combating material loss is essential to any industry, especially when the spent material is presumed to have health benefits. Further in

vivo studies are warranted to confirm the biological activities so that the DSM can be further explored for the re-use for ayurvedic formulations.

References

Adisakwattana, S., Sookkongwaree, K., Roengsumran, S., Petsom, A., Ngamrojnavanich, N., Chavasiri, W., Yibchok-Anun, S., (2004). Structure activity relationships of trans-cinnamic acid derivatives on R-glucosidase inhibition. *Bioorg. Med. Chem. Lett*. 14: 2893–2896. doi: 10.1016/j.bmcl.2004.03.037.

Anand, K. K., Singh, B., Saxena, A. K., Chandan, B. K., Gupta, V. N., Bhardwaj, V. (1997). 3, 4, 5-trihydroxy benzoic acid (gallic acid), the hepatoprotective principle in the fruits ofterminalia belerica-bioassay guided activity. *Pharmacological Research*. 36(4): 315-321. doi: 10.1006/phrs.1997.0236.

Aras, A., Bursal, E., Türkan, F., Tohma, H., Kılıç, Ö., Gülçin, İ., Köksal, E. (2019). Phytochemical Content, Antidiabetic, Anticholinergic, and Antioxidant Activities of Endemic Lecokia cretica Extracts. *Chemistry & biodiversity*, 16(10), e1900341. doi: 10.1002/cbdv.201900341.

Arha, G., (2017). Reducing wait time prediction in hospital emergency room: lean analysis using a random forest model. Master's thesis, university of tennessee. https://trace.tennessee.edu/utk_gradthes/4722

Arun, K.B., Chandran, J., Venugopal, V.V., Madhavankutty, T.S., Nisha, P., (2018). Spent cumin seeds generated from ayurvedic industry as a source of bioactive compounds for nutraceutical/functional food applications. *J. Food Process. Preserv.* 42(1): 3392. doi: 10.1111/jfpp.13392.

Asci, H., Ozmen, O., Ellidag, H. Y., Aydin, B., Bas, E., Yilmaz, N. (2017). The impact of gallic acid on the methotrexate-induced kidney damage in rats. *journal of food and drug analysis*. 25(4): 890-897. doi: 10.1016/j.jfda.2017.05.001.

Association of Official Analytical Chemistry (AOAC). Official Methods of Analysis, 15th ed.; Association of Official Analytical Chemists: Gaithersburg, MD, USA, 1990.

Awasthi, H.H., Pandey, A.K., (2015). Use of Dashamoola in Cervical Spondylosis: Past and Present Perspective. *J. AYUSH*. 4(1): 10-16.

Barros, R.G.C., Andrade, J.K.S., Denadai, M., Nunes, M.L., Narain, N., (2017). Evaluation of bioactive compounds potential and antioxidant activity in some Brazilian exotic fruit residues. *Food Res. Int*. 102: 84-92. doi: 10.1016/j.foodres.2017.09.082.

Brand-Williams, W., Cuvelier, M.E., Berset, C.L.W.T., (1995). Use of a free radical method to evaluate antioxidant activity. *LWT-Food Sci. Technol*. 28(1): 25-30. doi: 10.1016/S0023-6438(95)80008-5.

Chang, C.C., Yang, M.H., Wen, H.M., Chern, J.C., (2002). Estimation of total flavonoid content in propolis by two complementary colourimetric methods. *J. Food Drug Anal.* 10(3).

Chekroun-Bechlaghem, N., Belyagoubi-Benhammou, N., Belyagoubi, L., Gismondi, A., Nanni, V., Di Marco, G., Atik Bekkara, F. (2019). Phytochemical analysis and antioxidant activity of Tamarix africana, Arthrocnemum macrostachyum and Suaeda fruticosa, three halophyte species from Algeria. Plant Biosystems-An International Journal Dealing with all *Aspects of Plant Biology*, 153(6), 843-852. doi: 10.1080/11263504.2018.1555191.

Chen, Q. C., Zhang, W. Y., Jin, W., Lee, I. S., Min, B. S., Jung, H. J., Bae, K. (2010). Flavonoids and isoflavonoids from Sophorae Flos improve glucose uptake in vitro. *Planta Med.* 76(1): 79–81. doi: 10.1055/s-0029-1185944.

Chiou, S. Y., Sung, J. M., Huang, P. W., Lin, S. D. (2017). Antioxidant, antidiabetic, and antihypertensive properties of Echinacea purpurea flower extract and caffeic acid derivatives using in vitro models. *Journal of medicinal food,* 20(2), 171-179. doi: 10.1089/jmf.2016.3790.

Cremonini, E., Fraga, C.G. and Oteiza, P.I., (2019). (–)-Epicatechin in the control of glucose homeostasis: Involvement of redox-regulated mechanisms. *Free Radical Biology and Medicine*. 130: pp.478-488. doi: 10.1016/j.freeradbiomed.2018.11.010.

Cuellar, M. A., Quiñones, N., Vera, V., Salas, C. O., Estévez, J. C., Estévez, R. J. (2015). Preliminary Studies on the Synthesis of (–)-Shikimic Acid Based 1, 2, 3, 4-Tetrahydrobenzo [b] phenanthridine-7, 12-diones. *Synlett*, 26(04): 552-556. doi: 10.1055/s-0034-1379948.

Das S.N., Chatterjee S., (1995). Long term toxicity study of ART-400. *Indian Indg Med*., 16 (2): 117-123.

Deb P.K., Ghosh R., Chakraverty R., Debnath R., Das L., Bhakta T., (2014). Phytochemical and Pharmacological Evaluation of Fruits of Solanum indicum Linn. *Int. J. Pharm. Sci. Rev. Res.*, 25(2): 28-32.

Dehghan, H., Sarrafi, Y., Salehi, P. (2016). Antioxidant and antidiabetic activities of 11 herbal plants from Hyrcania region, *Iran. journal of food and drug analysis*, 24(1), 179-188. doi: 10.1016/j.jfda.2015.06.010.

Du, G., Jin, L., Han, X., Song, Z., Zhang, H., Liang, W. (2009). Naringenin: a potential immunomodulator for inhibiting lung fibrosis and metastasis. *Cancer research*. 69(7): 3205-3212. doi: 10.1158/0008-5472.

Engeli, S., Birkenfeld, A.L., Badin, P.M., Bourlier, V., Louche, K., Viguerie, N., Thalamas, C., Montastier, E., Larrouy, D., Harant, I., Glisezinski, I., (2012). Natriuretic peptides enhance the oxidative capacity of human skeletal muscle. *J. Clin. Invest.* 122(12): 4675-4679. doi: 10.1172/JCI64526.

Fraga, C.G. & Oteiza, P.I., (2011). Dietary flavonoids: role of (−)-epicatechin and related procyanidins in cell signaling. *Free Radical Biology and Medicine.* 51(4): pp.813-823. doi: 10.1016/j.freeradbiomed.2011.06.002.

Frankel, E.N., Meyer, A.S., (2000). The problems of using one-dimensional methods to evaluate multifunctional food and biological antioxidants. *J. Sci. Food Agric*. 80(13): 1925-1941. doi: 10.1002/1097-0010(200010)80:13<1925.

Govindarajan, R., Rastogi, S., Vijayakumar, M., Shirwaikar, A., Rawat, A.K.S., Mehrotra, S., Pushpangadan, P., (2003). Studies on the antioxidant activities of Desmodium gangeticum. *Biol. Pharm Bull.* 26(10): 1424-1427. doi: 10.1248/bpb.26.1424.

Green L.C., Wagner D.A., Glogowski, J., (1982). Analysis of nitrate, nitrite, and [15N] nitrate in biological fluids. Anal Biochem 126: 131–138. doi: 10.1016/0003-2697(82)90118-x.

Guitard, R., Paul, J.F., Nardello-Rataj, V., Aubry, J.M., (2016). Myricetin, rosmarinic and carnosic acids as superior natural antioxidant alternatives to α-tocopherol for the preservation of omega-3 oils. *Food Chem.* 21: 284-295. doi: 10.1016/j.foodchem.2016.06.038.

Hanhineva, K., Törrönen, R., Bondia-Pons, I., Pekkinen, J., Kolehmainen, M., Mykkänen, H., Poutanen, K., (2010). Impact of dietary polyphenols on carbohydrate metabolism. *Int. J. Mol. Sci*. 11(4): 1365-1402. doi: 10.3390/ijms11041365.

Hao, X., Wu, X., Shen, G., Wen, L., Li, H., Huang, Q. (2015). Thermodynamic models for determination of the solubility of (-)-shikimic acid in different pure solvents and in (H2O+ ethanol) binary solvent mixtures. The Journal of Chemical Thermodynamics. 88: 8-14. doi: 10.1016/j.jct.2015.04.009.

Ho, H. H., Chang, C. S., Ho, W. C., Liao, S. Y., Wu, C. H., Wang, C. J. (2010). Anti-metastasis effects of gallic acid on gastric cancer cells involves inhibition of NF-κB activity and downregulation of PI3K/AKT/small GTPase signals. *Food Chem. Toxicol.* 48(8-9): 2508-2516. doi: 10.1016/j.fct.2010.06.024.

Hodgson, J.M., Chan, S.Y., Puddey, I.B., Devine, A., Wattanapenpaiboon, N., Wahlqvist, M.L., Lukito, W., Burke, V., Ward, N.C., Prince, R.L., Croft, K.D., (2004). Phenolic acid

metabolites as biomarkers for tea-and coffee-derived polyphenol exposure in human subjects. *Br. J. Nutr*. 91(2): 301-305. doi: 10.1079/BJN20031046.

Irshad, S., Singh, J., Kakkar, P., Mehrotra, S., (2009). Molecular characterization of Desmodium species - An important ingredient of 'Dashmoola' by RAPD analysis. *Fitoterapia.* 80(2): 115-118. doi: 10.1016/j.fitote.2008.11.004.

Jadon, A., Bhadauria, M., Shukla, S. (2007). Protective effect of Terminalia belerica Roxb. and gallic acid against carbon tetrachloride induced damage in albino rats. *Journal of ethnopharmacology.* 109(2): 214-218. doi: 10.1016/j.jep.2006.07.033.

Junior, O. C., Lima, N. M., Silva, M. G., Aguiar, V. B., Carli, G. P., Scherrer, E. C., Carli, A. P. (2020). In vitro and in vivo evaluation of anti-inflammatory activity and free radical scavenging potential of leaves extract from Anadenanthera colubrina. *Natural Product Research,* 1-5. doi: 10.1080/14786419.2020.1727472.

Kale R. H., Halde U. K., Biyani K. R., (2012). Protective Effect of Aqueous Extract of Uraria Picta on Acetaminophen Induced Nephrotoxicity in Rats. *International Journal of Research in Pharmaceutical and Biomedical Sciences.*, 3 (1): 110-113.

Karattu Veedu, K., Peringattu Kalarikkal, T., Jayakumar, N. and Gopalan, N.K., 2019. Anticorrosive Performance of Mangifera indica L. Leaf Extract-Based Hybrid Coating on Steel. *ACS Omega*, 4(6), pp.10176-10184. DOI: 10.1021/acsomega.9b00632

Karunagoda, K., Shukla, K., Donga, S., Tanna, C., Dei, L.P., (2010). A comparative study of Dashamoola Taila Matra Basti and Tila Taila Matra Basti in Kashtartava (dysmenorrhea). Ayu. 31(3): 305. doi: 10.4103/0974-8520.77154.

Kilic, I., Yeşiloğlu, Y., Bayrak, Y., (2014). Spectroscopic studies on the antioxidant activity of ellagic acid. Spectrochim. *Acta A Mol. Biomol. Spectrosc.* 130: 447-452. doi: 10.1016/j.saa.2014.04.052.

Kim, K. Y., Nguyen, T. H., Kurihara, H., & Kim, S. M. (2010). α-Glucosidase inhibitory activity of bromophenol purified from the red alga Polyopes lancifolia. *Journal of Food Science.*, 75: H145–H150.

Kumar, K.S., Ashish, G.R., Mony, R.S., Sundaresan, A., (2015). Comparative evaluation of the antioxidant and antidiabetic activity of different parts of Aegle marmelos and its chemical profiling using HPLC and HPTLC technique. *World J Pharm. Sci*. 4(09): 1107-21.

Kyriakis, E., Stravodimos, G.A., Kantsadi, A.L., Chatzileontiadou, D.S., Skamnaki, V.T., Leonidas, D.D., (2015). Natural flavonoids as antidiabetic agents. The binding of gallic and ellagic acids to glycogen phosphorylase b. *FEBS Lett*. 589(15): 1787-1794. doi: 10.1016/j.febslet.2015.05.013.

Lesjak, M., Beara, I., Simin, N., Pintać, D., Majkić, T., Bekvalac, K., Orčić, D., Mimica-Dukić, N., (2018). Antioxidant and anti-inflammatory activities of quercetin and its derivatives. J. *Funct. Foods*. 40: 68-75.

M Estevez, A., J Estevez, R. (2012). A short overview on the medicinal chemistry of (—)-shikimic acid. *Mini reviews in medicinal chemistry*, 12(14): 1443-1454. doi: 10.2174/138955712803832735.

Madlener, S., Illmer, C., Horvath, Z., Saiko, P., Losert, A., Herbacek, I., Fritzer-Szekeres, M. (2007). Gallic acid inhibits ribonucleotide reductase and cyclooxygenases in human HL-60 promyelocytic leukemia cells. *Cancer letters.* 245(1-2): 156-162. doi: 10.1016/j.canlet.2006.01.001.

Mizushima, Y., and Kobayashi, M., (1968). Interaction of anti-inflammatory drugs with serum proteins, especially with some biologically active proteins. *J of Pharma Pharmacol*; 20: 169-173. doi: 10.1111/j.2042-7158.1968.tb09718.x.

Mosmann, T., (1983). Rapid colourimetric assay for cellular growth and survival: Application to proliferation and cytotoxicity assays. *J. Immunol. Methods*. 65(1–2): 55–63. doi: 10.1016/0022-1759(83)90303-4.

Nagarkar, B., Jagtap, S., (2017). Effect of new polyherbal formulations DF1911, DF2112 and DF2813 on CFA induced inflammation in rat model. BMC Complement. *Alternative Med.* 17(1): 194. doi: 10.1186/s12906-017-1711-6.

Nagarkar, B., Jagtap, S., Narkhede, A., Nirmal, P., Pawar, N., Kuvalekar, A., Kulkarni, O., Harsulkar, A., (2013). Different Ayurvedic dosage forms of Dashamoola possess varied anti-inflammatory activity. *World J. Pharm. Pharmaceutic*. Sci. 2: 3118-36.

Nam, B., Rho, J. K., Shin, D. M., Son, J. (2016). Gallic acid induces apoptosis in EGFR-mutant non-small cell lung cancers by accelerating EGFR turnover. *Bioorganic & medicinal chemistry letters.* 26(19): 4571-4575. doi: 10.1016/j.bmcl.2016.08.083.

Nanda, G.C. & Tiwari, R.K., (2016). Shothahara activities of dashamoola dravyas as an anti-inflammatory formulation with special reference to charak. Ayushdhara., 2393: 9583 -9591.

Naveed, M., Hejazi, V., Abbas, M., Kamboh, A. A., Khan, G. J., Shumzaid, M., WenHua, L. (2018). Chlorogenic acid (CGA): A pharmacological review and call for further research. *Biomedicine & Pharmacotherapy.* 97: 67-74. doi: 10.1016/j.biopha.2017.10.064.

Navruz, A., Türkyılmaz, M., Özkan, M. (2016). Colour stabilities of sour cherry juice concentrates enhanced with gallic acid and various plant extracts during storage. *Food Chem.* 197: 150-160. doi: 10.1016/j.foodchem.2015.10.098.

Oteiza, P. I., Fraga, C. G., Mills, D. A., Taft, D. H. (2018). Flavonoids and the gastrointestinal tract: Local and systemic effects. *Molecular aspects of medicine*. 61: 41-49. doi: 10.1016/j.mam.2018.01.001.

Oyedepo, O.O., and Femurewa, A.J., (1995). Anti-protease and membrane stabilizing activities of extracts of Fagra zanthoxiloides, Olax subscorpioides and Tetrapleura tetraptera. *Int J of Pharmacong*; 33: 65-69. doi: 10.3109/13880209509088150.

Prabhu, G.R.D., Kiran, C.R., Sundaresan, A., Mony, R.S., Venugopalan, V.V., (2015). Process development studies for recovery of bio active isolates from spent black pepper generated from *ayurvedic industry. Ind. Crops Prod*. 66: 144-149.

Ramón-Gonçalves, M., Gómez-Mejía, E., Rosales-Conrado, N., León-González, M.E. and Madrid, Y., (2019). Extraction, identification and quantification of polyphenols from spent coffee grounds by chromatographic methods and chemometric analyses. *Waste Management*, 96, pp.15-24. doi: 10.1016/j.wasman.2019.07.009.

Randive, D.S., Adanaik, R.S., Nalawade, P.P., Patil, A.M., (2014). Studies on Standardization parameters for marketed formulations of Draksharishtha. *IJUPBS*. 3(4): 397-401.

Rao, M.L., Savithramma, N., (2011). Phytochemical screening of dasamoola-An Ayurvedic drug. *Int J Pharm Pharm Sci*. 3: 318-20.

Re, R., Pellegrini, N., Proteggente, A., Pannala, A., Yang, M., Rice-Evans, C., (1999). Antioxidant activity applying an improved ABTS radical cation decolourization assay. *Free Radic Biol Med.* 26(9-10): 1231-1237. doi: 10.1016/s0891-5849(98)00315-3.

Roidoung, S., Dolan, K.D., Siddiq, M., (2016). Gallic acid as a protective antioxidant against anthocyanin degradation and colour loss in vitamin-C fortified cranberry juice. *Food Chem.* 210: pp.422-427. doi: 10.1016/j.foodchem.2016.04.133.

Sakat, S., Juvekar, A. R., Gambhire M. N., (2010). In vitro antioxidant and anti-inflammatory activity of methanol extract of Oxalis corniculata Linn. International Journal of Pharma and *Pharmacological Sciences*. 2(1): 146-155.

Sekhon-Loodu, S., Rupasinghe, H. P. (2019). Evaluation of antioxidant, antidiabetic and antiobesity potential of selected traditional medicinal plants. *Frontiers in nutrition*, 6, 53. doi: 10.3389/fnut.2019.00053.

Silva, W., Torres-Gatica, M. F., Oyarzun-Ampuero, F., Silva-Weiss, A., Robert, P., Cofrades, S., Giménez, B. (2018). Double emulsions as potential fat replacers with gallic acid and quercetin nanoemulsions in the aqueous phases. *Food Chem*. 253: 71-78. doi: 10.1016/j.foodchem.2018.01.128.

Singleton, V.L., Rossi, J.A., (1965). Colorimetry of total phenolics with phosphomolybdic-phosphotungstic acid reagents. *AM. J. Enol. Viticult*. 16(3): 144-158.

Sobeh, M., Mahmoud, M. F., Abdelfattah, M. A., El-Beshbishy, H. A., El-Shazly, A. M., Wink, M. (2017). Albizia harveyi: phytochemical profiling, antioxidant, antidiabetic and hepatoprotective activities of the bark extract. *Medicinal Chemistry Research*, 26(12), 3091-3105. doi: 10.1007/s00044-017-2005-8.

Sorrentino, E., Succi, M., Tipaldi, L., Pannella, G., Maiuro, L., Sturchio, M., Tremonte, P. (2018). Antimicrobial activity of gallic acid against food-related Pseudomonas strains and its use as biocontrol tool to improve the shelf life of fresh black truffles. *International journal of food microbiology.* 266: 183-189. doi: 10.1016/j.ijfoodmicro.2017.11.026.

Stanek, N., and Jasicka-Misiak, I., 2018. HPTLC phenolic profiles as useful tools for the authentication of honey. *Food analytical methods*, 11(11), pp.2979-2989. DOI: 10.1007/s12161-018-1281-3

Sudhanshu, S.M., Rao, N., Menghani, E., (2012). Dashamularishta: Phytochemical and Antimicrobial Screening against effect of Environmental Pollution. *Int. J. Pharm. Sci. Res.* 3(9): 1000-1004.

Tungcharoen, P., Wattanapiromsakul, C., Tansakul, P., Nakamura, S., Matsuda, H., Tewtrakul, S. (2018). Antiinflammation constituents from Curcuma zedoaroides. *Phytotherapy research*, *32*(11), 2312-2320. doi: 10.1002/ptr.6173.

Vyas, M., Ashok, B.K., Ravishankar, B., Patgiri, B.J., Prajapati, P.K., (2011). A Comparative Anti-Inflammatory Activity of Brihatpanchamoola kwatha Prepared from Root Bark and Stem Bark. Inventi Rapid: *Ethnopharmacology.*

Wang, T.Y., Li, Q., Bi, K.S., (2018). Bioactive flavonoids in medicinal plants: Structure, activity and biological fate. *Asian J. Pharm. Sci.* 13(1): 12-23.

Xiao, Z., Storms, R., Tsang, A. (2006). A quantitative starch-iodine method for measuring alpha-amylase and glucoamylase activities. *Anal. Biochem*. 351(1): 146–148. doi: 10.1016/j.ab.2006.01.036.

Yoshioka, K. A. Z. U. M. I., Kataoka, T. O. M. O. K. O., Hayashi, T. O. M. O. K. O., Hasegawa, M., Ishi, Y., Hibasami, H. (2000). Induction of apoptosis by gallic acid in human stomach cancer KATO III and colon adenocarcinoma COLO 205 cell lines. *Oncology reports*. 7(6): 1221-1224. doi: 10.3892/or.7.6.1221.

Zeng, W., Jin, L., Zhang, F., Zhang, C. Liang, W., (2018). Naringenin as a potential immunomodulator in therapeutics. *Pharmacological research,* 135, pp.122-126. doi: 10.1016/j.phrs.2018.08.002.

Zou, M.H., Shi, C., Cohen, R.A., (2002). Oxidation of the zinc-thiolate complex and uncoupling of endothelial nitric oxide synthase by peroxynitrite. *J. Clin. Invest.* 109(6): 817-826. doi: 10.1172/JCI14442.

Chapter-4

Lignin nanoparticles from Ayurvedic industry spent materials: Applications in Pickering emulsions for curcumin and vitamin D_3 encapsulation

Abstract

Lignin nanoparticles (LNP), extracted from spent materials of Dashamoola Arishta (Ayurvedic formulation), shared a molecular weight of 14.42 kDa with commercial lignin. Processed into LNPs (496.43 ± 0.54 nm) via planetary ball milling, they demonstrated stability at pH 8.0 with a zeta potential of -32±0.27 mV. Operating as Pickering particles, LNP encapsulated curcumin and vitamin D_3 in sunflower oil, forming LnE+Cu+vD_3 nanoemulsions (particle size: 347.40±0.71 nm, zeta potential: -42.27±0.72 mV) with high encapsulation efficiencies (curcumin: 87.95±0.21%, vitamin D_3: 72.66 ± 0.11%). The LnE+Cu+vD_3 emulsion exhibited stability without phase separation over 90 days at room (27 ± 2 °C) and refrigeration (4 ± 1 °C) temperatures. Remarkably, LnE+Cu+vD_3 exhibited reduced toxicity, causing 29.32% and 34.99% cell death in L6 and RAW264.7 cells respectively, at the highest concentration (50 µg/mL). This underscores the potential valorisation of Ayurvedic industry spent materials for diverse industrial applications.

Keywords: Lignin nanoparticles, Ayurveda industry, Curcumin, Vitamin D_3, Pickering nanoemulsions.

Graphical abstract

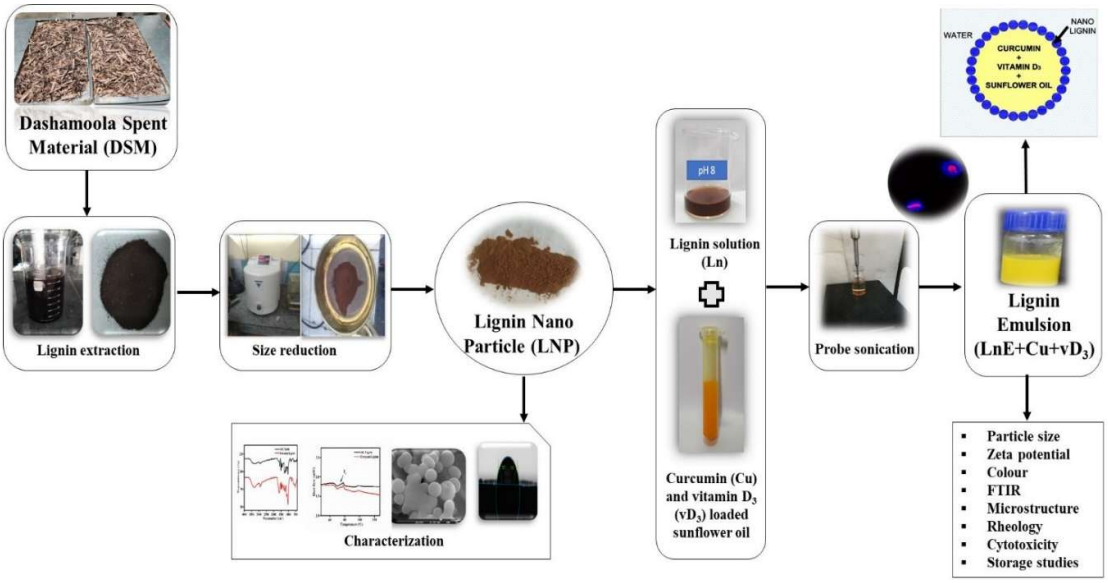

Fig. 2. Graphical abstract showing lignin extraction, nanoparticle formation, and emulsion preparation with curcumin and vitamin D_3.

Highlights

- Lignin nanoparticles (LNP) were produced from Ayurvedic spent materials
- LNPs were maximally stable, had lowest particle size and highest zeta potential at pH 8.0
- LNP produced stable Pickering emulsions and encapsulated curcumin and vitamin D_3
- These Pickering emulsions were stable for 90-day at refrigerated temperature
- There was no observable phase separation even at room temperature for 90 days

4.1. Introduction

Lignin is one of the most important components of the plant cell wall structure, and it is the second-most prevalent natural macromolecule after cellulose (Gordobil et al., 2018). It is an amorphous, heterogeneous molecule constituting phenylpropane units derived from three aromatic alcohols (coniferyl, p-coumaryl, and sinapyl). The chemical structure of lignin depends highly on the botanical origin, growing conditions of the plant, and the extraction process (Gordobil et al., 2018; Tortora et al., 2014; Rahman, et al., 2018; Zou et al., 2019). Agriculture, forestry and paper/pulp industry together create approximately 78 million metric tonnes of lignin as a by-product (Zou et al., 2019). Lignin is used in multiple sectors, encompassing biofuels (char, hydrogen, syngas, diesel), chemicals (polymers, dispersants, binders), agriculture (controlled release for pesticides/herbicides, heavy metal sequestration, humic acid formation, high-value fertilizers), human health applications (drug encapsulation, delivery, health-promoting functions), and UV protection in cosmetics (Schneider et al., 2021; Abraham et al., 2023).

Ayurveda is an indigenous form of traditional Indian medicinal science that has been practiced for thousands of years, with its roots dating back several millennia. It makes use of plant-based formulations to treat a wide range of illnesses (Randive et al., 2014). Dashamoola Arishta (DA) is an anti-inflammatory formulation and is one of the most effective and sought-after Ayurvedic preparations for inflammation-related ailments (Randive et al., 2014, Shukla et al., 2010, Nagarkar et al., 2013). It is prepared from the roots of ten different medicinal plants, primarily including Bilva (*Aegle marmelos*), Agnimantha (*Premna integrifolia*), Shyonaka (*Oroxylum indicum*), Patala (*Stereospermum suaveolens*), Gambhari (*Gmelina arborea*), Brihati (*Solanum indicum*), Kantakari (*Solanum xanthocarpum*), Shalaparni (*Desmodium gangeticum*), Prishnaparni (*Uraria picta*), Gokshura (*Tribulus terrestris*), as recorded in Ayurvedic texts (Vyas et al., 2011; Abraham et al., 2020). Ayurveda industry generates ~1000 tons of spent materials of dashamoola, hence forth referred to as dashamoola spent material

(DSM), after the arista production and is a rich source of lignocellulosic materials. Our earlier study showed that this DSM is rich in lignocellulosic content and that it can be valorised to be used in Ayurvedic industry and could converted into a sustainable, commercially viable source of lignin and cellulose (Abraham et al., 2020).

Naturally obtained biopolymeric materials including cellulose and pectin or their derivatives have lately seen increasing popularity as emulsion stabilizers (Hossain et al., 2021, Jiang and Hsieh, 2015, McClements et al., 2017). Micron and nanosized particles have been used as surface-active stabilizers for Pickering emulsions (Zou et al., 2019; Bertolo et al., 2019; Sipponen et al., 2018; Li et al, 2021). Pickering emulsions are stabilized by solid particles and are finding applications in foods, cosmetics and pharmaceuticals etc (Zou et al., 2019; Hossain et al., 2021). In addition to providing emulsifying and stabilizing properties, lignin and cellulose are known to protect light-sensitive compounds such as vitamins, oils, and food colour (Pandian et al., 2021; Sodeinde et al., 2021).

Several studies have touted curcumin's potential for providing health promoting functions to human against inflammation, oxidation-induced stresses cells (Anand et al., 2008). It is also known to promote immunomodulation (Ahsan et al., 1999). A recent study showed that the deficiency of Vitamin D_3 in the US population was associated with a higher incidence of COVID-19 infections and subsequent deaths among the Latino and Black populations (Ames et al., 2021). The intake of curcumin and vitamin D_3 was reported to provide relief from the infections and complications associated with COVID-19 (Ilie et al., 2020, Zahedipour et al., 2020, Rattis et al., 2021). Curcumin and vitamin D_3 are sensitive to environmental factors, and require to be stabilized by encapsulation. Encapsulated form of these compounds enables precise dosing and increased bioavailability, both of which are important for their efficacy.

In the above context, the current research aimed to isolate and characterize the lignin from DSM and convert it into nano lignin. Subsequently, the efficacy of nano lignin, utilized as a

Pickering particle in an O/W emulsion, was investigated for its ability to encapsulate curcumin and vitamin D_3, along with an assessment of their storage stability.

4.2. Material and methods

4.2.1. Material and chemicals

DSM for the study was kindly provided by Arya Vaidya Sala, Kottakal, Malappuram, Kerala, India. SD Fine Chemicals, Mumbai, India, supplied sulphuric acid (72% w/v), calcium carbonate. Laccase and cellulase enzymes were supplied by Zytex Biotech Pvt. Ltd, Andheri (E), Mumbai, India. Lignin standard was procured from Sigma Aldrich Chemicals Pvt. Ltd, Massachusetts, USA. Sisco Research Laboratories Pvt. Ltd., Mumbai, India, provided all the analytical-grade reagents utilized in the current study.

4.2.2. Isolation of lignin from DSM

The compositional analysis of DSM in terms of lignin, cellulose and hemicellulose was carried out according to National Renewable Energy Laboratory (NREL) protocol (Ruiz and Date, 1996). Lignin was extracted form DSM using alkaline extraction method (Si et al., 2015; Wunna et al., 2017). Briefly, DSM was suspended in 1% NaOH with 10% w/v loading. This mixture was heated at 121 ^{o}C for 1 h in an autoclave. Subsequently, the treated solid content was cooled to a room temperature before utilization with the cheese cloth. The supernatant (black liquor) obtained in this way was rendered acidic by lowering the pH to 2.0 using 10% H_2SO_4. The precipitate was recovered by centrifugation at 5000 x g for 15 minutes. The solid mass, lignin, obtained from the centrifugation step was freeze-dried at -80°C under a pressure of 10 Pa.

4.2.3. Preparation of nano lignin

Planetary ball mill (Pulverisette, Fritsch, Germany) running at 300 rpm and zirconium dioxide (ZrO_2) containers (50 mL) containing ZrO_2 balls (10 mm) was used for the size reduction of extracted lignin. All lignin samples were ground for 23 cycles in an argon environment (each

cycle had a (each cycle lasted for 5 minutes, followed by a 10-minute gap). After the ball milling, the powder was sieved through 63 mm sieve (Jayanth Scientific Instruments, Delhi, India).

4.2.4. Zeta potential and particle size

The droplet size and zeta potential of lignin was calculated from pH 4.0 to 10.0 using the Malvern Zeta sizer (Zeta Nano-ZS; Malvern Instruments, UK), which relies on the dynamic light scattering (DLS) principle.

4.2.5. Characterization of LNP

The lignin nanoparticles (LNP) were characterized in terms of NMR, GPC, FTIR, TGA, DSC, XRD and compared with that of Standard Lignin Powder (SLP). Further LNP was also characterized in terms of contact angle, SEM and TEM. The protocols for these tests are provided below.

4.2.5.1. Purity of extracted lignin

A two-step hydrolysis process was performed to analyse the chemical composition of the recovered lignin, focusing specifically on its carbohydrate, acid-soluble, and insoluble content (Ruiz and Ehrman, 1996). The polysaccharides content of the hydrolysate formed at the end of the two-step acid treatment was quantitated using the HPLC method, following the procedure outlined in Karthyani et al., 2017.

4.2.5.2. Functional group analysis of LNP using FTIR

FTIR analysis of the LNP was carried out using FTIR – ATR spectrometer (Perkin Elmer, USA) and the spectra were recorded from 4000 to 1000 cm^{-1} with a resolution of 4 cm^{-1}.

4.2.5.3. Determining the molecular weight of LNP

The gel permeation chromatography method was employed to determine the molecular weight of lignin. The method used a 300 × 7.8 mm Phenomenex Phenogel GPC column mounted on

a Shimadzu GPC unit connected to a photodiode array detector. The calibration and analysis were carried out as reported by Akhil et al., 2020.

4.2.5.4. NMR characterization of LNP: Molecular structure analysis

A previously reported ^{1}H-^{13}C NMR heteronuclear single-quantum coherence (HSQC) technique was used for analysing the LNP using an in-house Bruker Avance II 500 spectrometer (US). Sample preparation involved the addition of a 10 mg lignin sample in 1 mL d6-DMSO. The contours and cross peaks were identified and assigned according to the reported literature (Gabov et al., 2014, Ragauskas and Yoo, 2018).

4.2.5.5. Analysis of phenolic content

UV spectrometry was used to calculate the phenolic content of lignin. The assay was based on the change in the absorbance brought out by the ionisation of phenolic hydroxyl groups in alkaline conditions. The LNP was dissolved in a 0.2 M NaOH solution and dioxane. The total phenolic hydroxyl group and C-5 substitution (condensed Phenolic OH) were determined according to Goldmann et al., 2017.

4.2.5.6. Surface composition of LNP

The X-ray photoelectron spectroscopy (XPS) was used to determine the surface composition of lignin. PHI 5000 Versa Probe II (ULVAC-PHI Inc., USA) was used to determine the ratio of oxygen and carbon (O: C). The oxygen-to-carbon ratio directly provides details on the percentage of surface lignin. The equipment used a built-in micro-focused (200 μm, 15 kV) monochromatic Al-Kα X-Ray source ($h\nu$ =1486.6 eV) for carrying out the analysis (Mou et al., 2013).

4.2.5.7. Thermal degradation of LNP

Thermal gravimetric (TG) analyses of LNP and SLP were carried on a TA Q50 instrument. Sample (10 mg) was placed in the alumina crucible, heated in the temperature range 40-500 °C

at a heating rate of 10 $^{\circ}C\ min^{-1}$ in the presence of nitrogen (Moustaqim et al., 2018). The weight loss (%) versus temperature data were recorded.

4.2.5.8. Thermal characteristics of LNP

Differential scanning calorimetry (DSC) was employed to assess the thermal behavior, specifically focusing on the Glass Transition Temperature (Tg), of both LNP and SLP. Measurements were performed using DSC Q2000, TA Instruments, USA. Distilled water (6 L) was added to 3.0 mg of the sample and was transferred into pre-weighed aluminium sample pans. Samples were heated from 25 °C to 95 °C at a rate of 10 °C/min under a nitrogen environment. The onset temperature (TO) marks the initiation of phase transitions, peak temperature (TP), and conclusion temperature (TC) were measured using the Fit2D software (Sathyan and Nisha, 2022).

4.2.5.9. Crystalline and amorphous content of LNP

The wide-angle X-ray diffraction (WAXD) observations were captured using Xenocs' XEUSS SAXS/WAXS instrument in transmission mode to analyse the amorphous and crystalline content of LNP and SLP. Cu K radiation at 50 kV and 0.6 mA with a wavelength of 1.54 was used. Fit2D software was used to analyse the data after the 2D patterns were captured on a Mar345 picture plate. The degree of crystallinity was calculated by the ratio of the intensity of the crystalline peak to the total intensity according to Raveendran et al., 2011.

4.2.5.10. Contact angle

A thin film of LNP was made by dispersing 5% (w/v) LNP in distilled water on a spotless glass slide and dried at 85 $^{\circ}C$ for 30 min. A drop of distilled water (2 μL) was then added on the film surface, and their contact angle was determined using a drop shape analyzer (Model DSA30E, KRUSS GmBH, Hamburg, Germany; with Kruss Advance Software 1.7.0.8, Version 15).

4.2.5.11. Microscopic surface morphology

A specimen holder made of aluminium was coated with carbon tape before being filled with the sample, a thin layer of gold was applied using a gold/palladium sputter coater (SC7620, Emitech, Quorum Technologies Ltd, Kent, UK). Scanning electron microscopy (ZEISS; EVO 18, Germany) was used to analyze the microscopic surface texture of these samples under 15 KV of accelerating voltage, 10,000× magnification was used to capture the micrographs (Sathyan and Nisha, 2022).

4.2.5.12. Internal structure of LNP

Transmission electron microscopy **(**TEM) of the LNP was done using JOEL JEM F200 with STEM, EDS, and Gatan EELS and FEI Tecnai T30 with EDAX. This technique facilitated high-resolution imaging and detailed examination of the internal structure and composition of LNP at the nanoscale.

4.2.6. Preparation of O/W Pickering emulsions

Oil-in-water (O/W) Pickering emulsions were prepared using LNP as Pickering particle. LNP solutions of various concentrations (0, 500, 1000, 1500, 2000, 2500 ppm) at pH 8 were prepared and used. Sunflower oil (10% w/w) loaded with 50 ppm curcumin (Cu) and 50 ppm vitamin D_3 (vD_3) was used as the dispersed phase. Pickering emulsions {(1) LnE (LNP stabilized O/W emulsion of sunflower oil) and (2) LnE+Cu+vD_3 (LNP stabilized O/W emulsion of sunflower oil loaded with curcumin, and vitamin D_3)} were prepared by using a probe sonicator (VCX-750 Vibra cell, sonics & materials, USA) sonicating for 0, 15, 30, 45, 60 minutes (cycle 10 s on/10 s off, amplitude 50%). The resulting emulsions LnE+Cu+vD_3 were analysed in terms of particle size, ζ-potential, colour and stability at 4 °C and 27 °C for 90 days.

4.2.6.1. Rheological properties

A controlled stress rheometer was used to analyse the rheological properties (viscometric,

dynamic strain sweep, and dynamic frequency sweep behaviour) of two emulsions: LnE and LnE+Cu+vD_3 (MCR 102 Rheometer, Anton Paar GmbH, Ostfildern-Scharnhausen, Germany). A cone and plate geometry with a 25 mm diameter was employed in these tests. The gap between the cone and the plate was 0.105 mm. The viscometric was applied in a shear rate ranging from 0.01 to 100 s^{-1} to record shear rate versus viscosity data. During the dynamic strain sweep analysis, the strain for LnE and LnE+Cu+vD_3 was varied from 0.01 to 100%. The linear viscoelastic region (LVE) was determined from their strain sweep curve. The behaviour of the two emulsions, during dynamic frequency sweep was measured by varying the frequency from 0.01 to 100 rad/s (Sathyan and Nisha, 2022; Kavya, Jacob and Nisha, 2023).

4.2.6.2. Microstructure of emulsions

Microstructure of the emulsion was captured and analysed using a fluorescence microscope (Olympus fluorescence microscope IX83, Olympus corporation of Americas, Center Valley, USA) to understand whether LNP acted as a Pickering particle. LNP and the oil phase were stained with dye calcofluor white and nile red respectively. Emulsion (100 µL) was taken in a 96-well plate, stained with nile red (10%), kept for a few minutes, followed by adding calcofluor white (5mg/mL). Photographs were taken using a delta 512 EMCCD camera (photometrics, USA) (Bai et al., 2019).

4.2.6.3. Creaming index

Emulsions were transferred to15 mL graduated test tubes immediately after preparation and stored for 90 days at both room temperature (27°C) and refrigerating temperature (4°C). The amount of oil phase (in mL) that had separated from the emulsion was recorded every 15-day interval. Using Eq. (1), the percentage of separated oil (phase) was calculated using equation (1) (Huimin et al., 2014).

$$\text{Phase separation (\%)} = (VT/VE) \times 100 \quad (1).$$

Where, VT is the volume (mL) of the oil phase that was separated. VE is the total volume (mL) of emulsion used in the test.

4.2.6.4. Encapsulation efficiency

Encapsulation efficiency, representing the quantity of curcumin and Vitamin D_3 retained within the Pickering emulsion, was assessed using high-performance liquid chromatography (HPLC). To prepare samples for analysis, 1 mL of emulsion was mixed with 5 mL of methanol and stirred using a magnetic stirrer for 3 hours at 2,795× g. The mixture was then centrifuged at 55,900 × g for 10 minutes, supernatant was collected and filtered through a 0.22 µm PTFE syringe filter. The filtered sample was analyzed using a Prominence UFLC system (Shimadzu, Japan) containing LC-20AD system equipped with a column oven (CTO-20A), an autosampler injector (SIL-20AC), a diode array detector, and a Phenomenex Gemini C18 column (250 × 4.6 mm, 5 µm) (SPD-M20A). The analysis for curcumin and vitamin D_3 was carried out using an isocratic flow of 100% methanol as the mobile phase, with a flow rate set at 1 mL/min and an injection volume of 10 µL. Detection of the curcumin and vitamin D_3 fractions was performed at 420 nm and 261 nm, respectively, with retention times of 3.2 minutes for curcumin and 7.6 minutes for vitamin D_3. The column temperature was maintained at 40 °C throughout the analysis (Fig. 8 a-f).

The encapsulation efficiency (E.E) of Curcumin and Vitamin D_3 was determined using equation (2).

$$E.E.(\%) = \frac{mass\ of\ compound\ retained\ in\ the\ emulsion\ (mg)}{totla\ mass\ of\ compund\ used\ (mg)} \times 100 \qquad (2).$$

4.2.6.5. Cell viability assay

The L6 myoblast (NCCS, Pune, India) and RAW 264.7 (ATCC, Manassas, USA) cell lines were used in these tests. The cells grown in Dulbecco's modified eagle's medium (DMEM) supplemented with fetal bovine serum (10%) and a solution containing antibiotic-antimycotic

solution (1%) were kept in CO_2 incubator maintained at 37 °C and 5% CO_2. Cells were seeded in 96 well plates at a density of 1×10^4 cells/well for cell viability assays.

The toxicity of lignin solution (Ln) and lignin emulsion (LnE+Cu+vD_3) against RAW 264.7 and L6 myoblast cells was studied using MTT assay (Klapiszewski et al., 2013). The cell lines grown in 96 well-plates were incubated with varying DSME concentrations (10 - 500 µg/mL) for 24 h. After the incubation period, the cells in each well were washed and added with 100 µL of MTT (0.5 mg/mL) and incubated at 37 °C for 4 h in a CO_2 incubator. Following incubation, 100 µL of DMSO was added in each well and optical density was determined (570 nm, Synergy4 Biotek multiplate reader, USA) after 45 min (Mosmann et al., 1983). In the MTT assay, the viability of cells is related to the conversion of MTT (yellow colour) to formazan crystals (purple colour). The abovementioned conversion will happen only in metabolically viable cells. The intensity of the purple colour measured at 570 nm is directly correlated with the number of viable cells. Higher optical density indicates more viable cells, indicating their potential to convert MTT into formazan.

4.2.6.7. Storage stability

To evaluate the storage stability of the emulsions LnE+Cu+vD_3, they were stored at two temperatures: room temperature (27°C) and refrigerated temperature (4°C) for 90 days. During the storage period, the LnE+Cu+vD_3 was examined in 15 days' interval for changes in colour, particle size, and zeta potential.

4.2.7. Statistical analysis

Experiments were carried out in triplicate unless otherwise specified above. Results are presented as mean values and standard deviation (SD). The analysis of variance was carried out using one-way analysis of variance (ANOVA) with Dunnetts multiple comparison test using graph prism pad 5.0 statistical software versions and Microsoft Excel (2007). A 95% confidence level was used to confirm significant difference between any two mean values.

4.3. Results and discussion

4.3.1. Characterization of extracted lignin

4.3.1.1. Chemical composition

The composition of DSM was found to closely resemble that of typical lignocellulosic biomass, with cellulose 39.10 %, hemicellulose 30.56 %, and lignin 27.89%. Lignin, with a purity of 96.18%, was extracted through alkaline hydrolysis of DSM and then converted into LNP using ball milling, which was further characterised using various physicochemical methods. In order to understand the pH stability of LNP, surface charge across pH range of 4 to 10 was studied (Fig. 4.1a). Notably, the LNP solution exhibited negative surface charge in this pH range. At pH 8.0, the LNP solution had the zeta potential value of -32.40 ± 0.81 mV and particle size of 496.43 ± 0.54 nm) (Fig. 4.1b). The negative zeta potential values can be attributed to the surface hydroxyl and acidic groups becoming ionized when dispersed in an aqueous solution (Czaikoski et al., 2020, Klapiszewski et al., 2013). The difference in electrostatic interactions at various pH values may be correlated with the variation in particle sizes. At higher pH, cleavage of the β-O-4 linkage in lignin was observed, potentially leading to a reduction in particle size (Pradyawong et al., 2022).

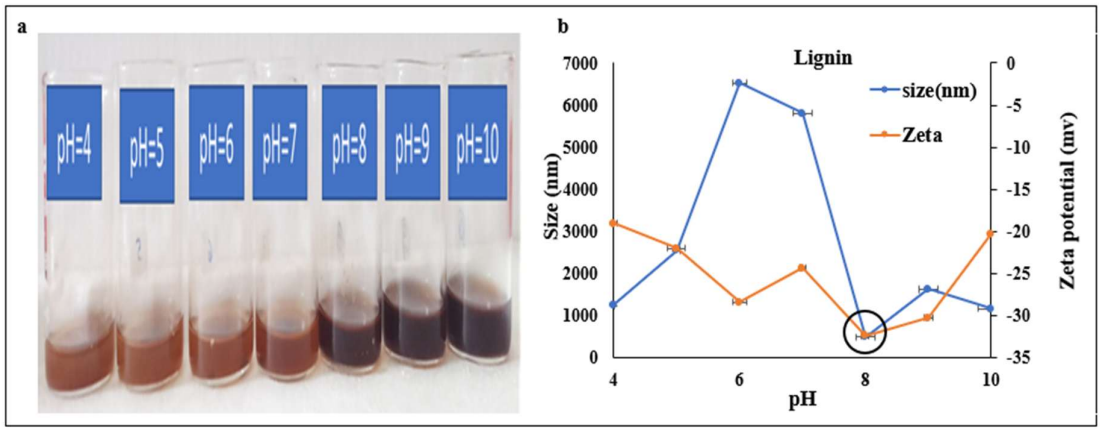

Fig. 4.1. (a) Images of lignin solution of pH 4-10, (b) Lignin solution size & zeta potential at pH 4-10

Further, chemical and structural characteristics of the LNP were compared with standard (commercially obtained) SLP. IR and NMR data indicated that SLP and LNP had guaiacyl (G), syringyl (S) and *p*-hydroxyl (H) units (Fig. 2a,b). However, the intensity of G unit was more pronounced in the aromatic region of the HSQC spectra as shown in Fig. 2b. The contour corresponding to G5 protons was wider suggesting the presence of higher guaiacyl units with unsubstituted C5 position. β-O-4 linkages of G and S units were also observed in the aliphatic region of the HSQC spectra along with β-β linkages (Balakshin et al., 2003). The IR spectra of SLP and LNP were close, indicating the similar structural composition, as shown in Fig. 2c.

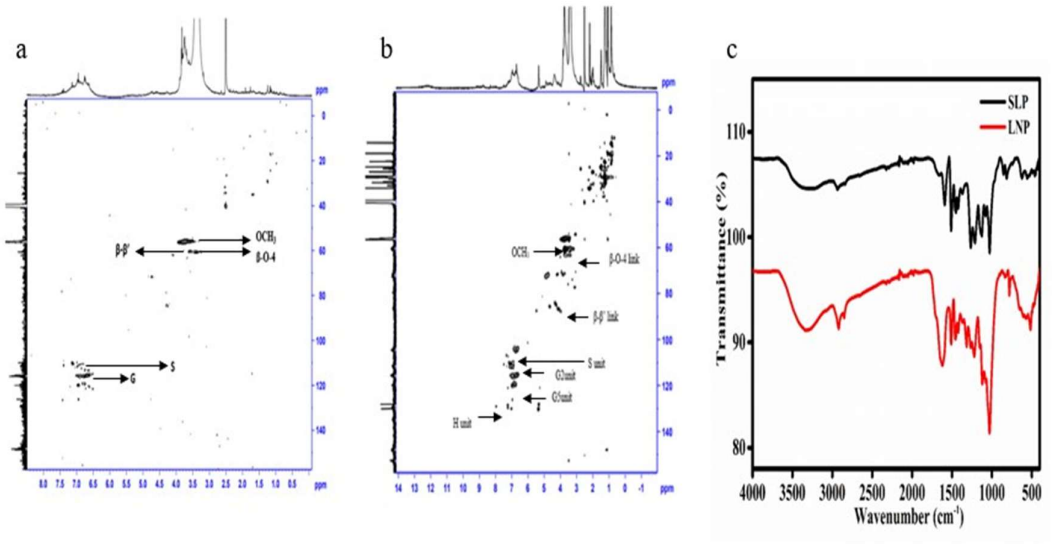

Fig. 4.2. (a) 2D-NMR spectroscopy of SLP, (b) 2D-NMR spectroscopy of LNP (c) FTIR spectroscopy of Standard Lignin Powder (SLP) and Lignin nanoparticles (LNP).

GPC data provided important insights into the structural heterogeneity, cross-linking or branching of the LNP in terms of molecular weight and Polydispersity index (PDI). LNP was found to have higher molecular weight than SLP (Table 4.1). PDI represents the heterogeneity of the macromolecule. Lignin is covalently bonded to polysaccharides, hemicelluloses in particular, which adds to its heterogeneity (Tarasov, et al., 2018). However, LNP had a lower PDI value than SLP, indicating better homogeneity. It is known that the β-O-4 linkages are

easily cleaved by alkali (Tarasov et al., 2018; Devendra et al., 2022). The NMR data indicated a higher number density of β-O-4 linkages in LNP, suggesting the presence of complex lignin-carbohydrate moieties. This may potentially lead to the blocking of inter-lignin β-O-4 linkages through steric hindrance, resulting in better homogeneity (Tarasov et al., 2018; Devendra et al., 2022).

Table 4.1: Lignin characterized by GPC, IR, UV

Lignin	**Molecular weight (KDa)**	**PDI**	**IR**	**Total phenolic and aliphatic OH in mmol/g (UV analysis)**
Extracted Lignin (LNP)	14.417	2.00	G-S-H lignin (1327,1514,833) C-H S unit (1120)	a) Phenolic OH: 2.134 b) C_5 substituted: 0.169
Standard Lignin (SLP)	12.634	2.30	Phenolic OH (3392), G>S(1510), C-O (1029)	a) Total Phenolic OH: 3.556 b) C_5 substituted: 1.860

The FTIR analysis revealed that LNP had a complex lignin structure, potentially with a broader range of phenolic constituents, while SLP had a simpler lignin structure with a higher concentration of phenolic OH groups (Devendra et al., 2022). The FTIR data of LNP indicated the presence of G-S-H lignin units (1327, 1514 cm^{-1}) and C-H S units (833 cm^{-1}), indicating a complex lignin structure. In contrast, standard lignin (SLP) showed a higher proportion of G units (1510 cm^{-1}) and phenolic OH groups (3392 cm^{-1}). These differences in lignin composition indicated that they had distinct reactivity profiles and would potentially be suitable for different applications (Tarasov, et al., 2018; Devendra et al., 2022). UV analysis (supplementary table

4.1) indicated that LNP had a lower total phenolic OH content (2.134 mmol/g) compared to SLP (3.556 mmol/g). A similar trend was observed in C5-substituted phenolic OH, with LNP measuring 0.169 mmol/g and SLP measuring 1.86 mmol/g. SLP contained a notably higher concentration of both total phenolic ~groups and C5 substituted phenolic OH groups compared to LNP. These data and underlying trends are comparable with those reported by Devendra et al., 2022 in the case of both condensed and uncondensed phenolic hydroxyl groups through absorbance changes upon ionization in an alkaline medium. The difference in phenolic content between LNP and SNP can have significant implications for their reactivity, chemical functionality, and suitability in various industrial applications.

4.3.1.2. Bonding and elemental composition

XPS analysis helps to identify the elemental composition, nature of bonding and the state of oxidation of a material (Mou et al., 2013). The survey spectrum of LNP and SLP revealed the presence of carbon and oxygen as shown in (Fig. 4.3a-f). The high-resolution C 1s spectrum of SLP revealed a peak at binding energy of 284.09 eV, attributed to C-C/C=C bonding in lignin. LNP had a lower binding energy of 284.69 eV. In addition, SLP showed peaks at 287 and 289 eV corresponding to C-O/C-OH, C=O/O-C=O in the C 1s spectrum. Meanwhile, the O1s spectrum of all three compounds showed a peak at 532.8 eV, indicating the presence of C-O in the structure. LNP showed an additional peak at 530.7 eV, indicative of C=O in the lignin structure. This can be attributed to the large polarizability of phenolic structure of lignin. As a result, the binding energy of the lignin was shifted to a lower value, specifically 532 eV. These spectral features showed that LNP had broad C1s and O1s peaks in comparison to commercial lignin which had C1s and O1s peaks at 284 and 532 eV, respectively (Mou et al., 2013).

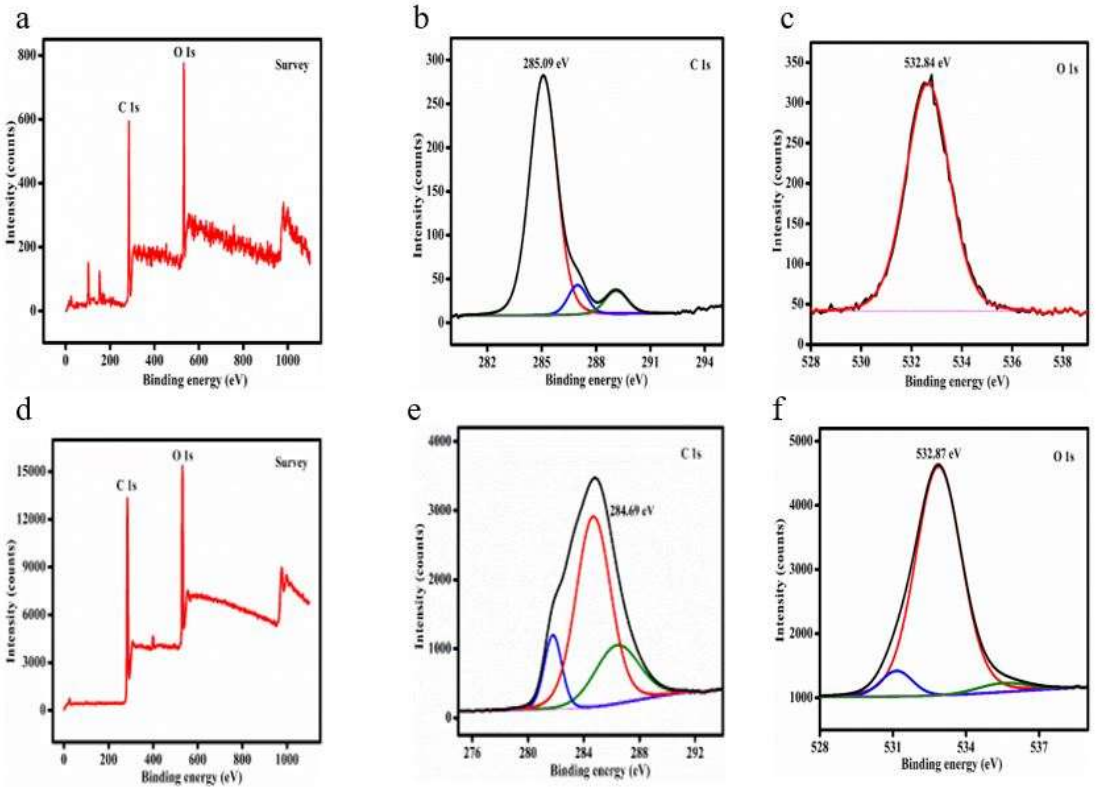

Fig. 4.3. (a) Survey spectrum of SLP, (b) XPS Curve Fitting of SLP carbon spectra, (c) XPS Curve Fitting of SLP oxygen spectra, (d) Survey spectrum of LNP, (e) XPS Curve Fitting of LNP carbon spectra, (f) XPS Curve Fitting of LNP oxygen spectra

4.3.1.3. Thermal behaviour

The thermal stability of extracted lignin was evaluated through TGA and DSC analysis. A steady decrease in the mass loss (weight loss) was observed from 40 to 100 °C in the TGA curve (Fig. 4.4a) of both LNP and SLP (7.60 and 11.17% respectively), which corresponded to the moisture loss (Moustaqim et al., 2018). Above 100 °C (post-dehydration), the TGA curve showed two peaks, which could be attributed to the decomposition of β-O-4 bonds and aliphatic hydroxyl groups around 200 °C and cleavage of the C-C bond and demethoxylation of phenolic lignin around 300 °C to 450 °C (Ragauskas and Yoo, 2018). There was a 44.22% weight loss between 150 and 300 °C with an onset temperature around 150 °C for LNP. This was followed by a 67.11% loss of mass between 300 to 450 °C whereas SLP showed a 54.95% weight loss

in the same temperature range. The degradation profile was similar to what is reported for lignin (Ragauskas and Yoo, 2018; Devendra et al., 2022). The difference in the mass loss during the thermal degradation of LNP and SLP could be attributed to the difference in their composition, which could be further inferred from the residual mass of 8.21% for SLP versus 6.02% for LNP at 800°C.

The DSC profile of LNP and SLP samples exhibited comparable thermal profiles, including water evaporation, lignin decomposition, and glass transition temperature as shown in Fig. 4.4b. LNP showed an endothermic peak below 100 °C, aligning with the evaporation of water. Additionally, an appearance of an exothermic peak around 200 °C suggested the decomposition of lignin, a finding that agrees well with Moustaqim et al., 2018's report. DSC analysis identified a similar glass transition temperature (T_g) of about 72 °C for both LNP and SLP.

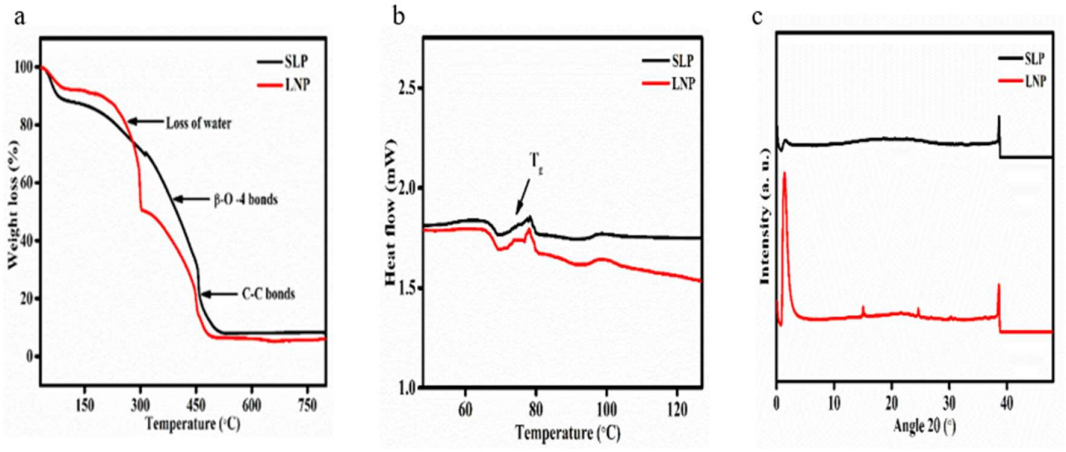

Fig. 4.4. Thermal and structural analyses of SLP and LNP: (a) TGA for thermal stability, (b) DSC for melting/crystallization behaviours and (c) XRD for crystalline structure

Fig. 4.4c showcases the XRD patterns of LNP and SLP. As compared to SLP, LNP exhibited sharp peaks at 18° and 23° which could be attributed to the presence of residual cellulose in LNP. LNP isolated through alkaline hydrolysis showed 96.18% purity and contained 3.18% cellulose, as compared to SLP's 98% purity and no cellulose. Similar spectrum for alkaline

extracted lignin is reported earlier which is correlated with its residual cellulose (Gomide et al. 2020). SLP showed a broad peak, indicative of its predominantly amorphous nature.

Overall, these structural analyses highlighted the importance of considering both thermal and structural characteristics when evaluating the potential application of LNP to encapsulate heat sensitive bioactive compounds (e.g., curcumin) and vitamins. The robust thermal stability of LNP makes it an excellent candidate for protecting these sensitive compounds during processing and ensuring their preservation in the final product.

4.3.1.4. Surface morphology and microstructure

The morphological features of LNP were studied using SEM and TEM to understand the morphological and microstructural properties. The SEM and TEM microstructure (Fig. 4.5a-c) showed that the LNP were spherical, and the size ranged from 200 to 300 nm. There was not a strong spread of size, and which indicated that ball milling can be used to produce LNP surface morphology of lignin nanoparticles.

With their small size, spherical shape, uniformity, and relatively narrow size range, these LNP are expected to be suitable for application in food formulations, especially as encapsulating shell materials and delivery vehicles. In the ensuing section presents their efficacy as Pickering particles to stabilize emulsions.

4.3.2. Characteristics of Pickering emulsion produced using LNP

In order to understand the hydrophobic/hydrophilic nature of LNP which is important for preparing emulsion, the contact angle was measured and was found to be 71.6° (Fig. 4.5d). This indicated that the LNP had hydrophilic in nature and could be considered to be suitable to produce O/W emulsions. It is expected for these LNPs (as Pickering particles) to adsorb at the oil-water interface and form a dense layer to prevent the droplet aggregation (McClements, 2015).

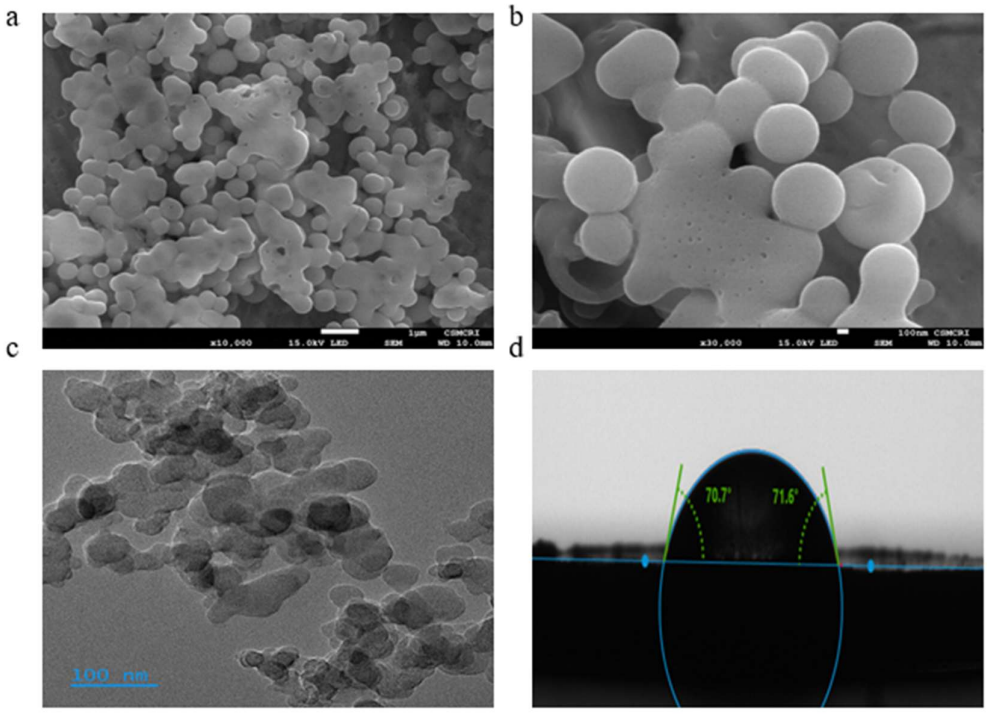

Fig. 4.5. Microscopic characterization of LNP: (a) SEM image at 10,000× magnification, (b) SEM image at 30,000× magnification, showcasing surface morphology, (c) TEM image revealing internal structure, and (d) Contact angle measurement demonstrating surface wettability of LNP

LNPs were used to prepare two Pickering emulsions: (1) LnE and (2) LnE+Cu+vD_3. These emulsions were prepared at pH 8.0 based on the pH stability information presented in section 3.1.1. Initial trials were carried to understand the composition of the emulsion (LnE) in terms of percentage of dispersed phase and the amount of LNP required. It was found that 10% of oil with 2000-2500 ppm of LNP produced stable LnE. Ultrasound was used to prepare emulsions using sonication time ranging from 15 to 60 min (Fig. 4.6a). Most stable emulsions were obtained at 45 min of sonication at LNP concentration of 2000 ppm, which are referred to LnE (Fig. 6a). Based on this experience, LnE+Cu+vD_3 emulsions with 10% sunflower oil and 2000 LNP loaded with curcumin and vitamin D_3 at concentrations of 500 ppm each, maintaining a

45-minutes of sonication. As the loading of curcumin and vitamin D_3 can affect the stability of the interface, we further evaluated the optimum LNP concentration by varying its concentration from 0 to 2500 ppm (Fig. 4.6b). The stability of emulsion was evaluated in terms of oil separation. The most stable LnE+Cu+vD_3 were obtained in the LNP concentrations of 2000 ppm and 2500 ppm. Ultimately, we chose the LNP concentration of 2000 ppm. (Li et al.,2021; Zhang et al., 2022).

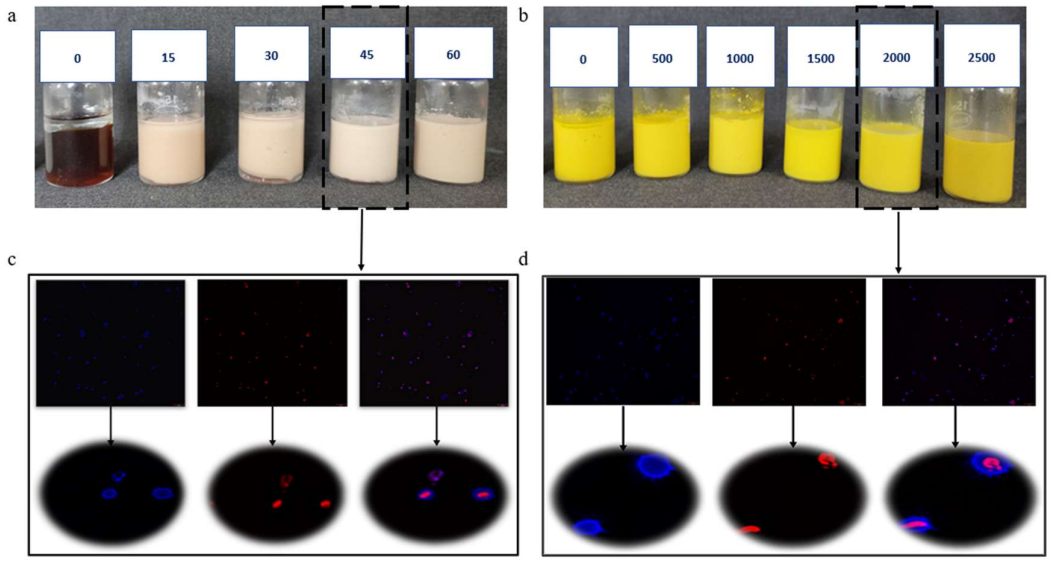

Fig. 4.6. (a) Formation of lignin emulsion through probe sonication at varying time intervals (0-60 min), (b) Influence of varying LNP concentration (0-2500 ppm) on curcumin and vitamin D_3-loaded lignin emulsion, (c) fluorescence microscopy images of LnE (d) fluorescence microscopy images of LnE+Cu+vD_3

The microstructure of the optimized emulsions, LnE and LnE+Cu+vD_3, was examined using fluorescent microscopy to ascertain the formation of Pickering emulsions. LNPs would be considered as Pickering particles if they could preferentially be adsorbed at the O/W interface and ensured emulsion stability. The organization of lignin and oil droplets in the freshly prepared emulsion (LnE) is presented Fig. 4.6c. The calcofluor dye (blue colour) indicated the presence of LNP while the Nile red stain (red colour) revealed the size of individual oil

droplets. The blue contour could be clearly observed surrounding the red-coloured oil droplets, illustrating how LNP were forming a layer entrapping them. In the case of the LnE+Cu+vD_3 emulsion, where curcumin and vitamin D_3 are solubilized in sunflower oil, the oil droplets were stained with Nile red and lignin with calcofluor dye (as shown in Fig. 4.6d). Again, the blue contour was observed to encircle the red-coloured oil droplets, demonstrating that LNP clearly acting as Pickering particles. Similar to our findings, Yuan et al., 2023 observed fluorescence microscopy images in which lignin, stained in blue (using calcofluor white), formed a contour around red-coloured oil droplets (stained with Nile red) created through high-energy microfluidization. These observations indicated that LNP can act as Pickering particles in oil-in-water emulsion systems.

4.3.2.1. Particle size and zeta potential

The particle size and zeta potential of LnE and LnE+Cu+vD_3 were significantly different (Table 4.2). LnE had larger particle size (546.83 ± 9.81) band small absolute value of zeta potential while LnE+Cu+vD_3 (347.40 ± 0.71) had smaller particle size higher absolute value of zeta potential. The smaller size of LnE+Cu+vD_3 indicated that this emulsion was more stable at the same time was containing curcumin and vitamin D_3 in the core. These compounds in LnE+Cu+vD_3 acted as natural surfactants, reducing the surface tension between oil and water phases, which helped to form smaller droplets. They modified the interfacial properties, possibly through steric hindrance and electrostatic repulsion, enhancing droplet stability against coalescence. Additionally, their incorporation could increase the viscosity of the continuous phase, further stabilizing the smaller droplets by impeding their movement (Zembyla et al., 2020). The negative zeta potential values for both formulations, especially the higher value in LnE+Cu+vD_3, underscored their electrostatic stability, which is important for broader application of LNP in food emulsions (Bertolo et al., 2019, Winuprasith, et al., 2018,

Saffarionpour and Diosady, 2022). This finding is also in accordance with previous research highlighting the role of kraft lignin in stabilizing O/W emulsions (Czaikoshi et al., 2020).

Table 4.2: Lignin emulsions of size, zeta, and colour values

Sample name	LnE	LnE+Cu+vD$_3$
Size (nm)	546.83 ± 9.81^a	347.40 ± 0.71^b
Zeta (Mv)	-35.53 ± 0.57^a	-42.265 ± 0.72^b
L*	73.93 ± 0.23^a	62.62 ± 1.25^b
a*	5.31 ± 0.03^a	3.893 ± 0.03^b
b*	13.53 ± 0.09^a	59.91 ± 0.71^b

Values are means ± SE (n = 3). Values with different superscript letter denotes significant difference between the sample ($p \leq 0.05$).

4.3.2.2. Colour analysis of emulsions

The colour analysis further revealed distinctions in LnE and LnE+Cu+vD$_3$ (Table 4.2). Notably, the colour values revealed that emulsions formulated with curcumin and vitamin D$_3$ exhibited a vibrant yellow hue, as evidenced by a substantial increase in the b* value. Specifically, the b* value rose from 13.53 ± 0.092 in LnE to 59.91 ± 0.716 in LnE+Cu+vD$_3$, a change attributed to the presence of curcumin. The above-mentioned differences in colour, particle size and zeta potential data indicated that the presence of curcumin and vitamin D$_3$ in the oil phase actually brought about positive impact on LNP-stabilized emulsions (Heger et al., 2014; Kharat et al., 2017).

4.3.2.3. Viscometrical and rheological behaviour of optimized emulsions

To understand the rheological characteristics of an emulsion stabilized by lignin, we compare the rheological behaviors of two emulsions: LnE and LnE+Cu+vD_3.The curves for LnE and LnE+Cu+vD_3 are illustrated in Fig. 7a-c. The viscosity-shear rate graph in Fig. 4.7a reveals that both LnE and LnE+Cu+vD_3 exhibit shear-thinning behavior, with viscosities decreasing as the shear rate increases. Specifically, the viscosity of LnE decreases from 6.94 to 0.0054 Pa.s as the shear rate varies from 0.01 to 20 s^{-1}, while for LnE+Cu+vD_3, it drops from 13.1 Pa.s to 0.00315 Pa.s over the same shear rate range. Notably, the decrease in viscosity values indicates that LnE+Cu+vD_3 is more susceptible to applied shear-induced deformation than LnE. This heightened susceptibility of LnE+Cu+vD_3 to shear-induced deformation, resulting in a more pronounced viscosity decrease compared to LnE, can be attributed to the impact of the added components Cu and vD_3. The presence of Cu and vD_3 likely alters the interfacial properties of the LNP-stabilized O/W emulsion droplets, potentially promoting droplet coalescence or disrupting the overall emulsion structure under shear forces. The pronounced shear-thinning behaviour observed in Pickering emulsions, indicative of weak associative interactions within the drop network structure, aligns with similar findings reported by Zhao et al., 2022.

The linear visco-elastic regions (LVE) of LnE and LnE+Cu+vD_3 are presented in Fig. 4.7b. In LnE, the G' (storage modulus) consistently exceeded G" (loss modulus) at higher strains, indicating a solid-like behaviour without a crossover between G' and G". Similarly, LnE+Cu+vD_3 showed a distinct trend with G' consistently surpassing G" across the entire strain range. The persistent G' dominance in LnE+Cu+vD_3 implies sustained solid-like behaviour and non-crossover of G' and G" in both LnE and LnE+Cu+vD_3 for stability assessment. The enhanced elastic property of LnE+Cu+vD_3 is attributed to the interface-stabilizing effect of lignin particle, curcumin and vitamin D_3. This, along with the reported G' dominance, implies

a prolonged solid-like structure, enhancing stability of O/W emulsions against droplet coagulation or aggregation during storage (Kavya, Jacob and Nisha, 2023).

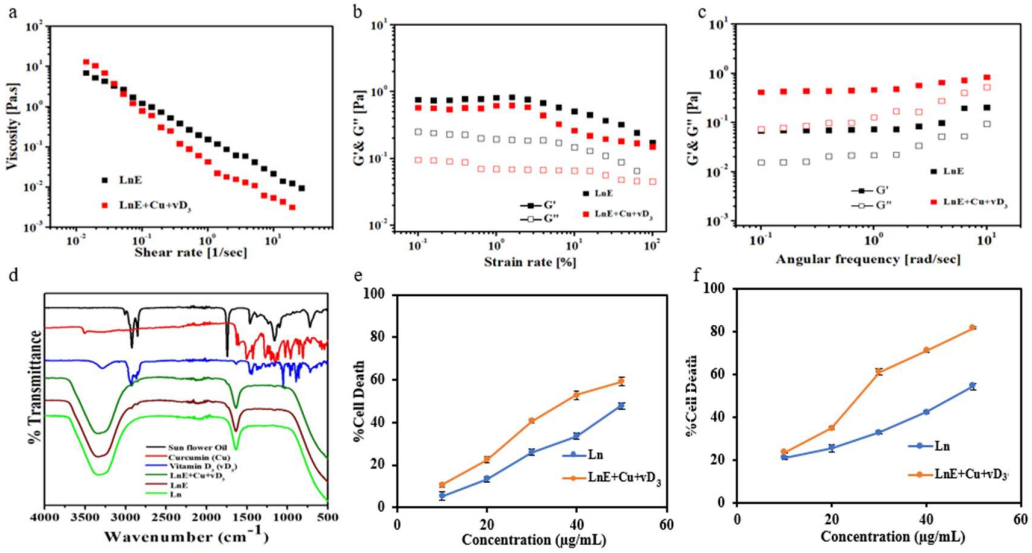

Fig. 4.7. (a) Viscosity curve, (b) amplitude sweep, (c) frequency sweep of LnE and LnE+Cu+vD$_3$, (d) FTIR analysis of lignin emulsions, (e) Analysis of toxicity of emulsion (Ln/ LnE+Cu+vD$_3$) against L6 (f) Analysis of toxicity of emulsion (Ln/ LnE+Cu+vD$_3$) against RAW264 respectively.

The frequency sweep results for LnE and LnE+Cu+vD$_3$ are presented in Fig. 4.7c. LnE consistently exhibited G' > G" across the applied frequency range, with no noticeable responses observed with an increase in frequency. Similarly, LnE+Cu+vD$_3$ showed G' > G", and there was no crossover between G' and G" values. The elasticity values of LnE+Cu+vD$_3$ were higher than those of LnE. These findings suggest that the lignin solution and the added components Cu and vD$_3$ in LnE+Cu+vD$_3$ retained their solid-like characteristics to a greater extent under non-destructive strain for a longer duration compared to LnE alone. This effect has been documented in these studies (Sannya and Nisha, 2022; Zhao et al., 2022) suggesting that the presence of Cu and vD$_3$ contributes to the prevention of droplet coagulation.

4.3.2.4. Molecular level of interactions among the components of emulsions

The FT-IR spectra of the Ln (lignin solutions), sunflower oil, curcumin (Cu), vitamin D_3 (vD_3), LnE and LnE+Cu+vD_3 are presented in Fig. 4.7d. The broad peaks in the range of 3600−3000 cm^{-1} in LnE+Cu+vD_3 correspond to OH bonds in carboxylic acid and free OH stretching bonds. These OH stretching vibrations indicates inter- or intra-molecular hydrogen bonds. In sunflower oil, a main peak was observed in the region 3000—2800 cm^{-1}. The bands in this region could be assigned to the symmetrical and asymmetrical C-H stretching vibration of the CH_2 and CH_3 aliphatic groups due to the alkyl residue of triglycerides (Bunaciu et al., 2012).

The main peak corresponding to the symmetrical and asymmetrical C-H stretching vibrations of the CH_2 and CH_3 aliphatic groups in sunflower oil is absent in both LnE and LnE+Cu+vD_3, suggesting the effective encapsulation of sunflower oil by lignin in these emulsions. Moreover, the FT-IR spectra showed characteristic bands for curcumin at 1438 (olefinic C-H bending vibration), 1510 (C=C vibrations), as well as 1597 and 1674 cm^{-1} (C-O stretching) (Nandiyanto et.al, 2017). In the case of vitamin D_3, the peaks at 2935 and 2874 cm^{-1} were related to alkyl C–H stretch. Several other C–H linkages were observed in the range of 1052–1460 cm^{-1} on the spectrum vitamin D_3. The peak around 1460 cm^{-1} was related to C–H vibration bending of the methylene group of vitamin D_3 (Hasanvand et al, 2018; Klapiszewski et al., 2013). Notably, in LnE+Cu+vD_3, the main characteristic peaks of curcumin and vitamin D_3 were not observed, indicating their encapsulation within the emulsion. These findings collectively underscored that the sunflower oil, curcumin, and vitamin D_3 formed the core of the emulsion system and supported the fact that LnE+Cu+vD_3 emulsion was stable. In the context of sunflower oil, the absence of its main characteristic peak in LnE and LnE+Cu+vD_3 suggested that sunflower oil was fully covered by lignin in these emulsions. Additionally, the absence of characteristic peaks of curcumin and vitamin D_3 in LnE+Cu+vD_3 confirmed the effective encapsulation of

these bioactive compounds in the emulsion. These findings showed that this Pickering emulsion could be used a carrier for the delivery of these functional ingredients.

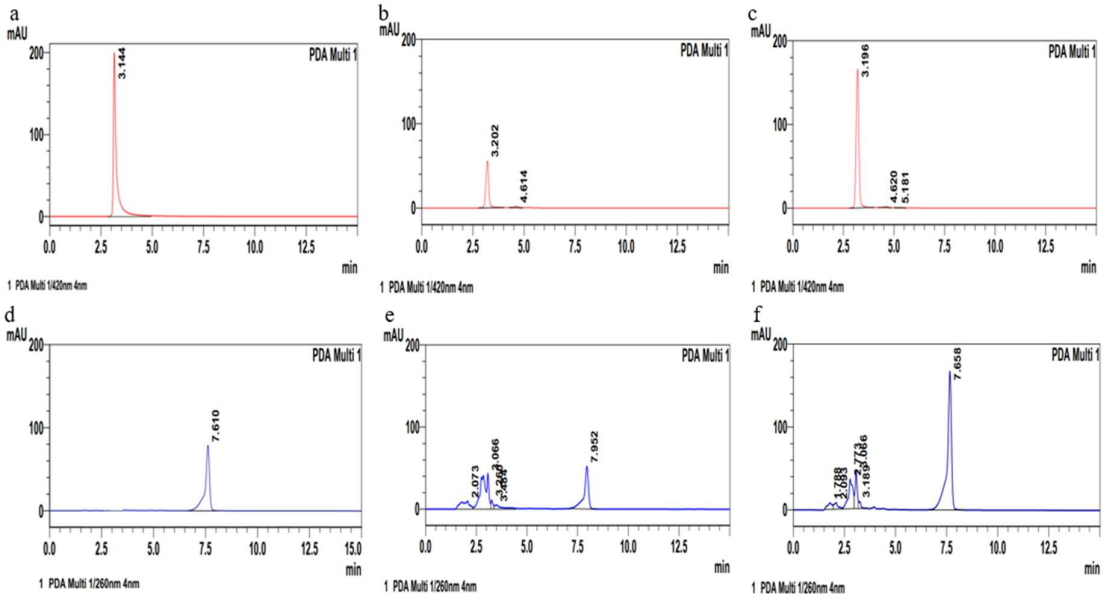

Fig. 4.8. Encapsulation efficiency of HPLC chromatograph (a) standard curcumin (b) curcumin without lignin emulsion (c) curcumin in LnE+Cu+vD_3 (d) standard vitamin D_3 (e) vitamin D_3 without lignin emulsion (f) vitamin D_3 in LnE+Cu+vD_3.

The encapsulation efficiency (EE) of curcumin and vitamin D_3 in the LnE+Cu+vD_3 are 87.95 ± 0.21% and 72.66 ± 0.11% respectively (Fig. 4.8a-f). In the absence of lignin as Pickering particle, the EE of curcumin and vitamin D_3 decreased to 30.43 ± 0.01% and 17.19 ± 0.03%. These results suggested that an LNP-based emulsion could encapsulate and protect these bioactive compounds.

4.3.3. Toxicity

To ensure biological safety, the toxicity of lignin solution (Ln) and the lignin emulsion (LnE+Cu+vD_3) against L6 and RAW264.7 cell lines was assessed by MTT assay. The results (Fig. 4.7e,f) showed that Ln at the highest concentration (50 µg/mL) induced 59.06% and 81.51% cell death in L6 and RAW264.7 cells, respectively. Meanwhile, cells treated with 50

µg/mL of LnE caused the death of 47.78% of L6 cells and 54.27% of RAW 264.7 cells. The IC_{50} values for Ln and LnE+Cu+vD_3 against L6 myoblast cells were as 58.68 ± 1.18 µg/mL and 37.43 ± 0.67 µg/mL, respectively. Whereas, the IC_{50} values for Ln and LnE+Cu+vD_3 against RAW264.7 cell lines were 46.62 ± 0.78 µg/mL and 28.49 ± 0.23 µg/mL, respectively. The cytotoxicity of lignin was low below 0.5 % w/w concentration which ensued in a dose-response relationship, for HT-29 cells and Caco-2 cells (Czaikoski., et al., 2020). Recent research has also reported a similarly low vitro cytotoxicity of lignin at low concentrations (0.1 mg/mL) (Yu et al., 2023).

4.3.4. Storage stability of Pickering emulsion

Storage stability of emulsions is an important parameter that determines their suitability in potential applications. We assessed the storage stability of the LnE+Cu+vD_3 emulsion by measuring the creaming index, particle size, zeta potential, and colour at both room temperature (27 ± 2 °C) and refrigerated temperature (4 ± 2 °C) over a period of 90 days. The results are presented in Fig. 4.10 a-c. The images provided in Fig. 4.9.

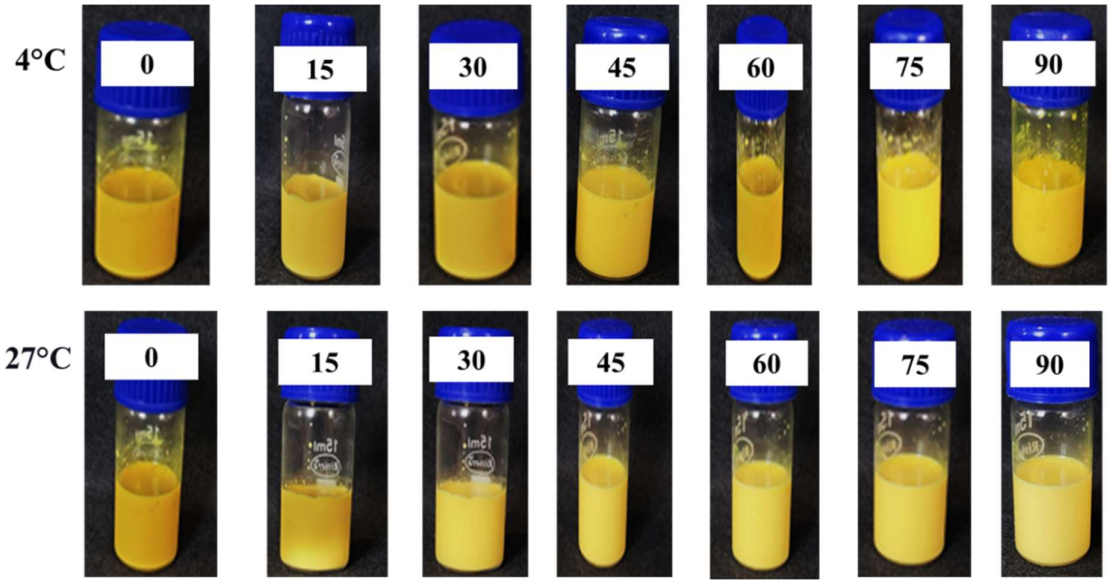

Fig. 4.9. Visual images of the stability of the emulsion (LnE+Cu+vD_3) at room temperature (27 ± 2 °C) and refrigerated temperature (4 ± 2 °C) across a 90-day period

Creaming index indicates the degree of stability of emulsions. There was no significant variation in the creaming index data during the entire storage period at both the condition. This observation indicated that the LNP produced Pickering emulsions could with stand potential coagulation and instability (Mirhosseini et al., 2008). This observation also complemented the overall resilience of the emulsion structure, as evidenced by size, zeta potential, and colour. The particle size of the emulsion increased substantially over time at room temperature, indicating a trend toward destabilization. However, the absence of phase separation in this case to indicted that the stability of the emulsion was not compromised. The increase of particle size in refrigerated emulsion was slow and gradual highlighting better stability compared to when stored at room temperature. This observation aligns with the broader understanding in emulsion science that lower temperatures are more suitable for better stability (Chen et al., 2021). Simultaneously, the zeta potential values, reflecting the repulsive forces between particles, showed a decreasing trend over time at room temperature, in line with the particle size, and hinted at higher likelihood of phase separation. The zeta potential of the emulsion on 90^{th} day at room temperature was -25.98 ± 0.51 mV while it was -30.87± 0.57 mV when stored at refrigerated condition. The fact that the magnitude of zeta potential of emulsion stored at room temperature for 90 days was still high supported the fact that no phase separation was observed in it. The samples stored under refrigeration maintained consistently higher zeta potential values, refrigeration temperature is conducive for storage stability of Pickering emulsions produced using LNP. These findings also showed that particle size and zeta potential greatly affected the stability of the LnE+Cu+vD_3 emulsion. The extended 90-day stability of emulsions stabilized by LNP, despite its relatively hydrophilic nature as indicated by a 70° contact angle, could be attributed to several key factors. These include the stabilization enhancements through surface modifications and functionalization of LNP, derived from their polyherbal spent source, to improve compatibility with the oil phase. This enabled adjustment of optimal oil-to-

water ratio in the emulsion formulation (Zembyla et al. 2020). Additionally, the small and uniform particle size of LNP offerred a protective effect against droplet coalescence. Its interactions with encapsulated curcumin and vitamin D_3 further contributed to the emulsion's stability. Chen et al., 2021 also reported that the shape and droplet diameter of lignin-stabilized emulsion remained unchanged upon 30 days of storage. Among the different types of lignin, the authors observed that kraft lignin had lower storage stability when stored for 28 days which was due to the presence of different functional groups (Czaikoski et al., 2020). Our findings are akin to those of earlier studies that colloidal systems of nanosized lignin were stable when the zeta potential values ranged between -35.1 mV and -32.4 mV (Bertolo et al., 2019).

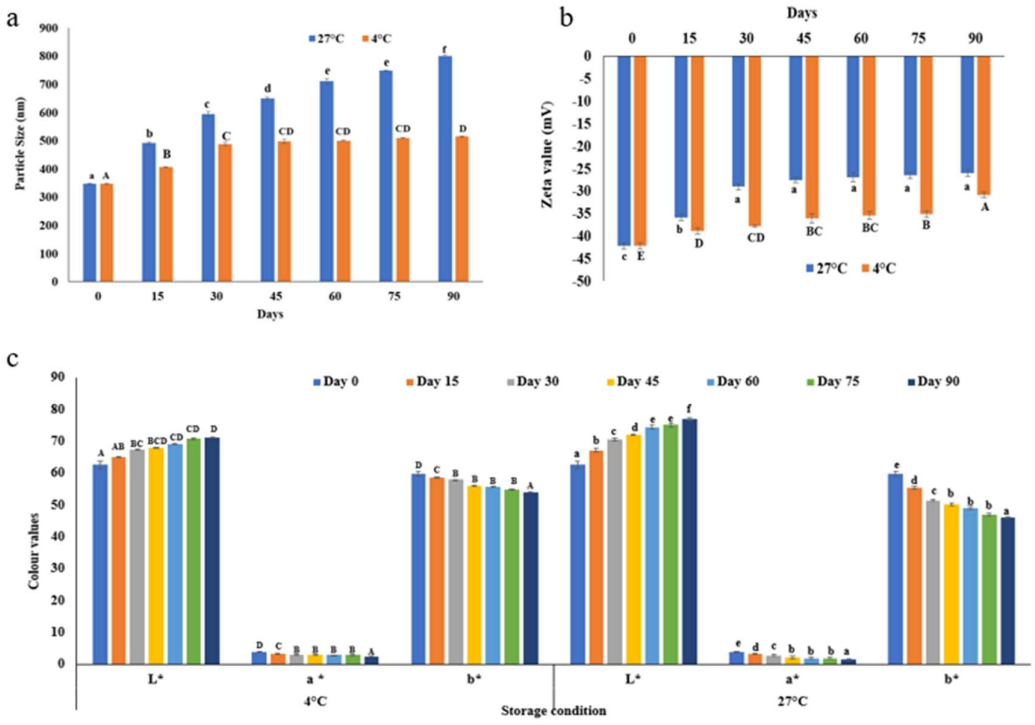

Fig. 4.10. (a) Particle size (b) zeta potential of LnE+Cu+vD_3 during storage (c) colour values of LnE+Cu+vD_3 during storage. The results are presented as mean ± standard deviation. Small letters indicate significant differences at 27°C, while capital letters signify significant differences at 4°C between the interval days ($p < 0.05$).

The colour parameters (L*a*b*) of LnE+Cu+vD_3 at the room and refrigerated storage temperatures are presented in Fig. 4.10c. At room temperature, significant changes in colour were observed over time, indicating the degradation of curcumin in the emulsion due to its inherent sensitivity at ambient temperatures. The degradation of curcumin at elevated temperatures, indicated by a change in colour, have also been reported in the literature (Kharat et al., 2017). In contrast, refrigerated conditions exhibited a notable colour stability as there was only slight decrease in the b* values upon 90 days of storage. This finding suggests that under refrigeration temperatures, the LNP stabilized Pickering emulsion system effectively preserves the colour integrity of curcumin and vitamin D_3. The observed stability resulted from the encapsulation of bioactives within the lipid droplets and their covering by LNP, providing a protective environment. In essence, these results indicated that the LnE+Cu+vD_3 had desirable stability both at room and refrigeration temperatures, although the room temperature had destabilizing tendency. Storing these LnE+Cu+vD_3 emulsion at refrigeration condition was conducive in terms of its minimal impact on particle size, zeta potential and colour stability.

4.4. Conclusion

The valorisation of lignin from dashamoola spent material (DSM) in the ayurvedic industry is important from a sustainability perspective, given lignin's enormous potential for food applications. Lignin nanoparticles (LNP) were produced from DSM aiming to use them as Pickering particles and further applying them to produce Pickering O/W emulsions. LNP with sufficiently high absolute value of zeta potential and sufficiently low particle size were synthesized. The findings of this study showed that stable Pickering emulsions incorporating curcumin and vitamin D_3 (LnE+Cu+vD_3) could be produced using LNP as Pickering particles. The particle size, zeta potential, and curcumin stability were reasonable at room temperature and highly stable at refrigerated temperature for 90 days. Curcumin and vitamin D_3 remained fully encapsulated in the oil phase and had no effect on the emulsion stability LNP network at

the oil-water interface. The encapsulation efficiency of bioactives in this emulsion system was also quite high (curcumin: 87.95±0.21%, vitamin D_3: 72.66 ± 0.11%). Therefore, this study offers an easy-to-implement valorisation pathway for DSM that can enhance the ayurvedic industry's economic performance. The LNP are expected to find greater applications in food industry in the future as emulsifiers.

References

Abraham, B., Reshmitha, T. R., Navami, M. M., George, L., Venugopalan, V. V., & Nisha, P. (2020). Phytochemical rich extract from the spent material generated from Industrial Dashamoola preparation (a medicinal Ayurvedic decoction) with antioxidant, antidiabetic and anti-inflammatory potential. *Industrial crops and products*, *151*, 112451. https://doi.org/10.1016/j.indcrop.2020.112451.

Abraham, B., Syamnath, V. L., Arun, K. B., Zahra, P. F., Anjusha, P., Kothakotta, A., & Nisha, P. (2023). Lignin-based nanomaterials for food and pharmaceutical applications: Recent trends and future outlook. *Science of The Total Environment*, 881, 163316. https://doi.org/10.1016/j.scitotenv.2023.163316.

Ahsan, H., Parveen, N., Khan, N. U., & Hadi, S. M. (1999). Pro-oxidant, anti-oxidant and cleavage activities on DNA of curcumin and its derivatives demethoxycurcumin and bisdemethoxycurcumin. *Chemico-biological interactions*, *121*(2), 161-175. https://doi.org/10.1016/S0009-2797(99)00096-4.

Akhil, G. H., Kariyil, B. J., Akshatha, G. D., Bhatt, S. V., Dhanusha, G., & John, R. (2020). Germinated seeds of Hordeum vulgare target extrinsic pathway of apoptosis in triple-negative breast cancer cells. *Pharmacognosy Magazine*, *16* (Suppl 3), S531-S539. doi:10.4103/pm.pm_123_20.

Ames, B. N., Grant, W. B., & Willett, W. C. (2021). Does the high prevalence of vitamin D deficiency in African Americans contribute to health disparities?. *Nutrients*, *13*(2), 499. https://doi.org/10.3390/nu13020499.

Anand, P., Thomas, S. G., Kunnumakkara, A. B., Sundaram, C., Harikumar, K. B., Sung, B., Tharakan, ST., Misra, K., Priyadarsini, IK., Rajasekharan, KN., & Aggarwal, B. B. (2008). Biological activities of curcumin and its analogues (Congeners) made by man and Mother Nature. *Biochemical pharmacology*, *76*(11), 1590-1611. https://doi.org/10.1016/j.bcp.2008.08.008.

Bai, L., Lv, S., Xiang, W., Huan, S., McClements, D. J., & Rojas, O. J. (2019). Oil-in-water Pickering emulsions via microfluidization with cellulose nanocrystals: 1. Formation and stability. *Food Hydrocolloids*, *96*, 699-708. https://doi.org/10.1016/j.foodhyd.2019.04.038.

Balakshin, M. Y., Capanema, E. A., Chen, & Gracz, H. S. (2003). Elucidation of the structures of residual and dissolved pine kraft lignins using an HMQC NMR technique. *Journal of agricultural and food chemistry*, 51(21), 6116-6127. https://doi.org/10.1021/jf034372d

Beliciu, C. M., & Moraru, C. I. (2011). The effect of protein concentration and heat treatment temperature on micellar casein–soy protein mixtures. *Food Hydrocolloids*, *25*(6), 1448-1460. https://doi.org/10.1016/j.foodhyd.2011.01.011.

Bertolo, M. R., de Paiva, L. B. B., Nascimento, V. M., Gandin, C. A., Neto, M. O., Driemeier, C. E., & Rabelo, S. C. (2019). Lignins from sugarcane bagasse: Renewable source of nanoparticles as Pickering emulsions stabilizers for bioactive compounds encapsulation. *Industrial crops and products*, *140*, 111591. https://doi.org/10.1016/j.indcrop.2019.111591.

Bunaciu, A. A., Fleschin, S., & Aboul-Enein, H. Y. (2022). Detection of sunflower oils adulteration by ATR-FTIR spectra. *Chemical Papers*, *76*(9), 5533-5539. https://doi.org/10.1007/s11696-022-02245-6.

Chen, K., Qian, Y., Wang, C., Yang, D., Qiu, X., & Binks, B. P. (2021). Tumor microenvironment-responsive, high internal phase Pickering emulsions stabilized by lignin/chitosan oligosaccharide particles for synergistic cancer therapy. *Journal of Colloid and Interface Science*, *591*, 352-362. https://doi.org/10.1016/j.jcis.2021.02.012.

Czaikoski, A., Gomes, A., Kaufmann, K. C., Liszbinski, R. B., de Jesus, M. B., & da Cunha, R. L. (2020). Lignin derivatives stabilizing oil-in-water emulsions: Technological aspects, interfacial rheology and cytotoxicity. *Industrial crops and products*, *154*, 112762. https://doi.org/10.1016/j.indcrop.2020.112762.

Demir, M., Demir, F., & Aygun, H. (2021). Vitamin D deficiency is associated with COVID-19 positivity and severity of the disease. *Journal of medical virology*, *93*(5), 2992-2999. https://doi.org/10.1002/jmv.26832.

Devendra, L. P., & Sukumaran, R. K. (2023). Comparative evaluation of lignin derived from different sugarcane bagasse pretreatments in the synthesis of wood adhesive. *BioEnergy Research*, *16*(1), 151-162. https://doi.org/10.1007/s12155-022-10450-0.

Gabov, K., Gosselink, R. J., Smeds, A. I., & Fardim, P. (2014). Characterization of lignin extracted from birch wood by a modified hydrotropic process. *Journal of agricultural and food chemistry*, *62*(44), 10759-10767. https://doi.org/10.1021/jf5037728.

García-Negrón, V., Kizzire, D. G., Rios, O., Keffer, D. J., & Harper, D. P. (2020). Elucidating nano and meso-structures of lignin carbon composites: A comprehensive study of feedstock and temperature dependence. *Carbon*, *161*, 856-869. https://doi.org/10.1016/j.carbon.2020.02.010.

Goldmann, W. M., Ahola, J., Mankinen, O., Kantola, A. M., Komulainen, S., Telkki, V. V., & Tanskanen, J. (2016). Determination of phenolic hydroxyl groups in technical lignins by ionization difference ultraviolet spectrophotometry (Δ ε-IDUS method). https://doi.org/10.3311/PPch.9269.

Gomide, R. A. C., de Oliveira, A. C. S., Rodrigues, D. A. C., de Oliveira, C. R., de Assis, O. B. G., Dias, M. V., & Borges, S. V. (2020). Development and characterization of lignin microparticles for physical and antioxidant enhancement of biodegradable polymers. *Journal of Polymers and the Environment*, 28, 1326-1334. https://doi.org/10.1007/s10924-020-01685-z

Gordobil, O., Herrera, R., Yahyaoui, M., İlk, S., Kaya, M., & Labidi, J. (2018). Potential use of kraft and organosolv lignins as a natural additive for healthcare products. *RSC advances*, *8*(43), 24525-24533. DOI: 10.1039/C8RA02255K.

Hasanvand, E., Fathi, M., & Bassiri, A. (2018). Production and characterization of vitamin D_3 loaded starch nanoparticles: effect of amylose to amylopectin ratio and sonication parameters. *Journal of food science and technology*, *55*, 1314-1324. https://doi.org/10.1007/s13197-018-3042-0.

Heger, M., van Golen, R. F., Broekgaarden, M., & Michel, M. C. (2014). The molecular basis for the pharmacokinetics and pharmacodynamics of curcumin and its metabolites in relation to cancer. *Pharmacological reviews*, *66*(1), 222-307. http://dx.doi.org/10.1124/pr.110.004044.

Hossain, K. M. Z., Deeming, L., & Edler, K. J. (2021). Recent progress in Pickering emulsions stabilised by bioderived particles. *RSC advances*, *11*(62), 39027-39044. DOI: 10.1039/D1RA08086E.

Huimin, X., Lin, L., Shilin, G., Elfalleh, W., Shenghua, H., Qinghai, S., & Ying, M. (2014). Formation, stability, and properties of an algae oil emulsion for application in UHT milk. *Food and Bioprocess Technology*, *7*, 567-574. https://doi.org/10.1007/s11947-013-1054-3.

Ilie, P. C., Stefanescu, S., & Smith, L. (2020). The role of vitamin D in the prevention of coronavirus disease 2019 infection and mortality. *Aging clinical and experimental research*, *32*(7), 1195-1198. doi.org/10.1007/s40520-020-01570-8.

Jiang, F., & Hsieh, Y. L. (2015). Holocellulose nanocrystals: amphiphilicity, oil/water emulsion, and self-assembly. *Biomacromolecules*, *16*(4), 1433-1441. https://doi.org/10.1021/acs.biomac.5b00240.

Karunagoda, K., Shukla, K., Donga, S., Tanna, C., & Dei, L. P. (2010). A comparative study of dashamoola taila matra basti and tila taila matra basti in kashtartava (dysmenorrhea). *Ayu*, *31*(3), 305. doi: 10.4103/0974-8520.77154.

Karthyani, S., Pandey, A., & Devendra, L. P. (2017). Delignification of cotton stalks using sodium cumene sulfonate for bioethanol production. *Biofuels*. 11, 431–440. https://doi.org/10.1080/17597269.2017.1370884.

Kavya, M., Jacob, A. R., & Nisha, P. (2023). Pectin emulsions and emulgels: Bridging the correlation between rheology and microstructure. *Food Hydrocolloids*, 143, 108868. https://doi.org/10.1016/j.foodhyd.2023.108868.

Kharat, M., Du, Z., Zhang, G., & McClements, D. J. (2017). Physical and chemical stability of curcumin in aqueous solutions and emulsions: Impact of pH, temperature, and molecular environment. *Journal of agricultural and food chemistry*, *65*(8), 1525-1532. https://doi.org/10.1021/acs.jafc.6b04815.

Klapiszewski, Ł., Nowacka, M., Milczarek, G., & Jesionowski, T. (2013). Physicochemical and electrokinetic properties of silica/lignin biocomposites. *Carbohydrate polymers*, *94*(1), 345-355. https://doi.org/10.1016/j.carbpol.2013.01.058.

Li, X., Shen, J., Wang, B., Feng, X., Mao, Z., & Sui, X. (2021). Acetone/water cosolvent approach to lignin nanoparticles with controllable size and their applications for pickering emulsions. *ACS Sustainable Chemistry & Engineering*, *9*(15), 5470-5480. https://doi.org/10.1021/acssuschemeng.1c01021.

McClements, D. J. (2015). *Food emulsions: principles, practices, and techniques*. CRC press. https://doi.org/10.1201/9781420039436.

McClements, D. J., Bai, L., & Chung, C. (2017). Recent advances in the utilization of natural emulsifiers to form and stabilize emulsions. *Annual review of food science and technology*, *8*, 205-236. https://doi.org/10.1146/annurev-food-030216-030154.

Mirhosseini, H., Tan, C. P., Hamid, N. S., & Yusof, S. (2008). Effect of Arabic gum, xanthan gum and orange oil contents on ζ-potential, conductivity, stability, size index and pH of orange beverage emulsion. *Colloids and Surfaces A: Physicochemical and Engineering Aspects*, *315*(1-3), 47-56. https://doi.org/10.1016/j.colsurfa.2007.07.007.

Mou, H. Y., Heikkilä, E., & Fardim, P. (2013). Topochemistry of alkaline, alkaline-peroxide and hydrotropic pretreatments of common reed to enhance enzymatic hydrolysis efficiency. *Bioresource technology*, *150*, 36-41. https://doi.org/10.1016/j.biortech.2013.09.093.

Mosmann, T. (1983). Rapid colorimetric assay for cellular growth and survival: application to proliferation and cytotoxicity assays. *Journal of immunological methods*, *65*(1-2), 55-63. https://doi.org/10.1016/0022-1759(83)90303-4.

Moustaqim, EL, M., El Kaihal, A., El Marouani, M., Men-La-Yakhaf, S., Taibi, M., Sebbahi, S., El Hajjaji & Kifani-Sahban, F. (2018). Thermal and thermomechanical analyses of lignin. *Sustainable chemistry and pharmacy*, *9*, 63-68. https://doi.org/10.1016/j.scp.2018.06.002.

Nagarkar, B., Jagtap, S., Narkhede, A., Nirmal, P., Pawar, N., Kuvalekar, A., Kulkarni, O., & Harsulkar, A. (2013). Different Ayurvedic dosage forms of Dashamoola possess varied anti-inflammatory activity. *World J Pharm Pharmaceutic Sci*, *2*, 3118-3136.

Nandiyanto, A. B. D., Wiryani, A. S., Rusli, A., Purnamasari, A., Abdullah, A. G., Widiaty, I., & Hurriyati, R. (2017). Extraction of curcumin pigment from Indonesian local turmeric with its infrared spectra and thermal decomposition properties. *In IOP Conference Series: Materials Science and Engineering, 180(1),012136*. DOI 10.1088/1757-899X/180/1/012136.

Pandian, B., Ramalingam, S., Sreeram, K. J., & Rao, J. R. (2021). Natural pigment: Preparation of brown pigment from lignin biomass for coloring application. *Dyes and Pigments*, *195*, 109704. https://doi.org/10.1016/j.dyepig.2021.109704.

Pradyawong, S., Shrestha, R., Li, P., Sun, X. S., & Wang, D. (2022). Effect of pH and pH-shifting on lignin–protein interaction and properties of lignin-protein polymers. *Journal of Polymers and the Environment*, 1-12. https://doi.org/10.1016/j.dyepig.2021.109704.

Ragauskas, A. J., & Yoo, C. G. (2018). Advancements in biomass recalcitrance: the use of lignin for the production of fuels and chemicals. *Frontiers in energy research*, *6*, 118. https://doi.org/10.3389/fenrg.2018.00118.

Rahman, UR O., Shi, S., Ding, J., Wang, D., Ahmad, S., Yu, H. (2018). Lignin nanoparticles: synthesis, characterization and corrosion protection performance. *New Journal of Chemistry,* 42(5), 3415-25. DOI: 10.1039/C7NJ04103A.

Randive, D. S., Adnaik, R. S., Nalawade, P. P., & Patil, A. M. (2014). Studies on standardization parameters for marketed formulations of draksharishtha. *International Journal of Pharma and Bio Sciences, 3*(4), 397-401.

Rattis, B. A., Ramos, S. G., & Celes, M. (2021). Curcumin as a Potential Treatment for COVID-19. *Frontiers in pharmacology*, 1068. https://doi.org/10.3389/fphar.2021.675287.

Ruiz, R., Ehrman, T, (1996), Determination of carbohydrates in biomass by high performance liquid chromatography. Laboratory analytical procedure, 2.

Sathyan, S., & Nisha, P. (2022). Optimization and characterization of porous starch from corn starch and application studies in emulsion stabilization. *Food and Bioprocess Technology*, *15*(9), 2084-2099. https://doi.org/10.1007/s11947-022-02843-y.

Saffarionpour, S., & Diosady, L. L. (2022). Curcumin, a potent therapeutic nutraceutical and its enhanced delivery and bioaccessibility by pickering emulsions. *Drug Delivery and Translational Research*, 1-34. https://doi.org/10.1007/s13346-021-00936-3.

Schneider, W. D. H., Dillon, A. J. P., & Camassola, M. (2021). Lignin nanoparticles enter the scene: A promising versatile green tool for multiple applications. *Biotechnology Advances*, 47, 107685. https://doi.org/10.1016/j.biotechadv.2020.107685.

Sekeri, S. H., Ibrahim, M. N. M., Umar, K., Yaqoob, A. A., Azmi, M. N., Hussin, M. H., & Malik, M. F. I. A. (2020). Preparation and characterization of nanosized lignin from oil palm (Elaeis guineensis) biomass as a novel emulsifying agent. *International journal of biological macromolecules*, *164*, 3114-3124. https://doi.org/10.1016/j.ijbiomac.2020.08.181.

Si, S., Chen, Y., Fan, C., Hu, H., Li, Y., Huang, J., & Tu, Y. (2015). Lignin extraction distinctively enhances biomass enzymatic saccharification in hemicelluloses-rich Miscanthus

species under various alkali and acid pretreatments. *Bioresource technology*, 183, 248-254. https://doi.org/10.1016/j.biortech.2015.02.031

Sindhu, R., Kuttiraja, M., Binod, P., Janu, K. U., Sukumaran, R. K., & Pandey, A. (2011). Dilute acid pretreatment and enzymatic saccharification of sugarcane tops for bioethanol production. *Bioresource Technology*, *102(23),* 10915-10921. https://doi.org/10.1016/j.biortech.2011.09.066.

Sipponen, M. H., Farooq, M., Koivisto, J., Pellis, A., Seitsonen, J., & Österberg, M. (2018). Spatially confined lignin nanospheres for biocatalytic ester synthesis in aqueous media. *Nature Communications*, 9(1), 2300. https://doi.org/10.1038/s41467-018-04715-6.

Sodeinde, K. O., Ojo, A. M., Olusanya, S. O., Ayanda, O. S., Adeoye, A. O., Dada, T. M., & Lawal, O. S. (2021). Cellulose isolated from Delonixregia pods: Characterisation and application in the encapsulation of vitamin A. *Industrial Crops and Products*, *160*, 113138. https://doi.org/10.1016/j.indcrop.2020.113138.

Tarasov, D., Leitch, M., & Fatehi, P. (2018). Lignin–carbohydrate complexes: properties, applications, analyses, and methods of extraction: a review. *Biotechnology for biofuels*, *11*(1), 1-28. https://doi.org/10.1186/s13068-018-1262-1.

Tao, H., Wang, P., Wu, F., Jin, Z., & Xu, X. (2016). Particle size distribution of wheat starch granules in relation to baking properties of frozen dough. *Carbohydrate Polymers*, *137*, 147-153. https://doi.org/10.1016/j.carbpol.2015.10.063.

Tortora, M., Cavalieri, F., Mosesso, P., Ciaffardini, F., Melone, F., & Crestini, C. (2014). Ultrasound driven assembly of lignin into microcapsules for storage and delivery of hydrophobic molecules. *Biomacromolecules*, *15*(5), 1634-1643. https://doi.org/10.1021/bm500015j.

Wang, B., Li, D., Wang, L. J., & Özkan, N. (2010). Effect of concentrated flaxseed protein on the stability and rheological properties of soybean oil-in-water emulsions. *Journal of Food Engineering*, *96*(4), 555-561. https://doi.org/10.1016/j.jfoodeng.2009.09.001.

Winuprasith, T., Khomein, P., Mitbumrung, W., Suphantharika, M., Nitithamyong, A., & McClements, D. J. (2018). Encapsulation of vitamin D_3 in pickering emulsions stabilized by nanofibrillated mangosteen cellulose: Impact on in vitro digestion and bioaccessibility. *Food hydrocolloids*, *83*, 153-164. https://doi.org/10.1016/j.foodhyd.2018.04.047.

Wunna, K., Nakasaki, K., Auresenia, J. L., Abella, L. C., & Gaspillo, P. A. D. (2017). Effect of alkali pretreatment on removal of lignin from sugarcane bagasse. *Chemical Engineering Transactions*, 56, 1831-1836. DOI:10.3303/CET1756306

Yuan, T., Zeng, J., Guo, D., Sun, Q., Wang, B., Sha, L., & Chen, K. (2023). Multiphasic lignocellulose-based suspension for oil-water interfacial stabilization: synergistic adsorption and phase behavior. *International Journal of Biological Macromolecules*, *224,* 1142-1151. https://doi.org/10.1016/j.ijbiomac.2022.10.198.

Yu, M., Xin, H., He, D., Zhu, C., Li, Q., Wang, X., & Zhou, J. (2023). Electrospray lignin nanoparticles as Pickering emulsions stabilizers with antioxidant activity, UV barrier properties and biological safety. *International Journal of Biological Macromolecules*, *238*, 123938. https://doi.org/10.1016/j.ijbiomac.2023.123938.

Zahedipour, F., Hosseini, S. A., Sathyapalan, T., Majeed, M., Jamialahmadi, T., Al-Rasadi, K., Banach, M., & Sahebkar, A. (2020). Potential effects of curcumin in the treatment of COVID-19 infection. *Phytotherapy Research*, *34*(11), 2911-2920. https://doi.org/10.1002/ptr.6738.

Zembyla, M., Murray, B. S., & Sarkar, A. (2020). Water-in-oil emulsions stabilized by surfactants, biopolymers and/or particles: A review. *Trends in Food Science & Technology,* 104, 49-59. https://doi.org/10.1016/j.tifs.2020.07.028

Zhao, X., Yang, X., Bao, Y., Guo, Y., Luo, J., Jiang, S., & Zhang, W. (2023). Construction of vitamin D delivery system based on pine nut oil Pickering emulsion: effect of phenols. *Journal of the Science of Food and Agriculture*, 103(8), 4034-4046. DOI 10.1002/jsfa.12363.

Zou, T., Sipponen, MH., Osterberg, M. (2019). Natural shape-retaining microcapsules with shells made of chitosan-coated colloidal lignin particles. *Frontiers in Chemistry,* 22,7:370. https://doi.org/10.3389/fchem.2019.00370.

Chapter-5

Nutrient-rich puffed snacks developed using blended flours and lignin Pickering emulsions containing curcumin and vitamin D_3

Abstract:

This study explores the use of blended flours and fortification with health-promoting compounds to improve the nutritional profile of extruded puffed snacks (EPS). Lignin particles extracted from the Ayurvedic spent materials were used to create lignin Pickering emulsions (LPE) for incorporating the lipophilic compounds, curcumin and vitamin D_3. A blended flour composed of pearl millet, spent coconut, and corn grits was used to replace 80% of the traditionally used corn grits. Fortification was achieved by incorporating LPE containing curcumin and vitamin D_3. Protein content, dietary fiber, texture profile, and structural integrity of the snacks were evaluated. Compared to a control made solely from corn grits, the EPS with blended flour showed higher protein (13.8%) and dietary fiber (19.2%) contents. However, the increase in protein and fiber content resulted in lower expansion ratios for EPS produced with the blended flour, with or without LPE. The EPS containing LPE had similar hardness, microstructure, fracturability, chewiness, and gumminess as those without LPE. Sensory analysis scores confirmed the acceptability of EPS and EPS containing LNP. Importantly, the inclusion of LPE enhanced the stability of curcumin (69.0%) and vitamin D_3 (65.7%), highlighting the protective encapsulation effect of lignin particles. This study underscores the potential of lignin-based Pickering emulsions loaded with lipophilic compounds, combined with blended flours, for producing nutrient-rich and health-promoting ready-to-eat snacks through extrusion.

Key words: Extrusion, Puffed snacks, Lignin, Pickering emulsion, Fortification, Blended flour, Curcumin, Vitamin D_3

Graphical abstract

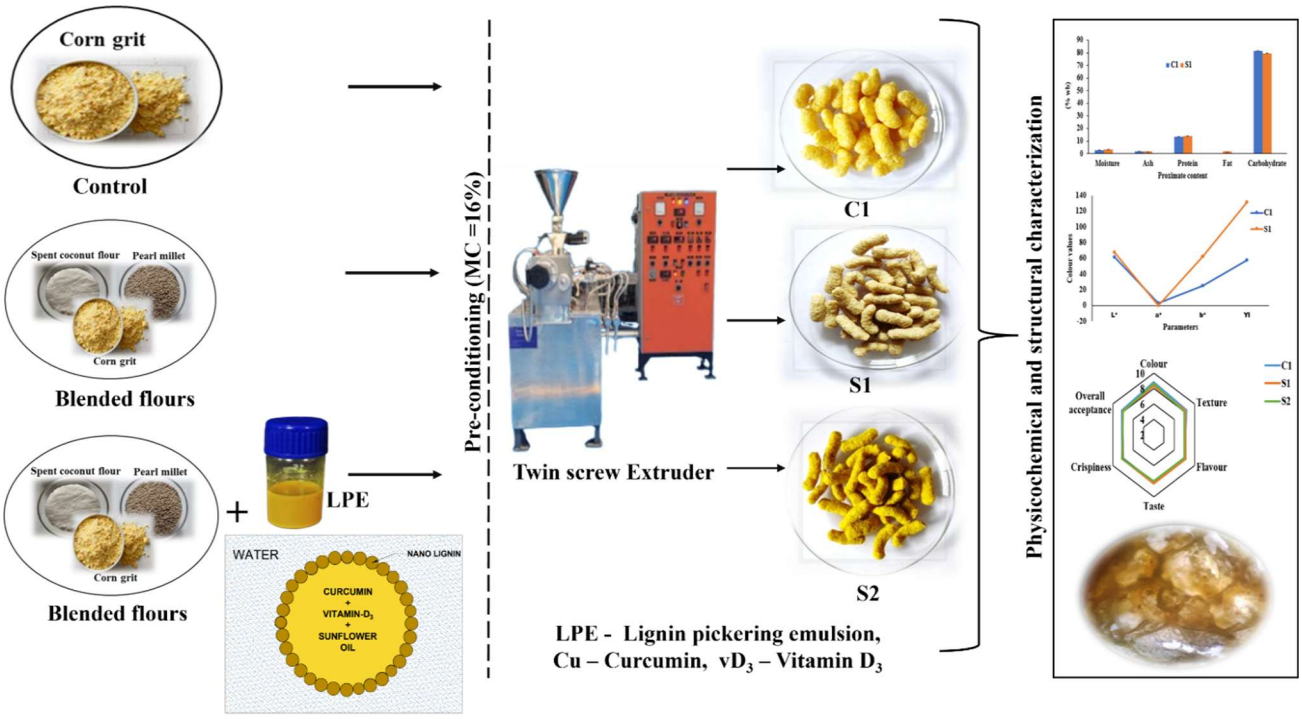

Fig. 3. Graphical abstract showing extruded snacks from blended flours and lignin Pickering emulsions with curcumin and vitamin D_3

Highlights:

- Extruded puffed snacks (EPS) were produced from blended flour of pearl millet, spent coconut flour, and corn grits
- EPS was infused with curcumin and vitamin D_3 encapsulated in lignin-based Pickering emulsion (LPE)
- EPS with LPE maintained texture, sensory appeal, and structural integrity
- LPE protected curcumin (69%) and vitamin D_3 (65%)
- LNP can be an effective carrier for delivery of functional ingredients in food products

5.1. Introduction

Extrusion cooking is a widely used industrial process that applies high pressure, heat, and mechanical force in a short time, resulting in significant transformations in food matrices. This method is effective for producing ready to eat (RTE) snacks with unique textures and flavors. The high-temperature short-time (HTST) nature of extrusion enables rapid cooking and facilitates the production of a wide variety of snack products (Abilmazhinov et al., 2023). However, the intense conditions can also degrade heat-sensitive nutrients like vitamins, essential fatty acids, and bioactive compounds, which poses a challenge in the development of nutritionally fortified snacks (Prabha et al., 2021).

Fortifying extruded snacks with bioactive and nutritional compounds has become increasingly important because it offers health benefits beyond basic nutrition (Dilrukshi et al., 2022). Traditional fortification methods typically involve the direct addition of vitamins, minerals, or other bioactive compounds to the food matrix before extrusion. However, these methods often result in significant nutrient losses due to the harsh processing conditions, thereby reducing the effectiveness of fortification (Onwulata, 2013). When carried out as a preceding step, microencapsulation protects bioactive compounds like omega-3 fatty acids and probiotics from the detrimental effects of extrusion by creating a protective barrier, thereby enhancing the nutritional quality of the final product (Feizollahi et al., 2018; Sultana et al., 2022). Pickering emulsions that are stabilized by solid particles rather than surfactants, are attracting increasing attention as delivery vehicles owing to their higher stability and better ability to protect the encapsulated bioactive compounds (Abraham et al., 2024). Studies have focused on improving the nutritional characteristics of extruded products by incorporating biopolymers, such as inulin and chitosan (Tsokolar-Tsikopoulos et al., 2015; Kumar et al., 2018). Incorporating inulin, a prebiotic fiber, into extruded snacks has been shown to enhance dietary fiber content, improve gut health, and boost

antioxidant activity, thereby making the snacks nutritionally superior (Tsokolar-Tsikopoulos et al., 2015). Another study highlighted the role of chitosan in enhancing the functional properties of proteins, reducing fat absorption during extrusion, and improving the textural attributes of snacks (Kumar et al., 2018).

Lignin, a natural biopolymer from plant cell walls, is gaining attention for its potential to create delivery systems that enhance the bioavailability of encapsulated bioactive compounds (Wang et al., 2023; Abraham et al., 2023). A recent study showed that lignin, as a Pickering particle, effectively protected sensitive nutrients like vitamins (e.g., vitamin D_3) and polyphenols (e.g., curcumin) from heat and mechanical degradation, while improving their stability and delivery (Abraham et al., 2024). Curcumin, a polyphenol found in turmeric, is well-known for its anti-inflammatory, antioxidant, and antimicrobial properties, while vitamin D_3 is essential for calcium absorption and bone health (Al-Azzawi et al., 2023). The combination of these bioactives in lignin-based Pickering emulsions represents a novel approach to fortification, particularly in high temperature processes like extrusion.

Extruded snacks are commonly made using corn flour, which is favored for its starch content that supports the puffing and expansion processes during extrusion. However, corn-based extruded snacks often lack significant nutritional value, as they are typically low in protein, fiber, and essential micronutrients (Amadeu et al., 2024, Ahmed et al., 2024). In developing nutritionally enhanced extruded snacks, the choice of raw materials is of prime importance, and blended flours offer a practical solution (Amadeu et al., 2024). These flour blends typically combine grains, tubers, legumes, and seeds, providing a balanced mix of proteins, carbohydrates, fibers, and micronutrients (Ahmed et al., 2024; Grasso, 2020). Ahmed et al., (2024) demonstrated that twin-screw extrusion can produce granules containing iron and vitamin D_3, using a blend of corn and

lentil flours as the carrier matrix. These granules exhibited excellent chemical stability and bioactive effects when tested on human osteoblast cells, suggesting potential applications for bone health. Grasso, (2020) reviewed the use of industrial by-products in extruded snacks, emphasizing nutritional and sustainability benefits. These studies highlight the versatility of blended flours in developing nutrient-rich extruded snacks. Spent coconut flour, a by-product of virgin coconut oil production, is rich in dietary fiber, protein, and antioxidants, making it an excellent ingredient to enhance the health benefits of snacks, particularly for gluten-free and vegan consumers (Shakeela et al., 2024). Similarly, pearl millet flour, rich in essential minerals and other nutrients, is derived from a crop known for its drought resilience (Longvah, 2017).

This study aimed to develop fortified extruded puffed snacks (EPS) using blends of pearl millet, corn grits, and spent coconut flour, enriched with LPE-encapsulated curcumin and vitamin D_3. The EPS were compared to a corn-based control for their physicochemical, textural, and sensory properties. The stability of the encapsulated bioactives (curcumin and vitamin D_3) was also compared to that of the non-encapsulated formulation. This research achieves improved stability of curcumin and vitamin D_3 while creating healthier snacks that contribute to improved micronutrient intake and support better overall nutrition.

5.2. Materials and methods

5.2.1. Materials

Lignin was isolated from Ayurvedic spent materials, converted to nano lignin using planetary mill (Pulverisette, Fritsch, Germany) as reported by Abraham et al., (2024). Spent coconut meal, a by-product of virgin coconut oil processing, was supplied by Apex Coco Solar Energy Pvt. Ltd. (Tamil Nadu, India). The residual oil was removed to produce spent coconut flour (SCF). Pearl millet and corn were sourced from the local market in Thiruvananthapuram, cleaned, ground into flour, and

sieved through a 200 mm mesh to achieve uniform particle size. Curcumin and cholecalciferol (Vitamin D_3) were procured from Sigma-Aldrich Chemicals Pvt. Ltd. (Massachusetts, USA). All other chemicals and reagents used in this study were of chromatography grade and were sourced from reliable local suppliers.

5.2.2. Preparation of O/W Pickering emulsions

Oil-in-water (O/W) Pickering emulsions were formulated using lignin nanoparticles as the stabilizing agent. LNP solution was prepared at a concentration of 2000 ppm at a pH of 8.0 Sunflower oil (10% w/w), containing 50 ppm of curcumin and 50 ppm of vitamin D_3 was used as the dispersed phase. This emulsion was prepared by sonicating with a VCX-750 Vibra Cell (Sonics & Materials, USA) for 45 min (using a 10 s on/10 s off cycle at 50% amplitude) according to the recent study by Abraham et al. (2024). The resulting Pickering emulsion (LPE) was used for fortification of the extruded snacks.

5.2.3. Preparation of extruded snacks

The composition of flour blend was determined through preliminary trials and contained 15% Spent Coconut Flour (SCF), 65% Pearl Millet Flour (PMF), and 20% Corn Grits (CG) on w/w basis. This formulation yielded extrudates with sensory and physical properties comparable to the control made with only corn grits. The control, prepared using only corn grit, is referred to as **C1**, and the product with optimized flour blend is denoted as **S1**.

This optimised flour blend was subsequently infused with LPE. The resulting LPE infused (which contained curcumin and vitamin D_3 as stated above) extrudates are referred to as **S2**.

5.2.4. Extrusion process

The blended flour (S1) was uniformly mixed using a laboratory-scale mixer (Basic Technology Private Ltd, Kolkata, India) and conditioned with 16 ± 1% water to achieve optimal expansion and

texture during extrusion cooking. The hydrated flour was equilibrated for 1 h at ambient temperature (30 ± 2 °C) in an airtight container before extrusion. After conditioning, the flour mixtures were extruded. For all the EPS the time and temperature were kept same.

Extrudates were prepared using a laboratory scale twin screw extruder employing hot extrusion technology (L-TSE, Basic Technology Private Ltd, Kolkata, India). The operating parameters of the extrusion process including screw speed, feed moisture content, and cooking temperature, were optimized through preliminary trials. The extrusion process is illustrated in Fig. 5.1. Before operation, the extruder was primed, and a 2 mm circular die was attached to the barrel end. The barrel was heated to 105 °C and 80 °C. The screw speed (350 rpm), feeder speed (10 rpm), and cutter speed (70 rpm) were adjusted via the main control panel. Once the desired barrel temperature was reached, the optimized flour blend was fed using a semi-automatic feeder, and the extruded product emerged from the die. The extrudates were cut uniformly by the cutter assembly, cooled to room temperature, and promptly packed into pouches. The extrudates were toasted in a conventional oven (Bajaj OTG oven, India) at 160 °C for 3 min. This temperature-time combination was determined through trials. The toasted extruded products were coated with refined sunflower oil and a seasoning agent (Symega Food Ingredients Limited, Cochin, Kerala, India) for sensory appeal.

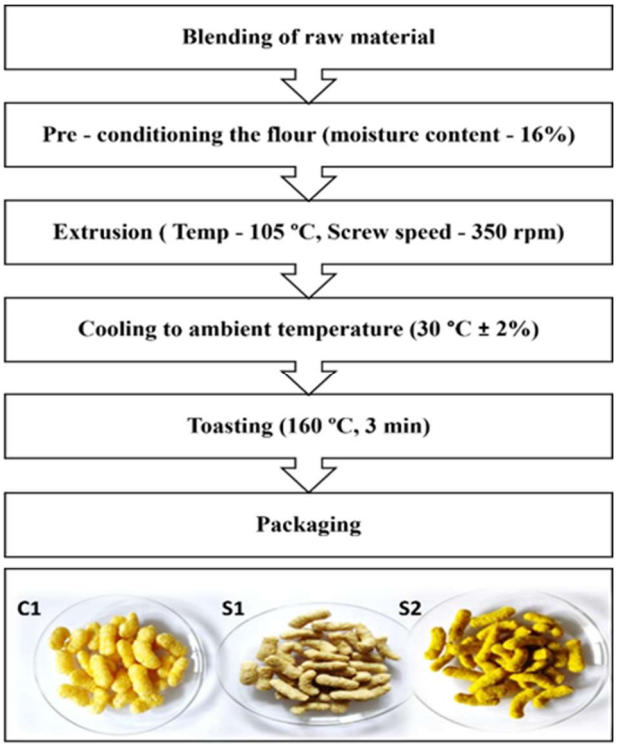

Fig. 5.1. Flowchart of extrusion process to produce EPS: C1 - Control, S1 – EPS with Composite flour, S2 – EPS with lignin-based Pickering emulsion fortified (LPE)

5.2.5. Analysis of the physical and functional attributes of extrudates

5.2.5.1. Proximate composition of flours and extrudates

Moisture, ash, fat, and protein contents were determined according to the procedures outlined by the AOAC (method 930.15, 923.03, 920.39) (1990). Samples were oven-dried at 105 °C, then transferred to a desiccator and allowed to cool to room temperature (32.0 ± 2°C). For determining ash content, the mass of the samples was recorded before and after the ashing step using a muffle furnace (550 °C for 6 h). Protein content was determined using Micro Kjeldahl method with nitrogen-to-protein conversion factor of 6.25. The fat content was determined via Soxhlet extraction. Total carbohydrate was determined by difference.

5.2.5.2. Estimation of dietary fiber

The dietary fiber content of EPS - S1, S2 and C1 was determined according to the Bureau of Indian Standards Method IS:11062, (1984) with a slight modification. Fat- and moisture-free samples were autoclaved with water, the pH was adjusted, and pepsin, pancreatin, and glucoamylase were added. The mixture was then incubated for enzymatic digestion. After incubation, the pretreated extract was centrifuged at 1,118,000 × g for 10 min to separate the residue and supernatant. The residue, containing insoluble fiber, was collected, washed three times with acetone and diethyl ether, and lyophilized to obtain a stable weight of insoluble dietary fiber. The supernatant, containing soluble fiber, was precipitated using ethanol and refrigerated overnight. It was then centrifuged (Model 7780; KUBOTA, Tokyo, Japan) again at 1,118,000 × g for 10 min, and the resulting residue was collected. This residue was washed three times with alcohol, acetone, and diethyl ether, then lyophilized in a pilot scale freeze dryer (SP Scientific VirTis Genesis 35L Pilot Lyophilizer, Warminster, USA) to achieve a constant weight, yielding the soluble dietary fiber (Arun et al., 2018).

5.2.5.3. Expansion ratio

The expansion ratio of an EPS was measured by comparing the diameter of the extruded product to that of the die (Tas & Shah, 2021). A digital vernier calliper (0.1 accuracy) was used to measure the diameter of ten randomly selected extrudates, and the mean value was recorded. The expansion ratio of the extrudates was calculated using equation (1).

$$\mathrm{ER} = \frac{\text{Cross sectional diameter of extrudate}}{\textit{Cross sectional diameter of the die opening}} \quad (1).$$

5.2.5.4. Bulk density

The length and diameter of ten EPS samples were measured using the digital vernier caliper. The mass of these 10 EPS samples was also measured. The bulk density was measured using equation (2) considering they were cylindrical in shape (Suri et al., 2020).

$$\text{Bulk density } (g/cm^3) = 4m/(\pi d^2 L) \quad (2).$$

Where, L is the length (cm), m is the mass (g) and d is the diameter (cm) of the extruded snacks, respectively.

5.2.5.5. Colour analysis

The colour parameters of the EPS were measured using a colourimeter (Hunter lab, Colour Flex EZ, Virginia, USA). The empty cuvette was calibrated initially using standard white and black plates. The hue of the samples was assessed on the L* (lightness), a*(red-green), and b* (yellow-blue) colour systems. To measure the colour values, the extruded products were pulverized and transferred into cylindrical glass sample cuvette, which were then placed in the sample port. The colour values were recorded after 10 rotations of each sample, with measurements taken in triplicate (Shakeela et al., 2022).

5.2.5.6. Texture analysis

The textural properties of extrudates were analyzed using a texture analyzer (TA. XT texture analyzer, Stable Microsystems, Surrey, England). Texture profile analysis (Stable Microsystems) was employed to measure properties such as hardness, gumminess, chewiness, fracturability. A 2 mm cylindrical probe was used in these measurements. The tests were carried out in compression mode using the following parameters: pre-test speed: 1 mm/s, post-test speed: 5 mm/s, test speed: 1 mm/s, trigger force: 5 g, distance (compression): 10 mm. The texture of EPS was analyzed at three different positions of the sample, and each sample was tested in triplicate.

5.2.5.7. Sensory analysis

Sensory analysis was conducted to evaluate the acceptability of extrudate snacks. A semi trained panel of 25 members, aged 25 to 45, assessed the samples based on appearance, colour, aroma, taste, and overall acceptance. Panelists were instructed to focus on one attribute at a time and cleanse their palate with water between each sample to prevent cross-sensory contamination. Participants were encouraged to provide candid feedback based on their overall sensory experience. A 9-point hedonic scale was used for the evaluation, with scores ranging from 1 ('dislike extremely'), 5 ('neither like nor dislike'), and 9 ('like extremely'), following the guidelines of ISO 4121:2003. The average score across all criteria was calculated to determine the sensory attributes (Wichchukit, 2015).

5.2.5.8. Cross sectional microscopic images

The microstructure of the EPS was observed using an Olympus CX41 microscope (Olympus, Shinjuku, Tokyo, Japan). Images of the surface morphology of the extrudates were captured at 4× magnification using a camera attached to the microscope and equipped with QCapture software (QImaging).

5.2.5.9. Observing microscopic morphology

The EPS were sliced and mounted onto an aluminum specimen holder using carbon tape. Prior to microscopic examination, a thin layer of gold was applied using a gold/palladium sputter coater (SC7620, Emitech, Quorum Technologies Ltd, Kent, UK). Scanning electron microscopy (ZEISS; EVO 18, Germany) was used to acquire and analyse the microscopic surface morphology of the extruded samples. The instrument operated at an accelerating voltage of 15 kV. Micrographs were captured at 500× magnification.

5.2.5.10. Stability of curcumin and vitamin D_3

The bioactive stability, representing the percentage retaining of curcumin and vitamin D_3 in the extruded product, was determined using a high-performance liquid chromatography with a diode-array detector (HPLC-DAD). For the analysis, 1 g of powdered EPS was mixed with 5 mL of methanol and magnetically stirred for 3 h. The methanolic extract was centrifuged at 1,118,000 × g for 10 min, and the supernatant was collected and filtered through a 0.22 µm PTFE syringe filter. The HPLC analysis was performed as previously described by the (Abraham et al., 2024). Briefly, a Prominence UFLC system (Shimadzu, Japan) was used, equipped with a Phenomenex Gemini C18 column (250 × 4.6 mm, 5 µm). The system operated with an isocratic flow of 100% methanol at a rate of 1 mL/min, with detection wavelengths of 420 nm for curcumin and 261 nm for vitamin D_3. Retention times for curcumin and vitamin D_3 were 3.2 min and 7.6 min, respectively. The column temperature was maintained at 40 °C throughout the analysis.

5.2.6. Statistical analysis

Experiments were carried out in triplicate except mentioned above. All analyses were conducted with three technical replicates, and the results are presented as mean ± standard deviation (SD). The data were subjected to analysis of variance (ANOVA) using GraphPad Prism 5.0 statistical software to determine if there were statistically significant differences between any two mean values or samples ($p < 0.05$).

5.3. Results and discussion

5.3.1. Nutritional profile of extruded snacks

The nutritional profiles of EPS are shown in Table 5.1. The fat content showed a slight increase in S2 (1.64 %), attributed to the inclusion of sunflower oil in the emulsion, while S1 (0.10 %) and C1 (0.08 %) showed comparatively lower fat levels. Variations in carbohydrate content were

observed, likely due to differences in ingredient composition, such as dietary fiber. Other parameters, including moisture and ash content, showed no significant differences among C1, S1, and S2. EPS produced using the blended flour showed significantly higher protein content as compared to C1. Typically, extruded snacks are made with corn flour to achieve better expansion and texture. However, it is low in protein and other essential nutrients. Over-reliance on this ingredient results in nutritionally deficient snacks with a high glycemic index. The use of blended flour in this study produced snacks with increased protein content (13.5%) in S1 against 9.8% in the corn-based control (C1). The increased protein content came from the spent coconut flour (SCF), a known protein-rich ingredient. SCF contains 25.5% protein, thus, it significantly contributed the protein content in the formulation. Additionally, pearl millet, with a reported protein content of 12.5% (Navami, 2024), further enhanced the protein profile of the blend. Similar increase in protein content was reported in enriched extrudates; for example, Gojiya et al., (2022) and group observed an increase in protein content from 14.0% to 26.7% when 10% to 40% defatted sesame flour was added in the formulation.

The addition of PMF and SCF to the blended flour significantly enhanced the dietary fiber content in the EPS. SCF contains 54.0% total dietary fiber, including 44.5% insoluble fiber and 9.5% soluble fiber. Similarly, pearl millet contributes to the fiber profile of S1, as it contains 11.5% total dietary fiber, comprising 9.1% insoluble fiber and 2.3% soluble fiber (Longvah, 2017). S1 contained significantly higher levels of total dietary fiber (18.9%), insoluble dietary fiber (14.2%), and soluble dietary fiber (4.6%) compared to C1, which had 13.0%, 9.6%, and 3.4%, respectively (Table 5.1). This increase in fiber content can be attributed to the contributions of pearl millet and SCF. A recent study (Karun et al., 2023) reported a 5% increase in protein content in extrudates with the addition of green gram and cowpea flour, along with a 3% reduction in total carbohydrate

content, making it a healthier snack option. Similarly, another study observed significant increases in protein (7.6% to 27.2%) and fiber content (0.1% to 2.6%) in extrudates with the incorporation of cowpea (10% to 30%) and whey protein concentrate (WPC) (5% to 20%) compared to the control. The formulation containing 15% cowpea and 5% WPC received the highest levels of acceptance, with a protein content of 14.6% and a total dietary fiber content of 1.6% (Dilrukshi et al., 2022). These findings highlight that use of blended flour containing fiber- and protein-rich ingredients can significantly improve the nutritional profile of extruded snacks (Amadeu et al., 2024; Delic et al., 2023). The snacks developed in this study were significantly dense in terms of protein and dietary fiber can be considered as healthier option.

Table 5.1: Nutritional profile of EPS from corn grit (C1) and blended flours (S1), blended flours infused with curcumin and vitamin D_3 (S2).

Composition (Wb %)	**C1**	**S1**	**S2**
Protein	9.8 ± 0.0^{a}	13.5 ± 0.1^{b}	13.8 ± 0.2^{b}
Moisture	2.9 ± 0.5^{a}	2.8 ± 0.1^{b}	3.3 ± 0.0^{c}
Fat	0.1 ± 0.2^{a}	0.1 ± 0.2^{a}	1.6 ± 0.1^{c}
Ash	1.4 ± 0.2^{a}	2.0 ± 0.1^{b}	1.74 ± 0.0^{b}
Carbohydrate	85.8 ± 0.2^{a}	81.6 ± 0.5^{b}	79.5 ± 0.1^{c}
Total dietary fiber	13.0 ± 0.2^{a}	18.9 ± 0.1^{b}	19.2 ± 0.1^{c}
Insoluble dietary fiber	9.6 ± 0.1^{a}	14.2 ± 0.1^{b}	14.6 ± 0.2^{b}
Soluble dietary fiber	3.4 ± 0.2^{a}	4.6 ± 0.1^{b}	4.6 ± 0.2^{b}

Different superscripts within the same row denote significant differences between the samples and control ($p > 0.05$; $n = 3$).

5.3.2. Bulk density and expansion ratio

The bulk density and expansion ratio are important indicators of texture, mouthfeel, and overall consumer acceptance of extruded snacks. Bulk density reflects the degree of puffing in extruded products and the blended flour and LPE are expected to alter the bulk density of the snack samples. As shown in Fig. 5.2a, the bulk density of S1 (0.70 g/cm³ and S2 (0.72 g/cm³) were higher than that of the control C1 (0.50 g/cm³). The similar bulk density values of S1 and S2 indicated that the incorporation of LPE did not significantly alter the physical or internal structure of the snacks. Bulk density is influenced by the interactions among starch, protein, and fiber components (Aussanasuwannakul, 2022). SCF is rich in dietary fiber, which enhances the compactness of extruded snacks and increases their bulk density. The observed increase in bulk density with the addition of dietary fiber suggests that higher fiber content contributes to a denser and more compact extrudate structure. Previous studies have shown that increased fiber content in extruded products correlates with higher bulk density.

The higher expansion ratios typically signify lighter, crispier textures. The control sample (C1) had the highest expansion ratio 4.01, while the expansion ratio of both S1 and S2 was only 37.2% of the control (Fig. 5.2b). The inclusion of soluble and insoluble fibers in extruded snacks significantly influences their physicochemical characteristics, particularly the expansion ratio and bulk density. The observed decrease in expansion ratio can be attributed to the increased protein and fiber content, resulting in a denser, less expanded structure. An increase of protein content also affects the extent and rate of starch gelatinization, which could lead to a decrease in the expansion ratio (Aussanasuwannakul, 2022). Studies have shown that incorporating dietary fibers from various sources, such as polydextrose, gum acacia, inulin, xanthan gum, and resistant starch, into corn-based feed reduces the expansion of extruded snacks. The addition of fiber increases the

viscosity of the starchy dough during extrusion, reducing the water available for gelatinization and thereby limiting starch expansion at the die (Han et al., 2017).

Fiber typically functions as an inert filler within the expanded starch matrix. At low concentrations, the fiber is insufficient to evenly distribute throughout the extrudate matrix. However, as its content increases, the starch matrix may become overwhelmed, causing it to collapse as fiber particles penetrate. This process ultimately reduces the expansion ratio. Previous study reported reduced expansion index values in extruded products containing okara and mung bean powder. This was attributed to the high fiber content (60.8% in okara; 15.2% in mung bean) and notable protein levels (26.5% in okara; 20.2% in mung bean) Aussanasuwannakul (2022). Similarly, extruded snacks made with 80–90% broken rice and 10–20% lupin flour, higher rice content increased the expansion index, whereas higher lupin flour content reduced it (Oliveira et al., 2015). During snack extrusion, dietary fiber significantly impacts starch gelatinization by competing with starch for available water. This competition reduces amylose leaching and limits the full gelatinization of amylose and amylopectin, potentially affecting amylose retrogradation and disrupting the structure of amylopectin. Additionally, fiber increases dough viscosity, disrupting the starch matrix and hindering expansion. These structural disruptions weaken the matrix, reducing the expansion ratio and producing denser snacks with higher bulk density and less puffiness. As a result, the texture of fiber-enriched snacks differs markedly from fiber-free products (Alam et al., 2016; Aussanasuwannakul, 2022).

The extruded product formulated with 15% spent coconut flour (SCF) and 65% pearl millet flour successfully replaced 80% of corn flour, marking a significant step toward replacing traditional corn-based snacks. Similarly, extruded snack developed using 80% pearl millet flour, 10% African

walnut flour, and 10% corn starch, which achieved moderate sensory acceptance (Sobowale et al., 2021).

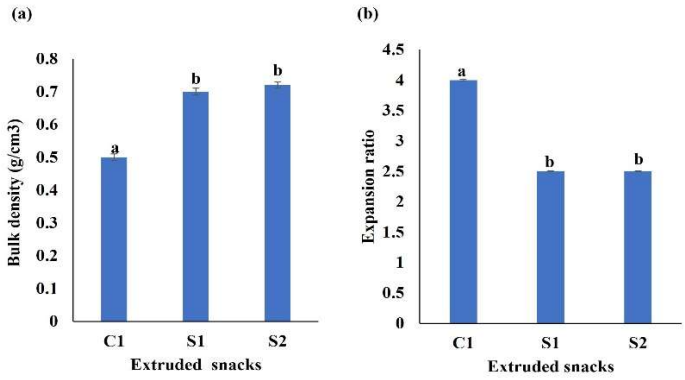

Fig. 5.2. (a) Bulk density (b) expansion ratio, content in the extrudates. Different letters denote significant difference between the samples ($p<0.05$).

5.3.3. Texture profile analysis

Texture attributes like hardness, fracturability, gumminess, and chewiness are essential for evaluating the quality and appeal of extruded snacks. Hardness affects the perception of freshness, while fracturability can be correlated with the crispiness. Gumminess indicates the effort required to chew, and chewiness influences the overall sensory experience. All of these attributes are vital for creating products that satisfy the consumers. The texture qualities of the extruded snacks are shown in Fig. 5.3. The increase in hardness observed in S1 and S2 compared to C1 is primarily due to the higher protein and fiber content from SCF and PMF, which disrupts the starch matrix, leading to reduced expansion and a denser texture. The strong relationship between hardness and expansion suggests that higher protein and fiber levels enable the formation of a compact structure that affects the overall texture. This type of relationship was also noted by Kumar et al., (2018), that fortification of snacks with chitosan, which was attributed to the increase in dietary fibre content. Similarly, an incorporation of 5 to 20% tomato pomace powder in extruded snacks was

found to increase in the hardness (Yagci et al., 2022). A protein-starch interaction that inhibited expansion might be attributed to an increase in hardness in sorghum-based extruded snacks when protein-rich soy meal flour was added up to 20% of formulation (Rodríguez-Vidal et al., 2017). The control sample (C1) had the highest chewiness when compared to S1 and S2. Earlier research also showed that the chewiness was significantly reduced from 1.63 N to 0.42 N when corn flour was supplemented with soy and chickpea flour about 20 - 40% (Shan et al., 2016). Gumminess of EPS increased with the addition of SCF and PMF compared to that of the control. Fiber acts as both a structure-forming and water-absorbing component, creating a denser matrix that resists deformation and thereby enhances gumminess. This aligns with previous studies showing that incorporating soy and chickpea flour into corn flour significantly increased gumminess, demonstrating a positive correlation between dietary fiber content and gumminess in extruded products. It is also reported that gumminess increased significantly from 0.33 N in the control to 1.99 N with when 20% soy and 20% chickpea flour substituted in corn flour (Shan et al., 2016). Fracturability is an important texture attribute that reflects the brittleness or crispness of a snack. A higher of fracturability value indicates that the snack can break with less force and indicates to a crunchy and crisp texture. In extruded snacks, it is affected by several factors, including the composition of the ingredients (e.g., starch, fiber, moisture, fat, or emulsifiers), the extrusion process parameters (e.g., temperature and pressure), and the extent of product expansion. It was observed that addition of fiber rich SCF and PMF resulted in a slight reduction in fracturability compared to that of the control. Fiber-rich ingredients, such as SCF and PMF, disrupt the continuous starch network, reducing product expansion and creating a denser texture. This compact structure absorbs more force before breaking, thereby reducing the product's brittleness. The lower expansion caused by high fiber content also decreases porosity, making the product less

brittle and slightly tougher to fracture. These findings are consistent with studies that reported similar effects when high-fiber ingredients, such as tomato pomace, were incorporated into extruded snacks, resulting in reduced fracturability due to the compact and dense structure (Yagci et al., 2022; Sinaki and Koksel, 2024).

Notably, the similar texture profiles of S1 and S2 suggest that incorporating lignin-based Pickering emulsions (containing curcumin and vitamin D_3) does not significantly alter the core textural properties of the snacks. This finding indicates that these emulsions can be used to fortify extruded snacks without compromising their overall texture profile, making them a promising option for enhancing nutritional value.

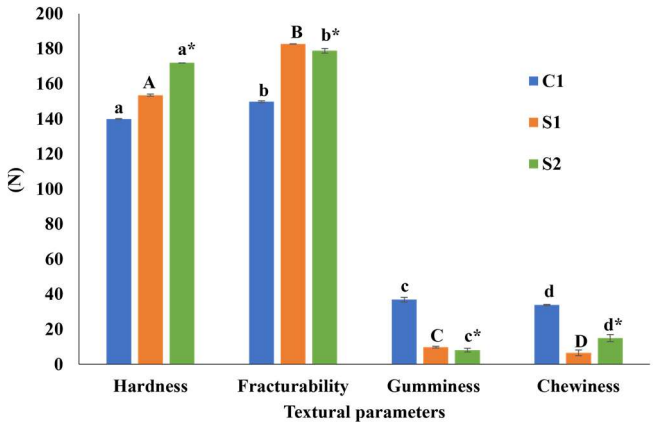

Fig. 5.3. Texture profile of extruded puffed snacks. All the parameters expressed in Newton (N). different letters denote significant difference in the values between the samples ($p<0.05$).

5.3.4. Colour analysis

The colour properties of the extruded snacks, as indicated by the L* (lightness), a* (red-green), b* (yellow-blue), and yellowness index (YI) values, showed significant variation among C1, S1, and S2 in terms of colour (Table 5.2). Sample C1 exhibited the highest lightness suggesting to a brighter appearance compared to the other samples. The a* and b* values of C1 indicated a more pronounced reddish and yellowish hue, contributing to its high yellowness index (YI = 80.86).

This is due to the presence of corn grits, whose yellow colour primarily comes from natural carotenoid pigments, particularly lutein and zeaxanthin.

In contrast, S1 displayed the lowest lightness and reduced a* and b* values, resulting in the lowest yellowness index (YI = 57.78). The lower colour intensity of S1 can be attributed to the incorporation of SCF and PMF, with the latter likely responsible for the darker colour. Pearl millet contributes to the dark colour of extrudates due to its high phenolic content, including tannins and flavonoids, which act as natural pigments. During extrusion, the high temperatures and pressures trigger the Maillard reaction, forming brown melanoidins that further enhance the dark colour. Pigments such as anthocyanins present in the bran layer of pearl millet further intensify the darkening effect during processing. It is reported that reactions such as Maillard browning, caramelization, pigment degradation, and lipid oxidation contribute to the reduction in lightness in extruded snacks (Zahari et al., 2021). S2, however, exhibited a markedly different colour profile. While its lightness was comparable to C1, the a* value shifted toward the green spectrum, and its b* value was significantly higher than the other samples, resulting in the highest yellowness index (YI = 131.26). This indicates that S2 had a strong yellow hue due to the presence of curcumin and lignin, which carry yellow and brown pigments (Abraham et al., 2024). The colour profile of the extruded snacks formulated in this work aligns with research showing that the addition of vegetable ingredients and other agricultural by-products to rice-, barley-, and corn-based extruded snacks improves their colour desirability (Gupta et al., 2008; Grasso, 2020; Brennan et al., 2013). Furthermore, the inclusion of lignin in extruded snacks not only supports the stability of bioactives like curcumin and vitamin D_3 but also enhances the product's visual appeal.

Table 5.2: Colour analysis of EPS at different combinations of blended flours.

Extruded puffed snack	L*	a*	b*	Yellowness index (YI)
C1	67.9 ± 0.1^{a}	3.9 ± 0.0^{a}	38.5 ± 0.2^{a}	80.9 ± 0.0^{a}
S1	61.5 ± 0.0^{b}	3.0 ± 0.0^{b}	24.9 ± 0.1^{b}	57.8 ± 0.1^{b}
S2	67.8 ± 0.3^{a}	-0.4 ± 0.0^{c}	62.2 ± 0.2^{c}	131.3 ± 0.5^{c}

Entries within the same column with different superscripts denote significant differences between the sample and control ($p > 0.05$; $n = 3$).

5.3.5. Sensory profile of snacks

The sensory profile of the EPS was evaluated to determine their potential acceptance by the consumers. Attributes such as colour, texture, flavor, and overall acceptability were evaluated (Fig. 5.4). All samples received mean scores above 8.0 out of 9 for each attribute, indicating high levels of acceptance among the panellists. The panellists noted the sample fortified with LPE (S2) had a distinct darker yellow hue compared to the control and the one produced using blended flour without fortifying with the emulsion yet received similar sensory score in texture, flavor, and crispiness.

The high sensory scores across all samples suggest that the inclusion of SCF and PMF did not negatively impact consumer acceptability. The positive sensory attributes of S1 and S2 snacks, including taste, texture, and crispness could be attributed to the unique combination of pearl millet and coconut flour, which created a distinct flavor profile compared to commercial snacks. The crispness was resulted from the extrusion process and the interaction of the ingredients.

The distinct darker yellow colour of the product fortified with LPE (S2) added a unique visual appeal without compromising texture and flavour. A similar result was observed with the addition

of tomato pomace powder to ready-to-eat (RTE) snacks. When included at levels of 5–10%, the snacks achieved the highest sensory scores. However, acceptability decreased at inclusion levels above 10% (Yagci et al., 2022). Likewise, Hoglund (2018) incorporated bilberry press cake into extruded snack formulations. Substitutions of up to 25% were tested, but products with 10% inclusion were the most preferred by panellists. In another study, oat flour was added at levels of 5–20% to extruded snacks. Formulations containing 10% oat flour achieved the highest overall sensory scores (Gumul et al., 2015). These studies highlighted that moderate inclusion levels of natural fiber-rich ingredients enhanced snack sensory appeal, whereas excessive amounts reduced acceptability. The findings confirm that the blend of SCF, PMF, and corn grits—fortified with LPE—improves the nutritional profile of extruded snacks while maintaining high sensory appeal. Notably, the blended flour in this study contained 15% SCF and 65% PMF, replacing 80% of corn grits in extruded puffed snacks while still delivering desirable sensory properties.

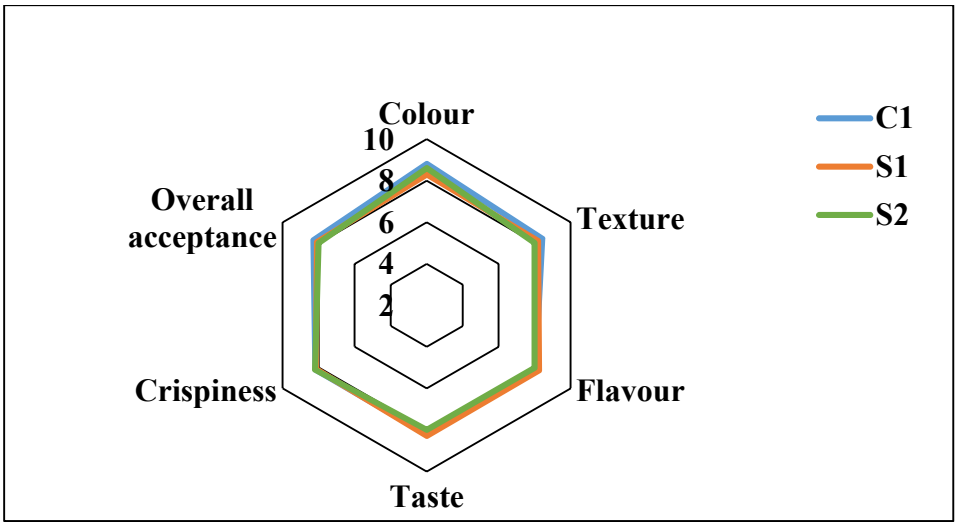

Fig. 5.4. Sensory profiles of extruded puffed snacks. corn grit (C1) and blended flour (S1), blended flour infused with curcumin and vitamin D_3 (S2).

5.3.6. Microstructural analysis

The microstructural analysis of EPS samples using an optical microscope (Fig. 5.5 a-c) revealed notable differences among C1, S1, and S2. The control sample (C1) displayed a uniform pore distribution with large, homogeneous edges, indicating greater expansion and aeration during extrusion. In contrast, S1 had smaller pores and a denser, less porous structure due to the higher fiber content in SCF and PMF, which promoted a more compact matrix. S2 showed a similar structure to S1 but with a distinct yellow hue caused by the presence of curcumin.

The microstructural characteristics of EPS samples—C1, S1, and S2—were examined through SEM (Fig. 5.5 d-f). Fig. 5.5d reveals a rough, fractured surface with air pockets formed during the extrusion process. This porous structure results from the expansion of starch and protein components at the end of the extrusion process. The visible cracks may be due to moisture evaporation and rapid expansion. In contrast, Fig. 5.5e shows a more fibrous, layered structure with elongated strands, suggesting partial melting of starches or proteins that solidify into fibrous formations, enhancing the snack's crunchiness. Fig. 5.5f displays a microstructure similar to that of the control (C1), indicating that LPE did not affect the EPS microstructure. Similar findings were reported in extruded snacks made from rice starch and pea protein blends, which showed an even distribution of proteins and carbohydrates throughout the porous structure (Philipp et al., 2017).

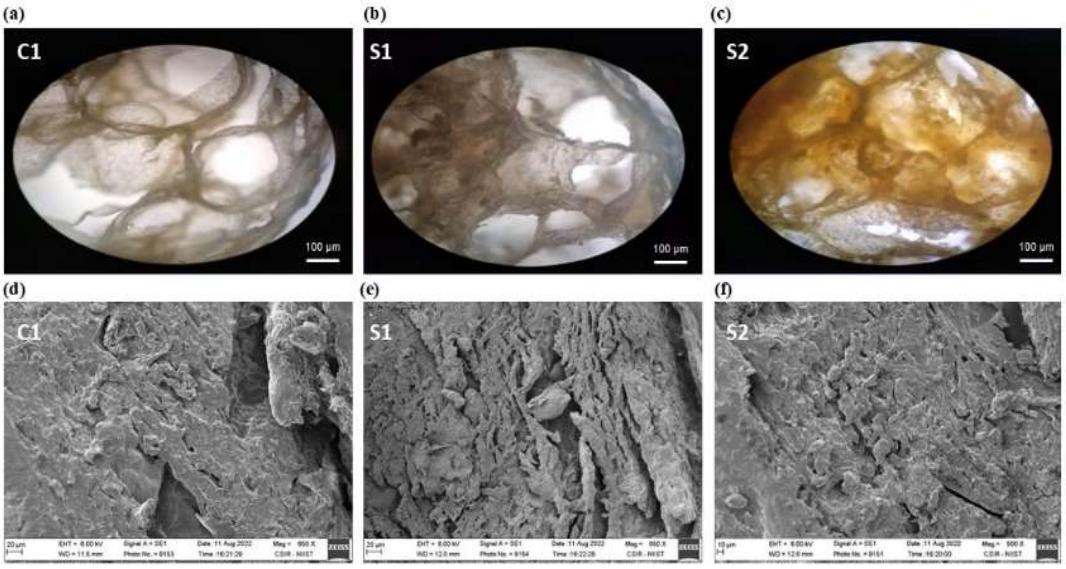

Fig. 5.5. Microscopic images, (a-c) optical microscopy images, (d-f) SEM images of extruded puffed snacks

5.3.7. Stability of bioactives in lignin-encapsulated extrudates

Emulsions stabilized by lignin show promise in encapsulating health-promoting compounds like vitamin D_3 and curcumin for fortifying snack products. Incorporating these bioactive compounds into extruded snacks can significantly enhance their nutritional profile. Preserving the stability of curcumin and vitamin D_3 within the emulsion is crucial for maintaining the health benefits of fortified snacks over time. To evaluate LPE's ability to protect curcumin and vitamin D_3 during extrusion, a control EPS (C2) was prepared by adding these compounds directly to the blended flour without emulsifying with lignin particles. The stability of curcumin and vitamin D_3 in C2 was then compared to that in the S2 sample. Fig. 5.6 (a-d) shows the chromatograms of the extrudates S2 and C2, showing the stability of curcumin and vitamin D_3 in the products. The bioactive stability of curcumin and vitamin D_3 in S2 was 69.0 and 65.7%, respectively. In contrast,

the stability of curcumin and vitamin D_3 significantly decreased to 7.4 and 8.2%, respectively in C2 (Fig. 5.6 g).

The significant difference in bioactive stability between S2 and C2 underscores the vital role of lignin as a protective agent in extrusion processes. Lignin acts as a stabilizer, shielding curcumin and vitamin D_3 from the harsh thermal conditions, thereby maintaining their integrity and activity. Without lignin, as observed in C2, the curcumin and vitamin D_3 are highly susceptible to thermal degradation their stability is compromised. These findings are in accordance with those of Bertolo (2019), in which lignin particles were shown to protect bioactive compound (curcumin) in food system. The notably higher stability of curcumin and vitamin D_3 in S2 underscores lignin's potential as a protective agent, demonstrating its suitability for the production of fortified extruded snacks. Lignin has also been shown to possess antioxidative properties, with the ability to protect oxygen-sensitive compounds (Dai et al., 2019). In this study, lignin's role as a Pickering particle was vital for successfully encapsulating curcumin and vitamin D_3, ensuring their stability during high-temperature extrusion (110 ± 2 °C). These findings align with existing literature, where lignin is consistently noted as an encapsulating and protective agent for bioactive compounds (Czaikoski, 2020; Dai et al., 2019).

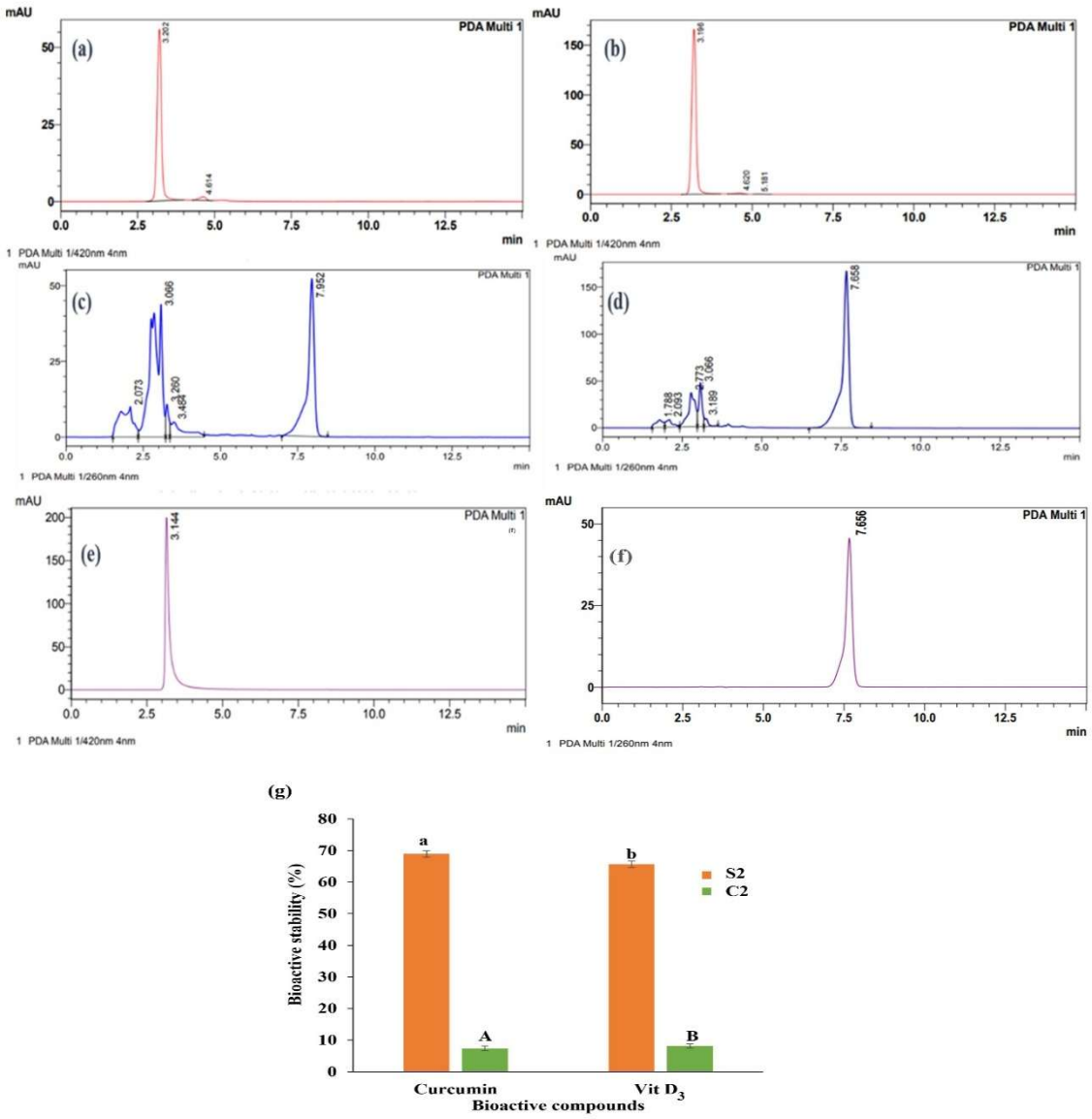

Fig. 5.6. HPLC chromatograms of extruded snacks showing bioactive stability: (a) Curcumin content in C2, (b) Curcumin content in S2, (c) Vitamin D_3 content in C2, (d) Vitamin D_3 content in S2 (e) Standard curcumin, (f) Standard vitamin D_3. (g) Bioactive stability of curcumin and vitamin D_3 in extruded snacks, different letter indicates significant difference in values between C2 and S2.

5.4. Conclusion

This study successfully developed and characterized nutritionally and functionally superior extruded puffed snacks (EPS). The EPS were formulated using a blend of spent coconut, pearl millet flour, corn grits, and lignin Pickering emulsions (LPE) in which curcumin and vitamin D_3 were encapsulated. Notably, 80% of the corn flour typically used in traditional snacks was replaced with the blended flour, resulting in increased protein and dietary fiber content. Although the expansion ratio, bulk density, and textural properties of the blended flour snacks were lower than those of traditional corn flour snacks, the inclusion of LPE enhanced their nutritional profile. The overall sensory acceptance of these snacks was comparable to conventional snacks, indicating their suitability as nutritionally enriched alternatives. The study also confirmed that curcumin and vitamin D_3 were effectively encapsulated within the snacks' matrix, with their structural integrity and bioactivity preserved during the extrusion process. Lignin played a vital role in maintaining the stability and bioavailability of curcumin and vitamin D_3 in the snacks. These findings highlight the potential of lignin-stabilized emulsions for incorporating bioactive compounds into healthier, ready-to-eat snacks.

References

Abilmazhinov, Y., Bekeshova, G., Nesterenko, A., Dibrova, Z., Ermolaev, V., Ponomarev, E. and Vlasova, V., 2023. A review on the improvement of extruded food processing equipment: extrusion cooking in food processing. Food Science and Technology, 43. https://doi.org/10.5327/fst.80621.

Abraham, B., Shakeela, H., Devendra, L. P., Arun, K. B., Ragavan, K. V., Brennan, C., & Nisha, P. (2024). Lignin nanoparticles from Ayurvedic industry spent materials: Applications in Pickering

emulsions for curcumin and vitamin D_3 encapsulation. *Food Chemistry*, *458*, 140284. https://doi.org/10.1016/j.foodchem.2024.140284.

Abraham, B., Shakeela, H., Devendra, L.P., Arun, K.B., Ragavan, K.V., Brennan, C., Mantri, N., Adhikari, B. and Nisha, P., 2024. Lignin nanoparticles from Ayurvedic industry spent materials: Applications in Pickering emulsions for curcumin and vitamin D_3 encapsulation. Food Chemistry, 458, p.140284. https://doi.org/10.1016/j.foodchem.2024.140284

Abraham, B., Syamnath, V.L., Arun, K.B., Zahra, P.F., Anjusha, P., Kothakotta, A., Chen, Y.H., Ponnusamy, V.K. and Nisha, P., 2023. Lignin-based nanomaterials for food and pharmaceutical applications: Recent trends and future outlook. Science of The Total Environment, 881, p.163316. https://doi.org/10.1016/j.scitotenv.2023.163316

Ahmed, J., Giri, B.R., Reza, M.A., Qasim, S.S.B., Thomas, L., Al-Attar, H. and Maniruzzaman, M., 2024. Twin-screw extrusion of vitamin D3/iron-blend granules in corn and lentil composite flours: Stability, microstructure, and interaction of vitamin D3 with human osteoblast cells. Journal of Food Science, 89(1), pp.435-449. https://doi.org/10.1111/1750-3841.16841

Alam, M. S., Kaur, J., Khaira, H., & Gupta, K. (2016). Extrusion and extruded products: changes in quality attributes as affected by extrusion process parameters: a review. *Critical reviews in food science and nutrition*, *56*(3), 445-473. doi.org/10.1080/10408398.2013.779568.

Al-Azzawi, M.A., Maftool, A.J., Al-Shimary, A.A. and Mohammed, A.A., 2023. A Comprehensive Review of Vitamin D3: Metabolism, Functions, and Clinical Implications. International Journal of Medical Science and Dental Health, 9(12), pp.37-46. https://doi.org/10.55640/ijmsdh-09-12-08

Amadeu, C.A., Martelli, S.M. and Vanin, F.M., 2024. Nutritional aspects of composite flours for baked and extruded products: A review. Cereal Chemistry, 101(3), pp.450-467. https://doi.org/10.1002/cche.10765

AOAC (Association of Official Analytical Chemists). Official methods of analysis. Assoc Anal Chem. 1990; 62:2742–4

Arun, K. B., Thomas, S., Reshmitha, T. R., Akhil, G. C., & Nisha, P. (2017). Dietary fibre and phenolic-rich extracts from Musa paradisiaca inflorescence ameliorates type 2 diabetes and associated cardiovascular risks. Journal of Functional Foods, 31, 198-207.

Aussanasuwannakul, A., Teangpook, C., Treesuwan, W., Puntaburt, K., & Butsuwan, P. (2022). Effect of the addition of soybean residue (okara) on the physicochemical, tribological, instrumental, and sensory texture properties of extruded snacks. *Foods*, *11*(19), 2967. https://doi.org/10.3390/foods11192967.

Bertolo, M. R., de Paiva, L. B. B., Nascimento, V. M., Gandin, C. A., Neto, M. O., Driemeier, C. E., & Rabelo, S. C. (2019). Lignins from sugarcane bagasse: Renewable source of nanoparticles as Pickering emulsions stabilizers for bioactive compounds encapsulation. Industrial Crops and Products, 140, Article 111591. https://doi.org/ 10.1016/j.indcrop.2019.111591.

Biradar, V.M., Kumar, P., Yallappa, M., Ramya, C.S., Nayak, P., Sekhar, M., Bhushan, S. and Babu, S., 2024. Sustainable nutricereal: a review on nutrient and bio-active composition and its potential health benefits of pearl millet. Int J Adv Biochem Res, 8(3S), pp.30-5. https://doi.org/10.33545/26174693.2024.v8.i3Sa.684

Brennan, M. A., Derbyshire, E., Tiwari, B. K., & Brennan, C. S. (2013). Integration of β-glucan fibre rich fractions from barley and mushrooms to form healthy extruded snacks. *Plant Foods for Human Nutrition*, *68*, 78-82. https://doi.org/10.1007/s11130-012-0330-0

Bureau of Indian Standards. (1984). Method for estimation of total dietary fibre in food stuffs. IS: 11062(1984). New Delhi, India: Indian Standards Institution.

Czaikoski, A., Gomes, A., Kaufmann, K. C., Liszbinski, R. B., de Jesus, M. B., & da Cunha, R. L. (2020). Lignin derivatives stabilizing oil-in-water emulsions: Technological aspects, interfacial rheology and cytotoxicity. Industrial Crops and Products, 154, Article 112762. https://doi.org/10.1016/j.indcrop.2020.112762.

Dai, L., Li, Y., Kong, F., Liu, K., Si, C., & Ni, Y. (2019). Lignin-based nanoparticles stabilized pickering emulsion for stability improvement and thermal-controlled release of trans-resveratrol. ACS Sustainable Chemistry & Engineering, 7(15), 13497-13504. https://pubs.acs.org/doi/full/10.1021/acssuschemeng.9b02966.

Delić, J., Ikonić, P., Jokanović, M., Peulić, T., Ikonić, B., Banjac, V., Vidosavljević, S., Stojkov, V. and Hadnađev, M., 2023. Sustainable snack products: Impact of protein-and fiber-rich ingredients addition on nutritive, textural, physical, pasting and colour properties of extrudates. Innovative Food Science & Emerging Technologies, 87, p.103419. https://doi.org/10.1016/j.ifset.2023.103419

Dias-Martins, A.M., Trombete, F.M., Cappato, L.P., Chávez, D.W., Santos, M.B. and Carvalho, C.W., 2024. Processing, composition, and technological properties of decorticated, sprouted, and extruded pearl millet (Pennisetum glaucum (L.) R. Br.) flours. Journal of Food Process Engineering, 47(2), p.e14561. https://doi.org/10.1111/jfpe.14561.

Dilrukshi, H.N., Torrico, D.D., Brennan, M.A. and Brennan, C.S., 2022. Effects of extrusion processing on the bioactive constituents, in vitro digestibility, amino acid composition, and antioxidant potential of novel gluten-free extruded snacks fortified with cowpea and whey protein concentrate. Food chemistry, 389, p.133107. https://doi.org/10.1016/j.foodchem.2022.133107.

Feizollahi, E., Hadian, Z. and Honarvar, Z., 2018. Food fortification with omega-3 fatty acids; microencapsulation as an addition method. Current Nutrition & Food Science, 14(2), pp.90-103. https://doi.org/10.2174/1573401313666170728151350

Ferreira, S. M., Capriles, V. D., & Conti-Silva, A. C. (2021). Breakfast cereals with inulin obtained through thermoplastic extrusion: Chemical characteristics and physical and technological properties. *LWT*, *137*, 110390. https://doi.org/10.1016/j.lwt.2020.110390.

Gojiya, D., Davara, P., Gohil, V., & Dabhi, M. (2022). Process standardization for formulating protein-augmented corn-based extrudates using defatted sesame flour (DSF): Sesame oil industry waste valorisation. Journal of Food Processing and Preservation, 46(12), e17203. https://doi.org/10.1111/jfpp.17203.

Grasso, S. (2020). Extruded snacks from industrial by-products: A review. *Trends in Food Science & Technology*, *99*, 284-294. https://doi.org/10.1016/j.tifs.2020.03.012.

Gumul, D., Ziobro, R., Gambuś, H., & Nowotna, A. (2015). Usability of residual oat flour in the manufacture of extruded corn snacks. *CyTA-Journal of Food*, *13*(3), 353-360. https://doi.org/10.1080/19476337.2014.984336

Gupta, M., Bawa, A. S., & Semwal, A. D. (2008). Effect of barley flour on development of rice-based extruded snacks. *Cereal Chemistry*, *85*(2), 115-122. https://doi.org/10.1094/CCHEM-85-2-0115.

Han, Y. J., & Tran, T. T. T. (2018). Corn snack with high fiber content: Effects of different fiber types on the product quality. Lwt, 96, 1-6. https://doi.org/10.1016/j.lwt.2018.05.014

Heeba S, Kavya M, Chinthu Udayarajan and Nisha P, (2024), Physicochemical Interactions of Spent Coconut Flour and Its Application in Developing Plant-Based Cheese Spread

Höglund, E., Eliasson, L., Oliveira, G., Almli, V. L., Sozer, N., & Alminger, M. (2018). Effect of drying and extrusion processing on physical and nutritional characteristics of bilberry press cake extrudates. *Lwt*, *92*, 422-428. https://doi.org/10.1016/j.lwt.2018.02.042.

Karun, G., Sukumar, A., Nagamaniammai, G., & Preetha, R. (2023). Development of multigrain ready-to-eat extruded snack and process parameter optimization using response surface methodology. Journal of Food Science and Technology, 60(3), 947-957. https://doi.org/10.1007/s13197-022-05390-8.

Kumar, R., Xavier, K.M., Lekshmi, M., Balange, A. and Gudipati, V., 2018. Fortification of extruded snacks with chitosan: Effects on techno functional and sensory quality. Carbohydrate polymers, 194, pp.267-273. https://doi.org/10.1016/j.carbpol.2018.04.050

Longvah, T., Ananthan, R., Bhaskarachary, K. and Venkaiah, K. (2017). Indian Food Composition Tables 2017, National Institute of Nutrition, Indian Council of Medical Research, Hyderabad, Telangana, India. https://www.nin.res.in/ebooks/IFCT2017.pdf

Moraru, C. I., & Kokini, J. L. (2003). Nucleation and expansion during extrusion and microwave heating of cereal foods. *Comprehensive reviews in food science and food safety*, *2*(4), 147-165.

Navami, M. M., Abraham, B., Archana, H., & Nisha, P. (2023). Nutritional profiling and quantitative analysis of amino acids and vitamins using LC–MS/MS in selected raw and germinated ancient grains. JSFA Reports, 3(8), 377-386. https://doi.org/10.1002/jsf2.141.

Oliveira, L. C., Rosell, C. M., & Steel, C. J. (2015). Effect of the addition of whole-grain wheat flour and of extrusion process parameters on dietary fibre content, starch transformation and mechanical properties of a ready-to-eat breakfast cereal. *International journal of food science & technology*, *50*(6), 1504-1514. https://doi.org/10.1111/ijfs.12778.

Onwulata, C.I., 2013. Microencapsulation and functional bioactive foods. Journal of Food Processing and Preservation, 37(5), pp.510-532. https://doi.org/10.1111/j.1745-4549.2012.00680.x

Pai, D. A., Blake, O. A., Hamaker, B. R., & Campanella, O. H. (2009). Importance of extensional rheological properties on fiber-enriched corn extrudates. *Journal of Cereal Science*, *50*(2), 227-234. https://doi.org/10.1016/j.jcs.2009.05.007.

Philipp, C., Oey, I., Silcock, P., Beck, S. M., & Buckow, R. (2017). Impact of protein content on physical and microstructural properties of extruded rice starch-pea protein snacks. Journal of Food Engineering, 212, 165-173. https://doi.org/10.1016/j.jfoodeng.2017.05.024

Piayura, S. and Itthivadhanapong, P., 2023. The effects of feed moisture and dried coconut meal content on the physicochemical, functional, and sensory properties of gluten-free Riceberry rice flour-based extruded snacks. Frontiers in Sustainable Food Systems, 7, p.1194594. https://doi.org/10.3389/fsufs.2023.1194594

Pitts, K. F., McCann, T. H., Mayo, S., Favaro, J., & Day, L. (2016). Effect of the sugar replacement by citrus fibre on the physical and structural properties of wheat-corn based extrudates. *Food and Bioprocess Technology*, *9*, 1803-1811. https://doi.org/10.1007/s11947-016-1764-4.

Prabha, K., Ghosh, P., Abdullah, S., Joseph, R.M., Krishnan, R., Rana, S.S. and Pradhan, R.C., 2021. Recent development, challenges, and prospects of extrusion technology. Future Foods, 3, p.100019. https://doi.org/10.1016/j.fufo.2021.100019

Rodríguez-Vidal, A., Martínez-Flores, H. E., González Jasso, E., Velázquez de la Cruz, G., Ramírez-Jiménez, A. K., & Morales-Sánchez, E. (2017). Extruded snacks from whole wheat supplemented with textured soy flour: Effect on instrumental and sensory textural characteristics. *Journal of texture studies*, *48*(3), 249-257. https://doi.org/10.1111/jtxs.12234.

Rodríguez-Vidal, A., Martínez-Flores, H. E., González Jasso, E., Velázquez de la Cruz, G., Ramírez-Jiménez, A. K., & Morales-Sánchez, E. (2017). Extruded snacks from whole wheat supplemented with textured soy flour: Effect on instrumental and sensory textural characteristics. *Journal of texture studies*, *48*(3), 249-257. https://doi.org/10.1111/jtxs.12234.

Sanusi, M.S., Sunmonu, M.O., Alasi, S.O., Adebiyi, A.A. and Tajudeen, A.A., 2023. Composition, bioactive constituents and glycemic index of brown rice-watermelon seeds extruded snacks as stimulated by extrusion conditions. Applied Food Research, 3(1), p.100287. https://doi.org/10.1016/j.afres.2023.100287

Shah, F. U. H., Sharif, M. K., Butt, M. S., & Shahid, M. (2017). Development of protein, dietary fiber, and micronutrient enriched extruded corn snacks. *Journal of texture studies*, *48*(3), 221-230. https://doi.org/10.1111/jtxs.12231.

Shakeela, H., Mini, N. M., Abraham, B., Natarajan, N., & Nisha, P. (2022). Influence of coating material and processing parameters on acrylamide formation in potato patties. *International Journal of Food Engineering*, *18*(5), 399-409. https://doi.org/10.1515/ijfe-2021-0337.

Shakeela, H., Mohan, K. and Nisha, P., 2024. Unlocking a nutritional treasure: health benefits and sustainable applications of spent coconut meal. Sustainable Food Technology, 2(3), pp.497-505. doi: 10.1039/D3FB00247K

Shruthi, V. H., Hiregoudar, S., & Nidoni, U. (2019). Evaluation of textural properties of corn based extruded products. 2405-2410. https://plantarchives.org/19-2/2405-2410%20(5310).pdf

Sobowale, S. S., Kewuyemi, Y. O., & Olayanju, A. T. (2021). Process optimization of extrusion variables and effects on some quality and sensory characteristics of extruded snacks from whole pearl millet-based flour. *SN Applied Sciences*, *3*, 1-12. https://doi.org/10.1007/s42452-021-04808-w.

Sinaki, N. Y., & Koksel, F. (2024). Effects of dietary fibre source and content and extrusion conditions on the physicochemical composition and physical quality of fibre-enriched lentil snacks. *International Journal of Food Science & Technology*, *59*(4), 2236-2248. https://doi.org/10.1111/ijfs.16943.

Sultana, M., Chan, E.S., Pushpamalar, J. and Choo, W.S., 2022. Advances in extrusion-dripping encapsulation of probiotics and omega-3 rich oils. Trends in Food Science & Technology, 123, pp.69-86. https://doi.org/10.1016/j.tifs.2022.03.006

Suri, S., Dutta, A., Shahi, N. C., Raghuvanshi, R. S., Singh, A., & Chopra, C. S. (2020). Numerical optimization of process parameters of ready-to-eat (RTE) iron rich extruded snacks for anaemic population. *Lwt*, *134*, 110164. https://doi.org/10.1016/j.lwt.2020.110164.

Tas, A. A., & Shah, A. U. (2021). The replacement of cereals by legumes in extruded snack foods: Science, technology and challenges. *Trends in Food Science & Technology*, *116*, 701-711. https://doi.org/10.1016/j.tifs.2021.08.016.

Tsokolar-Tsikopoulos, K.C., Katsavou, I.D. and Krokida, M.K., 2015. 'The effect of inulin addition on structural and textural properties of extruded products under several extrusion conditions' The effect of inulin addition on structural and textural properties of rice flour extrudates. Journal of food science and technology, 52, pp.6170-6181.

Wang, K., Zhu, M., Yang, Z., Bai, L., Huan, S., & Wang, C. (2023). Sustainable Production of Stable Lignin Nanoparticle-Stabilized Pickering Emulsions via Cellulose Nanofibril-Induced Depletion Effect. ACS Sustainable Chemistry & Engineering. https://doi.org/10.1021/acssuschemeng.3c01972

Wang, P., Fu, Y., Wang, L., Saleh, A. S., Cao, H., & Xiao, Z. (2017). Effect of enrichment with stabilized rice bran and extrusion process on gelatinization and retrogradation properties of rice starch. *Starch-Stärke*, *69*(7-8), 1600201. https://doi.org/10.1002/star.201600201.

Wichchukit, S., & O'Mahony, M. (2015). The 9-point hedonic scale and hedonic ranking in food science: some reappraisals and alternatives. *Journal of the Science of Food and Agriculture*, *95*(11), 2167-2178. https://doi.org/10.1002/jsfa.6993

Yadav, A., Niresh, A., Anmol, S., Kumar, S., Chaitali, S. and Satvika, C., 2023. Studies on development of technology for preparation of millet based extruded snack.

Yagci, S., Calıskan, R., Gunes, Z. S., Capanoglu, E., & Tomas, M. (2022). Impact of tomato pomace powder added to extruded snacks on the in vitro gastrointestinal behaviour and stability of bioactive compounds. *Food Chemistry*, *368*, 130847. https://doi.org/10.1016/j.foodchem.2021.130847

Zahari, I., Ferawati, F., Purhagen, J. K., Rayner, M., Ahlström, C., Helstad, A., & Östbring, K. (2021). Development and characterization of extrudates based on rapeseed and pea protein blends using high-moisture extrusion cooking. *Foods*, *10*(10), 2397. https://doi.org/10.3390/foods10102397.

Chapter-6

Cellulose and lignin nanoparticles from an Ayurvedic waste stream for essential oil-based active packaging to extend shelf life of perishable fruit

Abstract

Cellulose and lignin nanoparticles (NCP and LNP) were successfully extracted from Dashamoola spent material (DSM), a residue from an Ayurvedic decoction. The NCP had a particle size of 493.6 nm and a zeta potential of -30.9 mV, indicating good colloidal stability. FTIR confirmed the removal of non-cellulosic components, while TGA demonstrated thermal stability, with major degradation between 260°C and 350°C. XRD analysis indicated a semi-crystalline structure of nanocellulose. Oil-in-water emulsions of tea tree oil (TTO) were prepared using NCP (C at 4%), LNP (L at 4%), and a combination blend (2% each of C and L in CL_TTO), with 16% TTO, all in w/v. Among these, CL_TTO emulsions had the smallest particle size and highest stability. PVOH-based films, prepared with a 4% w/v mixture of CL_TTO emulsion, PVOH, and glycerol, demonstrated improved tensile strength, Young's modulus, water vapour barrier properties, and water repellence. These films blocked 95% UV transmittance, providing appreciable protection to light-sensitive products. PVOH-CL_TTO films also exhibited strong antioxidant activity (85% DPPH scavenging) and antimicrobial property against *E. coli*. These films extended the shelf life of strawberries by preserving lightness, firmness, and pH for 14 days under chilling (4°C). These findings highlight the potential of NCP and LNP obtained from DSM for producing sustainable active packaging which would valorizing Ayurvedic waste stream.

Keywords: Nano cellulose, Nano Lignin, Polyvinyl Alcohol, Emulsion, Active packaging film.

Graphical abstract

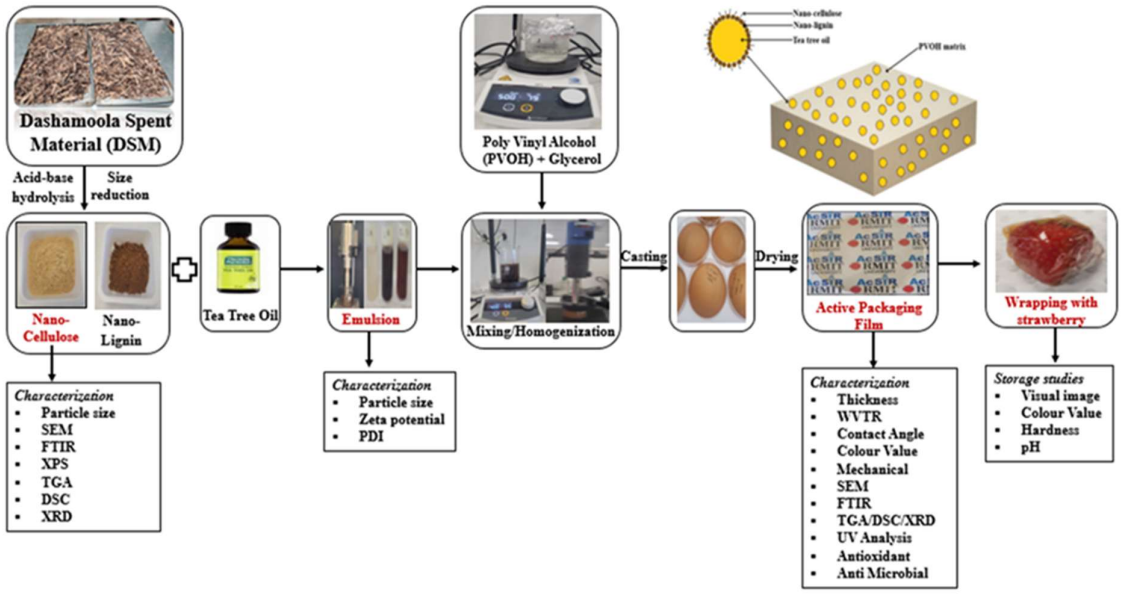

Fig. 4. Graphical abstract showing the process of obtaining cellulose and lignin from DSM and their application in making active packaging films.

Highlights

- Cellulose and lignin were extracted from Ayurvedic spent material and converted into nanoparticles.
- Cellulose and lignin nanoparticles were characterized using FTIR, XRD, TGA, and SEM.
- Tea tree oil emulsion stabilized by cellulose and lignin nanoparticles exhibited desirable stability.
- Incorporation of the emulsion in PVOH film enhanced strength and water vapor barriers.
- Films containing this emulsion extended the shelf life of strawberries for 14 days at 4°C.

6.1. Introduction

Sustainability and by-product valorisation are essential for advancing Sustainable Development Goals (SDGs) (Ahmad et al., 2024). The Ayurveda industry, rooted in traditional medicine, is gaining global significance as demand grows for natural and holistic healthcare products (Mukherjee et al., 2017). Indian Ayurvedic industry generates about 1000 ton/year Dashamoola spent material (DSM) as a byproduct of *Dashamoola arishta* production, which is rich in lignocellulosic materials including cellulose and lignin (Abraham et al., 2020; Abraham et al., 2023). Lignin is a complex organic polymer which offers UV-blocking and antioxidant properties, while cellulose is the most abundant biopolymer, which provides excellent mechanical strength and water vapour and oxygen barrier properties (Abraham et al., 2023; Tanpichai et al., 2022; Liu et al., 2021). Both lignin and cellulose have wide applications such as biocomposite production, textile, food, and pharmaceutical industries. As a part of active food packaging, they improve barrier properties, mechanical robustness. The incorporation of these natural materials coming from renewable sources into polymer systems contributes to sustainability (Abraham et al., 2023; Tanpichai et al., 2022).

Application of emulsion technology enhances the functionality of active packaging films by dispersing small droplets of hydrophobic substances in hydrophilic matrices. The uniformity of distribution and size of these droplets play important roles in determining the film's effectiveness (Cheng et al., 2024; Chen et al., 2024; Pandita et al., 2024). Emulsions help incorporate hydrophobic bioactive compounds or essential oils, such as tea tree oil (TTO), into hydrophilic biopolymer matrices, and help enhance the antioxidant and antimicrobial activities of the resulting packaging materials or films (Hanan et al., 2024; Dai et al., 2024; Pandita et al., 2024). TTO, derived from *Melaleuca alternifolia*, contains active compounds like terpinene-4-ol and γ-terpinene, which impart antibacterial and antioxidant properties (Brun et

al., 2019). These materials, along with biopolymer stabilizers such as cellulose and lignin, can greatly reduce moisture permeability and improve the barrier and protective functions of biodegradable polymer-based films (Yang et al., 2016; Hassan et al., 2024; Asgher et al., 2020; He et al., 2023).

Petroleum-based plastics dominate food packaging due to their cost-effectiveness and desirable mechanical and barrier properties; however, environmental concerns have increased interest in biodegradable alternatives (Sani et al., 2021; Salgado et al., 2021; Bhargava et al., 2020). Polyvinyl alcohol (PVOH) is a promising biodegradable polymer due to its hydrophilic, non-toxic nature, making it suitable for environment-friendly packaging applications (Panda et al., 2022). Although PVOH lacks inherent antioxidant properties, it can be fortified with natural additives like lignocellulose, curcumin, essential oils, and plant extracts to enhance its functionality (Haque et al., 2021; Roy et al., 2021; Debiagi et al., 2014; Luzi et al., 2022). However, there remains a significant gap in sustainable packaging solutions that not only enhance food preservation but also utilize natural, industry-derived byproducts including spent materials of Ayurvedic industry. In PVOH systems, cellulose and lignin provide UV-blocking properties, reduce moisture sensitivity, and reinforce mechanical strength under humid conditions, offering a sustainable alternative to inorganic fillers (Dudeja et al., 2023; Oun et al., 2022; Li et al., 2022; Cazon et al., 2019). Thus, the incorporation of lignin and nanocellulose derived from DSM into PVOH matrix could produce active and sustainable packaging materials for food application (Suganthi et al., 2020; Bahrami & Fattahi, 2021).

The increasing global population and changing dietary habits have significantly raised the demand for fresh fruits and vegetables (Nian et al., 2024). Strawberries (*Fragaria ananassa*), valued for their nutritional benefits and economic importance, are highly perishable and particularly susceptible to mechanical damage, moisture loss, texture softening, physiological degradation, and microbial spoilage (Lan et al., 2019). These factors rapidly degrade

strawberry quality, posing challenges for marketing and distribution (He et al., 2024; Bertolo et al., 2023). Although active packaging technologies using biopolymers infused with PVOH have been explored to extend the shelf life of perishable products, their effectiveness in maintaining the quality of strawberries and similarly perishable fruits over extended storage periods remains limited. It is of practical importance to apply the active packaging materials produced using lignin and nanocellulose from Ayurvedic spent materials (DSM as an example) and PVOH to extend the shelf life of perishable fruits (e.g., strawberries) (Nian et al., 2024).

The role of lignin nanoparticles in stabilizing emulsions was established in our earlier research (Abraham et al., 2024). This research investigates the effectiveness of cellulose and lignin nanoparticles derived from Ayurvedic residues in developing PVOH-based active packaging films infused with tea tree oil. The study evaluates the impact of these natural biopolymers on the films' morphological, mechanical, and functional properties, as well as their ability to extend the shelf life of perishable fruits. By exploring the utilisation of nanocellulose and lignin from Ayurvedic spent materials, this work contributes to sustainability and offers a viable, eco-friendly alternative to conventional plastics for food preservation.

6.2. Materials and methods

6.2.1. Raw material selection and source

The Dashamoola Spent Material (DSM) utilized in the research was generously supplied by Arya Vaidya Sala, located in Kottakal, Malappuram, Kerala, India (M/s. AVS Kottakal Ltd).

6.2.2. Chemicals and reagents

Analytical-grade sodium hydroxide (NaOH), sodium chlorite ($NaClO_2$), hydrochloric acid (HCl), and glacial acetic acid (CH_3COOH) were obtained from HiMedia, India. Petroleum ether was acquired from Sisco Research Laboratories Pvt. Ltd. (SRL), India. Cellulose powder (CAS number 9004-34-6, SCP), glycerol, 2,2-diphenyl-1-picrylhydrazyl (DPPH), and polyvinyl alcohol (Mw: 89,000-98,000 Da, fully hydrolyzed) were sourced from Sigma-

Aldrich Pty Ltd. (New South Wales, Australia). Tea tree oil (TTO) from Thursday Plantation was purchased from a local Chemist Warehouse outlet (Melbourne, Australia). Antibacterial assays were performed using the LB broth dilution method on *E. coli* strain 25922, sourced from New England Biolabs. All other reagents used in this study were of analytical-grade and supplied by Sigma-Aldrich Pty Ltd. (New South Wales, Australia).

6.2.3. Fruit selection

Strawberries (*Fragaria ananassa*) were selected as a representative fruit. Freshly harvested (within one day), the strawberries were sourced directly from Coles, Bundoora, Melbourne, Australia. The fruits were chosen based on uniform shape, size, colour, and absence of physical damage. After selection, the strawberries were gently washed with deionised water, dried using clean paper towels, chilled at 4 ± 1°C and 80 ± 5% relative humidity (RH), and used immediately.

6.2.4. Nano cellulose (NCP) and nano lignin (LNP) extraction from DSM

The compositional analysis of DSM was conducted following the National Renewable Energy Laboratory (NREL) protocol (Ruiz and Date, 1996) and reported in our previous paper (Abraham et al., 2024). The isolation of cellulose from DSM was adapted from the methodologies outlined by Silvério et al. (2013) and Dinçel Kasapoğlu et al. (2023), with slight modifications to suit the material. DSM was initially dried at 40 °C in a hot air oven and then ground into fine powder. This powder was suspended in a 1% NaOH solution with a 10% w/v loading and autoclaved at 121 °C for 1 h. After cooling to room temperature, the solid was separated from the liquid using cheesecloth and retained for further processing. The solid residue underwent acid treatment with 4% H_2SO_4 in an autoclave for 1 h. This process was repeated three times to ensure the removal of hemicellulose and partial lignin. Afterward, the acid-treated residue was cooled, centrifuged at 5000 × g for 15 min, and thoroughly washed with water until a neutral pH was achieved.

For bleaching, an equal volume mixture of 1.7% w/v $NaClO_2$ and an acetate buffer (pH-4.5) was used. The acetate buffer was prepared by dissolving 2.7 g of NaOH and 7.5 mL of glacial acetic acid in 100 mL of distilled water. The solid residue was treated with the bleaching solution at 80 °C for 3 h, until a uniform colour was achieved. After bleaching, the residue was cooled, centrifuged at 5000 × g for 10 min, and washed until neutral pH. Finally, the bleached residue was freeze-dried at −80 °C and 10 Pa, yielding fine cellulose powder. A planetary ball mill (Pulverisette, Fritsch, Germany) operating at 300 rpm, with zirconium dioxide (ZrO_2) containers (50 mL) and ZrO_2 balls (10 mm), was used to reduce the size of the extracted cellulose. The milling process was conducted in an argon environment to prevent oxidation and consisted of 23 cycles, with each cycle lasting 5 minutes followed by a 10-minute gap to prevent overheating. The cellulose powder composition was determined using the NREL method. The resulting nanocellulose powder (NCP) was stored in zip-lock pouches for further experimental analyses.

The procedure for the extraction and characterization of lignin nanoparticle (LNP) from DSM is detailed in our previous work (Abraham et al., 2024). Briefly, lignin was extracted from Dashamoola spent material (DSM) through alkaline hydrolysis followed by acid precipitation. The precipitated lignin was purified and processed into nanolignin using ball milling. The nanolignin particles were characterized for their size, morphology, and surface properties using techniques such as dynamic light scattering (DLS), Fourier-transform infrared spectroscopy (FTIR), and nuclear magnetic resonance (NMR). These methods confirmed the structural features, including β-O-4 linkages and guaiacyl, syringyl, and *p*-hydroxyphenyl units, as well as the thermal stability and surface charge characteristics essential for its potential applications.

6.2.5. Characterization of NCP

6.2.5.1. Particle size and zeta potential of NCP

The particle size of the NCP was measured using a dynamic light scattering method (Mastersizer 3000, Malvern Instruments Ltd., Malvern, UK). Samples were diluted in distilled water (pH 7) and agitated at 200 rpm for thorough dispersion. For Zeta potential analysis, the NCP samples were diluted 100 times using Milli Q water prior to measurements. The pH of the NCP aqueous solution is 7. The Zeta potential was measured with a Zetasizer (Nano-ZS, Malvern Instruments Ltd., Malvern, UK).

6.2.5.2. Observation of microstructure

The microstructure of the NCP was examined using a scanning electron microscope (SEM-Quanta200, Philips XL-30, Philips, Eindhoven, the Netherlands). The NCP powder samples were placed on silicon wafer pieces mounted on aluminium stubs using double-sided adhesive conductive carbon tape. The specimens were coated with a thin layer of iridium using a sputter coater to improve conductivity and to prevent the development of electrical charge in the samples during imaging. The SEM measurements were conducted at an acceleration voltage of 0.7 kV.

6.2.5.3. Functional group analysis of NCP using FTIR

FTIR analysis of NCP and Standard Cellulose Powder (SCP) was performed using an FTIR-ATR spectrometer (Perkin Elmer, USA). Spectra were recorded from 4000 to 1000 cm^{-1} with a 4 cm^{-1} resolution, allowing comparison of the functional groups in NCP and SCP. A total of 64 scans were recorded and averaged for each sample.

6.2.5.4. Thermal degradation of NCP

Thermal gravimetric (TG) analyses of NCP and SCP were carried on a TA Q50 instrument. Sample (10 mg) was placed in the alumina crucible, heated in the temperature range 40-500 °C at a heating rate of 10 $^{\circ}C\ min^{-1}$ in the presence of nitrogen (Moustaqim et al., 2018). The weight loss (%) versus temperature data were recorded.

6.2.5.5. Surface composition of NCP

X-ray photoelectron spectroscopy (XPS) was used to determine the surface compositions of NCP and SCP. A PHI 5000 Versa Probe II (ULVAC-PHI Inc., USA) was employed to analyse the oxygen-to-carbon (O:C) ratio, which provides insights into the percentage of lignin on the surface. The analysis was carried out using a micro-focused (200 μm, 15 kV) monochromatic Al-Kα X-ray source (hν = 1486.6 eV) (Mou et al., 2013).

6.2.5.6. Crystalline and amorphous content of NCP

The wide-angle X-ray diffraction (WAXD) analysis was performed using a Xenocs' XEUSS SAXS/WAXS instrument in transmission mode to analyse the amorphous and crystalline content of NCP and SCP. Cu Kα radiation at 50 kV and 0.6 mA with a wavelength of 1.54 Å was used. The 2D diffraction patterns were captured on a Mar345 image plate and analysed using Fit2D software. The degree of crystallinity was calculated as the ratio of the intensity of the crystalline peak to the total intensity, according to the method described by Sindhu et al. (2011).

6.2.6. Preparation and characterization of emulsions

NCP and LNP extracted from DSM were used to prepare emulsions with tea tree oil (TTO) as the oil phase, designated as C_TTO and L_TTO, respectively. An emulsion was also prepared using a combination of NCP (C) and LNP (L) with TTO as the oil phase, designated as CL_TTO. NCP, LNP, and their combination were mixed with TTO at specified concentrations: 4% w/v for C, 4% w/v for L, and 2% w/v each of C and L for CL, along with 16% w/v TTO in each emulsion. These mixtures were stirred at 35°C for 60 min at 300 rpm, followed by sonication (10 s on/off, 5 min, 50% amplitude) to obtain the final emulsions (Abraham et al., 2024).

6.2.6.1. Particle size and zeta potential

The particle (droplet) size and Zeta potential of the above-mentioned emulsions were measured using the Zetasizer (Nano-ZS, Malvern Instruments Ltd., Malvern, UK) at 25°C, as described

in section 6.2.5.1. The emulsion samples were diluted 10 times using Milli Q water for both particle size and Zeta potential measurements.

6.2.7. Film casting preparation

A polyvinyl alcohol (PVOH) solution was prepared by dissolving PVOH in water to achieve a concentration of 3% w/v. The PVOH solution was then blended with 1% w/v glycerol and stirred at 80 °C and 500 rpm for 60 min to ensure uniform mixing of glycerol with PVOH, as glycerol acts as a plasticiser. Each of the emulsion (C_TTO, L_TTO, or CL_TTO) was then added to the PVOH-glycerol solution and the mixture was stirred at 35°C for 60 min with a magnetic stirrer set at 300 rpm. To achieve homogeneity, the mixture was further homogenized using an IKA T25 Ultra Turrax homogenizer (Wilmington, USA) for 3 min at 5000 rpm and then probe-sonicated for 2 min (10 s on, 10 s off, at 50% amplitude). Finally, the solutions were degassed to remove entrapped air bubbles. Table 6.1. Shows the composition or formulation of the films.

The final step involved casting 15 mL of each mixture into a 10-cm diameter acrylic Petri dish and drying at room temperature (25 ± 2°C) for 48 h. The films were then conditioned over saturated magnesium chloride to achieve a constant relative humidity (RH-53%) environment before further testing or characterization (He et al., 2023). The resulting films, PVOH, PVOH-C_TTO, PVOH-L_TTO, and PVOH-CL_TTO, had total solid contents of 4% (w/w) as indicated in Table 6.1.

Table 6.1: Preparation ratio PVOH, PVOH-C_TTO, PVOH-L_TTO, and PVOH-CL_TTO

Code	PVOH (%)	Glycerol (%)	Cellulose (C) (%)	Lignin (L) (%)	TTO (%)	Total content (%)
PVOH	3.0	1	0	0	0	4
PVOH-C_TTO	2.8	1	0.04	0	0.16	4
PVOH-L_TTO	2.8	1	0	0.04	0.16	4
PVOH-CL_TTO	2.8	1	0.02	0.02	0.16	4

6.2.8. Characterization of films

6.2.8.1. Thickness of films

The thickness of the films was measured using a digital micrometer (Mitutoyo, Japan, precision up to 0.01 mm). Measurements were taken at 5 different locations on each film and averaged to ensure accuracy.

6.2.8.2. Water contact angle analysis

The water contact angle (WCA) was measured to evaluate the surface hydrophobicity of the films using an OCA-20 Contact Angle System (Data Physics Instruments, Germany) equipped with a Basler high-resolution camera. Rectangular film samples (20 mm × 80 mm) were positioned horizontally, and a 1 μL water droplet was applied to the surface. The WCA was determined by averaging the left and right angles from digital images, with at least ten measurements taken and averaged per film. All experiments were conducted at room temperature.

6.2.8.3. Water vapour transmission rate (WVTR)

The water vapour permeability of the films was measured using a Permatran-W system (Mocon, Minneapolis, USA) at 22 ± 1 °C. The wet side relative humidity (RH) was maintained at 80%, with a gradient of 70% RH across the films.

6.2.8.4. Measurement of colour parameters

The colour profile of the films was measured using a Chroma Meter CR–400 (Minolta, Japan) in terms of lightness (L*; black to white), redness (a*; green to red), and yellowness (b*; blue to yellow). The instrument was calibrated using a standard white plate, and measurements were taken at three points on each film. The total colour difference (ΔE) was calculated using equation (1) (Martinez-Alvarenga et al., 2014).

$$\Delta E=\sqrt{(L^*_{film}-L^*_{standard})^2+(a^*_{film}-a^*_{standard})^2+(b^*_{film}-b^*_{standard})^2} \quad (1)$$

6.2.8.5. Micro structure analysis

The microstructure of the films, including both surface and cross-sectional views, was analyzed using scanning electron microscopy (SEM), as described in section 2.5.2. Film samples, measuring approximately 5 mm × 5 mm, were mounted on aluminium stubs with conductive carbon tape and coated with a thin layer of iridium to enhance conductivity and prevent charging during imaging (He et al., 2023).

6.2.8.6. Measurement of mechanical properties

The mechanical properties of the four different of the films, including tensile strength, elongation at break, and Young's modulus, were determined using an Instron universal testing machine (model 4467, Instron Corporation, Massachusetts, USA) equipped with a 100-kN load cell. Data collection and analysis were performed using Bluehill software. Film strips, cut to approximately 5 mm × 50 mm, were conditioned at 53% RH for 48 h, following the ASTM D1708 standard. During the tensile test, each strip was placed between two clamps with an initial grip separation of 22 mm and subjected to a crosshead speed of 10 mm/min (Oladzadabbasabadi et al., 2024).

6.2.8.7. Thermal degradation of films

Thermal degradation of the films was determined using a thermogravimetric (TG) analysis, as described in section 6.2.5.4. Film samples (10 mg) were heated from 40 to 500 °C at a rate of 10 °C/min under nitrogen purge. The weight loss (%) versus temperature data were recorded, and DTG (Derivative Thermogravimetry) was also evaluated.

6.2.8.8. Thermal characteristics of films

Differential scanning calorimetry (DSC) was used to evaluate the thermal behavior of the films, specifically focusing on the glass transition temperature (T_g). Measurements were performed using a DSC Q2000 (TA Instruments, USA). Approximately 3.0 mg of the film sample was placed into pre-weighed aluminium pans. The samples were heated from 25 °C to 95 °C at a

rate of 10 °C/min under a nitrogen environment. The onset temperature (T_0), peak temperature (T_p), and conclusion temperature (T_x) were determined using the Fit2D software (Abraham et al.,2024).

6.2.8.9. Crystalline and amorphous content of films

The crystalline and amorphous contents of the films were determined using wide-angle X-ray diffraction (WAXD), as described in section 6.2.5.6.

6.2.8.10. Film transparency

The UV–Vis transmission through the films was measured across the 200–800 nm wavelength range using a UV–Vis spectrophotometer (UV-2600, Shimadzu, Kyoto, Japan). Film samples were cut to dimensions of 1.5 × 3 cm², and the absorption spectrum was recorded within the specified range (He et al., 2023).

6.2.8.11. Antioxidant properties of films

Antioxidant activity of the films was determined using DPPH scavenging activity. Film sample of 900 mg dipped in 18 mL of methanol and incubated at 25°C for 1 h with stirring (150 rpm). One mL of this methanolic extract was mixed with 2 mL of 0.06 mM DPPH solution and vortexed. The mixture was incubated in dark for 30 min at room temperature (25 ± 2°C). Absorbance was measured at 517 nm using a UV–vis spectrometer (Abraham et al., 2020). A control sample with methanol and DPPH was prepared, and antioxidant activity (%) was calculated using Equation (2).

$$DPPH\ activity\ (\%) = \left(\frac{Absorbance\ of\ control - Absorbance\ of\ film\ sample}{Absorbance\ of\ control}\right) * 100 \qquad (2)$$

6.2.8.12. Antibacterial assays of films

Antibacterial activity of the films was assessed using the LB broth dilution method against *Escherichia coli* strain 25922 (New England Biolabs). LB broth was prepared by dissolving 10 g/L tryptone, 5 g/L yeast extract, and 10 g/L NaCl in distilled water, and the pH was adjusted

to 7.0. The medium was sterilized by autoclaving at 121°C for 15 min. After cooling, *E. coli* was cultured in the LB broth overnight at 37°C with shaking at 100 rpm. Two mL of LB broth was added to each well of sterile 24-well plates, and film samples (1.5 cm × 1.5 cm) were transferred to the wells. A bacterial suspension (50 µL, 10^6 cells/mL) was inoculated into each well, with bacteria-only wells serving as controls. Bacterial growth was monitored over 18 h at 37°C with shaking at 100 rpm, and optical density was measured at 600 nm using a UV-Vis spectrophotometer.

6.2.9. Assessment of preservation effect on strawberry

The preservation performance of of the films on strawberries wrapped on them was evaluated at room temperature (22 ± 2°C) and under chilling condition (4 ± 1°C). Observations were recorded at room temperature on days 0, 2, and 4, while those under refrigeration were recorded on days 4, 8, and 14 (Lan et al., 2019). The assessed films for their ability to extend the shelf life of strawberries included plain polyvinyl alcohol (PVOH), and PVOH containing Pickering emulsion produced using NCP (C) and LNP (L) tea tree oil (PVOH-CL_TTO). Unwrapped strawberries (UW) were used for comparision.

6.2.9.1. Colour analysis of strawberry

The colour parameters of strawberries, unwrapped (UW) and wrapped in PVOH and PVOH-CL_TTO films, were measured using a chromameter CR–400. Measurements were taken at three random spots and the average L*, a*, and b* were recorded as described in section 2.8.4.

6.2.9.2. Hardness of strawberry

The hardness of strawberry samples was assessed using a texture analyzer (TA-XT2i, Stable Micro Systems) with a 50 kg load cell. The fruit samples were positioned on the platform to allow a 5 mm diameter aluminium probe to pierce the shoulders. A compression test was performed, and hardness was defined as the force (N) required to penetrate 50% of the sample height at a speed of 1 mm/s. The texture profile analysis (TPA) involved a two-cycles, with

pre-test, test, and post-test speeds of 5 mm/s, 1 mm/s, and 8 mm/s, respectively. Firmness was reported as the maximum force during the first compression.

6.2.9.3. pH of strawberry

A strawberry sample weighing 5 g was homogenised with 50 mL of distilled water and then filtered through a paper filter or muslin cloth. The pH of the filtrate was measured using a pH meter (Microprocessor Meter, HANNA Instruments, Romania)

6.2.10. Statistical analysis

Experiments were conducted in triplicate unless otherwise specified. Results are presented as mean values ± standard deviation (SD). Statistical analysis was performed using one-way analysis of variance (ANOVA) followed by Tukeys multiple comparison test, utilizing GraphPad Prism 5.0 and Microsoft Excel (2007). A 95% confidence level ($p < 0.05$) was used to determine significant differences between mean values.

6.3. Results and discussion

6.3.1. Characterisation of extracted lignin and cellulose from DSM

The lignocellulosic biomass of DSM used in this work contained 39.1% cellulose, 30.6% hemicellulose, and 27.9% lignin (Abraham et al., 2024). In our previous studies (Abraham et al., 2024), lignin was successfully isolated from DSM and converted into lignin nanoparticles (LNP) with a molecular weight of 14.42 kDa, which was comparable to that of commercial LNPs. The LNPs, produced using planetary ball milling to a size of 496.4 nm, demonstrated stability at pH 8.0 with a zeta potential of -32.0 mV. The authors (Abraham et al., 2024) used these LNPs as Pickering particles to produce oil-in-water (O/W) emulsion of sunflower oil, which remained stable for 90 days at room temperature. In this work, we further extracted NCP from DSM and characterised it. O/W emulsions of tea tree oil were produced using LNP and NCP, both separately and in combination.

The NCP powder obtained from DSM had a particle size of 493.6 nm (Fig. 6.1a) and a zeta potential of -30.9 mV. These values close to the size and surface charge of commonly reported cellulose nanoparticles (Li et al., 2022; Haque et al., 2021). Its purity was determined to be 93.7% cellulose and 4.9% hemicellulose, confirming the effective isolation of cellulose nanoparticles.

The SEM image in Fig. 6.1c represents the NCP obtained from the extracted cellulose (Fig. 6.1b) after planetary ball milling. As shown, the figures reveal morphological changes induced by the mechanical treatment. Fig. 6.1c depicts a more fragmented and irregular particle structure compared to the fibrillar network observed in Fig. 6.1b. This indicates that ball milling effectively reduced particle size and disrupted the cellulose fibres, resulting in smaller, more irregular particles. This level of reduction in size increases the surface area, which is beneficial for applications requiring enhanced reactivity or better dispersion in composite matrices (Nagarajan et al., 2019). The rougher surface morphology of these NCPs suggests potential for improved bonding with other materials in nanocomposites, making them suitable for applications such as emulsions and biodegradable packaging. FTIR data shown in Fig. 6.1d highlights the key structural characteristics of standard cellulose powder (SCP) and NCP powder, confirming the latter's high purity. The absorption bands around 3340 cm^{-1} and 1040 cm^{-1} correspond to O-H and C-O stretching vibrations, which are typical of cellulose structures. The absence of a peak at 1738 cm^{-1} in NCP indicates the successful removal of lignin, while the C=O stretching vibration associated with ester groups from hemicellulose confirms its partial removal (Soni et al., 2015). Additionally, bands at 1641 cm^{-1}, attributed to adsorbed water, and 1429 cm^{-1}, corresponding to CH_2 bending, further confirm the preservation of the cellulose structure in NCP (Trilokesh et al., 2019). The close similarity between the FTIR spectra of SCP and NCP indicates that the extraction of cellulose and its conversion into

nanoform did not alter the cellulose structure, making NCP suitable for applications in emulsions, biocomposites, and packaging (Li et al., 2019).

Thermogravimetric analysis (Fig. 6.1e) reveals a distinct two-stage thermal degradation process for both NCP and SCP. The initial weight loss, occurring below 125 °C, is attributed to the evaporation of bound water—an inherent characteristic of cellulose fibers. This stage underscores the hydrophilic nature of the material and its tendency to retain moisture. The second, more significant weight loss between 260 °C and 350 °C corresponds to the depolymerization of cellulose chains, a hallmark of cellulose thermal degradation. These findings not only confirm the thermal behaviour of NCP and SCP but also provide insights into their stability under elevated temperatures, a critical consideration for applications in biocomposites or thermally resilient materials (Trilokesh et al., 2019). Above 400 °C, they further degraded into inorganic char or ash similar to degradation of typical cellulosic materials (Soni et al., 2015). NCP exhibited slightly lower moisture retention in the initial stage (5.2% compared to 6.1% for SCP) and a marginally reduced weight loss during cellulose depolymerization (63.4% compared to 65.8% for SCP), likely due to its higher purity compared to SCP. The thermal stability of NCP was comparable to that of SCP, indicating its suitability for high-temperature applications such as bio-composites, where resistance to thermal degradation is critical (Li et al., 2019).

XRD analysis, shown in Fig. 6.1f, indicates that the NCP retains its semi-crystalline structure, similar to SCP. The prominent peak at 22.5° 2θ corresponds to the (002) plane, which is characteristic of cellulose I. A secondary peak is observed near 18° 2θ, attributed to the ($1\bar{1}0$) plane, further confirms the cellulose I allomorph (Candido et al., 2017). The similar crystallinity values observed in NCP and SCP indicate that the extraction and size reduction processes effectively preserved the cellulose's natural structure—an essential factor for its

functional applications. Crystallinity plays a key role in determining material properties such as mechanical strength and barrier functionality, both of which directly influence performance in bio-composites and packaging materials (Lu et al., 2012).

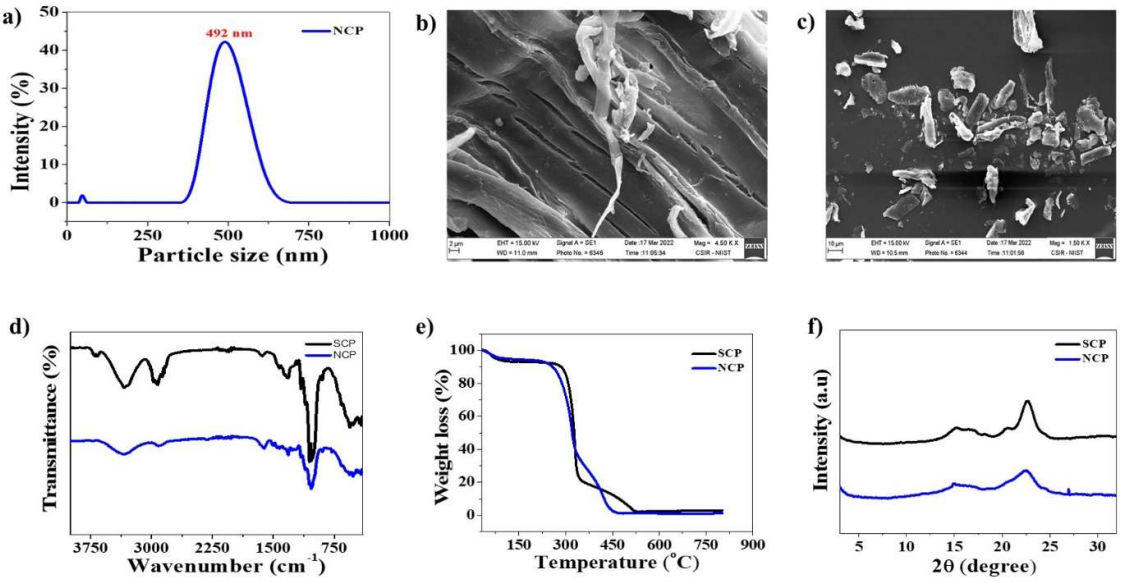

Fig. 6.1. Characteristics of nanocellulose powder (NCP) obtained from Dashamoola Spent Material (DSM): (a) particle size distribution, (b, c) SEM images with scale bars of 2 µm at ×4500 magnification and 10 µm at ×1500 magnification, respectively, (d) FTIR spectra, (e) TGA, and (f) XRD analysis.

6.3.2. Compositional analysis of NCP

X-ray photoelectron spectroscopy was used to assess the surface elemental composition and chemical states of the extracted nanocellulose powder (NCP), and the data is shown in Fig. 6.2. The survey spectra (Fig. 6.2a&b) for both standard cellulose and NCP revealed the predominance of carbon and oxygen, the primary constituents of cellulose. In the high-resolution C1s spectra (Fig. 6.2c&d), the extracted cellulose exhibited a peak at 284.72 eV, corresponding to the C-C and C-H bonds, similar to standard cellulose (Zhang et al., 2020). The minor shifts in binding energy likely resulted from slight changes in surface chemistry

during extraction, possibly due to residual non-cellulosic substances or environmental exposure. The O1s spectra (Fig. 6.2e&f) showed a peak at 532.62 eV, corresponding to hydroxyl and ether groups. This peak exhibited a slight shift compared to standard cellulose, suggesting surface interactions such as hydrogen bonding or electrostatic interactions that may have occurred during the extraction process (Zhang et al., 2020). These results suggest that the core chemical structure of cellulose remained largely intact in NCP with minimal surface modifications (Anari et al., 2024).

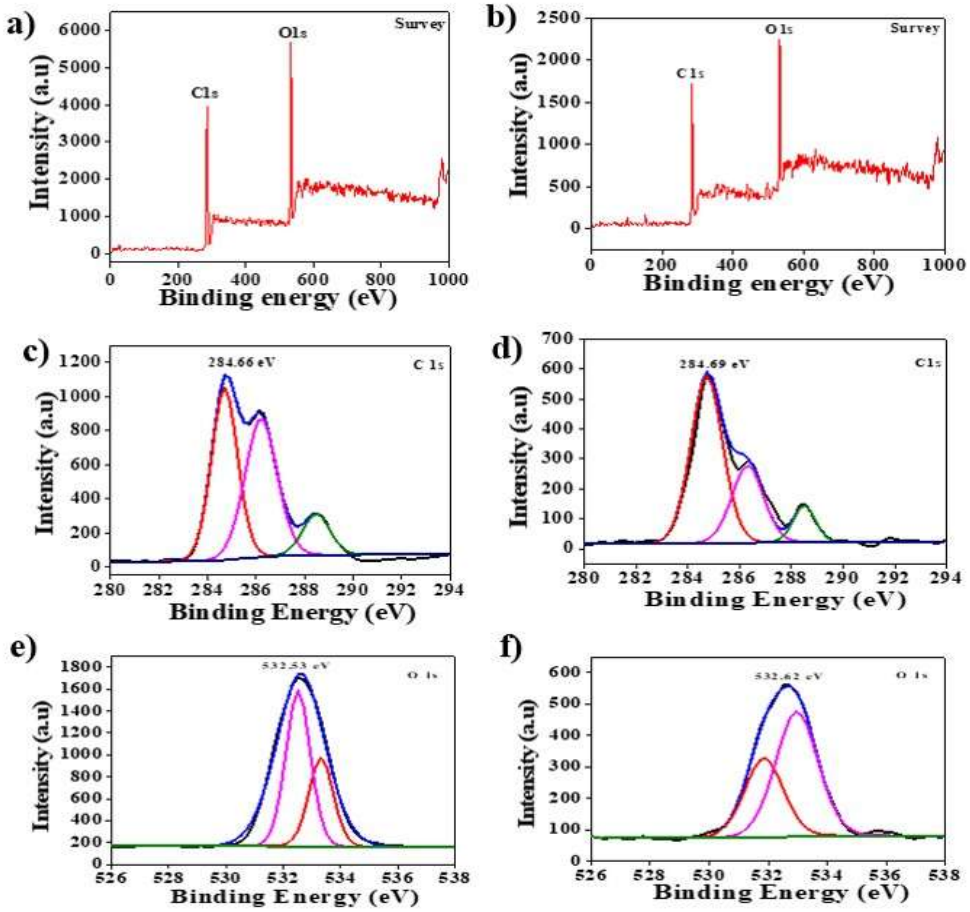

Fig. 6.2. XPS analysis of NCP obtained from Dashamoola spent material (DSM): (a) Survey spectrum of SCP, (b) Survey spectrum of NCP, (c) C1s spectrum of SCP, (d) C1s spectrum of NCP, (e) O1s spectrum of SCP, and (f) O1s spectrum of NCP.

6.3.3. Emulsion preparation and characterization

LNP and NCP are shown to possess significant potential in forming stable emulsions (Abraham et al., 2023; Zhu et al., 2021). Building on this information, O/W emulsions of tea tree oil (TTO) as dispersed phase with LNP (2%) and NCP (2%) were fabricated as detailed in section 2.6, where oil phase was 16%. The characteristics of emulsion stabilized by of NCP (i.e., C-TTO), LNP (i.e., L_TTO), and their combination (i.e., CL_TTO) are presented in Table 6.2. The particle size data revealed that C_TTO exhibited comparatively larger average particle size (620.9 nm) to that of L_TTO (593.2 nm) and CL_TTO (585.9 nm), suggesting that lignin may contribute to produce finer emulsions. The combination yielded the smallest particle size, as observed in CL_TTO, suggesting that this pairing is beneficial and could lead to the formation of more stable emulsions, which are desirable for producing active packaging films (Li et al., 2025; Pandita et al., 2024).

Zeta potential data also indicated that the combination was beneficial as CL_TTO (-39.4 mV) had the highest magnitude followed by L_TTO (-35.7 mV) and C_TTO (-32.6 mV). Higher magnitudes of zeta potential generally correlate with better emulsion stability due to higher electrostatic repulsion. The highest negative charge observed in CL_TTO aligns with its smallest particle size, this formulation would produce emulsion with higher stability (Pandita et al., 2023; Bai et al., 2018).

The polydispersity index (PDI) values, presented in Table 6.2, follow a similar trend. CL_TTO exhibited the lowest PDI, L_TTO fell in between, and C_TTO showed the highest. Lower PDI values indicate a narrower size distribution, which typically leads to higher stability. These findings align with recent studies that show combining biopolymers with emulsifying properties can enhance the stability of emulsions (Rehman et al., 2024). Photographs of these emulsions (Fig. 6.3) confirm that there was no phase separation in these emulsions. This high level of stability is promising for developing clear, stable active packaging films infused with

potent essential oils (He et al., 2023). Further, TTO infused bioactive PVOH films were developed using NCP, LNP and their mixtures as Pickering emulsifiers.

Table 6.2: Particle size, PDI and Zeta of emulsion tea tree oil with cellulose (C_TTO), lignin (L_TTO), and their combination (CL_TTO)

Emulsions	**C_TTO**	**L_TTO**	**CL_TTO**
Size (nm)	620.85 ± 10.38^{a}	593.19 ± 8.57^{b}	585.89 ± 4.08^{b}
PDI	0.511 ± 0.01^{a}	0.491 ± 0.05^{b}	0.409 ± 0.01^{c}
Zeta (mV)	-32.55 ± 0.89^{a}	-35.74 ± 0.92^{b}	-39.39 ± 0.43^{c}

Small letters indicate significant difference between the samples

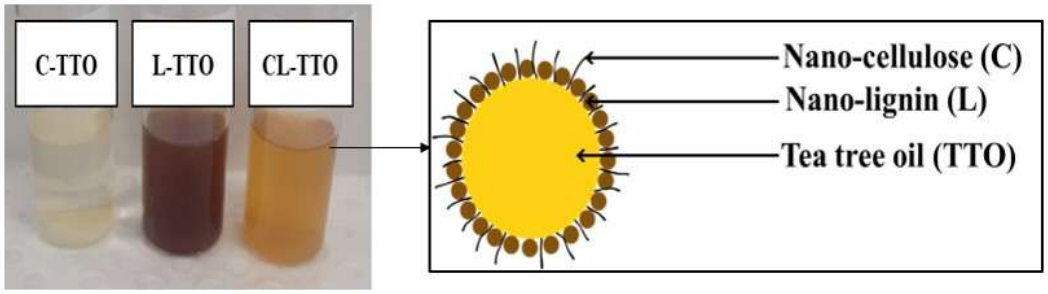

Fig. 6.3. Visual images of tea tree oil emulsions with cellulose (C_TTO), lignin (L_TTO), and their combination (CL_TTO), taken 5 minutes after preparation. A graphical representation of the CL_TTO emulsion is also shown.

6.3.4. Essential oil infused bioactives PVOH film and its characterization

Bioactive films were prepared using PVOH as the main matrix and infused with emulsified TTO essential oil. NCP, LNP, and their combinations, described above, served as Pickering emulsifiers. The films were then prepared by solution casting, as detailed in Section 6.2.7. Characterisation of these films examines how the infused C_TTO, L_TTO, and CL_TTO

emulsions influence their structural, mechanical, and functional properties, providing insights into the modifications imparted by lignin and cellulose within the PVOH matrix.

6.3.4.1. Physical properties of films

The thickness of the films (Table 6.3) showed a gradual increase across PVOH, PVOH-C_TTO, PVOH-L_TTO, and PVOH-CL_TTO films. Given the total non-water content, the addition of cellulose, lignin, and tea tree oil increased the thickness of these films. Thickness of films is an important parameter as it impacts their tensile strength and flexibility.

WVTR, which indicates a film's moisture barrier property, was highest in the PVOH film (349.3 g/m²·day). WVTR significantly decreased in the PVOH-CL_TTO film (170.7 g/m²·day), likely due to the presence of cellulose-lignin matrix, which creates a more complex diffusion path for water vapour enhancing barrier properties. In comparison, Zhou et al. (2022) reported a higher WVTR of 1400.6 g/m²·day for PVOH films containing chitin and lignin, while Lingait et al. (2024) reported a WVTR of 562.3 g/m²·day for PVOH films with pectin. These findings indicate that incorporating cellulose and lignin nanoparticles into PVOH-CL_TTO active films creates a more effective moisture barrier than similar composite films.

In contact angle measurements, values < 90° indicate hydrophilicity, while values > 90° indicate hydrophobicity. The PVOH film had a contact angle of 50.1° indicating its hydrophilic nature. The incorporation of NCP and LNP increased the contact angle of the films by 8° (PVOH-C_TTO) and 14° (PVOH-L_TTO). The combination of NCP and LNP increased the contact angle by 20° (PVOH-CL_TTO). These films remained hydrophilic in nature. Studies have reported contact angle values of 60° for lignin-containing PVOH films with a lignin content of 5% (Phansamarng et al., 2024) and 51° for PVOH films containing nanocellulose and Fe^{3+} together (Ren et al., 2024). The findings on WVTR and WCA suggest that the combined incorporation of NCP and LNP in PVOH films significantly enhances water

resistance, making them more resistance to water vapour transport and increase water repellence.

Colour analysis revealed significant changes in the optical properties of the PVOH films with the addition of NCP and LNP, and essential oils. As shown in Table 6.3, the control PVOH film had the highest L* value, indicating a lighter, more transparent appearance. In contrast, the LNP containing film (e PVOH-L_TTO) had the lowest L* value (81.3) indicating its darker hue attributed to lignin's natural chromophores, such as phenolic and carbonyl groups (Liu et al., 2024). This shift was accompanied by increased a* and b* values, producing a richer colour and enhancing the film's visual appeal.

The total colour difference (ΔE) also increased when LNP and NCP and essential oils were present in the films compared that the control film. This light dark hue was not only aesthetically pleasant but also added a light-shielding effect, potentially protecting packaged products from light-induced oxidative damage (Liu et al., 2024). Similar colour changes have been reported in κ-carrageenan films containing fenugreek extract (Farhan and Hani, 2020). These optical enhancements, combined with improved water vapour barrier properties, make these films more suitable than PVOH films to be used in moisture-sensitive packaging where both functionality and aesthetics are essential.

Table 6.3: Properties of PVOH-based films with tea tree oil, cellulose, and lignin, including thickness, contact angle, WVTR, colour parameters (L*, a*, b*), and total colour difference (ΔE).

	PVOH	PVOH-C_TTO	PVOH-L_TTO	PVOH-CL_TTO
Thickness (µm)	60.00 ± 10.00^{a}	70.00 ± 10.00^{a}	80.00 ± 10.00^{a}	80.00 ± 10.00^{a}
Contact angle (°)	50.12 ± 2.95^{a}	58.43 ± 0.90^{b}	64.13 ± 1.26^{c}	70.53 ± 0.90^{d}
WVTR (g/m²·day)	349.34 ± 3.06^{d}	191.42 ± 4.08^{c}	183.15 ± 2.42^{b}	170.71 ± 2.57^{a}
L*	91.89 ± 0.17^{d}	89.48 ± 0.37^{c}	81.27 ± 1.76^{a}	85.89 ± 0.84^{b}
a*	0.76 ± 0.04^{a}	1.15 ± 0.02^{b}	4.71 ± 0.11^{d}	2.25 ± 0.01^{c}
b*	0.19 ± 0.04^{a}	0.43 ± 0.18^{b}	9.87 ± 0.72^{d}	5.62 ± 0.13^{c}
ΔE		2.45 ± 0.82^{a}	13.00 ± 0.54^{c}	6.74 ± 0.69^{b}

Data are presented as mean ± standard deviation (n = 3) and the different superscripted alphabets in the same row indicate significant differences ($p < 0.05$) between the samples.

6.3.5. Surface morphology of films

The photographic images of the films (Fig. 6.4a) show a noticeable increase in opacity from the pure PVOH film to those containing NCP, LNP, and essential oil. The pure PVOH film appears highly transparent, reflecting its smooth and homogenous structure. The PVOH-C_TTO film showed only slight increase in opacity, indicating that the NCP does not introduce significant changes in transparency and opacity. The PVOH-L_TTO film exhibited the highest increase in chromaticity and opacity, attributed to the relatively higher concentration of LNP, which imparts its own distinct colour. he opacity and colour variation of the PVOH-CL_TTO film remained between those of PVOH and PVOH-L_TTO, suggesting that the colouring component originated from LNP, albeit at half the concentration present in PVOH-L_TTO. These alterations in colour and transparency underscore the impact of incorporating additives

on both the aesthetic and functional properties of the films, with potential implications for light transmission and barrier performance (Phansamarng et al., 2024; Ren et al., 2024).

SEM images (Fig. 6.4b) provided further insight into the surface morphology of the films. The pure PVOH film showed a smooth, uniform texture, indicating a pristine polymer matrix. In contrast, the PVOH-C_TTO and PVOH-L_TTO films exhibited rougher surfaces, with visible particle distributions suggesting the presence of additives within the PVOH matrix. This surface roughness is likely caused by phase separation, where the additives disrupt the matrix continuity, resulting in a textured surface. Such microscale surface variation is important in modulating surface wettability (Ren et al., 2024; Phansamarng et al., 2024; Zhang et al., 2021)

The cross-sectional SEM images (Fig. 6.4c) revealed distinct difference in the internal structure among the films. The pure PVOH film demonstrated a dense and uniform cross-section, indicating tightly packed polymer chains. In contrast, the PVOH-C_TTO film exhibited a stratified structure, indicative of layered microphase separation, while the PVOH-L_TTO film shows an eroded, uneven structure, likely due to lignin's tendency to aggregate within the matrix. The PVOH-CL_TTO film exhibited a three-phase microstructure, where interactions between PVOH, cellulose, and lignin produced a rough, layered internal structure. These morphological features, driven by polymer-additive interactions, give rise to the unique mechanical and barrier properties of the composite films (Zhang et al., 2021; Wang et al., 2024).

Mechanical flexibility tests (Fig. 6.4d) of the PVOH-CL_TTO film showed that it maintained its structural integrity under bending, stretching, twisting, and folding stresses without tearing or permanent deformation. These properties are essential for packaging applications, where materials must withstand mechanical forces during handling and transportation (Wang et al., 2024). The robust performance of PVOH-CL_TTO in these tests reinforces its suitability for use as a flexible packaging material.

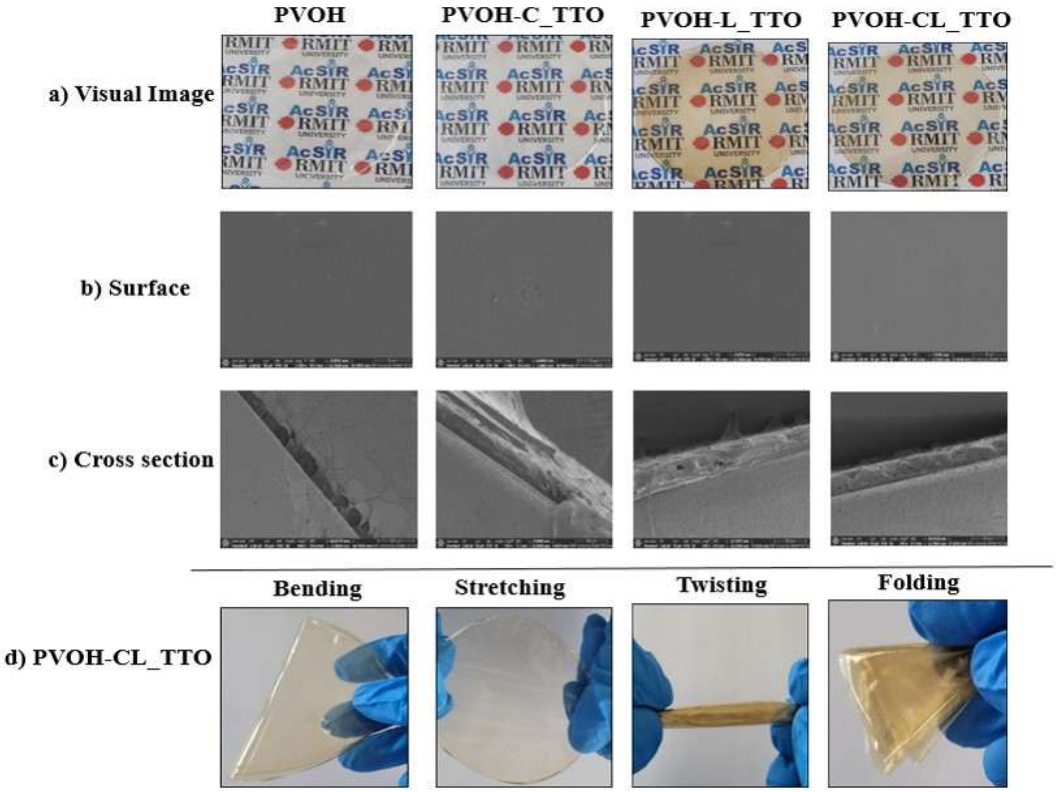

Fig. 6.4. Analysis of Polyvinyl Alcohol (PVOH) treatments showing (a) photographic appearance, (b) surface morphology with a scale bar of 50 µm at ×1500 magnification, (c) cross-sections with a scale bar of 300 µm at ×250 magnification, and (d) mechanical flexibility tests, including bending, stretching, twisting, and folding.

6.3.6. Mechanical properties of films

The mechanical properties of PVOH films, both with and without NCP, LNP, and TTO, demonstrate their considerable potential for active packaging applications. As shown in Fig. 6.5a, the stress-strain behaviour of these films revealed that PVOH-C_TTO exhibited significant robustness, withstanding a stress of up to 6.34 MPa before failure. This 20% increase of tensile strength over the unmodified PVOH film suggests that cellulose reinforcement significantly improves the load-bearing capacity of PVOH, making it suitable for packaging applications (Pirsa, 2024).

The Young's modulus (Fig. 6.5b) of PVOH-C_TTO film was the highest (48.78 MPa). This represents a substantial increase from the modulus of pure PVOH (24.75 MPa), indicating that the addition of cellulose creates a more rigid material, ideal for applications requiring resistance to deformation. Conversely, the PVOH-L_TTO and PVOH-CL_TTO composites exhibited lower moduli of 25.13 MPa and 34.92 MPa, respectively, suggesting a softer material that could be more appropriate for wrapping, where some flexibility is required (Li et al., 2022).

The elongation at break values (Fig. 6.5c), further illustrated the ductility of the PVOH composites. PVOH-L_TTO and PVOH-CL_TTO displayed remarkable elongation at break values of 100.04% and 102.27%, respectively—considerably higher than the 61.93% of the standard PVOH film. This level of flexibility allows the material to absorb impacts during transportation, reducing the likelihood of damage to packaged goods, which is particularly advantageous for fragile items (Akelah, 2013).

The tensile strength (Fig. 6.5d) data of the films showed that PVOH-C_TTO film had the highest tensile strength. Although PVOH-L_TTO and PVOH-CL_TTO had slightly lower tensile strength values. Thus, the NCP an LNP extracted from DSM improve the mechanical properties of PVOH, creating flexible packaging materials more suitable in food applications. The incorporation of essential oil (e.g., tea tree oil) imparts antibacterial properties (Section 6.3.8) without compromising the mechanical properties of these films (Borges et al., 2024).

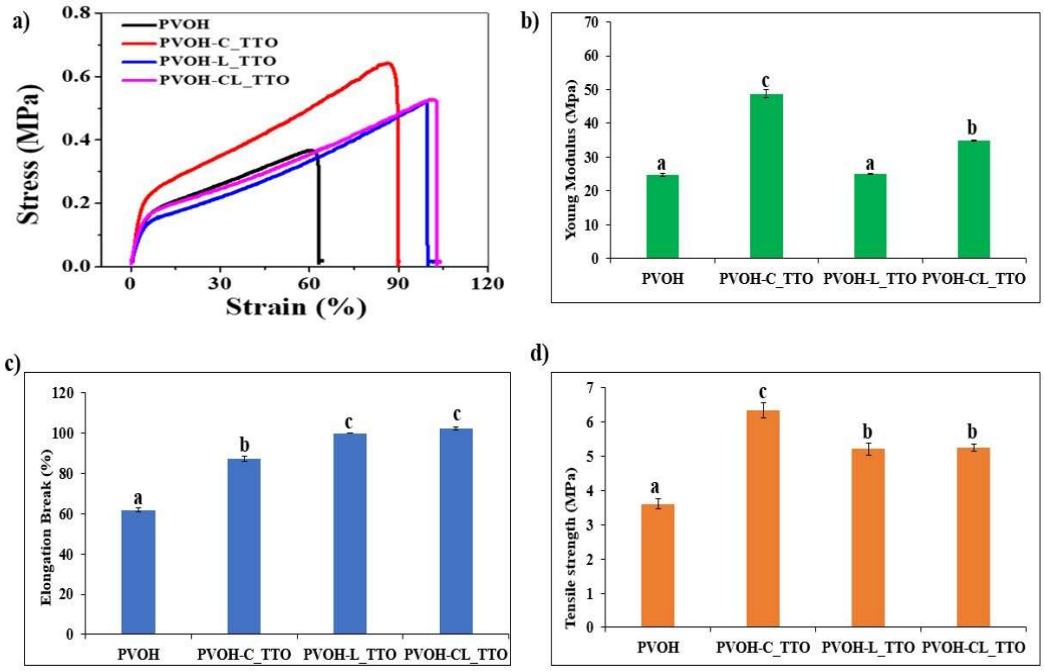

Fig. 6.5. Mechanical profiles of PVOH composites (a) Stress-strain curves (b) Young's modulus (c) Elongation at break and (d) Tensile strength.

6.3.7. FTIR, thermal properties and UV transmittance of films

The FT-IR spectra of PVOH films and with and without NCP and LNP shown in Fig. 6.6a provide key structural insights. The PVOH film exhibited characteristic asymmetric stretching vibrations of the hydroxyl (-OH) and methylene (CH_2) groups at around 3302 cm^{-1} and 2941 cm^{-1}. These peaks shifted in the spectra of PVOH containing, NCP and LNP individually and in combination, indicating interactions between PVOH and NCP, LNP and tea tree oil. Notably, PVOH-L_TTO showed strong absorption IR due to aromatic skeletal vibrations and C-H stretching in the 1600-1500 cm^{-1} and 1460 cm^{-1} regions, consistent with lignin's structure. The presence of cellulose in PVOH-C_TTO introduced notable changes in the fingerprint region (1200-900 cm^{-1}), where the C-O-C pyranose ring skeletal vibrations are observed (Szymanska-Chargot et al. 2015). The broad band around 3300 cm^{-1}, associated with the -OH stretching of cellulose and PVOH, indicated formation of intermolecular hydrogen bonding

(Zhang et al. 2011). In PVOH-CL_TTO, the spectrum is more complex due to interactions between lignin's aromatic structure and cellulose's hydroxyl groups, with additional influence from tea tree oil components such as terpinen-4-ol. These shifts reflect changes in the hydrogen bonding network that would impact the film's physical properties (He et al., 2023).

The thermogravimetric analysis (TGA) shown in Fig. 6.6b captures the thermal degradation behaviour of PVOH films with or without NCP, LNP and tea tree oil. The pure PVOH film showed a single-stage degradation starting around 300°C, with complete decomposition occurring by 400°C. In contrast, the PVOH-C_TTO film began to lose weight at a lower temperature (~250-260°C), likely due to the volatilization of tea tree oil components, with cellulose contributing to gradual weight loss beyond this point (Wang et al., 2021). The PVOH-L_TTO film exhibited lesser overall weight loss. It had a higher residual mass above 30%, attributable to lignin's tendency to form a char rather than volatilizing. The PVOH-L_TTO film was thermally stable up to 500°C compared to other films. The PVOH-CL_TTO film showed similar behaviour in terms of initial weight loss followed by lignin's char formation. These results highlight the fact that the NCP and LNP obtained from DSM can help produce thermally stable biodegradable active packaging.

The differential thermal gravimetric (DTG) analysis (Fig. 6.6c) further elucidates the decomposition profiles of these films. The pure PVOH film showed a sharp peak around 300°C, typical of its semi-crystalline structure (Bascón-Villegas et al., 2021). The addition of cellulose and tea tree oil in PVOH-C_TTO lowered the onset of thermal degradation to around 250°C, with another peak indicating that cellulose component was thermally stabile up to ~350°C (Wang et al., 2019). The broader DTG peak for PVOH-L_TTO (270-330°C) suggested to a staggered degradation, likely due to lignin's amorphous structure. The PVOH-CL_TTO composite exhibited a multi-modal DTG curve, suggesting sequential degradation of tea tree oil, cellulose, and lignin (Bascón-Villegas et al., 2021).

The Differential Scanning Calorimetry (DSC) analysis (Fig. 6.6d) illustrates the thermal transitions of PVOH-based films with NCP, LNP, and TTO. Pure PVOH exhibited a Tg of 85-90°C and a melting peak at 220-230°C, reflecting its semi-crystalline structure (Bascón-Villegas et al., 2021). The PVOH-C_TTO film showed a lower Tg (70-75°C) due to the plasticizing effect of TTO and a broad melting peak near 200-210°C, indicating disrupted crystallinity caused by cellulose (Wang et al., 2021). The PVOH-L_TTO film had a higher Tg (95-100°C) and a melting peak at 225-235°C, showing restricted polymer chain mobility and improved stability due to lignin. The PVOH-CL_TTO film exhibited intermediate thermal behaviour, with a Tg around 80-85°C and endothermic events at 180-200°C (cellulose) and 220-230°C (PVOH). These results highlight lignin's stabilizing effect and TTO's flexibility-enhancing properties, making PVOH-CL_TTO suitable for active packaging applications (Wang et al., 2021; Bascón-Villegas et al., 2021).

X-ray diffraction (XRD) patterns in Fig. 6.6e show the structural shifts in the PVOH composites. Pure PVOH exhibits sharp peaks at 2θ values around 19.5° and 40.5°, indicative of its semi-crystalline nature (Abdelghany et al., 2019). The PVOH-C_TTO sample reveals reduced peak intensity, suggesting decreased crystallinity due to hydrogen bonding disruptions by cellulose (Lu et al., 2012). PVOH-L_TTO displays slight peak broadening, particularly near 22°, indicating a less ordered structure due to lignin's amorphous nature. The PVOH-CL_TTO sample shows diminished peak intensity and additional shifts, indicating complex interactions between PVOH, cellulose, lignin, and tea tree oil, likely affecting the film’s mechanical and barrier properties (Wang et al., 2021).

The UV transmittance spectra (Fig. 6.6f) highlight the films' potential for active packaging. Pure PVOH film showed 55% UV transmittance, providing moderate UV protection. PVOH-C_TTO reduced the transmittance to 50%, with tea tree oil contributing antioxidants that protect within the 200-400 nm range. PVOH-L_TTO exhibited a substantial reduction in UV

transmittance, reaching 0%, thanks to lignin's UV-absorbing properties derived from its aromatic structure (Shikinaka et al., 2020). PVOH-CL_TTO showed 5% UV transmittance indicating a sound level of UV protection. In particular, incorporation of LNP enhanced the film's ability to block harmful UV rays, which is expected to help extend shelf life of UV-sensitive products.

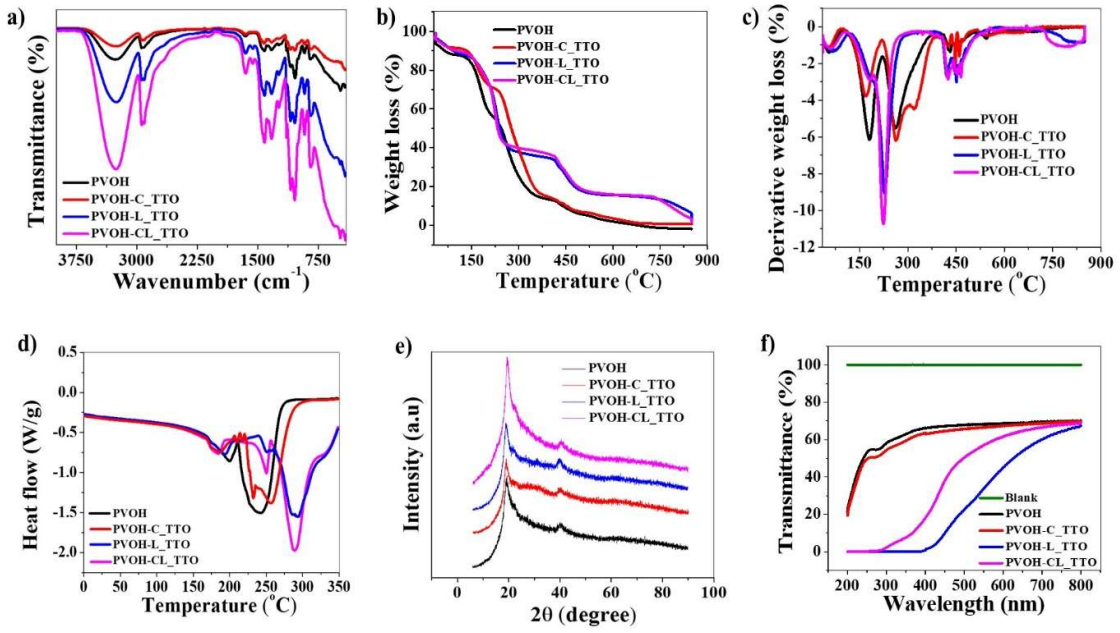

Fig. 6.6. Polyvinyl alcohol (PVOH)-based films with lignin, cellulose, and tea tree oil additives, showing (a) FTIR absorption spectra, (b) TGA thermograms, (c) DTG curves, (d) DSC thermograms, (e) XRD patterns, and (f) UV-Vis transmittance spectra. L= lignin, C= cellulose, TTO = tea tree oil.

6.3.8. Antioxidant and antimicrobial activity of films

The antioxidant activity of the films was evaluated using the DPPH radical scavenging method and the results are shown in Fig. 6.7a. The results indicated that the incorporation of lignin (PVOH-L_TTO) and a combination of lignin with essential oils (PVOH-CL_TTO) significantly enhanced the films' antioxidant properties. Specifically, the PVOH-CL_TTO film exhibited a DPPH scavenging activity of 85%, which is substantially higher than that of control

PVOH film (less than 20%). This enhancement is attributed to the phenolic compounds present in lignin and essential oils, which are known to neutralize free radicals (Barhoum et al, 2020; Basbasan et al., 2023). The presence of lignin and essential oils amplified the film's antioxidant effectiveness. In contrast, the pure PVOH film showed minimal activity, underscoring the importance of incorporating, particularly nano lignin to improve antioxidant capacity of active films.

The antimicrobial activity against *E. coli* is shown in Fig. 6.7b. The data showed that films containing lignin and essential oils (PVOH-L_TTO and PVOH-CL_TTO) significantly inhibited bacterial growth. Lignin's phenolic structure is known to contribute to its antimicrobial properties by disrupting bacterial cell walls and interfering with essential cellular processes (Li et al., 2023). The combination of lignin and essential oils in PVOH-CL_TTO further enhanced the antimicrobial effectiveness. Essential oils are known to possess antimicrobial properties against broad-spectrum of bacterial species (Wang et al., 2021). Thus, they provide additional antimicrobial benefits when combined with lignin. Conversely, the pure PVOH film showed negligible antimicrobial activity, indicating that PVOH lacks inherent antibacterial properties. These results highlight that the incorporation of lignin and essential oils imparts both antioxidant and antimicrobial functionalities to the films, making them suitable as active packaging materials.

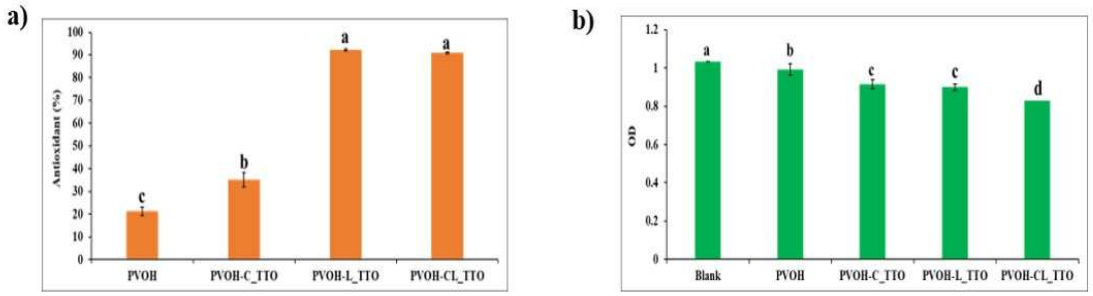

Fig. 6.7. a) Antioxidant (DPPH scavenging) and b) antimicrobial (E. coli inhibition) activities of pure PVOH films and PVOH films containing NCP, LNP and tea tree oil.

6.3.9. Application of films to extend the shelf-life of strawberries

In Fig. 6.8a and 6.8b, the performance of films in preserving shelf life of strawberries wrapped in them and stored at room temperature (22 ± 2°C) on the 0^{th}, 2^{nd}, and 4^{th} days, and under refrigeration (4 ± 1°C) on the 4^{th}, 8^{th}, and 14^{th} days. The assessed included plain polyvinyl alcohol (PVOH), and PVOH containing NCP and and LNP with tea tree oil (PVOH-CL_TTO). The unwrapped (UW) on strawberry was used as the control. Results indicated that PVOH-CL_TTO films provided the best preservation effects compared to the others. This superior performance is primarily due to UV barrier, antimicrobial properties imparted by lignin and tea tree oil, respectively. The presence of NCP increased the water vapour barrier. The PVOH-CL_TTO films effectively maintained the strawberries' colour, firmness, and pH. The enhanced colour retention and reduced browning were evident over time, while firmness was preserved, indicating reduced moisture loss and cellular breakdown. Furthermore, the pH stability observed in PVOH-CL_TTO-wrapped strawberries highlighted the film's ability to slow down spoilage. These findings confirm the potential of PVOH-CL_TTO films in extending the shelf-life and freshness of perishable fruits.

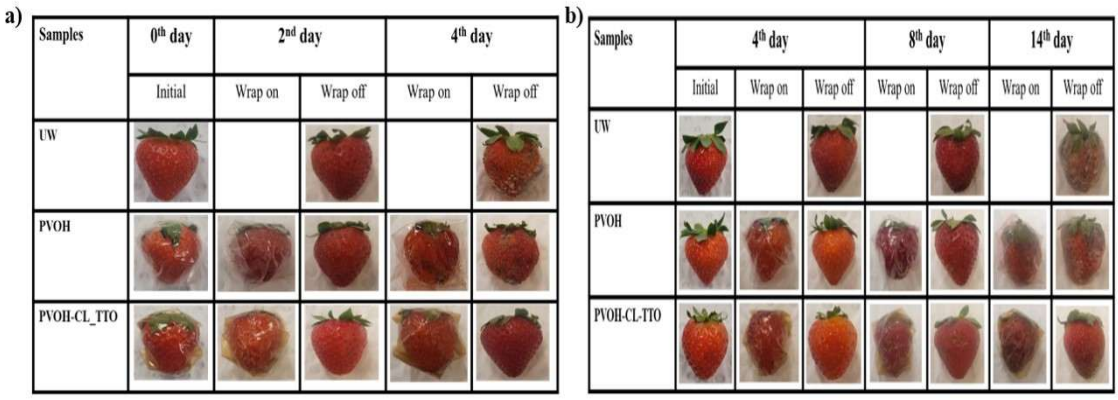

Fig. 6.8. Strawberry preservation studies: (a) Room temperature (22°C) storage observed at 0, 2, and 4 days; (b) Refrigeration (4°C) observed at 4, 8, and 14 days. Comparison of unwrapped (UW), plain PVOH and PVOH-CL_TTO wraps. C = cellulose, L = lignin, TTO = tea tree oil.

6.3.9.1. Storage studies of strawberry

The lightness (L*) of strawberries is a critical indicator of freshness. As shown in Fig. 6.9a, on day 0, all fresh samples had an initial L* value of 50.0. Over time, particularly at room temperature, a rapid decline in lightness was observed. For example, on day 2, unwrapped strawberries showed a significant drop of L* to 35.0, indicating rapid spoilage. In contrast, strawberries wrapped in PVOH and PVOH-CL_TTO films retained higher lightness values of 40.0 and 45.0, respectively, indicating a slower degradation process. By day 4, PVOH-CL_TTO films maintained a L* value of 42.0, outperforming both PVOH-wrapped samples (38.0) and unwrapped samples (30.0). Under refrigeration (4 ± 1°C), the decline in L* values was less severe across all samples. By day 14, PVOH-CL_TTO-wrapped strawberries retained an L* value of 35.0, while unwrapped samples fell to 25.0. This preservation effect could be attributed to the structural reinforcement provided by lignin and cellulose in the PVOH-CL_TTO films, as well as the antimicrobial properties of tea tree oil (Da silva et al., 2019; He et al., 2023). These findings indicate that PVOH-CL_TTO films could be used to extend the shelf life of fresh fruits (Basumatary et al., 2023).

The firmness is also an important parameter that reflects on the freshness of fruits. As shown in Fig. 6.9b, on day 0, all samples had firmness values between 6.8 N and 7.0 N reflecting their initial freshness. At room temperature, unwrapped strawberries showed a significant decline in firmness, by day 2, it dropped to 5.5 N, whereas strawberries wrapped in PVOH and PVOH-CL_TTO films retained higher firmness at 6.2 N and 6.5 N, respectively. By day 4, firmness of unwrapped strawberries further decreased to 4.8 N, while PVOH-CL_TTO-wrapped samples maintained firmness at 5.8 N. Under refrigerated/chilling condition, the decline in firmness was slower across all samples. By day 14, the firmness of unwrapped strawberries decreased to 4.2 N, while that of PVOH-CL_TTO-wrapped strawberries much higher level of firmness (5.5 N), reflecting the film's ability to preserve texture (Shen et al., 2023).

The variation of pH in stored strawberries is an important indicator of spoilage. As shown in Fig. 6.9c, on day 0, the pH of fresh samples ranged between 4.8 and 5.0. At room temperature, unwrapped strawberries showed a decline in pH to 4.5 by day 2, suggesting to a faster spoilage. In contrast, strawberries wrapped in PVOH and PVOH-CL_TTO films maintained pH values between 4.7 and 4.8, due to the antimicrobial properties of the films (Zhang et al., 2019). By day 4, unwrapped strawberries' pH dropped further to 4.3, while that of PVOH-CL_TTO samples remained at 4.7. Under refrigeration, the pH decline was more gradual. By day 14, unwrapped strawberries reached a pH of 4.2, while PVOH-CL_TTO samples maintained a stable pH of 4.7, demonstrating the effectiveness of these films in preserving strawberry by reducing spoilage rate (Basumatary et al., 2023; Shen et al., 2023). These results demonstrated the ability of PVOH-CL_TTO films in extending the shelf life of strawberries by preserving freshness, texture, and acidity.

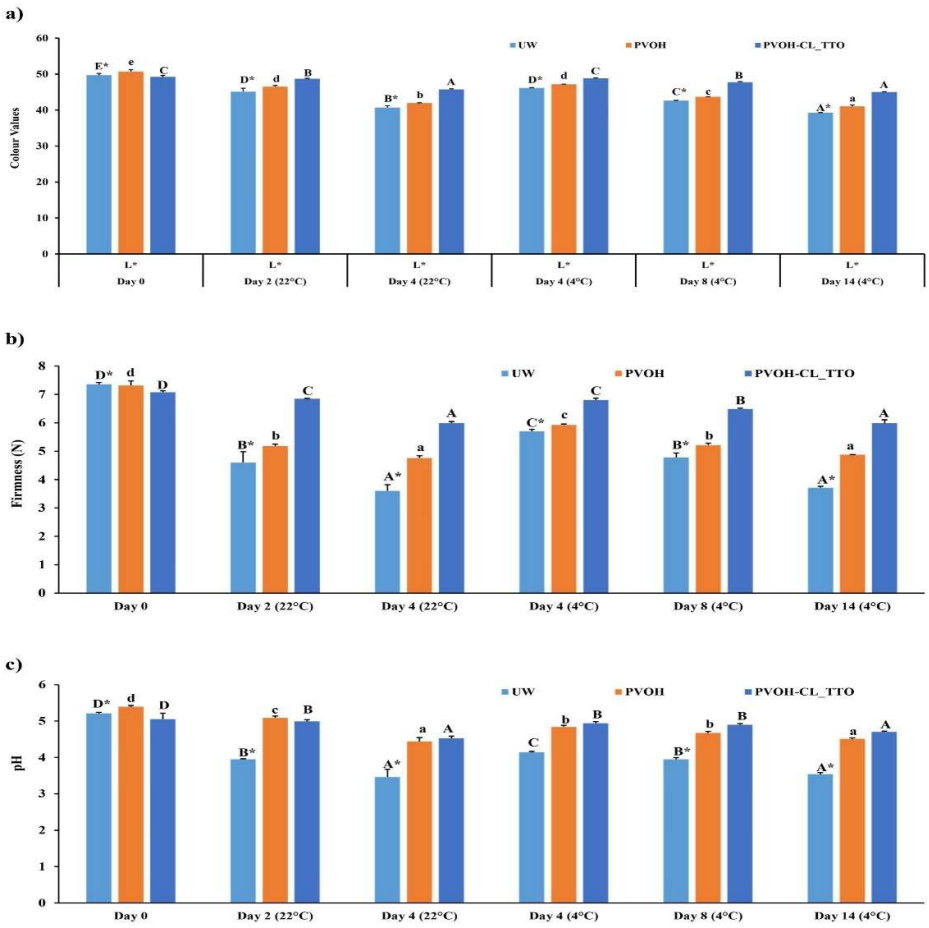

Fig. 6.9. Storage performance of strawberries wrapped in different films over 14 days at room (22 ± 2°C) and refrigerated (4 ± 1°C) conditions, with standard deviations: (a) colour (L*); (b) firmness (%); (c) pH. Films include UW, PVOH, and PVOH-CL_TTO. In (a), * shows significant differences between UW, lowercase letters for PVOH, and uppercase for PVOH-CL_TTO across days ($p < 0.05$).

6.4. Conclusion

Cellulose and lignin were successfully extracted from Dashamoola spent material (DSM) and converted into nanoparticles. The cellulose nanoparticles (NCP) showed excellent structural integrity, thermal stability, and potential for applications including in food packaging. Formation of emulsions and their characterisation revealed that combining lignin nanoparticles (LNP) and NCP enhanced the stability, uniformity of O/W emulsions using an essential oil

(tea tree oil) as the dispersed phase. Incorporating these emulsions into PVOH resulted in bioactive packaging materials with improved physical, mechanical, thermal, antioxidant, and antimicrobial properties. These active films were effective in extending the shelf life of strawberries, a model perishable fruit, up to 14 days in chilled condition. These findings highlight the potential of utilizing cellulose and lignin obtained from Ayurvedic industry's waste stream to develop sustainable, high-performance packaging solutions.

References

Abdelghany, AM, Menazea, AA, & Ismail, AM (2019). Synthesis, characterization, and antimicrobial activity of Chitosan/Polyvinyl Alcohol blend doped with Hibiscus Sabdariffa L. extract. *Journal of Molecular Structure*, *1197*, 603-609. https://doi.org/10.1016/j.molstruc.2019.07.089

Abraham, B., Reshmitha, T. R., Navami, M. M., George, L., Venugopalan, V. V., & Nisha, P. (2020). Phytochemical rich extract from the spent material generated from Industrial Dashamoola preparation (a medicinal Ayurvedic decoction) with antioxidant, antidiabetic and anti-inflammatory potential. *Industrial crops and products*, *151*, 112451. https://doi.org/10.1016/j.indcrop.2020.112451.

Abraham, B., Shakeela, H., Devendra, LP, Arun, KB, Ragavan, KV, Brennan, C., & Nisha, P. (2024). Lignin nanoparticles from Ayurvedic industry spent materials: Applications in Pickering emulsions for curcumin and vitamin D_3 encapsulation. Food Chemistry, 458, 140284. https://doi.org/10.1016/j.foodchem.2024.140284

Abraham, B., Syamnath, V. L., Arun, K. B., Zahra, P. F., Anjusha, P., Kothakotta, A., & Nisha, P. (2023). Lignin-based nanomaterials for food and pharmaceutical applications: Recent trends and future outlook. *Science of The Total Environment*, 881, 163316. https://doi.org/10.1016/j.scitotenv.2023.163316.

Ahmad, T., Esposito, F., & Cirillo, T. (2024). Valorization of Agro-Food By-Products: Advancing Sustainability and Sustainable Development Goals 2030 through Functional Compound Recovery. *Food Bioscience*, 105194.

Akelah, A., & Akelah, A. (2013). Polymers in food packaging and protection. *Functionalized polymeric materials in agriculture and the food industry*, 293-347. https://doi.org/10.1007/978-1-4614-7061-8_6

Anari, E. S., Soltanizadeh, N., & Fathi, M. (2024). The potential of DBD plasma pretreatment for the isolation of micro-and nano-cellulose fibers from the walnut shells. Carbohydrate Polymers, 327, 121692. https://doi.org/10.1016/j.carbpol.2023.121692

Asgher, M., Qamar, S.A., Bilal, M., & Iqbal, HM (2020). Bio-based active food packaging materials: Sustainable alternative to conventional petrochemical-based packaging materials. *Food Research International* , *137* , 109625. https://doi.org/10.1016/j.foodres.2020.109625

Bahrami, A., & Fattahi, R. (2021). Biodegradable carboxymethyl cellulose–polyvinyl alcohol composite incorporated with Glycyrrhiza Glabra L. essential oil: Physicochemical and antibacterial features. *Food science & nutrition,* 9(9), 4974-4985. https://doi.org/10.1002/fsn3.2449

Bai, L., Greca, L. G., Xiang, W., Lehtonen, J., Huan, S., Nugroho, R. W. N., & Rojas, O. J. (2018). Adsorption and assembly of cellulosic and lignin colloids at oil/water interfaces. Langmuir, 35(3), 571-588. https://doi.org/10.1021/acs.langmuir.8b01288

Barhoum, A., Jeevanandam, J., Rastogi, A., Samyn, P., Boluk, Y., Dufresne, A., & Bechelany, M. (2020). Plant celluloses, hemicelluloses, lignin, and volatile oils for the synthesis of nanoparticles and nanostructured materials. *Nanoscale* , *12* (45), 22845-22890. https://doi.org/10.1039/D0NR04795C

Basbasan, A. J., Hararak, B., Winotapun, C., Wanmolee, W., Chinsirikul, W., Leelaphiwat, P., & Boonruang, K. (2023). Lignin nanoparticles for enhancing physicochemical and antimicrobial properties of polybutylene succinate/thymol composite film for active packaging. *Polymers*, *15*(4), 989. https://doi.org/10.3390/polym15040989

Bascón-Villegas, I., Sánchez-Gutiérrez, M., Pérez-Rodríguez, F., Espinosa, E., & Rodríguez, A. (2021). Lignocellulose nanofibre obtained from agricultural wastes of tomato, pepper and eggplants improves the performance of films of polyvinyl alcohol (PVA) for food packaging. *Foods* , *10* (12), 3043. https://doi.org/10.3390/foods10123043

Basumatary, I. B., Mukherjee, A., Katiyar, V., & Kumar, S. (2022). Biopolymer-based nanocomposite films and coatings: Recent advances in shelf-life improvement of fruits and vegetables. *Critical Reviews in Food Science and Nutrition*, *62*(7), 1912-1935. https://doi.org/10.1080/10408398.2020.1848789

Bertolo, M. R., Dias, L. D., Lima, A. R., Aguiar, A. S., Alves, F., de Souza, M., & Junior, S. B. (2023). Photoantimicrobial chitosan-gelatin-pomegranate peel extract films for strawberries preservation: From microbiological analysis to in vivo safety assessment. *International Journal of Biological Macromolecules*, *253*, 127085. https://doi.org/10.1016/j.ijbiomac.2023.127085

Bhargava, N., Sharanagat, V. S., Mor, R. S., & Kumar, K. (2020). Active and intelligent biodegradable packaging films using food and food waste-derived bioactive compounds: A review. *Trends in Food Science & Technology*, 105, 385-401. https://doi.org/10.1016/j.tifs.2020.09.015

Borges, J. C., de Almeida Campos, L. A., Kretzschmar, E. A. M., & Cavalcanti, I. M. F. (2024). Incorporation of essential oils in polymeric films for biomedical applications. *International*

Journal of Biological Macromolecules , 132108. https://doi.org/10.1016/j.ijbiomac.2024.132108

Brun, P., Bernabè, G., Filippini, R., & Piovan, A. (2019). In vitro antimicrobial activities of commercially available tea tree (Melaleuca alternifolia) essential oils. *Current microbiology* , *76* , 108-116. https://doi.org/10.1007/s00284-018-1594-x

Candido, R. G., Godoy, G. G., & Gonçalves, A. R. (2017). Characterization and application of cellulose acetate synthesized from sugarcane bagasse. Carbohydrate polymers, 167, 280-289. https://doi.org/10.1016/j.carbpol.2017.03.057

Cazón, P., Velazquez, G., & Vázquez, M. (2019). Novel composite films from regenerated cellulose-glycerol-polyvinyl alcohol: Mechanical and barrier properties. *Food Hydrocolloids*, 89, 481-491. https://doi.org/10.1016/j.foodhyd.2018.11.012

Chen, M., Hu, Z., Zheng, H., Wang, J., & Xu, X. (2024). Antimicrobial polysaccharide hydrogels embedded with methyl-β-cyclodextrin/thyme oil inclusion complexes for exceptional mechanical performance and chilled chicken breast preservation. *International Journal of Biological Macromolecules* , *267* , 131586. https://doi.org/10.1016/j.ijbiomac.2024.131586

Cheng, Y., Cai, X., Zhang, X., Zhao, Y., Song, R., Xu, Y., & Gao, H. (2024). Applications in Pickering Emulsions of Enhancing Preservation Properties: Current Trends and Future Prospects in Active Food Packaging Coatings and Films. *Trends in Food Science & Technology*, 104643. https://doi.org/10.1016/j.tifs.2024.104643

Da Silva, J. S. P., Da Silva, J. M. F., Soares, B. G., & Livi, S. (2017). Fully biodegradable composites based on poly (butylene adipate-co-terephthalate)/peach palm trees fiber. *Composites Part B: Engineering*, 129, 117-123. https://doi.org/10.1016/j.compositesb.2017.07.088

Dai, T., Liu, Y., Wang, L., Yao, J., Zhu, G., Guo, B., & Zhang, M. (2024). PVA@ tea tree oil-emulsion core–shell microfiber membranes for extending the shelf life of fruits. *Journal of Applied Polymer Science* , *141* (10), e55038. https://doi.org/10.1002/app.55038

Debiagi, F., Kobayashi, R. K., Nakazato, G., Panagio, L. A., & Mali, S. (2014). Biodegradable active packaging based on cassava bagasse, polyvinyl alcohol and essential oils. *Industrial Crops and Products*, 52, 664-670. https://doi.org/10.1016/j.indcrop.2013.11.032

Dinçel Kasapoğlu, E., Kahraman, S., & Tornuk, F. (2023). Extraction optimization and characterization of cellulose nanocrystals from apricot pomace. *Foods* , *12* (4), 746. https://doi.org/10.3390/foods12040746

Dudeja, I., Mankoo, R. K., & Singh, A. (2023). Citric acid crosslinked ternary blended (polyvinyl alcohol, lignin, lemongrass essential oil/nanoemulsions) biopolymeric hydrogel films: structural, functional, antioxidant, antifungal and biodegradable properties. Journal of Food Measurement and Characterization, 17(4), 3774-3788. https://doi.org/10.1007/s11694-023-01905-9

Farhan, A., & Hani, N.M. (2020). Active edible films based on semi-refined κ-carrageenan: Antioxidant and colour properties and application in chicken breast packaging. *Food Packaging and Shelf Life* , *24* , 100476. https://doi.org/10.1016/j.fpsl.2020.100476

Hanan, E., Dar, A. H., Shams, R., & Goksen, G. (2024). New insights into essential oil nano emulsions loaded natural biopolymers recent development, formulation, characterization and packaging applications: A comprehensive review. *International Journal of Biological Macromolecules*, 135751. https://doi.org/10.1016/j.ijbiomac.2024.135751

Haque, A. N. M. A., Zhang, Y., & Naebe, M. (2021). A review on lignocellulose/poly (vinyl alcohol) composites: Cleaner approaches for greener materials. Cellulose, 1-24. https://doi.org/10.1007/s10570-021-04234-6

Haque, A. N. M. A., Zhang, Y., & Naebe, M. (2021). A review on lignocellulose/poly (vinyl alcohol) composites: Cleaner approaches for greener materials. Cellulose, 1-24. https://doi.org/10.1007/s10570-021-04234-6

Hassan, F., Mu, B., & Yang, Y. (2024). Natural polysaccharides and proteins-based films for potential food packaging and mulch applications: A review. *International Journal of Biological Macromolecules* , 129628. https://doi.org/10.1016/j.ijbiomac.2024.129628

He, Y., Ye, H. C., You, T. T., & Xu, F. (2023). Sustainable and multifunctional cellulose-lignin films with excellent antibacterial and UV-shielding for active food packaging. *Food Hydrocolloids*, *137*, 108355. https://doi.org/10.1016/j.foodhyd.2022.108355

He, Y., Ye, H. C., You, T. T., & Xu, F. (2023). Sustainable and multifunctional cellulose-lignin films with excellent antibacterial and UV-shielding for active food packaging. *Food Hydrocolloids*, *137*, 108355. https://doi.org/10.1016/j.foodhyd.2022.108355

He, Y., Ye, H. C., You, T. T., & Xu, F. (2023). Sustainable and multifunctional cellulose-lignin films with excellent antibacterial and UV-shielding for active food packaging. *Food Hydrocolloids*, *137*, 108355. https://doi.org/10.1016/j.foodhyd.2022.108355

He, Y., Ye, H. C., You, T. T., & Xu, F. (2023). Sustainable and multifunctional cellulose-lignin films with excellent antibacterial and UV-shielding for active food packaging. *Food Hydrocolloids*, *137*, 108355. https://doi.org/10.1016/j.foodhyd.2022.108355

Lan, W., Zhang, R., Ahmed, S., Qin, W., & Liu, Y. (2019). Effects of various antimicrobial polyvinyl alcohol/tea polyphenol composite films on the shelf life of packaged strawberries. *Lwt*, *113*, 108297. https://doi.org/10.1016/j.lwt.2019.108297

Li, K., Zhong, W., Li, P., Ren, J., Jiang, K., & Wu, W. (2023). Antibacterial mechanism of lignin and lignin-based antimicrobial materials in different fields. *International Journal of Biological Macromolecules* , 126281. https://doi.org/10.1016/j.ijbiomac.2023.126281

Li, N., Xiang, H. J., Hu, T. G., Qiu, W. P., Hong, Y. X., Huang, K. W., & Wen, P. (2025). Multifunctional electrospun nanofibrous film integrated with cinnamon essential oil emulsion stabilized by dealkali lignin for active packaging material. *Colloids and Surfaces A: Physicochemical and Engineering Aspects*, *704*, 135467. https://doi.org/10.1016/j.colsurfa.2024.135467

Li, Q., Wang, Y., Wu, Y., He, K., Li, Y., Luo, X., Li, B., Wang, C. & Liu, S. (2019). Flexible cellulose nanofibrils as novel pickering stabilizers: The emulsifying property and packing behavior. Food Hydrocolloids, 88, pp.180-189. https://doi.org/10.1016/j.foodhyd.2018.09.039

Li, X., Liu, Y., & Ren, X. (2022). Transparent and ultra-tough PVA/alkaline lignin films with UV shielding and antibacterial functions. *International Journal of Biological Macromolecules*, 216, 86-94. https://doi.org/10.1016/j.ijbiomac.2022.06.188

Li, X., Liu, Y., & Ren, X. (2022). Transparent and ultra-tough PVA/alkaline lignin films with UV shielding and antibacterial functions. *International Journal of Biological Macromolecules*, 216, 86-94. https://doi.org/10.1016/j.ijbiomac.2022.06.188

Lingait, D., Sethy, L. K., & Kumar, A. (2024). Biopolymer sporopollenin reinforced pectin/PVA composite films for sustainable packaging application. *Sustainable Chemistry and Pharmacy*, *41*, 101711. https://doi.org/10.1016/j.scp.2024.101711

Liu, B., Zhang, W., Zeng, J., Gong, N., Ying, G., Li, P., & Chen, K. (2024). Acid-catalyzed phenolation of lignin with tea polyphenol: Enhancing UV resistance and oxidation resistance for potential applications. *International Journal of Biological Macromolecules* , *267* , 131462. https://doi.org/10.1016/j.ijbiomac.2024.131462

Liu, Y., Ahmed, S., Sameen, D.E., Wang, Y., Lu, R., Dai, J., & Qin, W. (2021). A review of cellulose and its derivatives in biopolymer-based for food packaging applications. Trends in Food Science & Technology , 112 , 532-546. https://doi.org/10.1016/j.tifs.2021.04.016

Lu, P., & Hsieh, Y. L. (2012). Cellulose isolation and core–shell nanostructures of cellulose nanocrystals from chardonnay grape skins. Carbohydrate polymers, 87(4), 2546-2553. https://doi.org/10.1016/j.carbpol.2011.11.023

Lu, P., & Hsieh, Y. L. (2012). Cellulose isolation and core–shell nanostructures of cellulose nanocrystals from chardonnay grape skins. Carbohydrate polymers, 87(4), 2546-2553. https://doi.org/10.1016/j.carbpol.2011.11.023

Luzi, F., Del Buono, D., Orfei, B., Moretti, C., Buonaurio, R., Torre, L., & Puglia, D. (2022). Lemna minor aqueous extract as a natural ingredient incorporated in poly (vinyl alcohol)-based films for active food packaging systems. *Food Packaging and Shelf Life*, 32, 100822. https://doi.org/10.1016/j.fpsl.2022.100822

Martinez-Alvarenga, MS, Martinez-Rodriguez, EY, Garcia-Amezquita, LE, Olivas, GI, Zamudio-Flores, PB, Acosta-Muniz, CH, & Sepulveda, DR (2014). Effect of Maillard reaction conditions on the degree of glycation and functional properties of whey protein isolate–Maltodextrin conjugates. *Food Hydrocolloids* , *38* , 110-118. https://doi.org/10.1016/j.foodhyd.2013.11.006

Mou, H. Y., Heikkilä, E., & Fardim, P. (2013). Topochemistry of alkaline, alkaline-peroxide and hydrotropic pretreatments of common reed to enhance enzymatic hydrolysis efficiency. *Bioresource technology*, *150*, 36-41. https://doi.org/10.1016/j.biortech.2013.09.093.

Moustaqim, EL, M., El Kaihal, A., El Marouani, M., Men-La-Yakhaf, S., Taibi, M., Sebbahi, S., El Hajjaji & Kifani-Sahban, F. (2018). Thermal and thermomechanical analyses of

lignin. *Sustainable chemistry and pharmacy*, *9*, 63-68. https://doi.org/10.1016/j.scp.2018.06.002.

Nagarajan, K. J., Balaji, A. N., & Ramanujam, N. R. (2019). Extraction of cellulose nanofibers from cocos nucifera var aurantiaca peduncle by ball milling combined with chemical treatment. *Carbohydrate polymers*, *212*, 312-322. https://doi.org/10.1016/j.carbpol.2019.02.063

Nian, L., Wang, M., Sun, X., Zeng, Y., Xie, Y., Cheng, S., & Cao, C. (2024). Biodegradable active packaging: Components, preparation, and applications in the preservation of postharvest perishable fruits and vegetables. *Critical Reviews in Food Science and Nutrition*, *64* (8), 2304-2339. https://doi.org/10.1080/10408398.2022.2122924

Oladzadabbasabadi, N., Abraham, B., Ghasemlou, M., Ivanova, E. P., & Adhikari, B. (2024). Green synthesis of non-isocyanate hydroxyurethane and its hybridization with carboxymethyl cellulose to produce films. *International Journal of Biological Macromolecules* , *276* , 133617. https://doi.org/10.1016/j.ijbiomac.2024.133617

Oun, A. A., Shin, G. H., & Kim, J. T. (2022). Multifunctional poly (vinyl alcohol) films using cellulose nanocrystals/oregano and cellulose nanocrystals/cinnamon Pickering emulsions: Effect of oil type and concentration. *International Journal of Biological Macromolecules*, 194, 736-745. https://doi.org/10.1016/j.ijbiomac.2021.11.119

Panda, P. K., Sadeghi, K., & Seo, J. (2022). Recent advances in poly (vinyl alcohol)/natural polymer based films for food packaging applications: A review. *Food Packaging and Shelf Life*, 33, 100904. https://doi.org/10.1016/j.fpsl.2022.100904

Pandita, G., de Souza, C. K., Gonçalves, M. J., Jasińska, J. M., Jamróz, E., & Roy, S. (2024). Recent progress on Pickering emulsion stabilized essential oil added biopolymer-based film

for food packaging applications: A review. *International Journal of Biological Macromolecules*, 132067. https://doi.org/10.1016/j.ijbiomac.2024.132067

Pandita, G., de Souza, C.K., Gonçalves, M.J., Jasińska, J.M., Jamróz, E., & Roy, S. (2024). Recent progress on Pickering emulsion stabilized essential oil added biopolymer-based film for food packaging applications: A review. *International Journal of Biological Macromolecules* , 132067. https://doi.org/10.1016/j.ijbiomac.2024.132067

Phansamarng, P., Bacchus, A., Pour, F. H., Kongvarhodom, C., & Fatehi, P. (2024). Cationic lignin incorporated polyvinyl alcohol films for packaging applications. *Industrial Crops and Products*, *221*, 119217. https://doi.org/10.1016/j.indcrop.2024.119217

Pirsa, S. (2024). Cellulose-based cartons: production methods, modification, and smart/active packaging. *Cellulose*, *31*(6), 3421-3445. https://doi.org/10.1007/s10570-024-05826-8

Ren, Y., Fan, X., Cao, L., & Chen, Y. (2024). Water-resistant and barrier properties of poly (vinyl alcohol)/nanocellulose films enhanced by metal ion crosslinking. *International Journal of Biological Macromolecules*, 277, 134245. https://doi.org/10.1016/j.ijbiomac.2024.134245

Roy, S., & Rhim, J. W. (2021). Antioxidant and antimicrobial poly (vinyl alcohol)-based films incorporated with grapefruit seed extract and curcumin. *Journal of Environmental Chemical Engineering,* 9(1), 104694. https://doi.org/10.1016/j.jece.2020.104694

Ruiz, R., Ehrman, T, (1996), Determination of carbohydrates in biomass by high performance liquid chromatography. Laboratory analytical procedure, 2.

Salgado, P. R., Di Giorgio, L., Musso, Y. S., & Mauri, A. N. (2021). Recent developments in smart food packaging focused on biobased and biodegradable polymers. *Frontiers in Sustainable Food Systems*, 5, 630393. https://doi.org/10.3389/fsufs.2021.630393

Sani, M. A., Azizi-Lalabadi, M., Tavassoli, M., Mohammadi, K., & McClements, D. J. (2021). Recent advances in the development of smart and active biodegradable packaging materials. *Nanomaterials*, 11(5), 1331. https://doi.org/10.3390/nano11051331

Shen, Y., Seidi, F., Ahmad, M., Liu, Y., Saeb, M. R., Akbari, A., & Xiao, H. (2023). Recent advances in functional cellulose-based films with antimicrobial and antioxidant properties for food packaging. *Journal of Agricultural and Food Chemistry*, *71*(44), 16469-16487. https://doi.org/10.1021/acs.jafc.3c06004J.

Shikinaka, K., Nakamura, M., & Otsuka, Y. (2020). Strong UV absorption by nanoparticulated lignin in polymer films with reinforcement of mechanical properties. *Polymer*, *190*, 122254. https://doi.org/10.1016/j.polymer.2020.122254

Silvério, H.A., Neto, WPF, Dantas, N.O., & Pasquini, D. (2013). Extraction and characterization of cellulose nanocrystals from corncob for application as reinforcing agent in nanocomposites. *Industrial crops and products* , *44* , 427-436. https://doi.org/10.1016/j.indcrop.2012.10.014

Sindhu, R., Kuttiraja, M., Binod, P., Janu, K. U., Sukumaran, R. K., & Pandey, A. (2011). Dilute acid pretreatment and enzymatic saccharification of sugarcane tops for bioethanol production. *Bioresource Technology*, *102(23),* 10915-10921. https://doi.org/10.1016/j.biortech.2011.09.066.

Soni, B., & Mahmoud, B. (2015). Chemical isolation and characterization of different cellulose nanofibers from cotton stalks. Carbohydrate polymers, 134, 581-589. https://doi.org/10.1016/j.carbpol.2015.08.031

Suganthi, S., Vignesh, S., Kalyana Sundar, J., & Raj, V. (2020). Fabrication of PVA polymer films with improved antibacterial activity by fine-tuning via organic acids for food packaging applications. *Applied Water Science*, 10(4), 1-11. https://doi.org/10.1007/s13201-020-1162-y

Szymanska-Chargot, M., Chylinska, M., Kruk, B., & Zdunek, A. (2015). Combining FT-IR spectroscopy and multivariate analysis for qualitative and quantitative analysis of the cell wall composition changes during apple development. *Carbohydrate Polymers* , *115* , 93-103. https://doi.org/10.1016/j.carbpol.2014.08.039

Tanpichai, S., Boonmahitthisud, A., Soykeabkaew, N., & Ongthip, L. (2022). Review of the recent developments in all-cellulose nanocomposites: Properties and applications. Carbohydrate polymers , 286 , 119192. https://doi.org/10.1016/j.carbpol.2022.119192

Trilokesh, C., & Uppuluri, K. B. (2019). Isolation and characterization of cellulose nanocrystals from jackfruit peel. Scientific Reports, 9(1), 16709.| https://doi.org/10.1038/s41598-019-53412-x

Wang, H., Liu, X., Wu, M., & Huang, Y. (2024). Construction of multiple crosslinked networks for the preparation of high-performance lignin-containing cellulose nanofiber reinforced polyvinyl alcohol films. *International Journal of Biological Macromolecules*, 259, 129061. https://doi.org/10.1016/j.ijbiomac.2023.129061

Wang, Y., Li, J., Guo, X., Wang, H., Qian, F., & Lv, Y. (2021). Active biodegradable polyvinyl alcohol–hemicellulose/tea polyphenol films with excellent moisture resistance prepared via ultrasound assistance for food packaging. *Coatings*, *11*(2), 219. https://doi.org/10.3390/coatings11020219

Wang, Y., Li, J., Guo, X., Wang, H., Qian, F., & Lv, Y. (2021). Active biodegradable polyvinyl alcohol–hemicellulose/tea polyphenol films with excellent moisture resistance prepared via ultrasound assistance for food packaging. *Coatings*, *11*(2), 219. https://doi.org/10.3390/coatings11020219

Yang, W., Fortunati, E., Dominici, F., Giovanale, G., Mazzaglia, A., Balestra, G. M., & Puglia, D. (2016). Effect of cellulose and lignin on disintegration, antimicrobial and antioxidant

properties of PLA active films. *International journal of biological macromolecules*, *89*, 360-368. https://doi.org/10.1016/j.ijbiomac.2016.04.068

Zhang, H., Chen, Y., Wang, S., Ma, L., Yu, Y., Dai, H., & Zhang, Y. (2020). Extraction and comparison of cellulose nanocrystals from lemon (Citrus limon) seeds using sulfuric acid hydrolysis and oxidation methods. Carbohydrate polymers, 238, 116180. https://doi.org/10.1016/j.carbpol.2020.116180

Zhang, W., Yang, X., Li, C., Liang, M., Lu, C., & Deng, Y. (2011). Mechanochemical activation of cellulose and its thermoplastic polyvinyl alcohol ecocomposites with enhanced physicochemical properties. *Carbohydrate Polymers* , *83* (1), 257-263. https://doi.org/10.1016/j.carbpol.2010.07.062

Zhang, Y., Haque, ANMA, & Naebe, M. (2021). Lignin–cellulose nanocrystals from hemp hurd as light-colored ultraviolet (UV) functional filler for enhanced performance of polyvinyl alcohol nanocomposite films. *Nanomaterials* , *11* (12), 3425. https://doi.org/10.3390/nano11123425

Zhou, Q., Chen, J., Wang, C., Yang, G., Janaswamy, S., Xu, F., & Liu, Z. (2022). Preparation and characterization of lignin nanoparticles and chitin nanofibers reinforced PVA films with UV shielding properties. *Industrial Crops and Products* , *188* , 115669. https://doi.org/10.1016/j.indcrop.2022.115669

Zhu, M., Huan, S., Liu, S., Li, Z., He, M., Yang, G., & Bai, L. (2021). Recent development in food emulsion stabilized by plant-based cellulose nanoparticles. *Current Opinion in Colloid & Interface Science* , *56* , 101512. https://doi.org/10.1016/j.cocis.2021.101512

Chapter 7

General Conclusion, Discussion, and Recommendation

7.1. Overview of research work

This thesis addresses two important challenges faced by the Ayurvedic and allied sectors: the effective utilization of byproducts or spent material left over after the extraction of medicinally important compounds, and the development of eco-friendly, health-promoting products. To address these challenges, the research primarily focused on Dashamoola spent material (DSM), a lignocellulose-rich byproduct from Ayurvedic drug production that is generated in significant quantities. DSM was selected as a model due to its abundance and high potential to extract high-value phytochemicals, such as polyphenols, nanocellulose and lignin, for use as ingredients in nutraceutical, food, and packaging applications.

The first experimental chapter of this thesis involved a detailed characterization of DSM, revealing its rich phytochemical composition, including polyphenols such as gallic acid, shikimic acid, and epicatechin. These compounds, known for their antioxidant, antidiabetic, and anti-inflammatory properties, were extracted with higher yields by optimizing the extraction method. In vitro assays confirmed their antioxidative and other health-promoting properties, underscoring DSM's potential as a sustainable source of health-promoting ingredients. Furthermore, the recovery of these compounds at high yields demonstrates that this work offers an efficient valorisation pathway for Ayurvedic industrial byproducts.

In the second experimental chapter, lignin nanoparticles (LNPs) were produced from DSM using ball milling. These nanoparticles exhibited exceptional stability and effectiveness as Pickering particles, capable of stabilizing oil-in-water emulsions. The emulsions successfully encapsulated bioactive compounds, such as curcumin and vitamin D_3, achieving high encapsulation efficiency and stability for over 90 days under varying storage conditions. This part of the research highlighted the shielding capability of LNPs in protecting bioactive

compounds from degradation caused by environmental factors. This work also demonstrated the potential of lignin, a traditionally underutilized component, for industrial applications as an emulsifier and encapsulant.

In the third experimental chapter of this thesis, LNP-based Pickering emulsions were formulated and applied to nutrient-fortified extruded snacks. A flour blend comprising pearl millet, coconut spent flour (CSF), and corn grits was used to formulate these snacks, achieving a significantly improved nutritional profile. Encapsulation of curcumin and vitamin D_3 within these emulsions better preserved their bioavailability and enhanced stability during the high-temperature extrusion process, outperforming conventional fortification methods. These findings demonstrate that LNPs extracted from DSM spent material serve as highly effective Pickering emulsifiers and delivery vehicles for health-promoting yet unstable compounds, offering a novel approach to snack food fortification.

The fourth, or final, experimental chapter focused on developing biodegradable packaging films composed of polyvinyl alcohol (PVOH) infused with nanocellulose and nanolignin extracted from DSM. Nanocellulose contributed to structural reinforcement, while nanolignin provided UV-blocking properties and acted as an antioxidant. Tea tree oil an essential oil, was incorporated into these films to impart antibacterial functionality. Compared to PVOH-only films, the modified films exhibited improved mechanical and thermal properties. The enhanced antioxidant, UV-blocking, and antimicrobial properties of these films preserved freshness for a longer duration and reduced microbial load, thereby extending the shelf life of strawberries. Thus, nanocellulose and nanolignin extracted from DSM demonstrated potential as components of biodegradable and sustainable food packaging solutions. This application in food packaging also provides a pathway for value addition to DSM and other Ayurvedic waste materials.

Overall, this research provides an effective pathway for the valorisation of DSM by optimizing the extraction of antioxidants, cellulose, and lignin, and demonstrating their applications in nutrient fortification, emulsification, delivery systems, and active, biodegradable packaging. The outcomes highlight the potential of these DSM-derived materials for enhancing the functionality and sustainability of food and food packaging applications. This work establishes a foundation for future studies to further refine these materials and explore their use in other industrial processes.

7.2. Key findings, general discussion, and conclusion

7.2.1. Extraction and bioactive potential of phenolic compounds from DSM

The extraction process for bioactive compound-rich extracts from DSM was optimized, resulting in a higher yield. The extracts contained phenolic compounds, including gallic acid, shikimic acid, and epicatechin. These extracts, due to the presence of these compounds, exhibited strong antioxidant, antidiabetic, and anti-inflammatory activities, as confirmed by DPPH, ABTS, and protein denaturation assays. The antioxidant potential of the extract, reflected in its IC_{50} values, indicated a strong radical scavenging capacity. These findings align with existing studies confirming the role of polyphenols in mitigating oxidative stress.

In vitro studies revealed the cytoprotective and metabolic-regulating effects of phenolic compound-rich DSM extracts, highlighting their potential applications in nutraceuticals. These extracts exhibited significant α-amylase and α-glucosidase inhibitory activities, indicating their efficacy in glycemic control and their potential as viable candidates for developing health-promoting ingredients. These findings align with contemporary research on polyphenols and flavonoids, corroborating the bioactive potential of plant-derived polyphenols in health promotion (Olivares et al., 2018; Milke et al., 2018).

7.2.2. Development and application of lignin nanoparticles

Lignin nanoparticles (LNPs) extracted from DSM demonstrated exceptional properties as Pickering particles, enabling the stabilization of oil-in-water emulsions. These emulsions were used to encapsulate curcumin and vitamin D_3, achieving high encapsulation efficiencies of 87.9% and 72.6%, respectively. The emulsions remained stable for over 90 days, with no phase separation observed. Such stability highlights the structural integrity and protective capacity of LNPs under varying environmental conditions.

These findings mark a significant advancement in the valorisation of lignin, extracted from DSM, and pave the way for its broader application in the food, pharmaceutical, and other industries. Their stability and multifunctionality make them a compelling alternative to synthetic stabilizers. Studies by Grappa et al. (2024) and Lizundia et al. (2021) corroborate the multifunctional properties of lignin nanoparticles across diverse applications, reinforcing the outcomes of this research.

7.2.3. Fortification of extruded snacks using nanolignin from DSM

The development of nutrient-rich snacks using blended flour and LNP-based Pickering emulsions represents an innovation of practical importance. These snacks contained significantly higher protein (13.8%) and dietary fiber (19.2%) levels compared to conventional extruded snacks, addressing common nutritional deficiencies. These findings align with the role of high-protein and high-fiber ingredients in enhancing snack nutritional quality, as highlighted by Gomes et al. (2023).

The LNP-stabilized emulsions were utilized to encapsulate curcumin and vitamin D_3, which preserved their structural integrity during the extrusion process and enhanced their bioavailability. Incorporating these curcumin- and vitamin D_3-infused emulsions into extruded snacks further improved their health-promoting properties. The use of underutilized grains such

as pearl millet and byproducts like CSF highlights the potential to create nutritious snacks with sustainable ingredients and contributes towards overcoming malnutrition. Increased utilization of underutilized crops supports global food security, as emphasized by Geisen et al. (2021).

7.2.4. Creating active packaging films using NCP and LNP from DSM

Active packaging films developed using PVOH as the primary matrix and DSM-derived nanocellulose and nanolignin as additives demonstrated superior properties, including UV-blocking, antimicrobial activity, and moisture resistance. These films extended the shelf life of strawberries, a model perishable fruit, by preserving their colour, firmness, and pH for up to 14 days under chilled conditions. This work contributes to the growing trend of developing bio-based and biodegradable active packaging materials, as highlighted by Tan et al. (2021).

The research presented in this thesis on the use of DSM-derived materials, such as nanocellulose and nanolignin combined with essential oils, in developing active (antimicrobial, UV-blocking) biodegradable packaging films demonstrates their potential in sustainable packaging. These components can serve as valuable elements of eco-friendly alternatives to conventional plastics while also helping to extend the shelf life of perishable fruits. Similarly, Zhang et al. (2022) highlight the benefits of incorporating lignocellulosic materials into sustainable packaging solutions.

7.3. Contribution made by the thesis to the body of knowledge

This thesis makes a significant contribution to the body of knowledge by demonstrating how Ayurvedic spent materials, an underutilized resource, can be sustainably repurposed into high-value products, thereby contributing to the advancement of circular economy practices. It optimizes extraction and purification protocols to obtain nanocellulose and nanolignin from DSM at the highest yield levels and provides insights into their characteristics using advanced

analytical methods. These findings pave the way for their effective valorisation and application in areas such as healthy food development and biodegradable packaging.

The key contributions made by this thesis to the body of knowledge in the relevant field are outlined below.

1. **Extraction and characterization of phenolic compound-rich DSM extract (Chapter 3):** This study optimized process protocols to achieve the highest yield of phenolic compound-rich extracts from DSM. The major phenolic compounds were subsequently identified and characterized, confirming that DSM is a rich source of polyphenols and flavonoids. The findings demonstrate the potential of these extracts for developing health-promoting foods.
2. **Extraction, characterization, and application of lignin nanoparticles from DSM (Chapter 4):** This study optimized the extraction and purification protocols to obtain lignin from DSM and successfully converted it into lignin nanoparticles (LNPs). The LNPs were characterized using advanced analytical techniques to determine their structural, thermal, and functional properties. The findings demonstrate the potential of LNPs as UV-blocking agents and encapsulating materials, providing a scalable model for their integration into various industrial processes.
3. **Formulation and application of LNP-stabilized pickering emulsions for nutrient-rich snack fortification (Chapter 5):** This part of the work demonstrated that LNPs can be effectively used to formulate highly stable LNP-stabilized Pickering emulsions. It showed that these emulsions could successfully encapsulate bioactive compounds, such as curcumin and vitamin D_3, ensuring a high level of structural stability and preservation of bioactivity during extrusion into snacks. This study advances the science underpinning the application of LNPs derived from DSM in food systems,

highlighting their potential to create nutrient-rich emulsions and snacks with enhanced health-promoting properties. Additionally, it demonstrates that these enriched Pickering emulsions can be readily utilized to fortify snack products made from underutilized grains.

4. **Development of active packaging films using nanocellulose and LNPs derived from DSM (Chapter 6):** This work demonstrated that cellulose nanoparticles and lignin nanoparticles (LNPs) could be successfully incorporated into a PVOH matrix to reinforce its structure and impart UV-light blocking properties. It also showed that essential oils could be infused into these films to introduce antimicrobial functionality. The resulting films exhibited desirable UV-blocking and antimicrobial properties without compromising mechanical integrity or water vapor barrier performance. These films significantly extended the shelf life of strawberries, a perishable fruit, providing a realistic pathway for creating active and fully biodegradable packaging materials. This study establishes the feasibility of applying nanocellulose and LNPs derived from DSM in food packaging, contributing to their value addition.

These contributions collectively advance the body of knowledge on the effective valorisation of Ayurvedic spent materials, demonstrating optimized methods for extracting and characterizing the physicochemical properties of phenolic compound-rich extracts, nanocellulose, and lignin nanoparticles (LNPs). This research demonstrates real-life applications of these materials in creating stable emulsions, encapsulating health-promoting compounds, fortifying extruded products, and developing active biodegradable packaging. In essence, it provides a holistic pathway for the valorisation of Ayurvedic spent materials, using DSM as a model.

7.4. Recommendations for future work

Even though the research demonstrated the applications of ingredients derived from DSM, there are several other areas where further research would be vital:

1. **Scaling up of extraction process:** The extraction of phenolic compound-rich extracts, nanocellulose and LNP of DSM were carried out in laboratory scale. The scaling up of the extraction process including pilot plant trials and feasibility studies would provide valuable information to ascertain their successful commercial exploitation.
2. **Clinical trials for phenolic compound-rich extracts:** In vitro studies were carried out in this work to evaluate their health promoting aspects. Thus, clinical evaluations need to be undertaken to ascertain the safety human health-promotion aspects of DSM extracts. This step is essential for regulatory approvals and product safety.
3. **Broader applications of LNPs:** In this work, application of LNPs were applied to produce Pickering emulsions and to encapsulate curcumin and vitamin D_3. Their applications in drug delivery, cosmetics, and agricultural formulations need to be pursued to leverage their unique properties.
4. **Further expand the application in packaging films:** In this work, the nanocellulose and LNPs obtained from DSM were applied create a single prototype of active-biodegradable packaging. Its efficacy was tested in only one fruit (strawberry). Nanocellulose and LNPs from DSM can be incorporated in various natural polymer based and synthetic plastics as they bring unique re-enforcing and colouring and UV blocking properties. Their applications in synthetic yet biodegradable plastic such as PBAT, PBSA and PHAs greatly broaden their application.
5. **Cost-benefit analysis:** While this study refined the extraction methods and demonstrated the potential applications of DSM-derived ingredients, a detailed cost analysis of their extraction and processing is necessary. This includes assessing raw

material costs, processing efficiency, energy consumption, and scalability factors. A comprehensive economic evaluation will help determine the commercial viability of these materials obtained from DSM and other Ayurvedic waste streams.

There are many opportunities to undertake research and development to make use of DSM-derived materials. The approach taken in this study for value-adding DSM can be applied to other waste streams of Ayurvedic industry.

References

Olivares-Vicente, M., Barrajon-Catalan, E., Herranz-Lopez, M., Segura-Carretero, A., Joven, J., Encinar, J. A., & Micol, V. (2018). Plant-derived polyphenols in human health: Biological activity, metabolites and putative molecular targets. *Current drug metabolism*, 19 (4), 351-369. https://doi.org/10.2174/1389200219666180220095236

Milke, L., Aschenbrenner, J., Marienhagen, J., & Kallscheuer, N. (2018). Production of plant-derived polyphenols in microorganisms: current state and perspectives. *Applied Microbiology and Biotechnology*, *102*, 1575-1585. https://doi.org/10.1007/s00253-018-8747-5

Grappa, R., Venezia, V., Basta, L., Alfieri, M. L., Panzella, L., Verrillo, M., & Costantini, A. (2024). Green synthesis of stable lignin nanoparticles with reversible swelling behavior and enhanced multifunctional features. *ACS Sustainable Chemistry & Engineering*, *12*(28), 10653-10664. https://doi.org/10.1021/acssuschemeng.4c03783

Lizundia, E., Sipponen, M. H., Greca, L. G., Balakshin, M., Tardy, B. L., Rojas, O. J., & Puglia, D. (2021). Multifunctional lignin-based nanocomposites and nanohybrids. *Green Chemistry*, *23*(18), 6698-6760. https://doi.org/10.1039/D1GC01684A

Geisen, S., Krishnaswamy, K., & Myers, R. (2021). Physical and structural characterization of underutilized climate-resilient seed grains: millets, sorghum, and amaranth. *Frontiers in Sustainable Food Systems*, *5*, 599656. https://doi.org/10.3389/fsufs.2021.599656

Gomes, KS, Berwian, GF, Batistella, VMC, Bender, LE, Reinehr, CO, & Colla, LM (2023). Nutritional and technological aspects of the production of proteic extruded snacks added from novel raw materials. *Food and Bioprocess Technology*, *16* (2), 247-267. https://doi.org/10.1007/s11947-022-02887-0

Tan, C., Han, F., Zhang, S., Li, P., & Shang, N. (2021). Novel bio-based materials and applications in antimicrobial food packaging: Recent advances and future trends. *International Journal of Molecular Sciences*, *22* (18), 9663. https://doi.org/10.3390/ijms22189663

Zhang, X., Tanguy, N.R., Chen, H., Zhao, Y., Gnanasekar, P., Le Lagadec, R., & Yan, N. (2022). Lignocellulosic nanofibrils as multifunctional components for high-performance packaging applications. *Materials Today Communications*, *31*, 103630. https://doi.org/10.1016/j.mtcomm.2022.103630

AcSIR Course work

Code	Course work	Credits	Status
AcSIR-39-RM	Research Methodology Course ➢ Ethics, IP, Safety Communications ➢ Basic Mathematics & Statistical Methods ➢ Computer Applications & Informatics ➢ Tools and Techniques	4	Completed
BIO-NIIST-2-4106	Fundamentals of Food processing	2	Completed
BIO-NIIST-2-4108	Significance of food preservation	1	Completed
BIO-NIIST-2-4109	Thermal processing of foods	1	Completed
BIO-NIIST-3-4101	Seminar course	1	Completed
BIO-NIIST-3-4114	Prebiotics and Probiotics	1	Completed
BIO-NIIST-3-4116	Functional Foods and Nutraceuticals	2	Completed
CHE-NIIST-4-4101	Project Proposal Writing	2	Completed
CHE-NIIST-4-4102	Review Article Writing	2	Completed
CHE-NIIST-4-4103	CSIR-800 Project Work	4	Completed

ABSTRACT

Name of the student: Billu Abraham **Registration No: 10CC19A39002**
Faculty of study: Chemical Sciences **Year of submission: 2025**
CSIR Lab: CSIR NIIST **Name of the Supervisor/ Co-supervisor: Dr. Nisha P/ Dr. Anjineyulu Kothakota**

Title of the thesis: Technological Interventions for Value Addition of Polyherbal Spent Materials from Ayurvedic Industries

This thesis explores the valorization of Dashamoola spent material (DSM), a byproduct generated in large quantities during the preparation of Ayurvedic formulations like Dashamoolaarishta. The Ayurvedic industry produces substantial waste in the form of DSM, which is rich in lignocellulosic biomass, including lignin, cellulose, and hemicellulose, as well as bioactive polyphenols such as shikimic acid, gallic acid, and epicatechin. Traditionally discarded as waste, DSM represents untapped potential for sustainable and health-promoting applications, aligning with the principles of the circular economy and waste valorization.

This study focuses on:

1. Extracting and characterizing bioactive compounds from DSM using advanced chromatographic techniques, revealing potent antioxidant, antidiabetic, and anti-inflammatory activities.

2. Converting lignin from DSM into nanoparticles and using them to stabilize Pickering emulsions for encapsulating curcumin and vitamin D_3, ensuring improved stability and bioavailability.

3. Integrating these emulsions into the extrusion process to develop nutrient-fortified snacks with enhanced nutritional profiles and sensory qualities.

4. Utilizing DSM-derived lignin and cellulose to create active packaging films infused with tea tree oil, offering improved properties for sustainable food preservation.

The findings demonstrate the potential of DSM to provide innovative solutions for waste valorization while addressing critical global challenges in health, nutrition, and sustainability. This work underscores the importance of leveraging waste from the Ayurvedic industry as a resource for developing functional and eco-friendly products. By integrating sustainable practices into traditional medicine systems, the industry can reduce its environmental impact while creating economic and social value.

List of publications emanating from the thesis work

1. **Billu, A.,** Syamnath, V.L., Arun, K.B., Zahra, P.F., Anjusha, P., Kothakotta, A., Chen, Y.H., Ponnusamy, V.K., Nisha, P., (2023). Lignin-based nanomaterials for food and pharmaceutical applications: Recent trends and future outlook. *Science of The Total Environment*, p.163316. doi: 10.1016/j.scitotenv.2023.163316. *(This published review paper, is presented as Chapter 2B in this thesis).*
2. **Billu, A.,** Reshmitha, T. R., Navami, M. M., Liza George, Venugopal, V. V., Nisha, P. (2020). Phytochemical rich extract from the spent material generated from Industrial Dashamoola preparation (a medicinal Ayurvedic decoction) with antioxidant, antidiabetic and anti-inflammatory potential. *Industrial crops and products.* doi: 10.1016/j.indcrop.2020.112451. *(This published research paper is presented as Chapter 3 in this thesis).*
3. **Billu, A.,** Shakeela, H., Leena P, D., Arun, K. B., Vasanth, R., Brennan, C. S., Mantri, N., Adhikari, B., Nisha, P., (2024). Lignin Nanoparticles from Ayurvedic Industry Spent Materials: Applications in Pickering Emulsions for Curcumin and Vitamin D_3 Encapsulation. *Food Chemistry.* doi: 10.1016/j.foodchem.2024.140284. *(This published research paper is presented as Chapter 4 in this thesis).*
4. **Billu, A.,** Shakeela, H., Brennan, C. S., Mantri, N., Adhikari, B., Nisha, P. Nutrient-rich puffed snacks developed using blended flours and lignin Pickering emulsions containing curcumin and vitamin D_3. *RSC Sustainable Food Techology. (This published research paper is presented as Chapter 5 in this thesis).*
5. **Billu, A.,** Shakeela, H., Brennan, C. S., Mantri, N., Adhikari, B., Nisha, P. Cellulose and lignin nanoparticles from an Ayurvedic waste stream for essential oil-based active packaging to extend shelf life of perishable fruit. *International Journal of Biological Macromolecules. (This published research paper is presented as Chapter 6 in this thesis)*- Accepted.

List of manuscripts under revision: -

6. **Billu, A.,** Aziz, S., Brennan, C. S., Mantri, N., Adhikari, B., Nisha, P. Status and Prospects of Valorisation of Ayurvedic Spent Materials: Focus on Dashamoola By-products. *RSC Sustainable Food Technology***.** *(This review is presented as Chapter 2A in this thesis).*

List of publications not related to thesis

1. Shini, V. S., **Billu, A.,** Abhijith, S., & Nisha, P. 2024. Exploring the nutritional, physico chemical and hypoglycemic properties of green banana flours from unexploited banana cultivars of Southern India. *Sustainable Food Technology*. doi: 10.1039/d4fb00066h
2. Prabha, B., Krishnan, S. L., **Billu, A.,** Jayamurthy, P., & Radhakrishnan, K. V. 2024. An insight into the mechanistic role of (-)-Ampelopsin F from Vatica chinensis L. in inducing insulin secretion in pancreatic beta cells. *Bioorganic & Medicinal Chemistry*, 117695. doi: 10.1016/j.bmc.2024.117695.
3. Krishnan, G. V., **Billu, A.,** Lankalapalli, R. S., Bhaskaran Nair Saraswathy Amma, D. K., & Bhaskaran, K. (2024). Rice sheath blight disease control by native endophytic Bacillus subtilis from Kuttanad, a Globally Important Agricultural Heritage System. *New Zealand Journal of Botany*, 1-23. https://doi.org/10.1080/0028825X.2024.2394184
4. Navami MM., **Billu, A.,** Archana, H., & Nisha P., 2023. Nutritional profiling and quantitative analysis of amino acids and vitamins using LC-MS/MS in selected raw and germinated ancient grains. *Journal of the science of food and Agriculture Reports.* pp.343-404. doi: 10.1002/jsf2.141**.**
5. George, G., Shyni, G.L., Mohan, S., **Billu, A.,** Nisha, P., Ranjith, S., Rajankutty, K. and Raghu, K.G., 2023. In vitro and in vivo anti-inflammatory and anti-arthritic effect of Tinospora cordifolia via modulation of JAK/STAT pathway. *Inflammopharmacology*, pp.1-17. doi:10.1007/s10787-023-01155-7
6. Nidhina, K., **Billu, A**., Fontes-Candia, C., Martínez-Abad, A., Martínez-Sanz, M., Nisha, P., & López-Rubio, A. (2022). Physicochemical and functional properties of pectin extracted from the edible portions of jackfruit at different stages of maturity. *Journal of the Science of Food and Agriculture*. doi.org/10.1002/jsfa.12391
7. Poornima, M.S., Sindhu, G., **Billu, A.,** Sruthi, C.R., Nisha, P., Gogoi, P., Baishya, G. and Raghu, K.G., 2022. Pretreatment of hydroethanolic extract of Dillenia indica L. attenuates oleic acid induced NAFLD in HepG2 cells via modulating SIRT-1/p-LKB-1/AMPK, HMGCR & PPAR-α signaling pathways. *Journal of Ethnopharmacology*, p.115237. doi: 10.1016/j.jep.2022.115237
8. Arumugam, M., Udayan, A., Sabapathy, H., **Billu, A.,** 2021. Plant growth regulator triggered metabolomic profile leading to increased lipid accumulation in an edible marine microalga. *Journal of Applied Phycology*, *33*(3), pp.1353-1365. doi: 10.1007/s10811-021-02424-0**.**

9. George, G., Shyni, G.L., **Billu, A.,** Nisha, P. and Raghu, K.G., 2021. Downregulation of TLR4/MyD88/p38MAPK and JAK/STAT pathway in RAW 264.7 cells by Alpinia galanga reveals its beneficial effects in inflammation. *Journal of Ethnopharmacology*, *275*, p.114132. doi: 10.1016/j.jep.2021.114132.
10. Arun, K.B., Madhavan, A., **Billu, A.,** Balaji, M., Sivakumar, K.C., Nisha, P. and Kumar, A., (2020). Acetylation of isoniazid-a novel mechanism of isoniazid resistance in Mycobacterium tuberculosis. *Antimicrobial Agents and Chemotherapy*. doi: 10.1128/AAC.00456-20.
11. Heeba, S., Navami, M. M., **Billu, A**., Nayana, N., Nisha, P., 2020. Influence of coating material and processing parameters on acrylamide formation in potato patties and mitigation strategies. *International Journal of Food Engineering***.** doi: 10.1515/ijfe-2021-0337.
12. Nair, A., Basavaraja, D., **Billu, A.,** Nisha, P., Varughese, S., Purushothaman, J., Somappa, S.B., 2020. Advanced Glycation End-products (AGE) Trapping Agents: Design and Synthesis of Nature Inspired Indeno [2, 1-c] pyridinones. *Bioorganic Chemistry*, p.104375. doi: 10.1016/j.bioorg.2020.104375**.**
13. Makebe, Calister Wingang; Steve Carly, DESOBGO ZANGUE; Agwanande, Wilson Ambindei; **Billu A;** JONG Emmanuel, NSO; Nisha, P. 2020. Optimization of pectinase-assisted extraction of Annona muricata L. juice and the impact of liquefaction on the structure of pectin. *Journal of the science of food and Agriculture.* doi: 10.1002/jsfa.10600**.**
14. Arun, K.B., Dhanya, R., Chandran, J., **Billu, A.,** Sannya, S., Nisha, P. 2020. A comparative study to elucidate the biological activities of crude extracts from rice bran and wheat bran in cell line models. *Journal of Food Science and Technology*. doi: 10.1007/s13197-020-04353-1.

List of posters and orals presented

1. **Billu Abraham,** Nisha P, Nitin Mantri, Charles Brennan and Benu Adhikari. *Enhancing Nutritional Value: Development of Curcumin and Vitamin D_3-Enriched Extruded Snacks using a Sunflower Oil-Based Lignin-Stabilized Nano Pickering Emulsion.* Proceedings of Australasian American Oil Chemical Society (AAOCS) 2023 Conference – Future of Lipids: Health and Sustainability during 13th-15th November 2023, held on Newcastle, Australia (**Oral- AAOCS Student Travel Grant Award).**
2. **Billu Abraham**, Reshmitha T. R, Liza George, Venugopal V V and P. Nisha. *Antidiabetic and anti-inflammatory potential of phytochemicals from Dashamoola (a combination of the root of ten medicinal plants prescribed in Ayurveda) spent material generated from Ayurveda industry.* Proceedings of New Horizons in Biotechnology (NHBT) during 20th-24th November 2019, held on Thiruvananthapuram, Kerala **(Poster).**
3. **Billu Abraham.** Participated and made on online presentation in connection with Prof. Dr. A. Hisham Endowment Award 2021 contest held online at google meet platform on 11th September 2021 **(Oral)**.

Contributions to Academic Conferences

1. Enhancing nutritional value: Development of curcumin and vitamin D_3-enriched extruded snacks using a sunflower oil-based lignin-stabilized nano pickering emulsion

Billu Abraham[1,2,3]**,** *Nisha P*[*,1,2,3], Nitin Mantri[1], Charles Brennan[1] and Benu Adhikari*[*,1].

[1]Royal Melbourne Institute of Technology, Australia,
[2]Agro Processing and Technology Division,
CSIR-National Institute for Interdisciplinary Science and Technology, Council of Scientific and Industrial Research, Trivandrum, India-695019
[3]*Academy of Scientific and Innovative Research (AcSIR), New Delhi 110001, India*
** Corresponding authors: Email: pnisha@niist.res.in; Tel: +91 9846777133*
Email: benu.adhikari@rmit.edu.au; Tel: +61 3 992 59940

Abstract- This study aims to enhance food product nutrition to address the critical issue of micronutrient deficiencies affecting 2 billion people globally. It focuses on incorporating vital nutrients like curcumin and vitamin D_3 into extruded snacks by leveraging the solubility of these micronutrients in sunflower oil. However, due to the high temperatures prevailing in the extrusion processes, direct addition of these micronutrients is not possible; hence, we utilized lignin to stabilize a nano pickering emulsion before incorporating it into the snack formulation prior to the extrusion process. The lignin-stabilized emulsions (LSE) were produced through sonication and contained sunflower oil (10%), lignin (0.25%), vitamin D_3 (0.05%), and curcumin (0.05%). These LSEs were stable due to their small size (347 ± 0.7 nm) and high zeta potential (-42.62 ± 0.7 mV). Microscopic imaging revealed the Pickering nature of LSE. FTIR-ATR analysis confirmed the effective encapsulation of curcumin and vitamin D_3 in LSE. The effective encapsulation of curcumin in the LSE was further confirmed by the high yellowness index (131.26 ± 0.50) compared to Emulsion Without Lignin (EWL, 80.86 ± 0.04). Textural and sensory evaluation of LSE-incorporated snacks were similar to those snack samples that did not contain it. The HPLC analysis of LSE-incorporated snacks confirmed better encapsulation of curcumin (78.95 ± 0.5%) and vitamin D_3 (66.66 ± 0.6%) than in EWL (17.425 ± 0.2% curcumin, 8.185 ± 0.4% vitamin D_3). This research offers a promising pathway for the fortification of snack products with edible oil-soluble micronutrients and thus contributes to the global effort to combat micronutrient deficiencies (Billu A STOTEN 2023; 881:163316).

2. **Antidiabetic and anti-inflammatory potential of phytochemicals from Dashamoola (a combination of the root of ten medicinal plants prescribed in Ayurveda) spent material generated from Ayurveda industry**

Billu Abraham[1,2], T R Reshmitha[1,2], Liza George[1], V V Venugopalan[1], P Nisha[1,2]

[1]Agro Processing and Technology Division,

CSIR-National Institute for Interdisciplinary Science and Technology, Council of Scientific and Industrial Research, Trivandrum, India-695019

[2] Academy of Scientific and Innovative Research (AcSIR), New Delhi 110001, India

**Corresponding authors: P Nisha: Mobile: +91 9846777133*

Email: pnisha@niist.res.in, bp.nisha@yahoo.com

Abstract: Dashamoola (DA) is an age-old Ayurvedic formulation considered as the panacea for inflammation-related ailments. In DA preparations, water is used as the solvent and therefore, most of the time the active ingredients are not extracted out completely and remain in the spent material (DSM). In this study, initially, DSME was subjected to HPTLC analysis to check the presence of bioactive compounds and then compared with extracts of the fresh dashmoola (DE). TPC and TFC studies indicated the polyphenol and/or flavonoid-rich matrix. Subsequently, HPLC analysis of DSME confirmed the presence of polyphenols, especially flavonoids like myricetin (74.93±0.937 µg/mL). Antioxidant property of DSME was evaluated using DPPH (IC_{50} 68.17±0.184 µg/mL), ABTS (IC_{50} 17.8±1.03 µg/mL) and NO (IC_{50} 738±1.02 µg/mL) assays, which showed comparable IC_{50} values to that of the assay standards. The antidiabetic studies yielded promising results as inferred from α-amylase (IC_{50} 129.19±0.84 µg/mL) and α-glucosidase (IC_{50} 77.03±0.92 µg/mL) inhibition assays. The anti-inflammatory capability of DSME was evaluated using protein denaturation assay which showed an IC_{50} value of 61.17±0.004 µg/mL against 100.12±0.061 µg/mL that of Aspirin. DSME (IC_{50} of 60.8±0.003 µg/mL) closely contested with Aspirin (IC_{50} of 70.1±0.012 µg/mL) in proteinase inhibition assay. RAW 264.7 cells subjected to LPS-induced NO production further strengthens the scope of preliminary antioxidant results. Safety of DSME was established by MTT assay in L6 myoblast and RAW 264.7 cells with tolerability up to 500 µg/mL concentration. This study highlights the potential of DSME as a source of bioactives with immense nutraceutical/therapeutic properties.

3. Process for isolation of bioactives and development of ayurvedic nutraceutical food from Dashamoola spent material

Billu Abraham[1,2], P Nisha[1,2]

[1]Agro Processing and Technology Division,

CSIR-National Institute for Interdisciplinary Science and Technology, Council of Scientific and Industrial Research, Trivandrum, India-695019

[2] *Academy of Scientific and Innovative Research (AcSIR), New Delhi 110001, India*

**Corresponding authors: P Nisha: Mobile: +91 9846777133: Fax: + 91-471- 491712*

Email: pnisha@niist.res.in, bp.nisha@yahoo.com

Abstract: Dashamoola (combination of 10 medicinal plant roots) is a well-known ayurvedic arishtam used to improve the general health and immunity of an individual. In this study, we aim to evaluate the proximate composition and antioxidant potential of Dashamoola spent for the development of a value added product from ayurvedic waste. Dashamoola spent material was extracted in a soxhlet apparatus with 70% ethanol for 6 hours. The analysis of bioactive compounds presents in the freeze-dried spent extracts by phytochemical screening assays, antioxidant assays, chromatographic techniques such as HPTLC and HPLC. Proximate analysis showed that the carbohydrate content of spent was higher compare the moisture, protein, ash and fat. The phytochemical analysis showed that ethanolic extract of spent Dashamoola is rich in total phenolic and flavonoid content. Polyphenols were quantified using HPLC and confirmed by HPTLC. The antioxidant potential was assessed in terms of DPPH, ABTS and NO free radical scavenging activity.65.16% Crude fiber component is present in spent material. Dietary fibre from spent Dashamoola (IDF-85.36%, SDF-4.21%) was Isolated and quantified. Since spent dashamoola is rich in antioxidants and fibre, an attempt was made to develop a value added product - Dashamoola spent Squash and its quality parameters was estimated. The study thus, established the nutraceutical potential of the spent Dashamoola.

SCI PUBLICATION

Industrial Crops & Products 151 (2020) 112451

Contents lists available at ScienceDirect

Industrial Crops & Products

journal homepage: www.elsevier.com/locate/indcrop

Phytochemical rich extract from the spent material generated from Industrial Dashamoola preparation (a medicinal Ayurvedic decoction) with antioxidant, antidiabetic and anti-inflammatory potential

Billu Abraham[a,b], T R Reshmitha[a,b], M M Navami[a,b], Liza George[a], V V Venugopalan[a], P Nisha[a,b,*]

[a] Agro Processing and Technology Division, CSIR-National Institute for Interdisciplinary Science and Technology, Council of Scientific and Industrial Research, Trivandrum, 695019, India

[b] Academy of Scientific and Innovative Research (AcSIR), Ghaziabad, 201002, India

ARTICLE INFO

Keywords:
Dashamoola spent material
Phytochemical assay
Antioxidant activity
Antidiabetic activity
Anti-inflammatory activity

ABSTRACT

Dashamoola Arishta (DA), an age-old Ayurvedic formulation, is considered as panacea for inflammation-related ailments. As water is used as the solvent in DA preprations, the active ingredients are not extracted out completely and remain in the spent material (DSM). The phytochemicals extracted from DA and DSMDE using 70% (v/v) ethanol (DA & DSME respectively) were characterized using HPTLC which suggested retentsion of considerable amount of phytochemicals in DSME. Studies on the total phenolic and flavonoid content indicated polyphenol and/or flavonoid-rich matrix. LCMS/MS analysis of DSME confirmed the presence of polyphenols, especially shikimic acid (83.225 mg/g), gallic acid (51.261 mg/g), epicatechin (26.300 mg/g), naringenin (25.054 mg/g) and vanillic acid (14.147 mg/g). The antioxidant potential of DE and DSME evaluated in terms of DPPH (IC_{50} 98.19 & 68.17 μg/mL), ABTS (IC_{50} 44.2 & 17.8 μg/mL) and NO (IC_{50} 881 & 738 μg/mL) assays indicated better activity of DSME. DSME showed better antidiabetic potential as inferred from α-amylase and α-glucosidase inhibition assays. The anti-inflammatory capability of DSME was evaluated using protein denaturation assay which showed an IC_{50} value of 61.17 μg/mL against 95.04 & 100.12 μg/mL for DE and aspirin, resepctively. DSME (IC_{50} of 60.8 μg/mL) closely contested with aspirin (IC_{50} of 70.1 μg/mL) in the proteinase inhibition assay. RAW 264.7 cells subjected to LPS-induced NO production further strengthens the scope of preliminary antioxidant results. Safety of DSME was established by MTT assay in L6 myoblast and RAW 264.7 cells with tolerability reaching up to 500 μg/mL concentration. The present study indicate the potential of of DSM for further value addition, as a source of bioactives with immense nutraceutical/therapeutic properties.

1. Introduction

Ayurveda, an indigenous system of traditional medicine, is being practiced for over thousands of years. It generally focuses on plant-based medicines for the management of various diseases (Randive et al., 2014). Scientific validation of the traditional medicines are being attempted to trace clues regarding contributing factors in ameliorating debilitating disease conditions (Tungcharoen et al., 2018). Dashamoola is an ayurvedic polyherbal formulation prepared from ten different plant roots, in equal proportions, based on traditional Ayurvedic text 'Sahasrayogam'. The plants used in Dashamoola preparation are known to possess therapeutical potential against certain health ailments (Awasthi and Pandey (2015)) which include the roots of ten medicinal plans - five bigger plants called "Valiyapanchamoola" and five smaller plants called "Laghupanchamoola" as recorded in Ayurvedic texts (Vyas et al., 2011). Valiyapanchamoola is a combination of *Stereospermum suaveolens* (Patala) *Premna integrifolla* (Agnimantha), *Aegle marmelos* (Bilva/Indian Bael) *Gmelinaarborea* (Gamphari) and *Oroxylum indicum* (Shyonaka). Laghupanchamoola category includes *Desmodium gangeticum* (Shalaparni), *Uraria picta* (Prithakpami), *Solanum indicum* (Brihati root), *Solanum xanthocarpum* (Kanthakari) and *Tribulus terrestris* (Gokshura) (Nagarkar et al., 2013). All the plants in Dashmoola are endowed with medicinal properties, mainly anti-inflammatory, hypoglycemic, antihypertensive, vasodilator, analgesic, anti-cholestrolemic, antirheumatic, antioxidant and anti-fever (Nanda and Tiwari (2016)). In the above context, dashamoola plays a versatile role in the biological and pharmacological aspects (Rao and Savithramma (2011)). There are several products with "dashamoola" as the main ingredient as

* Corresponding author at: Agro Processing and Technology Division, CSIR-National Institute for Interdisciplinary Science and Technology, Council of Scientific and Industrial Research, Trivandrum, 695019, India.
E-mail addresses: pnisha@niist.res.in, bp.nisha@yahoo.com (P. Nisha).

https://doi.org/10.1016/j.indcrop.2020.112451
Received 30 January 2020; Received in revised form 28 March 2020; Accepted 6 April 2020

described in Ayurvedic classics (Karunagoda et al., 2010; Irshad et al., 2009). The need for dashamoola in the market is on the rise because of its utility in preparing various formulations (Nagarkar and Jagtap (2017); Sudhanshu et al., 2012).

Most of the Ayurvedic preparations use water as solvent, and therefore, the active ingredients are not extracted out completely. Therefore, a major part of the phytochemicals with potential biological activity may be retained in the spent material. Similar studies conducted on spent cumin (Arun et al., 2018) and black pepper (Prabhu et al., 2015) revealed the potential for value addition of Ayurvedic spent materials as a rich source of bioactives for further formulions in the form of functional foods and nutraceuticals.

Utilization of spent materials generated from Ayurveda industries have got great relevance as the availability of plant materials are getting diminished due to the high demand for the medicinal plants in various preparations and also due to the threat of extinction. The Ayurvedic industries are investigating possibilities for preserving the medicinal plants by various means. One such activity includes the utilization of spent materials for further value addition. In this context, spent materials generated from Ayurveda industries are investigated and found to possess promising biological activities (Arun et al., 2018). Some of the plants used in Dashamoola are becoming extinct, and therefore, the re-utilization of the spent materials for the ayurvedic/nutraceutical preparations, if found potential, could be of high relevance. The medicinal plants in the 'Dashamoola' are reported to possess antioxidant, anti-inflammatory and hypoglycemic action (Nanda and Tiwari (2016)). As Ayurvedic medicine preparations employ water-based decoctions of medicinal plants and other ingredients (Dashamoola in the present study), the spent materials (DS in the present study) may retain a major part of the bioactive phytochemicals. Based on this hypothesis, the objectives of the present study is to compare the phytochemical content of DS with that of fresh dashamoola extract and to evaluate its antioxidant, antidiabetic and anti-inflammatory potential. From this study, we expect to gain valuable information about the compounds that are retained in the spent materials and their potential in encompassing inflammation and diabetes.

2. Materials and methods

2.1. Chemicals and Plant material

2,2'-azino-bis(3-ethylbenzothiazoline-6-sulphonic acid) (ABTS), 2,2-diphenyl-1-picrylhydrazyl (DPPH), α-glucosidase, α-amylase, acarbose, trolox, ascorbic acid polyphenol standards, dulbecco's modified eagle's media (DMEM), fetal bovine serum (FBS), horse serum, rosiglitazone, 4-nitrophenyl α-D-glucopyranoside, 3-(4,5-dime thylthiazol-2-yl)-2,5-diphenyl tetrazolium bromide (MTT), gallic acid, dimethyl sulfoxide (DMSO), lipopolysaccharides(LPS), dexamethasone, aspirin, trypsin, casein, perchloric acid, Griess reagent were procured from Sigma Aldrich Chemicals (St. Louis, MO, USA). Folin–Ciocalteu reagent, sodium chloride (NaCl), ethylene diamine tetraacetic acid (EDTA), sodium carbonate (Na_2CO_3), tris-HCl, potassium hydroxide (KOH) were obtained from MERK. Trypsin-EDTA, antibiotic-antimycotic were purchased from Gibco Invitrogen (Carlsbad, CA, USA). 2-NBDG (2-(N-(7-nitrobenz-2-oxa-1,3-diazol-4-yl) amino)-2-deoxyglucose) was procured from Molecular Probe (Invitrogen Life Technologies, Carlsbad, CA, USA). All the reagents used were of high-quality analytical grade.

Fresh Dashamoola raw materials in the proportion as used for the Ayurveda preparations and corresponding spent Dashamoola materials were supplied by M/s. Kottakkal Arya Vaidyasala, Kottakkal, Kerala, India (M/s. AVS Kottakkal Ltd).

2.2. Proximate Composition and mineral analysis of Dashamoola Spent Materials (DSM)

Initially, moisture content (AOAC, 1990 method 930.15) of the oven-dried (105 °C) DSM was estimated in triplicates. For this, dried samples were allowed to cool in a desiccator before weighing. Weighed samples used for the estimation of ash content (AOAC, 1990 method 923.03) were heated (550 °C) in a muffle furnace with for 16 h. Micro-Kjeldahl method furnished protein content in the samples by converting resultant nitrogen to protein (multiplying by 6.25). Fat content was determined By using the soxhlet extraction method (AOAC, 1990 method 920.39) and the total carbohydrate content was calculated based on the difference method.

2.3. Preparation of the extracts

The dried raw and spent sample powder (40-60 mesh size) were extracted with 70% ethanol by hot extraction method using soxhlet apparatus lasting 6 hours. The extracts were filtered and then concentrated using a rotary evaporator (Heidolph, Germany). The concentrate was then lyophilized (VirTis Genesis, USA) and stored at −4 °C until use the lyophilized samples were then subjected to various analysis as described below.

2.4. High-Performance Thin Layer Chromatography (HPTLC)

The 70 % ethanolic extract of 1 g Fresh Dashamoola (DE) and 1 g spent Dashamoola (DSME) (10 mL) was dissolved in 10 mL of methanol. Pre-activated HPTLC Silica gel 60 F_{254} plates (10 × 10 cm; Merck, Darmstadt, Germany) was employed to perform chromatography. Then, the plates were submitted to densitometric scanning on a CAMAG scanner III at 490 nm. Using an automatic applicator in HPTLC (Linomat-V with N_2 flow, CAMAG Repostar 3, Switzerland), extracts were applied 8 mm above one end of each plate forming 6 mm wide bands. Before commencing chromatography, the plates were subjected to an activation process involving methanolic prewashing (60 °C for 5 minutes). Scanning speed of 40 mm s^{-1} and slit size of 5 × 0.45 mm were ensured for the analysis that utilized a mobile phase constituting Toluene: Ethyl acetate: Formic acid: Methanol (7:5:1:0.5). Plates were developed on a twin glass chamber (10 × 10 cm) filled with the mobile phase. Plates were then air-dried, derivatized, and then heated to 105 °C for 5 min. Derivatization of chromatogram makes use of the Camag glass reagent spray (5% sulfuric acid in methanol). After 30 minutes, plates were observed using Camag UV cabinet at 254 and 366 nm (Kumar et al., 2015).

2.5. Fourier transform infrared spectrum (FTIR)

FTIR spectroscopy was used for characterizing the functional groups of phytochemicals present in DE and DSME. The spectra were recorded using the Bruker FT-IR (Germany) spectrometer in the wavenumber range between 4000 to 400 cm^{-1}.

2.6. Phytochemical analysis of Spent Dashamoola

2.6.1. Determination of Total Phenolic Content (TPC)

Estimation of Phenolic content in DSME was done using Folin-Ciocalteau reagent with gallic acid (1-1000 µg/mL) serving as standard (Singleton and Rossi (1965)). Reaction mixtures containing 100-500 µL of DSME and Folin–Ciocalteu reagent (0.5 mL) mixed with 20% sodium carbonate were incubated for 90 minutes at 760 nm on a Shimadzu ultraviolet-visible 2600 (UV) spectrophotometer (Kyoto, Japan). The volume of the reaction mixtures were made up with distilled water. Gallic acid equivalent (mg/100 g) of DSME was plotted and the resulting standard curve was used for the quantification of polyphenols.

2.6.2. Determination of Total Flavonoid Content (TFC)

Flavonoid content in DSME was estimated by aluminum chloride method (Chang et al., 2002). Initially, varying concentrations of quercetin (20-100 µg) and DSME (100–500 µL) were prepared. To the samples, 0.3 mL of aluminium chloride (10%), sodium nitrite (5%) and 2 mL NaOH were added. The final volume (10 mL) of the reaction mixtures were attained by adding distilled water. After the reaction, absorbance of each sample was read at 510 nm using a spectrophotometer (Shimadzu ultraviolet-visible 2600 (UV) spectrophotometer (Kyoto, Japan).

2.7. Chemical profiling and quantification using LCMS/MS

The quantitative analysis of 28 compounds – catechol, catechin, quinine, naringenin, tocopherol, gallic acid, chlorogenic acid, epicatechin, syringic acid, vanillic acid, caffeic acid, epigallocatechin, ferulic acid, myricetin, quercetin, p-Coumaric acid, luteolin, apigenin, kaempferol, rutin, diadzein, hesperetin, shikimic acid, ellagic acid, morin, genistein, cinnamic acid and chrysin were performed by LC-MS/MS system (Nexera with LCMS-8045, Shimadzu Corporation, Kyoto, Japan) - HPLC (Nexera LC-30AD) equipped with an autosampler (SIL-30AC), temperature-controlled column oven (CTO-20AC) and prominence diode array detector (SPD-M20A) coupled to triple quadrupole mass spectrometer (Nexera with LCMS-8045, Shimadzu Corporation, Kyoto, Japan). Working standards were prepared by diluting the stock solution with water concentration ranging from 0.01- 1 µg/ml. The quantification of all the polyphenols was carried out on Shimadzu Shim-pack GISS C18 column (150 X 2.1 mm i.d, 1.9 µm) that used water / formic acid (100/0.1%) mobile phase for solvent A and 100 % methanol for solvent B. Polyphenols were eluted with a linear gradient system as follows: 0.5 – 1.9 min 5% of solvent B, 2.0 – 10.0 min 98% of solvent B, 10.1 – 15 min 98% of solvent B and 15.1 – 17 min 5% of solvent B, a flow rate of 0.3 mL/min, the injection volume was 10 µl and oven temperature of 40 °C. Positive and negative modes of multiple reaction-monitoring (MRM) mode were operated during LC-MS/MS with electrospray ionization (ESI). LC-MS/MS data were collected and processed by Lab Solutions software (Shimadzu, Kyoto, Japan). An interface temperature of 400 °C was conditioned for ionization, desolvation line temperature of 300 °C, heat block temperature of 400 °C, nebulizing gas flow (nitrogen) at 3 L/min and drying gas flow (nitrogen) at 10 L/min. Each calibration solution was analyzed in triplicate, and the average value of the results was used as the representative for each point. The results obtained are represented as polyphenols in µg/g with SD (n = 3). The values are statistically significant as F > F critical one-tail. Therefore the variances of the two populations are unequal. The analytical performance of the LC-MS/MS method is given in Table 1.

2.8. Antioxidant analysis of Dashamoola Spent Material

2.8.1. 2,2-diphenyl-1-picrylhydrazyl (DPPH) Radical Scavenging Activity

DPPH scavenging activity of DSME was estimated using a 130 mM DPPH solution. The reaction was allowed to take place between 2.5 mL of DPPH and 500 µL of DE / DSME (10 – 250 µg/mL) and ascorbic acid (1 – 10 µg/mL) (Brand-Williams et al., 1995). Following this, the mixture was vortexed and incubated in the dark for 90 minutes at 33 °C. The absorbance of the assay mixture was read at 517 nm using UV/VIS spectrophotometer 2600 (Shimadzu, Japan) at 517 nm. The following equation was used to calculate IC_{50} (µg/mL) values.

$$\%\,Inhibition = \frac{Absorbance\ ofControl - Absorbance\ of\ Sample}{Absorbance\ of\ Control} \times 100$$

2.8.2. 2, 2'-azino-bis (3-ethylbenzothiazoline-6-sulphonic acid) (ABTS) assay

ABTS assay uses radical cations prepared from 2 mM (0.0548 g in 50 ml) ABTS dissolved in distilled water (Re et al., 1999). Apart from ABTS, potassium persulfate 70 mM (0.0189 g in 1 mL) was also prepared. A reaction mixture containing 200 µL of potassium persulfate and 50 mL of ABTS were prepared and used post 2 hours of mixing. Solutions of DE and DSME were prepared at varying concentrations (1 – 100 µg/mL) by adding 0.3 mL of ABTS radical cation and 1.7 mL phosphate buffer (pH 7.4). Trolox (1 – 10 µg/mL) was used as positive control for the assay Absorbance was read at 734 nm, with triplicate values recorded for DE, DSME and Trolox.

Inhibition (%) = 100 x $(A_0\text{-}A_1)/A_0$

Where absorbance of the control and DE/DSME /standard are A_0 and A_1, respectively. IC_{50} values were determined from the curve obtained by plotting % inhibition and concentration. The IC_{50} value is indirectly proportional to antioxidant capacity.

2.8.3. Nitric oxide (NO) radical scavenging assay

Nitric oxide radical scavenging assay revolves around the production of nitrite ions and the subsequent spectrophotometric measurement of the resulting chromophore at 546 nm (Govindarajan et al., 2003). At physiological pH, nitric oxide gets released from sodium nitroprusside, which further reacts with oxygen to form nitrite ions. In the presence of nitric oxide scavengers, nitrite ion production plummets as these scavengers competitively use up the oxygen levels. Greiss reagent (1% sulphanilamide, 2% O-phosphoric acid and 0.1% of N-(1- naphthyl) ethylenediamine dihydrochloride) is used to estimate the nitrite ion concentration. Approximately 1 mL of sodium nitroprusside (5 mM) was mixed with varying concentrations of DE and DSME (200-1000 µg/ml) in phosphate buffer (pH 7.4, 0.1 M), followed by incubation at 25 °C for 2 h. Post incubation, 1.5 mL of Greiss reagent was added after the removal of the same volume of the reaction mixture. The resulting chromophore is formed in two steps- diazotization and coupling with Greiss reagent components. The absorbance of DE, DSME, ascorbic acid (10 – 500 µg/mL) and control tubes was measured at 546 nm after the formation of chromophores.

2.9. Antidiabetic assay of Dashamoola spent material

2.9.1. α -amylase inhibition assay

The assay method described by Xiao (Xiao et al., 2006) depends on the starch-iodine test for assessing α-amylase enzyme inhibition. The most active methanolic extract form was selected for the assay. Initially, varying concentrations of DE and DSME (50 – 250 µg/mL) extracts were added to the mixture followed by the addition of 0.02 M sodium phosphate buffer (pH 6.9) and 6 mM NaCl. 1 U/mL of porcine pancreatic α-amylase was added to all the mixtures which was then incubated at 50 °C for 30 min post addition of soluble starch (1% w/v). Finally, iodine reagent (5 mM I_2 and 5 mM KI) was added prior to stopping the reaction using 1 M HCl. Absorbance of the samples was read at 580 nm on a multiplate reader (Synergy 4 Biotek multiplate reader, USA). Wells without any extract was used as control and a known amylase inhibitor, Acarbose (1 – 25 µg/mL) was used as the positive control. The percentage of amylase enzyme inhibition was calculated using the following equation.

$$\%\,Inhibition = \frac{Absorbance\ ofControl - Absorbance\ of\ Sample}{Absorbance\ of\ Control} \times 100$$

2.9.2. α - glucosidase inhibition assay

α-glucosidase assay followed in this study is based on the procedure of Adisakwattana (Adisakwattana et al., 2004), with slight modifications. This assay aims at estimating the IC_{50} values of samples spectrophotometrically. Initially, 200 µL of DE and DSME (50 – 250 µg/mL) were premixed with 20 µL of α -glucosidase (1.25 U/mL) and was incubated at RT for 5 min. The extracts were dissolved in 50 mM potassium phosphate buffer (pH 6.8) before premixing. To the samples, 200 µL of 50 mM phosphate-buffered 4-nitrophenyl α-D-

Table 1
The analytical performance of the LC–MS/MS method of 28 compounds.

Compounds	R_t (min)	Parent ion (m/z)	Molecular Ion (m/z)	Ion Mode	CE (V)	Calibration equation	r^2	Linear Range (μg/L)	DL/QL (μg/L)
1. Catechol (PA)	1.87	111.20	78.95/64.10	+ve	−9/-25	y = 387.253x + 7.0483e + 006	0.986	5-50	0.07/0.23
2. Catechin (F)	6.75	291.20	139.10/165.05	+ve	−15/-13	y = 10393.1x-16953.5	0.993	5-150	2.20/6.68
3. Quinine (A)	6.88	325.20	307.10/184.05	+ve	−24/-28	y = 70839.3x + 3503.38	0.996	5-150	0.27/0.81
4. Naringenin (F)	7.28	273.20	153.05/147.15	+ve	−17/-21	y = 5753.24x-13117.0	0.992	5-150	0.78/2.37
5. Tocopherol (V)	12.87	429.50	163.15/205.05	+ve	−22/-23	y = 12257.5x-27446.3	0.993	5-150	2.31/7.01
6. Gallic acid (PA)	1.91	169.20	125.05/81.00	-ve	17/17	y = 2779.60x + 1214.12	0.992	5-150	3.20/9.70
7. Chlorogenic acid (PA)	6.81	353.00	191.20/92.90	-ve	16/43	y = 10282.0x + 16136.9	0.997	5-150	1.27/3.85
8. Epicatechin (F)	6.77	289.00	245.20/205.20	-ve	14/16	y = 2231.57x-3359.76	0.993	5-150	7.08/21.46
9. Syringic acid (PA)	7.20	197.20	182.20/123.05	-ve	14/24	y = 941.096x + 12146.4	0.996	5-150	10.44/31.65
10. Vanillic acid (PA)	6.79	167.20	152.10/108.10	-ve	17/19	y = 8887.775x + 2823.33	0.991	5-150	14.35/43.48
11. Caffeic acid (PA)	6.91	179.20	135.15/134.10	-ve	16/30	y = 31106.3x-2363.27	0.995	5-150	0.49/1.49
12. Epigallocatechin (F)	2.01	456.90	169.15/125.05	-ve	17/40	y = 904.191x-524.176	0.987	5-50	2.90/8.79
13. Ferulic acid (PA)	7.36	193.20	134.00/178.00	-ve	15/10	y = 2014.91x + 171906	0.992	5-50	4.37/13.23
14. Myricetin (F)	7.65	317.00	151.20/179.20	-ve	25/19	y = 15064.0x-14109.0	0.995	5-150	0.25/0.75
15. Quercetin (F)	7.92	301.20	151.05/179.00	-ve	22/18	y = 48446.6x + 52582.0	0.991	5-150	0.62/1.88
16. p-Coumaric acid (PA)	7.34	163.00	119.15/93.10	-ve	15/33	y = 12379.7x + 41113.6	0.992	5-150	2.13/6.46
17. Luteolin (F)	7.92	285.20	151.10/175.05	-ve	25/25	y = 29060.1x + 177101	0.991	5-150	0.27/0.83
18. Apigenin (F)	8.18	269.20	149.05/151.00	-ve	23/25	y = 26104.3x-13101.5	0.993	5-150	0.48/1.45
19. Kaempferol (F)	7.83	285.20	159.15/187.05	-ve	31/27	y = 1243.29x-487.739	0.993	5-150	1.44/4.36
20. Rutin (F)	7.34	609.20	300.00/301.15	-ve	38/34	y = 25186.6x + 9234.48	0.995	5-150	0.08/0.23
21. Diadzein (F)	7.91	252.90	208.20/224.15	-ve	29/25	y = 8324.16x-13781.5	0.981	5-150	0.71/2.16
22. Hesperetin (F)	7.86	301.20	164.10/286.05	-ve	25/18	y = 17857.8x-14187.8	0.993	5-150	0.57/1.73
23. Shikimic acid (PA)	1.76	172.90	111.20	-ve	11	y = 864.091x + 63809.9	0.969	5-150	5.79/17.55
24. Ellagic acid (PA)	7.56	300.90	185.10/145.20	-ve	31/40	y = 648.613x + 9964.71	0.992	5-150	2.28/6.92
25. Morin (F)	7.74	301.20	151.00/149.15	-ve	20/25	y = 49085.8x + 113300	0.994	5-150	0.59/1.79
26. Genistein (F)	7.81	269.20	133.20/132.05	-ve	31/46	y = 11955.6x-6477.21	0.990	5-150	0.59/1.79
27. Cinnamic acid (PA)	7.93	147.00	103.05	-ve	13	y = 628.783x + 1513.72	0.993	5-150	6.60/20.01
28. Chrysin (F)	8.39	252.90	62.95/143.20	-ve	32/27	y = 20464.6x-17508.2	0.996	5-150	0.41/1.26

PA – Phenolic acid, A- Alkaloid, F- Flavonoid, V- Vitamin
Rt – Retention time, DL- Detection Limit, QL- Quantitation Limit

glucopyranoside (1 mM) was added to initiate the reaction and incubated the reaction mixture for 20-minutes at room temperature. The addition of 500 μL of 1 M Na_2CO_3, terminates the reaction leaving a final volume of 1.5 mL in the reaction tubes. Quantity of p-nitrophenol released during the reaction was determined by reading samples at 405 nm using a microplate reader (BioTek Instruments Inc. Winooski, VT). Concentrations ranging from 10 – 100 μg/mL was used for acarbose (positive control). Glucosidase activity (IC_{50} values) of the extract was calculated based on the triplicate values obtained during spectrophotometric analysis.

$$\%\,Inhibition = \frac{Absorbance\ ofControl - Absorbance\ of\ Sample}{Absorbance\ of\ Control} \times 100$$

2.9.3. Glucose uptake assay

2.9.3.1. Cell culture conditions. L6 myoblast was obtained from NCCS, Pune, India. L6 Myoblasts were nurtured in Dulbecco's modified eagle's medium (DMEM) containing 10% fetal bovine serum (FBS) and 1% antibiotic-antimycotic solution. A humidified ambience (37 °C, 5% CO_2) was set up for the growth of the cells.The cells were seeded at a density of 1×10^3 cells/well on 24 well-plates and 96-well black plates (BD Biosciences, Franklin Lakes, NJ, United States) for different assays.

2.9.3.2. Cell viability assay. The cellular toxicity of DSME on L6 cells was determined by the MTT assay (Mosmann (1983)). The cells were seeded and cultured in 96 well plate for 24 h and then the cells were incubated with various concentrations of DSME (10 – 500 μg/mL) containing complete DMEM medium for 24 h. After incubation, 100 μL of MTT (0.5 mg/mL) was added to all wells and kept at dark for 4 h. After discarding the MTT medium, 200 μL of DMSO was added to solubilize the formed formazan by shaking. Then, the absorbance was measured at 570 nm using the microplate reader (Synergy4 Biotek multiplate reader, USA). The untreated cells were used as control.

2.9.3.3. Glucose uptake assay. Glucose uptake assay was done in differentiated L6 myoblast cell line as described by Chen (Chen et al., 2010) with minor modifications. Cells were seeded in 96-black well plates and allowed to differentiate into myotubes as described above. The assays were performed at 70% cell confluency, the cells were washed with phosphate-buffered saline (PBS), and treated with DSME extract at two different concentrations 50 μg/mL and 100 μg/mL in low glucose media for 24 hrs. After incubation, cells were incubated with 2-NBDG in PBS at 37 °C for 30 min. Cells were then incubated and subjected to washing with phosphate buffer (pH 7.4), and observed under confocal microscopy (Pathway 855, BD Bioscience, USA).

2.10. Anti-inflammatory activity of Spent Dashamoola

2.10.1. Inhibition of albumin denaturation

Anti-inflammatory activity of DE and DSME extract was determined using inhibition of albumin denaturation assay with minor modification (Mizushima and Kobayashi (1968) and Sakat et al., 2010). Different concentrations of DE and DSME (10 – 250 μg/mL) and 1% bovine albumin was mixed, and the pH of the mixture was adjusted using 1 N HCl. The Reaction mixture was incubated for 20 min at 37 °C, and then temperature increased to 60 °C for 30 min. After incubation, the samples were cooled and turbidity was read at 660 nm using a microplate reader (Synergy4 Biotek multiplate reader, USA). Reaction mixture without samples was used as control and aspirin (10 – 250 μg/mL) was used as standard. Experiments were done in triplicates. Percentage inhibition of protein denaturation was determined using the following equation:

Percentage inhibition = (Abs Control – Abs Sample) X 100/ Abs control

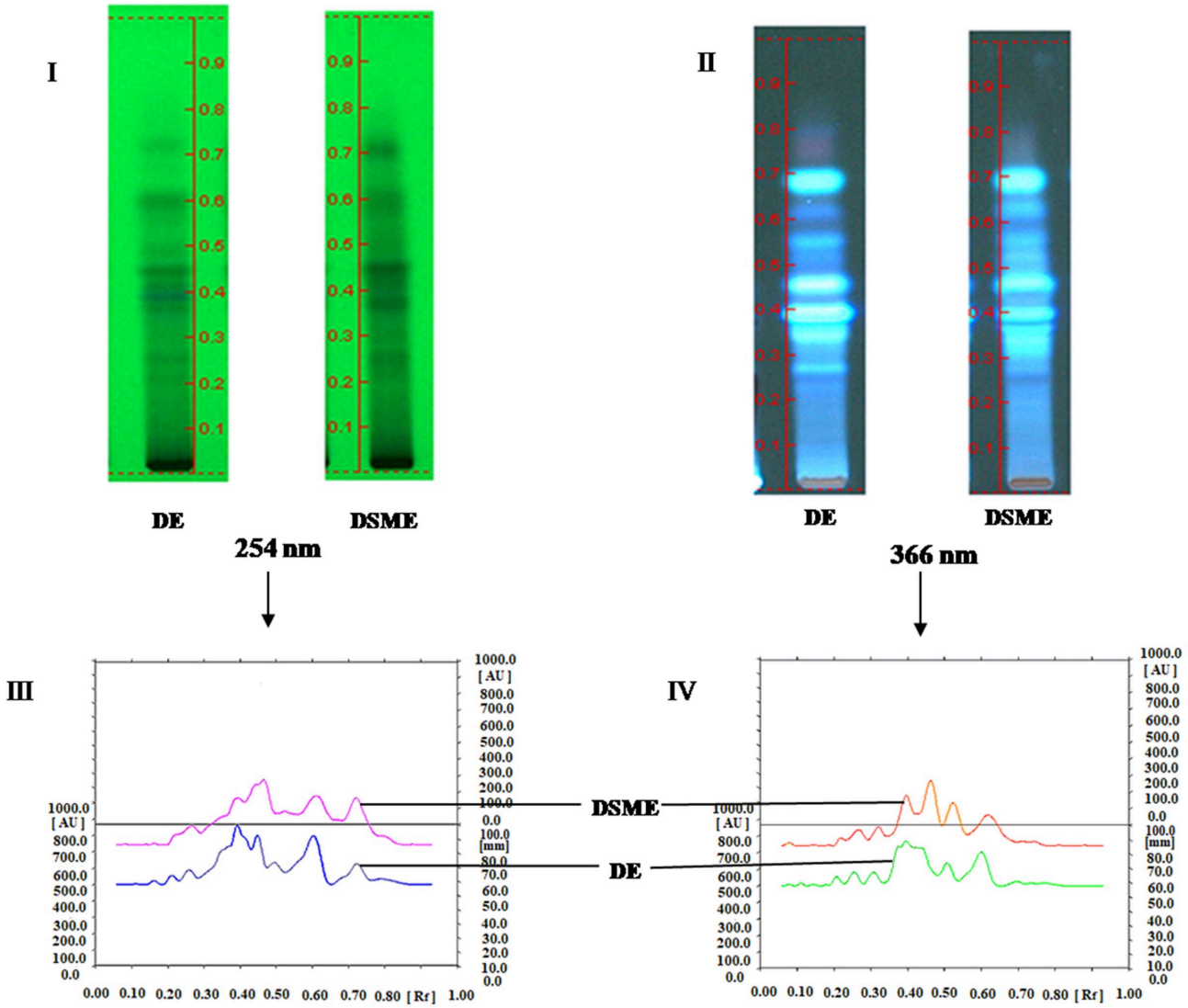

Fig. 1. TLC Plate views (I and II) and the corresponding HPTL chromatograms (III and IV) of DE, DSME at 254 and 366 nm.

2.10.2. Inhibition of antiproteinase action

The antiproteinase test was performed according to Oyedepo and Sakat with slight modification (Oyedepo and Femurewa (1995) and Sakat et al., 2010). The reaction mixture with 0.06 mg trypsin, 20 mM Tris HCl buffer (pH 7.4), and different concentrations (10 – 250 µg/ml) of DE / DSME and aspirin (10 – 250 µg/mL) was incubated for 5 min at 37 °C. Then, 0.8 % (w/v) casein was added to the mixture and incubated for 20 min to arrest the reaction. After incubation, 70% perchloric acid was added to the reaction mixture. Absorbance of the supernanant from the resulting cloudy suspension was read at 210 nm using multiplate reader (Synergy4 Biotek multiplate reader, USA) against buffer as blank and samples without extract as control. The experiments were done individually in triplicates. Percentage inhibition of proteinase inhibitory activity was determined using the equation below.

Percentage inhibition = (Abs control –Abs sample) X100/ Abs control

2.10.3. Nitric oxide inhibition assay

2.10.3.1. Cell culture conditions and cell viability. RAW 264.7 cells were procured from ATCC (American Type Culture Collection, Manassas, United States). The cells were maintained in the same way as described under 2.9.3.1. The cell viability was estimated using the MTT assay as per the protocol given under 2.9.3.2

2.10.3.2. Nitric oxide inhibition assay. NO released from immune cells was evaluated in the cultured supernatant media (Green et al., 1982). After pretreatment of DSME extract for 2 h, LPS (lipopolysaccharide, 5 µg/mL) was added to all the wells except that of the negative control. After 24 h incubation, all the treated cells in the culture media (100 µL) underwent treatment with 0.1 mL Griess reagent (1% sulfanilamide, 0.1% naphthylethylene diamine in 2.5% phosphoric acid solution) at ambient temperature for 10 min. The reaction mixture in the 96 well plates were then read at 540 nm using multiplate reader (Synergy4 Biotek multiplate reader, USA). Results were then calibrated using absorbance values obtained from dexamethasone standard.

2.11. Statistical analysis

Experimental data provided are mean ± SD (standard deviation) derived from triplicate measurements of values recorded from respective assays. All the data were then subjected Duncan's multiple range tests which is used to assess the significance of mean differences obtained during the initial one-way analysis of variance (ANOVA) using SPSS, standard version7.5.1 (SPSS Inc., USA) and the significance was

accepted at $p \leq 0.05$.

3. Results and discussion

3.1. Proximate analysis of DSM

Proximate analysis of Dashamoola Spent Material (DSM) serves to assess the macronutrient content in it. The proximate composition of DSM were, moisture content - 8.68 ± 0.070%; ash content 3.62 ± 0.049%; fat content 0.90 ± 0.007%; crude protein content: 3.34 ± 0.028% and carbohydrate content: 83.46 ± 0.431%. Thus carbohydrates turned out to be the major macronutrient in DSM.

3.2. Comparative evaluation of phytochemicals in DE and DSME by HPTLC

Preliminary evaluation of the phytochemical content of DE and DSME by HPTLC was performed to confirm the retention of bioactive compounds in the spent materials. First glimpse into the distribution pattern of bioactive compounds among DE and DSME was obtained through HPTLC. It is evident from the fluorescence behavior that DSME is enriched with phenolic compounds (Stanek and Jasicka-Misiak (2018)). HPTLC fingerprint yielded similar banding pattern and graphs for DE and DSME (Fig. 1). Interestingly, highest area (AU) was recorded by DSME (89874.8). Similar R_f values in DE and DSME indicates the presence of shared bioactive compounds in DSME which were retained even after industrial arishta preparation process (Table 2).

3.3. Fourier transform infrared spectroscopy (FTIR)

FTIR spectra of DE and DSME are depicted in Fig. 2. Presence of phenolic compounds and alcohols has created a broad band at 3334 cm^{-1} owing to the vibratory stretching of the − OH group. Peak formation at 1031 cm^{-1} is from the carboxylic acid carbonyl (C = O) groups contributed by the phenolics. Additionally, −CH bending vibrations (1450 − 1317 cm^{-1}), C − C stretching vibrations (1612 cm^{-1}) and aliphatic − CH stretching (2936 cm^{-1}) were also recorded (Karattu Veedu et al., 2019). Interestingly DSME was able to retain most of the functional groups from DE.

These striking similarities in HPTLC and FTIR analysis lead to further investigation of DSME using phytochemical assays and LC-MS/MS and other bioactive assays.

3.4. Determination of Total Phenolic Content (TPC) and Total Flavonoid Content (TFC) in DSME extract

Total phenolic content (TPC) was determined with gallic acid (1 mg/ml) as standard. A calibration curve was obtained that provided a linear equation, using which the phenolic content in DSME was calculated. Phenolic concentration in DSME (143.032 ± 5.0432 mg GAE/g dry weight) clearly suggested its potent antioxidant activity. Quercetin standard (1 mg/ml) was used to determine the total flavonoid content in DSME. The linear equation derived from the standard calibration plot was employed for the assessment of total flavonoids in the extract. Flavonoid content in the sample was estimated to be 62.92 ± 0.981 mg QE/g dry weight.

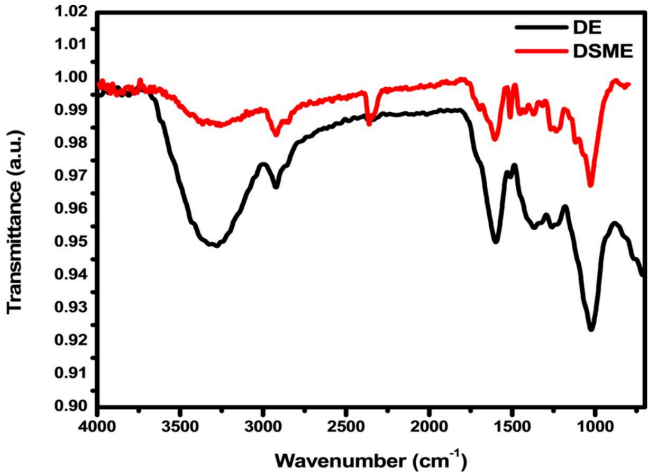

Fig. 2. FTIR spectra of Dashamoola raw extract (DE) & Dashamoola Spent Material Extract (DSME).

The total phenolic content of residue from bacaba fruit (Barros et al., 2017), spent coffee (Marina Ramón-Gonçalves et al., 2019) and spent cumin (Arun et al., 2018) was reported to be 0.11 GAE/g, 15.38 GAE/g, 9–29 mg GAE/g and 1.20 mg GAE/g, respectively. The flavonoid content bacaba fruit residue was 0.086 QE/g, coffee spent 11–27 mg QE/g DW, and spent cumin 3.10 mg QE/g DW. Compare to these reports, DSME possesses much higher phytochemicals.

3.5. Profiling and quantification of compounds using LC-MS/MS

A comparative LCMS/MS profiling of DE and DSME clearly suggest that DSME possess more phytochmeicals (Figs. 3). The corresponding chromatograms of the standard compounds, DSME and DE are given in supplementary Fig. 1, Fig. 2 and Fig. 3, respectively. These bioactive compounds are known for their effectiveness in curbing reactive oxidative species (ROS), diabetis, inflammation, cancer, and so on. Shikimic acid (83.225 mg/g) was found to be the most abundant one followed by gallic acid (51.261 mg/g), epicatechin (26.300 mg/g), naringenin (25.054 mg/g) and vanillic acid (14.147 mg/g) indicates the phytochemical richness of DSME in ameliorating disease conditions. Shikimic acid is the key ingredient of the oseltamivir phosphate, the drug used to treat human influenza (WHO, 1980) and alsos reported to possesses vital neuroprotective capability alongside a key role in preventing blood clots (M Estevez and J Estevez (2012)). Anticancer, herbicidal and antimicrobial role of shikimic acid makes it the starting material for the synthesis of the drugs (Cuellar et al., 2015) which is

Table 2
HPTLC data of DE and DSME at 254 nm.

DE				DSME			
Peak no.	R_f Value	Area (AU)	% Area	Peak no.	R_f Value	Area (AU)	% Area
1	0.16	374.2	0.61	1	-	-	-
2	0.21	1162.1	1.88	2	-	-	-
3	0.26	2532.5	4.10	3	0.27	5578.6	6.21
4	0.39	22992.6	37.26	4	0.39	17912.9	19.93
5	0.45	7651.4	12.40	5	0.46	22175.3	24.67
6	0.49	4536.5	7.36	6	0.52	9149.0	10.18
7	0.60	15380.6	24.93	7	0.61	18826.4	20.95
8	0.72	5356.3	8.68	8	0.72	14673.3	16.32
9	0.79	1717.2	2.78	9	0.79	1559.3	1.74
Total		61703.4	100%			89874.8	100%

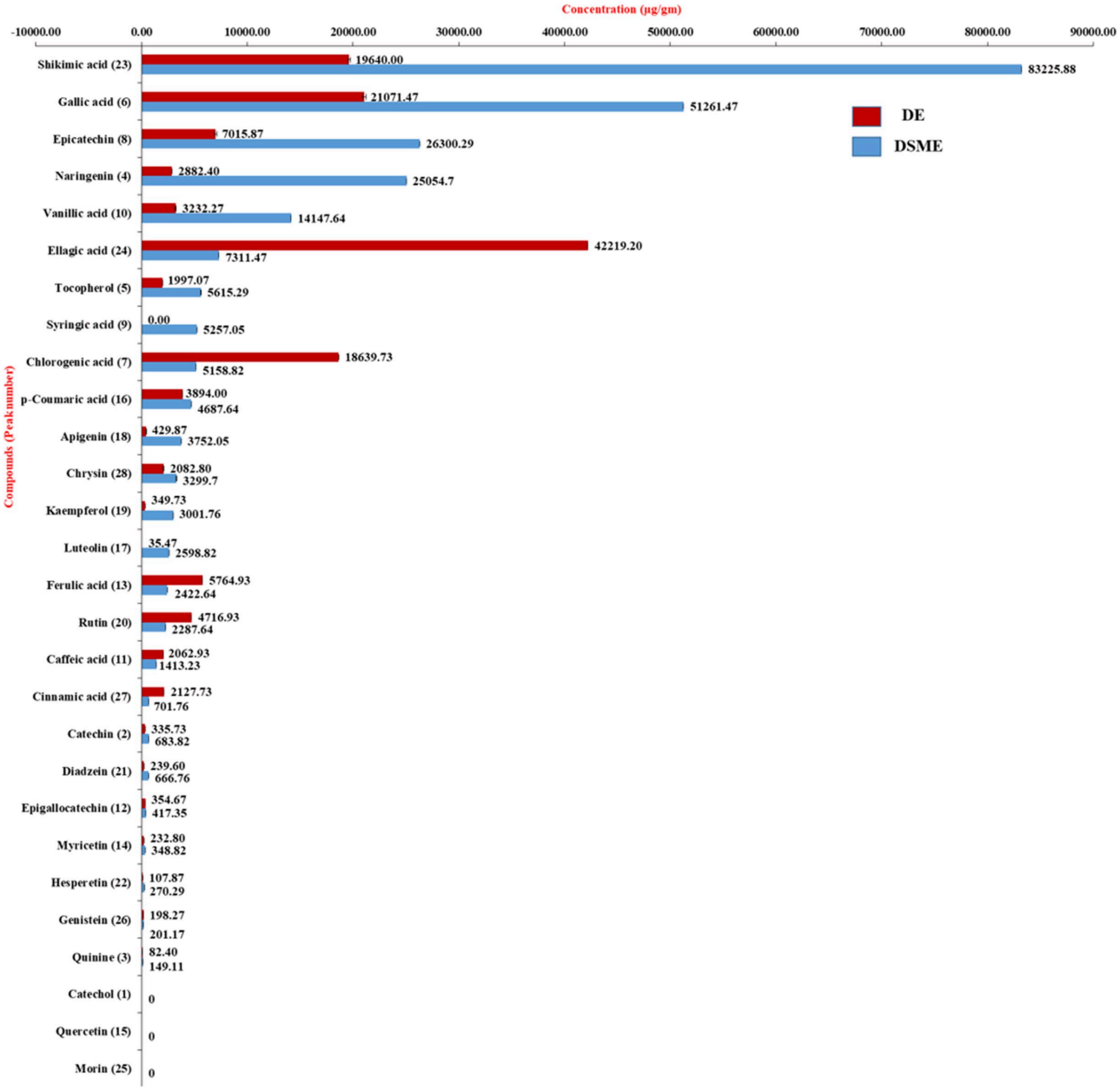

Fig. 3. LCMS/MS analysis of compounds in DE & DSME.

directly isolated from the plant source (Hao et al., 2015). Gallic acid ((3,4,5-trihydroxybenzoic acid) and chlorogenic acid (5.158 mg/g) have the ability to fight viral and microbial infections (Sorrentino et al., 2018) alongside stabilizing obesity and hypertension by affecting lipid metabolism (Naveed et al., 2018). Gallic acid is a potent bile stimulator with profound antioxidant efficacy (Anand et al., 1997), anticancerous (Asci et al., 2017; Ho et al., 2010; Yoshioka et al., 2000, Nam et al., 2016; Madlener et al., 2007), hepatoprotective (Jadon et al. (2007)). Antioxidant properties of gallic acid are leveraged for the natural color enhancement of fruit-based beverages (Navruz et al., 2016; Roidoung et al., 2016) and as an oxidation barrier in double emulsions (Silva et al., 2018). Studies based on epicatechin shed insight into improved insulin sensitivity and evading hyper and hypoglycemia in human test groups (Cremonini et al., 2019). By inhibiting NF-KB production (Fraga and Oteiza (2011)) and by exerting various protective actions on the gastrointestinal tract, epicatechin delivers direct benefit for the smooth functioning of the body (Oteiza et al., 2018). Naringenin is indeed a very interesting flavanone carrying a spectrum of biological activity ranging from anti-inflammatory, fibrosis and even neoplasm (Du et al., 2009; Zeng et al., 2018). Even though lesser in quantity when compared to other polyphenols, ellagic acid (7.311 mg/g), tocopherol (5.615 mg/g), syringic acid (5.257 mg/g), p-Coumaric acid (4.687 mg/g), apigenin (3.752 mg/g), chrysin (3.299 mg/g) were also identified and quantified. The trend followed by HPTLC was also observable in LCMS/MS results as the quantity of some of the detected compounds were more pronounced in DE (Fig. 3). The reason for this behavior could be attributed to the fact that 70% ethanol system used for extraction was efficient in leaching out compounds of varying polarities along with physical properties of the compounds, source of the plant materials used, etc. (Chekroun-Bechlaghem et al., 2019; Dehghan et al., 2016). Scientific investigations suggest that these polyphenols possess higher antioxidant capability (Guitard et al., 2016; Kilic et al., 2014; Lesjak et al., 2018; Hodgson et al., 2004; Kyriakis et al., 2015). From the LCMS/MS data, it can be inferred that DSME houses much promising biologically active of phenolic and flavonoid compounds as compared to some of the spent materials already reported (Marina Ramón-Gonçalves et al.,

Table 3
Antioxidant, anti-diabetic and anti-inflammation activity of DE and DSME.

Sample	Antioxidant Assays			Antidiabetic Assays		Anti-inflammatory Assays	
	DPPH (IC_{50} - μg/mL)	ABTS (IC_{50} - μg/mL)	NO (IC_{50} - μg/mL)	α-amylase (IC_{50} - μg/mL)	α-glucosidase (IC_{50} - μg/mL)	Albumin denaturation Inhibition (IC_{50} - μg/mL)	Proteinase Inhibition (IC_{50} - μg/mL)
Standard	Gallic acid	Trolox	Ascorbic acid	Acarbose	Acarbose	Aspirin	Aspirin
	2.3 ± 0.09	2.8 ± 0.32	238 ± 1.13	6.27 ± 0.92	54.67 ± 1.32	100.12 ± 0.061	70.1 ± 0.012
DE	98.19 ± 1.11	44.2 ± 0.98	881 ± 1.67	154.07 ± 1.57	102.91 ± 0.24	95.04 ± 0.019	78.6 ± 0.015
DSME	68.17 ± 1.54*	17.8 ± 1.03[a]	738 ± 1.02[a]	129.19 ± 0.84[a]	77.03 ± 0.92[a]	61.17 ± 0.004[a]	60.8 ± 0.003[a]

[a] Each value represents mean ± SD (standard deviation) from triplicate measurements. DSME significantly different from DE; (p value ≤0.05).

2019; Arun et al., 2018). Therefore, we explored the antioxidant activities of the extract further, by in vitro biochemical analysis. Therefore, we explored the antioxidant activities of the extract by in vitro biochemical analysis.

3.6. Evaluation of antioxidant efficiency

The degree of scavenging (expressed as IC_{50} value) of free radicals formed during various antioxidant assays is employed to assess the efficiency of a sample in curbing biological oxidation stress in vitro (Frankel and Meyer (2000)). The IC_{50} value (Table 3) of DE and DSME against DPPH free radical was found to be 98.19 ± 1.11, 68.17 ± 1.54 μg/mL, and that of standard gallic acid was 2.3 ± 0.09 μg/mL. ABTS assay is yet another tool that measures the extent of antioxidant capacity by trapping $ABTS^{+}$ free radicals. The results are expressed as TEAC value (Trolox equivalent antioxidant capacity) in comparison with the standard Trolox. TEAC of the sample is the concentration equivalent of extract to that of the activity shown by Trolox. TEAC values for 50% reduction in free radicals were 44.2 ± 0.98, 17.8 ± 1.03 and 2.8 ± 0.32 μg/ml for DE, DSME and Trolox, respectively. Nitric oxide (NO) production in the body is under the strict regulatory control of various biomolecules including hormones and cytokines. Although NO plays a vital role in maintaining cellular homeostasis, the overproduction of NO can be deleterious to physiological stability. NO can be viewed as markers of inflammation when expressed for a long period. In addition to inflammation, NO is also seen elevated in patients suffering from cancer, Parkinson's disease (PD), arthritis, and diabetes, (Zou et al., 2002). NO scavenging activity of methanolic extract of DE and DSME was 881 ± 1.67, 738 ± 1.02 μg/ml, respectively. The standard Vitamin C exhibited an IC_{50} value of 238 ± 1.13 μg/ml (Table 3).

3.7. In vitro antidiabetic assay

α-amylase found in the saliva and pancreatic juice is a hydrolizing enzyme that cleaves alpha 1, 4 glucosidic bonds in starch, thereby exposing the resulting oligosaccharides for the final conversion to glucose, leading to elevated blood glucose level (Hanhineva et al., 2010). On the other hand, α-glucosidases found in the intestinal cells aid absorption by catalyzing undigested carbohydrates to monosaccharides (Kim et al., 2010). Therefore, inhibitors of α-glucosidases and α-amylase are responsible for the lowering of postprandial blood sugar levels by delaying the availability of the respective enzymes. Hence, the antidiabetic potential of DE and DMSE was evaluated in terms of inhibition of the action of digestive enzymes. The α-amylase inhibition of DE and DSME recorded IC_{50} values of 154.07 ± 1.57 and 129.19 ± 0.84 μg/mL, respectively, whereas that of acarbose was 6.27 ± 0.92 μg/mL (Table 3). The IC_{50} values of DE and DSME in α -glucosidase inhibition assay were 102.91 ± 0.24 and 54.67 ± 1.32 μg/mL, respectively, while that of the standard (acarbose) was 77.03 ± 0.92 μg/mL (Table 3). It can be seen that DSME demonstrated superior activity over DE in all the test assays. This striking inhibitory potential of both the extract can be explained based on the molecular structure of the bioactive compounds present. Polyphenols and flavonoids are made of glycoside linkages, whose presence and structural variations cause enzyme inhibition (Wang et al., 2018). Plant extracts with high antioxidant potential have shown strong antidiabetic capacity during in vitro tests involving α-amylase and α-glucosidase enzymes (Sobeh et al., 2017; Sekhon-Loodu and Rupasinghe (2019)). Synergistic effect of bioactive compounds present in the samples including cholorogenic acid, caffeic acid, etc may be responsible for the activities of the extract (Chiou et al., 2017; Aras et al., 2019).

3.8. Glucose uptake assay

The role of skeletal muscle in rendering glucose homeostasis and oxidation is well documented (Engeli et al., 2012). Increasing the uptake of glucose by skeletal muscle cells has been one of the important targets for anti-diabetes therapy (Arha (2017)). It is known that glucose uptake mediated by the upregulation and expression of GLUT4 found in adipose tissue is key to an increase in sensitivity to insulin. In the case of type 2 diabetes, the cells including skeletal muscle cells fail to uptake glucose, creating an imbalance in the glucose homeostasis that leads to the onset of hyperglycemia. As DSME exhibited significant anti-diabetic properties, as established in the preliminary screening, it prompted us to carry out further studies to assess its efficacy in inducing glucose uptake in L6 myoblast.

Cytotoxicity effect of DSME on cell growth and survival was studied using the MTT assay. L6 myoblast cell lines were able to tolerate up to 500 μg/mL DSME while maintaining desirable cell viability of above 70% (Fig. 4). These results indicated that DSME extract did not cause any cytotoxicity in cells in vitro. Therefore, concentrations of DSME below this level (50 μg/mL and 100 μg/mL) were selected for the cellular experiments.

Glucose uptake efficacy of DSME was tested in glucose fluorescent analog, 2-NBDG (10 mM) L6 myoblast aided by confocal imaging Fig. 5 shows increased 2-NBDG uptake as evidenced by the increased fluorescent intensity in participant cells. However, the activity was less than the metformin, a standard drug used as the positive control, as can be noted from the higher fluorescent intensity under identical experimental conditions. As can be seen, the treatment of cells with DSME induced cellular uptake of 2-NBDG, indicating its intervention in diabetes management, presumably by GLUT4 translocation process.

3.9. In vitro anti-inflammatory assay

The anti-inflammatory activity of DSME was assessed in terms of inhibition of albumin denaturation, antiproteinase action, and NO production by RAW 264.7 cells.

3.9.1. Albumin denaturation inhibition by DSME extract

Protein denaturation is a process in which proteins lose their structural conformation due to external stress or any substances, such as strong base or acid or heat. When denatured, most of the proteins lose their biological function. Denaturation of proteins is known to be the main cause of inflammation (Mizushima and Kobayashi (1968) and Sakat et al., 2010). As a part of the examination of the mechanism of the anti-inflammatory activity of DE and DSME, its ability to inhibit protein

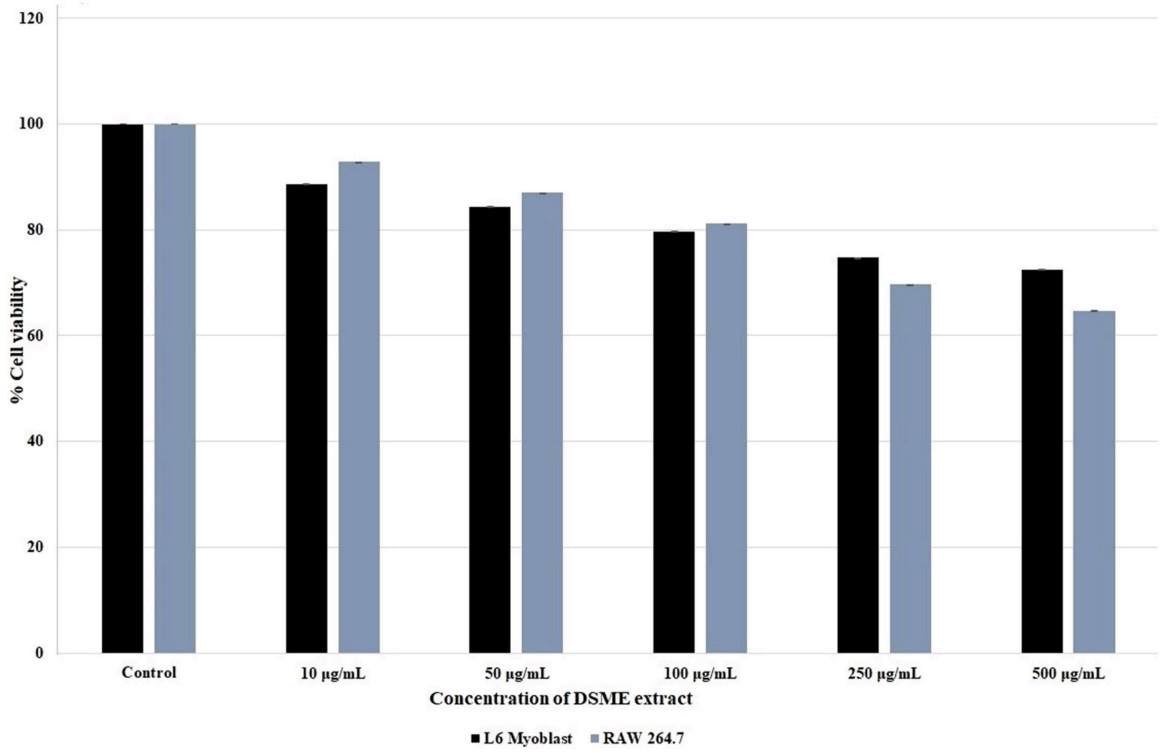

Fig. 4. The effect of DSME extract on L6 myoblast and RAW 264.7 cells viability by MTT assay (The data represents mean ± SD of three independent experiment).

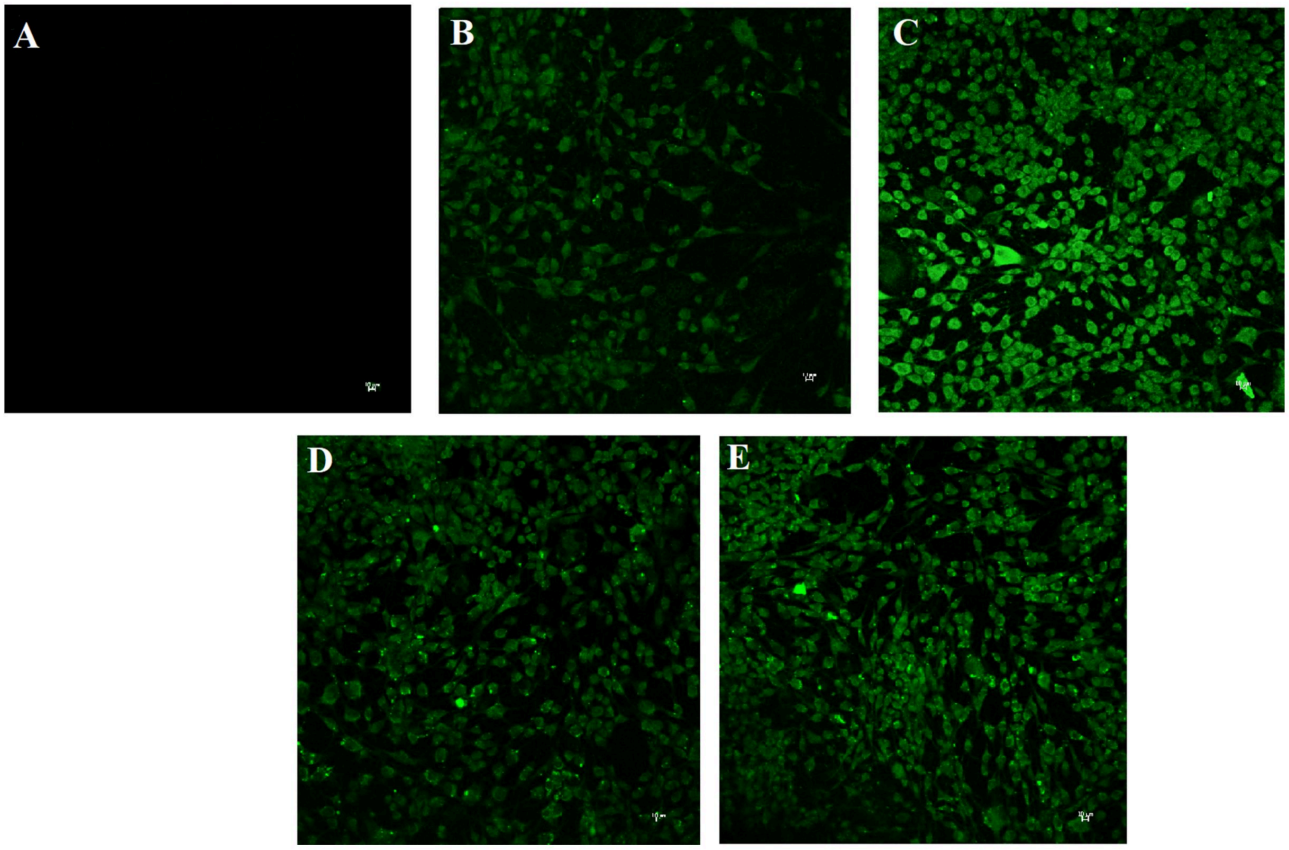

Fig. 5. Glucose uptake (2-NBDG) in L6 myoblast cells was observed under confocal microscopy (BD Falcon). Images A to E depicts A- Blank, B- control, C- Metformin, D- 50 µg/mL DSME, E- 100 µg/mL DSME.

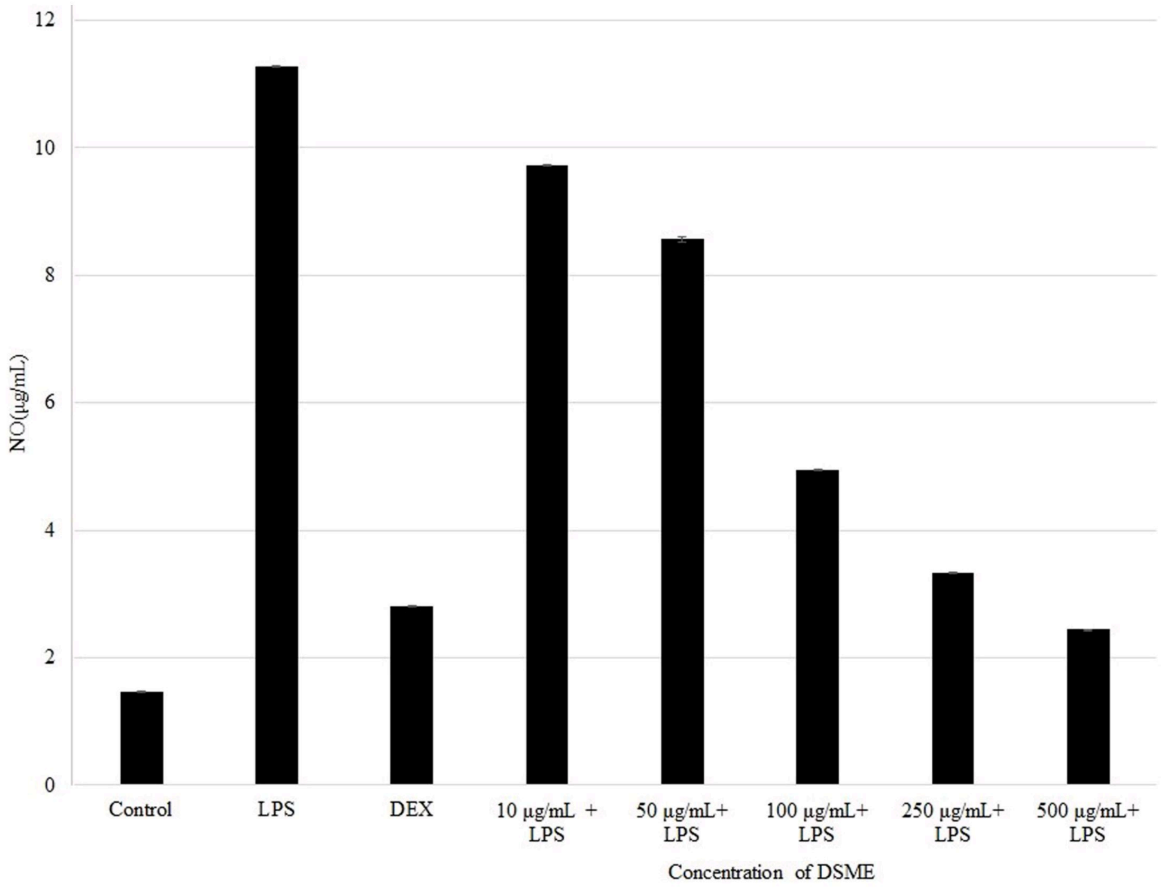

Fig. 6. NO Production inhibition assay by Griess reagent.

denaturation was studied. The results suggest that DSME extract was effective in inhibiting heat-induced albumin denaturation. DE and DSME demonstrated IC_{50} values of 95.04 ± 0.019 and 61.17 ± 0.004 µg/mL respectively against inhibition of protein denaturation that was much better than aspirin (100.12 ± 0.061 µg/mL), the standard anti-inflammation drug (Table 3). Thus, DSME resulted in higher inhibition when compared to DE and aspirin.

3.9.2. Proteinase inhibition by DSME extract

Proteinase enzymes (proteinases) have been associated with arthritic reactions. Neutrophils are known to be a rich source of proteinase and are confined inside cellular components like lysosomes. It was reported that the proteinase secreted by leukocytes plays an important role in the development of tissue damage during inflammatory reactions and a significant level of defense was provided by proteinase inhibitors. According to Das and Chatterjee (1995), a significant level of protection was provided by proteinase inhibitors. The IC_{50} value of DSME in anti-proteinase assay demonstrated 60.8 ± 0.003 µg/mL inhibitory activity whereas that of aspirin was 70.1 ± 0.012 µg/mL (Table 3). DE on the otherhand inhibited proteinase activity in a compatitive manner (IC_{50} 78.6 ± 0.015 µg/mL) but with less effectiveness than aspirin and DSME. DSME exhibited the highest anti-proteinase activity among all the test groups. The presence of bioactives in DSME might have contributed to their anti-inflammatory activity.

The cytotoxicity of the DSME on RAW 264.7 cells indicated cell viability above 70% on treatment of the cells with DSME at a concentration up to 500 µg/mL, and therefore, concentrations of DSME below this level (50 µg/mL and 100 µg/mL) were selected for other cellular experiments. DSME was also able to establish potent anti-inflammatory activity against LPS-induced NO formation in RAW 264.7 cell line (at 10–500 µg/mL concentrations) by significantly lowering nitrite concentration in nitrite estimation assay (Fig. 2).

3.9.3. Effect of DSME on NO production by RAW 264.7 cells

Estimation of inhibited NO produced by RAW 264.7 cells was carried out using Griess reagent. Cellular anti-inflammatory capability is reflected in the lowering of NO production post antigenic challenge. Unstimulated cells were found to produce fewer NO when compared to LPS treated (5 µg/mL) RAW 264.7 macrophage cells. Effectiveness of DSME extract (10–500 µg/mL) in neutralizing LPS-induced NO generation can be drawn from the results obtained in vitro (Fig. 6). At 500 µg/mL, it can be clearly seen that DSME was able to retard NO production in a concentration-dependent manner and exhibited an activity superior to the dexamethasone which served as the positive control. Evidence from this assay proves the potency of DSME in combating inflammation. There are instances in which ethanolic extract with high NO scavenging activity exhibited superior anti-inflammatory potential by impacting transcription factors leading to inhibition of cytokine production (Junior et al., 2020). Individual herbs that constitute Dashamoola were reported to have anti-inflammatory, antipyretic, analgesic properties, supported by various studies. Individual anti-inflammation contributions from *Uraria picta* root (Kale et al., 2012) and *Solanum indicum* Linn. fruits (Deb et al., 2014) have been documented in separate studies. Synergistic effects of the retained, flavonoids and phenolic acids in DSME could have attributed to the observed beneficial effects in vitro.

4. Conclusion

The study confirmed the retention of bioactive phytochmeicals in the spent dashamoola material. The HPTLC and LCMS/ms analysis of the DSME revealed the presence of phytochemicals wih immense

biological potential. Further studies on the antioxidant activities suggested promising activity which was better than the fresh extract itself. DSME demonsrated potential antidiabetic and anti-inflammatory capabilities in vitro. Retention of residual phytochemical in DSME with confirmed biological activity caters to the needs of several food, nutraceutical and pharmaceutical industries. If proven in vivo, the spent materilas from the related industries could be utilized for the further value addition e.g. development of nutraceutical products or active ingredeint isolation. Combating material loss is essential to any industry, especially when the spent material is presumed to have health benefits. Further in vivo studies are warranted to confirm the biological activities so that the DSM can be further explored for the re-use for ayurvedic formulations.

Authors contribution

B-A, TR-R, performed the experiments and data analysis. B-A, TR-R, and P-N wrote the manuscript. B-A, L-G, VV-V and P-N conceived and designed the study. P-N supervised the whole experimental work. B-A and P-N wrote and revised the manuscript.

Declaration of Competing Interest

The authors declare that they have no known competing financial interests or personal relationships that could have appeared to influence the work reported in this paper.

Acknowledgments

Authors are extremely grateful to Mr. Rajesh S Mony and Mr. Harikrishnan from M/s. Arya Vaidya Sala, Kottakkal (AVS: Kerala, India), for the technical support in identifying the thrust areas for value addition of the processed waste, and for providingthe spent materials.

References

Adisakwattana, S., Sookkongwaree, K., Roengsumran, S., Petsom, A., Ngamrojnavanich, N., Chavasiri, W., Yibchok-Anun, S., 2004. Structure activity relationships of trans-cinnamic acid derivatives on R-glucosidase inhibition. Bioorg. Med. Chem. Lett. 14, 2893–2896. https://doi.org/10.1016/j.bmcl.2004.03.037.

Anand, K.K., Singh, B., Saxena, A.K., Chandan, B.K., Gupta, V.N., Bhardwaj, V., 1997. 3, 4, 5-trihydroxy benzoic acid (gallic acid), the hepatoprotective principle in the fruits ofterminalia belerica-bioassay guided activity. Pharmacological Research 36 (4), 315–321. https://doi.org/10.1006/phrs.1997.0236.

Aras, A., Bursal, E., Türkan, F., Tohma, H., Kılıç, Ö., Gülçin, İ., Köksal, E., 2019. Phytochemical Content, Antidiabetic, Anticholinergic, and Antioxidant Activities of Endemic Lecokia cretica Extracts. Chemistry & biodiversity 16 (10), e1900341. https://doi.org/10.1002/cbdv.201900341.

Arha, G., 2017. Reducing Wait Time Prediction in Hospital Emergency Room: Lean Analysis Using a Random Forest Model.

Arun, K.B., Chandran, J., Venugopal, V.V., Madhavankutty, T.S., Nisha, P., 2018. Spent cumin seeds generated from ayurvedic industry as a source of bioactive compounds for nutraceutical/functional food applications. J. Food Process. Preserv. 42 (1), 3392. https://doi.org/10.1111/jfpp.13392.

Asci, H., Ozmen, O., Ellidag, H.Y., Aydin, B., Bas, E., Yilmaz, N., 2017. The impact of gallic acid on the methotrexate-induced kidney damage in rats. journal of food and drug analysis. Journal of Food and Drug Analysis 25 (4), 890–897. https://doi.org/10.1016/j.jfda.2017.05.001.

Association of Official Analytical Chemistry (AOAC), 1990. Official Methods of Analysis, 15th ed. Association of Official Analytical Chemists, Gaithersburg, MD, USA.

Awasthi, H.H., Pandey, A.K., 2015. Use of Dashamoola in Cervical Spondylosis: Past and Present Perspective. J. AYUSH. 4 (1), 10–16.

Barros, R.G.C., Andrade, J.K.S., Denadai, M., Nunes, M.L., Narain, N., 2017. Evaluation of bioactive compounds potential and antioxidant activity in some Brazilian exotic fruit residues. Food Res. Int. 102, 84–92. https://doi.org/10.1016/j.foodres.2017.09.082.

Brand-Williams, W., Cuvelier, M.E., Berset, C.L.W.T., 1995. Use of a free radical method to evaluate antioxidant activity. LWT-Food Sci. Technol. 28 (1), 25–30. https://doi.org/10.1016/S0023-6438(95)80008-5.

Chang, C.C., Yang, M.H., Wen, H.M., Chern, J.C., 2002. Estimation of total flavonoid content in propolis by two complementary colorimetric methods. J. Food Drug Anal. 10 (3).

Chekroun-Bechlaghem, N., Belyagoubi-Benhammou, N., Belyagoubi, L., Gismondi, A., Nanni, V., Di Marco, G., Atik Bekkara, F., 2019. Phytochemical analysis and antioxidant activity of Tamarix africana, Arthrocnemum macrostachyum and Suaeda fruticosa, three halophyte species from Algeria. Plant Biosystems-An International Journal Dealing with all Aspects of Plant Biology 153 (6), 843–852. https://doi.org/10.1080/11263504.2018.1555191.

Chen, Q.C., Zhang, W.Y., Jin, W., Lee, I.S., Min, B.S., Jung, H.J., Bae, K., 2010. Flavonoids and isoflavonoids from Sophorae Flos improve glucose uptake in vitro. Planta Med. 76 (1), 79–81. https://doi.org/10.1055/s-0029-1185944.

Chiou, S.Y., Sung, J.M., Huang, P.W., Lin, S.D., 2017. Antioxidant, antidiabetic, and antihypertensive properties of Echinacea purpurea flower extract and caffeic acid derivatives using in vitro models. Journal of medicinal food 20 (2), 171–179. https://doi.org/10.1089/jmf.2016.3790.

Cremonini, E., Fraga, C.G., Oteiza, P.I., 2019. (–)-Epicatechin in the control of glucose homeostasis: Involvement of redox-regulated mechanisms. Free Radical Biology and Medicine. 130, 478–488. https://doi.org/10.1016/j.freeradbiomed.2018.11.010.

Cuellar, M.A., Quiñones, N., Vera, V., Salas, C.O., Estévez, J.C., Estévez, R.J., 2015. Preliminary Studies on the Synthesis of (–)-Shikimic Acid Based 1, 2, 3, 4-Tetrahydrobenzo [b] phenanthridine-7, 12-diones. Synlett 26 (04), 552–556. https://doi.org/10.1055/s-0034-1379948.

Das, S.N., Chatterjee, S., 1995. Long term toxicity study of ART-400. Indian Indg Med. 16 (2), 117–123.

Deb, P.K., Ghosh, R., Chakraverty, R., Debnath, R., Das, L., Bhakta, T., 2014. Phytochemical and Pharmacological Evaluation of Fruits of Solanum indicum Linn. Int. J. Pharm. Sci. Rev. Res. 25 (2), 28–32.

Dehghan, H., Sarrafi, Y., Salehi, P., 2016. Antioxidant and antidiabetic activities of 11 herbal plants from Hyrcania region. Iran. journal of food and drug analysis 24 (1), 179–188. https://doi.org/10.1016/j.jfda.2015.06.010.

Du, G., Jin, L., Han, X., Song, Z., Zhang, H., Liang, W., 2009. Naringenin: a potential immunomodulator for inhibiting lung fibrosis and metastasis. Cancer research 69 (7), 3205–3212. https://doi.org/10.1158/0008-5472.

Engeli, S., Birkenfeld, A.L., Badin, P.M., Bourlier, V., Louche, K., Viguerie, N., Thalamas, C., Montastier, E., Larrouy, D., Harant, I., Glisezinski, I., 2012. Natriuretic peptides enhance the oxidative capacity of human skeletal muscle. J. Clin. Invest. 122 (12), 4675–4679. https://doi.org/10.1172/JCI64526.

Fraga, C.G., Oteiza, P.I., 2011. Dietary flavonoids: role of (−)-epicatechin and related procyanidins in cell signaling. Free Radical Biology and Medicine. 51 (4), 813–823. https://doi.org/10.1016/j.freeradbiomed.2011.06.002.

Frankel, E.N., Meyer, A.S., 2000. The problems of using one-dimensional methods to evaluate multifunctional food and biological antioxidants. J. Sci. Food Agric. 80 (13), 1925–1941. https://doi.org/10.1002/1097-0010(200010)80:13<1925.

Govindarajan, R., Rastogi, S., Vijayakumar, M., Shirwaikar, A., Rawat, A.K.S., Mehrotra, S., Pushpangadan, P., 2003. Studies on the antioxidant activities of Desmodium gangeticum. Biol. Pharm Bull. 26 (10), 1424–1427. https://doi.org/10.1248/bpb.26.1424.

Green, L.C., Wagner, D.A., Glogowski, J., 1982. Analysis of nitrate, nitrite, and [15N] nitrate in biological fluids. Anal Biochem 126, 131–138. https://doi.org/10.1016/0003-2697(82)90118-x.

Guitard, R., Paul, J.F., Nardello-Rataj, V., Aubry, J.M., 2016. Myricetin, rosmarinic and carnosic acids as superior natural antioxidant alternatives to α-tocopherol for the preservation of omega-3 oils. Food Chem. 21, 284–295. https://doi.org/10.1016/j.foodchem.2016.06.038.

Hanhineva, K., Törrönen, R., Bondia-Pons, I., Pekkinen, J., Kolehmainen, M., Mykkänen, H., Poutanen, K., 2010. Impact of dietary polyphenols on carbohydrate metabolism. Int. J. Mol. Sci. 11 (4), 1365–1402. https://doi.org/10.3390/ijms11041365.

Hao, X., Wu, X., Shen, G., Wen, L., Li, H., Huang, Q., 2015. Thermodynamic models for determination of the solubility of (-)-shikimic acid in different pure solvents and in (H2O + ethanol) binary solvent mixtures. The Journal of Chemical Thermodynamics. 88, 8–14. https://doi.org/10.1016/j.jct.2015.04.009.

Ho, H.H., Chang, C.S., Ho, W.C., Liao, S.Y., Wu, C.H., Wang, C.J., 2010. Anti-metastasis effects of gallic acid on gastric cancer cells involves inhibition of NF-κB activity and downregulation of PI3K/AKT/small GTPase signals. Food Chem. Toxicol. 48 (8-9), 2508–2516. https://doi.org/10.1016/j.fct.2010.06.024.

Hodgson, J.M., Chan, S.Y., Puddey, I.B., Devine, A., Wattanapenpaiboon, N., Wahlqvist, M.L., Lukito, W., Burke, V., Ward, N.C., Prince, R.L., Croft, K.D., 2004. Phenolic acid metabolites as biomarkers for tea-and coffee-derived polyphenol exposure in human subjects. Br. J. Nutr. 91 (2), 301–305. https://doi.org/10.1079/BJN20031046.

Irshad, S., Singh, J., Kakkar, P., Mehrotra, S., 2009. Molecular characterization of Desmodium species - An important ingredient of 'Dashmoola' by RAPD analysis. Fitoterapia 80 (2), 115–118. https://doi.org/10.1016/j.fitote.2008.11.004.

Jadon, A., Bhadauria, M., Shukla, S., 2007. Protective effect of Terminalia belerica Roxb. and gallic acid against carbon tetrachloride induced damage in albino rats. Journal of ethnopharmacology 109 (2), 214–218. https://doi.org/10.1016/j.jep.2006.07.033.

Junior, O.C., Lima, N.M., Silva, M.G., Aguiar, V.B., Carli, G.P., Scherrer, E.C., Carli, A.P., 2020. In vitro and in vivo evaluation of anti-inflammatory activity and free radical scavenging potential of leaves extract from Anadenanthera colubrina. Natural Product Research 1–5. https://doi.org/10.1080/14786419.2020.1727472.

Kale, R.H., Halde, U.K., Biyani, K.R., 2012. Protective Effect of Aqueous Extract of Uraria Picta on Acetaminophen Induced Nephrotoxicity in Rats. International Journal of Research in Pharmaceutical and Biomedical Sciences. 3 (1), 110–113.

Karattu Veedu, K., Peringattu Kalarikkal, T., Jayakumar, N., Gopalan, N.K., 2019. Anticorrosive Performance of Mangifera indica L. Leaf Extract-Based Hybrid Coating on Steel. ACS Omega 4 (6), 10176–10184. https://doi.org/10.1021/acsomega.9b00632.

Karunagoda, K., Shukla, K., Donga, S., Tanna, C., Dei, L.P., 2010. A comparative study of Dashamoola Taila Matra Basti and Tila Taila Matra Basti in Kashtartava (dysmenorrhea). Ayu. 31 (3), 305. https://doi.org/10.4103/0974-8520.77154.

Kilic, I., Yeşiloğlu, Y., Bayrak, Y., 2014. Spectroscopic studies on the antioxidant activity of ellagic acid. Spectrochim. Acta A Mol. Biomol. Spectrosc. 130, 447–452. https://

doi.org/10.1016/j.saa.2014.04.052.
Kim, K.Y., Nguyen, T.H., Kurihara, H., Kim, S.M., 2010. α-Glucosidase inhibitory activity of bromophenol purified from the red alga Polyopes lancifolia. Journal of Food Science. 75, H145–H150.
Kumar, K.S., Ashish, G.R., Mony, R.S., Sundaresan, A., 2015. Comparative evaluation of the antioxidant and antidiabetic activity of different parts of Aegle marmelos and its chemical profiling using HPLC and HPTLC technique. World J Pharm. Sci. 4 (09), 1107–1121.
Kyriakis, E., Stravodimos, G.A., Kantsadi, A.L., Chatzileontiadou, D.S., Skamnaki, V.T., Leonidas, D.D., 2015. Natural flavonoids as antidiabetic agents. The binding of gallic and ellagic acids to glycogen phosphorylase b. FEBS Lett. 589 (15), 1787–1794. https://doi.org/10.1016/j.febslet.2015.05.013.
Lesjak, M., Beara, I., Simin, N., Pintać, D., Majkić, T., Bekvalac, K., Orčić, D., Mimica-Dukić, N., 2018. Antioxidant and anti-inflammatory activities of quercetin and its derivatives. J. Funct. Foods. 40, 68–75.
M Estevez, A., J Estevez, R., 2012. A short overview on the medicinal chemistry of (—)-shikimic acid. Mini reviews in medicinal chemistry 12 (14), 1443–1454. https://doi.org/10.2174/138955712803832735.
Madlener, S., Illmer, C., Horvath, Z., Saiko, P., Losert, A., Herbacek, I., Fritzer-Szekeres, M., 2007. Gallic acid inhibits ribonucleotide reductase and cyclooxygenases in human HL-60 promyelocytic leukemia cells. Cancer letters 245 (1-2), 156–162. https://doi.org/10.1016/j.canlet.2006.01.001.
Mizushima, Y., Kobayashi, M., 1968. Interaction of anti-inflammatory drugs with serum proteins, especially with some biologically active proteins. J of Pharma Pharmacol 20, 169–173. https://doi.org/10.1111/j.2042-7158.1968.tb09718.x.
Mosmann, T., 1983. Rapid colourimetric assay for cellular growth and survival: Application to proliferation and cytotoxicity assays. J. Immunol. Methods. 65 (1–2), 55–63. https://doi.org/10.1016/0022-1759(83)90303-4.
Nagarkar, B., Jagtap, S., 2017. Effect of new polyherbal formulations DF1911, DF2112 and DF2813 on CFA induced inflammation in rat model. BMC Complement. Alternative Med. 17 (1), 194. https://doi.org/10.1186/s12906-017-1711-6.
Nagarkar, B., Jagtap, S., Narkhede, A., Nirmal, P., Pawar, N., Kuvalekar, A., Kulkarni, O., Harsulkar, A., 2013. Different Ayurvedic dosage forms of Dashamoola possess varied anti-inflammatory activity. World J. Pharm. Pharmaceutic. Sci. 2, 3118–3136.
Nam, B., Rho, J.K., Shin, D.M., Son, J., 2016. Gallic acid induces apoptosis in EGFR-mutant non-small cell lung cancers by accelerating EGFR turnover. Bioorganic & medicinal chemistry letters 26 (19), 4571–4575. https://doi.org/10.1016/j.bmcl.2016.08.083.
Nanda, G.C., Tiwari, R.K., 2016. Shothahara activities of dashamoola dravyas as an anti-inflammatory formulation with special reference to charak. Ayushdhara 2393, 9583–9591.
Naveed, M., Hejazi, V., Abbas, M., Kamboh, A.A., Khan, G.J., Shumzaid, M., WenHua, L., 2018. Chlorogenic acid (CGA): A pharmacological review and call for further research. Biomedicine & Pharmacotherapy. 97, 67–74. https://doi.org/10.1016/j.biopha.2017.10.064.
Navruz, A., Türkyılmaz, M., Özkan, M., 2016. Colour stabilities of sour cherry juice concentrates enhanced with gallic acid and various plant extracts during storage. Food Chem. 197, 150–160. https://doi.org/10.1016/j.foodchem.2015.10.098.
Oteiza, P.I., Fraga, C.G., Mills, D.A., Taft, D.H., 2018. Flavonoids and the gastrointestinal tract: Local and systemic effects. Molecular aspects of medicine 61, 41–49. https://doi.org/10.1016/j.mam.2018.01.001.
Oyedepo, O.O., Femurewa, A.J., 1995. Anti-protease and membrane stabilizing activities of extracts of Fagra zanthoxiloides, Olax subscorpioides and Tetrapleura tetraptera. Int J of Pharmacong 33, 65–69. https://doi.org/10.3109/13880209509088150.
Prabhu, G.R.D., Kiran, C.R., Sundaresan, A., Mony, R.S., Venugopalan, V.V., 2015. Process development studies for recovery of bio active isolates from spent black pepper generated from ayurvedic industry. Ind. Crops Prod. 66, 144–149.
Ramón-Gonçalves, M., Gómez-Mejía, E., Rosales-Conrado, N., León-González, M.E., Madrid, Y., 2019. Extraction, identification and quantification of polyphenols from spent coffee grounds by chromatographic methods and chemometric analyses. Waste Management 96, 15–24. https://doi.org/10.1016/j.wasman.2019.07.009.
Randive, D.S., Adanaik, R.S., Nalawade, P.P., Patil, A.M., 2014. Studies on Standardization parameters for marketed formulations of Draksharishtha. IJUPBS. 3 (4), 397–401.
Rao, M.L., Savithramma, N., 2011. Phytochemical screening of dasamoola-An Ayurvedic drug. Int J Pharm Pharm Sci. 3, 318–320.
Re, R., Pellegrini, N., Proteggente, A., Pannala, A., Yang, M., Rice-Evans, C., 1999. Antioxidant activity applying an improved ABTS radical cation decolorization assay. Free Radic Biol Med. 26 (9-10), 1231–1237. https://doi.org/10.1016/s0891-5849(98)00315-3.
Roidoung, S., Dolan, K.D., Siddiq, M., 2016. Gallic acid as a protective antioxidant against anthocyanin degradation and color loss in vitamin-C fortified cranberry juice. Food Chem. 210, 422–427. https://doi.org/10.1016/j.foodchem.2016.04.133.
Sakat, S., Juvekar, A.R., Gambhire, M.N., 2010. In vitro antioxidant and anti-inflammatory activity of methanol extract of Oxalis corniculata Linn. International Journal of Pharma and Pharmacological Sciences. 2 (1), 146–155.
Sekhon-Loodu, S., Rupasinghe, H.P., 2019. Evaluation of antioxidant, antidiabetic and antiobesity potential of selected traditional medicinal plants. Frontiers in nutrition 6, 53. https://doi.org/10.3389/fnut.2019.00053.
Silva, W., Torres-Gatica, M.F., Oyarzun-Ampuero, F., Silva-Weiss, A., Robert, P., Cofrades, S., Giménez, B., 2018. Double emulsions as potential fat replacers with gallic acid and quercetin nanoemulsions in the aqueous phases. Food Chem. 253, 71–78. https://doi.org/10.1016/j.foodchem.2018.01.128.
Singleton, V.L., Rossi, J.A., 1965. Colorimetry of total phenolics with phosphomolybdic-phosphotungstic acid reagents. AM. J. Enol. Viticult. 16 (3), 144–158.
Sobeh, M., Mahmoud, M.F., Abdelfattah, M.A., El-Beshbishy, H.A., El-Shazly, A.M., Wink, M., 2017. Albizia harveyi: phytochemical profiling, antioxidant, antidiabetic and hepatoprotective activities of the bark extract. Medicinal Chemistry Research 26 (12), 3091–3105. https://doi.org/10.1007/s00044-017-2005-8.
Sorrentino, E., Succi, M., Tipaldi, L., Pannella, G., Maiuro, L., Sturchio, M., Tremonte, P., 2018. Antimicrobial activity of gallic acid against food-related Pseudomonas strains and its use as biocontrol tool to improve the shelf life of fresh black truffles. International journal of food microbiology 266, 183–189. https://doi.org/10.1016/j.ijfoodmicro.2017.11.026.
Stanek, N., Jasicka-Misiak, I., 2018. HPTLC phenolic profiles as useful tools for the authentication of honey. Food analytical methods 11 (11), 2979–2989. https://doi.org/10.1007/s12161-018-1281-3.
Sudhanshu, S.M., Rao, N., Menghani, E., 2012. Dashamularishta: Phytochemical and Antimicrobial Screening against effect of Environmental Pollution. Int. J. Pharm. Sci. Res. 3 (9), 1000–1004.
Tungcharoen, P., Wattanapiromsakul, C., Tansakul, P., Nakamura, S., Matsuda, H., Tewtrakul, S., 2018. Antiinflammation constituents from Curcuma zedoaroides. Phytotherapy research 32 (11), 2312–2320. https://doi.org/10.1002/ptr.6173.
Vyas, M., Ashok, B.K., Ravishankar, B., Patgiri, B.J., Prajapati, P.K., 2011. A Comparative Anti-Inflammatory Activity of Brihatpanchamoola kwatha Prepared from Root Bark and Stem Bark. Inventi Rapid: Ethnopharmacology.
Wang, T.Y., Li, Q., Bi, K.S., 2018. Bioactive flavonoids in medicinal plants: Structure, activity and biological fate. Asian J. Pharm. Sci. 13 (1), 12–23.
Xiao, Z., Storms, R., Tsang, A., 2006. A quantitative starch-iodine method for measuring alpha-amylase and glucoamylase activities. Anal. Biochem. 351 (1), 146–148. https://doi.org/10.1016/j.ab.2006.01.036.
Yoshioka, K.A.Z.U.M.I., Kataoka, T.O.M.O.K.O., Hayashi, T.O.M.O.K.O., Hasegawa, M., Ishi, Y., Hibasami, H. (2000). Induction of apoptosis by gallic acid in human stomach cancer KATO III and colon adenocarcinoma COLO 205 cell lines. Oncology reports. 7: (6) 1221-1224 . doi:10.3892/or.7.6.1221.
Zeng, W., Jin, L., Zhang, F., Zhang, C., Liang, W., 2018. Naringenin as a potential immunomodulator in therapeutics. Pharmacological research 135, 122–126. https://doi.org/10.1016/j.phrs.2018.08.002.
Zou, M.H., Shi, C., Cohen, R.A., 2002. Oxidation of the zinc-thiolate complex and uncoupling of endothelial nitric oxide synthase by peroxynitrite. J. Clin. Invest. 109 (6), 817–826. https://doi.org/10.1172/JCI14442.

Food Chemistry 458 (2024) 140284

Contents lists available at ScienceDirect

Food Chemistry

journal homepage: www.elsevier.com/locate/foodchem

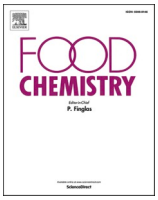

Lignin nanoparticles from Ayurvedic industry spent materials: Applications in Pickering emulsions for curcumin and vitamin D_3 encapsulation

Billu Abraham [a,c,d], Heeba Shakeela [a,c], Leena P. Devendra [b], K.B. Arun [e], K. Vasanth Ragavan [a,c], Charles Brennan [d], Nitin Mantri [d], Benu Adhikari [d,*], P. Nisha [a,c,d,*]

[a] Agro Processing and Technology Division, CSIR-National Institute for Interdisciplary Science and Technology, India
[b] Microbial Processing and Technology Division, CSIR-National Institute for Interdisciplinary Science and Technology, Council of Scientific and Industrial Research, Trivandrum 695019, India
[c] Academy of Scientific and Innovative Research (AcSIR), Ghaziabad 201002, India
[d] School of Science, RMIT University, Melbourne, VIC 3083, Australia
[e] Department of Life Science, Christ College (Deemed to be University), Bangalore, 560029, India

ARTICLE INFO

Keywords:
Lignin nanoparticles
Ayurveda industry
Curcumin
Vitamin D_3
Pickering nanoemulsions

ABSTRACT

Lignin nanoparticles (LNP), extracted from spent materials of Dashamoola Arishta (Ayurvedic formulation), shared a molecular weight of 14.42 kDa with commercial lignin. Processed into LNPs (496.43 ± 0.54 nm) via planetary ball milling, they demonstrated stability at pH 8.0 with a zeta potential of −32 ± 0.27 mV. Operating as Pickering particles, LNP encapsulated curcumin and vitamin D_3 in sunflower oil, forming LnE + Cu + vD_3 nanoemulsions (particle size: 347.40 ± 0.71 nm, zeta potential: −42.27 ± 0.72 mV) with high encapsulation efficiencies (curcumin: 87.95 ± 0.21%, vitamin D_3: 72.66 ± 0.11%). The LnE + Cu + vD_3 emulsion exhibited stability without phase separation over 90 days at room (27 ± 2 °C) and refrigeration (4 ± 1 °C) temperatures. Remarkably, LnE + Cu + vD_3 exhibited reduced toxicity, causing 29.32% and 34.99% cell death in L6 and RAW264.7 cells respectively, at the highest concentration (50 μg/mL). This underscores the potential valorization of Ayurvedic industry spent materials for diverse industrial applications.

1. Introduction

Lignin is one of the most important components of the plant cell wall structure, and it is the second-most prevalent natural macromolecule after cellulose (Gordobil et al., 2018). It is an amorphous, heterogeneous molecule constituting phenylpropane units derived from three aromatic alcohols (coniferyl, p-coumaryl, and sinapyl). The chemical structure of lignin depends highly on the botanical origin, growing conditions of the plant, and the extraction process (Gordobil et al., 2018; Rahman et al., 2018; Tortora et al., 2014; Zou et al., 2019). Agriculture, forestry and paper/pulp industry together create approximately 78 million metric tonnes of lignin as a by-product (Zou et al., 2019). Lignin is used in multiple sectors, encompassing biofuels (char, hydrogen, syngas, diesel), chemicals (polymers, dispersants, binders), agriculture (controlled release for pesticides/herbicides, heavy metal sequestration, humic acid formation, high-value fertilizers), human health applications (drug encapsulation, delivery, health-promoting functions), and UV protection in cosmetics (Abraham et al., 2023; Schneider et al., 2021).

Ayurveda is an indigenous form of traditional Indian medicinal science that has been practiced for thousands of years, with its roots dating back several millennia. It makes use of plant-based formulations to treat a wide range of illnesses (Randive et al., 2014). Dashamoola Arishta (DA) is an anti-inflammatory formulation and is one of the most effective and sought-after Ayurvedic preparations for inflammation-related ailments (Randive et al., 2014, Shukla et al., 2010, Nagarkar et al., 2013). It is prepared from the roots of ten different medicinal plants, primarily including Bilva (*Aegle marmelos*), Agnimantha (*Premna integrifolia*), Shyonaka (*Oroxylum indicum*), Patala (*Stereospermum suaveolens*), Gambhari (*Gmelina arborea*), Brihati (*Solanum indicum*), Kantakari (*Solanum xanthocarpum*), Shalaparni (*Desmodium gangeticum*), Prishnaparni (*Uraria picta*), Gokshura (*Tribulus terrestris*), as recorded in Ayurvedic texts (Vyas et al., 2011; Abraham et al., 2020). Ayurveda industry generates ~1000 tons of spent materials of dashamoola, hence forth referred to as dashamoola spent material (DSM), after the arista

* Corresponding authors at: School of Sciences, RMIT University, Melbourne, VIC 3083, Australia and Agro Processing and Technology Division, CSIR-NIIST, Thiruvananthapuram, Kerala 695019, India.
E-mail addresses: benu.adhikari@rmit.edu.au (B. Adhikari), pnisha@niist.res.in (P. Nisha).

https://doi.org/10.1016/j.foodchem.2024.140284
Received 25 January 2024; Received in revised form 27 March 2024; Accepted 28 June 2024
Available online 2 July 2024

production and is a rich source of lignocellulosic materials. Our earlier study showed that this DSM is rich in lignocellulosic content and that it can be valorised to be used in Ayurvedic industry and could converted into a sustainable, commercially viable source of lignin and cellulose (Abraham et al., 2020).

Naturally obtained biopolymeric materials including cellulose and pectin or their derivatives have lately seen increasing popularity as emulsion stabilizers (Hossain et al., 2021; Jiang & Hsieh, 2015; McClements et al., 2017). Micron and nanosized particles have been used as surface-active stabilizers for Pickering emulsions (Bertolo et al., 2019; Li et al., 2021; Sipponen et al., 2018; Zou et al., 2019). Pickering emulsions are stabilized by solid particles and are finding applications in foods, cosmetics and pharmaceuticals etc. (Hossain et al., 2021; Zou et al., 2019). In addition to providing emulsifying and stabilizing properties, lignin and cellulose are known to protect light-sensitive compounds such as vitamins, oils, and food color (Pandian et al., 2021; Sodeinde et al., 2021).

Several studies have touted curcumin's potential for providing health promoting functions to human against inflammation, oxidation-induced stresses cells (Anand et al., 2008). It is also known to promote immunomodulation (Ahsan et al., 1999). A recent study showed that the deficiency of Vitamin D_3 in the US population was associated with a higher incidence of COVID-19 infections and subsequent deaths among the Latino and Black populations (Ames et al., 2021). The intake of curcumin and vitamin D_3 was reported to provide relief from the infections and complications associated with COVID-19 (Ilie et al., 2020; Rattis et al., 2021; Zahedipour et al., 2020). Curcumin and vitamin D_3 are sensitive to environmental factors, and require to be stabilized by encapsulation. Encapsulated form of these compounds enables precise dosing and increased bioavailability, both of which are important for their efficacy.

In the above context, the current research aimed to isolate and characterize the lignin from DSM and convert it into nano lignin. Subsequently, the efficacy of nano lignin, utilized as a Pickering particle in an O/W emulsion, was investigated for its ability to encapsulate curcumin and vitamin D_3, along with an assessment of their storage stability.

2. Material and methods

2.1. Material and chemicals

DSM for the study was kindly provided by Arya Vaidya Sala, Kottakal, Malappuram, Kerala, India. SD Fine Chemicals, Mumbai, India, supplied sulphuric acid (72% *w/v*), calcium carbonate. Laccase and cellulase enzymes were supplied by Zytex Biotech Pvt. Ltd., Andheri (E), Mumbai, India. Lignin standard was procured from Sigma Aldrich Chemicals Pvt. Ltd., Massachusetts, USA. Sisco Research Laboratories Pvt. Ltd., Mumbai, India, provided all the analytical-grade reagents utilized in the current study.

2.2. Isolation of lignin from DSM

The compositional analysis of DSM in terms of lignin, cellulose and hemicellulose was carried out according to National Renewable Energy Laboratory (NREL) protocol (Ruiz & Ehrman, 1996). Lignin was extracted form DSM using alkaline extraction method (Si et al., 2015; Wunna et al., 2017). Briefly, DSM was suspended in 1% NaOH with 10% w/v loading. This mixture was heated at 121 °C for 1 h in an autoclave. Subsequently, the treated solid content was cooled to a room temperature before utilization with the cheese cloth. The supernatant (black liquor) obtained in this way was rendered acidic by lowering the pH to 2.0 using 10% H_2SO_4. The precipitate was recovered by centrifugation at 5000 x*g* for 15 min. The solid mass, lignin, obtained from the centrifugation step was freeze-dried at −80 °C under a pressure of 10 Pa.

2.3. Preparation of nano lignin

Planetary ball mill (Pulverisette, Fritsch, Germany) running at 300 rpm and zirconium dioxide (ZrO_2) containers (50 mL) containing ZrO_2 balls (10 mm) was used for the size reduction of extracted lignin. All lignin samples were ground for 23 cycles in an argon environment (each cycle had a (each cycle lasted for 5 min, followed by a 10-min gap). After the ball milling, the powder was sieved through 63 mm sieve (Jayanth Scientific Instruments, Delhi, India).

2.4. Zeta potential and particle size

The droplet size and zeta potential of lignin was calculated from pH 4.0 to 10.0 using the Malvern Zeta sizer (Zeta Nano-ZS; Malvern Instruments, UK), which relies on the dynamic light scattering (DLS) principle.

2.5. Characterization of LNP

The lignin nanoparticles (LNP) were characterized in terms of NMR, GPC, FTIR, TGA, DSC, XRD and compared with that of Standard Lignin Powder (SLP). Further LNP was also characterized in terms of contact angle, SEM and TEM. The protocols for these tests are provided below.

2.5.1. Purity of extracted lignin

A two-step hydrolysis process was performed to analyse the chemical composition of the recovered lignin, focusing specifically on its carbohydrate, acid-soluble, and insoluble content (Ruiz & Ehrman, 1996). The polysaccharides content of the hydrolysate formed at the end of the two-step acid treatment was quantitated using the HPLC method, following the procedure outlined in Karthyani et al., 2017.

2.5.2. Functional group analysis of LNP using FTIR

FTIR analysis of the LNP was carried out using FTIR – ATR spectrometer (Perkin Elmer, USA) and the spectra were recorded from 4000 to 1000 cm^{-1} with a resolution of 4 cm^{-1}.

2.5.3. Determining the molecular weight of LNP

The gel permeation chromatography method was employed to determine the molecular weight of lignin. The method used a 300 × 7.8 mm Phenomenex Phenogel GPC column mounted on a Shimadzu GPC unit connected to a photodiode array detector. The calibration and analysis were carried out as reported by Akhil et al., 2020.

2.5.4. NMR characterization of LNP: Molecular structure analysis

A previously reported $^{1}H—^{13}C$ NMR heteronuclear single-quantum coherence (HSQC) technique was used for analysing the LNP using an in-house Bruker Avance II 500 spectrometer (US). Sample preparation involved the addition of a 10 mg lignin sample in 1 mL d6-DMSO. The contours and cross peaks were identified and assigned according to the reported literature (Gabov et al., 2014; Ragauskas & Yoo, 2018).

2.5.5. Analysis of phenolic content

UV spectrometry was used to calculate the phenolic content of lignin. The assay was based on the change in the absorbance brought out by the ionization of phenolic hydroxyl groups in alkaline conditions. The LNP was dissolved in a 0.2 M NaOH solution and dioxane. The total phenolic hydroxyl group and C-5 substitution (condensed Phenolic OH) were determined according to Goldmann et al., 2016.

2.5.6. Surface composition of LNP

The X-ray photoelectron spectroscopy (XPS) was used to determine the surface composition of lignin. PHI 5000 Versa Probe II (ULVAC-PHI Inc., USA) was used to determine the ratio of oxygen and carbon (O: C). The oxygen-to-carbon ratio directly provides details on the percentage of surface lignin. The equipment used a built-in micro-focused (200 μm,

15 kV) monochromatic Al-Kα X-Ray source (hν =1486.6 eV) for carrying out the analysis (Mou et al., 2013).

2.5.7. Thermal degradation of LNP

Thermal gravimetric (TG) analyses of LNP and SLP were carried on a TA Q50 instrument. Sample (10 mg) was placed in the alumina crucible, heated in the temperature range 40–500 °C at a heating rate of 10 °C/min in the presence of nitrogen (Moustaqim et al., 2018). The weight loss (%) versus temperature data were recorded.

2.5.8. Thermal characteristics of LNP

Differential scanning calorimetry (DSC) was employed to assess the thermal behaviour, specifically focusing on the Glass Transition Temperature (Tg), of both LNP and SLP. Measurements were performed using DSC Q2000, TA Instruments, USA. Distilled water (6 L) was added to 3.0 mg of the sample and was transferred into pre-weighed aluminium sample pans. Samples were heated from 25 °C to 95 °C at a rate of 10 °C/min under a nitrogen environment. The onset temperature (TO) marks the initiation of phase transitions, peak temperature (TP), and conclusion temperature (TC) were measured using the Fit2D software (Sathyan & Nisha, 2022).

2.5.9. Crystalline and amorphous content of LNP

The wide-angle X-ray diffraction (WAXD) observations were captured using Xenocs' XEUSS SAXS/WAXS instrument in transmission mode to analyse the amorphous and crystalline content of LNP and SLP. Cu K radiation at 50 kV and 0.6 mA with a wavelength of 1.54 was used. Fit2D software was used to analyse the data after the 2D patterns were captured on a Mar345 picture plate. The degree of crystallinity was calculated by the ratio of the intensity of the crystalline peak to the total intensity according to Raveendran et al., 2011.

2.5.10. Contact angle

A thin film of LNP was made by dispersing 5% (*w/v*) LNP in distilled water on a spotless glass slide and dried at 85 °C for 30 min. A drop of distilled water (2 μL) was then added on the film surface, and their contact angle was determined using a drop shape analyzer (Model DSA30E, KRUSS GmBH, Hamburg, Germany; with Kruss Advance Software 1.7.0.8, Version 15).

2.5.11. Microscopic surface morphology

A specimen holder made of aluminium was coated with carbon tape before being filled with the sample, a thin layer of gold was applied using a gold/palladium sputter coater (SC7620, Emitech, Quorum Technologies Ltd., Kent, UK). Scanning electron microscopy (ZEISS; EVO 18, Germany) was used to analyse the microscopic surface texture of these samples under 15 KV of accelerating voltage, 10,000× magnification was used to capture the micrographs (Sathyan & Nisha, 2022).

2.5.12. Internal structure of LNP

Transmission electron microscopy (TEM) of the LNP was done using JOEL JEM F200 with STEM, EDS and Gatan EELS and FEI Tecnai T30 with EDAX. This technique facilitated high-resolution imaging and detailed examination of the internal structure and composition of LNP at the nanoscale.

2.6. Preparation of O/W Pickering emulsions

Oil-in-water (O/W) Pickering emulsions were prepared using LNP as Pickering particle. LNP solutions of various concentrations (0, 500, 1000, 1500, 2000, 2500 ppm) at pH 8 were prepared and used. Sunflower oil (10% *w/w*) loaded with 50 ppm curcumin (Cu) and 50 ppm vitamin D_3 (vD_3) was used as the dispersed phase. Pickering emulsions {(1) LnE (LNP stabilized O/W emulsion of sunflower oil) and (2) LnE + Cu + vD_3 (LNP stabilized O/W emulsion of sunflower oil loaded with curcumin, and vitamin D_3)} were prepared by using a probe sonicator (VCX-750 Vibra cell, sonics & materials, USA) sonicating for 0, 15, 30, 45, 60 min (cycle 10 s on/10 s off, amplitude 50%). The resulting emulsions LnE + Cu + vD_3 were analysed in terms of particle size, ζ-potential, color and stability at 4 °C and 27 °C for 90 days.

2.6.1. Rheological properties

A controlled stress rheometer was used to analyse the rheological properties (viscometric,

dynamic strain sweep, and dynamic frequency sweep behaviour) of two emulsions: LnE and LnE + Cu + vD_3 (MCR 102 Rheometer, Anton Paar GmbH, Ostfildern-Scharnhausen, Germany). A cone and plate geometry with a 25 mm diameter was employed in these tests. The gap between the cone and the plate was 0.105 mm. The viscometric was applied in a shear rate ranging from 0.01 to 100 s^{-1} to record shear rate versus viscosity data. During the dynamic strain sweep analysis, the strain for LnE and LnE + Cu + vD_3 was varied from 0.01 to 100%. The linear viscoelastic region (LVE) was determined from their strain sweep curve. The behaviour of the two emulsions, during dynamic frequency sweep was measured by varying the frequency from 0.01 to 100 rad/s (Kavya et al., 2023; Sathyan & Nisha, 2022).

2.6.2. Microstructure of emulsions

Microstructure of the emulsion was captured and analysed using a fluorescence microscope (Olympus fluorescence microscope IX83, Olympus corporation of Americas, Center Valley, USA) to understand whether LNP acted as a Pickering particle. LNP and the oil phase were stained with dye calcofluor white and nile red respectively. Emulsion (100 μL) was taken in a 96-well plate, stained with nile red (10%), kept for a few minutes, followed by adding calcofluor white (5 mg/mL). Photographs were taken using a delta 512 EMCCD camera (photometrics, USA) (Bai et al., 2019).

2.6.3. Creaming index

Emulsions were transferred to15 mL graduated test tubes immediately after preparation and stored for 90 days at both room temperature (27 °C) and refrigerating temperature (4 °C). The amount of oil phase (in mL) that had separated from the emulsion was recorded every 15-day interval. Using Eq. (1), the percentage of separated oil (phase) was calculated using eq. (1) (Huimin et al., 2014).

$$\text{Phase separation } (\%) = (VT/VE) \times 100 \quad (1)$$

where, VT is the volume (mL) of the oil phase that was separated. VE is the total volume (mL) of emulsion used in the test.

2.6.4. Encapsulation efficiency

Encapsulation efficiency, representing the quantity of curcumin and Vitamin D_3 retained within the Pickering emulsion, was assessed using high-performance liquid chromatography (HPLC). To prepare samples for analysis, 1 mL of emulsion was mixed with 5 mL of methanol and stirred using a magnetic stirrer for 3 h at 2795 ×*g*. The mixture was then centrifuged at 55,900 ×*g* for 10 min, supernatant was collected and filtered through a 0.22 μm PTFE syringe filter. The filtered sample was analysed using a Prominence UFLC system (Shimadzu, Japan) containing LC-20 CE system equipped with a column oven (CTO-20 A), an autosampler injector (SIL-20 AC), a diode array detector, and a Phenomenex Gemini C18 column (250 × 4.6 mm, 5 μm) (SPD-M20A). The analysis for curcumin and vitamin D_3 was carried out using an isocratic flow of 100% methanol as the mobile phase, with a flow rate set at 1 mL/min and an injection volume of 10 μL. Detection of the curcumin and vitamin D_3 fractions was performed at 420 nm and 261 nm, respectively, with retention times of 3.2 min for curcumin and 7.6 min for vitamin D_3. The column temperature was maintained at 40 °C throughout the analysis.

The encapsulation efficiency (E.E) of Curcumin and Vitamin D_3 was determined using eq. (2).

$$E.E.(\%) = \frac{mass\ of\ compound\ retained\ in\ the\ emulsion\ (mg)}{totla\ mass\ of\ compund\ used\ (mg)} \times 100 \quad (2)$$

2.6.5. Cell viability assay

The L6 myoblast (NCCS, Pune, India) and RAW 264.7 (ATCC, Manassas, USA) cell lines were used in these tests. The cells grown in Dulbecco's modified eagle's medium (DMEM) supplemented with fetal bovine serum (10%) and a solution containing antibiotic-antimycotic solution (1%) were kept in CO_2 incubator maintained at 37 °C and 5% CO_2. Cells were seeded in 96 well plates at a density of 1×10^4 cells/well for cell viability assays.

The toxicity of lignin solution (Ln) and lignin emulsion (LnE + Cu + vD_3) against RAW 264.7 and L6 myoblast cells was studied using MTT assay (Klapiszewski et al., 2013). The cell lines grown in 96 well-plates were incubated with varying DSME concentrations (10–500 μg/mL) for 24 h. After the incubation period, the cells in each well were washed and added with 100 μL of MTT (0.5 mg/mL) and incubated at 37 °C for 4 h in a CO_2 incubator. Following incubation, 100 μL of DMSO was added in each well and optical density was determined (570 nm, Synergy4 Biotek multiplate reader, USA) after 45 min (Mosmann, 1983). In the MTT assay, the viability of cells is related to the conversion of MTT (yellow color) to formazan crystals (purple color). The abovementioned conversion will happen only in metabolically viable cells. The intensity of the purple color measured at 570 nm is directly correlated with the number of viable cells. Higher optical density indicates more viable cells, indicating their potential to convert MTT into formazan.

2.6.6. Storage stability

To evaluate the storage stability of the emulsions LnE + Cu + vD_3, they were stored at two temperatures: room temperature (27 °C) and refrigerated temperature (4 °C) for 90 days. During the storage period, the LnE + Cu + vD_3 was examined in 15 days' interval for changes in color, particle size, and zeta potential.

2.7. Statistical analysis

Experiments were carried out in triplicate unless otherwise specified above. Results are presented as mean values and standard deviation (SD). The analysis of variance was carried out using one-way analysis of variance (ANOVA) with Dunnetts multiple comparison test using graph prism pad 5.0 statistical software versions and Microsoft Excel (2007). A 95% confidence level was used to confirm significant difference between any two mean values.

3. Results and discussion

3.1. Characterization of extracted lignin

3.1.1. Chemical composition

The composition of DSM was found to closely resemble that of typical lignocellulosic biomass, with cellulose 39.10%, hemicellulose 30.56%, and lignin 27.89%. Lignin, with a purity of 96.18%, was extracted through alkaline hydrolysis of DSM and then converted into LNP using ball milling, which was further characterized using various physicochemical methods. In order to understand the pH stability of LNP, surface charge across pH range of 4 to 10 was studied. Notably, the LNP solution exhibited negative surface charge in this pH range. At pH 8.0, the LNP solution had the zeta potential value of −32.40 ± 0.81 mV and particle size of 496.43 ± 0.54 nm) (Supplementary Fig. 1). The negative zeta potential values can be attributed to the surface hydroxyl and acidic groups becoming ionized when dispersed in an aqueous solution (Czaikoski et al., 2020; Klapiszewski et al., 2013). The difference in electrostatic interactions at various pH values may be the correlated with the variation in particle sizes. At higher pH, cleavage of the β-O-4 linkage in lignin was observed, potentially leading to a reduction in particle size (Pradyawong et al., 2022).

Further, chemical and structural characteristics of the LNP were compared with standard (commercially obtained) SLP. IR and NMR data indicated that SLP and LNP had guaiacyl (G), syringyl (S) and p-hydroxyl (H) units (Fig. 1a, b). However, the intensity of G unit was more pronounced in the aromatic region of the HSQC spectra as shown in Fig. 1b. The contour corresponding to G5 protons was wider suggesting the presence of higher guaiacyl units with unsubstituted C5 position. β-O-4 linkages of G and S units were also observed in the aliphatic region of the HSQC spectra along with β-β linkages (Balakshin et al., 2003). The IR spectra of SLP and LNP were close, indicating the similar structural composition, as shown in Fig. 1c.

GPC data provided important insights into the structural heterogeneity, cross-linking or branching of the LNP in terms of molecular weight and Polydispersity index (PDI). LNP was found to have higher molecular weight than SLP (Supplementary Table 1). PDI represents the heterogeneity of the macromolecule. Lignin is covalently bonded to polysaccharides, hemicelluloses in particular, which adds to its heterogeneity (Tarasov et al., 2018). However, LNP had a lower PDI value than SLP, indicating better homogeneity. It is known that the β-O-4 linkages are easily cleaved by alkali (Devendra & Sukumaran, 2023; Tarasov et al., 2018). The NMR data indicated a higher number density of β-O-4 linkages in LNP, suggesting the presence of complex lignin-carbohydrate moieties. This may potentially lead to the blocking of inter-lignin β-O-4 linkages through steric hindrance, resulting in better homogeneity (Devendra & Sukumaran, 2023; Tarasov et al., 2018).

The FTIR analysis revealed that LNP had a complex lignin structure, potentially with a broader range of phenolic constituents, while SLP had a simpler lignin structure with a higher concentration of phenolic OH groups (Devendra & Sukumaran, 2023). The FTIR data of LNP indicated the presence of G-S-H lignin units (1327, 1514 cm^{-1}) and C—H S units (833 cm^{-1}), indicating a complex lignin structure. In contrast, standard lignin (SLP) showed a higher proportion of G units (1510 cm^{-1}) and phenolic OH groups (3392 cm^{-1}). These differences in lignin composition indicated that they had distinct reactivity profiles and would potentially be suitable for different applications (Devendra & Sukumaran, 2023; Tarasov et al., 2018). UV analysis (supplementary Table 1) indicated that LNP had a lower total phenolic OH content (2.134 mmol/g) compared to SLP (3.556 mmol/g). A similar trend was observed in C5-substituted phenolic OH, with LNP measuring 0.169 mmol/g and SLP measuring 1.86 mmol/g. SLP contained a notably higher concentration of both total phenolic ~groups and C5 substituted phenolic OH groups compared to LNP. These data and underlying trends are comparable with those reported by Devendra et al., 2022 in the case of both condensed and uncondensed phenolic hydroxyl groups through absorbance changes upon ionization in an alkaline medium. The difference in phenolic content between LNP and SNP can have significant implications for their reactivity, chemical functionality, and suitability in various industrial applications.

3.1.2. Bonding and elemental composition

XPS analysis helps to identify the elemental composition, nature of bonding and the state of oxidation of a material (Mou et al., 2013). The survey spectrum of LNP and SLP revealed the presence of carbon and oxygen as shown in (Fig. 2a-f). The high-resolution C 1 s spectrum of SLP revealed a peak at binding energy of 284.09 eV, attributed to C-C/C=C bonding in lignin. LNP had a lower binding energy of 284.69 eV. In addition, SLP showed peaks at 287 and 289 eV corresponding to C-O/C-OH, C=O/O-C=O in the C 1 s spectrum. Meanwhile, the O1s spectrum of all three compounds showed a peak at 532.8 eV, indicating the presence of C—O in the structure. LNP showed an additional peak at 530.7 eV, indicative of C═O in the lignin structure. This can be attributed to the large polarizability of phenolic structure of lignin. As a result, the binding energy of the lignin was shifted to a lower value, specifically 532 eV. These spectral features showed that LNP had broad C1s and O1s peaks in comparison to commercial lignin which had C1s and O1s peaks

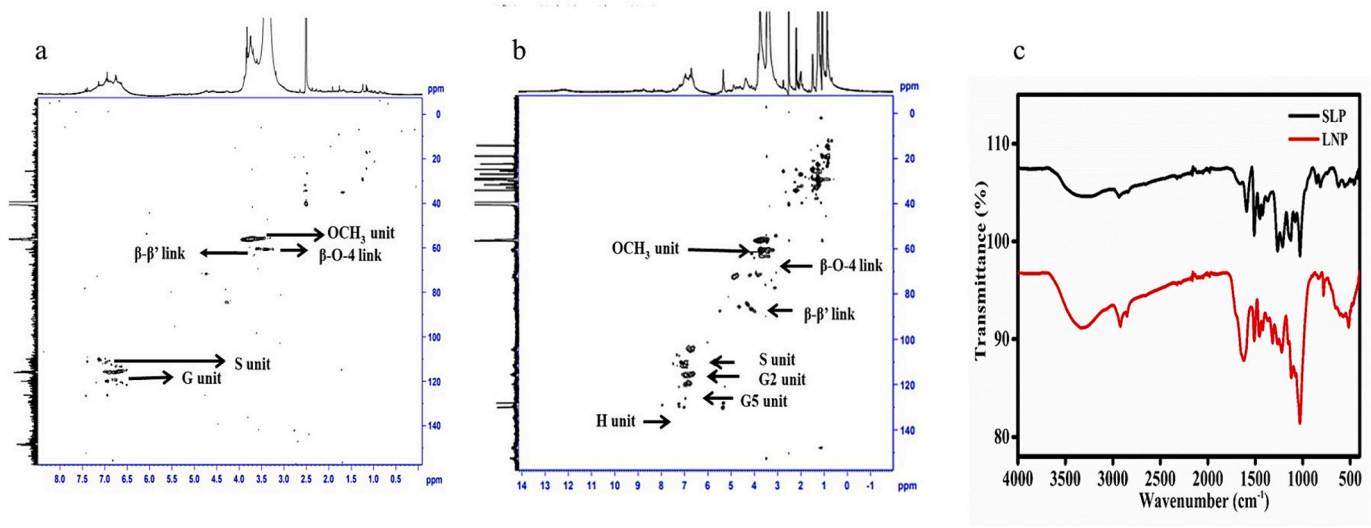

Fig. 1. (a) 2D-NMR spectroscopy of SLP, (b) 2D-NMR spectroscopy of LNP (c) FTIR spectroscopy of Standard Lignin Powder (SLP) and Lignin nanoparticles (LNP).

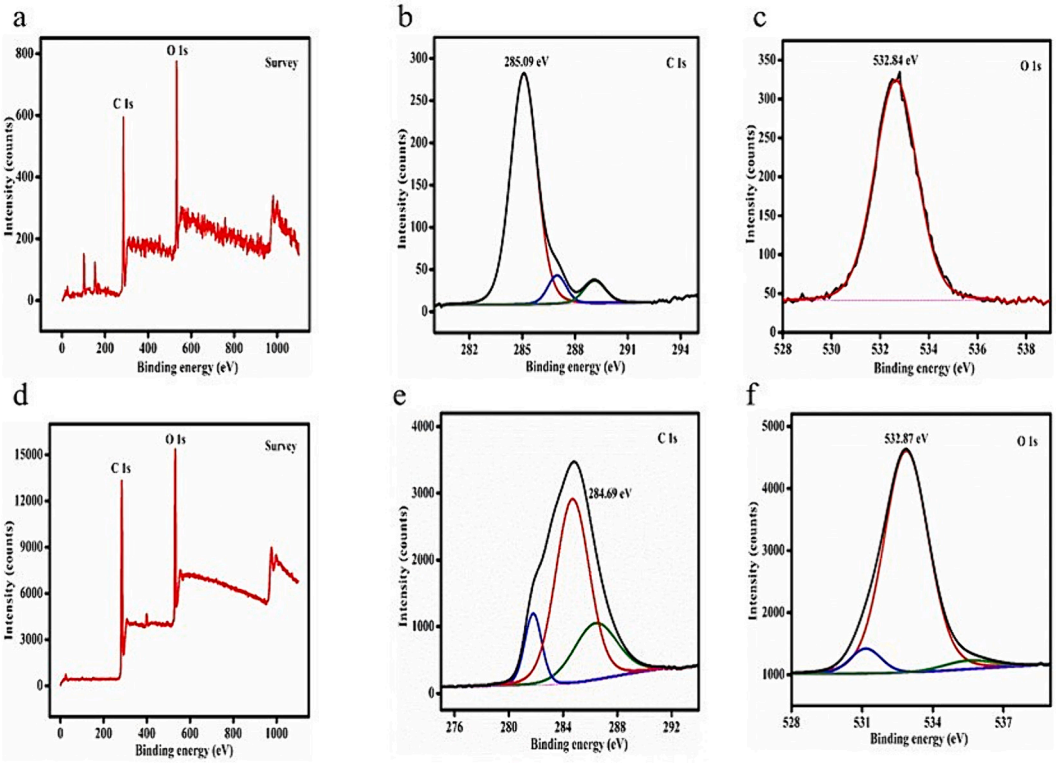

Fig. 2. (a) Survey spectrum of SLP, (b) XPS Curve Fitting of SLP carbon spectra, (c) XPS Curve Fitting of SLP oxygen spectra, (d) Survey spectrum of LNP, (e) XPS Curve Fitting of LNP carbon spectra, (f) XPS Curve Fitting of LNP oxygen spectra.

at 284 and 532 eV, respectively (Mou et al., 2013).

3.1.3. Thermal behaviour

The thermal stability of extracted lignin was evaluated through TGA and DSC analysis. A steady decrease in the mass loss (weight loss) was observed from 40 to 100 °C in the TGA curve (Fig. 3a) of both LNP and SLP (7.60 and 11.17% respectively), which corresponded to the moisture loss (Moustaqim et al., 2018). Above 100 °C (post-dehydration), the TGA curve showed two peaks, which could be attributed to the decomposition of β-O-4 bonds and aliphatic hydroxyl groups around 200 °C and cleavage of the C—C bond and demethoxylation of phenolic lignin around 300 °C to 450 °C (Ragauskas & Yoo, 2018). There was a 44.22% weight loss between 150 and 300 °C with an onset temperature around 150 °C for LNP. This was followed by a 67.11% loss of mass between 300 and 450 °C whereas SLP showed a 54.95% weight loss in the same temperature range. The degradation profile was similar to what is reported for lignin (Ragauskas & Yoo, 2018; Devendra et al., 2022). The difference in the mass loss during the thermal degradation of LNP and SLP could be attributed to the difference in their composition, which could be further inferred from the residual mass of 8.21% for SLP versus 6.02% for LNP at 800 °C.

The DSC profile of LNP and SLP samples exhibited comparable thermal profiles, including water evaporation, lignin decomposition, and glass transition temperature as shown in Fig. 3b. LNP showed an

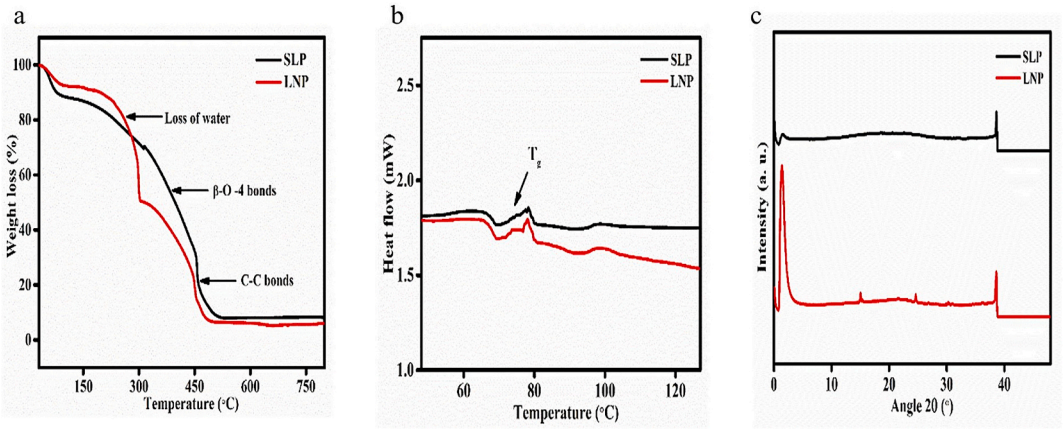

Fig. 3. Thermal and structural analyses of SLP and LNP: (a) TGA for thermal stability, (b) DSC for melting/crystallization behaviors and (c) XRD for crystalline structure.

endothermic peak below 100 °C, aligning with the evaporation of water. Additionally, an appearance of an exothermic peak around 200 °C suggested the decomposition of lignin, a finding that agrees well with Moustaqim et al., 2018's report. DSC analysis identified a similar glass transition temperature (T_g) of about 72 °C for both LNP and SLP.

Fig. 3c showcases the XRD patterns of LNP and SLP. As compared to SLP, LNP exhibited sharp peaks at 18° and 23° which could be attributed to the presence of residual cellulose in LNP. LNP isolated through alkaline hydrolysis showed 96.18% purity and contained 3.18% cellulose, as compared to SLP's 98% purity and no cellulose. Similar spectrum for alkaline extracted lignin is reported earlier which is correlated with its residual cellulose (Gomide et al., 2020). SLP showed a broad peak, indicative of its predominantly amorphous nature.

Overall, these structural analyses highlighted the importance of considering both thermal and structural characteristics when evaluating the potential application of LNP to encapsulate heat sensitive bioactive compounds (e.g., curcumin) and vitamins. The robust thermal stability of LNP makes it an excellent candidate for protecting these sensitive compounds during processing and ensuring their preservation in the final product.

3.1.4. *Surface morphology and microstructure*

The morphological features of LNP were studied using SEM and TEM to understand the morphological and microstructural properties. The SEM and TEM microstructure (Fig. 4a-c) showed that the LNP were spherical, and the size ranged from 200 to 300 nm. There was not a strong spread of size, and which indicated that ball milling can be used to produce LNP surface morphology of lignin nanoparticles.

With their small size, spherical shape, uniformity, and relatively narrow size range, these LNP are expected to be suitable for application in food formulations, especially as encapsulating shell materials and delivery vehicles. In the ensuing section presents their efficacy as Pickering particles to stabilize emulsions.

3.2. *Characteristics of Pickering emulsion produced using LNP*

In order to understand the hydrophobic/hydrophilic nature of LNP which is important for preparing emulsion, the contact angle was

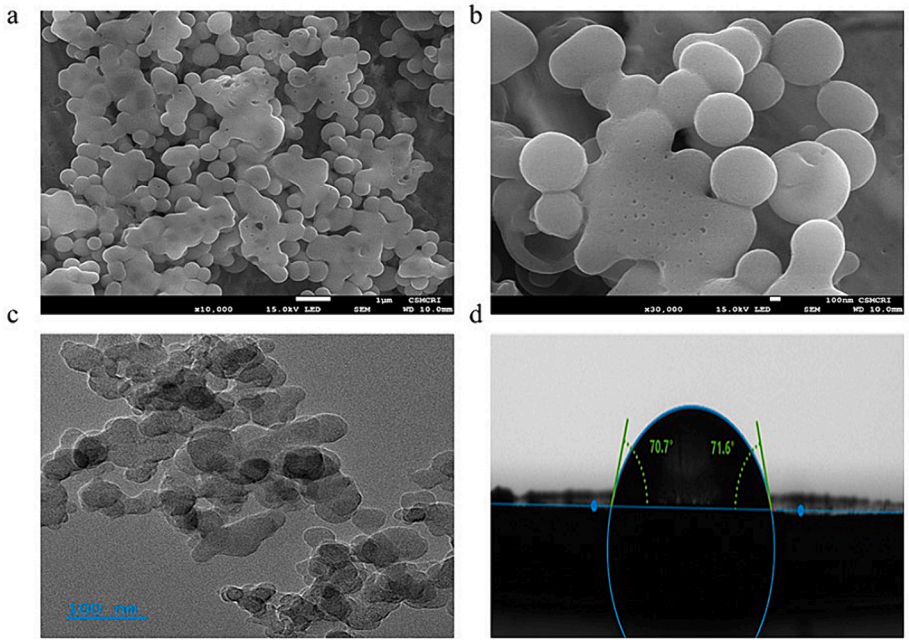

Fig. 4. Microscopic characterization of LNP: (a) SEM image at 10,000× magnification, (b) SEM image at 30,000× magnification, showcasing surface morphology, (c) TEM image revealing internal structure and (d) Contact angle measurement demonstrating surface wettability of LNP.

measured and was found to be 71.6° (Fig. 4 d). This indicated that the LNP had hydrophilic in nature and could be considered to be suitable to produce O/W emulsions. It is expected for these LNPs (as Pickering particles) to adsorb at the oil-water interface and form a dense layer to prevent the droplet aggregation (McClements, 2015).

LNPs were used to prepare two Pickering emulsions: (1) LnE and (2) LnE + Cu + vD_3. These emulsions were prepared a pH 8.0 based on the pH stability information presented in section 3.1.1. Initial trials were carried to understand the composition of the emulsion (LnE) in terms of percentage of dispersed phase and the amount of LNP required. It was found that 10% of oil with 2000–2500 ppm of LNP produced stable LnE. Ultrasound was used to prepare emulsions using sonication time ranging from 15 to 60 min (Fig. 5a). Most stable emulsions were obtained at 45 min of sonication at LNP concentration of 2000 ppm, which are referred to LnE (Fig. 5 a). Based on this experience, LnE + Cu + vD_3 emulsions with 10% sunflower oil and 2000 LNP loaded with curcumin and vitamin D_3 at concentrations of 500 ppm each, maintaining a 45-min of sonication. As the loading of curcumin and vitamin D_3 can affect the stability of the interface, we further evaluated the optimum LNP concentration by varying its concentration from 0 to 2500 ppm (Fig. 5b.). The stability of emulsion stability was evaluated in terms of oil separation. The most stable LnE + Cu + vD_3 were obtained in the LNP concentrations of 2000 ppm and 2500 ppm. Ultimately, we chose the LNP concentration of 2000 ppm. (Li et al., 2021; Zhang et al., 2022).

The microstructure of the optimized emulsions, LnE and LnE + Cu + vD_3, was examined using fluorescent microscopy to ascertain the formation of Pickering emulsions. LNPs would be considered as Pickering particles if they could preferentially be adsorbed at the O/W interface and ensured emulsion stability. The organization of lignin and oil droplets in the freshly prepared emulsion (LnE) is presented Fig. 5c. The calcofluor dye (blue color) indicated the presence of LNP while the Nile red stain (red color) revealed the size of individual oil droplets. The blue contour could be clearly observed surrounding the red-colored oil droplets, illustrating how LNP were forming a layer entrapping them. In the case of the LnE + Cu + vD_3 emulsion, where curcumin and vitamin D_3 are solubilized in sunflower oil, the oil droplets were stained with Nile red and lignin with calcofluor dye (as shown in Fig. 5d). Again, the blue contour was observed to encircle the red-colored oil droplets, demonstrating that LNP clearly acting as Pickering particles. Similar to our findings, Yuan et al., 2023 observed fluorescence microscopy images in which lignin, stained in blue (using calcofluor white), formed a contour around red-colored oil droplets (stained with nile red) created through high-energy microfluidization. These observations indicated that LNP can act as Pickering particles in oil-in-water emulsion systems.

3.2.1. *Particle size and zeta potential*

The particle size and zeta potential of LnE and LnE + Cu + vD_3 were significantly different (Table 1). LnE had larger particle size (546.83 ± 9.81) band small absolute value of zeta potential while LnE + Cu + vD_3 (347.40 ± 0.71) had smaller particle size higher absolute value of zeta potential. The smaller size of LnE + Cu + vD_3 indicated that this emulsion was more stable at the same time was containing curcumin and vitamin D_3 in the core. These compounds in LnE + Cu + vD_3 acted as natural surfactants, reducing the surface tension between oil and water phases, which helped to form smaller droplets. They modified the interfacial properties, possibly through steric hindrance and electrostatic repulsion, enhancing droplet stability against coalescence. Additionally, their incorporation could increase the viscosity of the continuous phase, further stabilizing the smaller droplets by impeding their movement (Zembyla et al., 2020). The negative zeta potential values for both formulations, especially the higher value in LnE + Cu + vD_3, underscored their electrostatic stability, which is important for

Table 1
Lignin emulsions of size, zeta, and color values.

Sample name	LnE	LnE + Cu + vD_3
Size (nm)	546.83 ± 9.81[a]	347.40 ± 0.71[b]
Zeta (Mv)	−35.53 ± 0.57[a]	−42.265 ± 0.72[b]
L*	73.93 ± 0.23[a]	62.62 ± 1.25[b]
a*	5.31 ± 0.03[a]	3.893 ± 0.03[b]
b*	13.53 ± 0.09[a]	59.91 ± 0.71[b]

Values are means ± SE ($n = 3$). Values with different superscript letter denotes significant difference between the sample ($p \leq 0.05$).

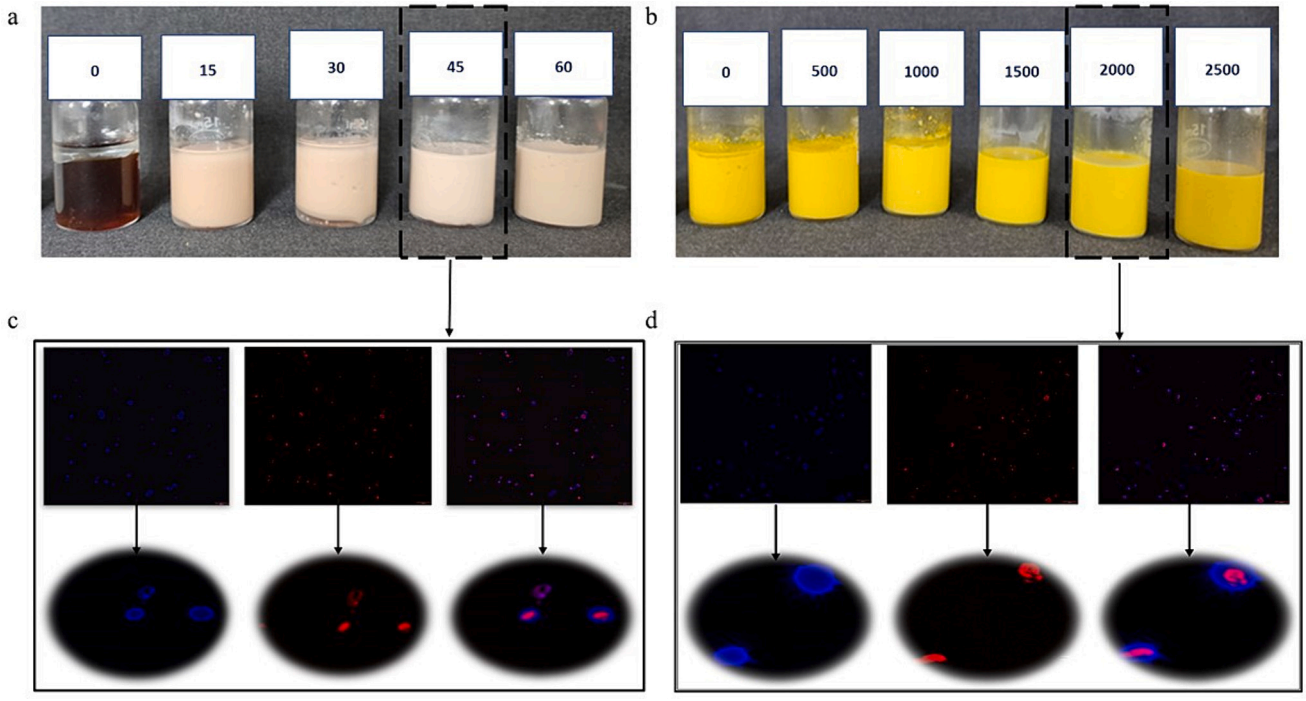

Fig. 5. (a) Formation of lignin emulsion through probe sonication at varying time intervals (0–60 min), (b) Influence of varying LNP concentration (0–2500 ppm) on curcumin and vitamin D3-loaded lignin emulsion, (c) fluorescence microscopy images of LnE (d) fluorescence microscopy images of LnE + Cu + vD_3.

broader application of LNP in food emulsions (Bertolo et al., 2019; Saffarionpour & Diosady, 2022; Winuprasith et al., 2018). This finding is also in accordance with previous research highlighting the role of kraft lignin in stabilizing O/W emulsions (Czaikoski et al., 2020).

3.2.2. Color analysis of emulsions

The color analysis further revealed distinctions in LnE and LnE + Cu + vD_3 (Table 1). Notably, the color values revealed that emulsions formulated with curcumin and vitamin D_3 exhibited a vibrant yellow hue, as evidenced by a substantial increase in the b* value. Specifically, the b* value rose from 13.53 ± 0.092 in LnE to 59.91 ± 0.716 in LnE + Cu + vD_3, a change attributed to the presence of curcumin. The above-mentioned differences in color, particle size and zeta potential data indicated that the presence of curcumin and vitamin D_3 in the oil phase actually brought about positive impact on LNP-stabilized emulsions (Heger et al., 2014; Kharat et al., 2017).

3.2.3. Viscometrical and rheological behaviour of optimized emulsions

To understand the rheological characteristics of an emulsion stabilized by lignin, we compare the rheological behaviors of two emulsions: LnE and LnE + Cu + vD_3.The curves for LnE and LnE + Cu + vD_3 are illustrated in Fig. 6a-c. The viscosity-shear rate graph in Fig. 6a reveals that both LnE and LnE + Cu + vD_3 exhibit shear-thinning behaviour, with viscosities decreasing as the shear rate increases. Specifically, the viscosity of LnE decreases from 6.94 to 0.0054 Pa.s as the shear rate varies from 0.01 to 20 s^{-1}, while for LnE + Cu + vD_3, it drops from 13.1 Pa.s to 0.00315 Pa.s over the same shear rate range. Notably, the decrease in viscosity values indicates that LnE + Cu + vD_3 is more susceptible to applied shear-induced deformation than LnE. This heightened susceptibility of LnE + Cu + vD_3 to shear-induced deformation, resulting in a more pronounced viscosity decrease compared to LnE, can be attributed to the impact of the added components Cu and vD_3. The presence of Cu and vD_3 likely alters the interfacial properties of the LNP-stabilized O/W emulsion droplets, potentially promoting droplet coalescence or disrupting the overall emulsion structure under shear forces. The pronounced shear-thinning behaviour observed in Pickering emulsions, indicative of weak associative interactions within the drop network structure, aligns with similar findings reported by Zhao et al., 2023.

The linear visco-elastic regions (LVE) of LnE and LnE + Cu + vD_3 are presented in Fig. 6b. In LnE, the G' (storage modulus) consistently exceeded G" (loss modulus) at higher strains, indicating a solid-like behaviour without a crossover between G' and G". Similarly, LnE + Cu + vD_3 showed a distinct trend with G' consistently surpassing G" across the entire strain range. The persistent G' dominance in LnE + Cu + vD_3 implies sustained solid-like behaviour and non-crossover of G' and G" in both LnE and LnE + Cu + vD_3 for stability assessment. The enhanced elastic property of LnE + Cu + vD_3 is attributed to the interface-stabilizing effect of lignin particle, curcumin and vitamin D_3. This, along with the reported G' dominance, implies a prolonged solid-like structure, enhancing stability of O/W emulsions against droplet coagulation or aggregation during storage (Kavya et al., 2023).

The frequency sweep results for LnE and LnE + Cu + vD_3 are presented in Fig. 6c. LnE consistently exhibited G' > G" across the applied frequency range, with no noticeable responses observed with an increase in frequency. Similarly, LnE + Cu + vD_3 showed G' > G", and there was no crossover between G' and G" values. The elasticity values of LnE + Cu + vD_3 were higher than those of LnE. These findings suggest that the lignin solution and the added components Cu and vD_3 in LnE + Cu + vD_3 retained their solid-like characteristics to a greater extent under non-destructive strain for a longer duration compared to LnE alone. This effect has been documented in this studies (Sannya and Nisha, 2022; Zhao et al., 2022) suggesting that the presence of Cu and vD_3 contributes to the prevention of droplet coagulation.

3.2.4. Molecular level of interactions among the components of emulsions

The FT-IR spectra of the Ln (lignin solutions), sunflower oil, curcumin (Cu), vitamin D_3 (vD_3), LnE and LnE + Cu + vD_3 are presented in Fig. 6d. The broad peaks in the range of 3600–3000 cm^{-1} in LnE + Cu + vD_3 correspond to OH bonds in carboxylic acid and free OH stretching bonds. These OH stretching vibrations indicates inter- or intra-molecular hydrogen bonds. In sunflower oil, a main peak was observed in the region 3000—2800 cm^{-1}. The bands in this region could be assigned to the symmetrical and asymmetrical C—H stretching vibration of the CH_2 and CH_3 aliphatic groups due to the alkyl residue of triglycerides (Bunaciu et al., 2022).

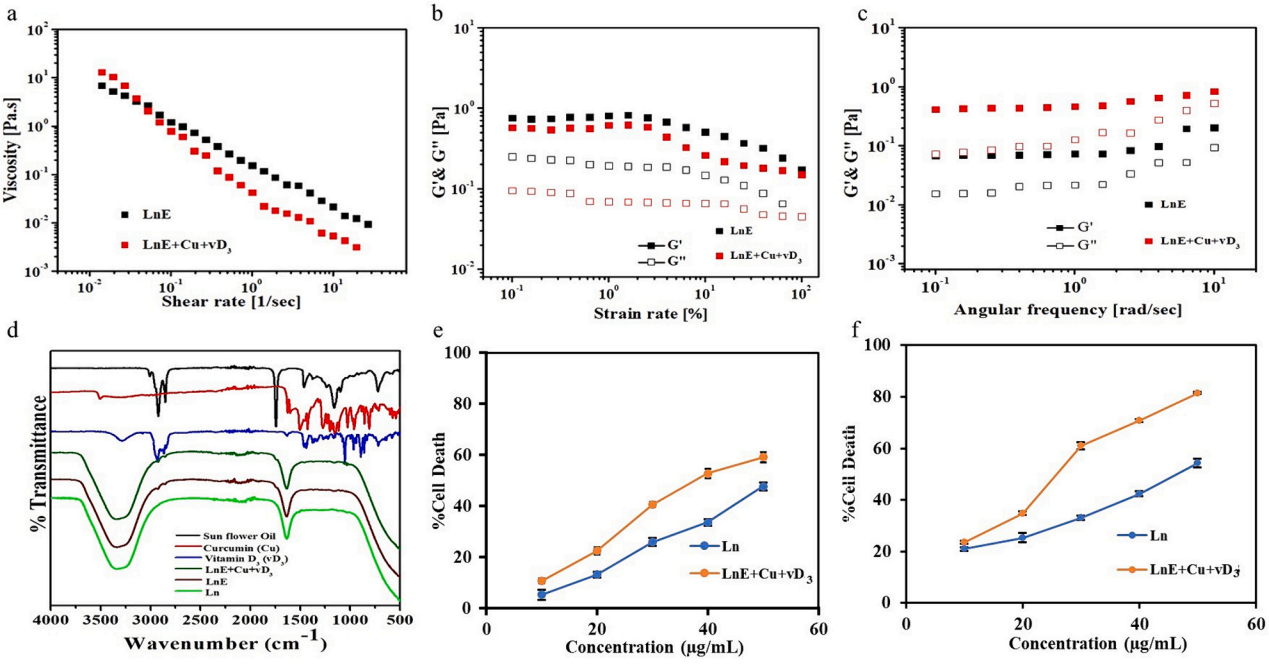

Fig. 6. (a) Viscosity curve, (b) amplitude sweep, (c) frequency sweep of LnE and LnE + Cu + vD_3, (d) FTIR analysis of lignin emulsions, (e) Analysis of toxicity of emulsion (Ln/ LnE + Cu + vD_3) against L6 (f) Analysis of toxicity of emulsion (Ln/ LnE + Cu + vD_3) against RAW264 respectively.

The main peak corresponding to the symmetrical and asymmetrical C—H stretching vibrations of the CH_2 and CH_3 aliphatic groups in sunflower oil is absent in both LnE and LnE + Cu + vD_3, suggesting the effective encapsulation of sunflower oil by lignin in these emulsions. Moreover, the FT-IR spectra showed characteristic bands for curcumin at 1438 (olefinic C—H bending vibration), 1510 (C═C vibrations), as well as 1597 and 1674 cm^{-1} (C—O stretching) (Nandiyanto et al., 2017). In the case of vitamin D_3, the peaks at 2935 and 2874 cm^{-1} were related to alkyl C—H stretch. Several other C—H linkages were observed in the range of 1052–1460 cm^{-1} on the spectrum vitamin D_3. The peak around 1460 cm^{-1} was related to C—H vibration bending of the methylene group of vitamin D_3 (Hasanvand et al., 2018; Klapiszewski et al., 2013). Notably, in LnE + Cu + vD_3, the main characteristic peaks of curcumin and vitamin D_3 were not observed, indicating their encapsulation within the emulsion. These findings collectively underscored that the sunflower oil, curcumin, and vitamin D_3 formed the core of the emulsion system and supported the fact that LnE + Cu + vD_3 emulsion was stable. In the context of sunflower oil, the absence of its main characteristic peak in LnE and LnE + Cu + vD_3 suggested that sunflower oil was fully covered by lignin in these emulsions. Additionally, the absence of characteristic peaks of curcumin and vitamin D_3 in LnE + Cu + vD_3 confirmed the effective encapsulation of these bioactive compounds in the emulsion. These findings showed that this Pickering emulsion could be used a carrier for the delivery of these functional ingredients.

The encapsulation efficiency (EE) of curcumin and vitamin D_3 in the LnE + Cu + vD_3 are 87.95 ± 0.21% and 72.66 ± 0.11% respectively (supplementary Fig. 2). In the absence of lignin as Pickering particle, the EE of curcumin and vitamin D_3 decreased to 30.43 ± 0.01% and 17.19 ± 0.03%. These results suggested that an LNP-based emulsion could encapsulate and protect these bioactive compounds.

3.3. Toxicity

To ensure biological safety, the toxicity of lignin solution (Ln) and the lignin emulsion (LnE + Cu + vD_3) against L6 and RAW264.7 cell lines was assessed by MTT assay. The results (Fig. 6 e, f) showed that Ln at the highest concentration (50 μg/mL) induced 59.06% and 81.51% cell death in L6 and RAW264.7 cells, respectively. Meanwhile, cells treated with 50 μg/mL of LnE caused the death of 47.78% of L6 cells and 54.27% of RAW 264.7 cells. The IC_{50} values for Ln and LnE + Cu + vD_3 against L6 myoblast cells were as 58.68 ± 1.18 μg/mL and 37.43 ± 0.67 μg/mL, respectively. Whereas, the IC_{50} values for Ln and LnE + Cu + vD3 against RAW264.7 cell lines were 46.62 ± 0.78 μg/mL and 28.49 ± 0.23 μg/mL, respectively. The cytotoxicity of lignin was low below 0.5% *w*/w concentration which ensued in a dose-response relationship, for HT-29 cells and Caco-2 cells (Czaikoski et al., 2020). Recent research has also reported a similarly low vitro cytotoxicity of lignin at low concentrations (0.1 mg/mL) (Yu et al., 2023).

3.4. Storage stability of Pickering emulsion

Storage stability of emulsions is an important parameter that determines their suitability in potential applications. We assessed the storage stability of the LnE + Cu + vD3 emulsion by measuring the creaming index, particle size, zeta potential, and color at both room temperature (27 ± 2 °C) and refrigerated temperature (4 ± 2 °C) over a period of 90 days. The results are presented in Fig. 7a-c. The images provided in Supplementary Fig. 3.

Creaming index indicates the degree of stability of emulsions. There was no significant variation in the creaming index data during the entire storage period at both the condition. This observation indicated that the LNP produced Pickering emulsions could with stand potential coagulation and instability (Mirhosseini et al., 2008). This observation also complemented the overall resilience of the emulsion structure, as

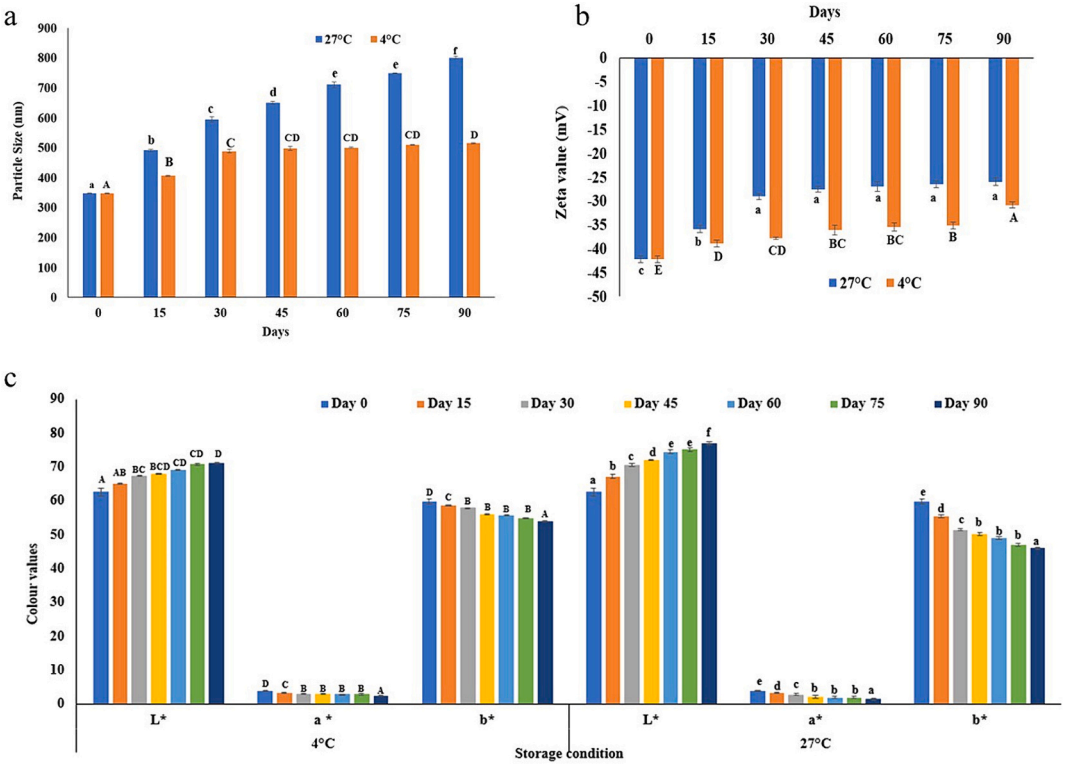

Fig. 7. (a) Particle size (b) zeta potential of LnE + Cu + vD_3 during storage (c) color values of LnE + Cu + vD_3 during storage. The results are presented as mean ± standard deviation. Small letters indicate significant differences at 27 °C, while capital letters signify significant differences at 4 °C between the interval days ($p < 0.05$).

evidenced by size, zeta potential, and color. The particle size of the emulsion increased substantially over time at room temperature, indicating a trend toward destabilization. However, the absence of phase separation in this case to indicted that the stability of the emulsion was not compromised. The increase of particle size in refrigerated emulsion was slow and gradual highlighting better stability compared to when stored at room temperature. This observation aligns with the broader understanding in emulsion science that lower temperatures are more suitable for better stability (Chen et al., 2021). Simultaneously, the zeta potential values, reflecting the repulsive forces between particles, showed a decreasing trend over time at room temperature, in line with the particle size, and hinted at higher likelihood of phase separation. The zeta potential of the emulsion on 90th day at room temperature was -25.98 ± 0.51 mV while it was -30.87 ± 0.57 mV when stored at refrigerated condition. The fact that the magnitude of zeta potential of emulsion stored at room temperature for 90 days was still high supported the fact that no phase separation was observed in it. The samples stored under refrigeration maintained consistently higher zeta potential values, refrigeration temperature is conducive for storage stability of Pickering emulsions produced using LNP. These findings also showed that particle size and zeta potential greatly affected the stability of the LnE + Cu + vD_3 emulsion. The extended 90-day stability of emulsions stabilized by LNP, despite its relatively hydrophilic nature as indicated by a 70° contact angle, could be attributed to several key factors. These include the stabilization enhancements through surface modifications and functionalization of LNP, derived from their polyherbal spent source, to improve compatibility with the oil phase. This enabled adjustment of optimal oil-to-water ratio in the emulsion formulation (Zembyla et al., 2020). Additionally, the small and uniform particle size of LNP offerred a protective effect against droplet coalescence. Its interactions with encapsulated curcumin and vitamin D_3 further contributed to the emulsion's stability. Chen et al., 2021 also reported that the shape and droplet diameter of lignin-stabilized emulsion remained unchanged upon 30 days of storage. Among the different types of lignin, the authors observed that kraft lignin had lower storage stability when stored for 28 days which was due to the presence of different functional groups (Czaikoski et al., 2020). Our findings are akin to those of earlier studies that colloidal systems of nanosized lignin were stable when the zeta potential values ranged between −35.1 mV and − 32.4 mV (Bertolo et al., 2019).

The color parameters (L*a*b*) of LnE + Cu + vD_3 at the room and refrigerated storage temperatures are presented in Fig. 7c. At room temperature, significant changes in color were observed over time, indicating the degradation of curcumin in the emulsion due to its inherent sensitivity at ambient temperatures. The degradation of curcumin at elevated temperatures, indicated by a change in color, have also been reported in the literature (Kharat et al., 2017). In contrast, refrigerated conditions exhibited a notable color stability as there was only slight decrease in the b* values upon 90 days of storage. This finding suggests that under refrigeration temperatures, the LNP stabilized Pickering emulsion system effectively preserves the color integrity of curcumin and vitamin D_3. The observed stability resulted from the encapsulation of bioactives within the lipid droplets and their covering by LNP, providing a protective environment. In essence, these results indicated that the LnE + Cu + vD_3 had desirable stability both at room and refrigeration temperatures, although the room temperature had destabilizing tendency. Storing these LnE + Cu + vD_3 emulsion at refrigeration condition was conducive in terms of its minimal impact on particle size, zeta potential and color stability.

4. Conclusion

The valorization of lignin from dashamoola spent material (DSM) in the ayurvedic industry is important from a sustainability perspective, given lignin's enormous potential for food applications. Lignin nanoparticles (LNP) were produced from DSM aiming to use them as Pickering particles and further applying them to produce Pickering O/W emulsions. LNP with sufficiently high absolute value of zeta potential and sufficiently low particle size were synthesized. The findings of this study showed that stable Pickering emulsions incorporating curcumin and vitamin D_3 (LnE + Cu + vD_3) could be produced using LNP as Pickering particles. The particle size, zeta potential and curcumin stability were reasonable at room temperature and highly stable at refrigerated temperature for 90 days. Curcumin and vitamin D_3 remained fully encapsulated in the oil phase and had no effect on the emulsion stability LNP network at the oil-water interface. The encapsulation efficiency of bioactives in this emulsion system was also quite high (curcumin: $87.95 \pm 0.21\%$, vitamin D_3: $72.66 \pm 0.11\%$). Therefore, this study offers an easy-to-implement valorization pathway for DSM that can enhance the ayurvedic industry's economic performance. The LNP are expected to find greater applications in food industry in the future as emulsifiers.

Supplementary data to this article can be found online at https://doi.org/10.1016/j.foodchem.2024.140284.

CRediT authorship contribution statement

Billu Abraham: Writing – original draft, Methodology, Investigation, Data curation, Conceptualization. **Heeba Shakeela:** Writing – original draft, Data curation. **Leena P. Devendra:** Methodology, Investigation. **K.B. Arun:** Validation, Investigation, Data curation. **K. Vasanth Ragavan:** Conceptualization, Funding acquisition, Methodology, Project administration, Resources, Supervision, Writing – review & editing. **Charles Brennan:** Investigation. **Nitin Mantri:** Investigation. **Benu Adhikari:** Writing – review & editing, Validation, Supervision. **P. Nisha:** Conceptualization, Funding acquisition, Methodology, Project administration, Resources, Supervision, Writing – review & editing.

Declaration of competing interest

The authors declare no conflict of interest.
The authors declare that there are no conflicts of interest

Data availability

Data will be made available on request.

Acknowledgments

The authors wish to thank CSIR-NIIST and RMIT for providing facilities. And providing fellowship to the first author. Special thanks to Dr. T.S. Madhavankutty, Mr. Rajesh S Mony and Mr. Harikrishnan of M/s. Arya Vaidya Sala, Kottakkal (AVS: Kerala, India), for technical support and providing the spent materials for this work. The authors also acknowledge the Department of Science and Technology, Government of India, for partially funding the project. We are thankful to Kiran Mohan for assistance in TEM and Kavya Mohan for rheology related tests.

References

Abraham, B., Reshmitha, T. R., Navami, M. M., George, L., Venugopalan, V. V., & Nisha, P. (2020). Phytochemical rich extract from the spent material generated from industrial Dashamoola preparation (a medicinal Ayurvedic decoction) with antioxidant, antidiabetic and anti-inflammatory potential. *Industrial Crops and Products, 151*, Article 112451. https://doi.org/10.1016/j.indcrop.2020.112451

Abraham, B., Syamnath, V. L., Arun, K. B., Zahra, P. F., Anjusha, P., Kothakotta, A., & Nisha, P. (2023). Lignin-based nanomaterials for food and pharmaceutical applications: Recent trends and future outlook. *Science of the Total Environment, 881*, Article 163316. https://doi.org/10.1016/j.scitotenv.2023.163316

Ahsan, H., Parveen, N., Khan, N. U., & Hadi, S. M. (1999). Pro-oxidant, anti-oxidant and cleavage activities on DNA of curcumin and its derivatives demethoxycurcumin and bisdemethoxycurcumin. *Chemico-Biological Interactions, 121*(2), 161–175. https://doi.org/10.1016/S0009-2797(99)00096-4

Akhil, G. H., Kariyil, B. J., Akshatha, G. D., Bhatt, S. V., Dhanusha, G., & John, R. (2020). Germinated seeds of Hordeum vulgare target extrinsic pathway of apoptosis in triple-negative breast cancer cells. *Pharmacognosy Magazine, 16*(Suppl. 3), S531–S539. https://doi.org/10.4103/pm.pm_123_20

Ames, B. N., Grant, W. B., & Willett, W. C. (2021). Does the high prevalence of vitamin D deficiency in African Americans contribute to health disparities? *Nutrients, 13*(2), 499. https://doi.org/10.3390/nu13020499

Anand, P., Thomas, S. G., Kunnumakkara, A. B., Sundaram, C., Harikumar, K. B., Sung, B., … Aggarwal, B. B. (2008). Biological activities of curcumin and its analogues (congeners) made by man and mother nature. *Biochemical Pharmacology, 76*(11), 1590–1611. https://doi.org/10.1016/j.bcp.2008.08.008

Bai, L., Lv, S., Xiang, W., Huan, S., McClements, D. J., & Rojas, O. J. (2019). Oil-in-water Pickering emulsions via microfluidization with cellulose nanocrystals: 1. *Formation and stability. Food Hydrocolloids, 96*, 699–708. https://doi.org/10.1016/j.foodhyd.2019.04.038

Balakshin, M. Y., Capanema, E. A., & Chen, & Gracz, H. S.. (2003). Elucidation of the structures of residual and dissolved pine Kraft lignins using an HMQC NMR technique. *Journal of Agricultural and Food Chemistry, 51*(21), 6116–6127. https://doi.org/10.1021/jf034372d

Bertolo, M. R., de Paiva, L. B. B., Nascimento, V. M., Gandin, C. A., Neto, M. O., Driemeier, C. E., & Rabelo, S. C. (2019). Lignins from sugarcane bagasse: Renewable source of nanoparticles as Pickering emulsions stabilizers for bioactive compounds encapsulation. *Industrial Crops and Products, 140*, Article 111591. https://doi.org/10.1016/j.indcrop.2019.111591

Bunaciu, A. A., Fleschin, S., & Aboul-Enein, H. Y. (2022). Detection of sunflower oils adulteration by ATR-FTIR spectra. *Chemical Papers, 76*(9), 5533–5539. https://doi.org/10.1007/s11696-022-02245-6

Chen, K., Qian, Y., Wang, C., Yang, D., Qiu, X., & Binks, B. P. (2021). Tumor microenvironment-responsive, high internal phase Pickering emulsions stabilized by lignin/chitosan oligosaccharide particles for synergistic cancer therapy. *Journal of Colloid and Interface Science, 591*, 352–362. https://doi.org/10.1016/j.jcis.2021.02.012

Czaikoski, A., Gomes, A., Kaufmann, K. C., Liszbinski, R. B., de Jesus, M. B., & da Cunha, R. L. (2020). Lignin derivatives stabilizing oil-in-water emulsions: Technological aspects, interfacial rheology and cytotoxicity. *Industrial Crops and Products, 154*, Article 112762. https://doi.org/10.1016/j.indcrop.2020.112762

Devendra, L. P., & Sukumaran, R. K. (2023). Comparative evaluation of lignin derived from different sugarcane bagasse pretreatments in the synthesis of wood adhesive. *Bioenergy Research, 16*(1), 151–162. https://doi.org/10.1007/s12155-022-10450-0

Gabov, K., Gosselink, R. J., Smeds, A. I., & Fardim, P. (2014). Characterization of lignin extracted from birch wood by a modified hydrotropic process. *Journal of Agricultural and Food Chemistry, 62*(44), 10759–10767. https://doi.org/10.1021/jf5037728

Goldmann, W. M., Ahola, J., Mankinen, O., Kantola, A. M., Komulainen, S., Telkki, V. V., & Tanskanen, J. (2016). *Determination of phenolic hydroxyl groups in technical lignins by ionization difference ultraviolet spectrophotometry (Δ ε-IDUS method)*. https://doi.org/10.3311/PPch.9269

Gomide, R. A. C., de Oliveira, A. C. S., Rodrigues, D. A. C., de Oliveira, C. R., de Assis, O. B. G., Dias, M. V., & Borges, S. V. (2020). Development and characterization of lignin microparticles for physical and antioxidant enhancement of biodegradable polymers. *Journal of Polymers and the Environment, 28*, 1326–1334. https://doi.org/10.1007/s10924-020-01685-z

Gordobil, O., Herrera, R., Yahyaoui, M., İlk, S., Kaya, M., & Labidi, J. (2018). Potential use of Kraft and organosolv lignins as a natural additive for healthcare products. *RSC Advances, 8*(43), 24525–24533. https://doi.org/10.1039/C8RA02255K

Hasanvand, E., Fathi, M., & Bassiri, A. (2018). Production and characterization of vitamin D 3 loaded starch nanoparticles: Effect of amylose to amylopectin ratio and sonication parameters. *Journal of Food Science and Technology, 55*, 1314–1324. https://doi.org/10.1007/s13197-018-3042-0

Heger, M., van Golen, R. F., Broekgaarden, M., & Michel, M. C. (2014). The molecular basis for the pharmacokinetics and pharmacodynamics of curcumin and its metabolites in relation to cancer. *Pharmacological Reviews, 66*(1), 222–307. https://doi.org/10.1124/pr.110.004044

Hossain, K. M. Z., Deeming, L., & Edler, K. J. (2021). Recent progress in Pickering emulsions stabilised by bioderived particles. *RSC Advances, 11*(62), 39027–39044. https://doi.org/10.1039/D1RA08086E

Huimin, X., Lin, L., Shilin, G., Elfalleh, W., Shenghua, H., Qinghai, S., & Ying, M. (2014). Formation, stability, and properties of an algae oil emulsion for application in UHT milk. *Food and Bioprocess Technology, 7*, 567–574. https://doi.org/10.1007/s11947-013-1054-3

Ilie, P. C., Stefanescu, S., & Smith, L. (2020). The role of vitamin D in the prevention of coronavirus disease 2019 infection and mortality. *Aging Clinical and Experimental Research, 32*(7), 1195–1198. https://doi.org/10.1007/s40520-020-01570-8

Jiang, F., & Hsieh, Y. L. (2015). Holocellulose nanocrystals: Amphiphilicity, oil/water emulsion, and self-assembly. *Biomacromolecules, 16*(4), 1433–1441. https://doi.org/10.1021/acs.biomac.5b00240

Karthyani, S., Pandey, A., & Devendra, L. P. (2017). Delignification of cotton stalks using sodium cumene sulfonate for bioethanol production. *Biofuels, 11*, 431–440. https://doi.org/10.1080/17597269.2017.1370884

Kavya, M., Jacob, A. R., & Nisha, P. (2023). Pectin emulsions and emulgels: Bridging the correlation between rheology and microstructure. *Food Hydrocolloids, 143*, Article 108868. https://doi.org/10.1016/j.foodhyd.2023.108868

Kharat, M., Du, Z., Zhang, G., & McClements, D. J. (2017). Physical and chemical stability of curcumin in aqueous solutions and emulsions: Impact of pH, temperature, and molecular environment. *Journal of Agricultural and Food Chemistry, 65*(8), 1525–1532. https://doi.org/10.1021/acs.jafc.6b04815

Klapiszewski, Ł., Nowacka, M., Milczarek, G., & Jesionowski, T. (2013). Physicochemical and electrokinetic properties of silica/lignin biocomposites. *Carbohydrate Polymers, 94*(1), 345–355. https://doi.org/10.1016/j.carbpol.2013.01.058

Li, X., Shen, J., Wang, B., Feng, X., Mao, Z., & Sui, X. (2021). Acetone/water cosolvent approach to lignin nanoparticles with controllable size and their applications for Pickering emulsions. *ACS Sustainable Chemistry & Engineering, 9*(15), 5470–5480. https://doi.org/10.1021/acssuschemeng.1c01021

McClements, D. J. (2015). *Food emulsions: principles, practices, and techniques. CRC press*. https://doi.org/10.1201/9781420039436

McClements, D. J., Bai, L., & Chung, C. (2017). Recent advances in the utilization of natural emulsifiers to form and stabilize emulsions. *Annual Review of Food Science and Technology, 8*, 205–236. https://doi.org/10.1146/annurev-food-030216-030154

Mirhosseini, H., Tan, C. P., Hamid, N. S., & Yusof, S. (2008). Effect of Arabic gum, xanthan gum and orange oil contents on ζ-potential, conductivity, stability, size index and pH of orange beverage emulsion. *Colloids and Surfaces A: Physicochemical and Engineering Aspects, 315*(1–3), 47–56. https://doi.org/10.1016/j.colsurfa.2007.07.007

Mosmann, T. (1983). Rapid colorimetric assay for cellular growth and survival: Application to proliferation and cytotoxicity assays. *Journal of Immunological Methods, 65*(1–2), 55–63. https://doi.org/10.1016/0022-1759(83)90303-4

Mou, H. Y., Heikkilä, E., & Fardim, P. (2013). Topochemistry of alkaline, alkaline-peroxide and hydrotropic pretreatments of common reed to enhance enzymatic hydrolysis efficiency. *Bioresource Technology, 150*, 36–41. https://doi.org/10.1016/j.biortech.2013.09.093

Moustaqim, E. L. M., El Kaihal, A., El Marouani, M., Men-La-Yakhaf, S., Taibi, M., Sebbahi, S., … Kifani-Sahban, F. (2018). Thermal and thermomechanical analyses of lignin. *Sustainable Chemistry and Pharmacy, 9*, 63–68. https://doi.org/10.1016/j.scp.2018.06.002

Nagarkar, B., Jagtap, S., Narkhede, A., Nirmal, P., Pawar, N., Kuvalekar, A., Kulkarni, O., & Harsulkar, A. (2013). Different Ayurvedic dosage forms of Dashamoola possess varied anti-inflammatory activity. *World J Pharm Pharmaceutic Sci, 2*, 3118–3136.

Nandiyanto, A. B. D., Wiryani, A. S., Rusli, A., Purnamasari, A., Abdullah, A. G., Widiaty, I., & Hurriyati, R. (2017). Extraction of curcumin pigment from Indonesian local turmeric with its infrared spectra and thermal decomposition properties. *In IOP Conference Series: Materials Science and Engineering, 180*(1), Article 012136. https://doi.org/10.1088/1757-899X/180/1/012136

Pandian, B., Ramalingam, S., Sreeram, K. J., & Rao, J. R. (2021). Natural pigment: Preparation of brown pigment from lignin biomass for coloring application. *Dyes and Pigments, 195*, Article 109704. https://doi.org/10.1016/j.dyepig.2021.109704

Pradyawong, S., Shrestha, R., Li, P., Sun, X. S., & Wang, D. (2022). Effect of pH and pH-shifting on lignin–protein interaction and properties of lignin-protein polymers. *Journal of Polymers and the Environment, 1-12*. https://doi.org/10.1016/j.dyepig.2021.109704

Ragauskas, A. J., & Yoo, C. G. (2018). Advancements in biomass recalcitrance: The use of lignin for the production of fuels and chemicals. *Frontiers in Energy Research, 6*, 118. https://doi.org/10.3389/fenrg.2018.00118

Rahman, U. R. O., Shi, S., Ding, J., Wang, D., Ahmad, S., & Yu, H. (2018). Lignin nanoparticles: Synthesis, characterization and corrosion protection performance. *New Journal of Chemistry, 42*(5), 3415–3425. https://doi.org/10.1039/C7NJ04103A

Randive, D. S., Adnaik, R. S., Nalawade, P. P., & Patil, A. M. (2014). Studies on standardization parameters for marketed formulations of draksharishtha. *International Journal of Pharma and Bio Sciences, 3*(4), 397–401.

Rattis, B. A., Ramos, S. G., & Celes, M. (2021). Curcumin as a potential treatment for COVID-19. *Frontiers in Pharmacology, 1068*. https://doi.org/10.3389/fphar.2021.675287

Ruiz, R., & Ehrman, T. (1996). Determination of carbohydrates in biomass by high performance liquid chromatography. *Laboratory analytical procedure, 2*.

Saffarionpour, S., & Diosady, L. L. (2022). Curcumin, a potent therapeutic nutraceutical and its enhanced delivery and bioaccessibility by Pickering emulsions. *Drug Delivery and Translational Research, 1-34*. https://doi.org/10.1007/s13346-021-00936-3

Sathyan, S., & Nisha, P. (2022). Optimization and characterization of porous starch from corn starch and application studies in emulsion stabilization. *Food and Bioprocess Technology, 15*(9), 2084–2099. https://doi.org/10.1007/s11947-022-02843-y

Schneider, W. D. H., Dillon, A. J. P., & Camassola, M. (2021). Lignin nanoparticles enter the scene: A promising versatile green tool for multiple applications. *Biotechnology Advances, 47*, Article 107685. https://doi.org/10.1016/j.biotechadv.2020.107685

Si, S., Chen, Y., Fan, C., Hu, H., Li, Y., Huang, J., & Tu, Y. (2015). Lignin extraction distinctively enhances biomass enzymatic saccharification in hemicelluloses-rich Miscanthus species under various alkali and acid pretreatments. *Bioresource Technology, 183*, 248–254. https://doi.org/10.1016/j.biortech.2015.02.031

Sipponen, M. H., Farooq, M., Koivisto, J., Pellis, A., Seitsonen, J., & Österberg, M. (2018). Spatially confined lignin nanospheres for biocatalytic ester synthesis in aqueous media. *Nature Communications, 9*(1), 2300. https://doi.org/10.1038/s41467-018-04715-6

Sodeinde, K. O., Ojo, A. M., Olusanya, S. O., Ayanda, O. S., Adeoye, A. O., Dada, T. M., & Lawal, O. S. (2021). Cellulose isolated from Delonixregia pods: Characterisation and application in the encapsulation of vitamin A. *Industrial Crops and Products, 160*, Article 113138. https://doi.org/10.1016/j.indcrop.2020.113138

Tarasov, D., Leitch, M., & Fatehi, P. (2018). Lignin–carbohydrate complexes: Properties, applications, analyses, and methods of extraction: A review. *Biotechnology for Biofuels, 11*(1), 1–28. https://doi.org/10.1186/s13068-018-1262-1

Tortora, M., Cavalieri, F., Mosesso, P., Ciaffardini, F., Melone, F., & Crestini, C. (2014). Ultrasound driven assembly of lignin into microcapsules for storage and delivery of hydrophobic molecules. *Biomacromolecules, 15*(5), 1634–1643. https://doi.org/10.1021/bm500015j

Winuprasith, T., Khomein, P., Mitbumrung, W., Suphantharika, M., Nitithamyong, A., & McClements, D. J. (2018). Encapsulation of vitamin D3 in Pickering emulsions stabilized by nanofibrillated mangosteen cellulose: Impact on in vitro digestion and bioaccessibility. *Food Hydrocolloids, 83*, 153–164. https://doi.org/10.1016/j.foodhyd.2018.04.047

Wunna, K., Nakasaki, K., Auresenia, J. L., Abella, L. C., & Gaspillo, P. A. D. (2017). Effect of alkali pretreatment on removal of lignin from sugarcane bagasse. *Chemical Engineering Transactions, 56*, 1831–1836. https://doi.org/10.3303/CET1756306

Yu, M., Xin, H., He, D., Zhu, C., Li, Q., Wang, X., & Zhou, J. (2023). Electrospray lignin nanoparticles as Pickering emulsions stabilizers with antioxidant activity, UV barrier properties and biological safety. *International Journal of Biological Macromolecules, 238*, Article 123938. https://doi.org/10.1016/j.ijbiomac.2023.123938

Yuan, T., Zeng, J., Guo, D., Sun, Q., Wang, B., Sha, L., & Chen, K. (2023). Multiphasic lignocellulose-based suspension for oil-water interfacial stabilization: Synergistic adsorption and phase behavior. *International Journal of Biological Macromolecules, 224*, 1142–1151. https://doi.org/10.1016/j.ijbiomac.2022.10.198

Zahedipour, F., Hosseini, S. A., Sathyapalan, T., Majeed, M., Jamialahmadi, T., Al-Rasadi, K., … Sahebkar, A. (2020). Potential effects of curcumin in the treatment of COVID-19 infection. *Phytotherapy Research, 34*(11), 2911–2920. https://doi.org/10.1002/ptr.6738

Zembyla, M., Murray, B. S., & Sarkar, A. (2020). Water-in-oil emulsions stabilized by surfactants, biopolymers and/or particles: A review. *Trends in Food Science & Technology, 104*, 49–59. https://doi.org/10.1016/j.tifs.2020.07.028

Zhao, X., Yang, X., Bao, Y., Guo, Y., Luo, J., Jiang, S., & Zhang, W. (2023). Construction of vitamin D delivery system based on pine nut oil Pickering emulsion: Effect of phenols. *Journal of the Science of Food and Agriculture, 103*(8), 4034–4046. https://doi.org/10.1002/jsfa.12363

Zou, T., Sipponen, M. H., & Osterberg, M. (2019). Natural shape-retaining microcapsules with shells made of chitosan-coated colloidal lignin particles. *Frontiers in Chemistry, 22*(7), 370. https://doi.org/10.3389/fchem.2019.00370

Sustainable Food Technology

ROYAL SOCIETY OF CHEMISTRY

PAPER

View Article Online
View Journal

Cite this: DOI: 10.1039/d4fb00378k

Nutrient-rich puffed snacks developed using blended flours and lignin Pickering emulsions containing curcumin and vitamin D_3

Billu Abraham, [abd] Heeba Shakeela,[ab] Pavithra Pathrakadavil Ajayan,[c] Charles Brennan,[d] Nitin Mantri,[d] Benu Adhikari *[de] and Nisha P. *[abd]

This study explores the use of blended flours and fortification with health-promoting compounds to improve the nutritional profile of extruded puffed snacks (EPS). Lignin particles extracted from Ayurvedic spent materials were used to create lignin Pickering emulsions (LPEs) for incorporating the lipophilic compounds, curcumin and vitamin D_3. A blended flour composed of pearl millet, spent coconut, and corn grits was used to replace 80% of the traditionally used corn grits. Fortification was achieved by incorporating LPE containing curcumin and vitamin D_3. Protein content, dietary fiber, texture profiles, and structural integrity of the snacks were evaluated. Compared to a control made solely from corn grits, the EPS with blended flour showed higher protein (13.8%) and dietary fiber (19.2%) contents. However, the increase in protein and fiber content resulted in lower expansion ratios for EPS produced with the blended flour, with or without LPE. The EPS containing LPE had similar hardness, microstructure, fracturability, chewiness, and gumminess as those without LPE. Sensory analysis scores confirmed the acceptability of both EPS and EPS containing LPE. Importantly, the inclusion of LPE enhanced the stability of curcumin (69.0%) and vitamin D_3 (65.7%), highlighting the protective encapsulation effect of lignin particles. This study underscores the potential of lignin-based Pickering emulsions loaded with lipophilic compounds, combined with blended flours, for producing nutrient-rich and health-promoting ready-to-eat snacks through extrusion.

Received 17th December 2024
Accepted 10th February 2025

DOI: 10.1039/d4fb00378k

rsc.li/susfoodtech

Sustainability spotlight

The sustainability goals of this study align with SDG 2 (Zero Hunger), SDG 3 (Good Health and Well-being) and SDG 12 (Responsible Consumption and Production). By utilizing nutrient-dense blended flours and lignin particles derived from agricultural and Ayurvedic waste, the study promotes food waste valorization and a circular economy. Fortifying snacks with curcumin and vitamin D_3 addresses nutritional deficiencies, while producing affordable, shelf-stable, and health-promoting ready-to-eat snacks enhances food security and supports sustainable food innovation.

1. Introduction

Extrusion cooking is a widely used industrial process that applies high pressure, heat, and mechanical force in a short time, resulting in significant transformations in food matrices. This method is effective for producing ready to eat (RTE) snacks with unique textures and flavors. The high-temperature short-time (HTST) nature of extrusion enables rapid cooking and facilitates the production of a wide variety of snack products.[1] However, the intense conditions can also degrade heat-sensitive nutrients like vitamins, essential fatty acids, and bioactive compounds, which poses a challenge in the development of nutritionally fortified snacks.[2]

Fortifying extruded snacks with bioactive and nutritional compounds has become increasingly important because it offers health benefits beyond basic nutrition.[3] Traditional fortification methods typically involve the direct addition of vitamins, minerals, or other bioactive compounds to the food matrix before extrusion. However, these methods often result in significant nutrient losses due to the harsh processing conditions, thereby reducing the effectiveness of fortification.[4] When carried out as a preceding step, microencapsulation protects bioactive compounds like omega-3 fatty acids and probiotics from the detrimental effects of extrusion by creating a protective

[a]Agro Processing and Technology Division, National Institute for Interdisciplinary Science and Technology (CSIR-NIIST), Thiruvananthapuram, Kerala, India. E-mail: pnisha@niist.res.in; Tel: +91 9846777133

[b]Academy of Scientific and Innovative Research (AcSIR), Ghaziabad 201002, India

[c]Department of Food Science and Technology, Kerala University of Fisheries and Ocean Studies (KUFOS), Kerala, India

[d]School of Science, RMIT University, Melbourne, VIC 3083, Australia. E-mail: benu.adhikari@rmit.edu.au; p.nisha@rmit.edu.au; Tel: +61 3 992 59940

[e]Centre for Advanced Materials and Industrial Chemistry (CAMIC), RMIT University, Melbourne, VIC 3001, Australia

barrier, thereby enhancing the nutritional quality of the final product.[5,6] Pickering emulsions that are stabilized by solid particles rather than surfactants have attracted increasing attention as delivery vehicles owing to their higher stability and better ability to protect encapsulated bioactive compounds.[7] Studies have focused on improving the nutritional characteristics of extruded products by incorporating biopolymers, such as inulin and chitosan.[8,9] Incorporating inulin, a prebiotic fiber, into extruded snacks has been shown to enhance dietary fiber content, improve gut health, and boost antioxidant activity, thereby making the snacks nutritionally superior.[8] Another study highlighted the role of chitosan in enhancing the functional properties of proteins, reducing fat absorption during extrusion, and improving the textural attributes of snacks.[9]

Lignin, a natural biopolymer derived from plant cell walls, is gaining attention for its potential to create delivery systems that enhance the bioavailability of encapsulated bioactive compounds.[10,11] A recent study showed that lignin, as a Pickering particle, effectively protects sensitive nutrients like vitamins (*e.g.*, vitamin D_3) and polyphenols (*e.g.*, curcumin) from heat and mechanical degradation, while improving their stability and delivery.[7] Curcumin, a polyphenol found in turmeric, is well-known for its anti-inflammatory, antioxidant, and antimicrobial properties, while vitamin D_3 is essential for calcium absorption and bone health.[12] The combination of these bioactives in lignin-based Pickering emulsions represents a novel approach for fortification, particularly in high temperature processes like extrusion.

Extruded snacks are commonly made using corn flour, which is favored for its high starch content that supports the puffing and expansion processes during extrusion. However, corn-based extruded snacks often lack significant nutritional value, as they are typically low in protein, fiber, and essential micronutrients.[13,14] In developing nutritionally enhanced extruded snacks, the choice of raw materials is of prime importance, and blended flours offer a practical solution.[13] These flour blends typically combine grains, tubers, legumes, and seeds, providing a balanced mix of proteins, carbohydrates, fibers, and micronutrients.[14,15] Ahmed *et al.* demonstrated that twin-screw extrusion can produce granules containing iron and vitamin D_3, using a blend of corn and lentil flours as the carrier matrix. These granules exhibited excellent chemical stability and bioactive effects when tested on human osteoblast cells, suggesting their potential applications for bone health.[14] Grasso reviewed the use of industrial by-products in extruded snacks, emphasizing nutritional and sustainability benefits.[15] These studies highlight the versatility of blended flours in developing nutrient-rich extruded snacks. Spent coconut flour, a by-product of virgin coconut oil production, is rich in dietary fiber, protein, and antioxidants, making it an excellent ingredient to enhance the health benefits of snacks, particularly for gluten-free and vegan consumers.[16] Similarly, pearl millet flour, rich in essential minerals and other nutrients, is derived from a crop known for its drought resilience.[17]

This study aimed to develop fortified extruded puffed snacks (EPS) using blends of pearl millet, corn grits, and spent coconut flour, enriched with LPE-encapsulated curcumin and vitamin D_3. The EPSs were compared to a corn-based control for their physicochemical, textural, and sensory properties. The stability of the encapsulated bioactives (curcumin and vitamin D_3) was also compared to that of the non-encapsulated formulation. This research achieves improved stability of curcumin and vitamin D_3 while creating healthier snacks that contribute to improved micronutrient intake and support better overall nutrition.

2. Materials and methods

2.1. Materials

Lignin was isolated from Ayurvedic spent materials and converted to nano lignin using a planetary mill (Pulverisette, Fritsch, Germany), as reported by Abraham.[7] Spent coconut meal, a by-product of virgin coconut oil processing, was supplied by Apex Coco Solar Energy Pvt. Ltd (Tamil Nadu, India). The residual oil was removed to produce spent coconut flour (SCF). Pearl millet and corn were sourced from the local market in Thiruvananthapuram, cleaned, ground into flour, and sieved through a 200 mm mesh to achieve uniform particle size. Curcumin and cholecalciferol (vitamin D_3) were procured from Sigma-Aldrich Chemicals Pvt. Ltd (Massachusetts, USA). All other chemicals and reagents used in this study were of chromatography grade and were sourced from reliable local suppliers.

2.2. Preparation of O/W Pickering emulsions

Oil-in-water (O/W) Pickering emulsions were formulated using lignin nanoparticles as the stabilizing agent. LNP solution was prepared at a concentration of 2000 ppm at a pH of 8.0. Sunflower oil (10% w/w), containing 50 ppm curcumin and 50 ppm vitamin D_3 was used as the dispersed phase. This emulsion was prepared by sonicating with a VCX-750 Vibra Cell (Sonics & Materials, USA) for 45 min (using a 10 s on/10 s off cycle at 50% amplitude) according to the recent study.[7] The resulting Pickering emulsion (LPE) was used for fortification of the extruded snacks.

2.3. Preparation of extruded snacks

The composition of the flour blend was determined through preliminary trials and contained 15% Spent Coconut Flour (SCF), 65% Pearl Millet Flour (PMF), and 20% Corn Grits (CG) on a w/w basis. This formulation yielded extrudates with sensory and physical properties comparable to the control made with only corn grits. The control, prepared using only corn grit, is referred to as C1, and the product with optimized flour blend is denoted as S1.

This optimised flour blend was subsequently infused with LPE. The resulting LPE infused (which contained curcumin and vitamin D_3 as stated above) extrudates are referred to as S2.

2.4. Extrusion process

The blended flour (S1) was uniformly mixed using a laboratory-scale mixer (Basic Technology Private Ltd, Kolkata, India) and conditioned with 16 ± 1% water to achieve optimal expansion and texture during extrusion cooking. The hydrated flour was equilibrated for 1 h at ambient temperature (30 ± 2 °C) in an airtight container before extrusion. After conditioning, the flour

mixtures were extruded. For all the EPSs, the time and temperature were kept the same.

Extrudates were prepared using a laboratory scale twin screw extruder employing hot extrusion technology (L-TSE, Basic Technology Private Ltd, Kolkata, India). The operating parameters of the extrusion process including screw speed, feed moisture content, and cooking temperature, were optimized through preliminary trials. The extrusion process is illustrated in Fig. 1. Before operation, the extruder was primed, and a 2 mm circular die was attached to the barrel end. The barrel was heated to 105 °C and 80 °C. The screw speed (350 rpm), feeder speed (10 rpm), and cutter speed (70 rpm) were adjusted *via* the main control panel. Once the desired barrel temperature was reached, the optimized flour blend was fed using a semi-automatic feeder, and the extruded product emerged from the die. The extrudates were cut uniformly using a cutter assembly, cooled to room temperature, and promptly packed into pouches. The extrudates were toasted in a conventional oven (Bajaj OTG oven, India) at 160 °C for 3 min. This temperature–time combination was determined through trials. The toasted extruded products were coated with refined sunflower oil and a seasoning agent (Symega Food Ingredients Limited, Cochin, Kerala, India) for sensory appeal.

2.5. Analysis of the physical and functional attributes of extrudates

2.5.1. Proximate composition of flours and extrudates. Moisture, ash, fat, and protein contents were determined according to the procedures outlined by the AOAC.[18] Samples were oven-dried at 105 °C, and then transferred to a desiccator and allowed to cool to room temperature (32.0 ± 2 °C). For determining ash content, the mass of the samples was recorded before and after the ashing step using a muffle furnace (550 °C for 6 h). Protein content was determined using the Micro Kjeldahl method with a nitrogen-to-protein conversion factor of 6.25. The fat content was determined *via* Soxhlet extraction. Total carbohydrate was determined by difference.

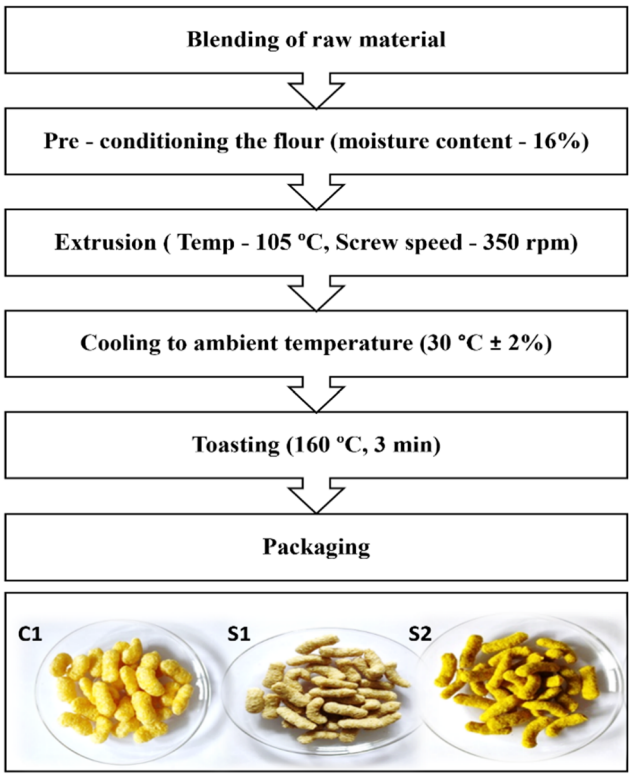

Fig. 1 Flowchart of the extrusion process for producing EPS: C1 – control, S1 – EPS with blended flour, and S2 – EPS with lignin-based Pickering emulsion (LPE) fortification.

2.5.2. Estimation of dietary fiber. The dietary fiber content of EPSs – S1, S2 and C1 – was determined according to the Bureau of Indian Standards Method with a slight modification.[19] Fat- and moisture-free samples were autoclaved with water, the pH was adjusted, and pepsin, pancreatin, and glucoamylase were added. The mixture was then incubated for enzymatic digestion. After incubation, the pretreated extract was centrifuged at 1 118 000 × *g* for 10 min to separate the residue and supernatant. The residue, containing insoluble fiber, was collected, washed three times with acetone and diethyl ether, and lyophilized to obtain a stable weight of insoluble dietary fiber. The supernatant, containing soluble fiber, was precipitated using ethanol and refrigerated overnight. It was then centrifuged (Model 7780; KUBOTA, Tokyo, Japan) again at 1 118 000 × *g* for 10 min, and the resulting residue was collected. This residue was washed three times with alcohol, acetone, and diethyl ether, and then lyophilized in a pilot scale freeze dryer (SP Scientific VirTis Genesis 35L Pilot Lyophilizer, Warminster, USA) to achieve a constant weight, yielding the soluble dietary fiber.[20]

2.5.3. Expansion ratio. The expansion ratio of an EPS was measured by comparing the diameter of the extruded product to that of the die.[21] A digital vernier calliper (0.1 accuracy) was used to measure the diameter of ten randomly selected extrudates, and the mean value was recorded. The expansion ratio of the extrudates was calculated using eqn (1).

$$\mathrm{ER} = \frac{\text{cross sectional diameter of extrudate}}{\text{cross sectional diameter of the die opening}}. \quad (1)$$

2.5.4. Bulk density. The length and diameter of ten EPS samples were measured using a digital vernier caliper. The mass of these 10 EPS samples was also measured. The bulk density was measured using eqn (2) considering they were cylindrical in shape.[22]

$$\text{Bulk density (g cm}^{-3}) = 4m/(\pi d^2 L). \quad (2)$$

where, L is the length (cm), m is the mass (g) and d is the diameter (cm) of the extruded snacks, respectively.

2.5.5. Colour analysis. The colour parameters of the EPS were measured using a colorimeter (Hunter lab, Colour Flex EZ, Virginia, USA). The empty cuvette was calibrated initially using standard white and black plates. The hue of the samples was assessed on the L^* (lightness), a^* (red-green), and b^* (yellow-blue) colour systems. To measure the color values, the extruded products were pulverized and transferred into cylindrical glass sample cuvettes, which were then placed in the

sample port. The color values were recorded after 10 rotations of each sample, with measurements taken in triplicate.[23]

2.5.6. Texture analysis. The textural properties of extrudates were analyzed using a texture analyzer (TA. XT texture analyzer, Stable Microsystems, Surrey, England). Texture profile analysis (Stable Microsystems) was employed to measure properties such as hardness, gumminess, chewiness, fracturability. A 2 mm cylindrical probe was used in these measurements. The tests were carried out in compression mode using the following parameters: pre-test speed: 1 mm s^{-1}, post-test speed: 5 mm s^{-1}, test speed: 1 mm s^{-1}, trigger force: 5 g, and distance (compression): 10 mm. The texture of EPSs was analyzed at three different positions of the sample, and each sample was tested in triplicate.

2.5.7. Sensory analysis. Sensory analysis was conducted to evaluate the acceptability of extrudate snacks. A semi trained panel of 25 members, aged 25 to 45, assessed the samples based on appearance, color, aroma, taste, and overall acceptance. Panelists were instructed to focus on one attribute at a time and cleanse their palate with water between samples to prevent cross-sensory contamination. Participants were encouraged to provide candid feedback based on their overall sensory experience. A 9-point hedonic scale was used for the evaluation, with scores ranging from 1 ('dislike extremely'), 5 ('neither like nor dislike'), and 9 ('like extremely'), following the guidelines of ISO 4121:2003. The average score across all criteria was calculated to determine the sensory attributes.[24]

2.5.8. Cross-sectional microscopic images. The microstructure of the EPS was observed using an Olympus CX41 microscope (Olympus, Shinjuku, Tokyo, Japan). Images of the surface morphology of the extrudates were captured at 4× magnification using a camera attached to the microscope and equipped with QCapture software (QImaging).

2.5.9. Observing microscopic morphology. The EPSs were sliced and mounted onto an aluminum specimen holder using carbon tape. Prior to microscopic examination, a thin layer of gold was applied using a gold/palladium sputter coater (SC7620, Emitech, Quorum Technologies Ltd, Kent, UK). Scanning electron microscopy (ZEISS; EVO 18, Germany) was used to acquire and analyse the microscopic surface morphology of the extruded samples. The instrument operated at an accelerating voltage of 15 kV. Micrographs were captured at 500× magnification.

2.5.10. Stability of curcumin and vitamin D_3. The bioactive stability, representing the percentage retention of curcumin and vitamin D_3 in the extruded product, was determined using high-performance liquid chromatography with a diode-array detector (HPLC-DAD). For the analysis, 1 g of powdered EPS was mixed with 5 mL of methanol and magnetically stirred for 3 h. The methanolic extract was centrifuged at 1 118 000 × *g* for 10 min, and the supernatant was collected and filtered through a 0.22 μm PTFE syringe filter. The HPLC analysis was performed as previously described by the authors.[7] Briefly, a Prominence UFLC system (Shimadzu, Japan) was used, equipped with a Phenomenex Gemini C18 column (250 × 4.6 mm, 5 μm). The system operated with an isocratic flow of 100% methanol at a rate of 1 mL min^{-1}, with detection wavelengths of 420 nm for curcumin and 261 nm for vitamin D_3. Retention times for curcumin and vitamin D_3 were 3.2 min and 7.6 min, respectively. The column temperature was maintained at 40 °C throughout the analysis.

2.6. Statistical analysis

Experiments were carried out in triplicate, except where otherwise mentioned. All analyses were conducted with three technical replicates, and the results are presented as mean ± standard deviation (SD). The data were subjected to analysis of variance (ANOVA) using GraphPad Prism 5.0 statistical software to determine if there were statistically significant differences between any two mean values or samples ($p < 0.05$).

3. Results and discussion

3.1. Nutritional profile of extruded snacks

The nutritional profiles of EPS are shown in Table 1. The fat content showed a slight increase in S2 (1.64%), attributed to the inclusion of sunflower oil in the emulsion, while S1 (0.10%) and C1 (0.08%) showed comparatively lower fat levels. Variations in carbohydrate content were observed, likely due to differences in ingredient composition, such as dietary fiber. Other parameters, including moisture and ash content, showed no significant differences among C1, S1, and S2. EPS produced using the blended flour showed significantly higher protein content as compared to C1. Typically, extruded snacks are made with corn flour to achieve better expansion and texture. However, it is low in protein and other essential nutrients. Over-reliance on corn flour results in nutritionally deficient snacks with a high glycemic index. The use of blended flour in this study produced snacks with increased protein content (13.5%) in S1 against 9.8% in the corn-based control (C1). The increased protein content resulted from the spent coconut flour (SCF), a known protein-rich ingredient. SCF contains 25.5% protein; thus, it significantly contributed the protein content in the formulation. Additionally, pearl millet, with a reported protein content of 12.5%,[25] further enhanced the protein profile of the blend. A similar increase in protein content was reported in enriched extrudates; for example, Gojiya *et al.* observed an increase in

Table 1 Nutritional profile of EPSs made from corn grit (C1), blended flours (S1), and blended flours infused with curcumin and vitamin D_3 (S2)[a]

Composition (Wb%)	C1	S1	S2
Protein	9.8 ± 0.0^{a}	13.5 ± 0.1^{b}	13.8 ± 0.2^{b}
Moisture	2.9 ± 0.5^{a}	2.8 ± 0.1^{b}	3.3 ± 0.0^{c}
Fat	0.1 ± 0.2^{a}	0.1 ± 0.2^{a}	1.6 ± 0.1^{c}
Ash	1.4 ± 0.2^{a}	2.0 ± 0.1^{b}	1.74 ± 0.0^{b}
Carbohydrate	85.8 ± 0.2^{a}	81.6 ± 0.5^{b}	79.5 ± 0.1^{c}
Total dietary fiber	13.0 ± 0.2^{a}	18.9 ± 0.1^{b}	19.2 ± 0.1^{c}
Insoluble dietary fiber	9.6 ± 0.1^{a}	14.2 ± 0.1^{b}	14.6 ± 0.2^{b}
Soluble dietary fiber	3.4 ± 0.2^{a}	4.6 ± 0.1^{b}	4.6 ± 0.2^{b}

[a] Different superscripts within the same row denote significant differences between the samples and control ($p > 0.05$; $n = 3$).

protein content from 14.0% to 26.7% when 10% to 40% defatted sesame flour was added into the formulation.[26]

The addition of PMF and SCF to the blended flour significantly enhanced the dietary fiber content in the EPS. SCF contains 54.0% total dietary fiber, including 44.5% insoluble fiber and 9.5% soluble fiber. Similarly, pearl millet contributes to the fiber profile of S1, as it contains 11.5% total dietary fiber, comprising 9.1% insoluble fiber and 2.3% soluble fiber.[17] S1 contained significantly higher levels of total dietary fiber (18.9%), insoluble dietary fiber (14.2%), and soluble dietary fiber (4.6%) compared to C1, which contained 13.0%, 9.6%, and 3.4%, respectively (Table 1). This increase in fiber content can be attributed to the contributions of pearl millet and SCF. A recent study reported a 5% increase in protein content in extrudates with the addition of green gram and cowpea flour, along with a 3% reduction in total carbohydrate content, making it a healthier snack option.[27] Similarly, another study reported significant increases in protein (7.6% to 27.2%) and fiber content (0.1% to 2.6%) in extrudates with the incorporation of cowpea (10% to 30%) and whey protein concentrate (WPC) (5% to 20%) compared to the control. The formulation containing 15% cowpea and 5% WPC achieved the highest acceptance, with a protein content of 14.6% and a total dietary fiber content of 1.6%.[3] These findings highlight that the use of blended flour containing fiber- and protein-rich ingredients can significantly improve the nutritional profile of extruded snacks.[13,28] The snacks developed in this study were significantly dense in protein and dietary fiber and can be considered a healthier option.

3.2. Expansion ratio and bulk density

The expansion ratio and bulk density are important indicators of texture, mouthfeel, and overall consumer acceptance of extruded snacks. Bulk density reflects the degree of puffing in extruded products and the blended flour and LPE are expected to alter the bulk density of the snack samples. As shown in Fig. 2a, the bulk density of S1 (0.70 g cm^{-3}) and S2 (0.72 g cm^{-3}) were higher than that of the control C1 (0.50 g cm^{-3}). The similar bulk density values of S1 and S2 indicated that the incorporation of LPE did not significantly alter the physical or internal structure of the snacks. Bulk density is influenced by the interactions among starch, protein, and fiber components.[29] SCF is rich in dietary fiber, which enhances the compactness of extruded snacks and increases their bulk density. The observed increase in bulk density with the addition of dietary fiber suggests that higher fiber content contributes to a denser and more compact extrudate structure. Previous studies have shown that increased fiber content in extruded products correlates with higher bulk density.

The higher expansion ratios typically signify lighter, crispier textures. The control sample (C1) had the highest expansion ratio of 4.01, while the expansion ratio of both S1 and S2 was only 37.2% of that of the control (Fig. 2b). The inclusion of soluble and insoluble fibers in extruded snacks significantly influences their physicochemical characteristics, particularly the expansion ratio and bulk density. The observed decrease in the expansion ratio can be attributed to the increased protein and fiber content, resulting in a denser, less expanded structure. An increase in protein content also affects the extent and rate of starch gelatinization, which could lead to a decrease in the expansion ratio.[29] Studies have shown that incorporating dietary fibers from various sources, such as polydextrose, gum acacia, inulin, xanthan gum, and resistant starch, into corn-based feed reduces the expansion of extruded snacks.[30] The addition of fiber increases the viscosity of the starchy dough during extrusion, reducing the water available for gelatinization and thereby limiting starch expansion at the die.[31]

Fiber typically functions as an inert filler within the expanded starch matrix. At low concentrations, the fiber is insufficient to be evenly distributed throughout the extrudate matrix. However, as its content increases, the starch matrix may become overwhelmed, causing it to collapse as fiber particles penetrate. This process ultimately reduces the expansion ratio.[32] A previous study reported reduced expansion index values in extruded products containing okara and mung bean powder. This was attributed to the high fiber content (60.8% in okara; 15.2% in mung bean) and notable protein levels (26.5% in okara; 20.2% in mung bean).[32] Similarly, extruded snacks made with 80–90% broken rice and 10–20% lupin flour showed that higher rice content increased the expansion index, whereas higher lupin flour content reduced it.[33]

During snack extrusion, dietary fiber significantly impacts starch gelatinization by competing with starch for available water. This competition reduces amylose leaching and limits the full gelatinization of amylose and amylopectin, potentially affecting amylose retrogradation and disrupting the structure of amylopectin. Additionally, fiber increases dough viscosity, disrupting the starch matrix and hindering expansion. These structural disruptions weaken the matrix, reducing the expansion ratio and producing denser snacks with higher bulk density and less puffiness. As a result, the texture of fiber-enriched snacks differs markedly from fiber-free products.[29,34]

The extruded product formulated with 15% spent coconut flour (SCF) and 65% pearl millet flour successfully replaced 80% of corn flour, marking a significant step toward replacing traditional corn-based snacks. Similarly, an extruded snack developed using 80% pearl millet flour, 10% African walnut flour, and 10% corn starch achieved moderate sensory acceptance.[35]

3.3. Texture profile analysis

Texture attributes like hardness, fracturability, gumminess, and chewiness are essential for evaluating the quality and appeal of extruded snacks. Hardness affects the perception of freshness, while fracturability can be correlated with the crispiness. Gumminess indicates the effort required to chew, and chewiness influences the overall sensory experience. All of these attributes are vital for creating products that satisfy the consumers. The texture qualities of the extruded snacks are shown in Fig. 3. The increase in hardness observed in S1 and S2 compared to C1 is primarily due to the higher protein and fiber content from SCF and PMF, which disrupt the starch matrix,

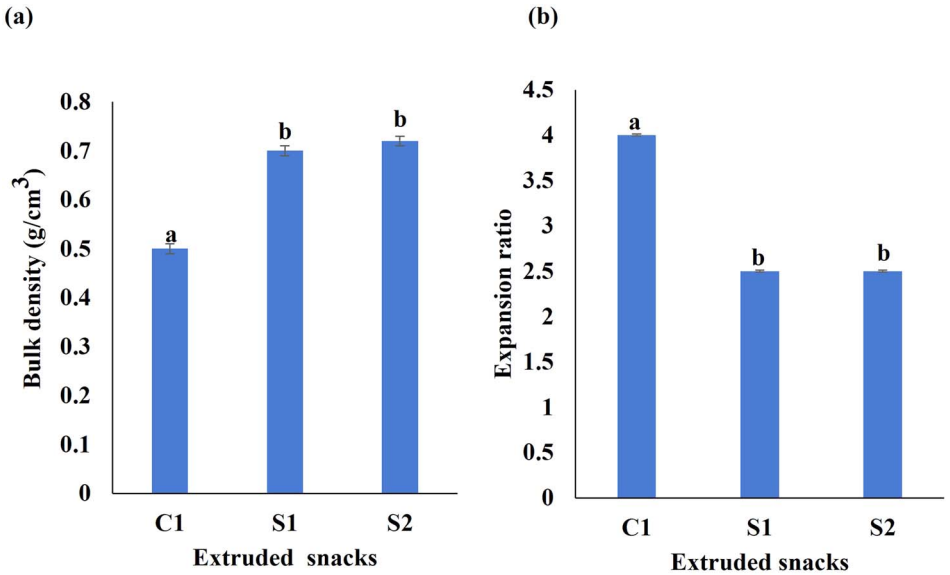

Fig. 2 (a) Bulk density and (b) expansion ratio content in the extrudates. Different letters denote significant differences between the samples ($p < 0.05$).

leading to reduced expansion and a denser texture. The strong relationship between hardness and expansion suggests that higher protein and fiber levels enable the formation of a compact structure that affects the overall texture. This type of relationship was also noted by Kumar *et al.*,[9] who found that fortification of snacks with chitosan led to the increase in dietary fibre content. Similarly, the incorporation of 5 to 20% tomato pomace powder in extruded snacks was found to increase hardness.[36] A protein–starch interaction that inhibited expansion might be attributed to an increase in hardness in sorghum-based extruded snacks when protein-rich soy meal flour was added up to 20% of the formulation.[37] The control sample (C1) had the highest chewiness compared to S1 and S2. Earlier research also showed that chewiness was significantly reduced from 1.63 N to 0.42 N when corn flour was supplemented with soy and chickpea flour about 20–40%.[38] The gumminess of EPS increased with the addition of SCF and PMF compared to the control. Fiber acts as both a structure-forming and water-absorbing component, creating a denser matrix that resists deformation and thereby enhances gumminess. This aligns with previous studies showing that incorporating soy and chickpea flour into corn flour significantly increases gumminess, demonstrating a positive correlation between dietary fiber content and gumminess in extruded products. It has also been reported that gumminess increased significantly from 0.33 N in the control to 1.99 N when 20% soy and 20% chickpea flour were substituted for corn flour.[38] Fracturability is an important texture attribute that reflects the brittleness or crispness of a snack. A higher fracturability value indicates that the snack can break with less force, indicating its crunchy and crisp texture. In extruded snacks, it is affected by several factors, including the composition of the ingredients (*e.g.*, starch, fiber, moisture, fat, or emulsifiers), the extrusion process parameters (*e.g.*, temperature and pressure), and the extent of product expansion. It was observed that the addition of fiber rich SCF and PMF resulted in a slight reduction in fracturability compared to the control. Fiber-rich ingredients, such as SCF and PMF, disrupt the continuous starch network, reducing product expansion and creating a denser texture. This compact structure absorbs more force before breaking, thereby reducing the product's brittleness. The lower expansion caused by high fiber content also decreases porosity, making the product less brittle and slightly tougher to fracture. These findings are consistent with studies that reported similar effects when high-fiber ingredients, such as tomato pomace, were incorporated into extruded snacks, resulting in reduced fracturability due to the compact and dense structure.[36,39]

Notably, the similar texture profiles of S1 and S2 suggest that incorporating lignin-based Pickering emulsions (containing curcumin and vitamin D_3) does not significantly alter the core

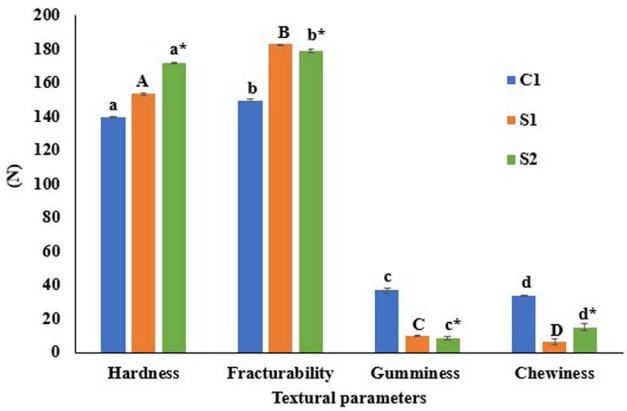

Fig. 3 Texture profile of extruded puffed snacks. All the parameters expressed in Newton (N). Different letters denote significant differences in the values between the samples ($p < 0.05$).

Table 2 Colour analysis of EPSs formulated with different combinations of blended flours[a]

Extruded puffed snack	L^*	a^*	b^*	Yellowness index (YI)
C1	67.9 ± 0.1^a	3.9 ± 0.0^a	38.5 ± 0.2^a	80.9 ± 0.0^a
S1	61.5 ± 0.0^b	3.0 ± 0.0^b	24.9 ± 0.1^b	57.8 ± 0.1^b
S2	67.8 ± 0.3^a	-0.4 ± 0.0^c	62.2 ± 0.2^c	131.3 ± 0.5^c

[a] Entries within the same column with different superscripts denote significant differences between the sample and control ($p > 0.05$; $n = 3$).

textural properties of the snacks. This finding indicates that these emulsions can be used to fortify extruded snacks without compromising their overall texture profile, making them a promising option for enhancing nutritional value.

3.4. Color analysis

The color properties of the extruded snacks, as indicated by the L^* (lightness), a^* (red-green), b^* (yellow-blue), and yellowness index (YI) values, showed significant variation among C1, S1, and S2 in terms of colour (Table 2). Sample C1 exhibited the highest lightness value suggesting a brighter appearance compared to the other samples. The a^* and b^* values of C1 indicated a more pronounced reddish and yellowish hue, contributing to its high yellowness index (YI = 80.86). This is due to the presence of corn grits, whose yellow colour primarily results from natural carotenoid pigments, particularly lutein and zeaxanthin.

In contrast, S1 displayed the lowest lightness value and reduced a^* and b^* values, resulting in the lowest yellowness index (YI = 57.78). The lower colour intensity of S1 can be attributed to the incorporation of SCF and PMF, with the latter likely responsible for the darker colour. Pearl millet contributes to the dark color of extrudates due to its high phenolic content, including tannins and flavonoids, which act as natural pigments. During extrusion, the high temperatures and pressures trigger the Maillard reaction, forming brown melanoidins that further enhance the dark color. Pigments such as anthocyanins present in the bran layer of pearl millet further intensify the darkening effect during processing. It has been reported that reactions such as Maillard browning, caramelization, pigment degradation, and lipid oxidation contribute to the reduction in lightness of extruded snacks.[40] S2, however, exhibited a markedly different colour profile. While its lightness was comparable to that of C1, the a^* value shifted toward the green spectrum, and its b^* value was significantly higher than that of other samples, resulting in the highest yellowness index (YI = 131.26). This indicates that S2 had a strong yellow hue due to the presence of curcumin and lignin, which carry yellow and brown pigments.[7] The colour profile of the extruded snacks formulated in this work aligns with research showing that the addition of vegetable ingredients and other agricultural by-products to rice-, barley-, and corn-based extruded snacks improves their colour desirability.[15,41,42] Furthermore, the inclusion of lignin in extruded snacks not only supports the stability of bioactives like curcumin and vitamin D_3 but also enhances the product's visual appeal.

3.5. Sensory profile of snacks

The sensory profile of the EPSs was evaluated to determine their potential acceptance by the consumers. Attributes such as color, texture, flavor, and overall acceptability were evaluated (Fig. 4). All samples received mean scores above 8.0 out of 9 for each attribute, indicating a high level of acceptance among the panellists. The panellists noted that the sample fortified with LPE (S2) had a distinct darker yellow hue compared to both the control and the one produced using blended flour without the emulsion fortification, yet it received similar sensory scores for texture, flavor, and crispiness.

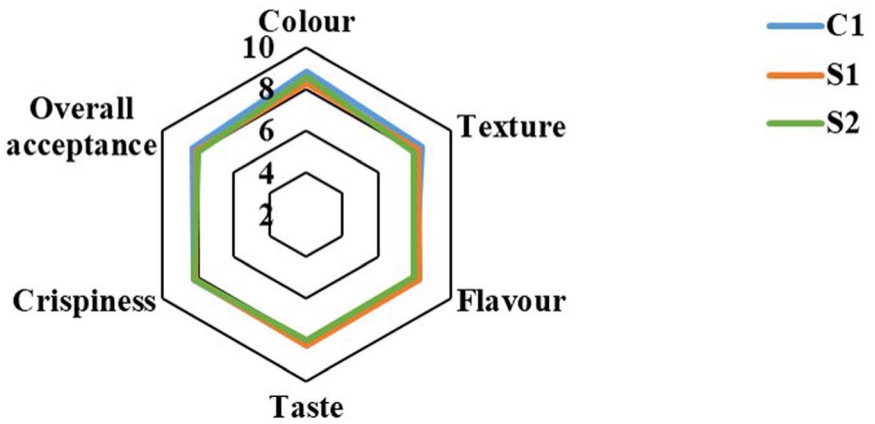

Fig. 4 Sensory profiles of extruded puffed snacks. Corn grit (C1) and blended flours (S1), blended flours infused with curcumin and vitamin D_3 (S2).

The high sensory scores across all samples suggest that the inclusion of SCF and PMF did not negatively impact consumer acceptability. The positive sensory attributes of S1 and S2 snacks, including taste, texture, and crispness could be attributed to the unique combination of pearl millet and coconut flour, which created a distinct flavor profile compared to commercial snacks. The crispness resulted from the extrusion process and the interaction of the ingredients.

The distinct darker yellow colour of the product fortified with LPE (S2) enhanced its visual appeal without compromising texture and flavour. A similar result was observed with the addition of tomato pomace powder to ready-to-eat (RTE) snacks. When included at levels of 5–10%, the snacks achieved the highest sensory scores. However, acceptability decreased at inclusion levels above 10%.[36] Likewise, Hoglund[43] incorporated bilberry press cake into extruded snack formulations. Substitutions of up to 25% were tested, but products with 10% inclusion were the most preferred by panellists. In another study, oat flour was added at levels of 5–20% to extruded snacks. Formulations containing 10% oat flour achieved the highest overall sensory scores.[44] These studies highlighted that moderate inclusion levels of natural fiber-rich ingredients enhanced snack sensory appeal, whereas excessive amounts reduced acceptability. The findings confirm that the blend of SCF, PMF, and corn grits—fortified with LPE—improves the nutritional profile of extruded snacks while maintaining strong sensory appeal. Notably, the blended flour in this study contained 15% SCF and 65% PMF, replacing 80% of corn grits in extruded puffed snacks while still delivering desirable sensory properties.

3.6. Microstructural analysis

The microstructural analysis of EPS samples using an optical microscope (Fig. 5a–c) revealed notable differences among C1, S1, and S2. The control sample (C1) displayed a uniform pore distribution with large, homogeneous edges, indicating greater expansion and aeration during extrusion. In contrast, S1 had smaller pores and a denser, less porous structure due to the higher fiber content in SCF and PMF, which promoted a more compact matrix. S2 showed a similar structure to S1 but with a distinct yellow hue caused by the presence of curcumin.

The microstructural characteristics of EPS samples—C1, S1, and S2—were examined through SEM (Fig. 5d–f). Fig. 5d reveals a rough, fractured surface with air pockets formed during the extrusion process. This porous structure results from the expansion of starch and protein components at the end of the extrusion process. The visible cracks may be due to moisture evaporation and rapid expansion. In contrast, Fig. 5e shows a more fibrous, layered structure with elongated strands, suggesting partial melting of starch or proteins that solidify into fibrous formations, enhancing the snack's crunchiness. Fig. 5f displays a microstructure similar to that of the control (C1), indicating that LPE did not affect the EPS microstructure. Similar findings were reported in extruded snacks made from rice starch and pea protein blends, which showed an even distribution of proteins and carbohydrates throughout the porous structure.[45]

3.7. Stability of bioactives in lignin-encapsulated extrudates

Emulsions stabilized by lignin show promise in encapsulating health-promoting compounds like vitamin D_3 and curcumin for fortifying snack products.[11] Incorporating these bioactive compounds into extruded snacks can significantly enhance their nutritional profile. Preserving the stability of curcumin and vitamin D_3 within the emulsion is crucial for maintaining the health benefits of fortified snacks over time. To evaluate LPE's ability to protect curcumin and vitamin D_3 during extrusion, a control EPS (C2) was prepared by adding these compounds directly to the blended flour without emulsifying with lignin particles. The stability of curcumin and vitamin D_3 in C2 was then compared to that in the S2 sample. Fig. 6 shows

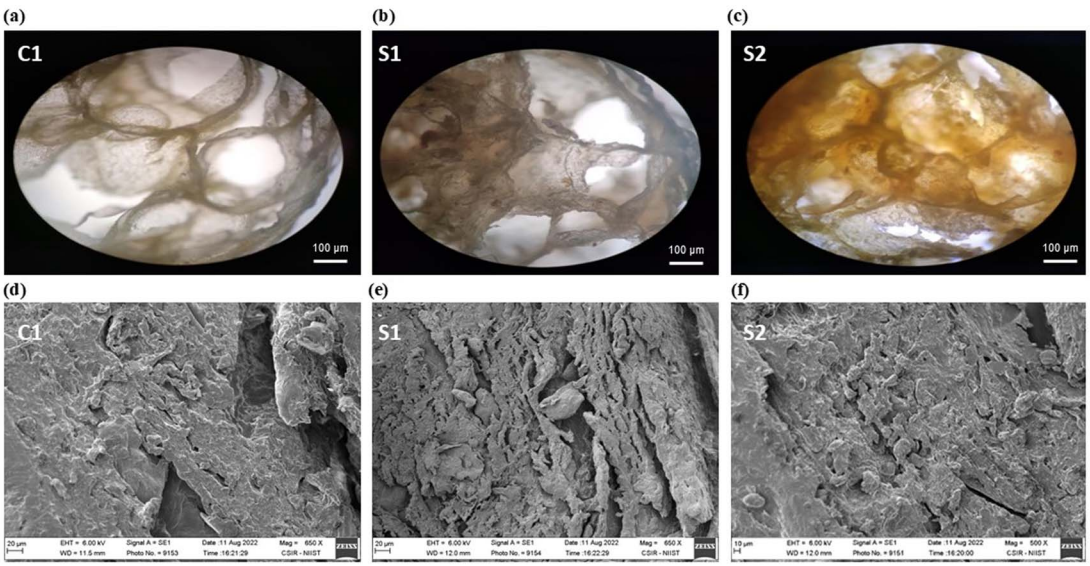

Fig. 5 Microscopic images, (a–c) optical microscopy images, and (d–f) SEM images of extruded puffed snacks.

the chromatograms of the extrudates S2 and C2, showing the stability of curcumin and vitamin D_3 in the products. The bioactive stability of curcumin and vitamin D_3 in S2 was 69.0 and 65.7%, respectively. In contrast, the stability of curcumin and vitamin D_3 significantly decreased to 7.4 and 8.2%, respectively in C2. These results indicate that lignin stabilised emulsions effectively protect curcumin and vitamin D_3 during the extrusion process.

The significant difference in bioactive stability between S2 and C2 underscores the vital role of lignin as a protective agent in extrusion processes. Lignin acts as a stabilizer, shielding curcumin and vitamin D_3 from the harsh thermal conditions, thereby maintaining their integrity and activity. Without lignin, as observed in C2, curcumin and vitamin D_3 are highly susceptible to thermal degradation their stability is compromised. These findings are in accordance with those of Bertolo,[46] which demonstrated that lignin particles protect bioactive

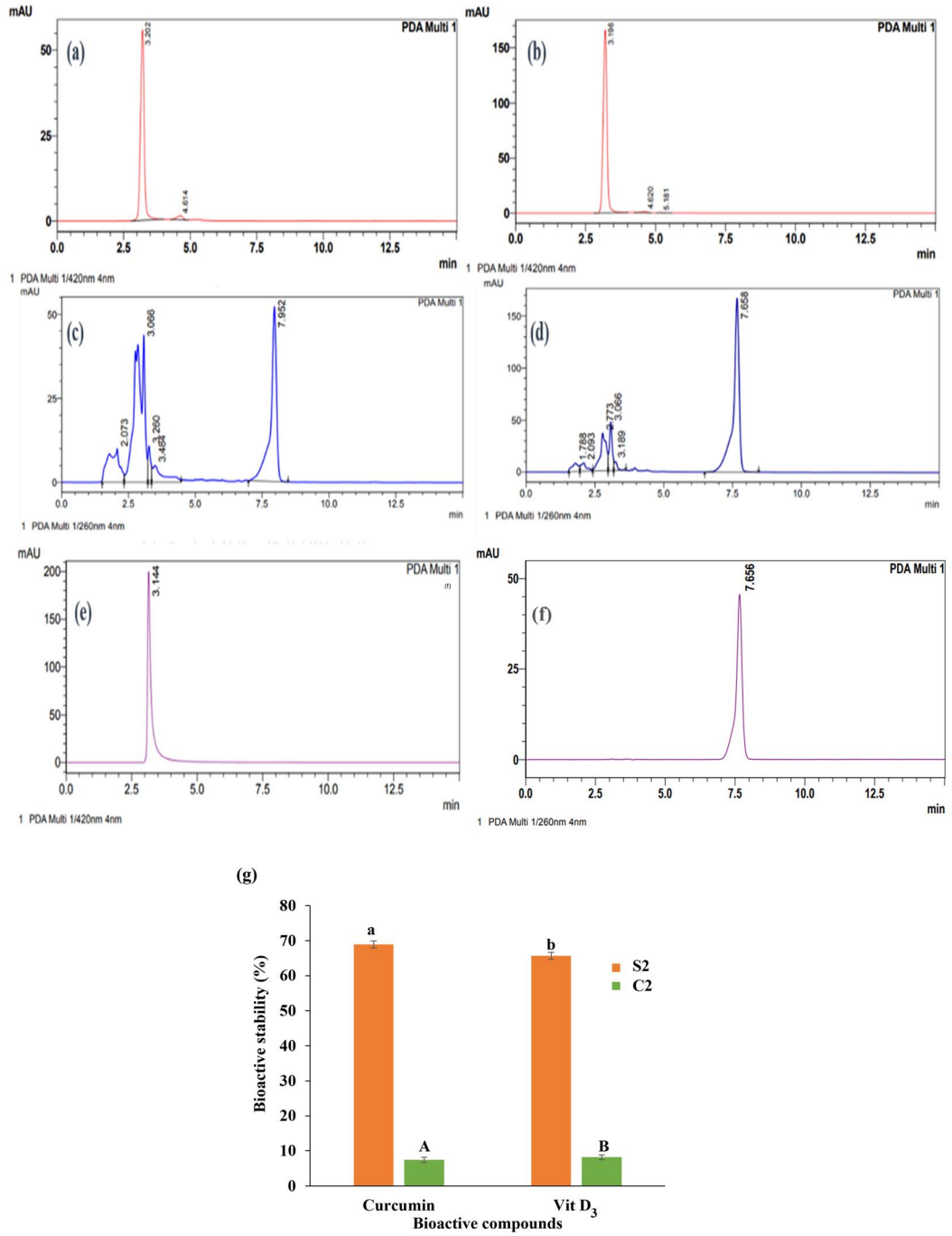

Fig. 6 HPLC chromatograms of extruded snacks showing bioactive stability: (a) curcumin content in C2, (b) curcumin content in S2, (c) vitamin D_3 content in C2, (d) vitamin D_3 content in S2 (e) standard curcumin, and (f) standard vitamin D_3. (g) Bioactive stability of curcumin and vitamin D_3 in extruded snacks; different letters denote significant differences in values between C2 and S2.

compounds (such as curcumin) in food systems. The notably higher stability of curcumin and vitamin D_3 in S2 underscores lignin's potential as a protective agent, demonstrating its suitability for the production of fortified extruded snacks. Lignin has also been shown to possess antioxidative properties, with the ability to protect oxygen-sensitive compounds.[47] In this study, lignin's role as a Pickering particle was vital for successfully encapsulating curcumin and vitamin D_3, ensuring their stability during high-temperature extrusion (110 ± 2 °C). These findings align with the existing literature, where lignin is consistently highlighted as an encapsulating and protective agent for bioactive compounds.[47,48]

4. Conclusion

This study successfully developed and characterized nutritionally and functionally superior extruded puffed snacks (EPSs). The EPSs were formulated using a blend of spent coconut, pearl millet flour, corn grits, and lignin Pickering emulsions (LPE) in which curcumin and vitamin D_3 were encapsulated. Notably, 80% of the corn flour typically used in traditional snacks was replaced with the blended flour, resulting in increased protein and dietary fiber content. Although the expansion ratio, bulk density, and textural properties of the blended flour snacks were lower than those of traditional corn flour snacks, the inclusion of LPE enhanced their nutritional profile. The overall sensory acceptance of these snacks was comparable to that of conventional snacks, indicating their suitability as nutritionally enriched alternatives. The study also confirmed that curcumin and vitamin D_3 were effectively encapsulated within the snacks' matrix, with their structural integrity and bioactivity preserved during the extrusion process. Lignin played a vital role in maintaining the stability and bioavailability of curcumin and vitamin D_3 in the snacks. These findings highlight the potential of lignin-stabilized emulsions for incorporating bioactive compounds into healthier, ready-to-eat snacks.

Data availability

The data for the manuscript can be made available on request.

Author contributions

Billu Abraham: conceptualization, data curation, investigation, methodology, validation, writing – original draft preparation. Heeba Shakeela: data curation, writing – draft preparation. Pavithra P.: methodology, investigation. Charles Brennan: investigation, data analysis. Nitin Mantri: investigation, data interpretation. Benu Adhikari: supervision, validation, writing – review & editing. Nisha P.: conceptualization, project administration, resources, supervision, validation, visualization, writing – review & editing.

Conflicts of interest

The authors declare that there are no conflicts of interest regarding the publication of this paper.

Acknowledgements

The authors gratefully acknowledge CSIR-NIIST and RMIT for providing the necessary facilities and support for this research. The first author expresses gratitude for the CSIR-SRF direct fellowship. The partial financial support from the Department of Science and Technology, Government of India, is also acknowledged. Special thanks to Mr Pratheesh Kumar for assistance with extrusion processing and Mr Hareesh for conducting SEM analysis.

References

1 Y. Abilmazhinov, G. Bekeshova, A. Nesterenko, Z. Dibrova, V. Ermolaev, E. Ponomarev and V. Vlasova, *Food Sci. Technol.*, 2023, **43**, DOI: **10.5327/fst.80621**.
2 K. Prabha, P. Ghosh, S. Abdullah, R. M. Joseph, R. Krishnan, S. S. Rana and R. C. Pradhan, *Future Foods*, 2021, **3**, 100019, DOI: **10.1016/j.fufo.2021.100019**.
3 H. N. Dilrukshi, D. D. Torrico, M. A. Brennan and C. S. Brennan, *Food Chem.*, 2022, **389**, 133107, DOI: **10.1016/j.foodchem.2022.133107**.
4 C. I. Onwulata, *J. Food Process. Preserv.*, 2013, **37**, 510–532, DOI: **10.1111/j.1745-4549.2012.00680.x**.
5 E. Feizollahi, Z. Hadian and Z. Honarvar, *Curr. Nutr. Food Sci.*, 2018, **14**, 90–103, DOI: **10.2174/1573401313666170728151350**.
6 M. Sultana, E. S. Chan, J. Pushpamalar and W. S. Choo, *Trends Food Sci. Technol.*, 2022, **123**, 69–86, DOI: **10.1016/j.tifs.2022.03.006**.
7 B. Abraham, H. Shakeela, L. P. Devendra, K. B. Arun, K. V. Ragavan, C. Brennan, N. Mantri, B. Adhikari and P. Nisha, *Food Chem.*, 2024, **458**, 140284, DOI: **10.1016/j.foodchem.2024.140284**.
8 K. C. Tsokolar-Tsikopoulos, I. D. Katsavou and M. K. Krokida, *J. Food Sci. Technol.*, 2015, **52**, 6170–6181, DOI: **10.1007/s13197-015-1718-2**.
9 R. Kumar, K. M. Xavier, M. Lekshmi, A. Balange and V. Gudipati, *Carbohydr. Polym.*, 2018, **194**, 267–273, DOI: **10.1016/j.carbpol.2018.04.050**.
10 K. Wang, M. Zhu, Z. Yang, L. Bai, S. Huan and C. Wang, *ACS Sustainable Chem. Eng.*, 2023, **11**, 9132–9142, DOI: **10.1021/acssuschemeng.3c01972**.
11 B. Abraham, V. L. Syamnath, K. B. Arun, P. F. Zahra, P. Anjusha, A. Kothakotta, Y. H. Chen, V. K. Ponnusamy and P. Nisha, *Sci. Total Environ.*, 2023, **881**, 163316, DOI: **10.1016/j.scitotenv.2023.163316**.
12 M. A. Al-Azzawi, A. J. Maftool, A. A. Al-Shimary and A. A. Mohammed, *Int. J. Med. Sci. Dent. Health*, 2023, **9**(12), 37–46, DOI: **10.55640/ijmsdh-09-12-08**.
13 C. A. Amadeu, S. M. Martelli and F. M. Vanin, *Cereal Chem.*, 2024, **101**(3), 450–467, DOI: **10.1002/cche.10765**.
14 J. Ahmed, B. R. Giri, M. A. Reza, S. S. B. Qasim, L. Thomas, H. Al-Attar and M. Maniruzzaman, *J. Food Sci.*, 2024, **89**(1), 435–449, DOI: **10.1111/1750-3841.16841**.
15 S. Grasso, *Trends Food Sci. Technol.*, 2020, **99**, 284–294, DOI: **10.1016/j.tifs.2020.03.012**.

16 H. Shakeela, K. Mohan and P. Nisha, *Sustainable Food Technol.*, 2024, **2**(3), 497–505, DOI: **10.1039/D3FB00247K**.
17 T. Longvah, R. Ananthan, K. Bhaskarachary and K. Venkaiah, *Indian Food Composition Tables 2017*, National Institute of Nutrition, Indian Council of Medical Research, Hyderabad, Telangana, India, 2017, **https://www.nin.res.in/ebooks/IFCT2017.pdf**.
18 AOAC, *Official Methods of Analysis*, Association of Official Analytical Chemists, 1990, vol. **62**, pp. , pp. 2742–2744.
19 Bureau of Indian Standards, *Method for Estimation of Total Dietary Fibre in Food Stuffs*, Indian Standards Institution, New Delhi, India, 1984, p. , p. 11062.
20 K. B. Arun, S. Thomas, T. R. Reshmitha, G. C. Akhil and P. Nisha, *J. Funct. Foods*, 2017, **31**, 198–207.
21 A. A. Tas and A. U. Shah, *Trends Food Sci. Technol.*, 2021, **116**, 701–711, DOI: **10.1016/j.tifs.2021.08.016**.
22 S. Suri, A. Dutta, N. C. Shahi, R. S. Raghuvanshi, A. Singh and C. S. Chopra, *LWT–Food Sci. Technol.*, 2020, **134**, 110164, DOI: **10.1016/j.lwt.2020.110164**.
23 H. Shakeela, N. M. Mini, B. Abraham, N. Natarajan and P. Nisha, *Int. J. Food Eng.*, 2022, **18**(5), 399–409, DOI: **10.1515/ijfe-2021-0337**.
24 S. Wichchukit and M. O'Mahony, *J. Sci. Food Agric.*, 2015, **95**(11), 2167–2178, DOI: **10.1002/jsfa.6993**.
25 M. M. Navami, B. Abraham, H. Archana and P. Nisha, *JSFA Rep.*, 2023, **3**(8), 377–386, DOI: **10.1002/jsf2.141**.
26 D. Gojiya, P. Davara, V. Gohil and M. Dabhi, *J. Food Process. Preserv.*, 2022, **46**(12), e17203, DOI: **10.1111/jfpp.17203**.
27 G. Karun, A. Sukumar, G. Nagamaniammai and R. Preetha, *J. Food Sci. Technol.*, 2023, **60**(3), 947–957, DOI: **10.1007/s13197-022-05390-8**.
28 J. Delić, P. Ikonić, M. Jokanović, T. Peulić, B. Ikonić, V. Banjac, S. Vidosavljević, V. Stojkov and M. Hadnađev, *Innovative Food Sci. Emerging Technol.*, 2023, **87**, 103419, DOI: **10.1016/j.ifset.2023.103419**.
29 A. Aussanasuwannakul, C. Teangpook, W. Treesuwan, K. Puntaburt and P. Butsuwan, *Foods*, 2022, **11**(19), 2967, DOI: **10.3390/foods11192967**.
30 Y. J. Han and T. T. T. Tran, *LWT–Food Sci. Technol.*, 2018, **96**, 1–6, DOI: **10.1016/j.lwt.2018.05.014**.
31 D. A. Pai, O. A. Blake, B. R. Hamaker and O. H. Campanella, *J. Cereal Sci.*, 2009, **50**(2), 227–234, DOI: **10.1016/j.jcs.2009.05.007**.
32 P. Wang, Y. Fu, L. Wang, A. S. Saleh, H. Cao and Z. Xiao, *Starch/Staerke*, 2017, **69**(7–8), 1600201, DOI: **10.1002/star.201600201**.
33 L. C. Oliveira, C. M. Rosell and C. J. Steel, *Int. J. Food Sci. Technol.*, 2015, **50**(6), 1504–1514, DOI: **10.1111/ijfs.12778**.
34 M. S. Alam, J. Kaur, H. Khaira and K. Gupta, *Crit. Rev. Food Sci. Nutr.*, 2016, **56**(3), 445–473, DOI: **10.1080/10408398.2013.779568**.
35 S. S. Sobowale, Y. O. Kewuyemi and A. T. Olayanju, *SN Appl. Sci.*, 2021, **3**, 1–12, DOI: **10.1007/s42452-021-04808-w**.
36 S. Yagci, R. Calıskan, Z. S. Gunes, E. Capanoglu and M. Tomas, *Food Chem.*, 2022, **368**, 130847, DOI: **10.1016/j.foodchem.2021.130847**.
37 A. Rodríguez-Vidal, H. E. Martínez-Flores, E. González Jasso, G. Velázquez de la Cruz, A. K. Ramírez-Jiménez and E. Morales-Sánchez, *J. Texture Stud.*, 2017, **48**(3), 249–257, DOI: **10.1111/jtxs.12234**.
38 F. U. H. Shah, M. K. Sharif, M. S. Butt and M. Shahid, *J. Texture Stud.*, 2017, **48**(3), 221–230, DOI: **10.1111/jtxs.12231**.
39 N. Y. Sinaki and F. Koksel, *Int. J. Food Sci. Technol.*, 2024, **59**(4), 2236–2248, DOI: **10.1111/ijfs.16943**.
40 I. Zahari, F. Ferawati, J. K. Purhagen, M. Rayner, C. Ahlström, A. Helstad and K. Östbring, *Foods*, 2021, **10**(10), 2397, DOI: **10.3390/foods10102397**.
41 M. Gupta, A. S. Bawa and A. D. Semwal, *Cereal Chem.*, 2008, **85**(2), 115–122, DOI: **10.1094/CCHEM-85-2-0115**.
42 M. A. Brennan, E. Derbyshire, B. K. Tiwari and C. S. Brennan, *Plant Foods Hum. Nutr.*, 2013, **68**, 78–82, DOI: **10.1007/s11130-012-0330-0**.
43 E. Hoglund, L. Eliasson, G. Oliveira, V. L. Almli, N. Sozer and M. Alminger, *LWT–Food Sci. Technol.*, 2018, **92**, 422–428, DOI: **10.1016/j.lwt.2018.02.042**.
44 D. Gumul, R. Ziobro, H. Gambuś and A. Nowotna, *CyTA–J. Food*, 2015, **13**(3), 353–360, DOI: **10.1080/19476337.2014.984336**.
45 C. Philipp, I. Oey, P. Silcock, S. M. Beck and R. Buckow, *J. Food Eng.*, 2017, **212**, 165–173, DOI: **10.1016/j.jfoodeng.2017.05.024**.
46 M. R. Bertolo, L. B. B. de Paiva, V. M. Nascimento, C. A. Gandin, M. O. Neto, C. E. Driemeier and S. C. Rabelo, *Ind. Crops Prod.*, 2019, **140**, 111591, DOI: **10.1016/j.indcrop.2019.111591**.
47 L. Dai, Y. Li, F. Kong, K. Liu, C. Si and Y. Ni, *ACS Sustainable Chem. Eng.*, 2019, **7**(15), 13497–13504, DOI: **10.1021/acssuschemeng.9b02966**.
48 A. Czaikoski, A. Gomes, K. C. Kaufmann, R. B. Liszbinski, M. B. de Jesus and R. L. da Cunha, *Ind. Crops Prod.*, 2020, **154**, 112762, DOI: **10.1016/j.indcrop.2020.112762**.

International Journal of Biological Macromolecules xxx (xxxx) 142877

Contents lists available at ScienceDirect

International Journal of Biological Macromolecules

journal homepage: www.elsevier.com/locate/ijbiomac

Cellulose and lignin nanoparticles from an Ayurvedic waste stream for essential oil-based active packaging to extend shelf life of strawberries

Billu Abraham [a, b, c], Nazila Oladzadabbasabadi [c], Heeba Shakeela [a, b], Charles Brennan [c], Nitin Mantri [c], Nisha P [a, bc, *], Benu Adhikari [c, d, **]

[a] Agro Processing and Technology Division, CSIR-National Institute for Interdisciplinary Science and Technology, Council of Scientific and Industrial Research, Trivandrum 695019, India
[b] Academy of Scientific and Innovative Research (AcSIR), Ghaziabad 201002, India
[c] School of Science, RMIT University, Melbourne, VIC 3083, Australia
[d] Centre for Advanced Materials and Industrial Chemistry (CAMIC), RMIT University, Melbourne, VIC 3001, Australia

ARTICLE INFO

Keywords:
Nanocellulose
Nanolignin
Polyvinyl alcohol
Emulsion
Active packaging film

ABSTRACT

Cellulose and lignin nanoparticles (NCP and LNP) were successfully extracted from Dashamoola spent material (DSM), a residue from an Ayurvedic decoction. NCP had a particle size of 493.6 nm and a zeta potential of −30.9 mV, indicating good colloidal stability. FTIR confirmed the removal of non-cellulosic components, while TGA demonstrated thermal stability, with major degradation between 260 °C and 350 °C. A semi-crystalline structure of nanocellulose was indicated via XRD analysis. Oil-in-water emulsions of tea tree oil (TTO) were prepared using NCP (C at 4 %), LNP (L at 4 %), and a combination blend (2 % each of C and L in CL_TTO), with 16 % TTO, all in w/v. Among these, CL_TTO emulsions had the smallest particle size and highest stability. PVOH-based films, prepared with a 4 % w/v mixture of CL_TTO emulsion, PVOH, and glycerol, demonstrated improved tensile strength, Young's modulus, water vapour barrier properties, and water repellence. These films blocked 95 % UV transmittance, providing appreciable protection to light-sensitive products. PVOH-CL_TTO films also exhibited strong antioxidant activity (85 % DPPH scavenging) and antimicrobial property against *E. coli*. These films extended the shelf life of strawberries by preserving lightness, firmness, and pH for 14 days under chilling (4 °C). These findings highlight the potential of NCP and LNP obtained from DSM for producing sustainable active packaging which would valorizing Ayurvedic waste stream.

1. Introduction

Sustainability and by-product valorization are essential for advancing Sustainable Development Goals (SDGs) [1–3]. The Ayurveda industry, rooted in traditional medicine, is gaining global significance as demand grows for natural and holistic healthcare products [4]. Indian Ayurvedic industry generates about 1000 ton/year Dashamoola spent material (DSM) as a byproduct of *Dashamoola arishta* production, which is rich in lignocellulosic materials including cellulose and lignin [5,6]. Lignin is a complex organic polymer which offers UV-blocking and antioxidant properties, while cellulose is abundant and this biopolymer provides mechanical strength, and water vapour and oxygen barrier properties [6–9]. Both lignin and cellulose have wide applications such as biocomposite production, textile, food, and pharmaceutical industries. As a part of active food packaging, they improve barrier properties, mechanical robustness. The incorporation of these natural materials coming from renewable sources into polymer systems contributes to sustainability [6,8].

Emulsion technology has the prospect of enhancing the functionality of active packaging films by dispersing small droplets of hydrophobic substances in hydrophilic matrices. The uniformity of this distribution, together with the size of these droplets, plays an important role in determining the effectiveness of the film [10–12]. Emulsions help incorporate hydrophobic bioactive compounds and essential oils, such as tea tree oil (TTO), into hydrophilic biopolymer matrices, and this has the potential to enhance the antioxidant and antimicrobial activities of the resulting packaging materials or films [12–14]. TTO, derived from *Melaleuca alternifolia*, contains active compounds, including terpinene-4-ol and γ-terpinene, which impart antibacterial and antioxidant properties [15]. These materials, along with biopolymer stabilizers such as

* Correspondence to: N. P, Agro Processing and Technology Division, CSIR-National Institute for Interdisciplinary Science and Technology, Council of Scientific and Industrial Research, Trivandrum 695019, India.
** Correspondence to: B. Adhikari, Centre for Advanced Materials and Industrial Chemistry (CAMIC), RMIT University, Melbourne, VIC 3001, Australia.
E-mail addresses: pnisha@niist.res.in (N. P), benu.adhikari@rmit.edu.au (B. Adhikari).

https://doi.org/10.1016/j.ijbiomac.2025.142877
Received 13 December 2024; Received in revised form 25 March 2025; Accepted 4 April 2025
0141-8130/

cellulose and lignin, can reduce moisture permeability and improve the barrier and protective functions of biodegradable polymer-based films [16–19].

Petroleum-based plastics dominate food packaging due to their cost-effectiveness and desirable mechanical and barrier properties; however, environmental concerns have increased interest in biodegradable alternatives [20–22]. Polyvinyl alcohol (PVOH) is a promising biodegradable polymer due to its hydrophilic, non-toxic nature, making it suitable for environment-friendly packaging applications [23]. Although PVOH lacks inherent antioxidant properties, it can be fortified with natural additives like lignocellulose, curcumin, essential oils, and plant extracts to enhance its functionality [24–27]. However, there remains a significant gap in sustainable packaging solutions that not only enhance food preservation but also utilize natural, industry-derived byproducts including spent materials of the Ayurvedic industry. In PVOH systems, cellulose and lignin provide UV-blocking properties, reduce moisture sensitivity, and reinforce mechanical strength under humid conditions, offering a sustainable alternative to inorganic fillers [28–31]. Thus, the incorporation of lignin and nanocellulose derived from DSM into PVOH matrix could produce active and sustainable packaging materials for food application [32,33].

The increasing global population and changing dietary habits have significantly raised the demand for fresh fruits and vegetables [34]. Strawberries (*Fragaria ananassa*), valued for their nutritional benefits and economic importance, are highly perishable and particularly susceptible to mechanical damage, moisture loss, texture softening, physiological degradation, and microbial spoilage [35]. These factors rapidly degrade strawberry quality, posing challenges for marketing and distribution [36,37]. Although active packaging technologies using biopolymers infused with PVOH have been explored to extend the shelf life of perishable products, their effectiveness in maintaining the quality of strawberries over extended storage periods remains limited. It is practically important to apply active packaging materials made from nanolignin and nanocellulose derived from Ayurvedic spent materials (e.g., DSM) and PVOH to extend the shelf life of perishable fruits such as strawberries [34].

Our earlier work indicated that lignin nanoparticles play a role in stabilizing emulsions [38]. This new study investigates the effectiveness of cellulose and lignin nanoparticles derived from Ayurvedic residues in developing PVOH-based active packaging films infused with tea tree oil. The study evaluates the impact of these natural biopolymers on the films' morphological, mechanical, and functional properties, as well as their ability to extend the shelf life of strawberries. By exploring the utilisation of nanocellulose and lignin from Ayurvedic spent materials, this work contributes to sustainability and offers a viable, eco-friendly alternative to conventional plastics for food preservation.

2. Materials and methods

2.1. Raw material selection and source

The Dashamoola Spent Material (DSM) utilized in the research was generously supplied by Arya Vaidya Sala, located in Kottakal, Malappuram, Kerala, India (M/s. AVS Kottakal Ltd).

2.2. Chemicals and reagents

Analytical-grade sodium hydroxide (NaOH), sodium chlorite ($NaClO_2$), hydrochloric acid (HCl), and glacial acetic acid (CH_3COOH) were obtained from HiMedia, India. Petroleum ether was acquired from Sisco Research Laboratories Pvt. Ltd. (SRL), India. Cellulose powder (CAS number 9004-34-6, SCP), glycerol, 2,2-diphenyl-1-picrylhydrazyl (DPPH), and polyvinyl alcohol (Mw: 89,000–98,000 Da, fully hydrolyzed) were sourced from Sigma-Aldrich Pty Ltd. (New South Wales, Australia). Tea tree oil (TTO) from Thursday Plantation was purchased from a local Chemist Warehouse outlet (Melbourne, Australia). Antibacterial assays were performed using the LB broth dilution method on *E. coli* strain 25922, sourced from New England Biolabs. All other reagents used in this study were of analytical-grade and supplied by Sigma-Aldrich Pty Ltd. (New South Wales, Australia).

2.3. Fruit selection

Strawberries (*Fragaria ananassa*) were selected as a representative fruit. Freshly harvested (within one day), the strawberries were sourced directly from Coles, Bundoora, Melbourne, Australia. The strawberries were chosen based on uniform shape, size, colour, and absence of physical damage. After selection, the strawberries were gently washed with deionised water, dried using clean paper towels, chilled at 4 ± 1 °C and 80 ± 5 % relative humidity (RH), and used immediately.

2.4. Nanocellulose (NCP) and nanolignin (LNP) extraction from DSM

The compositional analysis of DSM was conducted following the National Renewable Energy Laboratory (NREL) protocol [39] and reported in our previous paper [38]. The isolation of cellulose from DSM was adapted from the methodologies outlined by Silvério et al. [40,41], with slight modifications to suit the material. DSM was initially dried at 40 °C in a hot air oven and then ground into fine powder. This powder was suspended in a 1 % NaOH solution with a 10 % w/v loading and autoclaved at 121 °C for 1 h. After cooling to room temperature, the solid was separated from the liquid using cheesecloth and retained for further processing. The solid residue underwent acid treatment with 4 % H_2SO_4 in an autoclave for 1 h. This process was repeated three times to ensure the removal of hemicellulose and partial lignin. Afterward, the acid-treated residue was cooled, centrifuged at 5000 ×*g* for 15 min, and thoroughly washed with water until a neutral pH was achieved.

For bleaching, an equal volume mixture of 1.7 % w/v $NaClO_2$ and an acetate buffer (pH -4.5) was used. The acetate buffer was prepared by dissolving 2.7 g of NaOH and 7.5 mL of glacial acetic acid in 100 mL of distilled water. The solid residue was treated with the bleaching solution at 80 °C for 3 h, until a uniform colour was achieved. After bleaching, the residue was cooled, centrifuged at 5000 ×*g* for 10 min, and washed until neutral pH. Finally, the bleached residue was freeze-dried at −80 °C and 10 Pa, yielding fine cellulose powder. A planetary ball mill (Pulverisette, Fritsch, Germany) operating at 300 rpm, with zirconium dioxide (ZrO_2) containers (50 mL) and ZrO_2 balls (10 mm), was used to reduce the size of the extracted cellulose. The milling process was conducted in an argon environment to prevent oxidation and consisted of 23 cycles, with each cycle lasting 5 min followed by a 10-min gap to prevent overheating. The cellulose powder composition was determined using the NREL method. The resulting nanocellulose powder (NCP) was stored in zip-lock pouches for further experimental analyses.

The procedure for the extraction and characterization of lignin nanoparticle (LNP) from DSM is detailed in our previous work [38]. Briefly, lignin was extracted from Dashamoola spent material (DSM) through alkaline hydrolysis followed by acid precipitation. The precipitated lignin was purified and processed into nanolignin using ball milling. The LNPs were characterized for their size, morphology, and surface properties using techniques such as dynamic light scattering (DLS), Fourier-transform infrared spectroscopy (FTIR), and nuclear magnetic resonance (NMR). These methods confirmed the structural features, including β-O-4 linkages and guaiacyl, syringyl, and *p*-hydroxyphenyl units, as well as the thermal stability and surface charge characteristics essential for its potential applications.

2.5. Characterization of NCP

2.5.1. Particle size and zeta potential of NCP

The particle size of the NCP was measured using a dynamic light scattering method (Mastersizer 3000, Malvern Instruments Ltd., Malvern, UK). Samples were diluted in distilled water (pH 7) and agitated at 200 rpm for thorough dispersion. For Zeta potential analysis, the NCP samples were diluted 100 times using Milli Q water prior to measurements. The pH of the NCP aqueous solution is 7. The Zeta potential was measured with a Zetasizer (Nano-ZS, Malvern Instruments Ltd., Malvern, UK).

2.5.2. Observation of microstructure

The microstructure of the NCP was examined using a scanning electron microscope (SEM-Quanta200, Philips XL-30, Philips, Eindhoven, the Netherlands). The NCP powder samples were placed on silicon wafer pieces mounted on aluminium stubs using double-sided adhesive conductive carbon tape. The specimens were coated with a thin layer of iridium using a sputter coater to improve conductivity and to prevent the development of electrical charge in the samples during imaging. The SEM measurements were conducted at an acceleration voltage of 0.7 kV.

2.5.3. Functional group analysis of NCP using FTIR

FTIR analysis of NCP and Standard Cellulose Powder (SCP) was performed using an FTIR-ATR spectrometer (Perkin Elmer, USA). Spectra were recorded from 4000 to 1000 cm^{-1} with a 4 cm^{-1} resolution, allowing comparison of the functional groups in NCP and SCP. A total of 64 scans were recorded and averaged for each sample.

2.5.4. Thermal degradation of NCP

Thermogravimetric (TG) analyses of NCP and SCP were performed using a TA Instruments Q50 instrument (USA). Sample (10 mg) was placed in the alumina crucible, heated in the temperature range 40–500 °C at a heating rate of 10 °C/min in the presence of nitrogen [42]. The weight loss (%) versus temperature data were recorded.

2.5.5. Surface composition of NCP

X-ray photoelectron spectroscopy (XPS) was used to determine the surface compositions of NCP and SCP. A PHI 5000 Versa Probe II (ULVAC-PHI Inc., USA) was employed to analyse the oxygen-to-carbon (O:C) ratio, which provides insights into the percentage of lignin on the surface. The analysis was carried out using a micro-focused (200 μm, 15 kV) monochromatic Al-Kα X-ray source ($h\nu$ = 1486.6 eV) [43].

2.5.6. Crystalline and amorphous content of NCP

The Wide-angle X-ray diffraction (WAXD) analysis was performed using a Xenocs XEUSS SAXS/WAXS instrument (France) in transmission mode to examine the amorphous and crystalline content of NCP and SCP. Cu Kα radiation at 50 kV and 0.6 mA with a wavelength of 1.54 Å was used. The 2D diffraction patterns were captured on a Mar345 image plate and analyzed using Fit2D software. The degree of crystallinity was calculated as the ratio of the intensity of the crystalline peak to the total intensity, according to the method described by Sindhu et al. [44].

2.6. Preparation and characterization of emulsions

NCP and LNP extracted from DSM were used to prepare emulsions with tea tree oil (TTO) as the oil phase, designated as C_TTO and L_TTO, respectively. An emulsion was also prepared using a combination of NCP (C) and LNP (L) with TTO as the oil phase, designated as CL_TTO. NCP, LNP, and their combination were mixed with TTO at specified concentrations: 4 % w/v for C, 4 % w/v for L, and 2 % w/v each of C and L for CL, along with 16 % w/v TTO in each emulsion. These mixtures were stirred at 35 °C for 60 min at 300 rpm, followed by sonication (10 s on/off, 5 min, 50 % amplitude) to obtain the final emulsions [38].

2.6.1. Particle size and zeta potential

The particle (droplet) size and Zeta potential of the above-mentioned emulsions were measured using the Zetasizer (Nano-ZS, Malvern Instruments Ltd., Malvern, UK) at 25 °C, as described in Section 2.5.1. The emulsion samples were diluted 10 times using Milli Q water for both particle size and Zeta potential measurements.

2.7. Film casting preparation

A polyvinyl alcohol (PVOH) solution was prepared by dissolving PVOH in water to achieve a concentration of 3 % w/v. The PVOH solution was then blended with 1 % w/v glycerol and stirred at 80 °C and 500 rpm for 60 min to ensure uniform mixing of glycerol with PVOH, as glycerol acts as a plasticiser. Each of the emulsion (C_TTO, L_TTO, or CL_TTO) was then added to the PVOH-glycerol solution and the mixture was stirred at 35 °C for 60 min with a magnetic stirrer set at 300 rpm. To achieve homogeneity, the mixture was further homogenized using an IKA T25 Ultra Turrax homogenizer (Wilmington, USA) for 3 min at 5000 rpm and then probe-sonicated for 2 min (10 s on, 10 s off, at 50 % amplitude). Finally, the solutions were degassed to remove entrapped air bubbles. Table 1 shows the composition or formulation of the films.

The final step involved casting 15 mL of each mixture into a 10-cm diameter acrylic Petri dish and drying at room temperature (25 ± 2 °C) for 48 h. The films were then conditioned over saturated magnesium chloride to achieve a constant relative humidity (RH-53 %) environment before further testing or characterization [19]. The resulting films, PVOH, PVOH-C_TTO, PVOH-L_TTO, and PVOH-CL_TTO, had total solid contents of 4 % (w/w) as indicated in Table 1.

2.8. Characterization of films

2.8.1. Thickness of films

The thickness of the films was measured using a digital micrometer (Mitutoyo, Japan, precision up to 0.01 mm). Measurements were taken at 5 different locations on each film and averaged to ensure accuracy.

2.8.2. Water contact angle analysis

The water contact angle (WCA) was measured to evaluate the surface hydrophobicity of the films using an OCA-20 Contact Angle System (Data Physics Instruments, Germany) equipped with a Basler high-resolution camera. Rectangular film samples (20 mm × 80 mm) were positioned horizontally, and a 1 μL water droplet was applied to the surface. The WCA was determined by averaging the left and right angles from digital images, with at least ten measurements taken and averaged per film. All experiments were conducted at room temperature.

2.8.3. Water vapour transmission rate (WVTR)

The water vapour permeability of the films was measured using a Permatran-W system (Mocon, Minneapolis, USA) at 22 ± 1 °C. The wet side relative humidity (RH) was maintained at 80 %, with a gradient of 70 % RH across the films.

Table 1
Preparation ratio PVOH, PVOH-C_TTO, PVOH-L_TTO, and PVOH-CL_TTO.

Code	PVOH (%)	Glycerol (%)	Cellulose (C) (%)	Lignin (L) (%)	TTO (%)	Total content (%)
PVOH	3	1	0	0	0	4
PVOH-C_TTO	2.8	1	0.04	0	0.16	4
PVOH-L_TTO	2.8	1	0	0.04	0.16	4
PVOH-CL_TTO	2.8	1	0.02	0.02	0.16	4

2.8.4. Measurement of colour parameters

The colour profile of the films was measured using a Chroma Meter CR–400 (Minolta, Japan) in terms of lightness (L*; black to white), redness (a*; green to red), and yellowness (b*; blue to yellow). The instrument was calibrated using a standard white plate, and measurements were taken at three points on each film. The total colour difference (ΔE) was calculated using Eq. (1) [45].

$$\Delta E = \sqrt{\left(L^*_{film} - L^*_{standard}\right)^2 + \left(a^*_{film} - a^*_{standard}\right)^2 + \left(b^*_{film} - b^*_{standard}\right)^2} \quad (1)$$

2.8.5. Micro structure analysis

The microstructure of the films, including both surface and cross-sectional views, was analyzed using scanning electron microscopy (SEM), as described in Section 2.5.2. Film samples, measuring approximately 5 mm × 5 mm, were mounted on aluminium stubs with conductive carbon tape and coated with a thin layer of iridium to enhance conductivity and prevent charging during imaging [19].

2.8.6. Measurement of mechanical properties

The mechanical properties of the four different of the films, including tensile strength, elongation at break, and Young's modulus, were determined using an Instron universal testing machine (model 4467, Instron Corporation, Massachusetts, USA) equipped with a 100-kN load cell. Data collection and analysis were performed using Bluehill software. Film strips, cut to approximately 5 mm × 50 mm, were conditioned at 53 % RH for 48 h, following the ASTM D1708 standard. During the tensile test, each strip was placed between two clamps with an initial grip separation of 22 mm and subjected to a crosshead speed of 10 mm/min [46].

2.8.7. Thermal degradation of films

Thermal degradation of the films was determined using a thermogravimetric (TG) analysis, as described in Section 2.5.4. Film samples (10 mg) were heated from 40 to 500 °C at a rate of 10 °C/min under nitrogen purge. The weight loss (%) versus temperature data were recorded, and DTG (Derivative Thermogravimetry) was also evaluated.

2.8.8. Thermal characteristics of films

Differential scanning calorimetry (DSC) was used to evaluate the thermal behaviour of the films, specifically focusing on the glass transition temperature (T_g). Measurements were performed using a DSC Q2000 (TA Instruments, USA). Approximately 3.0 mg of the film sample was placed into pre-weighed aluminium pans. The samples were heated from 25 °C to 95 °C at a rate of 10 °C/min under a nitrogen environment. The onset temperature (T_0), peak temperature (T_p), and conclusion temperature (T_x) were determined using the Fit2D software [38].

2.8.9. Crystalline and amorphous content of films

The crystalline and amorphous contents of the films were determined using wide-angle X-ray diffraction (WAXD), as described in Section 2.5.6.

2.8.10. Film transparency

The UV–Vis transmission through the films was measured across the 200–800 nm wavelength range using a UV–Vis spectrophotometer (UV-2600, Shimadzu, Kyoto, Japan). Film samples were cut to dimensions of 1.5 × 3 cm^2, and the absorption spectrum was recorded within the specified range [19].

2.8.11. Antioxidant properties of films

Antioxidant activity of the films was determined using DPPH scavenging activity. Film sample of 900 mg dipped in 18 mL of methanol and incubated at 25 °C for 1 h with stirring (150 rpm). One mL of this methanolic extract was mixed with 2 mL of 0.06 mM DPPH solution and vortexed. The mixture was incubated in dark for 30 min at room temperature (25 ± 2 °C). Absorbance was measured at 517 nm using a UV–vis spectrometer [5]. A control sample with methanol and DPPH was prepared, and antioxidant activity (%) was calculated using Eq. (2).

$$\text{DPPH activity (\%)} = \left(\frac{\text{Absorbance of control} - \text{Absorbance of film sample}}{\text{Absorbance of control}}\right) * 100 \quad (2)$$

2.8.12. Antibacterial assays of films

Antibacterial activity of the films was assessed using the LB broth dilution method against *Escherichia coli* strain 25922 (New England Biolabs). LB broth was prepared by dissolving 10 g/L tryptone, 5 g/L yeast extract, and 10 g/L NaCl in distilled water, and the pH was adjusted to 7.0. The medium was sterilized by autoclaving at 121 °C for 15 min. After cooling, *E. coli* was cultured in the LB broth overnight at 37 °C with shaking at 100 rpm. Two mL of LB broth was added to each well of sterile 24-well plates, and film samples (1.5 cm × 1.5 cm) were transferred to the wells. A bacterial suspension (50 μL, 10^6 cells/mL) was inoculated into each well, with bacteria-only wells serving as controls. Bacterial growth was monitored over 18 h at 37 °C with shaking at 100 rpm, and optical density was measured at 600 nm using a UV–Vis spectrophotometer.

2.9. Assessment of preservation effect on strawberry

The preservation performance of the films on strawberries wrapped on them was evaluated at room temperature (22 ± 2 °C) and under chilling condition (4 ± 1 °C). Observations were recorded at room temperature on days 0, 2, and 4, while those under refrigeration were recorded on days 4, 8, and 14 [35]. The assessed films for their ability to extend the shelf life of strawberries included plain polyvinyl alcohol (PVOH), and PVOH containing Pickering emulsion produced using NCP (C) and LNP (L) tea tree oil (PVOH-CL_TTO). Unwrapped strawberries (UW) were used for comparison.

2.9.1. Colour analysis of strawberry

The colour parameters of strawberries, unwrapped (UW) and wrapped in PVOH and PVOH-CL_TTO films, were measured using a chromameter CR–400. Measurements were taken at three random spots and the average L*, a*, and b* were recorded as described in Section 2.8.4.

2.9.2. Hardness of strawberry

The hardness of strawberry samples was assessed using a texture analyzer (TA-XT2i, Stable Micro Systems) with a 50 kg load cell. The strawberry samples were positioned on the platform to allow a 5 mm diameter aluminium probe to pierce the shoulders. A compression test was performed, and hardness was defined as the force (N) required to penetrate 50 % of the sample height at a speed of 1 mm/s. The texture profile analysis (TPA) involved a two-cycles, with pre-test, test, and post-test speeds of 5 mm/s, 1 mm/s, and 8 mm/s, respectively. Firmness was reported as the maximum force during the first compression.

2.9.3. pH of strawberry

A strawberry sample weighing 5 g was homogenized with 50 mL of distilled water and then filtered through a paper filter or muslin cloth. The pH of the filtrate was measured using a pH meter (Microprocessor Meter, HANNA Instruments, Romania).

2.10. Statistical analysis

Experiments were conducted in triplicate unless otherwise specified. Results are presented as mean values ± standard deviation (SD). Statistical analysis was performed using one-way analysis of variance

(ANOVA) followed by Tukey's multiple comparison test, utilizing GraphPad Prism 5.0 and Microsoft Excel (2007). A 95 % confidence level ($p < 0.05$) was used to determine significant differences between mean values.

3. Results and discussion

3.1. Characterization of extracted lignin and cellulose from DSM

The lignocellulosic biomass of DSM used in this work contained 39.1 % cellulose, 30.6 % hemicellulose, and 27.9 % lignin [38]. In our previous studies [38], lignin was successfully isolated from DSM and converted into lignin nanoparticles (LNP) with a molecular weight of 14.42 kDa, which was comparable to that of commercial LNPs. The LNPs, produced using planetary ball milling to a size of 496.4 nm, demonstrated stability at pH 8.0 with a zeta potential of −32.0 mV. These LNPs have been used as Pickering particles to produce oil-in-water (O/W) emulsion of sunflower oil, which remained stable for 90 days at room temperature [38]. In this work, we further extracted NCP from DSM and characterized it. O/W emulsions of tea tree oil were produced using LNP and NCP, both separately and in combination.

The NCP powder obtained from DSM had a particle size of 493.6 nm (Fig. 1a) and a zeta potential of −30.9 mV. These values close to the size and surface charge of commonly reported cellulose nanoparticles [24,30]. Its purity was determined to be 93.7 % cellulose and 4.9 % hemicellulose, confirming the effective isolation of cellulose nanoparticles.

The SEM image in Fig. 1c represents the NCP obtained from the extracted cellulose (Fig. 1b) after planetary ball milling. As shown, the figures reveal morphological changes induced by the mechanical treatment. Fig. 1c depicts a more fragmented and irregular particle structure compared to the fibrillar network observed in Fig. 1b. This indicates that ball milling effectively reduced particle size and disrupted the cellulose fibers, resulting in smaller, more irregular particles. This level of reduction in size increases the surface area, which is beneficial for applications requiring enhanced reactivity or better dispersion in composite matrices [47]. The rougher surface morphology of these NCPs suggests potential for improved bonding with other materials in nanocomposites, making them suitable for applications such as emulsions and biodegradable packaging. FTIR data shown in Fig. 1d highlights the key structural characteristics of standard cellulose powder (SCP) and NCP powder, confirming the latter's high purity. The absorption bands around 3340 cm^{-1} and 1040 cm^{-1} correspond to O—H and C—O stretching vibrations, which are typical of cellulose structures. The absence of a peak at 1738 cm^{-1} in NCP indicates the successful removal of lignin, while the C═O stretching vibration associated with ester groups from hemicellulose confirms its partial removal [48]. Additionally, bands at 1641 cm^{-1}, attributed to adsorbed water, and 1429 cm^{-1}, [38] corresponding to CH_2 bending, and this confirms the preservation of the cellulose structure in NCP [49]. The close similarity between the FTIR spectra of SCP and NCP indicates that the extraction of cellulose and its conversion into nanoform did not alter the cellulose structure, making NCP suitable for applications in emulsions, biocomposites, and packaging [50].

Thermogravimetric analysis (Fig. 1e) reveals a distinct two-stage thermal degradation process for both NCP and SCP. The initial weight loss, occurring below 125 °C, is attributed to the evaporation of bound water—an inherent characteristic of cellulose fibers. This stage underscores the hydrophilic nature of the material and its tendency to retain moisture. The second, more significant weight loss between 260 °C and 350 °C corresponds to the depolymerization of cellulose chains, a hallmark of cellulose thermal degradation. These findings not only confirm the thermal behaviour of NCP and SCP but also provide insights into their stability under elevated temperatures, a critical consideration for applications in biocomposites or thermally resilient materials [49]. Above 400 °C, they further degraded into inorganic char or ash similar to degradation of typical cellulosic materials [48]. NCP exhibited slightly lower moisture retention in the initial stage (5.2 % compared to 6.1 % for SCP) and a marginally reduced weight loss during cellulose depolymerization (63.4 % compared to 65.8 % for SCP), likely due to its higher purity compared to SCP. The thermal stability of NCP was comparable to that of SCP, indicating its suitability for high-temperature applications such as bio-composites, where resistance to thermal degradation is critical [50].

XRD analysis, shown in Fig. 1f, indicates that the NCP retains its semi-crystalline structure, similar to SCP. The prominent peak at 22.5° 2θ corresponds to the (002) plane, which is characteristic of cellulose I. A secondary peak is observed near 18° 2θ, attributed to the ($\bar{1}$10) plane, further confirms the cellulose I allomorph [51]. The similar crystallinity values observed in NCP and SCP indicate that the extraction and size reduction processes effectively preserved the cellulose's natural structure—an essential factor for its functional applications. Crystallinity plays a key role in determining material properties such as mechanical strength and barrier functionality, both of which directly influence performance in bio-composites and packaging materials [52].

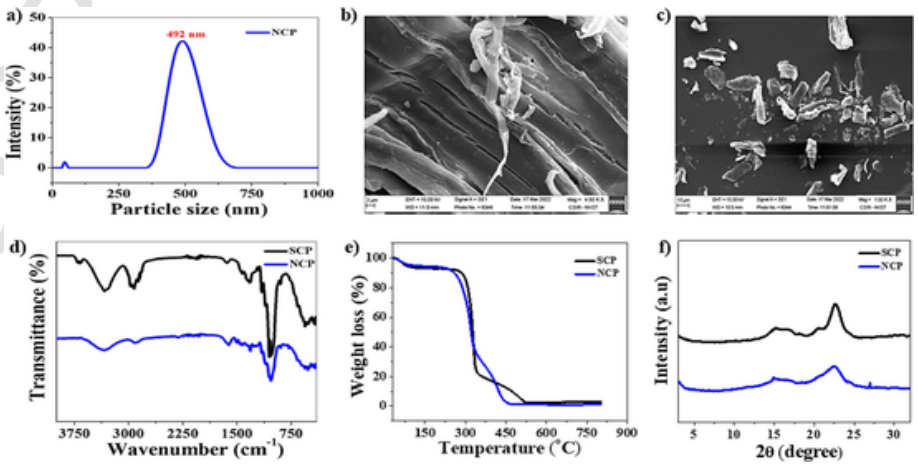

Fig. 1. Characteristics of nanocellulose powder (NCP) obtained from Dashamoola Spent Material (DSM): (a) particle size distribution, (b, c) SEM images with scale bars of 2 μm at ×4500 magnification and 10 μm at ×1500 magnification, respectively, (d) FTIR spectra, (e) TGA, and (f) XRD analysis.

3.2. Compositional analysis of NCP

X-ray photoelectron spectroscopy was used to assess the surface elemental composition and chemical states of the extracted nanocellulose powder (NCP), and the data is shown in Fig. 2. The survey spectra (Fig. 2a & b) for both standard cellulose and NCP revealed the predominance of carbon and oxygen, the primary constituents of cellulose. In the high-resolution C1s spectra (Fig. 2c & d), the extracted cellulose exhibited a peak at 284.72 eV, corresponding to the C—C and C—H bonds, similar to standard cellulose [53]. The minor shifts in binding energy likely resulted from slight changes in surface chemistry during extraction, possibly due to residual non-cellulosic substances or environmental exposure. The O1s spectra (Fig. 2e & f) showed a peak at 532.62 eV, corresponding to hydroxyl and ether groups. This peak exhibited a slight shift compared to standard cellulose, suggesting surface interactions such as hydrogen bonding or electrostatic interactions that may have occurred during the extraction process [53]. These results suggest that the core chemical structure of cellulose remained largely intact in NCP with minimal surface modifications [54].

3.3. Emulsion preparation and characterization

LNP and NCP are shown to possess significant potential in forming stable emulsions [6,55]. Building on this information, O/W emulsions of tea tree oil (TTO) as dispersed phase with LNP (2 %) and NCP (2 %) were fabricated as detailed in Section 2.6, where oil phase was 16 %. The characteristics of emulsion stabilized by of NCP (i.e., C-TTO), LNP (i.e., L_TTO), and their combination (i.e., CL_TTO) are presented in Table 2. The particle size data revealed that C_TTO exhibited comparatively larger average particle size (620.9 nm) to that of L_TTO (593.2 nm) and CL_TTO (585.9 nm), suggesting that lignin may contribute to produce finer emulsions [56]. The combination yielded the smallest particle size, as observed in CL_TTO, suggesting that this pairing is beneficial and could lead to the formation of more stable emulsions, which are desirable for producing active packaging films [9,12].

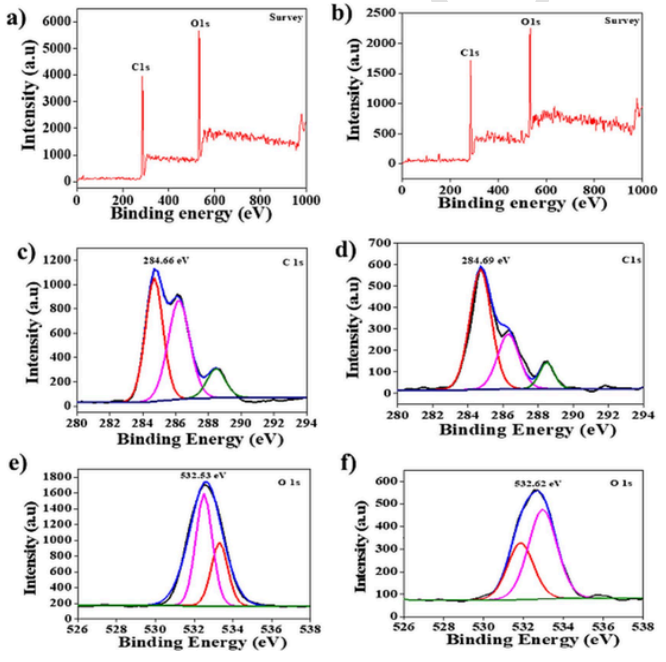

Fig. 2. XPS analysis of NCP obtained from Dashamoola spent material (DSM): (a) Survey spectrum of SCP, (b) Survey spectrum of NCP, (c) C1s spectrum of SCP, (d) C1s spectrum of NCP, (e) O1s spectrum of SCP, and (f) O1s spectrum of NCP.

Table 2
Particle size, PDI and Zeta of emulsion tea tree oil with cellulose (C_TTO), lignin (L_TTO), and their combination (CL_TTO).

Emulsions	C_TTO	L_TTO	CL_TTO
Size (nm)	620.85 ± 10.38[a]	593.19 ± 8.57[b]	585.89 ± 4.08[b]
PDI	0.511 ± 0.01[a]	0.491 ± 0.05[b]	0.409 ± 0.01[c]
Zeta (mV)	−32.55 ± 0.89[a]	−35.74 ± 0.92[b]	−39.39 ± 0.43[c]

Small letters indicate significant difference between the samples.

Zeta potential data also indicated that the combination was beneficial as CL_TTO (−39.4 mV) had the highest magnitude followed by L_TTO (−35.7 mV) and C_TTO (−32.6 mV). Higher magnitudes of zeta potential generally correlate with better emulsion stability due to higher electrostatic repulsion. The highest negative charge observed in CL_TTO aligns with its smallest particle size, this formulation would produce emulsion with higher stability [57,58].

The polydispersity index (PDI) values, presented in Table 2, follow a similar trend. CL_TTO exhibited the lowest PDI, L_TTO fell in between, and C_TTO showed the highest. Lower PDI values indicate a narrower size distribution, which typically leads to higher stability. These findings align with recent studies that show combining biopolymers with emulsifying properties can enhance the stability of emulsions [59]. Photographs of these emulsions (Fig. 3) confirm that there was no phase separation in these emulsions. This high level of stability is promising for developing clear, stable active packaging films infused with potent essential oils [19]. Further, TTO infused bioactive PVOH films were developed using NCP, LNP and their mixtures as Pickering emulsifiers.

3.4. Essential oil infused bioactives PVOH film and its characterization

Bioactive films were prepared using PVOH as the main matrix and infused with emulsified TTO essential oil. NCP, LNP, and their combinations, described above, served as Pickering emulsifiers. The films were then prepared by solution casting, as detailed in Section 2.7. Characterization of these films examines how the infused C_TTO, L_TTO, and CL_TTO emulsions influence their structural, mechanical, and functional properties, providing insights into the modifications imparted by lignin and cellulose within the PVOH matrix.

3.4.1. Physical properties of films

The thickness of the films (Table 3) showed a gradual increase across PVOH, PVOH-C_TTO, PVOH-L_TTO, and PVOH-CL_TTO films. Given the total non-water content, the addition of cellulose, lignin, and tea tree oil increased the thickness of these films. Thickness of films is an important parameter as it impacts their tensile strength and flexibility.

WVTR, which indicates a film's moisture barrier property, was highest in the PVOH film (349.3 g/m^2·day). WVTR significantly decreased in the PVOH-CL_TTO film (170.7 g/m^2·day), likely due to the presence of cellulose-lignin matrix, which creates a more complex diffusion path for water vapour enhancing barrier properties. In comparison, Zhou et

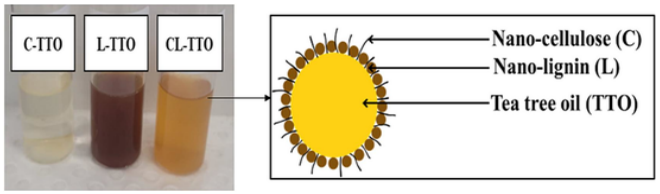

Fig. 3. Visual images of tea tree oil emulsions with cellulose (C_TTO), lignin (L_TTO), and their combination (CL_TTO), taken 5 min after preparation. A graphical representation of the CL_TTO emulsion is also shown.

Table 3
Properties of PVOH-based films with tea tree oil, cellulose, and lignin, including thickness, contact angle, WVTR, colour parameters (L*, a*, b*), and total colour difference (ΔE).

	PVOH	PVOH-C_TTO	PVOH-L_TTO	PVOH-CL_TTO
Thickness (μm)	60.00 ± 10.00^{a}	70.00 ± 10.00^{a}	80.00 ± 10.00^{a}	80.00 ± 10.00^{a}
Contact angle (°)	50.12 ± 2.95 ^{a}	58.43 ± 0.90^{b}	64.13 ± 1.26^{c}	70.53 ± 0.90^{d}
WVTR (g/m^{2}·day)	349.34 ± 3.06^{d}	191.42 ± 4.08^{c}	183.15 ± 2.42^{b}	170.71 ± 2.57^{a}
L*	91.89 ± 0.17^{d}	89.48 ± 0.37^{c}	81.27 ± 1.76^{a}	85.89 ± 0.84^{b}
a*	0.76 ± 0.04^{a}	1.15 ± 0.02^{b}	4.71 ± 0.11^{d}	2.25 ± 0.01^{c}
b*	0.19 ± 0.04 ^{a}	0.43 ± 0.18^{b}	9.87 ± 0.72^{d}	5.62 ± 0.13^{c}
ΔE		2.45 ± 0.82^{a}	13.00 ± 0.54^{c}	6.74 ± 0.69^{b}

Data are presented as mean ± standard deviation (n = 3) and the different superscripted alphabets in the same row indicate significant differences ($p < 0.05$) between the samples.

al. [60] reported a higher WVTR of 1400.6 g/m^{2}·day for PVOH films containing chitin and lignin, while Lingait et al. [61] reported a WVTR of 562.3 g/m^{2}·day for PVOH films with pectin. These findings indicate that incorporating cellulose and lignin nanoparticles into PVOH-CL_TTO active films creates a more effective moisture barrier than similar composite films.

In contact angle measurements, values <90° indicate hydrophilicity, while values >90° indicate hydrophobicity. The PVOH film had a contact angle of 50.1° indicating its hydrophilic nature. The incorporation of NCP and LNP increased the contact angle of the films by 8° (PVOH-C_TTO) and 14° (PVOH-L_TTO). The combination of NCP and LNP increased the contact angle by 20° (PVOH-CL_TTO). These films remained hydrophilic in nature. Studies have reported contact angle values of 60° for lignin-containing PVOH films with a lignin content of 5 % [62] and 51° for PVOH films containing nanocellulose and Fe^{3+} together [63]. The findings on WVTR and WCA suggest that the combined incorporation of NCP and LNP in PVOH films significantly enhances water resistance, making them more resistance to water vapour transport and increase water repellence.

Colour analysis revealed significant changes in the optical properties of the PVOH films with the addition of NCP and LNP, and essential oils. As shown in Table 3, the control PVOH film had the highest L* value, indicating a lighter, more transparent appearance. In contrast, the LNP containing film (e PVOH-L_TTO) had the lowest L* value (81.3) indicating its darker hue attributed to lignin's natural chromophores, such as phenolic and carbonyl groups [64]. This shift was accompanied by increased a* and b* values, producing a richer colour and enhancing the film's visual appeal.

The total colour difference (ΔE) also increased when LNP and NCP and essential oils were present in the films compared that the control film. This light dark hue was not only aesthetically pleasant but also added a light-shielding effect, potentially protecting packaged products from light-induced oxidative damage [64]. Similar colour changes have been reported in κ-carrageenan films containing fenugreek extract [65]. These optical enhancements, combined with improved water vapour barrier properties, make these films more suitable than PVOH films to be used in moisture-sensitive packaging where both functionality and aesthetics are essential.

3.5. Surface morphology of films

The photographic images of the films (Fig. 4a) show a noticeable increase in opacity from the pure PVOH film to those containing NCP, LNP, and essential oil. The pure PVOH film appears highly transparent, reflecting its smooth and homogenous structure. The PVOH-C_TTO film showed only slight increase in opacity, indicating that the NCP does not introduce significant changes in transparency and opacity. The PVOH-L_TTO film exhibited the highest increase in chromaticity and opacity, attributed to the relatively higher concentration of LNP, which imparts its own distinct colour. The opacity and colour variation of the PVOH-CL_TTO film remained between those of PVOH and PVOH-L_TTO, suggesting that the colouring component originated from LNP, albeit at half the concentration present in PVOH-L_TTO. These alterations in colour and transparency underscore the impact of incorporating additives on both the aesthetic and functional properties of the films, with potential implications for light transmission and barrier performance [62,63].

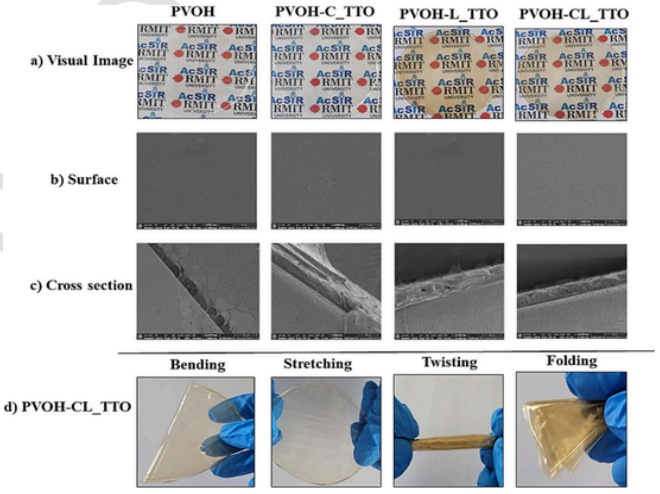

Fig. 4. Analysis of Polyvinyl Alcohol (PVOH) treatments showing (a) photographic appearance, (b) surface morphology with a scale bar of 50 μm at ×1500 magnification, (c) cross-sections with a scale bar of 300 μm at ×250 magnification, and (d) mechanical flexibility tests, including bending, stretching, twisting, and folding.

SEM images (Fig. 4b) provided further insight into the surface morphology of the films. The pure PVOH film showed a smooth, uniform texture, indicating a pristine polymer matrix. In contrast, the PVOH-C_TTO and PVOH-L_TTO films exhibited rougher surfaces, with visible particle distributions suggesting the presence of additives within the PVOH matrix. This surface roughness is likely caused by phase separation, where the additives disrupt the matrix continuity, resulting in a textured surface. Such microscale surface variation is important in modulating surface wettability [62,63,66].

The cross-sectional SEM images (Fig. 4c) revealed distinct difference in the internal structure among the films. The pure PVOH film demonstrated a dense and uniform cross-section, indicating tightly packed polymer chains. In contrast, the PVOH-C_TTO film exhibited a stratified structure, indicative of layered microphase separation, while the PVOH-L_TTO film shows an eroded, uneven structure, likely due to lignin's tendency to aggregate within the matrix. The PVOH-CL_TTO film exhibited a three-phase microstructure, where interactions between PVOH, cellulose, and lignin produced a rough, layered internal structure. These morphological features, driven by polymer-additive in-

teractions, give rise to the unique mechanical and barrier properties of the composite films [66,67].

Mechanical flexibility tests (Fig. 4d) of the PVOH-CL_TTO film showed that it maintained its structural integrity under bending, stretching, twisting, and folding stresses without tearing or permanent deformation. These properties are essential for packaging applications, where materials must withstand mechanical forces during handling and transportation [67]. The robust performance of PVOH-CL_TTO in these tests reinforces its suitability for use as a flexible packaging material.

3.6. Mechanical properties of films

The mechanical properties of PVOH films, both with and without NCP, LNP, and TTO, demonstrate their considerable potential for active packaging applications. As shown in Fig. 5a, the stress-strain behaviour of these films revealed that PVOH-C_TTO exhibited significant robustness, withstanding a stress of up to 6.34 MPa before failure. This 20 % increase of tensile strength over the unmodified PVOH film suggests that cellulose reinforcement significantly improves the load-bearing capacity of PVOH, making it suitable for packaging applications [68].

The Young's modulus (Fig. 5b) of PVOH-C_TTO film was the highest (48.78 MPa). This represents a substantial increase from the modulus of pure PVOH (24.75 MPa), indicating that the addition of cellulose creates a more rigid material, ideal for applications requiring resistance to deformation. Conversely, the PVOH-L_TTO and PVOH-CL_TTO composites exhibited lower moduli of 25.13 MPa and 34.92 MPa, respectively, suggesting a softer material that could be more appropriate for wrapping, where some flexibility is required [30].

The elongation at break values (Fig. 5c), further illustrated the ductility of the PVOH composites. PVOH-L_TTO and PVOH-CL_TTO displayed remarkable elongation at break values of 100.04 % and 102.27 %, respectively—considerably higher than the 61.93 % of the standard PVOH film. This level of flexibility allows the material to absorb impacts during transportation, reducing the likelihood of damage to packaged goods, which is particularly advantageous for fragile items [69].

The tensile strength (Fig. 5d) data of the films showed that PVOH-C_TTO film had the highest tensile strength. Although PVOH-L_TTO and PVOH-CL_TTO had slightly lower tensile strength values. Thus, the NCP an LNP extracted from DSM improve the mechanical properties of PVOH, creating flexible packaging materials more suitable in food applications. The incorporation of essential oil (e.g., tea tree oil) imparts antibacterial properties (Section 3.8) without compromising the mechanical properties of these films [70].

3.7. FTIR, thermal properties and UV transmittance of films

The FT-IR spectra of PVOH films and with and without NCP and LNP shown in Fig. 6a provide key structural insights. The PVOH film exhibited characteristic asymmetric stretching vibrations of the hydroxyl (—OH) and methylene (CH_2) groups at around 3302 cm^{-1} and 2941 cm^{-1}. These peaks shifted in the spectra of PVOH containing, NCP and LNP individually and in combination, indicating interactions between PVOH and NCP, LNP and tea tree oil. Notably, PVOH-L_TTO showed strong absorption IR due to aromatic skeletal vibrations and C—H stretching in the 1600–1500 cm^{-1} and 1460 cm^{-1} regions, consistent with lignin's structure. The presence of cellulose in PVOH-C_TTO introduced notable changes in the fingerprint region (1200–900 cm^{-1}), where the C—O—C pyranose ring skeletal vibrations are observed [71]. The broad band around 3300 cm^{-1}, associated with the —OH stretching of cellulose and PVOH, indicated formation of intermolecular hydrogen bonding. In PVOH-CL_TTO, the spectrum is more complex due to interactions between lignin's aromatic structure and cellulose's hydroxyl groups, with additional influence from tea tree oil components such as terpinen-4-ol. These shifts reflect changes in the hydrogen bonding network that would impact the film's physical properties [19].

The thermogravimetric analysis (TGA) shown in Fig. 6b captures the thermal degradation behaviour of PVOH films with or without NCP, LNP and tea tree oil. The pure PVOH film showed a single-stage degradation starting around 300 °C, with complete decomposition occurring by 400 °C. In contrast, the PVOH-C_TTO film began to lose weight at a lower temperature (~250–260 °C), likely due to the volatilization of tea tree oil components, with cellulose contributing to gradual weight loss beyond this point [72]. The PVOH-L_TTO film exhibited lesser overall weight loss. It had a higher residual mass above 30 %, attributable to lignin's tendency to form a char rather than volatilizing. The PVOH-

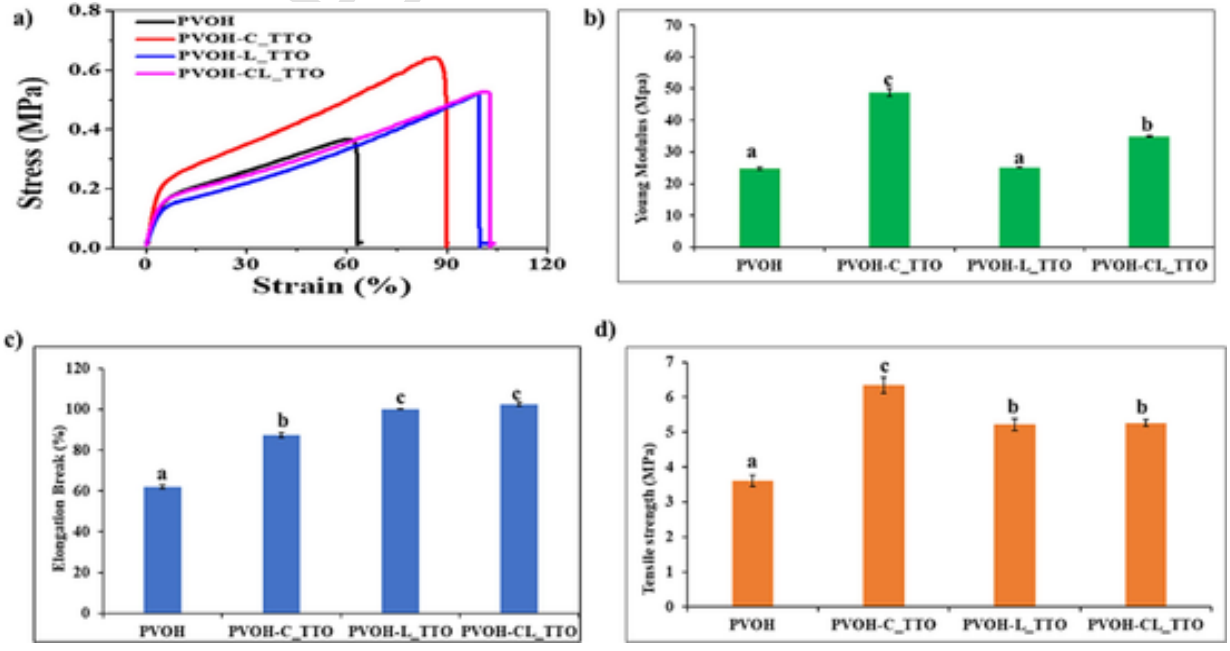

Fig. 5. Mechanical profiles of PVOH composites (a) Stress-strain curves (b) Young's modulus (c) Elongation at break and (d) Tensile strength.

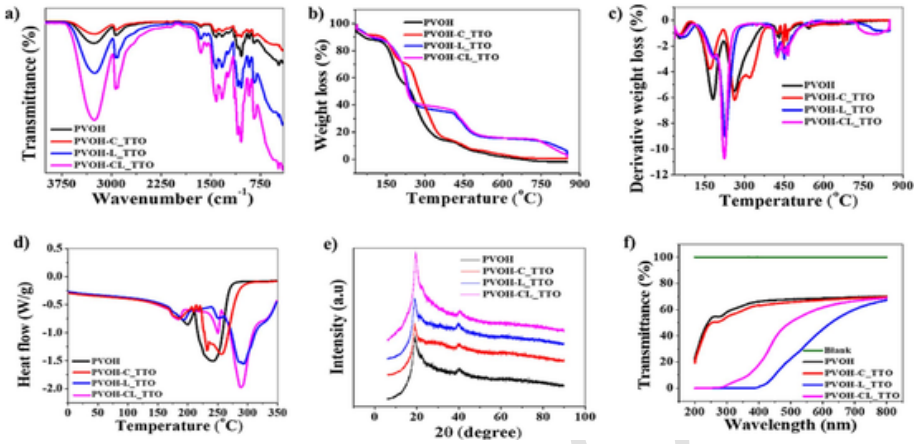

Fig. 6. Polyvinyl alcohol (PVOH)-based films with lignin, cellulose, and tea tree oil additives, showing (a) FTIR absorption spectra, (b) TGA thermograms, (c) DTG curves, (d) DSC thermograms, (e) XRD patterns, and (f) UV–Vis transmittance spectra. L = lignin, C = cellulose, TTO = tea tree oil.

L_TTO film was thermally stable up to 500 °C compared to other films. The PVOH-CL_TTO film showed similar behaviour in terms of initial weight loss followed by lignin's char formation. These results highlight the fact that the NCP and LNP obtained from DSM can help produce thermally stable biodegradable active packaging.

The differential thermal gravimetric (DTG) analysis (Fig. 6c) further illustrates the decomposition profiles of these films. The pure PVOH film showed a sharp peak around 300 °C, typical of its semi-crystalline structure [73]. The addition of cellulose and tea tree oil in PVOH-C_TTO lowered the onset of thermal degradation to around 250 °C, with another peak indicating that cellulose component was thermally stabile up to ~350 °C [74]. The broader DTG peak for PVOH-L_TTO (270–330 °C) suggested to a staggered degradation, likely due to lignin's amorphous structure. The PVOH-CL_TTO composite exhibited a multi-modal DTG curve, suggesting sequential degradation of tea tree oil, cellulose, and lignin [73].

The Differential Scanning Calorimetry (DSC) analysis (Fig. 6d) illustrates the thermal transitions of PVOH-based films containing NCP, LNP, and TTO. Pure PVOH exhibited a Tg of 87 °C and a melting peak at 225 °C, confirming its semi-crystalline nature [75]. The PVOH-C_TTO film showed a lower Tg (72 °C) due to the plasticizing effect of TTO, with a broad melting peak near 205 °C, indicating disrupted crystallinity [75]. The PVOH-L_TTO film exhibited a higher Tg (97 °C) and a melting peak at 230 °C, suggesting restricted polymer chain mobility and enhanced thermal stability due to lignin [76]. The PVOH-CL_TTO film displayed intermediate behaviour, with a Tg of 83 °C and endothermic events at 190 °C and 225 °C. These findings highlight lignin's stabilizing effect and TTO's flexibility-enhancing properties, making PVOH-CL_TTO a promising material for active packaging applications [75,76].

X-ray diffraction (XRD) patterns in Fig. 6e show the structural shifts in the PVOH composites. Pure PVOH exhibits sharp peaks at 2θ values around 19.5° and 40.5°, indicative of its semi-crystalline nature [77]. The PVOH-C_TTO sample reveals reduced peak intensity, suggesting decreased crystallinity due to hydrogen bonding disruptions by cellulose [52]. PVOH-L_TTO displays slight peak broadening, particularly near 22°, indicating a less ordered structure due to lignin's amorphous nature. The PVOH-CL_TTO sample shows diminished peak intensity and additional shifts, indicating complex interactions between PVOH, cellulose, lignin, and tea tree oil, likely affecting the film's mechanical and barrier properties [72].

The UV transmittance spectra (Fig. 6f) highlight the films' potential for active packaging. Pure PVOH film showed 55 % UV transmittance at 315–320 nm, providing moderate UV protection. PVOH-C_TTO reduced the transmittance to 50 %, with tea tree oil contributing antioxidants that protect within the 200–400 nm range. PVOH-L_TTO exhibited a substantial reduction in UV transmittance, reaching 0 %, thanks to lignin's UV-absorbing properties derived from its aromatic structure [78]. PVOH-CL_TTO showed 5 % UV transmittance indicating a sound level of UV protection. In particular, incorporation of LNP enhanced the film's ability to block harmful UV rays, which is expected to help extend shelf life of UV-sensitive products.

3.8. Antioxidant and antimicrobial activity of films

The antioxidant activity of the films was evaluated using the DPPH radical scavenging method and the results are shown in Fig. 7a. The results indicated that the incorporation of lignin (PVOH-L_TTO) and a combination of lignin with essential oils (PVOH-CL_TTO) significantly enhanced the films' antioxidant properties. Specifically, the PVOH-CL_TTO film exhibited a DPPH scavenging activity of 85 %, which is substantially higher than that of control PVOH film (< 20 %). This enhancement is attributed to the phenolic compounds present in lignin and essential oils, which are known to neutralize free radicals [79–81]. The presence of lignin and essential oils amplified the film's antioxidant effectiveness. In contrast, the pure PVOH film showed minimal activity,

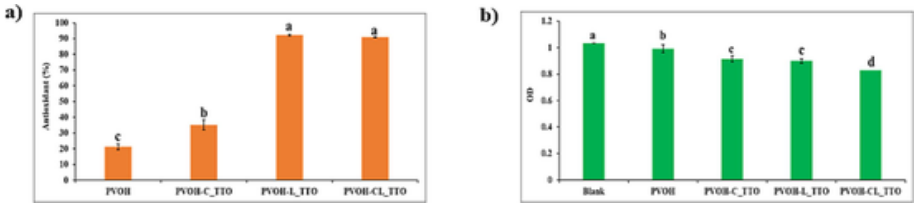

Fig. 7. a) Antioxidant (DPPH scavenging) and b) antimicrobial (*E. coli* inhibition) activities of pure PVOH films and PVOH films containing NCP, LNP and tea tree oil.

underscoring the importance of incorporating, particularly nanolignin to improve antioxidant capacity of active films.

The antimicrobial activity against *E. coli* is shown in Fig. 7b. The data showed that films containing lignin and essential oils (PVOH-L_TTO and PVOH-CL_TTO) significantly inhibited bacterial growth. Lignin's phenolic structure is known to contribute to its antimicrobial properties by disrupting bacterial cell walls and interfering with essential cellular processes [82]. The combination of lignin and essential oils in PVOH-CL_TTO further enhanced the antimicrobial effectiveness. Essential oils are known to possess antimicrobial properties against broad-spectrum of bacteria and fungal species [72,83]. Thus, they provide additional antimicrobial benefits when combined with lignin. Conversely, the pure PVOH film showed negligible antimicrobial activity, indicating that PVOH lacks inherent antibacterial properties. Thus the incorporation of lignin and essential oils imparts both antioxidant and antimicrobial functionalities to the films, making them suitable as active packaging materials.

3.9. Application of films to extend the shelf-life of strawberries

In Fig. 8a and b, the performance of films in preserving shelf life of strawberries wrapped in them and stored at room temperature (22 ± 2 °C) on the 0th, 2nd, and 4th days, and under refrigeration (4 ± 1 °C) on the 4th, 8th, and 14th days. The assessed included plain polyvinyl alcohol (PVOH), and PVOH containing NCP and LNP with tea tree oil (PVOH-CL_TTO). The unwrapped (UW) on strawberry was used as the control. Results indicated that PVOH-CL_TTO films provided the best preservation effects compared to the others. This superior performance is primarily due to UV barrier, antimicrobial properties imparted by lignin and tea tree oil, respectively. The presence of NCP increased the water vapour barrier. The PVOH-CL_TTO films effectively maintained the strawberries' colour, firmness, and pH. The enhanced colour retention and reduced browning were evident over time, while firmness was preserved, indicating reduced moisture loss and cellular breakdown. Furthermore, the pH stability observed in PVOH-CL_TTO-wrapped strawberries highlighted the film's ability to slow down spoilage. These findings confirm the potential of PVOH-CL_TTO films in extending the shelf-life and freshness of strawberries.

3.9.1. Storage studies of strawberry

The lightness (L*) of strawberries is a critical indicator of freshness. As shown in Fig. 9a, on day 0, all fresh samples had an initial L* value of 50.0. Over time, particularly at room temperature, a rapid decline in lightness was observed. For example, on day 2, unwrapped strawberries showed a significant drop of L* to 35.0, indicating rapid spoilage. In contrast, strawberries wrapped in PVOH and PVOH-CL_TTO films retained higher lightness values of 40.0 and 45.0, respectively, indicating a slower degradation process. By day 4, PVOH-CL_TTO films maintained a L* value of 42.0, outperforming both PVOH-wrapped samples (38.0) and unwrapped samples (30.0). Under refrigeration (4 ± 1 °C), the decline in L* values was less severe across all samples. By day 14, PVOH-CL_TTO-wrapped strawberries retained an L* value of 35.0, while unwrapped samples fell to 25.0. This preservation effect could be attributed to the structural reinforcement provided by lignin and cellulose in the PVOH-CL_TTO films, as well as the antimicrobial properties of tea tree oil [19,84]. These findings indicate that PVOH-CL_TTO films could be used to extend the shelf life of fresh fruits [85].

The firmness is also an important parameter that reflects on the freshness of sugar- and acid-rich fruits such as strawberries. As shown in Fig. 9b, on day 0, all samples had firmness values between 6.8 N and 7.0 N reflecting their initial freshness. At room temperature, unwrapped strawberries showed a significant decline in firmness, by day 2, it dropped to 5.5 N, whereas strawberries wrapped in PVOH and PVOH-CL_TTO films retained higher firmness at 6.2 N and 6.5 N, respectively. By day 4, firmness of unwrapped strawberries further decreased to 4.8 N, while PVOH-CL_TTO-wrapped samples maintained firmness at 5.8 N. Under refrigerated/chilling condition, the decline in firmness was slower across all samples. By day 14, the firmness of unwrapped strawberries decreased to 4.2 N, while that of PVOH-CL_TTO-wrapped strawberries much higher level of firmness (5.5 N), reflecting the film's ability to preserve texture [86].

The variation of pH in stored strawberries is an important indicator of spoilage. As shown in Fig. 9c, on day 0, the pH of fresh samples ranged between 4.8 and 5.0. At room temperature, unwrapped strawberries showed a decline in pH to 4.5 by day 2, suggesting to a faster spoilage. In contrast, strawberries wrapped in PVOH and PVOH-CL_TTO films maintained pH values between 4.7 and 4.8, due to the antimicrobial properties of the films [87]. By day 4, unwrapped strawberries' pH dropped further to 4.3, while that of PVOH-CL_TTO samples remained at 4.7. Under refrigeration, the pH decline was more gradual. By day 14, unwrapped strawberries reached a pH of 4.2, while PVOH-CL_TTO samples maintained a stable pH of 4.7, demonstrating the effectiveness of these films in preserving strawberry by reducing spoilage rate [85,86]. These results demonstrated the ability of PVOH-CL_TTO films in extending the shelf life of strawberries by preserving freshness, texture, and acidity.

The long-term stability of active films depends on their ability to withstand temperature fluctuations, humidity, and mechanical stress [72]. High humidity can compromise the film's moisture barrier, while temperature variations may affect its thermal stability and bioactive properties. Additionally, prolonged storage could reduce the film's antimicrobial efficiency due to the degradation of its antimicrobial compounds. Future studies should focus on enhancing the durability of active films under the most likely storage conditions.

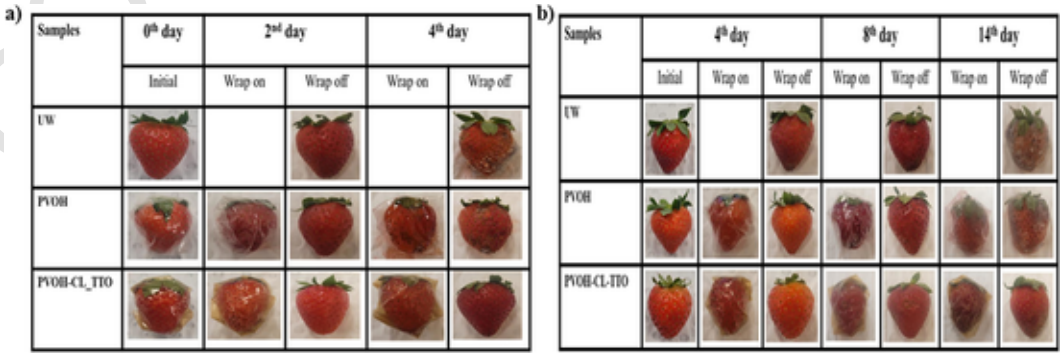

Fig. 8. Strawberry preservation studies: (a) Room temperature (22 °C) storage observed at 0, 2, and 4 days; (b) Refrigeration (4 °C) observed at 4, 8, and 14 days. Comparison of unwrapped (UW), plain PVOH and PVOH-CL_TTO wraps. C = cellulose, L = lignin, TTO = tea tree oil.

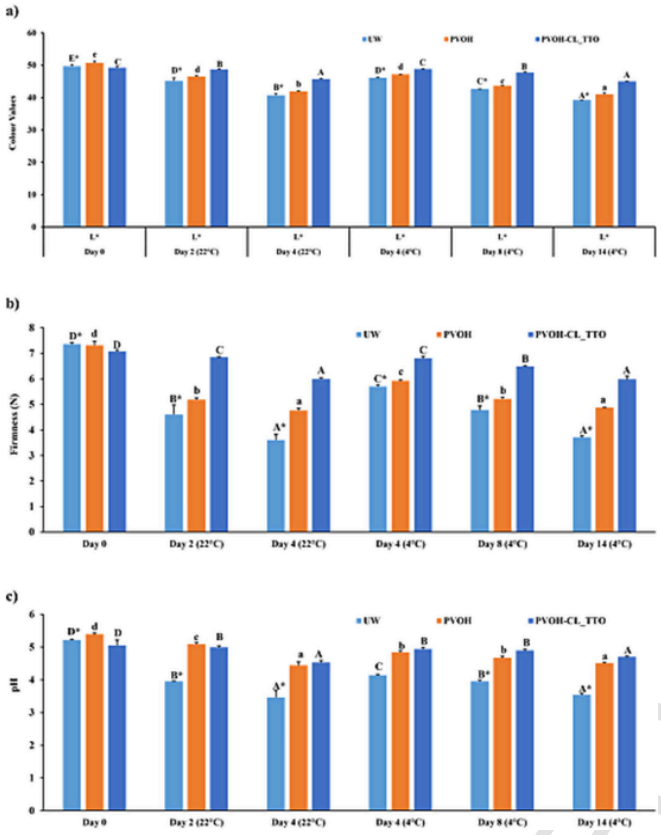

Fig. 9. Storage performance of strawberries wrapped in different films over 14 days at room (22 ± 2 °C) and refrigerated (4 ± 1 °C) conditions, with standard deviations: (a) Colour (L*); (b) Firmness (%); (c) pH. Films include UW, PVOH, and PVOH-CL_TTO. In (a), * shows significant differences between UW, lowercase letters for PVOH, and uppercase for PVOH-CL_TTO across days ($p < 0.05$).

4. Conclusion

Cellulose and lignin were successfully extracted from Dashamoola spent material (DSM) and converted into nanoparticles. The cellulose nanoparticles (NCP) showed excellent structural integrity, thermal stability, and potential for applications including in food packaging. Formation of emulsions and their characterization revealed that combining lignin nanoparticles (LNP) and NCP enhanced the stability, uniformity of O/W emulsions using an essential oil (tea tree oil) as the dispersed phase. Incorporating these emulsions into PVOH resulted in bioactive packaging materials with improved physical, mechanical, thermal, antioxidant, and antimicrobial properties. These active films were effective in extending the shelf life of strawberries up to 14 days in chilled condition. These findings highlight the potential of utilizing cellulose and lignin obtained from Ayurvedic industry's waste stream to develop sustainable, high-performance packaging solutions.

CRediT authorship contribution statement

Billu Abraham: Writing – original draft, Methodology, Investigation, Formal analysis, Data curation, Conceptualization. **Nazila Oladzadabbasabadi:** Validation, Methodology, Investigation. **Heeba Shakeela:** Writing – original draft, Methodology, Data curation. **Charles Brennan:** Project administration, Investigation. **Nitin Mantri:** Supervision, Investigation. **Nisha P:** Writing – review & editing, Supervision, Funding acquisition, Conceptualization. **Benu Adhikari:** Writing – review & editing, Visualization, Validation, Supervision, Methodology, Funding acquisition, Conceptualization.

Uncited reference

[56]

Declaration of competing interest

The authors declare no conflict of interest.

Acknowledgments

The authors gratefully acknowledge CSIR-NIIST, India, and RMIT, Australia, for providing the necessary facilities and support for this research. The first author extends sincere gratitude for the CSIR-SRF direct fellowship. Financial support was provided as part of the AcSIR-RMIT cotutelle PhD program. Nisha P acknowledge DST/TDT/WMT/Biomedical/2021/04 for the initial financial support. The authors acknowledge the technical support provided by RMIT Microscopy & Microanalysis Facility (RMMF) of the University. Special thanks to Yogeshwar Aher for conducting the antibacterial analysis and to Dr. Chaitali for carrying out the SEM analysis.

Data availability

Data will be made available on request.

References

[1] T. Ahmad, F. Esposito, T. Cirillo, Valorization of agro-food by-products: advancing sustainability and Sustainable Development Goals 2030 through functional compound recovery, Food Biosci. (2024) 105194, https://doi.org/10.1016/j.fbio.2024.105194.
[2] M. Gavahian, Opinion on the prospects of emerging food processing technologies to achieve sustainability in the industry by reduced energy consumption, waste reduction and valorization, and improved food nutrition, Int. J. Food Sci. Technol. 59 (2024) 8135–8140, https://doi.org/10.1111/ijfs.17525.
[3] S. Ospina-Maldonado, H. Martin-Gómez, G.A. Cardoso-Ugarte, From waste to wellness: a review on the harness of food industry by-products for sustainable functional food production, Int. J. Food Sci. Technol. 59 (2024) 8680–8692, https://doi.org/10.1111/ijfs.17571.
[4] P.K. Mukherjee, S. Banerjee, C.K. Katiyar, S. Sharma, N. Chattopadhyay, Traditional medical system (TMS) for sustainable healthcare in India, Drug Discov. Drug Dev. Indian Narrat. (2021) 1–36, https://doi.org/10.1007/978-981-15-8002-4_1.
[5] B. Abraham, T.R. Reshmitha, M.M. Navami, L. George, V.V. Venugopalan, P. Nisha, Phytochemical rich extract from the spent material generated from Industrial Dashamoola preparation (a medicinal Ayurvedic decoction) with antioxidant, antidiabetic and anti-inflammatory potential, Ind. Crop. Prod. 151 (2020) 112451, https://doi.org/10.1016/j.indcrop.2020.112451.
[6] B. Abraham, H. Shakeela, L.P. Devendra, K.B. Arun, K.V. Ragavan, C. Brennan, P. Nisha, Lignin nanoparticles from Ayurvedic industry spent materials: applications in Pickering emulsions for curcumin and vitamin D_3 encapsulation, Food Chem. 458 (2024) 140284, https://doi.org/10.1016/j.foodchem.2024.140284.
[7] B.K. Ndwandwe, S.P. Malinga, E. Kayitesi, B.C. Dlamini, Recent developments in the application of natural pigments as pH-sensitive food freshness indicators in biopolymer-based smart packaging: challenges and opportunities, Int. J. Food Sci. Technol. 59 (2024) 2148–2161, https://doi.org/10.1111/ijfs.16990.
[8] S. Tanpichai, A. Boonmahitthisud, N. Soykeabkaew, L. Ongthip, Review of the recent developments in all-cellulose nanocomposites: properties and applications, Carbohydr. Polym. 286 (2022) 119192, https://doi.org/10.1016/j.carbpol.2022.119192.
[9] Y. Liu, S. Ahmed, D.E. Sameen, Y. Wang, R. Lu, J. Dai, W. Qin, A review of cellulose and its derivatives in biopolymer-based food packaging applications, Trends Food Sci. Technol. 112 (2021) 532–546, https://doi.org/10.1016/j.tifs.2021.04.016.
[10] M. Chen, Z. Hu, H. Zheng, J. Wang, X. Xu, Antimicrobial polysaccharide hydrogels embedded with methyl-β-cyclodextrin/thyme oil inclusion complexes for exceptional mechanical performance and chilled chicken breast preservation, Int. J. Biol. Macromol. 267 (2024) 131586, https://doi.org/10.1016/j.ijbiomac.2024.131586.
[11] Y. Cheng, X. Cai, X. Zhang, Y. Zhao, R. Song, Y. Xu, H. Gao, Applications in Pickering emulsions of enhancing preservation properties: current trends and future prospects in active food packaging coatings and films, Trends Food Sci. Technol. (2024) 104643, https://doi.org/10.1016/j.tifs.2024.104643.
[12] G. Pandita, C.K. de Souza, M.J. Gonçalves, J.M. Jasińska, E. Jamróz, S. Roy,

Recent progress on Pickering emulsion stabilized essential oil added biopolymer-based film for food packaging applications: a review, Int. J. Biol. Macromol. (2024) 132067, https://doi.org/10.1016/j.ijbiomac.2024.132067.
[13] E. Hanan, A.H. Dar, R. Shams, G. Goksen, New insights into essential oil nano emulsions loaded natural biopolymers: recent development, formulation, characterization and packaging applications—a comprehensive review, Int. J. Biol. Macromol. (2024) 135751, https://doi.org/10.1016/j.ijbiomac.2024.135751.
[14] T. Dai, Y. Liu, L. Wang, J. Yao, G. Zhu, B. Guo, M. Zhang, PVA@ tea tree oil-emulsion core–shell microfiber membranes for extending the shelf life of fruits, J. Appl. Polym. Sci. 141 (2024) e55038, https://doi.org/10.1002/app.55038.
[15] P. Brun, G. Bernabè, R. Filippini, A. Piovan, *In vitro* antimicrobial activities of commercially available tea tree (*Melaleuca alternifolia*) essential oils, Curr. Microbiol. 76 (2019) 108–116, https://doi.org/10.1007/s00284-018-1594-x.
[16] W. Yang, E. Fortunati, F. Dominici, G. Giovanale, A. Mazzaglia, G.M. Balestra, D. Puglia, Effect of cellulose and lignin on disintegration, antimicrobial and antioxidant properties of PLA active films, Int. J. Biol. Macromol. 89 (2016) 360–368, https://doi.org/10.1016/j.ijbiomac.2016.04.068.
[17] F. Hassan, B. Mu, Y. Yang, Natural polysaccharides and proteins-based films for potential food packaging and mulch applications: a review, Int. J. Biol. Macromol. (2024) 129628, https://doi.org/10.1016/j.ijbiomac.2024.129628.
[18] M. Asgher, S.A. Qamar, M. Bilal, H.M. Iqbal, Bio-based active food packaging materials: sustainable alternative to conventional petrochemical-based packaging materials, Food Res. Int. 137 (2020) 109625, https://doi.org/10.1016/j.foodres.2020.109625.
[19] Y. He, H.C. Ye, T.T. You, F. Xu, Sustainable and multifunctional cellulose-lignin films with excellent antibacterial and UV-shielding for active food packaging, Food Hydrocoll. 137 (2023) 108355, https://doi.org/10.1016/j.foodhyd.2022.108355.
[20] M.A. Sani, M. Azizi-Lalabadi, M. Tavassoli, K. Mohammadi, D.J. McClements, Recent advances in the development of smart and active biodegradable packaging materials, Nanomaterials 11 (2021) 1331, https://doi.org/10.3390/nano11051331.
[21] P.R. Salgado, L. Di Giorgio, Y.S. Musso, A.N. Mauri, Recent developments in smart food packaging focused on biobased and biodegradable polymers, Front. Sustain. Food Syst. 5 (2021) 630393, https://doi.org/10.3389/fsufs.2021.630393.
[22] N. Bhargava, V.S. Sharanagat, R.S. Mor, K. Kumar, Active and intelligent biodegradable packaging films using food and food waste-derived bioactive compounds: a review, Trends Food Sci. Technol. 105 (2020) 385–401, https://doi.org/10.1016/j.tifs.2020.09.015.
[23] P.K. Panda, K. Sadeghi, J. Seo, Recent advances in poly (vinyl alcohol)/natural polymer-based films for food packaging applications: a review, Food Packag. Shelf Life 33 (2022) 100904, https://doi.org/10.1016/j.fpsl.2022.100904.
[24] A.N.M.A. Haque, Y. Zhang, M. Naebe, A review on lignocellulose/poly (vinyl alcohol) composites: cleaner approaches for greener materials, Cellulose 1–24 (2021), https://doi.org/10.1007/s10570-021-04234-6.
[25] S. Roy, J.W. Rhim, Antioxidant and antimicrobial poly (vinyl alcohol)-based films incorporated with grapefruit seed extract and curcumin, J. Environ. Chem. Eng. 9 (2021) 104694, https://doi.org/10.1016/j.jece.2020.104694.
[26] F. Debiagi, R.K. Kobayashi, G. Nakazato, L.A. Panagio, S. Mali, Biodegradable active packaging based on cassava bagasse, polyvinyl alcohol and essential oils, Ind. Crop. Prod. 52 (2014) 664–670, https://doi.org/10.1016/j.indcrop.2013.11.032.
[27] F. Luzi, D. Del Buono, B. Orfei, C. Moretti, R. Buonaurio, L. Torre, D. Puglia, *Lemna minor* aqueous extract as a natural ingredient incorporated in poly (vinyl alcohol)-based films for active food packaging systems, Food Packag. Shelf Life 32 (2022) 100822, https://doi.org/10.1016/j.fpsl.2022.100822.
[28] I. Dudeja, R.K. Mankoo, A. Singh, Citric acid crosslinked ternary blended (polyvinyl alcohol, lignin, lemongrass essential oil/nanoemulsions) biopolymeric hydrogel films: structural, functional, antioxidant, antifungal and biodegradable properties, J. Food Meas. Charact. 17 (2023) 3774–3788, https://doi.org/10.1007/s11694-023-01905-9.
[29] A.A. Oun, G.H. Shin, J.T. Kim, Multifunctional poly (vinyl alcohol) films using cellulose nanocrystals/oregano and cellulose nanocrystals/cinnamon Pickering emulsions: effect of oil type and concentration, Int. J. Biol. Macromol. 194 (2022) 736–745, https://doi.org/10.1016/j.ijbiomac.2021.11.119.
[30] X. Li, Y. Liu, X. Ren, Transparent and ultra-tough PVA/alkaline lignin films with UV shielding and antibacterial functions, Int. J. Biol. Macromol. 216 (2022) 86–94, https://doi.org/10.1016/j.ijbiomac.2022.06.188.
[31] P. Cazón, G. Velazquez, M. Vázquez, Novel composite films from regenerated cellulose-glycerol-polyvinyl alcohol: mechanical and barrier properties, Food Hydrocoll. 89 (2019) 481–491, https://doi.org/10.1016/j.foodhyd.2018.11.012.
[32] S. Suganthi, S. Vignesh, J. Kalyana Sundar, V. Raj, Fabrication of PVA polymer films with improved antibacterial activity by fine-tuning via organic acids for food packaging applications, Appl Water Sci 10 (2020) 1162, https://doi.org/10.1007/s13201-020-1162-y.
[33] A. Bahrami, R. Fattahi, Biodegradable carboxymethyl cellulose–polyvinyl alcohol composite incorporated with *Glycyrrhiza glabra* L. essential oil: physicochemical and antibacterial features, Food Sci. Nutr. 9 (2021) 4974–4985, https://doi.org/10.1002/fsn3.2449.
[34] L. Nian, M. Wang, X. Sun, Y. Zeng, Y. Xie, S. Cheng, C. Cao, Biodegradable active packaging: components, preparation, and applications in the preservation of postharvest perishable fruits and vegetables, Crit. Rev. Food Sci. Nutr. 64 (2024) 2304–2339, https://doi.org/10.1080/10408398.2022.2122924.
[35] W. Lan, R. Zhang, S. Ahmed, W. Qin, Y. Liu, Effects of various antimicrobial polyvinyl alcohol/tea polyphenol composite films on the shelf life of packaged strawberries, LWT 113 (2019) 108297, https://doi.org/10.1016/j.lwt.2019.108297.
[36] Z. He, Efforts towards Effective Robotic Strawberry Harvesting (PhD Dissertation), Washington State University, 2024.
[37] M.R. Bertolo, L.D. Dias, A.R. Lima, A.S. Aguiar, F. Alves, M. de Souza, S.B. Junior, Photoantimicrobial chitosan-gelatin-pomegranate peel extract films for strawberries preservation: from microbiological analysis to in vivo safety assessment, Int. J. Biol. Macromol. 253 (2023) 127085, https://doi.org/10.1016/j.ijbiomac.2023.127085.
[38] B. Abraham, V.L. Syamnath, K.B. Arun, P.F. Zahra, P. Anjusha, A. Kothakotta, P. Nisha, Lignin-based nanomaterials for food and pharmaceutical applications: recent trends and future outlook, Sci. Total Environ. 881 (2023) 163316, https://doi.org/10.1016/j.scitotenv.2023.163316.
[39] R. Ruiz, T. Ehrman, Determination of Carbohydrates in Biomass by High Performance Liquid Chromatography, Laboratory Analytical Procedure-002, NREL/MRI, Golden, CO, 1996.
[40] H.A. Silvério, W.P.F. Neto, N.O. Dantas, D. Pasquini, Extraction and characterization of cellulose nanocrystals from corncob for application as reinforcing agent in nanocomposites, Ind. Crop. Prod. 44 (2013) 427–436, https://doi.org/10.1016/j.indcrop.2012.10.014.
[41] E. Dinçel Kasapoğlu, S. Kahraman, F. Tornuk, Extraction optimization and characterization of cellulose nanocrystals from apricot pomace, Foods 12 (2023) 746, https://doi.org/10.3390/foods12040746.
[42] E.L.M. Moustaqim, A. El Kaihal, M. El Marouani, S. Men-La-Yakhaf, M. Taibi, S. Sebbahi, K. El Hajjaji, F. Kifani-Sahban, Thermal and thermomechanical analyses of lignin, Sustain. Chem. Pharm. 9 (2018) 63–68, https://doi.org/10.1016/j.scp.2018.06.002.
[43] H.Y. Mou, E. Heikkilä, P. Fardim, Topochemistry of alkaline, alkaline-peroxide and hydrotropic pretreatments of common reed to enhance enzymatic hydrolysis efficiency, Bioresour. Technol. 150 (2013) 36–41, https://doi.org/10.1016/j.biortech.2013.09.093.
[44] R. Sindhu, M. Kuttiraja, P. Binod, K.U. Janu, R.K. Sukumaran, A. Pandey, Dilute acid pretreatment and enzymatic saccharification of sugarcane tops for bioethanol production, Bioresour. Technol. 102 (2011) 10915–10921, https://doi.org/10.1016/j.biortech.2011.09.066.
[45] M.S. Martinez-Alvarenga, E.Y. Martinez-Rodriguez, L.E. Garcia-Amezquita, G.I. Olivas, P.B. Zamudio-Flores, C.H. Acosta-Muniz, D.R. Sepulveda, Effect of Maillard reaction conditions on the degree of glycation and functional properties of whey protein isolate–maltodextrin conjugates, Food Hydrocoll. 38 (2014) 110–118, https://doi.org/10.1016/j.foodhyd.2013.11.006.
[46] N. Oladzadabbasabadi, B. Abraham, M. Ghasemlou, E.P. Ivanova, B. Adhikari, Green synthesis of non-isocyanate hydroxyurethane and its hybridization with carboxymethyl cellulose to produce films, Int. J. Biol. Macromol. 276 (2024) 133617, https://doi.org/10.1016/j.ijbiomac.2024.133617.
[47] K.J. Nagarajan, A.N. Balaji, N.R. Ramanujam, Extraction of cellulose nanofibers from *Cocos nucifera* var aurantiaca peduncle by ball milling combined with chemical treatment, Carbohydr. Polym. 212 (2019) 312–322, https://doi.org/10.1016/j.carbpol.2019.02.063.
[48] B. Soni, B. Mahmoud, Chemical isolation and characterization of different cellulose nanofibers from cotton stalks, Carbohydr. Polym. 134 (2015) 581–589, https://doi.org/10.1016/j.carbpol.2015.08.031.
[49] C. Trilokesh, K.B. Uppuluri, Isolation and characterization of cellulose nanocrystals from jackfruit peel, Sci. Rep. 9 (2019) 16709, https://doi.org/10.1038/s41598-019-53412-x.
[50] Q. Li, Y. Wang, Y. Wu, K. He, Y. Li, X. Luo, B. Li, C. Wang, S. Liu, Flexible cellulose nanofibrils as novel Pickering stabilizers: the emulsifying property and packing behavior, Food Hydrocoll. 88 (2019) 180–189, https://doi.org/10.1016/j.foodhyd.2018.09.039.
[51] R.G. Candido, G.G. Godoy, A.R. Gonçalves, Characterization and application of cellulose acetate synthesized from sugarcane bagasse, Carbohydr. Polym. 167 (2017) 280–289, https://doi.org/10.1016/j.carbpol.2017.03.057.
[52] P. Lu, Y.L. Hsieh, Cellulose isolation and core–shell nanostructures of cellulose nanocrystals from chardonnay grape skins, Carbohydr. Polym. 87 (2012) 2546–2553, https://doi.org/10.1016/j.carbpol.2011.11.023.
[53] H. Zhang, Y. Chen, S. Wang, L. Ma, Y. Yu, H. Dai, Y. Zhang, Extraction and comparison of cellulose nanocrystals from lemon (*Citrus limon*) seeds using sulfuric acid hydrolysis and oxidation methods, Carbohydr. Polym. 238 (2020) 116180, https://doi.org/10.1016/j.carbpol.2020.116180.
[54] E.S. Anari, N. Soltanizadeh, M. Fathi, The potential of DBD plasma pretreatment for the isolation of micro-and nano-cellulose fibers from walnut shells, Carbohydr. Polym. 327 (2024) 121692, https://doi.org/10.1016/j.carbpol.2023.121692.
[55] M. Zhu, S. Huan, S. Liu, Z. Li, M. He, G. Yang, L. Bai, Recent development in food emulsion stabilized by plant-based cellulose nanoparticles, Curr. Opin. Colloid Interface Sci. 56 (2021) 101512, https://doi.org/10.1016/j.cocis.2021.101512.
[56] N. Li, H.J. Xiang, T.G. Hu, W.P. Qiu, Y.X. Hong, K.W. Huang, P. Wen, Multifunctional electrospun nanofibrous film integrated with cinnamon essential oil emulsion stabilized by dealkali lignin for active packaging material, Colloids Surf. A Physicochem. Eng. Asp. 704 (2025) 135467, https://doi.org/10.1016/j.colsurfa.2024.135467.
[57] G. Pandita, C.K. de Souza, M.J. Gonçalves, J.M. Jasińska, E. Jamróz, S. Roy, Recent progress on Pickering emulsion stabilized essential oil added biopolymer-based film for food packaging applications: a review, Int. J. Biol. Macromol. (2024) 132067, https://doi.org/10.1016/j.ijbiomac.2024.132067.
[58] L. Bai, L.G. Greca, W. Xiang, J. Lehtonen, S. Huan, R.W.N. Nugroho, O.J. Rojas, Adsorption and assembly of cellulosic and lignin colloids at oil/water interfaces, Langmuir 35 (2018) 571–588, https://doi.org/10.1021/acs.langmuir.8b01288.
[59] K. Rehman, T. Kanwal, A.A. Shuja, S. Saifullah, S.U. Simjee, M.R. Shah, Development and characterization of palmitoyl-modified arginine containing

curcumin-loaded niosomal vesicles for improved antioxidant and anticancer activities, Colloid Polym. Sci. 302 (2024) 1671–1685, https://doi.org/10.1007/s00396-024-05299-y.
[60] Q. Zhou, J. Chen, C. Wang, G. Yang, S. Janaswamy, F. Xu, Z. Liu, Preparation and characterization of lignin nanoparticles and chitin nanofibers reinforced PVA films with UV shielding properties, Ind. Crop. Prod. 188 (2022) 115669, https://doi.org/10.1016/j.indcrop.2022.115669.
[61] D. Lingait, L.K. Sethy, A. Kumar, Biopolymer sporopollenin reinforced pectin/PVA composite films for sustainable packaging application, Sustain. Chem. Pharm. 41 (2024) 101711, https://doi.org/10.1016/j.scp.2024.101711.
[62] P. Phansamarng, A. Bacchus, F.H. Pour, C. Kongvarhodom, P. Fatehi, Cationic lignin incorporated polyvinyl alcohol films for packaging applications, Ind. Crop. Prod. 221 (2024) 119217, https://doi.org/10.1016/j.indcrop.2024.119217.
[63] Y. Ren, X. Fan, L. Cao, Y. Chen, Water-resistant and barrier properties of poly (vinyl alcohol)/nanocellulose films enhanced by metal ion crosslinking, Int. J. Biol. Macromol. 277 (2024) 134245, https://doi.org/10.1016/j.ijbiomac.2024.134245.
[64] B. Liu, W. Zhang, J. Zeng, N. Gong, G. Ying, P. Li, K. Chen, Acid-catalyzed phenolation of lignin with tea polyphenol: enhancing UV resistance and oxidation resistance for potential applications, Int. J. Biol. Macromol. 267 (2024) 131462, https://doi.org/10.1016/j.ijbiomac.2024.131462.
[65] A. Farhan, N.M. Hani, Active edible films based on semi-refined κ-carrageenan: antioxidant and color properties and application in chicken breast packaging, Food Packag. Shelf Life 24 (2020) 100476, https://doi.org/10.1016/j.fpsl.2020.100476.
[66] Y. Zhang, A.N.M.A. Haque, M. Naebe, Lignin–cellulose nanocrystals from hemp hurd as light-colored ultraviolet (UV) functional filler for enhanced performance of polyvinyl alcohol nanocomposite films, Nanomaterials 11 (2021) 3425, https://doi.org/10.3390/nano11123425.
[67] H. Wang, X. Liu, M. Wu, Y. Huang, Construction of multiple crosslinked networks for the preparation of high-performance lignin-containing cellulose nanofiber reinforced polyvinyl alcohol films, Int. J. Biol. Macromol. 259 (2024) 129061, https://doi.org/10.1016/j.ijbiomac.2023.129061.
[68] S. Pirsa, Cellulose-based cartons: production methods, modification, and smart/active packaging, Cellulose 31 (2024) 3421–3445, https://doi.org/10.1007/s10570-024-05826-8.
[69] A. Akelah, A. Akelah, Polymers in food packaging and protection, in: Functionalized Polymeric Materials in Agriculture and the Food Industry, Springer, 2013, pp. 293–347, https://doi.org/10.1007/978-1-4614-7061-8_6.
[70] J.C. Borges, L.A. de Almeida Campos, E.A.M. Kretzschmar, I.M.F. Cavalcanti, Incorporation of essential oils in polymeric films for biomedical applications, Int. J. Biol. Macromol. (2024) 132108, https://doi.org/10.1016/j.ijbiomac.2024.132108.
[71] M. Szymanska-Chargot, M. Chylinska, B. Kruk, A. Zdunek, Combining FT-IR spectroscopy and multivariate analysis for qualitative and quantitative analysis of the cell wall composition changes during apple development, Carbohydr. Polym. 115 (2015) 93–103, https://doi.org/10.1016/j.carbpol.2014.08.039.
[72] Y. Wang, J. Li, X. Guo, H. Wang, F. Qian, Y. Lv, Active biodegradable polyvinyl alcohol–hemicellulose/tea polyphenol films with excellent moisture resistance prepared via ultrasound assistance for food packaging, Coatings 11 (2021) 219, https://doi.org/10.3390/coatings11020219.
[73] I. Bascón-Villegas, M. Sánchez-Gutiérrez, F. Pérez-Rodríguez, E. Espinosa, A. Rodríguez, Lignocellulose nanofibre obtained from agricultural wastes of tomato, pepper and eggplants improves the performance of films of polyvinyl alcohol (PVA) for food packaging, Foods 10 (2021) 3043, https://doi.org/10.3390/foods10123043.
[74] H. Wang, M. Zhang, J. Hu, H. Du, T. Xu, C. Si, Sustainable preparation of surface functionalized cellulose nanocrystals and their application for Pickering emulsions, Carbohydr. Polym. 297 (2022) 120062, https://doi.org/10.1016/j.carbpol.2022.120062.
[75] J.I. Castro, C.H. Valencia-Llano, M.E. Valencia Zapata, Y.J. Restrepo, J.H. Mina Hernandez, D.P. Navia-Porras, C.D. Grande-Tovar, Chitosan/polyvinyl alcohol/tea tree essential oil composite films for biomedical applications, Polymers 13 (2021) 3753, https://doi.org/10.3390/polym13213753.
[76] J. Huang, Q. Guo, R. Zhu, Y. Liu, F. Xu, X. Zhang, Facile fabrication of transparent lignin sphere/PVA nanocomposite films with excellent UV-shielding and high strength performance, Int. J. Biol. Macromol. 189 (2021) 635–640, https://doi.org/10.1016/j.ijbiomac.2021.08.167.
[77] A.M. Abdelghany, A.A. Menazea, A.M. Ismail, Synthesis, characterization and antimicrobial activity of chitosan/polyvinyl alcohol blend doped with *Hibiscus sabdariffa* L. extract, J. Mol. Struct. 1197 (2019) 603–609, https://doi.org/10.1016/j.molstruc.2019.07.089.
[78] X. Dong, J. Shang, T. Xiao, R. Song, X. Sheng, N. Li, Q. Ping, A facile method to fabricate sustainable bamboo ethanol lignin/carboxymethylcellulose films with efficient anti-ultraviolet and insulation properties, Int. J. Biol. Macromol. 273 (2024) 132959, https://doi.org/10.1016/j.ijbiomac.2024.132959.
[79] G. Akhouy, A.K. Eticha, C. Dogan, N. Dogan, M.D. Calisir, A. Toptas, F. Aziz, Y. Akgul, Electro-blown micro-nanofibrous mats with *Origanum elongatum* essential oil for enhancing the shelf life of tomato (*Solanum lycopersicum*), Int. J. Food Sci. Technol. 59 (2024) 9512–9522, https://doi.org/10.1111/ijfs.17600.
[80] A. Barhoum, J. Jeevanandam, A. Rastogi, P. Samyn, Y. Boluk, A. Dufresne, M. Bechelany, Plant celluloses, hemicelluloses, lignin, and volatile oils for the synthesis of nanoparticles and nanostructured materials, Nanoscale 12 (2020) 22845–22890, https://doi.org/10.1039/D0NR04795C.
[81] A.J. Basbasan, B. Hararak, C. Winotapun, W. Wanmolee, W. Chinsirikul, P. Leelaphiwat, K. Boonruang, Lignin nanoparticles for enhancing physicochemical and antimicrobial properties of polybutylene succinate/thymol composite film for active packaging, Polymers 15 (2023) 989, https://doi.org/10.3390/polym15040989.
[82] K. Li, W. Zhong, P. Li, J. Ren, K. Jiang, W. Wu, Antibacterial mechanism of lignin and lignin-based antimicrobial materials in different fields, Int. J. Biol. Macromol. 252 (2023) 126281, https://doi.org/10.1016/j.ijbiomac.2023.126281.
[83] L. Hernández-García, X. Molinos, P. Manzanares, J.F. Marcos, P.V. Martínez-Culebras, Comparing the activity and interactions of the antifungal protein PeAfpA with conventional fungicides and food preservatives against mycotoxigenic fungi, Int. J. Food Sci. Technol. 59 (2024) 9326–9335, https://doi.org/10.1111/ijfs.17575.
[84] J.S.P. Da Silva, J.M.F. Da Silva, B.G. Soares, S. Livi, Fully biodegradable composites based on poly (butylene adipate-co-terephthalate)/peach palm trees fiber, Compos. Part B Eng. 129 (2017) 117–123, https://doi.org/10.1016/j.compositesb.2017.07.088.
[85] I.B. Basumatary, A. Mukherjee, V. Katiyar, S. Kumar, Biopolymer-based nanocomposite films and coatings: recent advances in shelf-life improvement of fruits and vegetables, Crit. Rev. Food Sci. Nutr. 62 (2022) 1912–1935, https://doi.org/10.1080/10408398.2020.1848789.
[86] Y. Shen, F. Seidi, M. Ahmad, Y. Liu, M.R. Saeb, A. Akbari, H. Xiao, Recent advances in functional cellulose-based films with antimicrobial and antioxidant properties for food packaging, J. Agric. Food Chem. 71 (2023) 16469–16487, https://doi.org/10.1021/acs.jafc.3c06004.
[87] Y. Zhang, W. Jiang, Effective strategies to enhance ultraviolet barrier ability in biodegradable polymer-based films/coatings for fruit and vegetable packaging, Trends Food Sci. Technol. 139 (2023) 104139, https://doi.org/10.1016/j.tifs.2023.104139.

Science of the Total Environment 881 (2023) 163316

Contents lists available at ScienceDirect

Science of the Total Environment

journal homepage: www.elsevier.com/locate/scitotenv

Lignin-based nanomaterials for food and pharmaceutical applications: Recent trends and future outlook

Billu Abraham [a,b,c], V.L. Syamnath [a], K.B. Arun [d], P.M. Fathima Zahra [e], P. Anjusha [e], Anjhinaeyulu Kothakotta [a,b], Yi-Hsun Chen [f,*], Vinoth Kumar Ponnusamy [c,g,h,i,j,**], P. Nisha [a,b,***]

[a] Agro Processing and Technology Division, CSIR-National Institute for Interdisciplinary Science and Technology, Council of Scientific and Industrial Research, Trivandrum 695019, India
[b] Academy of Scientific and Innovative Research (AcSIR), Ghaziabad 201002, India
[c] Research Center for Precision Environmental Medicine, Kaohsiung Medical University (KMU), Kaohsiung City 807, Taiwan
[d] Department of Life Sciences, Christ (Deemed to be University), Bangalore 29, India
[e] College of Agriculture, Vellayani, Kerala Agricultural University, India
[f] Division of Gastroenterology, Department of Internal Medicine, Kaohsiung Medical University Hospital, Kaohsiung Medical University, Kaohsiung City, Taiwan
[g] Department of Medicinal and Applied Chemistry, Kaohsiung Medical University (KMU), Kaohsiung City 807, Taiwan
[h] Department of Medical Research, Kaohsiung Medical University Hospital (KMUH), Kaohsiung City 807, Taiwan
[i] Department of Chemistry, National Sun Yat-sen University (NSYSU), Kaohsiung City 804, Taiwan
[j] Ph.D. Program of Aquatic Science and Technology, College of Hydrosphere Science, National Kaohsiung University of Science and Technology (NKUST), Kaohsiung City 811, Taiwan

HIGHLIGHTS

- Lignin and nanolignin are biodegradable, biocompatible, and nontoxic.
- Nanolignin as nanoparticles as an affordable and sustainable substitute.
- Eco-friendly synthesis of lignin and nanolignin and their facile applications
- Lignin and nanolignin have applications in food, medicine, pharmacy and cosmetics.
- Nanolignin applications in biorefinery, agriculture, and bioremediation

GRAPHICAL ABSTRACT

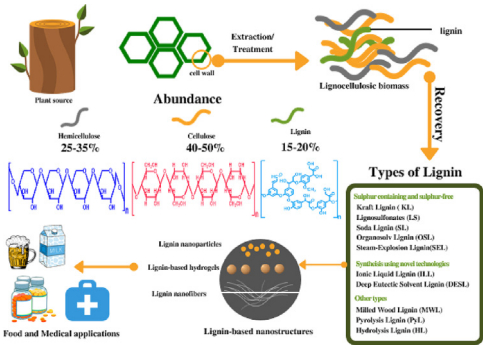

ARTICLE INFO

Editor: Huu Hao Ngo

Keywords:
Lignin
Nanolignin
Antioxidant activity
Nutrient delivery
Drug delivery

ABSTRACT

Small particles of size ranging from 1 to 100 nm are referred to as nanoparticles. Nanoparticles have tremendous applications in various sectors, including the areas of food and pharmaceutics. They are being prepared from multiple natural sources widely. Lignin is one such source that deserves special mention due to its ecological compatibility, accessibility, abundance, and low cost. This amorphous heterogeneous phenolic polymer is the second most abundant molecule in nature after cellulose. Apart from being used as a biofuel source, lignin is less explored for its potential at a nano-level. In plants, lignin exhibits cross-linking structures with cellulose and hemicellulose. Numerous advancements have taken place in synthesizing nanolignins for manufacturing lignin-based materials to benefit from the untapped potential of lignin in high-value-added applications. Lignin and lignin-based nanoparticles have numerous

* Correspondence to: Y.-H. Chen, Division of Gastroenterology, Department of Internal Medicine, Kaohsiung Medical University Hospital, Kaohsiung Medical University, Kaohsiung City, Taiwan.
** Correspondence to: V.K. Ponnusamy, Department of Medicinal and Applied Chemistry, & Research Center for Precision Environmental Medicine, Kaohsiung Medical University (KMU), Kaohsiung City 807, Taiwan.
*** Correspondence to: P. Nisha, Agro Processing and Technology Division, CSIR-National Institute for Interdisciplinary Science and Technology, Council of Scientific and Industrial Research, Trivandrum 695019, India.
E-mail addresses: jayshung1985@gmail.com (Y.-H. Chen), kumar@kmu.edu.tw (V.K. Ponnusamy), pnisha@niist.res.in (P. Nisha).

http://dx.doi.org/10.1016/j.scitotenv.2023.163316
Received 12 January 2023; Received in revised form 5 March 2023; Accepted 2 April 2023
Available online 5 April 2023

applications, but in this review, we are mainly focusing on the applications in the food and pharmaceutical sectors. The exercise we undertake has great relevance as it helps scientists and industries gain valuable insights into lignin's capabilities and exploit its physical and chemical properties to facilitate the development of future lignin-based materials. We have summarized the available lignin resources and their potential in the food and pharmaceutical industries at various levels. This review attempts to understand various methods adopted for the preparation of nanolignin. Furthermore, the unique properties of nano-lignin-based materials and their applications in fields including the packaging industry, emulsions, nutrient delivery, drug delivery hydrogels, tissue engineering, and biomedical applications were well-discussed.

Contents

1. Introduction . . . 3
2. Sources of lignin . . . 3
3. Applications of lignin . . . 3
   - 3.1. Food industry applications . . . 6
     - 3.1.1. Food emulsion . . . 8
     - 3.1.2. Food packaging . . . 8
     - 3.1.3. Nutrient delivery . . . 10
   - 3.2. Pharmaceutical applications . . . 10
     - 3.2.1. Hydrogels for drug delivery . . . 10
   - 3.3. Drug delivery and tissue engineering applications . . . 10
     - 3.3.1. Drug delivery applications . . . 10
     - 3.3.2. Tissue engineering applications . . . 11
   - 3.4. Lignin composites and its biological activity . . . 11
     - 3.4.1. Antioxidant activity . . . 11
     - 3.4.2. Antimicrobial properties . . . 12
     - 3.4.3. Lignin composites for drug delivery systems . . . 12
     - 3.4.4. Lignin composites for wound healing . . . 12
     - 3.4.5. Lignin for disease prevention . . . 12
4. Recent trends in lignin research: nanolignin . . . 13
   - 4.1. The rationale for nanolignin preparation . . . 13
     - 4.1.1. Nanolignin from mechanical processes . . . 13
     - 4.1.2. Nanolignin from solvent shifting method . . . 13
     - 4.1.3. Nanolignin from pH shifting technique . . . 13
     - 4.1.4. Nanolignin from template-based synthesis technique . . . 13
     - 4.1.5. Nanolignin from ice-segregation-induced self-assembly method . . . 13
     - 4.1.6. Nanolignin from aerosol process . . . 13
     - 4.1.7. Nanolignin from electrospinning method . . . 13
     - 4.1.8. Nanolignin from supercritical fluid processes . . . 13
     - 4.1.9. Nanolignin from solvent antisolvent precipitation . . . 13
     - 4.1.10. Nanolignin from acoustic cavitation assisted nanoparticles preparation. . . . 16
     - 4.1.11. Nanolignin from SERSL . . . 16
     - 4.1.12. Nanolignin from green synthesis process . . . 16
     - 4.1.13. Nanolignin from hydroxymethylation . . . 16
     - 4.1.14. Nanolignin from wheat pulping black liquor . . . 16
     - 4.1.15. Nanolignin from supercritical antisolvent technology . . . 16
     - 4.1.16. Nanolignin from chemomechanical methods . . . 16
     - 4.1.17. Nanolignin from self-assembly . . . 16
   - 4.2. Applications of nanolignin . . . 17
     - 4.2.1. Food packaging . . . 17
     - 4.2.2. Nanolignin as a radical scavenger/antioxidant . . . 17
     - 4.2.3. Nanolignin as a carrier . . . 17
     - 4.2.4. Solid and porous particles/structures . . . 18
     - 4.2.5. Nanolignin for oral disease and tissue regeneration . . . 18
     - 4.2.6. Nanolignin as a UV blocker . . . 18
     - 4.2.7. Nanolignin as adsorbent . . . 19
     - 4.2.8. Nanolignin as supercapacitor . . . 19
     - 4.2.9. Nanolignin as surfactant . . . 19
   - 4.3. United Nations sustainable development goal (UNSDG) achieved with the development of nanolignins . . . 19
5. Future perspectives . . . 19
6. Conclusion. . . . 19

CRediT authorship contribution statement . . . 19
Data availability . . . 19
Declaration of competing interest . . . 19
Acknowledgment . . . 19
References . . . 19

1. Introduction

The principal components of plant biomass created by plants consist of cellulose, hemicellulose, and lignin. Lignin is the most widely distributed aromatic polymer, and it participates with cellulose and hemicellulose to shape and toughen plant cell walls. According to recent reports, the paper industry produces nearly 50 million tons of biomass by-products annually worldwide. Unfortunately, 98 % of this organic chunk is either burned for generating energy or disposed of directly into sewage systems, leading to serious environmental consequences. That leaves 2 % of the biomass material for industrial use, especially for creating valuable lignin-based products (Pham et al., 2023). Lignin also accounts for one-fifth of the total biomass available on the planet (Pham et al., 2023; Bajwa et al., 2019). Together, they form a reinforced structure resembling a supra-molecular scaffold capable of providing physical and chemical durability to the cell when encountering infections and enzymatic and chemical destruction (Xie et al., 2018). Mostly lignin (up to 35 %) gets stored in the middle lamella of plants like jute, cotton, industrial hemp, and wood pulp. Lignin types viz. lignosulfonates (88 %), kraft lignin (9 %), and the emerging sulfur-free organosolv accounting for 2 % represent the lignin market. By 2025, lignin's valuation is expected to reach $913.1 million if current trends continue (Pham et al., 2023; Bajwa et al., 2019). Lignin has a variety of industrial applications, including sterile biomedical device modules, food packaging materials, toughened entities for tissue engineering, and deliverable drug carriers, among others. Lignin also adds value to consumer goods owing to its intrinsic UV shielding qualities, antioxidant capability, chemical stability, and physical toughness. Several publications discuss how lignin helps in value addition and shelf-life extension (Akbarian et al., 2022).

Augustin Pyramus de Candolle et al introduced the moniker lignum, and Peter Klason proposed a coniferyl alcohol-packed lignin skeleton to explain the chemical composition of lignin (Bajwa et al., 2019). Lignin is a polymer made up of three monolignols-*p*-hydroxyphenyl (H), guaiacyl (G), and syringyl (S) units. Substituted phenolic groups like p-coumaryl, coniferyl, and sinapyl are spatially ordered in a lignin biomolecule, allowing for a wide range of functional entities and linkages. The interplay between H, G, and S units in lignin contributes to their heterogeneity, yielding numerous functional groups and linkages. About 50 % of all linkages come from the aryl ether-O-4 linkage (Sethupathy et al., 2022).

Previously, the only way to obtain organic constituents and usable energy was from lignin-loaded industrial spent materials and their residues. The H, S, and G subunits produced by the radical coupling process of phenylpropanoid units provide the structural foundation for lignin (Ma et al., 2018). Because of their heterogeneous character, recovering lignin in its native state for structural elucidation becomes laborious. Recent near-perfect recoveries of milled wood lignin (MWL) and cellulolytic enzyme lignin (CEL) provide a resolution to this problem to an extent (Bertella and Luterbacher, 2020). Previous lignin research focused on its role in the pulp and paper industry, as lignin was dumped as waste by the industry. Because of that, studies were limited to structural elucidation and chemical profiling (Sharma et al., 2020).

In their natural form, lignins are polysaccharide-bound structures entangled in cellulose and hemicellulose with irregular distribution patterns (Sharma et al., 2020). Plant source, treatment criteria, extraction plan, and other factors influence the physicochemical properties of lignin. Agricultural and industrial by-products such as pulp and paper (Tortora et al., 2014), bagasse (Bertolo et al., 2019), herbal and agro-waste materials (Abraham et al., 2020), wood, and other organic wastes have copious amounts of lignin. In contrast, individual plant parts, grass, and other organic wastes yield significantly low levels of lignin (Sethupathy et al., 2022).

Recently, lignin-derived composites have drawn the attention of researchers and industrialists since their nanoforms improved durability and added multitudinous value to products such as rubber, textiles, and other materials (Ajith et al., 2021). Compared to nano-sized lignins, native lignin fails to deliver the expected interaction and performance-boosting capabilities when treated as a single entity (Parvathy et al., 2020). When impregnated with gluten-containing nanostructures, nanolignins exhibited improved thermal, mechanical, UV-shielding, and water-sensing capacity. Nanolignins combined with chitosan have shown up to 83 % methyl orange scavenging capabilities in contaminated water systems. A study found that the morphology of lignin nanoparticles provides better dispersibility and stability for up to two months. They produced uniformly dispersed nanolignins using acoustic irradiation sans chemical intervention (Gilca et al., 2015). Encapsulating cationic polyelectrolyte layers onto nanolignins loaded with silver ions can form biodegradable and eco-friendly fill-in for silver nanoparticles. The polyelectrolyte surface facilitates contact with the bacterial cell membrane and it kills a wide range of bacteria, particularly quaternary-amine-resistant *Ralstonia* sp., *Pseudomonas aeruginosa*, and *E. coli*, when combined with silver ions (Richter et al., 2015).

Many applications involving lignin are in the pipeline, and the need for superior materials to improve performances and evade life threats is rising. Therefore, we think it is high time to shed light on these overlooked abundant, ecofriendly, and biocompatible components.

2. Sources of lignin

The significant sources of lignin include plants and agro-processing residues. In India, ayurvedic industries also yield tons of spent materials as biowaste, a resource used for lignin production. The different sources of lignin are summarized in Table 1. Moreover, a Pine variety called Brazilwood, bamboo species such as *Bambusa vulgaris* and *Chusquea oxylepis*, *Festuca arundinacea* belonging to grass species, elephant grass (*Pennisetum purpureum*), *Zea mays*, red clover, bagasse (*Saccharum hibridas*) from sugar cane, and lucerne (*Medicago sativa*) are all good sources of lignin (Haghdan et al., 2016).

Using agricultural by-products for lignin synthesis has several advantages on the techno-economic-environmental front due to the accessibility to various eco-friendly methods. The agro-processing residual biomass generates economically viable homogeneous nanoscale coatings and sterile biopolymeric materials for food packaging. Sugar cane, rice, wheat, and maize are the four crops that contribute the most lignocellulosic biomass to the global agro-industry, with the remainder of the crops contributing only marginally. Bioethanol synthesis from lignin-rich agricultural by-products using environmentally friendly technology involving enzymes and engineered yeasts has the potential to contribute to energy security (Haldar et al., 2022).

The Ayurveda drug industry uses over a thousand plants and plant parts to manufacture various drugs. Dumping these biowastes exacerbates the accumulation of a large volume of industrial biomass in landfills (Vinardell and Mitjans, 2017). Several studies point to the judicious use of plant-based spent materials containing lignin portions. Our team has already revealed the potential of water-miscible bioactive trapped inside massive chunks of lignocellulose spent material abandoned by the Ayurveda medicine industry (Abraham et al., 2020). Due to incomplete extraction with popular solvents mentioned in Ayurvedic texts (water, milk, ghee, oil, etc.), herbal leftovers remained a reservoir of phytochemicals till further extraction. Vinardell et al. investigated the biological significance of lignin fractions generated from the babul tree (*Acacia nilotica*), a medicinal herb used in ayurvedic decoctions.

A primary extraction method of lignin from spent materials is described in Fig. 1. In addition, a study by Vinardell et al. supports using biotransformed lignin from medicinal plants in the food, pharmaceutical, and cosmetic industries (Vinardell and Mitjans, 2017). Various extraction techniques for lignin and their advantages and disadvantages are discussed in Table 2.

3. Applications of lignin

Lignin shows a wide range of potential applications in various industrial sectors, particularly in the food and pharmaceutical industries (Fig. 2).

Table 1
Major sources and classifications of lignin.

Source	Image	Classification	References
Wood		Sulfite lignin (Lignosulfonates)	Lora, 2008
Wood (Black liquors)		Kraft lignin	Ekeberg et al., 2006
Non-wood fibers, annual plants		Soda lignin (Alkali lignin)	Gosselink et al., 2004
Annual plants		Aquasolv lignin	Zhuang et al., 2016
Methanol extracts of fresh birch (*Betula pendula*) xylem		Brauns' lignins	Hiltunen et al., 2006
Middle lamella of the plant cell walls	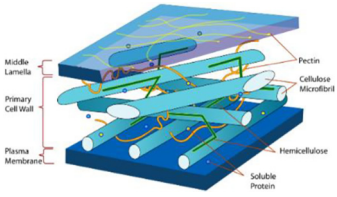	Milled wood lignin (Björkman's lignin)	Claudia et al., 2011
Residue left after polysaccharides hydrolysis of the carbohydrates in finely milled wood		Milled wood enzyme lignin (MWEL)	Agrawal et al., 2014
Solvent-soluble fraction of MWEL		Cellulase enzyme lignin	Agrawal et al., 2014

Table 1 (*continued*)

Source	Image	Classification	References
Hardwood and wheat straw		Organosolv lignin	Prakash et al., 2015
Insoluble residue portion after removing the ash by concentrated acid hydrolysis of the plant tissues	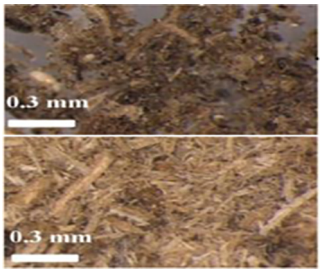	Klason lignin	Chen, 2015
Hardwood species such as aspen		Steam explosion lignin	Gellerstedt and Henriksson, 2008
Corn stalk		Organosolv ethanol lignin (OEL)	Wang et al., 2019
Bamboo	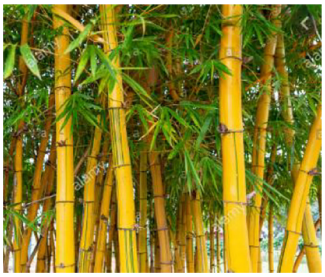	Lignin–carbohydrate complexes	Huang et al., 2018
Artocarpus heterophyllus		Bio composite lignin–chitosan	Jaganathan et al., 2018

(continued on next page)

Table 1 (*continued*)

Source	Image	Classification	References
Birch wood		Poly (lactic acid)–lignin biocomposites	Spiridon and Tanase, 2018
Oil palm empty fruit bunches		Lignocellulosic	Medina et al., 2016
Avermectin encapsulated with acetylated lignin and benzoylated lignin		Pulp-making black liquor	Zhou et al., 2019

3.1. Food industry applications

The food industry constantly strives to find new functional entities to improve the quality of food that leaves factories. Such functional foods will contain health-promoting components that can improve nutrient absorption by filtering out undesirable chemicals in the gastrointestinal tract (Gil-Chávez et al., 2019).

The zero-waste concept is a widely held concept that dictates the maximum utilization of plant-derived raw materials. Several allied and non-allied sectors will benefit if the agro-food industries fixate on adopting

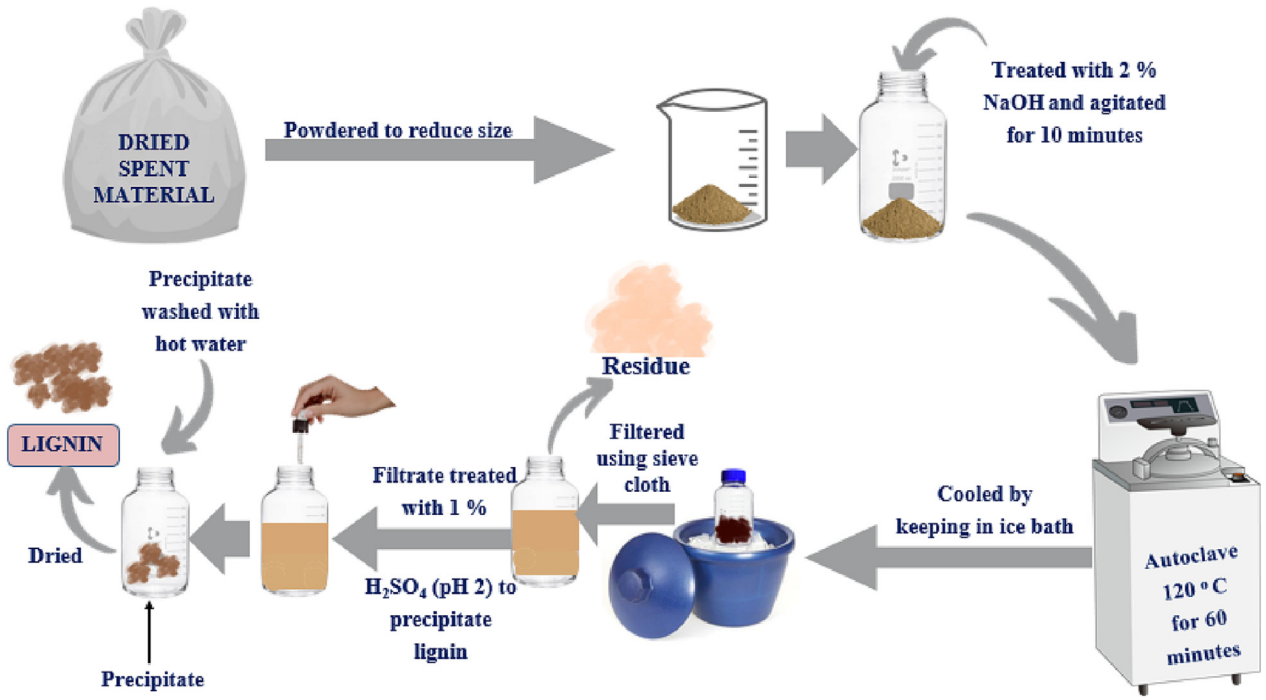

Fig. 1. Lignin extraction method using alkali condition.

Table 2
Extraction techniques, advantages, disadvantages, and application of lignin-sourced raw materials.

Raw material	Extraction method	Advantages	Disadvantages	Application	References
Wood	Aqueous dioxane extraction of milled wood	Better selectivity for the hydrolysis of lignin. This extraction process significantly increased yield and methoxyl content of the isolated lignin.	Dioxane is not recommendable from an environmental perspective as it uses toxic solvents	Agriculture, manufacturing, cosmetics, construction, and biomedicine	Lora, 2008; Chen, 2015
Wood (Black liquors)	Hydrophobic Interaction Chromatography (HIC) method to separate lignosulphonates and kraft lignins into seven distinctive peaks according to hydrophobicity	Water soluble	Complexity and irregularity of the molecular structure of lignin.	As dispersion agent in concrete, in ceramics, as dispersants in textile dyeing, in pesticides, and as binders in briquetting and animal feed	Sun et al., 2015, 2016; Ekeberg et al., 2006
Non-wood fibers, annual plants	Novel, sulfur chemical free-pulping process, which called the NovaFiber process	Anti-oxidant, UV stabilizer and low cost of lignin	Heterogeneity, odour and colour problems of lignin-based products.	Functional additive in commodity plastics like polyethylene and polypropylene	Gosselink et al., 2004
Annual plants	Liquid hot water pretreatment of lignocellulosic biomass.	Minimizes the formation of degradation products, Reduces high water consumption and energy input	The residual lignin, structural characteristics, high solid loading and end products negatively influence enzymatic hydrolysis of cellulose	Production of high value-added products and biorefinery of cellulosic ethanol.	Zhuang et al., 2016; Zhang et al., 2022
Methanol extracts of fresh birch (*Betula pendula*) xylem	Brauns lignin extracted with neutral alcoholic solvents.	Attractive light colour of the wood	Vacuum drying of sawn birch timber (dark in colour) causes discolouration.	Woodworking industry, wood panel products	Hiltunen et al., 2006
Middle lamella of the spruce (*Picea abies* and *Picea mariana*) and beech (Fagus) wood	Bjorkman method with slight modification. The biomass is saturated with toluene prior to milling (48 h) and the milled material is mixed with 1,4-dioxone/water solution and is stirred (24 h) at ambient temperature. After centrifugation, evaporate solvent from supernatants to separate milled wood lignin.	Quicker extraction method. Structural changes of lignin is relatively small during the separation process	Extraction is difficult due to the chemical bonds that exist between lignin and the carbohydrates. Lignin has a very high molecular weight and may form a three-dimensional network.	Anti-microbial and anti-HIV effects. It used as biological carriers.	Claudia et al., 2011
Finely Milled wood	Lignin isolated from Finely-milled wood, the cellulolytic enzymes are used.	Prevents scaling in hot and cooling waters and dissolves micronutrients in liquid fertilizers. Plentiful functional groups and low toxicity	Some carbohydrate cannot be removed by prolonged and repetitive enzymatic treatments or by purification methods during lignin isolation. Lower durability, poor fiber-matrix adhesion	As sequestering agents, as a dispersant in battery, as a dust suppressant, as a food additives, in cement, and in blends.	Ganasan et al., 2022; Agrawal et al., 2014
Hardwood and wheat straw	Methanol/H_2O(60/40,v/v); 0.1%HCl; 85 °C, 4 h.	The treatment of Hardwood and wheat straw with aqueous organic acids is very well suitable for separation of lignins.	Extraction efficiency is very less	Antioxidant additive in pharmaceuticals, cosmetics and the food industries.	Prakash et al., 2015
Insoluble residue portion after removing the ash by concentrated acid hydrolysis of the plant tissues	Benzene and Ethanol; 72 % conc. H_2SO_4 (30 °C, 4 h); diluted to 3 % (2 h); the insoluble substrate is weighed as lignin	Most direct and the most reliable method	Unstable physical and chemical properties	As packaging materials.	Chen, 2015
Hardwood species such as aspen	Comprehensive milling of the plant material, followed by solvent extraction with dioxane and further purification	More amount of lignin can be isolated.	Presence of minor carbohydrate impurities	Catalysts, adsorbents, ion exchangers	Gellerstedt and Henriksson, 2008
Corn stalk	Ionic liquids including [Hnmp]Cl, [Hnmp]CH_3SO_3 and [Hnmp]H_2PO_4:Acetone/water(1:1,v/v), 50–90 °C, 30–180 min	Ionic liquids provides a good environment for lignin extraction and enzymatic hydrolysis for corn stalk	Ionic liquids is their relatively high cost compared to conventional organic solvents	Suitable for adhesive formulation or other composite biomass applications due to better thermal stability	Wang et al., 2019
Bamboo	Formic acid/Acetic acid/water(30/50/20,%v/v), 50–107 °C, 30–180 min	Produces a light-colored acetic acid bamboo lignin microsphere with excellent UV absorbance. Has a small particle size and large interval space	It shows less unsaturated structure and fewer methoxyl groups.	Addresses the staining issue and facilitates the marketing promotion of lignin sunscreens.	Zhang et al., 2019
Artocarpus heterophyllus fruit peels	Treat fruit peel powder with dil H_2SO_4 (0.2 mol/L, 180 °C, 300 W); the resultant product 0.1 g dissolved in 7 mL of H_2SO_4 and microwave irradiation, filtration; washed with DD water; dried at 100 °C.	Higher porosity of lignin encouraged the water availability into the polymeric network of biocomposites	Sulfuric acid requiring neutralization and purification.	Wound healing (skin burns).	Jaganathan et al., 2018
Birch wood	Extracted with Hydrotopic solution with the addition of formic acid and hydrogen peroxide	Use of environmentally friendly hydrotopic process to extract lignin from industrial birch wood chips	Hydrotopic solvents are not cost effective.	Biomedical applications.	Spiridon and Tanase, 2018
Oil palm empty fruit bunches	93 %(w/w) acetic acid aqueous;0.3 % (w/w) HCl; 115 °C, 3 h.	Majority are lignocellulosic materials, consisting of an estimated cellulosic content of 30–50 %, 15–35 % of hemicelluloses and about 20–30 % of lignin.	Lower strength, variable quality and poor moisture resistance.	Cosmetics, pharmaceutical, polymers resins and biofuels.	Medina et al., 2016; Zhen et al., 2021
Avermectin (AVM) encapsulated with acetylated lignin (ACAL) and benzoylated lignin (BZAL)	ACAL and BZAL were obtained from the chemical modification of alkali lignin with CH_3COCl and C_7H_5ClO, respectively	Lignin used as shell material to prepare AVM-loaded nanospheresshowed good controlled release and anti-photolysis properties	Low yield of production and irreugalar morphology.	Tissue engineering or regeneration, artificial muscles, and strong underwater antifouling materials.	Zhou et al., 2019

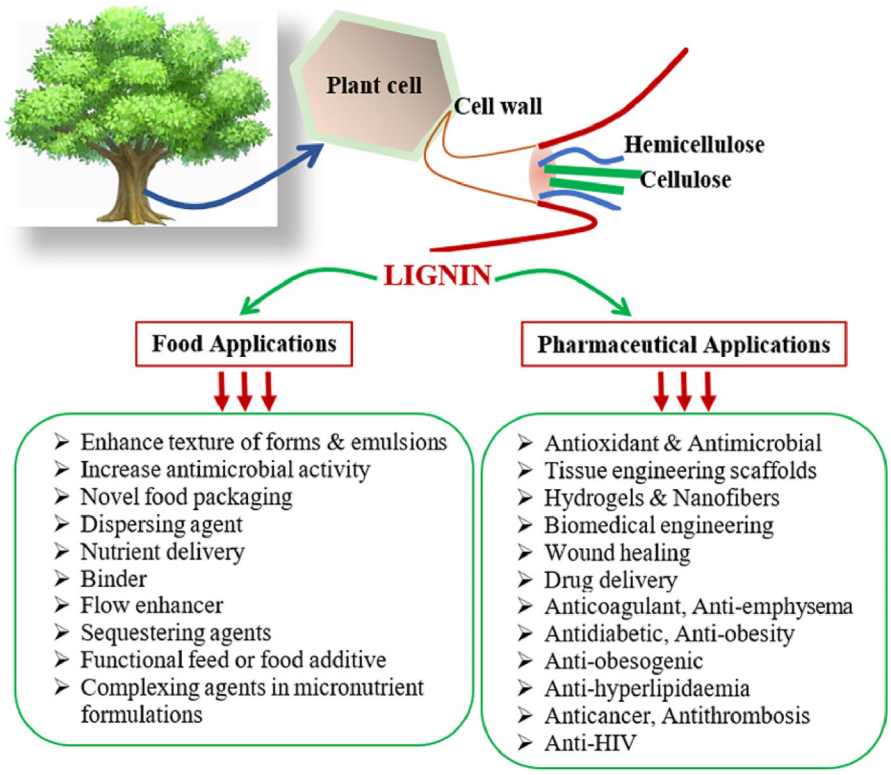

Fig. 2. Various applications of lignin materials.

such a policy for a low-cost alternative out of lignocellulosic biomass (Sharma et al., 2020). Moreover, various applications of lignin-sourced raw materials in food industries are depicted in Table 3.

3.1.1. Food emulsion

An emulsion is a stable concoction of unblendable liquids due to phase separation. The emulsification process allows unblendable liquids to stabilize and remain as a single unit. Food emulsions exhibit phase separation due to their inherent instability (Nypelö et al., 2015). The adsorptive nature of certain emulsifiers and their ability to lower the interfacial tension allows for the synthesis of finely divided emulsion. The food industry uses emulsions to make products, such as mayonnaise, salad creams, and beverages. The pharmaceutical industry uses it to make medications like ointments, and cosmetic and personal care products, including creams, lotions, sunscreens, hair sprays, and many more. A cohort from Finland demonstrated the application of wood-based lignin as a stabilizer, thickener, and texture enhancer in yogurt, baked, and meat products (Aura, 2018). As evidenced by Gil-Chávez et al., calorie-free lignin used to make fluffy muffins can be a replacement for egg components used for the baking process. In addition to being indigestible, lignin-rich foods help lower blood cholesterol and total calories (Gil-Chávez et al., 2019).

Kraft lignin modified with tannic acid has the potential to stabilize oil. Additionally, during ring-opening polymerization through re-oxidation, tannic acid yielded a form of lignin with improved carboxylate density and solubility. These types of lignin have potential applications in stabilizing oil (hexadecane) in water emulsion systems (Gharehkhani et al., 2018). In addition, lignosulfonates are part of pest and herb-controlling formulations, colorants, and pigments as stabilizers (Calvo-Flores and Dobado, 2010). By tweaking the acidity and salinity, it is possible to enhance the stabilizing properties of amphiphilic lignin obtained from soda and kraft lignin. The new functionalized lignins formed were due to molecular affinity between the two liquid phases (Rojas et al., 2007).

3.1.2. Food packaging

The food industry is looking for greener alternatives to traditional food packaging materials due to the adverse consequences of petroleum-derived materials, aluminum cans, and perfluorinated organic compounds (PFCs) (Tayeb et al., 2020). Due to its crosslinking properties, lignin finds application in food-grade biofilms to have a unique spatial arrangement that aids flexibility and stability (Sharma et al., 2020). Consumer products with lignin-incorporated packaging materials containing chitosan have a longer shelf life because they are impervious to moisture and pathogenic bacteria (Yang et al., 2016). Recently, biofilms reinforced with lignin were developed from oil palm black liquor spent materials using glycerol. These films demonstrated increased plasticity and thermal, mechanical, and water-repellent properties (Bhat et al., 2013).

Javed et al. exploited the incorporation of ammonium zirconium carbonate (AZC) cross-linker onto affixed lignin to improve the storage modulus of pure starch, thereby preventing or reducing coating dissolution of the support material (Javed et al., 2018). Tayeb et al. used a type of filtration to create ultrathin biopolymer wafer (16 g/m^2) coatings of lignin-containing cellulose nanofibrils (LCNF) and cellulose nanofibrils (CNF). Both LCNF and CNF favored physical and chemical properties such as tensile strength, water vapor permeability, moisture repellency, and oxygen transmission rate. When incubated with cooking oils, LCNF performed well as a leak-proof coating with improved mechanical qualities, giving a leak-free environment for five months. The findings show that wood-derived lignin candidates may outperform traditional fluorocarbon methods (Tayeb et al., 2020).

Cationic wood nanofiber (CWNF) biofilms derived from cationized sawdust contain lignin as a critical component. The lignin component of the system improved UV and oxygen shielding capability and optical transparency while quelling oxygen transmission and swelling tendencies under stimulated conditions, either alone or in combination. According to the study, such eco-friendly CWNF will eventually phase out oil-featured plastics from the packaging sector one day. Their application in electronic equipment such as solar batteries is due to their excellent UV absorbing

Table 3
Summary of the studies on the food applications of lignin.

Product	Usage	Feedstock lignin	Lignin content (wt%)	Reaction/process condition	References
Wood-derived products	Texture improvers, thickening agent, emulsion, foam stabilizers, reduce oxidation in food products	Kraft lignin	Up to 80 %	Evaluation of 1- and 2-naphthol, formaldehyde (chemical additives) during hydrothermal pre-treatments of pine, birch, and willow wood followed by the incorporation of the residual hydrolysis lignin in polylactic acid (PLA)-based composites.	Aura, 2018
Wood-derived products	For baking muffins, to substitute whole eggs and egg yolks	VTT tested lignin	15 or 25 %	By hot pressing from four different industrial sources	Gil-Chávez et al., 2019
Water-soluble lignin with a high anionic charge density	Stabilizer for oil (hexadecane) in water (O/W) emulsions	Water-soluble lignin	20–32 %	Initially, lignin and tannic acid underwent both oxidation and transesterification reactions. Later, re-oxidized tannic acid afforded a ring-opened product that enhanced carboxylate group content and hydrophilicity of modified lignin.	Gharehkhani et al., 2018
Vanillin	Flavoring agent in foods and beverages	Lignin sulfonates or kraft lignin	N/A	Oxidation reaction was catalyzed with recycled copper catalyst.	Calvo-Flores and Dobado, 2010
Polymeric amphiphiles	Stabilization of emulsions	Kraft and soda lignin	4–5 %	Reaction condition involves oxidation with recycled copper catalyst. Emulsions with various oils (including crude oils) can be formulated and their properties rationalized according to lignin surface activity as a function of pH and salinity.	Rojas et al., 2007
Paper-Based Oil Barrier Packaging	Holding commercially available cooking oils without leakage for over five months and excellent resistance to grease.	Lignin-containing cellulose nanofibrils	23 %	The process involves a filtration technique that mimics the addition of material at the wet end of a paper machine. Thin films (16 g/m2) from lignin-containing cellulose nanofibrils and cellulose nanofibrils form on paper substrates. Further analyses reveal the surface, barrier and mechanical attributes of the samples.	Tayeb et al., 2020
Biopolymer-based packaging substance	Filler material in biopolymer-based packaging	Lignocellulosic biomass	15 % to 25 %	Valorization of agri-food- industrial by-products	Sharma et al., 2020
Novel sago starch-based food packaging films	Good thermo mechanical properties, barrier properties, and seal strength with improved water resistance.	Lignin isolated from oil palm black liquor waste.	1, 2, 3, 4 and 5 % v/w.	Prepared through casting method from sago palm (*Metroxylon sagu*) starch (in the form of film matrix with 30 % w/w glycerol as plasticizer) by adding lignin isolated from oil palm black liquor waste (from empty fruit bunch), as a reinforcing material (1, 2, 3, 4 and 5 % v/w).	Bhat et al., 2013
Plasticized starchy films	Modifying tensile resistance	Lignosulfonates	10 %	Films were prepared from wheat starch and crude commercial lignosulfonates in the presence of glycerol, either by thermal moulding or by casting.	Baumberger et al., 1997
Lignin-containing coatings	Packaging materials	Kraft lignin	19–17 %	Starch solution was added to the lignin solution, stirred at 100–300 rpm, followed by the addition of glycerol and AZC solution.	Javed et al., 2018
Lignin-containing cellulose nanofibrils (LCNF)	Packaging materials	Kraft lignin	N/A	Thin films (16 g/m^2) from LCNF and CNF were formed on paper substrates through filtration technique.	Tayeb et al., 2020
Lignin-containing cationic wood nanofiber (CWNF) films	Packaging materials	Unbleached spruce sawdust	28.6 wt%	CWNF films were fabricated using the solvent-casting method: CWNF suspension was diluted, sonicated for 10 min, poured on a polystyrene tray and stored at 50 % relative humidity (RH).	Sirviö et al., 2020
Lignin esterified with TOFA	Barrier material in fiber-based packaging material	Softwood lignin		Lignin esterified with tall oil fatty acid (TOFA) and tested as barrier material in fiber-based packaging material.	Tammineneta l., 2014 T. Tamminen T. Ropponen H. Eva-Lena K Poppius-Levlin, 2014

capability (Sirviö et al., 2020). Tamminen et al. proposed esterified softwood lignin as a model packaging material capable of generating a uniform coat on paperboard. This wood-based barrier architecture utilizes tall oil fatty acid-mediated esterification and is a more environmentally friendly and long-lasting alternative to its oil-based counterparts (Tamminen et al.,2014).

3.1.3. Nutrient delivery

The use of nanoparticles to distribute nutrients has emerged as a promising field in the functional food business, attracting the attention of scientists and academics alike. The sole purpose of the diet is to ensure that the nutrient content of the consumed food gets delivered to the consumer with minimal loss. Gil-Chávez et al. cite a patent filed by the Dutch company DSM that turned lignin into a makeshift transport molecule for vitamins and natural coloring components like carotenoids (Gil-Chávez et al., 2019). Another study by Dinari using the atom transfer radical polymerization (ATRP) method underpins the ability of lignin-derived nanogels as a potent delivery vehicle for curcumin (CUR). The synthesized lignin-based nanogels (lignin-g-P(NIPAM-co-DMAEMA) nanogel (LNDNG) exhibited superior curcumin loading capacity (49.69 %), encapsulation efficiency (92.62 %) and cumulative release amount (65.36 % after 72 h), making it a promising candidate for the safe and efficient future nutrient delivery system (Dinari et al., 2021).

3.2. Pharmaceutical applications

3.2.1. Hydrogels for drug delivery

Hydrogel technology's applications in designing novel drug delivery systems and smart hydrogels have grown in stature, and it has never looked back. Hydrogels, as smart polymers, have been at the forefront of setting industry standards for better targeted and controlled drug administration for many years (TCDD). Smart hydrogels are non-toxic, biodegradable, and biocompatible, making them ideal for replacing conventional hydrogels (Domínguez-Robles et al., 2018, 2019a,b).

Because of the hydrophilic nature of the biopolymer, chemical and physical variants of hydrogels can retain large amounts of water in their intrinsic 3D framework (Ahmed, 2015). The hydrophilicity of monomeric and polymeric subunits (chemically induced) is essential to forming stable biopolymers. Such biopolymers will have cross-linked fabric and a rigid covalent backbone. In contrast, physical hydrogels rely heavily on network formation mediated by weak intermolecular forces (IMF) and shape-restricting molecular entanglements (Truong et al., 2021). Hydrogels are part of regenerative medicine as a moisture-controlling ingredient in food packaging and the development of diagnostic devices (Ahmed, 2015).

Techniques used to synthesize lignin-derived hydrogels include a) cross-linking, b) atom transfer radical polymerization (ATRP) and reversible addition-fragmentation chain-transfer (RAFT), c) polymerization and copolymerization, d) ultrasonication, and e) wet spinning, methods.

3.2.1.1. Cross-linking method. Crosslinking prevents hydrophilic components of hydrogel from dissolution upon coming in contact with an aqueous environment. Larrañeta et al demonstrated a convenient method to synthesize lignin-based hydrogels for biomedical purposes from high molecular weight lignin by fusing lignin with poly(ethylene glycol) and poly(methyl vinyl ether-co-maleic acid) via esterification. The investigators managed to cross-link the numerous alcohol groups present in the selected lignin with GAN (Gantrez) as the crosslinker and used PEG molecules with varying molecular weights to reinforce the final material. They also showed how to accelerate the solid-state synthesis using microwave (MW). Apart from GAN, other investigators, such as Sharma et al., used N, N -methylenebisacrylamide (MBAm) as a cross-linking agent, known for working effectively as a cross-linking agent and a monomer that improves efficiency, production, and swelling capacity of the resultant graft (Dacrory et al., 2018).

3.2.1.2. ATRP and RAFT methods. The ATRP (atom transfer radical polymerization) method utilizes the reactivity of organic halide precursor and monomeric forms of acrylonitrile to produce lignin-based hydrogels. On the other hand, Azobisisobutyronitrile (AIBN) initiator-lignin core complex achieves polymerization through radical reaction.

RAFT and ATRP ensue by regulating radicals by reversibly converting active polymeric radicals to produce dormant polymer chains (Truong et al., 2021). Although effective at synthesizing hydrogels, both techniques own drawbacks, such as substandard influence over molecular weight and distribution. Also, it is nearly impossible to create such hydrogels with preset capabilities and a stable copolymer structure.

3.2.1.3. Copolymerization method. Copolymerization of lignin-derived hydrogels from diverse monomeric species can be achieved by treating catalytic initiators, cross-linking agents, or graft copolymerization. For instance, lignosulfonate g-acrylic acid hydrogels from acrylic acid when copolymerized with lignosulfonates. Acrylamide monomer-mediated graft copolymerization is also a viable technique for synthesizing lignin hydrogels. Copolymerization is advantageous because it affords stable forms of commercial-grade biopolymers with improved mechanical properties and impact strength (Nguyen et al., 2022; Wu et al., 2017).

3.2.1.4. Ultrasonication method. This method exploits the rheological changes affecting reaction media when subjected to high-frequency sound waves. The sound waves cause low-pressure areas in the medium and create cavitation bubbles. Controlling the properties of these cavitation bubbles makes it possible to afford hydrogels (Sharma and Kumar, 2020). Lignosulphonate-grafted poly (acrylic acid-*co*-poly (vinyl pyrrolidone) was produced by subjecting the pH-dependent methodology to ultrasonication (Wang et al., 2016a, 2016b). The low monomer conversion and high power requirements for ultra-sonication reduce its industrial applications.

3.2.1.5. Wet spinning method. Generating a sustainable bio-based material on a sub-micron scale is economical and eco-friendly. With the introduction of shear stress, the approach self-assembles the growing hydrogel and then reshapes it in a multi-hierarchical arrangement. A prepolymer, a coagulation solution, and a receiving pool with a collector roller are the three essential components of traditional wet spinning. Wet spinning is a helpful way of assisting tissue regeneration, cell communication, and other biomimetic structures without compromising the functionality and architecture of the anticipated biological product.

3.3. Drug delivery and tissue engineering applications

3.3.1. Drug delivery applications

Polyethylene glycol (PEG) is a suitable candidate for the hydro-gelling of working models for drug delivery purposes. Another recent innovation in hydrogel-assisted drug delivery is the reactive extrusion procedure. In response to the catalytic impact of sodium hypophosphite, lignin, and related biopolymers undergo plasticization. As a result, citric acid backbones hold the network together. The formed hydrogels exhibited superior swelling properties when regulated by pH and acted as a switch to control the diffusion of liquids and particles. Furthermore, extruding hydrogels with a catalyst reduces the likelihood of degradation, making the reactive extrusion method a viable choice for systemic drug transportation (Farhat et al., 2017).

Using lignin-derived hydrogels as a sterile surface-spanning coating material for medical devices can save lives (Spiridon, 2018; Spiridon and Tanase, 2018). Concerns about resistant superbugs and cross-contamination during equipment handling and drug elution led to the development of a hydrogel with antimicrobial capabilities and the ability to keep the proposed medicine inside the hydrophobic bubble for up to four days. This achievement was accomplished by esterifying lignin with PEG and poly (methyl vinyl ether-*co*-maleic acid), resulting in a fluid absorption capability of 500 %. Larrañeta et al. found that PEG 10,000 coatings were

effective against a wide range of pathogenic microorganisms, including *S. aureus* and *Proteus mirabilis* (Larrañeta et al., 2018).

Recent studies established the role of sodium lignosulphonate-grafted poly (acrylic acid-*co*-poly (vinyl pyrrolidone) hydrogel (SLS-g-P(AA-*co*-PVP) as a drug delivery platform. They investigated amoxicillin uptake, transportation, and release in simulated conditions without the involvement of enzymes, which helped evade the gastric milieu's acidic conditions. The researchers evaluated the elasticity of the concerned hydrogels in intestine-like settings and discovered that pH significantly impacted the hydrogel's releasing capabilities. Swelling ratios of hydrogels were also a factor in determining the biopolymer's ability to retain water (Wang et al., 2016a, 2016b).

Inert and biocompatible characteristics of cellulose allow for bypassing the immune reaction that would otherwise be impossible with lignin alone. A cost-effective cellulose-lignin pair successfully prolonged the release of bioactive chemicals like phenolics. The complex can enhance desired output in all living systems by securing bioactive lignin inside the cellulose covering. The more swelling capacity a hydrogel has, the more polyphenols it can hold, which, in turn, is determined by the amount of lignin it contains. Hydrogels of this type are a good fit for drug delivery systems. A recent study tried to achieve a controlled release of metronidazole and lysozyme standards. The results from the experiment revealed that the desired effect came from the viscosity of the hydrogel (Dong et al., 2018).

3.3.2. Tissue engineering applications

Tissue engineering is an area of research concerned with developing biocompatible alternatives for restoring, maintaining, and improving tissue integrity and performance. Scaffolding techniques, facilitated by the characteristics of both synthetic and natural polymers, are used in biological substitutes. Tissue engineering has typically used cells from the source material and factors that guide the regular functioning of tissues. To provide the appropriate extracellular environment ex vivo, several biomimetic components and structural proteins, such as elastin and collagen, are combined.

The coupling of chitin and lignin facilitates the production of nonwoven polymer composites with a natural feel and acceptability. Such biocompatible tissue scaffolds resembled an extracellular matrix (ECM). After undergoing mild electrospinning, they enhanced optimal tissue regeneration without inducing immunogenicity. In addition, their interaction promoted wound healing and anti-inflammatory and anti-aging effects on a nanometric level (Morganti et al., 2018).

In one of the electro-spun methods, multi-component biomaterials containing chitin, lignin, and poly(glycerol sebacate) (PGS) gained bactericidal properties against *E. coli* and *Staphylococcus aureus* (Yin et al., 2018). The amount of PGS in the solution contributes to the structural integrity and strength of the hybrid biopolymer, and an optimum level of 15 % offers maximum mechanical strength. This lignin-based hybrid is ideal for wound dressing because its ECM mimics the microstructure of the unwoven network and has antibacterial properties (Abudula et al., 2018).

Ultra-fine biopolymers are formed by ring-opening polymerization when lignin combines with polyesters (polycaprolactone, PCL, and poly (L-lactic acid), PLLA). These polymers have fibrous 3D networks that can reach nanoscale thickness. Electrospinning takes place without a solvent, and the resulting biomaterial provides optimum conditions for cell growth and multiplication while also providing the necessary mechanical strength. Lignin must be kept between 10 % and 30 % to achieve these benefits (Kai et al., 2017). PCL featured lignin-based biopolymers created via the electrospinning method to yield ECM-like ultra-fine polymeric structures with 10 % wt lignin. Such scaffolds have outstanding elastic characteristics, bio-eco compatibility, pore size, and void fraction at optimum levels. Moreover, optimum pore size and void fraction of the nanocomposites are prerequisites for adequate cell adhesion and development (Salami et al., 2017).

A group of researchers used a solvent-less ring-opening polymerization approach involving lignin/PCL to create an antioxidant-rich bio scaffold capable of assisting in the regeneration, growth, and translational enhancement of neurons and supporting cells, including Schwann cells at various developmental stages. Experiments with hematopoietic cells from the bone marrow also yielded similar results (Wang et al., 2018). Copolymerization occurs when lignin interacts with PCL and polymethyl methacrylate (PMMA). These non-immunogenic electro-spun nanostructures afford biomaterials with superior properties favoring proper cell proliferation and adhesion (Kai et al., 2015).

When lignin and alginate gelatinize in CO_2, aerogels with physical and rheological properties ideal for tissue engineering are formed. By limiting the solubility of the alginate component, lignin was observed to enhance the functioning of the produced aerogels by creating a niche conducive to average cell growth, differentiation, and adhesion. In addition, the inherent stability of lignin aided in slowing the biopolymer's degradation rate, boosting bone tissue regeneration (Quraishi et al., 2015).

Lignin is a biomolecule that can change the intrinsic mechanical properties of other substances, allowing them to participate in bone tissue regeneration via tissue engineering. For example, lignin derived from OPEFB's (oil palm empty fruit bunches) black lye promotes preferential crosslinking of epichlorohydrin (ESH) following acid treatment, resulting in hydrogels with mechanical qualities required for a solid 3D network. The optimal lignin/agarose hydrogel includes 5 % lignin and agarose each, with a maximum ESH content of 10 mL (Sathawong et al., 2018). Similarly, adding 3 % lignin to chitosan improves the tensile strength and stiffness of the bone tissue fabrication candidate (Wang et al., 2016a, 2016b). The resulting PLA/lignin mesh enhanced tensile strength when reinforced with lignin (7–15 %), which was impossible with a lower amount of lignin. The human osteosarcoma cell line did not show any form of immune response to such a composite structure (Spiridon and Tanase, 2018). Because of their potential to solve solubility issues and unique thermal behavior, bioactive integrated metal implants produced from bio/eco-friendly scaffolds like organosolv/lignin are utilized to repair fractured bone tissue and regain functionality. When mixed with hydroxyapatite at varying concentrations, organosolv/lignin improved the bioactivity of titanium implants. Replacing titanium with silver makes the produced biomaterial more antibacterial, especially against *S. aureus* (Ganasan et al., 2022; Erakovic et al., 2014).

Heat treatment of wood constituents impacts the chemical makeup and the overall mechanical capabilities of polymer-ridden timber matrices. It is capable of creating implants with dimensional stability and low moisture content. To determine the lifetime of such biopolymer implants, regular histometrical and histological evaluations are necessary. During postoperative radiological follow-up in a trial with birch wood-derived bone implants for rabbit femur bone regeneration, the trabecular bone region of the affected femur supported the implant via intracondylar implantation. In addition to birch wood, other researchers used beech, juniper, and ash wood for biomaterial-assisted bone healing (Rekola et al., 2009).

3.4. Lignin composites and its biological activity

3.4.1. Antioxidant activity

Daily, biological systems produce reactive oxygen species (ROS) such as H_2O_2, superoxide ions, NO_3^-, NaClO, and OH due to various routine metabolic activities involving oxygen. These toxic chemical entities severely threaten the proper functioning of cells and tissues, increasing the risk of developing life-threatening and debilitating health problems over time. When ROS affects the stable existence of biomolecules in cells, premature aging, cancer, type 2 diabetes, and autoimmune disorders start forming (Liguori et al., 2018).

Researchers used poly (butylene succinate) via hot-melt extrusion to produce lignin-based composite materials with antioxidant potential (Domínguez-Robles et al., 2019a, 2019b). Previous studies have reported free radicals to be inhibited by lignin-carbohydrate complexes (LCCs) derived from poplar and bamboo. By up-regulating the antioxidant activity of the concerned enzymes, these complexes successfully scavenged reactive oxygen species (ROS) in both animal models (zebrafish) and in vitro (RAW 264.7 cells) (Dong et al., 2019). Lignin binds to PLA and castor oil to create customizable composites that can form fibrous interlocks when 3D printed.

Following extrusion at 200 °C, these composites achieve exceptional antioxidant and mechanical characteristics essential for biomedical and wound healing applications. An optimal mesh can accommodate up to 3 % (w/w) lignin content in its filamentous PLA structure (Domínguez-Robles et al., 2019a, 2019b). Lignin-based biomaterials are also employed to counteract the onset of ROS-mediated hyperglycemia. The α-amylase activity of *Acacia nilotica* lignin-rich wood produced promising in vitro free radical scavenging results (Barapatre et al., 2015). In another study involving lignin-derived metabolic intervention for curbing hyperglycemia, lignosulfonic acid (LS) was able to non-competitively inhibit the activity of the intestinal α-glucosidase enzyme and lower the absorption of 2-deoxy-glucose by glucose transporters (Hasegawa et al., 2015). Lignophenols (LPs) have been shown to play a crucial role in the chemoprotective aspect of Streptozotocin-induced diabetic nephropathy and localized oxidative stress. LPs commit to this by increasing oxygen delivery to the damaged organ and combating the mechanisms that cause glomerular fibrosis and MCR-mRNA expression (Sato et al., 2009).

3.4.2. Antimicrobial properties

Sepsis is one of the most common causes of death in the world. The systemic invasion of microbes triggers it (Demirci et al., 2018); hence, keeping medical devices, pharmaceuticals, and consumer items free of infectious agents becomes a challenging task (Greenhalgh et al., 2019). The synergistic effect of various phenolic groups and benzene moieties in lignin nanoparticles leads to bactericidal properties (Zhang et al., 2019; Reshmy et al., 2022). Acacia wood lignin, combined with poly vinyl alcohol (PVA) and AgNF (silver nanofibers), generates 3D networks that are resistant to microbial diseases. In a standard agar well diffusion test, such scaffoldings were efficient against *B. circulans* (1.3 0.08 cm) and *E. coli* (1.1 0.05 cm). Nanofibrous mats like these can be found in specialized applications such as membrane filters, sterile textiles, and wound-healing dressings (Aadil et al., 2018).

The chitosan/LS nanoparticles are another fascinating lignin-featured combination that works effectively against *E. coli, S. aureus*, and *B. subtilis* unfavorable effects. The lignin portion was found to decimate the bacterial presence, as demonstrated by the turbidimetric test (Kim et al., 2013). Lee et al. successfully created a system based on Lignin/PVA composite networks with near-100 % antibacterial efficacy against *S. aureus* and excellent UV shielding (UPF >50). PVA nanostructures containing lignin-decorated t-MWNTs (thin multi-walled nanotubes) inhibited the growth of *S. aureus* strains by 68.7 % after 18 h compared to PVA nanofibers, according to another study by the same research group. Such thermally stable reinforced nanofibers are excellent for initiating dermal wound healing (Lee et al., 2018).

Biocompatible silver-doped lignin mats (Silver/hydroxyapatite/lignin) with superior bactericidal capability against *Pseudomonas aeruginosa, S. aureus,* and *Candida famata* provide an industrial application for the development of implants requiring immunologically inert biofilms (Janković et al., 2015). Lignin nanoparticles (LNPs) can form multifunctional ternary systems with chitosan and PVA, thereby enhancing the antimicrobial and antioxidant potential of the resulting composite hydrogels. Both 1 and 3-wt% LNPs incorporated hydrogels exhibited antagonistic activity toward the growth of *S. aureus* 8325–4 and *E. coli* RB, allowing for their use in the packaging industry, wound healing fabrics, and targeted drug delivery systems. Moreover, LNP hydrogels synergistically improved the overall physical stability of the entire structure, making this versatile composite association a valuable addition to the pipeline (Yang et al., 2018). In a recent contribution, biomaterial featuring lignin/chitosan against *E. coli* and *Klebsiella* yielded a zone of inhibition of ~0.9 mm and ~1.1 mm for *E. coli* and *Klebsiella*, respectively (Jaganathan et al., 2018). The way the herpes simplex virus (HSV-1) undergoes inhibition by the nonsulfated cinnamic acid-derived lignopolymer ascertains the antiviral nature of lignin. The study found the overall efficacy of carboxylated lignopolymer to be 1000 times better at restricting the cellular entry of enveloped viruses than previous anti-HIV drug candidates.

Lignosulfonic acid inhibits the replication of the R5 and X4 virus types and HSV-2 through various cellular mechanisms, including blocking the gp120 viral protein from T cell adhesion and preventing CD4 + T cell bystander activation from already infected T cells. It is worth noting that this achievement was accomplished without compromising the efficacy of popular antivirals like acyclovir, LabyA1, or PRO2000 (Gordts et al., 2015). *Pimpinella anisum* has antiviral lignin-carbohydrate-protein complexes effective against common viruses infecting humans li HCMV, HSV-1, HSV-2, and measles. Upon treating these extracts with RAW 264.7 cells, they increased cytokine levels, as demonstrated by the increased IL-1 and IL-10 (Lee et al., 2011).

3.4.3. Lignin composites for drug delivery systems

A subpar maize starch biofilm may be efficiently transformed into a very stable pH-dependent (inversely proportional) drug delivery system with better thermal and mechanical properties by adding 2 wt% hazelnut-derived lignin. In a traditional in vitro release assay that lasted ten days, such thermoplastics successfully transported and delivered the standard antibiotic ciprofloxacin, with peak release occurring within 60 min. Lignin-graft-PDLA (LG-g-PDLA), a superior antioxidative and anticancer filler, improves the properties of an otherwise hostile environment created by PLLA nanocomposites for light-sensitive drugs like trans-resveratrol (t-RSV). The filler efficiently shields the drug from UV radiation after it forms a stereo complex and actively participates in the prolonged release of t-RSV, which can be fine-tuned by changing the filler content. LG-g-PDLA also improved the system's overall toughness and thermal stability (Liu et al., 2018).

3.4.4. Lignin composites for wound healing

Wound dressing fabric influences how the injured region initiates and promotes healing. Currently, sterile garments and fibers such as cotton wool, gauze bandages, and various cotton composites meet the requirement. An optimal dressing material allows for proper ventilation, pain relief, the absorption of serosanguinous discharge from wounds, and the prevention of sepsis. Recent advances in lignin research aim to develop user-friendly biocompatible dressing materials that keep the wound hydrated while meeting other healing requirements (Ravishankar et al., 2019).

Physical cross-links involving ionic bonds from an inherently weak chitosan-PVA composite permit 3D scaffolds of lignin-based hydrogels capable of withstanding stress levels (up to 46.87 MPa) required to evade deformation due to tensile strain. Histomorphological analysis of murine wound models suggested accelerated regeneration and increased protein adsorption capacity. Other benefits of such hydrogels include improved antibacterial and antioxidative activities and the ability to condition wound sites by regulating biological factors for appropriate healing, making them suitable for wound dressing (Zhang et al., 2019). A biocompatible hydrogel made of chitosan and alkali lignin with substantial wound regeneration potential was mentioned in a recent study. The hydrogel responded remarkably well in a scratch assay featuring mouse fibroblast cell lines (NIH 3 T3). The bio composite was able to regulate cell migration which is imperative for wound healing (Ravishankar et al., 2019).

Bacterial cellulose dehydrogenase polymer, a biofilm made from microbial cellulose and lignin, was created to improve wound healing and reduce pain while preventing infection. The large swelling capacity and bactericidal activity are helpful for therapies that require sustained drug release, such as delayed wound healing (Zmejkoski et al., 2018). The same researchers had previously created a hydrogel (DHP-Alg) compatible with human epithelial cells and had antibacterial activity against *Staphylococcus aureus*, *Pseudomonas aeruginosa*, *Salmonella Typhimurium*, and *Listeria monocytogenes* strains. When blended in 1:2 (*w/v*) of DHP: Alg(alginate), the participating hydrogel exhibited good MICs or minimal inhibitory concentrations (0.002–0.90 mg/mL) and MBCs (0.004–1.25 mg/mL) (Spasojević et al., 2016).

3.4.5. Lignin for disease prevention

Lignin is the major component of the medication $CDSO_3$, used to treat emphysema, a lung disease marked by ruptured alveoli and shortness of

breath. Here, low molecular weight lignin (LMWLs) with sulfated caffeic acid moiety ameliorated the disease condition by down-regulating neutrophil elastase (an aberrant protein marker), oxidation, and inflammation. As a result, its efficacy as a biocompatible anti-emphysema agent with triple benefits was established beyond doubt. The flow of blood through arteries is affected by high cholesterol levels. The presence of total cholesterol in the blood increases the risk of life-threatening illnesses like myocardial infarction and stroke. Lignophenols reduce cholesterol levels by regulating oleic acid-induced apo-B lipoproteins produced by HepG2 cells (Norikura et al., 2010a, 2010b). The research reveals that LP interventions at the transcriptional and translational levels are responsible for the desired result (Saluja et al., 2013). The pharmaceutical applications of lignin are summarized in Table 4.

4. Recent trends in lignin research: nanolignin

4.1. The rationale for nanolignin preparation

The most attractive features of lignocellulosic residues are their eco-friendliness, availability, and inherent bioactive characteristics. By harnessing the powers of nanotechnology, nanolignin has the potential to drive future nano-based medical interventions, diagnostics, and food sectors. Environmental and nanotechnology research is gaining traction due to the constant development of recyclable lignin-containing biomass. Several scientific improvements and patents relevant to enhanced lignin use, particularly in nano lignin-based products, have been made in the last decade (Dey et al., 2022). Common nanolignin preparation method is represented in Fig. 3. A comparison of lignin and nanolignin are described in Table 5. The following section discusses the available methods to synthesize nanolignin from native lignin.

4.1.1. Nanolignin from mechanical processes

The milling process is one of the most widely used methods for synthesizing nanolignins from plant sources. It is a cost-effective technique for obtaining lignins with nanomolecular particle sizes (Sharma and Kumar, 2020). For example, homogenizing 5 g/L kraft lignin at 15 K rpm for 4 h yields 500 nm kraft lignin-derived nanolignin. Furthermore, a sonication-based acoustic approach produces stable 10–20 nm nanolignin with a uniform dispersion of 0.7 % lignin suspension derived from wheat straw and Sarkanda grass. 20 kHz sound waves and 600 W input for an hour in a homogenous stable nanodispersion of size 10–20 nm are ideal circumstances for such nanoscale formation without free radicals (Gilca et al., 2015).

4.1.2. Nanolignin from solvent shifting method

Under the effect of polarity considerations of the involved lignin substrates, a strictly regulated solvent shift approach can produce mid-sized nanolignins despite their low yield. Dimethyl sulfoxide, acetone/water, tetrahydrofuran, and acetone are the chosen solvents for this procedure (Sharma and Kumar, 2020). Using tetrahydrofuran and water, the solvent-shifting approach produced small nanolignin with a particle size of 221 ± 10 nm, whereas kraft lignin created lignin nanoparticles with a 200–500 nm size (Figueiredo et al., 2017).

4.1.3. Nanolignin from pH shifting technique

Stable nanostructures with densely arranged lignin moieties form by precipitating extremely porous lignin nanoparticles by shifting the pH. Such stable nanoparticles are the result of two independent stages. The first attempt features Indulin AT in ethylene glycol solution followed by adding aqueous HCl. The second method uses a mixture of lignin and aqueous sodium hydroxide, which produces the required precipitates when combined with HNO_3. The first approach yielded pH stable (1–9) biodegradable nanoparticles. The second method produced environmentally safe nanolignins that are stable below pH 5. Lignin sourced nanostructures do not affect the growth of model microorganisms such as *Chlamydomonas reinhardtii* and *Saccharomyces cerevisiae*, ensuring cell viability (Sharma and Kumar, 2020).

4.1.4. Nanolignin from template-based synthesis technique

Caicedo et al. used template synthesis to create lignin-derived nanomaterials. The process is initiated by Schiff's base reaction between the aldehyde groups of thioglycolate lignin and their amino counterparts in the activated alumina membrane (APTES). Polymerization starts after adding hydroxycinnamaldehydes, hydroxycinnamates, or hydroxycinnamyl alcohols in the presence of appropriate catalysts such as HRP (horseradish peroxidase) and H_2O_2. As a result, nanotubes with 15 nm thick walls and nanowires with a 200 nm inner diameter form. These nanomaterials can also be bio-functionalized after being placed on the lignin base layer. (Caicedo et al., 2012). Reductant-mediated template synthesis of lignin molecules affords uniformly dispersed 45–55 nm pseudo spherical silver nanoparticles with antimicrobial activity. Although template synthesis has various advantages, it is also responsible for the toxicity factor of surfactants such as SDS and CTAB. Other limiting factors that undermine the overall effectiveness of this method are issues related to purification and the removability of source materials (Sharma and Kumar, 2020).

4.1.5. Nanolignin from ice-segregation-induced self-assembly method

Initially, a monomer unit-containing solution is frozen (Sharma and Kumar, 2020). As a result of this process, ice crystals form, which continue to develop and segregate the polymer phase. Under the effect of a revolving drum (300 rpm) and liquid nitrogen (77 K) as a coolant, homogenous lignin nanofiber scaffolds form with alkali lignin as the source material (Spender et al., 2012).

4.1.6. Nanolignin from aerosol process

Using an atomizer, this approach creates a continuous loop of aerosol. After passing through a heating tube, the aerosol is captured by a low-pressure impactor, which collects the sorted fractions of the required nanoparticle. This highly reproducible one-step method accurately assembles dried nanoparticles based on size and shape. This approach helps produce lignin nanoparticles with particle sizes ranging from 30 to 200 nm (Sharma and Kumar, 2020).

4.1.7. Nanolignin from electrospinning method

The electrospinning method requires a polymer solution as a starting material for nanolignin formation. The mixture can travel through a 100 m wide nozzle that acts as an electrode/auxiliary electrode system after being mixed with an appropriate solvent. For nanolignin production using the electrospinning process, the desired *E*-field level is 100–500 kV/m (Sharma and Kumar, 2020).

4.1.8. Nanolignin from supercritical fluid processes

Nanolignin synthesis with supercritical fluids like CO_2 is beneficial since it is inexpensive, non-flammable, and non-toxic (Sharma and Kumar, 2020). CO_2 also has a favorable critical temperature and pressure of 304.3 K and 7.4 MPs, making it an ideal choice for supercritical fluid-mediated processes. Fine lignin nanoparticles of 144 nm are formed by reacting CO_2 and acetone with lignin at 30 MPs and 35 °C. The compressed CO_2 antisolvent Technique can make environmentally friendly LNPs (Myint et al., 2016). The process starts by pumping CO_2 to a cooler kept at 258.2 K and then transferring it to the precipitator, where it gets liquefied. Following the stabilization of the precipitating unit, lignin solution was added to the obtained lignin nanoparticles after weighing. The resulting mixture was subjected to sonication for half an hour at room temperature and sprayed via a nozzle dictated by flow rate presets. The particles that make it to the filter paper are collected. CO_2 immiscible compounds are not suitable for this Technique (Sharma and Kumar, 2020).

4.1.9. Nanolignin from solvent antisolvent precipitation

The slow addition of a prepared lignin solution to an antisolvent such as water is used in this procedure. Polarity of antisolvent differs from that of the organic solvent used to dissolve lignin before antisolvent treatment. Water is a popular antisolvent because lignin is immiscible or sparingly soluble (Sharma and Kumar, 2020). In one work, both soft (alkali lignin) and

Table 4
Summary of the studies on the pharmaceutical applications of lignin.

Product	Usage	Feedstock lignin	Lignin content (wt%)	Reaction/process condition	References
Drug delivery hydrogels	Drug delivery systems	Kraft lignin	Up to 80 %	Used micro-extruder at 120 °C for 2 or 5 min of recirculation and 20 to 200 wt% citric acid.	Farhat et al., 2017
PEG-lignin hydrogels	Medical material coatings based on their resistance to infection and the ability to release drugs over several days.	Klason lignin and acid soluble lignin	10 % (w/w)	7.5 g of Ethanol/water (70 % v/v) containing 10 % (w/w) of LIG, 5 % (w/w) of GAN and 5 % (w/w) of GLY or PEG dried for 48 h, oven-dried at 80 °C for 24 h and placed in an ethanol/water (70 % v/v) solution for a week.	Larrañeta et al., 2018
SLS-g-P(AA-co-PVP) hydrogels	Deliver amoxicillin drug to the intestine.	Sodium Lignosulphonate	N/A	Involves free-radical polymerization- SLS and sodium hydrate mixing, followed by the addition of acrylic acid, PVP, NMBA and APS. The whole solution was stirred for an additional 30 min and transferred to an ultrasonic reactor.	Wang et al., 2016a, 2016b
Cellulose–lignin hydrogels	Controlled release of polyphenols by lignin.	Steam explosion lignin from aspen wood	N/A	Cross-linking reaction between cellulose in alkaline solution, lignin and epichlorohydrin for 8 h, at 80 °C.	Ciolacu et al., 2012
Microcrystalline cellulose hydrogel	Lignin controlled release of drug metronidazole.	N/A	6.3 %	Hydrolysis of bleached cellulose fibers and unbleached brown fibers. The mechanical treatment after hydrolysis enables dispersal of the cellulose into gel-like material.	Dong et al., 2018
Collagen hydrogels	Lignin controlled release rate of the cancer drug doxorubicin	Alkali lignin	N/A	Promotes the formation of layer-by-layer films using tannic acid and lignin dipped into collagen hydrogel for 30 s and then washing twice in pH-adjusted distilled water for 15 s each.	Choi et al., 2016
Pectin and lignin hydrogels	Deliver β-glucuronidase and estrogens	Wheat stems lignin and oak lignin	5 %	4 % citrus pectin heated to 40 °C, extruded into 100 mL of a 0.34 M aqueous CaCl2 solution and mixed with 2.5 % lignin.	Borisenkov et al., 2015
Scaffolds of chitin-lignin	Support cellular activity, optimize tissue regeneration without eliciting any undesirable local or systemic response	N/A	N/A	Nanoscale lignin obtained by the solution-precipitation method was allowed to complex with chitin nanofibril.	Morganti et al., 2018
Scaffolds of Chitin/lignin/poly (glycerol sebacate)	Create hybrid nonwoven scaffolds.	Bio-lignin	0.1 wt%	Chitin nanofibrils (30 wt%),bio-lignin, PEO (7 wt%) mixed with (deionized water(62.9 wt%) to produce the sol-gel mixture followed by the mixing of sol-gel and PGS solutions via electrospinning.	Abudula et al., 2018
Lignin-based copolymer	Tissue engineering	Alkali lignin	10–30 wt%	Alkali lignin, ε-caprolactone, L-lactide, and tin(II) 2-ethylhexanoate were mixed, stirred (130 °C,24 h, N2atm), and cooled. Added chloroform and centrifuged to obtain supernatant which was then washed with ether/ methanol mixed solvent and dried(50 °C,24 h)	Kai et al., 2017
Polymeric scaffold fibers	Enhance the biological response of the cells with the mechanical signals	N/A	10 wt% Lignin	Varying ratios (100, 95:5, 90:10, and 85:15) of lignin was added to the PCL solution containing 1 L dichloromethane. The mixture was stirred for 1 h, sonicated for 20 s, and applied into a 1-mL syringe of ELS. Desired scaffolds form on aluminum foil attached to the rotating drum.	Salami et al., 2017
Scaffolds of PCL/lignin nanofibers	Promote cell proliferation of both BMSCs and Schwann cells, enhance myelin basic protein expressions of Schwann cells, stimulate neurite outgrowth of DRG neurons and exhibit antioxidant properties	Alkali lignin	N/A	After reacting ε-caprolactone (6 g) with Tin(II) 2-ethyl hexanoate (0.5 wt% of monomer as the catalyst) and purging with N2 for 30 min, the mixture underwent stirring at 130 °C for 24 h. The resulting mixture was dissolved in chloroform, and the unreacted lignin was centrifuged at 5000 rpm for 5 min. The precipitate (lignin-PCL) was collected and dried in a vacuum oven at 50 °C for 24 h.	Wang et al., 2018
Aerogels using alginate and lignin	Scaffolds for tissue engineering	N/A	N/A	0.5 mL of DHP in DMSO was added to sodium alginate (0.2 g) in 9.5 mL of distilled water. Further addition of 0.5 % (w/ v) CaCl2 yielded the gel.	Quraishi et al., 2015
Lignin/hydroxyapatite and lignin/β-tricalcium phosphate systems	Bone tissue engineering	Brazilian wood biomass lignin	20 % and 40 %	HA and β-TCP were obtained by wet precipitation synthesis, dried at 110 °C for 4 h and mixed with lignin. The resulting mix was transformed into disks under pressure and sintered at 900 °C/1 h.	Mansur et al., 2005
Lignin-agarose hydrogel	Higher mechanical properties than pure agarose gels	Kraft black liquor	5 %	Chemical cross linking of 5 %lignin and 5 % agarose by 10 mL of epichlorohydrin	Sathawong et al., 2018
Lignin-chitosan microfibers	Influence mechanical properties	Alkali lignin	3 %	Chitosan (0.15 g) was mixed with 10 mL of 1 % acetic acid solution and was then stirred at 700 rpm for 4 h. Further addition of lignin accompanied by stirring at 700 rpm for 24 h and subsequent wet spinning technique facilitates fabrication.	Wang et al., 2016a, 2016b
(PLA)-lignin composites	Reduce crystallization of poly (lactic acid)	Kraft lignin	15 %	PLA and lignin was dried (48 h, 40 °C), batches melt mixed with PLA in the micro-compounding system, extrude injection moulded	Anwer et al., 2015
PLA-lignin composites	Increase the tensile strength	Organosolv lignin from birch wood and Kraft lignin from softwood	7–15 %	PLA pellets (50 °C) and lignin (80 °C) were dried, compounding procedure at 175 °C for 10 min, 60 rpm, compression moulding, using a Carver press.	Spiridon and Tanase, 2018
Hydroxyapatite/lignin composite coatings	Bioactive coating for titanium implants	Organosolv lignin	0.5–10 %	Electrophoretic deposition of HAP/Lig and Ag/HAP/Lig coatings on Titanium-HAP/Lig and Ag/HAP/Lig suspensions via ultrasonication lasting 30 min. Titanium plate forms the working electrode with an EPD voltage range of 50 to 100 V and deposition time ranging from 30 s to 5 min.	Erakovic et al., 2014
Heat-treated birch wood	Osteoconductivity	N/A	N/A	The wood material was heated at 140 °C and 200 °C under normal atmospheric pressure for 2 h.	Rekola et al., 2009
Lignin\PBS composites	Antibacterial and antioxidant properties	kraft lignin	up to 15 % w/w	Employed brabender plastograph internal mixing machine for adding lignin to PBS matrix at 150 °C, 80 rpm and 10 min. The mixture was cooled, milled using a blade mill and stored.	Domínguez-Robles et al., 2019a, 2019b
Lignin-carbohydrate complexes	Prevent the reduction of antioxidant enzyme activity.	LCC from bamboo and poplar	44.1 %–47.8 %	RAW 264.7 cells were co-incubated with ROS fluorescent probe for 30 min after adding 50 μg/mL LCCs-Bjorkman solution and 100 μmol/L of H_2O_2. Evaluation of ROS was achieved by the Flow cytometry technique.	Dong et al., 2019

3D printed meshes	Wound healing	Kraft lignin	0.5 to 3 %	Vortexed PLA pellets (40 g) and castor oil (40 μL) before adding and vortexing lignin and tetracycline powder. Allows for the extrusion of filaments, discs and squares and 3D-printed using Ultimaker 3FFF system.	Domínguez-Robles et al., 2019a, 2019b
Alkali lignin	To act against hyperglycemia	Alkali lignin	N/A	Alkali lignin extraction and microbial biotransformation by ligninolytic fungus.	Barapatre et al., 2015
Lignosulfonic acid	Suppress the rise in blood glucose level	N/A	N/A	LS acid was added to 0.2 U/mL alpha-glucosidase in 50 mM PBS and incubated for 30 min at 25 °C. Added PNP Gluc solution followed by Na_2CO_3 to terminate the reaction.	Hasegawa et al., 2015
Lignophenols	Excess oxidative stress, infiltration and activation of macrophages and glomerular expansion in STZ-induced diabetic kidneys	N/A	N/A	The LPs were mixed with a standard commercial laboratory diet and provided to diabetic rats	Sato et al., 2009
PVA/Acacia wood lignin/silver nanofibers	Act against *B. circulans* and *E. coli*	Acacia wood lignin	1 wt%	PVA and lignin were blended in a 9:1 ratio in 10 mL of methanol: water (60:40) and stirred for 2 h. Stirred again after adding silver nanoparticles and then sonicated.	Aadil et al., 2018
Chitosan/lignosulfonates nanoparticles	Antagonist for *S. aureus*, *E. coli* and *B. subtilis*	Hardwood lignin	N/A	Sonochemical formation of particles by incorporation of CS and LS solutions, 30 mL and 15 mL, respectively, in the presence of 5 mL of the organic phase (vegetal oil).	Kim et al., 2013
Lignin/(PVA) nanocomposite fibers	99.9 % reduction rate against *S.aureus,* excellent UV protection	Alkali lignin	50 and 85 wt%	The lignin/PVA solutions was stirred at 80 °C for 6 h and then electrospun under various spinning conditions.	Lee et al., 2019
Lignin/decorated thin multi-walled carbon nanotubes in poly (vinylalcohol) nanocomposites	68.7 % bacterial growth decrease of *S. aureus*	N/A	N/A	tMWNTs were synthesized via chemical vapor deposition (CVD) method and was added to lignin solutions and subjected to sonication.	Lee et al., 2018
Silver/hydroxyapatite/lignin thin films	Act against the microbial colonization of *S. aureus, P. aeruginosa* and *C. famata*	Organosolv Lignin	1 % w/v	Ag: HA powders (10 % w/v) and Lig (1 % w/v) were dissolved in distilled water, vortexed and flash-frozen in a liquid nitrogen-cooled copper container. Later, it was mounted on a cryogenic holder, rotated at 10 rpm and irradiated with a laser beam.	Janković et al., 2015
Gelatin/lignin films	Inhibitors for *B. subtilis*			H-bonding between gelatin-lignin via cholinium citrate.	Mehta and Kumar, 2019
Polyvinyl alcohol/lignin/chitosan hydrogels	Greater than 95 % cell reduction in *E. coli* and >85 % in *S. aureus*	Pristine lignin	1 and 3 %	PVA was diluted in deionized water at 20 % (wt/v) under magnetic stirring at 90 °C for 4 h. An aqueous dispersion of LNPs was added and sonicated for 5 min at 40 % amplitude. Chitosan was dissolved in water containing glacial acetic acid (1 % v/v) under magnetic stirring at 40 °C for 12 h and was mixed with PVA/LNPs solution.	Yang et al., 2018
Polylactide/silver/lignin nanoparticles	100 % cell reduction of L. *monocytogenes*	Organosolv lignin	40 mg	PLA (4 g) was added to the AgNPs solution and stirred continuously at 22 ± 2 °C for 48 h. The mix was cast onto a Teflon film-coated glass plate, dried, and then conditioned in a humidity chamber.	Shankar et al., 2018
Artocarpus heterophyllus peel lignin/chitosan Biocomposites	Inhibition zone for *E. coli* and *Klebsiella*	*Artocarpus heterophyllus* peel lignin	1 %,3 %,5 %	Lignin was added to chitosan medium (15 mg in 10 mL of 1 % acetic acid), sonicated at 100 W for 5 h and fabricated via freezing drying methods.	Jaganathan et al., 2018
Carboxylated lignin polymer	Act as an antagonist to HIV-1, dengue, Kaposi's sarcoma-associated herpes virus, and hepatitis C virus.	Caffeic acid and ferulic acid lignin	N/A	Caffeic/ferulic acid and H2O2 were added to 50 mL of 10 mg HRP in 10 mM sodium phosphate buffer at pH 8 for 5 h.	Thakkar et al., 2010
Lignosulfonic acid	Anti-HIV and anti-HSV activity	N/A	2.5 %	Mice exposed to HSV-2 G suspension were treated with 50 μL of 2.5 % LA, 5 % acyclovir, 1 % tenofovir for 5 days.	Gordts et al., 2015
Lignin-Carbohydrate-Protein Complexes	Antiviral activity against herpes simplex virus type1 and type 2, human cytomegalovirus (HCMV) and measles virus	*Pimpinella anisum* lignin		HSV-2 suspension and precooled (3 h) LCC were mixed at 40C, washed with PBS wash (3 times) before diluting (10-fold PBS) the cell pellet. Finally, added vero cell monolayers (35 mm dish) and performed a plaque assay.	Lee et al., 2011
Lignin– starch biodegradable films	Release of Ciprofloxacin	Alkali lignin	1.2, 1.6, 2.0 and 2.4 wt%	Starch and lignin were added to 20 mL water (constant stirring at 100 °C) containing 0.5 mL glycerol as a plasticizer and heated for 5 min. Dried biofilms were placed in vials containing 15 mL of Ciprofloxacin (172 mg/L) for 72 h at 208 °C and dried at 408 °C	Çalgeris et al., 2012
Drug-loaded poly(L-lactide)/lignin stereocomplex film	Release of trans -resveratrol	Alkaline lignin	10 % (w/w)	PLLA and LG-g-PDLA were dissolved in chloroform, sonicated for 5 min and trans-RSV acetone solution appended. The mixture was poured onto a smooth and framed PTFE plate and kept in a 40 °C vacuum.	Liu et al., 2018; Sun et al., 2015, 2016
Banana-chitosan film	Wound healing	N/A	N/A	Chitosan powder was dissolved in 2 % acetic acid solution and stirred for 4 h with 1 mL glycerol as a plasticizer. Mixed with banana peel powder, dried at 40 °C for 24 h followed by another drying at 40 °C for 4 h.	Rihayat et al., 2019
Lignin–chitosan–PVA composite hydrogel	Wound healing	Sulfite papermaking pulp lignin	10 wt%	Chitosan dissolved in acetic acid solution (500 rpm for 5 h), PVA dissolved into water (90 °C,6 h) and lignin dissolved into deionized water (500 rpm,5 h). The solution was mixed (1000 rpm, 5 h) and frozen at −18 °C for 8 h.	Zhang et al., 2019
Chitosan-alkali lignin hydrogel	Wound healing	Alkali lignin	10 %	Hydrogels and crosslinked films of chitosan and alkali lignin obtained by ionotropic cross-linking.	Ravishankar et al., 2019
Bacteria cellulose and lignin model polymer (BCDHP)	Wound healing		N/A	DHP synthesis by the action of CA, H2O2, and horseradish peroxidase prepared in phosphate buffer(pH 7.3). DHP was centrifuged and washed in double-distilled water. Finally, the precipitate was air-dried and dissolved in a 5 % dimethyl sulfoxide (DMSO) water solution.	Zmejkoski et al., 2018
DHP-alginate hydrogel	Wound healing		1 % (w/v)	DHP in DMSO solution and sodium alginate solution were mixed and CaCl2 0.5 % w/v was added.	Spasojević et al., 2016
Unsulfated or sulfated low molecular weight lignins	Therapeutic use in emphysema	Caffeic acid, ferulic acid or sinapic acid	N/A	LMWLs were synthesized chemoenzymatically from three 4-hydroxycinnamic acids.	Saluja et al., 2013
Lignophenols	Regulation of apo-B secretion, decreases cellular total cholesterol	Native lignin from Japanese cedar	N/A	Phase-separation system consisting of cresol and sulfuric acid.	Norikura et al., 2010a, 2010b

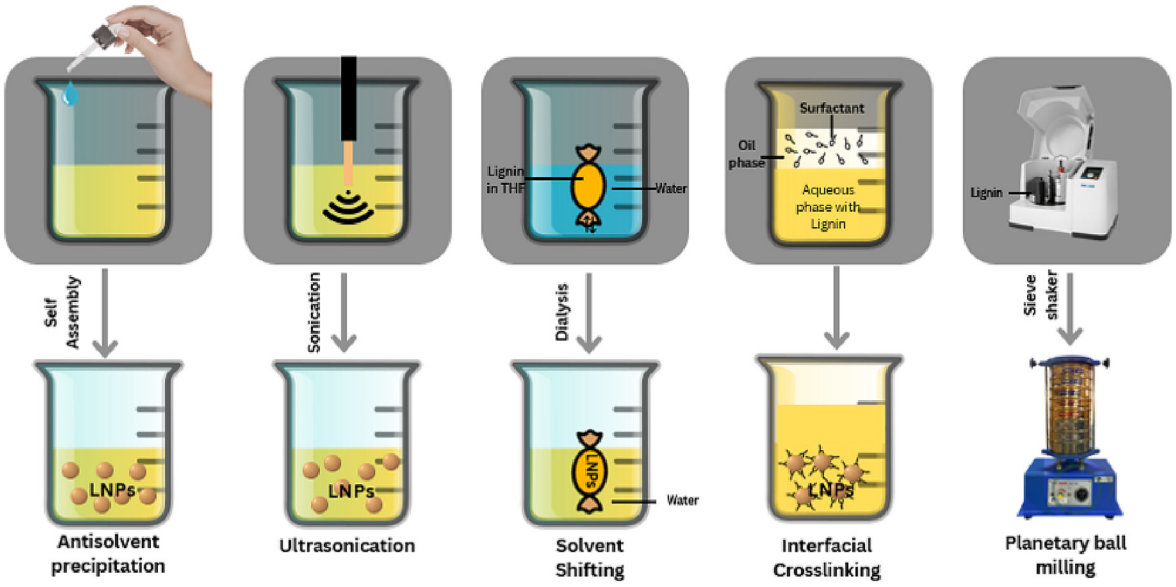

Fig. 3. Common preparation method of nanolignin.

hardwood (dioxin lignin) lignins were treated with the antisolvent precipitation approach to produce 80 to 104 nm lignin particles (ALNP and DLNP) with strong UV shielding and radical scavenging properties. For this, the contributors employed acetone and water with constant stirring (300 rpm) at 20 °C (Yearla and Padmasree, 2016). The Technique's drawbacks include the colloid system's instability, the shape of the formed nanoparticles, and the solvents' irremovable nature (Sharma and Kumar, 2020).

4.1.10. Nanolignin from acoustic cavitation assisted nanoparticles preparation

Gilca et al. prepared stable lignin nanoparticles from lignin (0.7 %) suspension by taking advantage of this method. The aqueous solution was then subjected to acoustic treatment via an ultrasonic probe outputting a 20 KHz frequency at 600 W for an hour. The resulting uniform nanosuspension was allowed to dry under mild conditions (Gilca et al., 2015).

4.1.11. Nanolignin from SERSL

Steam exploded rice straw lignin (SERSL) is an alternative source for the synthesis of LNPs. Initially, castor oil (20 wt%) and SERSL solution mixture underwent stirring to afford a homogenous solution. By maintaining a nitrogen setting, 20 mL HCl (1 M) was introduced in drops at 50 °C for 4 h. Nascent lignin nanoparticles formed were subjected to thorough washing with water and ethanol until a pH of 7 was reached (Rahman et al., 2018).

4.1.12. Nanolignin from green synthesis process

The use of precursor materials (kraft lignin and organosolv) in a unique technique for manufacturing LNPs resulted in nanoparticles with diameters ranging from 45 to 250 nm. Kraft (Indulin AT) guided synthesis begins when a solution of 0.25 g kraft in 50 mL ethylene glycol is vortexed (30 min) and filtered through a 0.45 μm pore size syringe filter. Particles emerge after quickly adding 1–3 mL of 0.025 M nitric acid to 5 mL of the filtered solution in a scintillation vial with continual shaking (Yang et al., 2016, 2018, 2019). The acetone/organosolv stock solution (0.25 organosolv in 50 mL acetone) was subjected to the same initial vortexing and filtration stages in the second approach. Finally, supersaturated lignin was phase-separated into LNPs by adding 9.2 mL water to a 1 mL filtrate solution (Richter et al., 2016).

4.1.13. Nanolignin from hydroxymethylation

Popa et al. demonstrated the role of hydroxymethylation in the synthesis of lignin nanoparticles in a study. Initially, 10 g of lignin derived from wheat straw and Sarkanda grass produced lignin suspension in water (47 mL) upon stirring continuously at room temperature for 120 min. The resulting lignin dispersion was then treated with a 50 % solution containing 1.29 g sodium hydroxide and a 25 % solution containing 3.14 g ammonium hydroxide while mechanically shaken for 2 h (for catalysis). A 37 % solution containing 6.7 g formaldehyde was allowed to react for 4 h in the next phase, kept at 85 °C. Next, a recovery stage with 1 N HCl (pH 2) yielded a precipitate, centrifuged to obtain a solid phase. The portion was washed twice with water and dried to obtain LNPs (Popa et al., 2011).

4.1.14. Nanolignin from wheat pulping black liquor

This method is suitable for transforming non-uniform clusters of lignin-derived polymers into uniformly distributed spherical colloidal nanoparticles. In one such study, pulping black liquor formed the source of alkali lignin, which was then purified and acetylated. For that, acetylated lignin-tetrahydrofuran (ACL–THF) solution (1 mg/mL) was prepared by adding tetrahydrofuran to the solution followed by water. The hydrophobic nature of acetylated lignin molecules in the ACL-THF solution started to promote the formation of colloids, as evidenced by the sudden rise in the scattered light intensity of the solution. The critical water content of 44 vol% facilitated the formation of spherical colloids (Qian et al., 2014a, 2014b).

4.1.15. Nanolignin from supercritical antisolvent technology

The supercritical antisolvent approach is a viable way to produce lignin-based nanoparticles from rugose wood elements. It comprises a combination of techniques, including precipitation, dissolution, centrifugation, and CO_2 supercritical equipment. They used carbonic acid as the antisolvent of choice in the patented technology for producing industrial-grade xylogen NPs (Zhiqiang et al., 2011).

4.1.16. Nanolignin from chemomechanical methods

This patented chemo-mechanical process enabled the synthesis of size-controlled xylogen nanoparticles with a particle size of up to 26 nm. The procedure begins with alkali treatment of the extract, followed by grinding to a particle size of <0.2 mm and freeze-drying the colloid sol to obtain xylogen NPs with an average particle size of 30 nm (Zhiming et al., 2013).

4.1.17. Nanolignin from self-assembly

When used as fillers in natural rubber, stable lignin nanoparticles of 100 nm made from industrial sulfate lignin accelerated vulcanization. Colloidal LPCs were mixed with a 2 % poly (diallyl dimethylammonium chloride) (PDADMAC) solution in an alkaline pH to make these electrostatically assembled NR/LPCs (Natural Rubber/ Lignin-Poly (diallyl

Table 5
Comparison of typical lignin and nanolignin.

Properties	Normal lignin	Nanolignin	References
Mechanical properties	Good mechanical properties	**Advantages:** Improved stiffness, strength, toughness, thermal stability and barrier properties. Performs better in comparison to traditional composites due to the higher specific surface of the nanofillers.	Cai et al., 2008
UV blocking	Better UV blocking property due to phenolic, ketone and other chromophores	**Advantages:** 30 % increase in UV protective activity exhibits a broader absorption band in the longer wavelength region and shows a shoulder toward the longer wavelength region SPF value of the sunscreens increases with decreasing size of lignin colloidal spheres.	Li et al., 2016
Antimicrobial property	Successful antimicrobial properties against various microorganisms due to the polyphenolic compounds of lignin	**Advantages:** Increased antimicrobial effect due to huge surface area, more functional and polyphenolic sidechains on their surface, and increased contact area.	Nada et al., 1989
Radical-scavenging capacity, reducing power, and superoxide radical scavenging activity.	Effective free-radical scavenger, capable of reducing oxygen radicals, retard and inhibit oxidation reactions	**Advantages:** Nanoscale polar OS lignin has improved radical-scavenging capacity, reducing power, superoxide radical scavenging activity and water solubility than non-nano scale lignin.	Dizhbite et al., 2004
Pickering emulsion	Under acidic conditions at pH 4, lignin forms particles with an average size of 182 nm. These particles form a Pickering emulsion.	**Advantages:** Nanoparticles grafted with surface-active polymer chains can decrease surface and interfacial tensions and create stable Pickering emulsions.	Wei et al., 2012
Carbonized lignin nanofibers	Produced carbon fibers from commercially available Kraft lignin.	**Advantages:** Increased tensile strength and modulus of carbon fibers were observed with decreasing fiber diameter.	Kadla et al., 2002
Adsorption capacity	Lignin-derived adsorbing materials exhibited relatively low adsorption capacity and poor affinity for specific heavy metal ions due to small surface areas (large size) and lack of functionalities. For example, 31.6 mg/g was the adsorption capacity of alkaline lignin for Cr(VI).	**Advantages:** Excellent adsorption capability toward different kinds of heavy metal ions Ex: lignin-based nano-trap (LBNT). LBNT is expected to possess reduced particle size for enhancing diffusion and contacting frequency, strong metal binding groups on the surface affordable to different kinds of heavy metal ions with excellent adsorption capability, and the surface-dispersed binding sites in control of loading heavy metal ions facilitating further multiple use.	Albadarin et al., 2011

dimethylammonium chloride) (PDADMAC) complexes (LPCs) composites (pH 12). The obtained solution was coprecipitated with H_2SO_4 (pH 2), yielding a mixture. Filtering, washing, and vacuum drying at 50 °C culminate in fabricating the NR/LPCs nanocomposites (Jiang et al., 2013).

4.2. Applications of nanolignin

Despite lignin's universal abundance, it is seldom considered for high-end applications. Because of their particle size and surface area, biopolymers such as lignin exhibit remarkable physical and chemical properties (Gilca et al., 2015; Gîlca and Popa, 2013). Large and highly complex compounds like lignin can be broken down to nanoscale levels. Nanolignin has the advantage of being mechanically and thermally stable particles with superior antioxidant, bactericidal, UV shielding, and stabilizing capabilities than native lignin molecules (Gupta et al., 2015). By valorizing the input feedstock, nanometric lignin particles can leverage the biorefining sector (Ponnusamy et al., 2019; Akbarian et al., 2022). The following section discusses the application of nanoscale lignin in different aspects (Fig. 4).

4.2.1. Food packaging

The biggest challenge faced by the food packaging industry is the lack of low-cost, biodegradable packaging with antimicrobial properties. Since impending contamination hazards threaten each packaging stage, the development of nanometric kraft lignin labeled with silver NPs could be one such solution. For this, Indulin AT was precipitated by pH shifting and treated with Ag-NPs in an aqueous $AgNO_3$ solution. These silver-tagged lignin NPs were able to efficiently neutralize both gram-negative and gram-positive food-borne pathogens (Richter et al., 2015).

Yang's team contributed to the industry by developing a three-component polymeric covering that had shown significant action against *Pseudomonas syringae* pv. tomato (Pst), a plant pathogen. LNPs and cellulose nanocrystals were deposited on PLA with and without a glycidyl methacrylate (GMA) graft using a melt extrusion method. The reinforced PLA biofilm (1 and 3 wt% of lignin) also exhibited good UV protection and nucleation. By incorporating chitosan in the skeleton, the same group executed solvent casting with binary and ternary coatings. As a result, PVA/CH/LNP nanocomposites could suppress *Erwinia carotovora* subsp. *carotovora* and *Xanthomonas arboricola pv. Pruni*. These encouraging findings highlight the efficacy and use of lignin nanoparticles as a safe and low-cost food packaging option (Yang et al., 2016).

4.2.2. Nanolignin as a radical scavenger/antioxidant

LNPs impart antioxidant functionality to systems courtesy of functional groups and inherent complexity. These factors promote hydrogen donation, an antagonist of oxidation and free radical formation (Chauhan, 2020). The antioxidant and radical scavenging potential of nanometric lignin composites are one of the most sought-after entities in the present-day food, pharma, and cosmetic industries. Lu et al. employed acetone as a solvent and supercritical CO_2 as an antisolvent. Upon estimation, the reducing power and radical scavenging potential of the nanolignins showed improvements (Lu et al., 2012).

Transparent polymeric composite structures of PLA-fused LNPs with strong antioxidant properties were recently described (Tian et al., 2017). In an investigation, dioxane lignin nanoparticles (DLNP) and alkali lignin nanoparticles (ALNP) were effective in protecting *E. coli* against radiation-induced death. Compared to the control, nano lignin production using an alkaline solution precipitation approach had a 3.3 times greater free radical scavenging capability. The nanolignin's bioavailability, smaller dimensions, and larger surface area are most likely to have contributed to the nanolignin's potency (Yearla and Padmasree, 2016).

4.2.3. Nanolignin as a carrier

Biocompatible substrates like lignin, both at micron and sub-micron levels) with low immunogenicity are used for a targeted treatment regime. Capsular, hollow, and porous forms, and solid structures with pores, are two types of lignin nanocarriers (Akbarian et al., 2022).

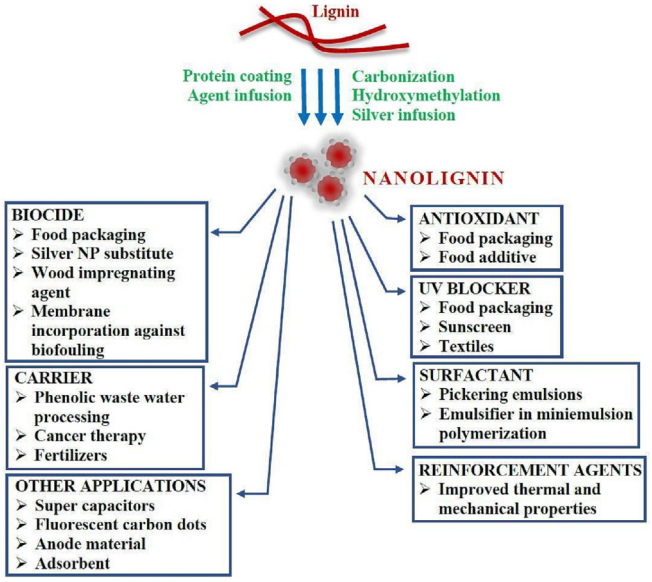

Fig. 4. Applications of nanolignin.

A lignosulfonate capsule with hollow porous structures carrying hydrophobic bioactive molecules, such as coumarin-6, is an example of a pH-sensitive nanometric drug carrier. Embedding β-thiopropionate (acid-labile functionality) on the shell surface enables drug delivery to the target site in response to a matching pH. These acoustically synthesized capsular carriers with allyl-grafts typically have a 50–300 nm diameter range and are formed in an oil-in-water emulsion system (Chen et al., 2016). Tortora et al. explored the production of coumarin-6 microcapsular carriers generated from kraft lignin. 0.3 to 1.1 μm sized microcapsules can be produced by a high-frequency acoustic-driven synthesis of oil-laden lignin microcapsules at the water/oil portion of oil in water emulsion. Furthermore, after internalization into hamster ovary cells, this method showed low immunogenicity and toxicity (Tortora et al., 2014). The release patterns of coumarin were similar in both cases. When loaded with bioactive supplements like polyphenols and essential oils, these nanocapsules have the potential to cure skin-related ailments (Akbarian et al., 2022).

Yiamsawas et al. developed stable lignin-derived nanocapsules of 150–200 nm diameter at the water-cyclohexane interface. Reduced cross-linking agent (lignosulfonic acid), enzyme degradation, increased temperature, and inversely proportional pH levels improved the release rates of the resulting nanocarriers. The same authors also describe an effective 2-propylpyridine-loaded kraft lignin-derived nanocapsules possessing an oil phase and lignin core (Yiamsawas et al., 2017).

Cytotoxicity of carbon nanotubes to living cells restricts their application in the human body. The ability of biocompatible lignin nanotubes to transfect HeLa cells after DNA adsorption makes them an appropriate solution to this problem. In a study comparing the cytotoxicity of both nanostructures on HeLa cells, lignin nanotubes exhibited a tolerance threshold ten times higher than carbon nanotubes. Recently, self-assembled micelles of lignin (SLRM) origin that encapsulated horseradish peroxidase (HRP) enzyme inside its hydrophilic core exhibited improved enzymatic activity upon immobilization. The SLRM core structure boosts HRP's overall activity, enabling bioremediation of phenol-contaminated wastewater at pH 4 (Zhong et al., 2016). Reusable colloidal cationic lignin nanospheres enable ester synthesis by helping to attach entrapped hydrolases onto the platform (Sipponen et al., 2018). The pH of the medium impacts the stability of novel biocompatible LNPs encapsulating water-soluble Rhodamine 6G. Green synthesis of nanoparticles utilizing a hydrotropic solution includes self-assembling LNPs made of aqueous sodium p-toluene sulfonate. These nanoparticles demonstrated a long-term drug release profile while encapsulating hydrophobic molecules with 90 % efficiency (Chen et al., 2018).

4.2.4. Solid and porous particles/structures

The use of novel bionanomaterials and nanocarriers is important in the fight against neoplasm. Shortcomings of conventional and targeted cancer therapies lie in the mode of delivery of the proposed drug. LNPs tasked to encapsulate test compounds against cancer must preserve the target medication from premature degradation and allow for ligand-assisted tumor penetration. Modifying LNPs with targeting entities help to attain enhanced cellular interaction during the treatment. Various cell lines treated with complex spherical LNPs containing iron molecules (Fe-LNPs and Fe_3O_4-LNPs) exhibited low polydispersity, low toxicity, insignificant in vitro hemolysis, and H_2O_2 generation at a stable pH of 7.4. Also, BZL (benzazulenein) cancer cell lines' cytotoxic effect was boosted by pure lignin nanoparticles (Figueiredo et al., 2017). The use of magnetic Resveratrol (RSV)-loaded lignin nanoparticles (AL/RSV/Fe3O4 NPs) in cytological and animal experiments was a success against proliferating cancer cells. The work focused on creating green chemistry-based self-assembled AL-based unmodified lignin nanocomposites. The magnetic drug-loaded delivery method improved long-term drug release, allowing optimal drug accumulation and tumor shrinkage (Dai et al., 2017). The overall performance of these innovative technologies makes it possible to test them in real-world circumstances.

4.2.5. Nanolignin for oral disease and tissue regeneration

As a virus-inhibiting agent, solubilized nanolignin in the form of [125I]-labeled LCC (lignin carbohydrate complex) has medical potential (Sakagami et al., 2017). A recent study examined the effect of combining electropositive chitin nanofibrils (CN) with LNPs. The bactericidal and anti-inflammatory capabilities of the formed CN-LG particles (163 nm) possessed a wide range of industrial and medicinal applications, including skin-related disorders. CN-LG matrix helps tissue regeneration by establishing a barrier against microbial proliferation at the wound site, in addition to being a chemoattractant. Also, these compounds can be administered to in vitro cultures of human keratinocytes and human mesenchymal stromal cells for potential use in skin contact applications (Danti et al., 2019).

4.2.6. Nanolignin as a UV blocker

Lignin is an excellent candidate for a sun blocker ingredient in some lignin-derived sunscreens since it is non-oxidizable. The addition of LNPs enhanced the native SPF value of plain creams significantly (1.03 versus 1.26–2.23 for amalgamations) (Chauhan, 2020). In another study, when exposed to 400 nm light, a transparent PLA-tagged LNP matrix containing 4 wt% LNPs offered UV protection of up to 80 % (Tian et al., 2017). Value-addition of sunscreens with photoprotective LNPs/ZnO sourced from *Agave tequilana* enhanced the SPF value of the sunscreen as evidenced by the extent of blocking of UV-B and UV-C rays (Hernandez et al., 2016). The poly (butylene adipate-coterephthalate) (PBAT) matrix forms biofilms with improved mechanical and thermal stability when combined with various LNP combinations of melanin core-shell nanoparticles (MNP) and lignin-melanin core-shell nanoparticles (LMNP). Poly(butylene adipate-coterephthalate) (PBAT) matrix associates with various LNP combinations of melanin core-shell nanoparticles (MNP) and lignin−melanin core−shell nanoparticles (LMNP) to form biofilms with enhanced mechanical and thermal stability. Also, they absorbed >80 % of incoming UV-B rays when NPs concentrations ranged between 0.5 and 5.0 wt% (Xing et al., 2019). A study dedicated to investigating the effect of the development of sunscreens with lignin and lignin-based colloidal micelles of different shapes and sizes revealed that of all blend types, sunscreen with colloidal spheres exhibited the most protection owing to the presence of phenolic groups in lignin molecules.

Although UV-absorbing clothes containing LNPs are rare, they protect from damaging UV rays without impairing the fabric's basic texture. A study found that nanolignins with silicone emulsion offered the garments antibacterial and antistatic properties. Such application-level initiatives could lead to the development of fabrics that protect wearers from more challenging environmental threats like viruses and fungi in the future. The role of nanolignins as a versatile finish agent is detailed in a study

that used lignin obtained from coconut fibers to treat cotton and linen textiles. Apart from being UV resistant, both fabrics showed significant action against *S. aureus* and *K. pneumonia*. The antioxidant capacity of the participating nanolignin impregnated fabrics was confirmed by their radical scavenging activity (Juikar and Vigneshwaran, 2017).

4.2.7. Nanolignin as adsorbent

Xiao's team had previously produced a functionalized metal-organic scaffold that efficiently scavenges heavy metal ions and microorganisms. Their study further bolstered its bactericidal property against *E. coli* (99.68 %) and *S. aureus* (99.76 %) when tagged with silver metal (Xiao et al., 2018; Liu et al., 2022).

4.2.8. Nanolignin as supercapacitor

LNPs can act as excellent ultra-capacitors when conditioned with a KOH (6 M) electrolyte solution. Activation of lignin-derived microspheres and precursors (LAC-M and LAC—P) resulted in profound capacitive (at 50 mV/s) and rate performance (at a particular current range of 0.05–100 A/g) features. When soda lignin from spruce wood is carbonized and activated, carbon fibers (ACFs) with submicron thickness and high porosity form. These acts can be used as ultra-capacitors with a storage capacity of 8.1 Wh/kg. A study that investigated alkaline lignin as ultra-capacitors vouched for the ability of the resulting fibrous mats to be used as an anode material in a conventional Li-ion battery. Such composites are expected to have a specific capacity of 445 mAh/g and a capacitance retention rate of about 90 % after 6000 charge/discharge cycles (Yu et al., 2018).

4.2.9. Nanolignin as surfactant

In the food and pharmaceutical industry, the use of submicron-level (320 nm) kraft lignin NPs as surfactants form a stable Pickering emulsion with different-sized hexadecane droplets. These lignin-derived surfactants offer a cost-effective and recyclable form of lignin NPs (182 nm) that renders pH responsiveness to styrene-in-water Pickering emulsions by generating insoluble particles at pH 4. RAFT-mediated grafting of kraft lignin particles with polyacrylamide functionality yields polymer-grafted lignin nanoparticles (PGLNs) that control aggregation strength without affecting interfacial interactions required to form Pickering emulsions. Furthermore, the emulsion's comparatively rapid creaming property did not affect Ostwald's ripening and coalescence for months (Qian et al., 2014a, 2014b).

4.3. United Nations sustainable development goal (UNSDG) achieved with the development of nanolignins

The use of nanolignins can guide the development of sustainable and environment-friendly food and pharmaceutical products (United Nations World Tourism Organization, 2018), which aligns with the United Nations Sustainable Development Goal 12 (UNSDG 12) - Responsible Consumption and Production. Nanolignin-derived products can also give access to the costly healthcare system because it follows UNSDG 3, which endorses Good Health and Well-being. Additionally, food and pharmaceutical applications containing nanolignins components can potentially create more job opportunities and hence support the UNSDG 8 - Decent Work and Economic Growth. Furthermore, lignin-based nanomaterials also contribute to UNSDG 13 - Climate Action as it addresses some environmental problems facing the food and pharmaceutical industries, such as waste and pollution.

5. Future perspectives

Lignin, an undervalued natural polymer, is rapidly gaining importance, especially with the application of nano-technological innovations. Most patents involving lignin deal with the production of nanolignin, which shows the vast potential of nanolignin. Based on our current knowledge of lignin and lignin nanoparticles and considering the existing gaps in technologies adopted for nanoparticle development, we have to enlist future actions that are feasible enough to overcome the hurdles in this area. It is necessary that studies should focus on the following areas in order to meet sustainable standards and ensure their safety and effectiveness, greener processes for the synthesis of lignin and nanolignin that use more affordable, environmentally friendly, and easily recoverable solvents are essential. To accomplish lignin and nanolignin industrialization and speedy commercialization, scale-up processes may call for investments in large-scale, quick, low-cost, energy-efficient in manufacturing methods. It is essential to do a life cycle analysis of a nanolignin biorefinery. Discovering and creating new nanolignin that could substitute carbon-intensive synthetic nanoparticles and nanoparticles made from other natural sources are novel applications of nanolignin. The viability and marketing of nanolignins will be improved by this. Prior to clinical trials, the safety, interactions, and efficacy of freshly synthesized lignin and nanolignins should be assessed using in silico, in vitro, and in vivo approaches. These results are necessary to obtain regulatory agency permission and move on to the next phase of nano lignin utilization.

6. Conclusion

A comparison between lignin and nano lignin shows vastly improved properties for nanolignin than non-nanolignin. This includes enhanced mechanical, UV blocking, radical-scavenging capacity, reducing power, superoxide radical scavenging activity, ability to form pickering emulsion, and adsorption capacity for nanolignin. The unique properties of lignin and nano lignin enable its application in other fields like the packaging industry, emulsions, nutrient delivery, drug delivery hydrogels, tissue engineering, and biomedical applications, which will be an excellent opening for human needs. Since these nanoscale and non-nano scale lignin has a wide range of properties, lignin applications will continue to undergo extensive research in the coming years. The findings and insights included in this review will give a different perspective on the potential applications of nanolignins in the food and pharma industries. The article also analyses the challenges and opportunities presented by useful nanolignins, which help researchers, policymakers, and industry professionals plan their nano-lignin-centred investigations with a clear mind about the possible challenges and limitations of the technology.

CRediT authorship contribution statement

Billu Abraham: Conceptualization, Visualization, Writing – original draft. **V.L. Syamnath:** Conceptualization, Writing – original draft. **K.B. Arun:** Visualization, Writing – original draft. **P.M. Fathima Zahra:** Resources, Writing – original draft. **P. Anjusha:** Resources, Writing – original draft. **Anjhinaeyulu Kothakotta:** Resources, Writing – original draft. **Yi-Hsun Chen:** Conceptualization, Visualization, Resources, Supervision. **Vinoth Kumar Ponnusamy:** Conceptualization, Resources, Visualization, Supervision, Writing – review & editing. **P. Nisha:** Conceptualization, Visualization, Project administration, Resources, Supervision, Writing – review & editing.

Data availability

No data was used for the research described in the article.

Declaration of competing interest

The authors declare that they have no known competing financial interests or personal relationships that could have appeared to influence the work reported in this paper.

Acknowledgment

Billu and Dr. P. Nisha acknowledge Department of Science & Technology (DST Project No. GAP1286), New Delhi, India, for the financial support and Billu acknowledges CSIR, New Delhi, India, for the Senior Research Fellowship. We thank the Director, CSIR-NIIST, Thiruvananthapuram, for providing the necessary facilities. This work was supported partially by

the Research Center for Precision Environmental Medicine, Kaohsiung Medical University, Kaohsiung, Taiwan from The Featured Areas Research Center Program within the framework of the Higher Education Sprout Project by the Ministry of Education (MOE) in Taiwan and by Kaohsiung Medical University Research Center Grant (KMUTC112A01). This work was also supported financially by the grant MOST-110-2113-M-037-009- from the Ministry of Science and Technology, Taiwan.

References

Aadil, K.R., Mussatto, S.I., Jha, H., 2018. Synthesis and characterization of silver nanoparticles loaded poly (vinyl alcohol)-lignin electrospun nanofibers and their antimicrobial activity. Int. J. Biol. Macromol. 120, 763–767. https://doi.org/10.1016/j.ijbiomac.2018.08.109.

Abraham, B., Reshmitha, T.R., Navami, M.M., George, L., Venugopalan, V.V., Nisha, P., 2020. Phytochemical rich extract from the spent material generated from Industrial dashamoola preparation (a medicinal ayurvedic decoction) with antioxidant, antidiabetic and anti-inflammatory potential. Ind. Crop. Prod. 151, 112451. https://doi:10.1016/j.indcrop.2020.112451.

Abudula, T., Gzara, L., Simonetti, G., Alshahrie, A., Salah, N., Morganti, P., Chianese, A., Fallahi, A., Tamayol, A., Bencherif, S.A., Memic, A., 2018. The effect of poly (glycerol sebacate) incorporation within hybrid chitin-lignin sol–gel nanofibrous scaffolds. Materials 11 (3), 451. https://doi.org/10.3390/ma11030451.

Agrawal, A., Kaushik, N., Biswas, S., 2014. Derivatives & applications of lignin – an insight. Scitech. J. 01 (7), 30–36.

Ahmed, E.M., 2015. Hydrogel: preparation, characterization, and applications: a review. J. Adv. Res. 6 (2), 105–121. https://doi.org/10.1016/j.jare.2013.07.006.

Ajith, M.P., Aswathi, M., Priyadarshini, E., Rajamani, P., 2021. Recent innovations of nanotechnology in water treatment: a comprehensive review. Bioresour. Technol. 342, 126000. https://doi.org/10.1016/J.BIORTECH.2021.126000.

Akbarian, A., Andooz, A., Kowsari, E., Ramakrishna, S., Asgari, S., Cheshmeh, Z.A., 2022. Challenges and opportunities of lignocellulosic biomass gasification in the path of circular bioeconomy. Bioresour. Technol., 127774 https://doi.org/10.1016/j.biortech.2022.127774.

Albadarin, A.A.H., Al-Muhtaseb, N.A., Al-laqtah, G.M., Walker, S.J., Allen, M.N.M., Ahmad, 2011. Biosorption of toxic chromium from aqueous phase by lignin: mechanism, effect of other metal ions and salts. Chem. Eng. J. 169, 20–30. https://doi.org/10.1016/j.cej.2011.02.044.

Anwer, M.A.S., Naguib, H.E., Celzard, A., Fierro, V., 2015. Comparison of the thermal, dynamic mechanical and morphological properties of PLA-lignin & PLA-tannin particulate green composites. Compos. PartB 82, 92–99. https://doi.org/10.1016/j.compositesb.2015.08.028.

Aura, A., 2018. MLM Wood components to boost the quality of food products. Wood components to boost the quality of food products [media]. Available from http://www.vttresearch.com/media/news/wood-components-to-boostthe-quality-of-food-products.

Bajwa, D., Pourhashem, G., Ullah, A.H., Bajwa, S., 2019. A concise review of current lignin production, applications, products and their environment impact. Ind. Crop. Prod. 139. https://doi:10.1016/j.indcrop.2019.111526.

Barapatre, A., Aadil, K.R., Tiwary, B.N., Jha, H., 2015. In vitro antioxidant and antidiabetic activities of biomodified lignin from Acacia nilotica wood. Int. J. Biol. Macromol. 75, 81–89. https://doi.org/10.1016/j.ijbiomac.2015.01.012.

Baumberger, S., Lapierre, C., Monties, B., Lourdin, D., Colonna, B., 1997. Preparation and properties of thermally moulded and cast lignosulfonates-starch blends. Ind. Crop. Prod. 6, 253–258.

Bertella, S., Luterbacher, J.S., 2020. Lignin functionalization for the production of novel materials. Trends Chem. 2 (5), 440–453. https://doi.org/10.1016/j.trechm.2020.03.001.

Bertolo, M.R.V., Brenelli de Paiva, L.B., Nascimento, V.M., Gandin, C.A., Neto, M.O., Driemeier, C.E., Rabelo, S.C., 2019. Lignins from sugarcane bagasse: renewable source of nanoparticles as Pickering emulsions stabilizers for bioactive compounds encapsulation. Ind. Crop. Prod. 140, 111591. https://doi:10.1016/j.indcrop.2019.111591.

Bhat, R., Abdullah, N., Din, R.H., Tay, G.S., 2013. Producing novel sago starch-based food packaging films by incorporating lignin isolated from oil palm black liquor waste. J. Food Eng. 119, 707–713.

Borisenkov, M.F., Karmanov, A.P., Kocheva, L.S., Markov, P.A., Istomina, E.I., Bakutova, L.A., Popov, S.V., 2015. Adsorption of β-glucuronidase and estrogens on pectin/lignin hydrogel particles. Int. J. Polym. Mater. 65 (9), 433–441. https://doi.org/10.1080/00914037.2015.1129955.

Cai, X., Riedl, B., Zhang, S.Y., Wan, H., 2008. The impact of the nature of nanofillers on the performance of wood polymer nanocomposites. Compos. A: Appl. Sci. Manuf. 39, 727–737. https://doi.org/10.1016/j.compositesa.2008.02.004.

Caicedo, H.K., Dempere, L.A., Vermerris, W., 2012. Template-mediated synthesis and biofunctionalization of flexible lignin-based nanotubes and nanowires. Nanotechnology 23, 105605–105617. https://doi.org/10.1088/0957-4484/23/10/105605.

Çalgeris, İ., Çakmakçı, E., Ogan, A., Kahraman, M.V., Kayaman-Apohan, N., 2012. Preparation and drug release properties of lignin–starch biodegradable films. Starch 64 (5), 399–407. https://doi.org/10.1002/star.201100158.

Calvo-Flores, F.G., Dobado, J.A., 2010. Lignin as renewable raw material. ChemSusChem 3 (11), 1227–1235.

Chauhan, P.S., 2020. Lignin nanoparticles: Eco-friendly and versatile tool for new era. Bioresour. Technol. Rep. 9, 100374.

Chen, H., 2015. Lignocellulose biorefinery feedstock engineering. Lignocellulose Biorefin. Eng, pp. 37–86.

Chen, L., Zhou, X., Shi, Y., Gao, B., Wu, J., Kirk, T.B., Xue, W., 2018. Green synthesis of lignin nanoparticle in aqueous hydrotropic solution toward broadening the window for its processing and application. Chem. Eng. J. 346, 217–225. https://doi:10.1016/j.cej.2018.04.020.

Chen, N., Dempere, L.A., Tong, Z., 2016. Synthesis of pH-responsive lignin-based nanocapsules for controlled release of hydrophobic molecules. ACS Sustain. Chem. Eng. 4 (10), 5204–5211. https://doi:10.1021/acssuschemeng.6b01209.

Choi, D., Heo, J., Park, J.H., Jo, Y., Jeong, H., Chang, M., Hong, J., 2016. Nano-film coatings onto collagen hydrogels with desired drug release. J. Ind. Eng. Chem. 36, 326–333. https://doi.org/10.1016/j.jiec.2016.02.023.

Ciolacu, D., Oprea, A.M., Anghel, N., Cazacu, G., Cazacu, M., 2012. New cellulose–lignin hydrogels and their application in controlled release of polyphenols. Mater. Sci. Eng. C 32 (3), 452–463. https://doi.org/10.1016/j.msec.2011.11.018.

Claudia, C., Federica, M., Marco, S., 2011. Milled wood lignin: a linear oligomer. Biomacromolecules 12, 3928–3935.

Dacrory, S., Abou-Yousef, H., Abouzeid, R.E., Kamel, S., Abdel-aziz, M.S., El-badry, M., 2018. Antimicrobial cellulosic hydrogel from olive oil industrial residue. Int. J. Biol. Macromol. 117, 179–188. https://doi.org/10.1016/j.ijbiomac.2018.05.179.

Dai, L., Liu, R., Hu, L.Q., Zou, Z.F., Si, C.L., 2017. Lignin nanoparticle as a novel green carrier for the efficient delivery of resveratrol. ACS Sustain. Chem. Eng. 5 (9), 8241–8249. https://doi:10.1021/acssuschemeng.7b01903.

Danti, S., Trombi, L., Fusco, A., Azimi, B., Lazzeri, A., Morganti, P., Donnarumma, G., 2019. Chitin nanofibrils and nanolignin as functional agents in skin regeneration. Int. J. Mol. Sci. 20 (11), 2669. https://doi:10.3390/ijms20112669.

Demirci, F., Yildirim, K., Kocer, H.B., 2018. Antimicrobial open-cell polyurethane foams with quaternary ammonium salts. J. Appl. Polym. Sci. 135 (9), 45914. https://doi.org/10.1002/app.45914.

Dey, N., Kumar, G., Vickram, A.S., Mohan, M., Singhania, R.R., Patel, A.K., Dong, C.D., Anbarasu, K., Thanigaivel, S., Ponnusamy, V.K., 2022. Nanotechnology-assisted production of value-added biopotent energy-yielding products from lignocellulosic biomass refinery–a review. Bioresour. Technol. 344, 126–171. https://doi.org/10.1016/j.biortech.2021.126171.

Dinari, A., Abdollahi, M., Sadeghizadeh, M., 2021. Design and fabrication of dual responsive lignin-based nanogel via "grafting from" atom transfer radical polymerization for curcumin loading and release. Sci. Rep. 11 (1), 1962. https://doi.org/10.1038/s41598-021-81393-3.

Dizhbite, T., Telysheva, G., Jurkjane, V., Viesturs, U., 2004. Characterization of the radical scavenging activity of lignins - natural antioxidants. Bioresour. Technol. 95, 309–317. https://doi.org/10.1016/j.biortech.2004.02.024.

Domínguez-Robles, J., Larrañeta, E., Fong, M.L., Martin, N.K., Irwin, N.J., Mutjé, P., Delgado-Aguilar, M., 2019. Lignin/poly (butylene succinate) composites with antioxidant and antibacterial properties for potential biomedical applications. Int. J. Biol. Macromol. 145, 92–99. https://doi.org/10.1016/j.ijbiomac.2019.12.146.

Domínguez-Robles, J., Martin, N., Fong, M., Stewart, S., Irwin, N., Rial-Hermida, M., Larrañeta, E., 2019. Antioxidant PLA composites containing lignin for 3D printing applications: a potential material for healthcare applications. Pharmaceutics 11 (4), 165. https://doi.org/10.3390/pharmaceutics11040165.

Domínguez-Robles, J., Peresin, M.S., Tamminen, T., Rodríguez, A., Larrañeta, E., Jääskeläinen, A.S., 2018. Lignin-based hydrogels with "super-swelling" capacities for dye removal. Int. J. Biol. Macromol. 115, 1249–1259. https://doi.org/10.1016/j.ijbiomac.2018.04.044.

Dong, H., Zheng, Yu, P., Jiang, Q., Wu, Y., Huang, C., Yin, B., 2019. Characterization and application of lignin-carbohydrate complexes from lignocellulosic materials as antioxidant for scavenging in vitro and in vivo reactive oxygen species. ACS Sustain. Chem. Eng. 8 (1), 256–266. https://doi.org/10.1021/acssuschemeng.9b05290.

Dong, Y., Paukkonen, H., Fang, W., Kontturi, E., Laaksonen, T., Laaksonen, P., 2018. Entangled and colloidally stable microcrystalline cellulose matrices in controlled drug release. Int. J. Pharm. 548 (1), 113–119. https://doi.org/10.1016/j.ijpharm.2018.06.022.

Ekeberg, D., Gretland, K.S., Gustafsson, J., Bråten, S.M., 2006. Characterisation of lignosulphonates and Kraft lignin by hydrophobic interaction chromatography. Anal. Chim. Acta 565 (1), 121–128.

Erakovic, S., Jankovic, A., Tsui, G.C.P., Tang, C.Y., Miskovic-Stankovic, V., Stevanovic, T., 2014. Novel bioactive antimicrobial lignin containing coatings on titanium obtained by electrophoretic deposition. Int. J. Mol. Sci. 15, 12294–12322.

Farhat, W., Venditti, R., Mignard, N., Taha, M., Becquart, F., Ayoub, A., 2017. Polysaccharides and lignin based hydrogels with potential pharmaceutical use as a drug delivery system produced by a reactive extrusion process. Int. J. Biol. Macromol. 104, 564–575. https://doi.org/10.1016/j.ijbiomac.2017.06.037.

Figueiredo, P., Lintinen, K., Kiriazis, A., Hynninen, V., Liu, Z., Bauleth-Ramos, T., Rahikkala, A., Correia, A., Kohout, T., Sarmento, B., Yli-Kauhaluoma, J., Hirvonen, J., Ikkala, O., Kostiainen, M.A., Santos, H.A., 2017. In vitro evaluation of biodegradable lignin-based nanoparticles for drug delivery and enhanced antiproliferation effect in cancer cells. Biomaterials 121, 97–108. https://doi.org/10.1016/j.biomaterials.2016.12.034.

Ganasan, E., Mohd Yusoff, H., Azmi, A.A., Chia, P.W., Lam, S.S., Kan, S.Y., Teo, C.K., 2022. Food additives for the synthesis of metal nanoparticles: a review. Environ. Chem. Lett., 1–14 https://doi.org/10.1007/s10311-022-01473-2.

Gellerstedt, G., Henriksson, G., 2008. Lignins: major sources, structure and properties. In: Belgacem, M.N., Gandini, A. (Eds.), Monomers, Polymers And Composites From Renewable Resources, pp. 201–224.

Gharehkhani, S., Ghavidel, N., Fatehi, P., 2018. Kraft lignin-tannic acid as a green stabilizer for oil/water emulsion. ACS Sustain. Chem. Eng. 2370–2379.

Gîlca, I.A., Popa, V.I., 2013. Study on biocidal properties of some nanoparticles based on epoxy lignin. Cellul. Chem. Technol. 47, 3–4.

Gilca, I.A., Popa, V.I., Crestini, C., 2015. Obtaining lignin nanoparticles by sonication. Ultrason. Sonochem. 23, 369–375. https://doi:10.1016/j.ultsonch.2014.08.02.

Gil-Chávez, J., Gurikov, P., Hu, X., Meyer, R., Reynolds, W., Smirnova, I., 2019. Application of novel and technical lignins in food and pharmaceutical industries: structure-function relationship and current challenges. Biomass Convers. Biorefinery https://doi.org/10.1007/s13399-019-00458-6.

Gordts, S.C., Férir, G., D'huys, T., Petrova, M.I., Lebeer, S., Snoeck, R., Schols, D., 2015. The low-cost compound lignosulfonic acid (LA) exhibits broad-spectrum anti-HIV and anti-HSV activity and has potential for microbicidal applications. PLOS One 10 (7), e0131219. https://doi.org/10.1371/journal.pone.0131219.

Gosselink, R., Snijder, M., Kranenbarg, A., Keijsers, E., de Jong, E., Stigsson, L., 2004. Characterisation and application of Nova Fiber lignin. Ind. Crop. Prod. 20, 191–203.

Greenhalgh, R., Dempsey-Hibbert, N.C., Whitehead, K.A., 2019. Antimicrobial strategies to reduce polymer biomaterial infections and their economic implications and considerations. Int. Biodeterior. Biodegrad. 136, 1–14. https://doi.org/10.1016/j.ibiod.2018.10.005.

Gupta, A.K., Mohanty, S., Nayak, S.K., 2015. Influence of addition of vapor grown carbon fibers on mechanical, thermal and biodegradation properties of lignin nanoparticle filled bio-poly (trimethylene terephthalate) hybrid nanocomposites. RSC Adv. 5 (69), 56028–56036. https://doi:10.1039/c5ra07828h.

Haghdan, S., Renneckar, S., Smith, G.D., 2016. Sources of lignin. Lignin in Polym. Compos, pp. 1–11.

Haldar, D., Shabbirahmed, A.M., Singhania, R.R., Chen, C.W., Dong, C.D., Ponnusamy, V.K., Patel, A.K., 2022. Understanding the management of household food waste and its engineering for sustainable valorization-a state-of-the-art review. Bioresour. Technol., 127390 https://doi.org/10.1016/j.biortech.2022.127390.

Hasegawa, Y., Kadota, Y., Hasegawa, C., Kawaminami, S., 2015. Lignosulfonic acid-induced inhibition of intestinal glucose absorption. J. Nutr. Sci. Vitaminol. 61 (6), 449–454. https://doi.org/10.3177/jnsv.61.449.

Hernandez, G.J.M., Escalante, A., Murillo Vazquez, R.N., Delgado, E., Gonzalez, F.J., Toriz, G., 2016. Use of agave tequilana-lignin and zinc oxide nanoparticles for skin photoprotection. J. Photochem. Photobiol. 163, 156–161. https://doi.org/10.1016/j.jphotobiol.2016.08.027.

Hiltunen, E., Alvila, L., Pakkanen, T.T., 2006. Characterization of brauns' lignin from fresh and vacuum-dried birch (Betula pendula) wood. Wood Sci. Technol. 40, 575.

Huang, C., Tang, S., Zhang, W., Tao, Y., Lai, C., Li, X., Yong, Q., 2018. Unveiling the structural properties of lignin–carbohydrate complexes in bamboo residues and its functionality as antioxidants and immunostimulants. ACS Sustain. Chem. Eng. 69, 12522–12531.

Jaganathan, G., Manivannan, K., Lakshmanan, S., Sithique, M.A., 2018. Fabrication and characterization of Artocarpus heterophyllus waste derived lignin added chitosan biocomposites for wound dressing application. Sustain. Chem. Pharm. 10, 27–32. https://doi.org/10.1016/j.scp.2018.08.002.

Janković, A., Eraković, S., Ristoscu, C., 2015. Structural and biological evaluation of lignin addition to simple and silver-doped hydroxyapatite thin films synthesized by matrix-assisted pulsed laser evaporation. J. Mater. Sci. Mater. Med. 26 (1), 17. https://doi.org/10.1007/s10856-014-5333-y.

Javed, A., Ullsten, H., Rättö, P., Järnström, L., 2018. Lignin-containing coatings for packaging materials. Nord. Pulp Pap.Res. J. 33 (3), 548–556.

Jiang, C., He, H., Jiang, H., Ma, L., Jia, D.M., 2013. Nano-lignin filled natural rubber composites: preparation and characterization. Express Polym. Lett. 7 (5), 480–493. https://doi.org/10.3144/expresspolymlett.2013.44.

Juikar, S.J., Vigneshwaran, N., 2017. Microbial production of coconut fiber nanolignin for application onto cotton and linen fabrics to impart multifunctional properties. Surf. Interfaces 9, 147–153. https://doi:10.1016/j.surfin.2017.09.006.

Kadla, J., Kubo, S., Venditti, R., Gilbert, R., Compere, A., Griffith, W., 2002. Lignin-based carbon fibers for composite fiber applications. Carbon 40, 2913–2920. https://doi.org/10.1016/S0008-6223(02)00248-8 N. Y.

Kai, D., Jiang, S., Low, Z.W., Loh, X.J., 2015. Engineering highly stretchable lignin-based electrospun nanofibers for potential biomedical applications. J. Mater. Chem. A B 3 (30), 6194–6204. https://doi.org/10.1039/c5tb00765h.

Kai, D., Zhang, K., Jiang, L., Wong, H.Z., Li, Z., Zhang, Z., Loh, X.J., 2017. Sustainable and antioxidant lignin–polyester copolymers and nanofibers for potential healthcare applications. ACS Sustain. Chem. Eng. 5, 6016–6025. https://doi.org/10.1021/acssuschemeng.7b00850.

Kim, S., Fernandes, M.M., Matamá, T., Loureiro, A., Gomes, A.C., Cavaco-Paulo, A., 2013. Chitosan–lignosulfonates sono-chemically prepared nanoparticles: characterisation and potential applications. Colloids Surf. B 103, 1–8. https://doi.org/10.1016/j.colsurfb.2012.10.033.

Larrañeta, E., Imízcoz, M., Toh, J.X., Irwin, N.J., Ripolin, A., Perminova, A., Donnelly, R.F., 2018. Synthesis and characterization of lignin hydrogels for potential applications as drug eluting antimicrobial coatings for medical materials. ACS Sustain. Chem. Eng. 6 (7), 9037–9046. https://doi.org/10.1021/acssuschemeng.8b01371.

Lee, E., Song, Y., Lee, S., 2019. Crosslinking of lignin/poly (vinyl alcohol) nanocomposite fiber webs and their antimicrobial and ultraviolet-protective properties. Tex. Res. J. 89 (1), 3–12. https://doi.org/10.1177/0040517517736468.

Lee, E.S., Kim, Y.O., Ha, Y.M., Lim, D., Hwang, J.Y., Kim, J., Park, M., Cho, J.W., Jung, Y.C., 2018. Antimicrobial properties of lignin-decorated thinmulti-walled carbon nanotubes in poly (vinyl alcohol) nanocomposites. Eur. Polym. J. 105, 79–84. https://doi.org/10.1016/j.eurpolymj.2018.05.014.

Lee, J.B., Yamagishi, C., Hayashi, K., Hayashi, T., 2011. Antiviral and immunostimulating effects of lignin-carbohydrate-protein complexes from Pimpinella anisum. Biosci. Biotechnol. Biochem. 75 (3), 459–465. https://doi.org/10.1271/bbb.100645.

Li, H., Deng, Y., Wu, H., Ren, Y., Qiu, X., Zheng, D., Li, C., 2016. Self-assembly of kraft lignin into nanospheres in dioxane-water mixtures. Holzforschung 70, 725–731. https://doi:10.1515/hf-2015-0238.

Liguori, I., Russo, G., Curcio, F., Bulli, G., Aran, L., Della-Morte, D., Gargiulo, G., Testa, G., Cacciatore, F., Bonaduce, D., Abete, P., 2018. Oxidative stress, aging, and diseases. Clin. Interv. Aging 26 (13), 757–772. https://doi:10.2147/CIA.S158513.

Liu, J., Wu, J., Lu, Y., Zhang, H., Hua, Q., Bi, R., Rojas, O., Renneckar, S., Fan, S., Xiao, Z., Saddler, J., 2022. The pre-addition of "blocking" proteins decreases subsequent cellulase adsorption to lignin and enhances cellulose hydrolysis. Bioresour. Technol., 128276 https://doi.org/10.1016/j.biortech.2022.128276.

Liu, R., Dai, L., Zou, Z., Si, C., 2018. Drug-loaded poly (L-lactide)/lignin stereocomplex film for enhancing stability and sustained release of trans-resveratrol. Int. J. Biol. Macromol. 119, 1129–1136. https://doi.org/10.1016/j.ijbiomac.2018.08.040.

Lora, J., 2008. Industrial commercial lignins: sources, properties and applications. Monomers, Polymers And Composites From Renewable Resources. Elsevier, pp. 225–241.

Lu, Q., Zhu, M., Zu, Y., Liu, W., Yang, L., Zhang, Y., ... Li, W., 2012. Comparative antioxidant activity of nanoscale lignin prepared by a supercritical antisolvent (SAS) process with non-nanoscale lignin. Food Chem. 135 (1), 63–67. https://doi.org/10.1016/j.foodchem.2012.04.070.

Ma, Z., Wang, J., Zhou, H., Zhang, Y., Yang, Y., Liu, X., Wang, S., 2018. Relationship of thermal degradation behavior and chemical structure of lignin isolated from palm kernel shell under different process severities. Fuel Process. Technol. 181, 142–156.

Mansur, H.S., Mansur, A.A., Bicallho, S.M., 2005. Lignin-hydroxyapatite/tricalcium phosphate biocomposites: SEM/EDX and FTIR characterization. Key Eng. Mater. 284–286, 745–748. https://doi.org/10.4028/www.scientific.net/KEM.284-286.745.

Medina, J.D.C., Woiciechowski, A.L., Filho, A.Z., Bissoqui, L., Noseda, M.D., Vandenberghe, L.P.de S., Zawadzki, S.F., Soccol, C.R., 2016. Biological activities and thermal behavior of lignin from oil palm empty fruit bunches as potential source of chemicals of added value. Ind. Crops Prod. 94, 630–637.

Mehta, M.J., Kumar, A., 2019. Ionic liquid stabilized gelatin-lignin films: a potential UV-shielding material with excellent mechanical and antimicrobial properties. Chem. Eur. J. 25 (5), 1269–1274. https://doi.org/10.1002/chem.201803763.

Morganti, P., Danti, S., Coltelli, M.B., 2018. Chitin and lignin to produce biocompatible tissues. Res. Clin. Dermatol. 1, 5–11.

Myint, A.A., Lee, H.W., Seo, B., Son, W.S., Yoon, J., Yoon, T.J., Lee, Y.W., 2016. One pot synthesis of environmentally friendly lignin nanoparticles with compressed liquid carbon dioxide as an antisolvent. Green Chem. 18 (7), 2129–2146. https://doi.org/10.1039/c5gc02398j.

Nada, A.M.A., El-Diwany, A.I., Elshafei, A.M., 1989. Infrared and antimicrobial studies on different lignins. Acta Biotechnol. 9, 295–298. https://doi.org/10.1002/abio.370090322.

Nguyen, N.T.T., Nguyen, L.M., Nguyen, T.T.T., Liew, R.K., Nguyen, D.T.C., Van Tran, T., 2022. Recent advances on botanical biosynthesis of nanoparticles for catalytic, water treatment and agricultural applications: a review. Sci. Total Environ., 154160 https://doi.org/10.1016/j.scitotenv.2022.154160.

Norikura, T., Mukai, Y., Fujita, S., Mikame, K., Funaoka, M., Sato, S., 2010. Lignophenols decrease oleate-induced apolipoprotein-B secretion in HepG2 cells. Basic Clin. Pharmacol. Toxicol. 107 (4), 813–817. https://doi.org/10.1111/j.1742-7843.2010.00575.x.

Norikura, T., Mukai, Y., Fujita, S., Mikame, K., Funaoka, M., Sato, S., 2010. Lignophenols decrease oleate-induced apolipoprotein-B secretion in HepG2 cells. Basic Clin. Pharmacol. Toxicol. 107 (4), 813–817. https://doi.org/10.1111/j.1742-7843.2010.00575.x.

Nypelö, T.E., Carrillo, C.A., Rojas, O.J., 2015. Lignin supracolloids synthesized from (W/O) microemulsions: use in the interfacial stabilization of Pickering systems and organic carriers for silver metal. Soft Matter 11, 2046–2054. https://doi.org/10.1039/c4sm02851a.

Parvathy, G., Sethulekshmi, A.S., Jayan, J.S., Raman, A., Saritha, A., 2020. Lignin based nanocomposites: synthesis and applications. Process Saf. Environ. Prot. 145, 395–410. https://doi:10.1016/j.psep.2020.11.017.

Pham, C.D., Dang, M.D., Ly, T.B., Tran, K.D., Vo, N.T., Do, N.H., Le, P.K., 2023. A review of the extraction methods and advanced applications of lignin-silica hybrids derived from natural sources. Int. J. Biol. Macromol., 123175 https://doi.org/10.1016/j.ijbiomac.2023.123175.

Ponnusamy, V.K., Nguyen, D.D., Dharmaraja, J., Shobana, S., Banu, J.R., Saratale, R.G., Chang, S.W., Kumar, G., 2019. A review on lignin structure, pretreatments, fermentation reactions and biorefinery potential. Bioresour. Technol. 271, 462–472. https://doi.org/10.1016/j.biortech.2018.09.070.

Popa, V.I., Capraru, A.M., Grama, S., Malutan, T., 2011. Nanoparticles based on modified lignins with biocide properties. Cellul. Chem. Technol. 45 (3), 221–226. https://www.researchgate.net/publication/265234734_Nanoparticles_based_on_modified_lignins_with_biocide_properties.

Prakash, A., Singh, R., Balagurumurthy, B., Bhaskar, T., Arora, A.K., Puri, S.K., 2015. Thermochemical valorization of lignin. In: Pandey, A., Bhaskar, T., Sukumaran, R.K. (Eds.), Recent Advances in Thermo-Chemical Conversion of Biomass, pp. 455–478.

Qian, Y., Deng, Y., Qiu, X., Li, H., Yang, D., 2014. Formation of uniform colloidal spheres from lignin, a renewable resource recovered from pulping spent liquor. Green Chem. 16 (4), 2156. https://doi.org/10.1039/c3gc42131g.

Qian, Y., Zhang, Q., Qiu, X., Zhu, S., 2014. CO2-responsive diethylaminoethyl-modified lignin nanoparticles and their application as surfactants for CO2/N2-switchable Pickering emulsions. Green Chem. 16, 4963–4968. https://doi.org/10.1039/C4GC01242A.

Quraishi, S., Martins, M., Barros, A.A., Gurikov, P., Raman, S.P., Smirnova, I., Reis, R.L., 2015. Novel non-cytotoxic alginate–lignin hybrid aerogels as scaffolds for tissue engineering. J. Supercrit. Fluids 105, 1–8. https://doi.org/10.1016/j.supflu.2014.12.026.

Rahman, O.ur, Shi, S., Ding, J., Wang, D., Ahmad, S., Yu, H., 2018. Lignin nanoparticles: synthesis, characterization and corrosion protection performance. New J. Chem. 42 (5), 3415–3425. https://doi.org/10.1039/c7nj04103a.

Ravishankar, K., Venkatesan, M., Desingh, R.P., Mahalingam, A., Sadhasivam, B., Subramaniyam, R., Dhamodharan, R., 2019. Biocompatible hydrogels of chitosan-alkali lignin for potential wound healing applications. Mater. Sci. Eng. C 102, 447–457. https://doi.org/10.1016/j.msec.2019.04.038.

Rekola, J., Aho, A.J., Gunn, J., Matinlinna, J., Hirvonen, J., Viitaniemi, P., Vallittu, P.K., 2009. The effect of heat treatment of wood on osteoconductivity. Acta Biomater. 5 (5), 1596–1604. https://doi.org/10.1016/j.actbio.2009.01.018.

Reshmy, R., Balakumaran, P.A., Divakar, K., Philip, E., Madhavan, A., Pugazhendhi, A., Sirohi, R., Binod, P., Awasthi, M.K., Sindhu, R., 2022. Microbial valorization of lignin: prospects and challenges. Bioresour. Technol. 344, 126240. https://doi.org/10.1016/j.biortech.2021.126240.

Richter, A.P., Bharti, B., Armstrong, H.B., Brown, J.S., Plemmons, D., Paunov, V.N., Velev, O.D., 2016. Synthesis and characterization of biodegradable lignin nanoparticles with

tunable surface properties. Langmuir 32 (25), 6468–6477. https://doi.org/10.1021/acs.langmuir.6b01088.
Richter, A.P., Brown, J.S., Bharti, B., Wang, A., Gangwal, S., Houck, K., Cohen Hubal, E.A., Paunov, V.N., Stoyanov, S.D., Velev, O.D., 2015. An environmentally benign antimicrobial nanoparticle based on a silver-infused lignin core. Nat. Nanotechnol. 10, 817–823. https://doi.org/10.1038/nnano.2015.141.
Rihayat, T., Suryani, Siregar, J.P., Zaimahwati, Salmyah, Helmi, Sariadi, Fitria, Satriananda, Putra, A., Fona, Z., Juanda, Raudah, Mawaddah, Nurhanifa, Riskina, S., Syahputra, W., Jaafar, J., 2019. Wound dressing based on banana peels waste and chitosan by strengthening lignin as wound healing medicine. IOP Conf. Ser.: Mater. Sci. Eng. C 506, 012056. https://doi.org/10.1088/1757-899x/506/1/012056.
Rojas, O.J., Bullon, J., Ysambertt, F., Forgiarini, A., Salager, J.L., Argyropoulos, D., 2007. Lignins as Emulsion Stabilizers. 953, pp. 182–199. https://doi.org/10.1021/bk-2007-0954.ch012.
Sakagami, H., Sheng, H., Yasui, T., Fukuchi, K., Oizumi, T., Ohno, H., Nakashima, H., 2017. Therapeutic potential of solubilized nanolignin against oral diseases. In: Andronescu, E., Grumezescu, A.M. (Eds.), Nanostructures for Oral Medicine, pp. 545–576 https://doi.org/10.1016/b978-0-323-47720-8.00019-5.
Salami, M.A., Kaveian, F., Rafienia, M., Samandari, S.S., Khandan, A., Naeimi, M., 2017. Electrospun polycaprolactone/lignin-based nanocomposite as a novel tissue scaffold for biomedical applications. J.Med. Signals Sensors 7 (4), 228–238. https://doi.org/10.4103/jmss.JMSS_11_17.
Saluja, B., Thakkar, J.N., Li, H., Desai, U.R., Sakagami, M., 2013. Novel low molecular weight lignins as potential anti-emphysema agents: in vitro triple inhibitory activity against elastase, oxidation and inflammation. Pulm. Pharmacol. Ther. 26 (2), 296–304. https://doi.org/10.1016/j.pupt.2012.12.009.
Sathawong, S., Sridach, W., Techato, K., 2018. Lignin: isolation and preparing the lignin based hydrogel. J. Environ. Chem. Eng. 6 (5), 5879–5888.
Sato, S., Mukai, Y., Yamate, J., Norikura, T., Morinaga, Y., Mikame, K., Fujita, S., 2009. Lignin-derived lignophenols attenuate oxidative and inflammatory damage to the kidney in streptozotocin-induced diabetic rats. Free Radic. Res. 43 (12), 1205–1213. https://doi.org/10.3109/10715760903247264.
Sethupathy, S., Morales, G.M., Gao, L., Wang, H., Yang, B., Jiang, J., Sun, J., Zhu, D., 2022. Lignin valorization: status, challenges and opportunities. Bioresour. Technol., 126696 https://doi.org/10.1016/j.biortech.2022.126696.
Shankar, S., Rhim, J.W., Won, K., 2018. Preparation of poly (lactide)/lignin/silver nanoparticles composite films with UV light barrier and antibacterial properties. Int. J. Biol. Macromol. 107, 1724–1731. https://doi.org/10.1016/j.ijbiomac.2017.10.038.
Sharma, S., Kumar, A. (Eds.), 2020. Lignin. Springer Series on Polymer And Composite Materials, p. 298 https://doi.org/10.1007/978-3-030-40663-9.
Sharma, S., Sharma, A., Mulla, S.I., Pant, D., Sharma, T., Kumar, A., 2020. Lignin as potent industrial biopolymer: An introduction. In: Sharma, S., Kumar, A. (Eds.), Lignin: Biosynthesis And Transformation for Industrial Applications, pp. 1–15 https://doi.org/10.1007/978-3-030-40663-9_1.
Sipponen, M.H., Farooq, M., Koivisto, J., Pellis, A., Seitsonen, J., Österberg, M., 2018. Spatially confined lignin nanospheres for biocatalytic ester synthesis in aqueous media. Nat. Commun. 9 (1), 2300. https://doi:10.1038/s41467-018-04715-6.
Sirviö, J.A., Ismail, M.Y., Zhang, K., Tejesvi, M.V., Ämmälä, A., 2020. Transparent lignin-containing wood nanofiber films with UV-blocking, oxygen barrier, and anti-microbial properties. J. Mater. Chem. A 8, 7935–7946.
Spasojević, D., Zmejkoski, D., Glamočlija, J., Nikolić, M., Soković, M., Milošević, V., Radotić, K., 2016. Lignin model compound in alginate hydrogel: a strong antimicrobial agent with high potential in wound treatment. Int. J. Antimicrob. Agents 48 (6), 732–735. https://doi.org/10.1016/j.ijantimicag.
Spender, J., Demers, A.L., Xie, X., Cline, A.E., Earle, M.A., Ellis, L.D., Neivandt, D.J., 2012. Method for production of polymer and carbon nanofibers from water-soluble polymers. Nano Lett. 12, 3857–3860. https://doi.org/10.1021/nl301983d.
Spiridon, I., 2018. Biological and pharmaceutical applications of lignin and its derivatives: a minireview. Cellul. Chem. Technol. 52 (7–8), 543–550.
Spiridon, I., Tanase, C.E., 2018. Design, characterization and preliminary biological evaluation of new lignin-PLA biocomposites. Int. J. Biol. Macromol. 114, 855–863.
Sun, Y., Ma, Y., Fang, G., Ren, S., Fu, Y., 2016. Controlled pesticide release from porous composite hydrogels based on lignin and polyacrylic acid. Bioresources 11 (1), 2361–2371.
Sun, Y., Yang, L., Lu, X., He, C., 2015. Biodegradable and renewable poly (lactide)–lignin composites: synthesis, interface and toughening mechanism. J. Mater. Chem. A 3, 3699–3709. https://doi.org/10.1039/C4TA05991C.
Tamminenetal.,2014T. Tamminen T. Ropponen H. Eva-Lena K Poppius-Levlin ., 2014. Functionalized lignin and method of producing the same. United States Patent No. 2014/0243511A1. Available at: https://patentimages.storage.googleapis.com/02/05/ad/8b6bff013f0857/US20140243511A1.pdf.
Tayeb, H.A., Tajvidi, M., Bousfield, D., 2020. Paper-based oil barrier packaging using lignin-containing cellulose nanofibrils. Molecules 25 (6), 1344.
Thakkar, J.N., Tiwari, V., Desai, U.R., 2010. Nonsulfated, cinnamic acid-based lignins are potent antagonists of HSV-1 entry into cells. Biomacromolecules 11 (5), 1412–1416. https://doi.org/10.1021/bm100161u.
Tian, D., Hu, J., Chandra, R.P., Saddler, J.N., Lu, C., 2017. Valorizing recalcitrant cellulolytic enzyme lignin via lignin nanoparticles fabrication in an integrated biorefinery. ACS Sustain. Chem. Eng. 5 (3), 2702–2710. https://doi.org/10.1021/acssuschemeng.6b03043.
Tortora, M., Cavalieri, F., Mosesso, P., Ciaffardini, F., Melone, F., Crestini, C., 2014. Ultrasound driven assembly of lignin into microcapsules for storage and delivery of hydrophobic molecules. Biomacromolecules 15 (5), 1634–1643. https://doi:10.1021/bm500015j.
Truong, N.P., Jones, G.R., Bradford, K.G.E., 2021. A comparison of RAFT and ATRP methods for controlled radical polymerization. Nat. Rev. Chem. 5, 859–869. https://doi.org/10.1038/s41570-021-00328-8.
United Nations World Tourism Organization, 2018. Tourism And the Sustainable Development Goals–Journey to 2030.
Vinardell, M.P., Mitjans, M., 2017. Lignins and their derivatives with beneficial effects on human health. Int. J. Mol. Sci. 18 (6), 1219.
Wang, J., Tian, L., Luo, B., Ramakrishna, S., Kai, D., Loh, X.J., Mo, X., 2018. Engineering PCL/lignin nanofibers as an antioxidant scaffold for the growth of neuron and Schwann cell. Colloids Surf.B 169, 356–365. https://doi.org/10.1016/j.colsurfb.2018.05.021 2016.08.014.
Wang, K., Loo, L.S., Goh, K.L., 2016. A facile method for processing lignin reinforced chitosan biopolymer microfibres: optimising the fibre mechanical properties through lignin type and concentration. Mater. Res. Express 3, 035301.
Wang, L., Ago, M., Borghei, M., Ishaq, A., Papageorgiou, A.C., Lundahl, M., Rojas, O.J., 2019. Conductive carbon microfibers derived from wet-spzun lignin/nanocellulose hydrogels. ACS Sustain. Chem. Eng. 7 (6), 6013–6022. https://doi.org/10.1021/acssuschemeng.8b06081.
Wang, X., Zhou, Z., Guo, X., He, Q., Chen, H., Ge, C., 2016. Ultrasonic-assisted synthesis of sodium lignosulfonate-grafted poly (acrylic acid-co-poly (vinyl pyrrolidone) hydrogel for drug delivery. RSC Adv. 6 (42), 35550–35558. https://doi.org/10.1039/C6RA03398A.
Wei, Z., Yang, Y., Yang, R., Wang, C., 2012. Alkaline lignin extracted from furfural residues for pH-responsive Pickering emulsions and their recyclable polymerization. Green Chem. 14, 3230. https://doi.org/10.1039/C2GC36278C.
Wu, S., Zhang, Y., Han, J., Xie, Z., Xu, J., Guo, B., 2017. Copolymerization with polyether segments improves the mechanical properties of biodegradable polyesters. ACS Omega 2 (6), 2639–2648. https://doi.org/10.1021/acsomega.7b00517.
Xiao, D., Ding, W., Zhang, J., Ge, Y., Wu, Z., Li, Z., 2018. Fabrication of a versatile lignin-based nano-trap for heavy metal ion capture and bacterial inhibition. Chem. Eng. J. https://doi.org/10.1016/j.cej.2018.10.037.
Xie, M., Muchero, W., Bryan, A.C., Yee, K., Guo, H.B., Zhang, J., 2018. A 5-enolpyruvylshikimate 3-phosphate synthase functions as a transcriptional repressor in populus. Plant Cell 30, 1645–1660. https://doi:10.1105/tpc.18.00168.
Xing, Q., Buono, P., Ruch, D., Dubois, P., Wu, L., Wang, W.J., 2019. Biodegradable UV blocking films through core-shell lignin-melanin nanoparticles in poly (butylene adipate-co-terephthalate). ACS Sustain. Chem. Eng. 7, 4147–4157. https://doi.org/10.1021/acssuschemeng.8b05755.
Yang, M., Zhao, W., Singh, S., Simmons, B., Cheng, G., 2019. On the solution structure of kraft lignin in ethylene glycol and its implication for nanoparticle preparation. Nanoscale Adv. 1, 299–304. https://doi.org/10.1039/C8NA00042E.
Yang, W., Fortunati, E., Bertoglio, F., Owczarek, J.S., Bruni, G., Kozanecki, M., Kenny, J.M., Torre, L., Visai, L., Puglia, D., 2018. Polyvinyl alcohol/chitosan hydrogels with enhanced antioxidant and antibacterial properties induced by lignin nanoparticles. Carbohydr. Polym. 181, 275–284. https://doi.org/10.1016/j.carbpol.2017.10.084.
Yang, W., Owczarek, J.S.S., Fortunati, E., Kozanecki, M., Mazzaglia, A., Balestra, G.M.M., Kenny, J.M.M., Torre, L., Puglia, D., 2016. Antioxidant and antibacterial lignin nanoparticles in polyvinyl alcohol/chitosan films for active packaging. Ind. Crop. Prod. 94, 800–811. https://doi.org/10.1016/j.indcrop.2016.09.061.
Yearla, S.R., Padmasree, K., 2016. Preparation and characterisation of lignin nanoparticles: evaluation of their potential as antioxidants and UV protectants. J. Exp. Nanosci. 11, 289–302. https://doi.org/10.1080/17458080.2015.1055842.
Yiamsawas, D., Beckers, S.J., Lu, H., Landfester, K., Wurm, F.R., 2017. Morphology-controlled synthesis of lignin nanocarriers for drug delivery and carbon materials. ACS Biomater. Sci. Eng. 3, 2375–2383. https://doi.org/10.1021/acsbiomaterials.7b00278.
Yin, H., Liu, L., Wang, X., Wang, T., Zhou, Y., Liu, B., Lü, X., 2018. A novel flocculant prepared by lignin nanoparticles-gelatin complex from switch grass for the capture of Staphylococcus aureus and Escherichia coli. Colloids Surf. A Physicochem. Eng. Asp. 545, 51–59. https://doi:10.1016/j.colsurfa.2018.02.033.
Yu, B., Chang, Z., Zhang, Y., Wang, C., 2018. Preparation and formation mechanism of size-controlled lignin based microsphere by reverse phase polymerization. Mater. Chem. Phys. 203, 97–105. https://doi:10.1016/j.matchemphys.2017.08.039.
Zhang, X., Zhou, Y., Xiong, W., Wei, W., Jiang, W., 2022. Co-production of xylose, lignin, and ethanol from eucalyptus through a choline chloride-formic acid pretreatment. Bioresour. Technol. 359, 127502. https://doi.org/10.1016/j.biortech.2022.127502.
Zhang, Y., Jiang, M., Zhang, Y., Cao, Q., Wang, X., Han, Y., Zhou, J., 2019. Novel lignin–chitosan–PVA composite hydrogel for wound dressing. Mater. Sci. Eng. C 104, 110002. https://doi.org/10.1016/j.msec.2019.110002.
Zhen, X., Li, H., Xu, Z., Wang, Q., Zhu, S., Wang, Z., Yuan, Z., 2021. Facile synthesis of lignin-based epoxy resins with excellent thermal-mechanical performance. Int. J. Biol. Macromol. 182, 276–285. https://doi:10.1016/J.IJBIOMAC.2021.03.203.
Zhimingetal.,2013L. Zhiming L. Chao W. Haiying , 2013. Preparation method of nanolignin with controllable particle size. Chinese Patent CN. 103145999A. https://patents.google.com/patent/CN103145999A/en.
Zhiqiangetal.,2011S. Zhiqiang S. Wenfeng Z. Jun Z. Baoyou Z.Y. Bin Y. Lei Z. Baishi Z. Xiuhua Z. Jian H. Luming , 2011. Method for preparing nano lignin by using supercritical anti-solvent technology. Chinese Patent CN. 102002165A. https://patents.google.com/patent/CN102002165A/en.
Zhong, X., Qian, Y., Huang, J., Yang, D., Deng, Y., Qiu, X., 2016. Fabrication of lignosulfonate vesicular reverse micelles to immobilize horseradish peroxidase. Ind. Eng. Chem. Res. 55, 2731–2737. https://doi.org/10.1021/acs.iecr.5b04939.
Zhou, Y., Wang, D., Yang, D., Qiu, X., Li, Y., 2019. Avermectin loaded nanosphere prepared from acylated alkali lignin showed anti-photolysis property and controlled release performance. Ind. Crop. Prod. 137, 453–459.
Zhuang, X., Wang, W., Yu, Q., Qi, W., Wang, Q., Tan, X., Zhou, G., Yuan, Z., 2016. Liquid hot water pretreatment of lignocellulosic biomass for bioethanol production accompanying with high valuable products. Bioresour. Technol. 199, 68–75.
Zmejkoski, D., Spasojević, D., Orlovska, I., Kozyrovska, N., Soković, M., Glamočlija, J., Radotić, K., 2018. Bacterial cellulose-lignin composite hydrogel as a promising agent in chronic wound healing. Int. J. Biol. Macromol. 118, 494–503. https://doi.org/10.1016/j.ijbiomac.2018.06.067.